Comparative Biogeography of Dune-Restricted Insects in the Desert Southwest

By

Matthew H Van Dam

A dissertation submitted in partial satisfaction of the

requirements for the degree of

Doctor of Philosophy

in

Environmental Science, Policy and Management

in the

Graduate Division

of the

University of California, Berkeley

Committee in charge:

Professor Kipling W. Will, Chair
Professor Rosemary Gillespie
Professor Jimmy McGuire

Fall 2013

Abstract

Comparative Biogeography of Dune-Restricted Insects in the Desert Southwest

by

Matthew H Van Dam

Doctor of Philosophy in Environmental Science, Policy and Management

University of California, Berkeley

Professor Kipling W. Will, Chair

The focus of my thesis is on the biogeography of dune-restricted insects, there are three main inquiries I addressed in my thesis: **(1)** Testing the effect distance may have on dispersal in the sand dunes fauna of the desert Southwest of North America. **(2)** A statistical evaluation of phylogenetic signal contained in different character systems in *Trigonoscuta*, using novel reproductive characters to delimit species. **(3)** Incorporating more precise natural history data into niche modeling and an evaluation of its effect on adaptation to climate change in the giant flower-loving flies *Rhaphiomidas*.

(1) I am specifically testing the hypothesis that Pleistocene river corridors mediated dispersal among sand dune-restricted taxa and aquatic taxa found in desert springs. From the seven different genera of dune restricted taxa and four aquatic desert taxa I examined, it appears that some taxa have used river corridors of sandy habitat to disperse. Although the patterns are largely concordant they differ markedly in dispersal times. Some having long distance dispersal occurring in the Pleistocene while others only disperse at the local level having disjunct distributions the result of much older vicariance events. Using both the phylogenetic pattern and date estimates allows for my conclusions not to be drawn from pattern alone. In addition I examined the effect distance has on jump dispersal and vicariance. I incorporated GIS estimates of dispersal distance in a connectivity matrix to model the connectivity of river corridors. Model selection was then used to see if the constraints and distance effect improved the fit of the model to the data, indicating if there was an actual effect of the Pleistocene river corridors used as dispersal pathways. This application of patterns, distance and dates allows for more statistical testing of biogeographic hypothesis and has implications for biogeography as a whole to explicitly test the effect of distance on biogeographic reconstructions.

(2) The genus *Trigonoscuta* consists of 65 described species with 98 subspecies. I investigated the validity of these species using a combined approach of morphology and molecular data to be able to properly delimit and reliably identify the species. For delimiting the species I examined the morphology of the male endophallus. The endophallus is the internal structure of the male genitalia, which is everted during mating. I derived a novel technique to evert the endophallus consistently. The characters of the endophallus alone repeated the relationships seen in the molecular data and provided

characters to delimit and describe species using morphological criteria. Using the consistency index (CI), I evaluated the contribution of each morphological character across all the equally most parsimonious trees. I then used this data to see if there was statistical support for which character system provided more phylogenetic resolution. This supported the idea that using the endophallus outperformed more traditional characters and should be utilized in phylogenetic reconstruction more often.

(3) I explored how partitioning climate data by day influences niche model predictions, as estimated by the MaxEnt machine-learning algorithm, for taxa with constrained phenologies. I utilized the giant flower-loving flies *Rhaphiomidas* because of their discrete phenologies as my focal taxon. I compared the results of partitioned by day data with WorldClim data that is partitioned by moth to examine what effect using more precise data has on species distribution models. I also examined how phylogenetic signal in both life history traits and climate tolerances can be used to identify how they adapt to different climates.

Acknowledgements

There are a good many people I would like to thank. I will go through in chronological order as to when I met them as best I can. First I would like to thank my Mom, Dad, and brother Alex. As I am a twin direct family is listed together. I would like to thank both of my parents for the support they gave me when I was little encouraging me in what ever I did. I would also like to thank here my Grandparents. To Grandpa Bob thanks for also encouraging me in my pursuits, I always was enthralled by all the storied you had in the Solomon Islands during WWII. I would also like to give thanks to my late Grandma Harriett far that as well. I would also especially like to thank Opa Herman and Grammie Barbara for their strong encouragement and help over the many years; I could not have been so successful with out you. To my late father, thanks for encouraging me to always do my best and encouraging and helping with all of the insect collecting when I was young. Ironically the hobby of collecting is what I am getting paid to do now so it was more valuable than we could have known. I wish you were still around so I could have your counsel on life issues as only you could, it is really sad to not have you around. To Mom I can truly see and partially relate to how hard it must have been to move on with life and not despair, your example of finding a way forward gives me some optimism in life. I would also like to thank here a dear friend on the family who also passed away too soon, only about a year after my dad when I was in the third year of grand school. Bill Baker you were one of the most inspirational people I have ever met your spirit of exploration and stories of travels plant collecting in South and Central America gave me the desire to do the same. I would now like to thank my brother. You were a huge help in the beginning of the thesis helping in collecting samples and working with me on publications. I hope we can still go collecting in the future if our careers do not take us too far apart, oh what we have sacrificed for these degrees and careers far too much. Time with people we can never get back.

Looking forward now. I would like to thank Art Evens and Rosser Garrison for their encouragement when I was young getting me into the nuts and bolts of insect identification and collecting. I would also like to thank Brian Brown for getting me interested in perusing work on *Rhaphiomidas*. As well Rick Rogers and Greg Ballmer with help collecting. I would like to thank Doug Yanega for his help during undergrad improving my identification skills as well as being a good friend. I would also like to thank Charlie O'Brien for his help with *Trigonoscuta* and encouragement to work on weevils. I would like to thank my advisor Kip Will, for being a good advisor and always having his door open to my many questions, as well as reviewing my many grants and papers. Especially for not discouraging me or being harsh on my many ideas, I really needed the perspective you provided. I would also like to thank Rosie Gillespie for having her door open and being so kind and helping with the many letters I have asked for. I would also like to thank George Roderick for giving encouragement and perspective on ideas I should peruse. I would also like to thank Ted Papenfuss for his many stories of collecting reptiles and interest in my ideas, it was very nice to have. I would also like to thank Jimmy McGuire for his careful edits of my thesis and suggestions.

To my grad school friends, there are so many to name who have been so kind over the years. Thanks to Michael Brewer for help with using the big computer in Rosie's lab, as well as being extremely generous with your time and being a good friend. I would also like to thank Lauren and Andy Rominger for being good friends and helping me with learning R, I could not have done it with out you both. I would also like to thank Nick Matzke for his help with the biogeographic analyses and being a good friend. I would like to give a special thanks to Brad Balukjian for being a very good friend over the years and helping me to see things for what they are and always giving me sound advice. You have been a great friend I probably would have quit if it were not for the balance in life you helped me to see. I look forward to reading the many articles and books you will write. I would also like to thank Meghan Cullpepper for your friendship in and out of lab it is so nice to have good friends. I would like to give a very special, special thanks to Athena Lam. Your kindness and love have made me be able to survive these last and most trying years. It has really been a great joy to have you in my life and I hope we will have many more years together. I would not have been able to finish without your love. From the time I first met you, you gave my life hope and caring when there was none. I am truly thankful for having you in my life.

The utility of the endophallus as a character system in *Trigonoscuta* (Coleoptera: Curculionidae) a statistical evaluation

ABSTRACT: In this study two different morphological character systems were evaluated as to the relative amount of phylogenetic signal they contain. The endophallic and external morphology character systems were statistically tested for their levels of homoplasy. The results demonstrate that the endophallic character system had a significantly higher average consistency index CI level, over the external characters. Additionally the morphological data supported the same clades, as did the molecular data. The results also demonstrate the utility of a comprehensive approach to evaluate characters, where by each character was evaluated over all of the equally most parsimonious trees. Additionally, the morphological data strongly influenced the results of the combined molecular and morphological analyses.

Key Words: Coleoptera, Curculionidae, endophallus, integrative taxonomy, molecular and morphological data, homoplasy

INTRODUCTION

The use of multiple independent lines of phylogenetic evidence to arrive at the best estimation of a phylogeny is one of the core principles of phylogenetics. How one evaluates the characters going into the analyses is of key importance as the characters are the foundation of the analyses. Despite the tremendous amount of data available through genome wide sequencing techniques, morphological data still play a pivotal role in phylogenetic reconstruction. For instance they are the only available data that allow for the incorporation of fossil taxa. This has become of great importance in total evidence dating analyses (Ronquist et al., 2012, Wood et al., 2012). Here I present a comprehensive method of character evaluation based on the widely used consistency index (CI) of Kluge and Farris (1969). The approach presented here is an improvement over methods that rely on a single best tree by which the characters' level of homoplasy are judged, as CI values vary between trees. Insect genitalia and external morphology are two character systems that are evaluated using this method. In addition to testing the amount of homoplasy present in these subsets of morphological characters, the second aim of this paper is to provide a phylogeny-based classification of *Trigonoscuta* weevils. To accomplish this, two different lines of evidence were used to arrive at a robust phylogenetic hypothesis for *Trigonoscuta*. Both morphological and molecular data are used to reconstruct phylogenetic hypotheses for the genus. Combined morphological and molecular data sets and the molecular data alone were tested using different topological constraints to find which topology was most probable given the data.

Insect genitalia have been used in a variety of studies from species delimitations to model systems of sexual selection (Puniamoorthy et al. 2010, Higginson et al. 2012). Studies of sexual selection involving insect genitalia have focused primarily on the post-copulatory mechanisms of selection (Dybas and Dybas 1981, Presgraves et al. 1999, Pitnick et al. 1999, Minder et al. 2005, Holman et al. 2007, Rugman-Jones and Eady 2008, Higginson et al. 2012), with only a few linking the interactions between the

endophallus and female genitalia (Eberhard 1993, Arnqvist et al. 2002, Takami 2002, Takami and Sota 2007, Ronn et al. 2007, Matsumura and Yoshizawa 2010). In cases of species delimitation, male genitalia have been the primary character system for differentiation. For species of Coleoptera, the median lobe of the aedeagus is typically included in species descriptions, with the endophallus much more rarely discussed. The endophallus is the structure that is placed into the bursacopulatrix to deliver sperm and accessory fluids, and so is in direct contact with the female internal structures (Dungelhoef and Schmitt 2010). Given this, there is high likelihood that the endophallus could bear evidence for both species boundaries and phylogenetic relationships. Despite the possibility it could be the bearer of important evidence, endophallus morphology is only commonly used for certain taxa (e.g. in Carabidae Allen 1972, Berlov 1992, Angus et al. 2000, Will 2002, Sasakawa and Kubota 2007), but remains little studied among many polyphagan groups like weevils. The utility of the endophallus and over-all genitalic morphology as an indicator of reproductive isolation is perhaps surprisingly not well studied (Coyne and Orr 2004). The "lock and key" hypothesis, although used extensively in the systematics literature, has only been tested in a few instances (Eberhard 1985, 1992, Shapiro and Porter 1989, Sota and Kubota 1998, Tanabe and Sota 2008). The diversity of forms seen in beetle genitalia is extensive, promoted by drift in allopatry or as a reproductive isolating mechanism in sympatry or sexual selection. Whatever the cause of this morphological diversity, its utility as a character system is worthy of investigation. In this study, I explore the phylogenetic signal provided by the endophallus, which I suspect to be an overlooked character system for weevils.

The first studies of the endophallus in Coleoptera were by Verhoeff (1895) and Jeannel (1911). Sharp and Muir (1912) first reviewed the endophallus throughout Coleoptera, followed by a more thorough examination by Sharp (1918). More recently the endophallus has been examined in the Adephaga, Curculionoidea, and Chrysomeloidea, demonstrating its utility for species delimitation (Schoof 1942, Gilbert 1964, Silfverberg 1972, Howden 1982, Thompson 1988, Anderson 1987, Liebherr 1994, Whitehead and Ball 1997, Angus et al. 2000, Takami and Sota 2007, Tracy and Robbins 2009). Many of these authors found species-diagnostic variation in the endophallus, although several of these authors remarked on the difficulty of extraction and inflation of the organ (Anderson 1987, Tracy and Robbins 2009). Few studies have quantified the information that the endophallus provides relative to other character systems. Thompson (1988) remarked on how endophalli of *Leptostethus* weevils, were useful in identifying species groups for which external characters may be misleading. Additionally, Anderson (1987) used the endopahlli to resolve species groups in the weevil tribe Cleonini. Other studies have evaluated the use of endophallic sclarites in order to assess their phylogenetic utility (Tarasov and Solodovnikov 2011). The present study will be the first to fully explore the phylogenetic signal contributed by the endophallus using a thorough examination of summary statistics.

A single genus may be highly variable in endophallus form (Thompson 1988, Anderson 1987). Thompson (1988) and Anderson (1987) used this variation to inform their reconstruction of relationships with in their respective taxa of study. The placement and position of the sclerites on the endophallus also provides characters in addition to the shapes of endophallus lobes. The endophallus provides many characters other than those

present in the median lobe, which is the morphological structure typically used in species descriptions and phylogenetic analyses (Anderson 1987).

Taxonomic Background

The Curculionidae compose some 40,000 species (Oberprieler et al. 2007). The weevil subfamily Entiminae – known as broad-snouted weevils – represent approximately 30% of all weevil species (Kuschel 1995). The naming of this large group is complicated in and of itself, however, and weevil systematists generally agree upon its putative monophyly (see Alonso-Zaraaga and Lyal (1999) for the nomenclatural history of changes). Entiminae monophyly is supported by the rostrum not being sexually dimorphic, with adults bearing a scar from the deciduous cusp on the mandibles (Thompson 1992). Kissinger's (1964) key to the genera of North American weevils split the current concept of Entiminae into five different less inclusive subfamilies (Leptopiinae, Eremninae, Tanymecinae, Brachyrininae, and Thylacitinae). He also gave keys with characters to many tribes within Entiminae, but lacked defining characters for tribal placement of *Trigonoscuta*. O'Brien and Wibmer (1982) followed his classification and provided a taxonomic list of synonyms for weevils of North and Central America. Attempts to clarify the different groups within Entiminae were tentatively proposed by Marvaldi (1997,1998) using adult and larval characters, dividing this large subfamily into 5 different tribes. Alonso-Zaraaga and Lyal (1999) have Entiminae split amongst 54 different tribes. They do not give any justification other than taxonomic priority for tribal composition amongst the many genera of weevils. *Trigonoscuta* is currently placed in the Geonemini (Barynotini is a junior synonym) (Alonso-Zaraaga and Lyal 1999). However, its hypothesized relatives *Strangaliodes* are currently placed in the Tropiphorini as well as other allied genera such as *Miloderes* (Pierce 1975, pers. comm. C. O'Brien 2009).

Trigonoscuta represents some 65 species and 90 subspecies, most of which are geographical isolates; however, there are many that are apparently sympatric (Pierce 1975). From this study I consider there to be at most 9 sympatric species with 64 species being geographical isolates not readily distinguishable by morphology. *Trigonoscuta* has a distribution that covers Californian coastal dunes as well as dunes of the Mojave and Sonoran deserts. In addition, each one of the California Channel Islands has its own endemic species. Pierce (1975) designated four different subgenera *Eremocatoecus* Pierce 1975 (desert species), *Nesocatoecus* Peirce 1975 (Channel Island species), *Panormus* (Casey) (Point Reyes and Monterey, CA) and *Trigonoscuta* (s. str.) Motschulsky (remaining Pacific coast north of Mexico). *Trigonoscuta* is highly restricted to sand dunes, feeding on a variety of dune plants. All the members of this genus are entirely flightless. Adults bury themselves under the sand during the day and are active on the surface of the sand and on plants at night. Most *Trigonoscuta* are known from only one sand dune system, and most species are allopatric (Pierce 1975). Some authors have questioned the validity of the species that he described, especially the sympatric species, as they show little if any external morphological variation (Anderson 2002, Evans and Hogue 2006). Studies of *Trigonoscuta* endophalli will give additional evidence as to the validity of sympatric species proposed by Pierce (1975).

METHODS.

Taxon Sampling

Specimens were collected over the course of three years (2008-2011) and included the published range of *Trigonoscuta* as well as samples from Baja California and Sonora, Mexico that are well outside of the previously documented range. The total number of locations is over 200 (Fig. 1). Specimens were preserved in 95% ethanol stored on ice in the field and then transferred to a -20°C. Specimens were left intact and various parts dissected later during DNA extraction. Outgroups were selected from putative sister taxa to *Trigonoscuta* (Pierce 1975), as well as other North American dune restricted weevils (*Miloderes*). The ingroup taxa were selected from each of the known populations, treated as locations of non-interconnected sand dunes described in Pierce (1975), as well as localities from museum specimens (CAS, CDFA, COB, EMEC, LACM, UCD, UCR). For each location (isolated sand dune), individual specimens were treated as separate taxa so as not to bias the sampling by imposing previous taxonomic concepts. A maximum of 12 individuals were sampled per isolated dune, with an average of four, excluding US coastal species of *Trigonoscuta*. This was done to allow for the assessment of the level of incomplete lineage sorting between samples or instances of mitochondrial introgression.

Extraction, PCR, sequencing and alignment

DNA extraction was performed by dissecting male genitalia and or removing a hind leg. Each specimen was soaked in the DNAEasy® tissue kit's extraction buffer (with proteinase K) overnight, followed by completion of the manufacturer's DNA extraction protocol for animal tissue. The specimens and their associated parts were vouchered and used in subsequent morphological studies. Three gene regions were used in this study: the mitochondrial gene COI, and the nuclear genes Arginine Kinase and EF1-Alpha. For primer sequences, see supplementary documents Table 1. PCR was performed by using 12.5 ul GoTaq Master Mix (including DNTPs, buffer, taq and dye; Promega Corporation, Madison, WI), 1.25 ul 10lM forward and reverse primer, 7.0 ul water, and 1.0 ul template DNA yielding a 25ul reaction. PCR products were purified with Exosap-IT (US Biochemical Corporation, Cleveland, OH). Sanger sequencing was performed at UC Berkeley's DNA Sequencing Facility. Contigs were assembled and edited in Geneious Pro v. 4.6.4 (Biomatters Ltd.). Sequences were aligned by ClustalW-2.0.10 (Larkin et al. 2007) with settings set to GAPOPEN=90.0, GAPEXT=10. Sequences were color-coded by amino acid in Mesquite version 2.71 (Build 514) (Maddison and Maddison 2009) and checked by eye for stop codons.

Morphological coding

The morphological data matrix was constructed in Mesquite, version 2.71 (build 514) (Maddison and Maddison 2009). A total of 44 multistate characters were used to score a total of 131 taxa. The specimens were coded by location (their individual sand dunes), except for some of the coastal specimens that showed little variation along the Pacific coast. Homology statements for the endophallus are positional, with the apex of the median lobe at the base of the endophallus and the transfer apparatus at the apex of the

endophallus. All positions for endophallic characters are defined relative to these landmarks.

Phylogenetic Analyses

Parsimony reconstruction of morphological data and assessing the difference in homoplasy of morphological character systems.

The character matrix was analyzed with TNT ver. 1.1 (Goloboff et al., 2003) using the ‘‘traditional search’’ option to find the most parsimonious trees under the following parameters: memory set to hold 1,000,000 trees; 1000 replicates with tree bisection–reconnection (TBR) branch swapping and saving 1000 trees per replicate. The parenthetical trees from TNT were converted to Newick trees. Autapomophies and parsimony uninformative characters were removed. Each tree was then assigned branch lengths of 1. The resulting trees were then scored for consistency index (CI), retention index (RI), and rescaled consistency index (RCI) values for each individual character in a tree. Mean values and standard deviation were calculated for each character. These analyses were performed in R (R Development Core Team 2011) using the packages APE (Paradis et al., 2004), phangorn (Schliep 2011), and BioGeoBEARS (Matzke 2013), as well as with an additional custom R script (appendix 1). Characters were scored for theses metrics individually on all equally most parsimonious trees to evaluate their phylogenetic informativeness. These procedures were performed so that outliers could be identified and reexamined or taken out of future analyses. This approach is also advantageous for evaluating character systems relative to others through statistical examination rather than relying on character means based on a single tree. In order to test whether the two character systems are statistically distinct, a Wilcoxon signed-rank test was performed, with this statistic chosen because the distribution of CI means failed to follow a normal distribution (Fig. 5). A final metric was used to assess how the different trees partitioned the homoplasy (concentrated or dispersed over the tree) using Sang’s AUCC (1995), which was done to investigate if there were any noticeable differences in how the homoplasy was partitioned i.e. on one branch or over many. This metric could be used to identify a particular tree, which may be an outlier for how a character’s history is reconstructed.

Bayesian Phylogenetic Reconstruction.

For analyses of DNA data, each sequence was partitioned by codon position. This partitioning strategy was selected because it has been demonstrated repeatedly that incorporating different rates of DNA evolution for each codon position outperforms single partitioning strategies (Seago et al. 2011, Brandley et al. 2005, Fyler et al. 2005). Model selection was performed in MrModeltest2 (Nylander, 2002). The GTR+I+G model was selected for each of the partitions using the Akaike information criterion (AIC) for model selection. Bayesian analyses were performed in MrBayes v3.2.1 (Ronquist et al., 2012), using two parallel runs each with four simultaneous Markov chains (1 cold and 3 heated) for 20,000,000 generations, sampling every 1,000 generations. Convergence and stationarity of the MCMC chains were assessed in the program Tracer v1.4.1 (Rambaut and Drummond 2008). The first 10,000 samples were removed as burn-in, and 50% majority rule consensus trees for the molecular and

morphological trees were inspected visually for differences in topology for further testing. A combined Bayesian analysis of morphological and molecular data was performed. The Mk1 model (Lewis, 2001), with a gamma distribution for rate heterogeneity, was used for the morphological data in the combined analyses. Visualization of the different topologies was performed in DensiTree version 2.0.1. Before the combined analyses were performed, different partitions of across-site rate variation were run in MrBayes to see if there was a preferred partitioning strategy for the two character systems. First the morphological data was treated as a single partition with either gamma-distributed or equal across-site rate variation. For the second set of analyses, two partitions were set, one for the endophallic characters, and the other for the external characters. The endophallic characters were set as equal and the external characters were set with either equal or gamma-distributed across-site rate-variation.

In cases for which there was conflict between trees built with molecular characters alone and with combined morphological and molecular characters, further phylogenetic reconstructions were performed under identical conditions presented above except with a prior constraint implemented to test the monophyly of a clade, in this case the Sonoran Desert Species group 3 (see results for the definition of this species group). This was done in order to test if there was a significant difference between two topological hypotheses. Bayes factors were calculated as by Brown and Lemmon (2007), ($2\ln(BF21) = 2[\ln(HM2) - \ln(HM1)]$).

For both the morphological across-site rate variation and constrained topologies analyses, the topological unconstrained or single partition model was H1 and the topological constrained or two morphological partition model was H2. Here we were able to utilize the stepping-stone (SS) model in MrBayes3.2.2. Each analysis was run for $20x10^6$ MCMC generations sampling every 1000. The burn-in was 50% as in preliminary analyses convergence was reached by this point. Using stepping-stone sampling based on 50 steps with 1000 generations within each step estimated the marginal likelihoods. The average between the two runs were used in calculations of the Bayes factors. Prior topological constraints of the Sonoran Desert Species group 3 being monophyletic were placed on both the full set of taxa for which only molecular data was available (Fig. 16), and on a subset of 131 taxa including only molecular data (Fig 18), and on the combined morphological and molecular data (Fig. 20).

RESULTS

Phylogenetic Analyses

Parsimony reconstruction of morphological data

Forty-two parsimony-informative characters were retained from an original slate of 44 characters. Two characters, numbers 11 and 35 from the initial matrix, were removed because they proved uninformative. A total of 131 specimens were included in the morphological analyses. The same number of populations was included in the parsimony reconstruction as for the larger 418-specimen Bayesian analysis. Only a singe individual represented each sampling location, as including more individuals vastly increased the tree space to be searched. Each individual from the molecular analyses was examined in the morphological analyses to ensure that individual populations were not composed of

different morphotypes. In addition, specimens from museum collections were examined where specific locations could be confirmed. The analyses yielded a total of 100 most parsimonious trees, each with 174 steps. The strict consensus tree (Fig. 7), was different from that of the molecular tree, but the major species groups were always monophyletic except in the 418-taxa Bayesian analyses. The subgenera were all polyphyletic except for *Nesocatoecus*, with *Trigonoscuta* (s. str.) and *Panormus* forming a polyphyletic assemblage. Also, *Eremocatoecus* was rendered polyphyletic with the inclusion of undescribed taxa from Baja California Mexico. When the endophallus characters were examined alone, they produced a strict consensus tree that matched the topology of the molecular tree with regard to the subgenera, except for the placements of Sonoran Desert Species groups 2 and 5 (see discussion section for species groups), which together were found to be the sister group of all other members of the genus.

Assessing relative homoplasy of morphological character systems.

Mean and standard deviation values for the CI, RI, and RIC were calculated for each character across the 100 most parsimonious trees (Table 1-2). In order to assess if there was a significantly better CI value for the endophallic verses external characters of *Trigonoscuta,* mean values were first examined for normality in order to use the appropriate test for significance. Values were summed according to their CI values to create a histogram (Fig. 5) as well as to identify the range of values around the mean (Fig. 4). As the CI values for the non-endophallic characters did not form a normal distribution, when looking at a histogram of their values (Fig. 5), the Shapiro-Wilk normality test was performed on the CI mean values with a p-value = 0.000002409, so the data is significantly not normally distributed. Confirming that the CI mean values are not normally distributed requires a non-parametric test to see if the character systems are significantly different. A Wilcoxon rank sum test with continuity correction was performed to assess significance in the two character systems. The results show that the endophallic characters are significantly greater in CI value than those of the non-endophallic characters (p-value = 0.002323). When comparing the mean CI values with CI values of the strict consensus tree, the Wilcoxon rank sum test shows that they were not significantly different (p-value = 0.5945). The AUCC values did not indicate that there was any one tree that greatly differed in the partitioning of homoplasy from the others with a minimum value of 0.1180476 and a maximum of 0.1256429 (Fig. 6), but visual inspection of the trees across this range found very different topologies.

Bayesian phylogenetic reconstruction of morphological and genetic data

A total of 418 specimens were sequenced for 855 base pairs of COI. After the initial tree was constructed based on this extensively sampled mtDNA data set, single individuals from each of the major clades were selected for sequencing for EF1alpha (Fig. 13) and aginine kinase (ArgK) (Fig. 14) to see if nuclear gene trees yielded congruent topologies. The relationships between the four major clades of *Trigonoscuta* were represented in all three of the gene trees ((Coast, Channel Island), ((Sonoran Colorado Desert, Baja California), (Mojave Desert))). The gene tree of ArgK did not resolve clades for the Sonoran Desert species groups (see discussion for definitions of Sonoran Desert species groups) (Fig. 14). In addition, a putative sister taxon, *Plenaschopsis pilosisquama*

Blaisdell 1925, was placed inside *Trigonoscuta* in both mitochondrial and nuclear gene trees. Each of the desert populations sampled produced a monophyletic clade from the COI data (Fig 15). The only population samples that did not form monophyletic clades were those on the Pacific Coast, and some of the Channel Island clades. In addition, the subgenera *Trigonoscuta* (s. str.) and *Panormus* formed a polyphyletic assemblage. The subgenus *Eremocatoecus* formed a polyphyletic assemblage of desert species. The only subgenus that formed a monophyletic group is the Channel Island species of *Nesocatoecus.*

Before analyzing a data set combining molecular and morphological data, Bayes factors were compared between different partitioning strategies of across-site rate variation (Table 4). For the morphological portioning model selection we were able to use the stepping-stone estimates of the marginal likelihood. Partitioning the morphological data favored the single partition model, results were all significantly above 20 showing strong support. Since there was not any benefit to adding an extra parameter (partition), I selected the across site rate variation distribution with the best likelihood. As there is not any difference in the number of parameters between the distributions, the likelihoods can be directly compared; only the shapes of the prior controlling across-site rate variation are changed. The single partition gamma distribution of across-site rate-variation was chosen for the combined analyses, as this had the best likelihood score. The initial Bayesian phylogenetic reconstructions yielded some topologies that conflicted greatly with the cladistic hypotheses presented by morphological trees. The main and most striking conflict was the spitting of two of the Sonoran desert species groups 3 and 5, rendering them polyphyletic (see discussion for group definitions). An analysis was run with monophyly enforced for Sonoran Desert species group 3, with little impact according to Bayes factors (Table 3). There was negligible difference between the constrained and unconstrained phylogenies for the combined molecular and morphological data set. On the 131-terminal set with just molecular data, Bayes factors showed weak preference for the constrained analyses (Bayes factor =14.6), where an absolute value from 3-20 is considered support for the hypothesis in question. The full 418-taxa analysis showed strong preference for the unconstrained analysis with a Bayes factor of -27.11.

DISCUSSION

Divisions of *Trigonoscuta*

From the morphological and molecular data, 10 well-defined species groups can be recognized although there is ambiguity as to how they are all interrelated. Rather than define these groups as subgenera or separate genera they will simply be listed as species groups of *Trigonoscuta*. I define these groups because it is necessary to establish monophyletic groups for further analyses of their biogeography or ecological habits. The following discussion will describe the support for these 10 divisions.

Pacific Coast Species group 1, is composed of the Channel Island species the subgenus *Trigonoscuta* (s. str.) and *Nesocatoecus.* **Synapomorphies:** basal lobe of the endophallus bifurcated, distal apex of the rostrum faintly impressed, difference in scale

size between the pronotum and elytra (Fig. 2 B), parallel sides to the pronotum, transverse sulcus of rostrum not V-shaped, eyes emarginate (Fig. 2 F). The subgenus *Trigonoscuta* (s. str.), composed of the Pacific coast species of *Trigonoscuta* north of the desert regions of Baja California. The subgenus *Panormus* has no support, as there are no morphological syanpomorphies that support this group and the molecular data also fails to support this subegenus as distinct from the subgenus *Trigonoscuta* (s. str.).

Pacific Coast Species group 2, consists of the subgenus *Nesocatoecus* Channel Island species and a single land-locked species only know from the central valley of California near Kettleman City. **Synapomorphy**: dorsally bifurcated lobes of the endophallus (Fig 3 G).

Dale Lake Species group, is represented by Mojave Desert species of the Dale Lake Complex. **Synapomorphies:** inverted distal half of the endophallus (Fig. 3 A), a basal dorsal lobe that is U-shaped with strong patches of microtrichae, hind tibia corbel plates conical (Fig. 2 C). Placement of this group differs between molecular and morphological analyses when external characters are included.

The remaining desert species are supported by the synapomorphies of the apical impression of the rostrum raised, and an intermittent comb of setae on front tibia.

The next division contains 5 distinct species groups endemic to the Sonoran Desert. They are united based on the distal lobe of the endophallus tri-lobed (Fig 3 C,F,H), endophallus dorsal basal lobe expanded (Fig. 3 C,D,F,H), the fore tibia bent, hind tibia corbels with fine spines.

Sonoran Desert Species group 1, Colorado Desert species of the Gran Desierto. **Synapomorphies:** half inverted endophallus (Fig 3 H), lateral basal lobes greatly expanded, basal lobe reduced to a prominent hump, non-imbricate scales, scales uniformly white.

Sonoran Desert Species group 2, represents the species of the southern Pacific Coast of Baja California (south of Guerrero Negro). **Synapomorphies:** M-shaped transfer apparatus of the endophallis, wing-like formation of the lateral lobes (Fig 3 D), highly reduced middle section of the endophallus, spine-like scales of the hind tibia corbels (Fig 2 D).

Sonoran Desert Species group 3, composed of species on the coastal dunes of the Sea of Cortez South of San Felipe and in Sonora S of Puerto Peñasco. **Synapomorphies:** Gradually rounded basal lobe of the endophallus ending near middle (Fig 3 F), lateral margins expanded, forming narrow wing-shape, dorsal basal lobe with narrow hump, transfer apparatus short, with no ventral process.

Sonoran Desert Species group 4, represented by species that occupy the Colorado Desert portion of the Sonoran desert. **Synapomorphies**: endophallus entirely inverted (Fig. 3 C), should be noted here that this inversion is independent and not homologous with those of *Trigonoscuta* of the Rice and Opal Mountain dunes, as the scleratized base of the endophallus is parallel rater than perpendicular to the median lobe (Fig. 3 E), lateral basal lobes conical, transfer apparatus short, with a triangular base.

Sonoran Desert Species group 5, is represented by the Pacific coast species of Baja California. **Synapomorphies**: endophallus basal lateral lobes expanded, pointed towards transfer apparatus, setal comb of front tibia thin, hair-like (Fig. 2 A)

Mojave Desert Species group, This complex of species is confined mostly to the Mojave Desert but with some members present in the Colorado Desert region of the

Sonoran Desert. **Synapomorphies**: endophallus distal ventral lobe simple (Fig. 3 B), transfer apparatus robust, elongate.

Assessing differences in homoplasy of morphological character systems.

In this contribution, the strategy used to compare the two character systems was to fully explore CI values for each character over all of the equally most parsimonious trees. This was done to give a robust estimate of the homoplasy and signal present in the characters that was not reliant upon a randomly chosen "best" or consensus tree, as in Song and Bucheli (2010), Strong (2011), Tarasov and Solodovnikov (2011), Franz (2013). CI values for an entire tree are uninformative for character evaluation because the changes in character coding (unless performed individually) cannot be traced back to any one particular character. In addition, consensus estimates will be lower than any one of the most parsimonious trees, although in this case, not significantly different. If one hopes to actually improve the coding of a morphological character, the approach of picking a single most parsimonious tree from which to base decisions regarding whether to include or exclude the character could be positively misleading, as there are many alternative trees with different topologies (Fig. 10). Therefore, I chose to take a statistical approach to evaluate a character's information across all equally most parsimonious trees. The mean values of each character, along with standard deviations and ranges, provide a more robust estimate as to the information present in each character. Why should this approach be taken? I advocate not using a single "best" tree or consensus tree for character evaluation because of the statistical nuance. For example, if you were trying to measure the difference between two treatments and only based your analysis on a single replicate out of many, any reasonable person would agree that this is insufficient to accurately test the difference between two different treatments when replicates are likely to vary. The same could be said for evaluating character systems with a single "best" tree or consensus tree, when you have many different equally most parsimonious trees. As far as using a consensus tree this may or may not be an equivalent representation of each character type's mean CI value. I would advocate to at least test to see if they are different as opposed to working under untested assumptions.

The results from the AUCC metric (Fig. 6) show that at either end of the range, there are strikingly different topologies (Figs. 8-9). Tree 29 (max AUCC) is nearly the same as tree 81 with the lowest AUCC except for the optimization of a few characters that support splitting the Mojave Desert species group into two different clades (Characters 16 and 32 (Figs 11-12)). The topology of tree 29 more closely resembles that of the molecular data, with species found along the Mojave River drainage forming two separate sub-clades, each from a different sand dune system.

The results from the Wilcoxon rank sum test show that the endophallic characters had significantly less homoplasy than the external morphological characters. Although the level of significance is marginal, the results support observations made in Coleopteran systems (Tarasov and Solodovnikov 2011). The results presented here suggest that most of the endophallic characters have few deep-level synapomorphies within *Trigonoscuta*. One reason for this may be that the endophalli are so different between species groups that synapomorphies linking them are absent. In addition, the endophalli contain a limited number of positional homologies. The molecular data also

present a similar pattern where the relationships between species groups are similarly unresolved or show low posterior probability at the same nodes.

The impact of adding morphological characters in resolving phylogenetic hypotheses

The results from the different constrained analyses are quite telling. For the combined data, topological constraints uniting Sonoran Desert species group 3 was unequivocal between constrained and unconstrained searches (Table 3). Both analyses gave virtually identical results, and the addition of this constraint is unwarranted in this case as indicated by the Bayes factor. However when the morphological characters are removed, the Sonoran Desert species group 3 dissolved into a polytomy. In this case, the Bayes factors indicated support for the constrained model of the 131 sample set. This could indicate that the molecular data alone does not provide sufficient evidence to resolve the deep nodes in the Sonoran Desert species groups 2-5. When we look at the large taxa set of 418 samples, the Bayes factors indicates support for the unnstrained analyses. The results of the three separate analyses suggest several different explanations for the alternation of support for the monophyly of the Sonoran Desert species group 3. One possibility is that the COI data is insufficient to resolve these deeper nodes. Another is that the unconstrained topology is more optimal than constrained analyses of the 418 taxa, but perhaps less optimal than the topology presented in the subsample of 131 taxa. What is clear however, is that the addition of morphological characters provides strong evidence that the Sonoran Desert species group 3 is monophyletic and that the signature of the morphological data is not swamped out by that of the COI sequence data. These results are similar to those of Baker et al. (1998) and Wahlberg et al. (2005), in that the morphology contributed support (as seen in more resolution and higher posterior probabilities) to the phylogenetic hypotheses. In the aforementioned studies they relied upon parsimony analyses solely, and only looked at statistical support values of the incongruence index of Mickevitch and Farris (1981), and did not test topological constraints. Their results are still comparable even though they used different metrics for testing the contribution of morphological data.

CONCLUSIONS

From this study the utility of the endophallus as a character system is clearly demonstrated. This character system out-performs the external characters in *Trigonoscuta* by having a significantly higher CI value. The findings also support those of Tarasov and Solodovnikov (2011), who also found that the phylogenetic signal in this character system is equivalent to or greater than characters drawn from external morphology. Additionally, the statistical approach of evaluating individual character-performance across all equally most parsimonious trees gives a more complete picture as to the performance of the characters. This comprehensive method of examining characters will hopefully enhance and expedite the process by which we evaluate characters going into our analyses, as this is an objective way of evaluating a characters' informativeness. A second major finding is that the use of even a simple amount of morphological data has a positive impact in finding the most probable phylogenetic hypothesis.

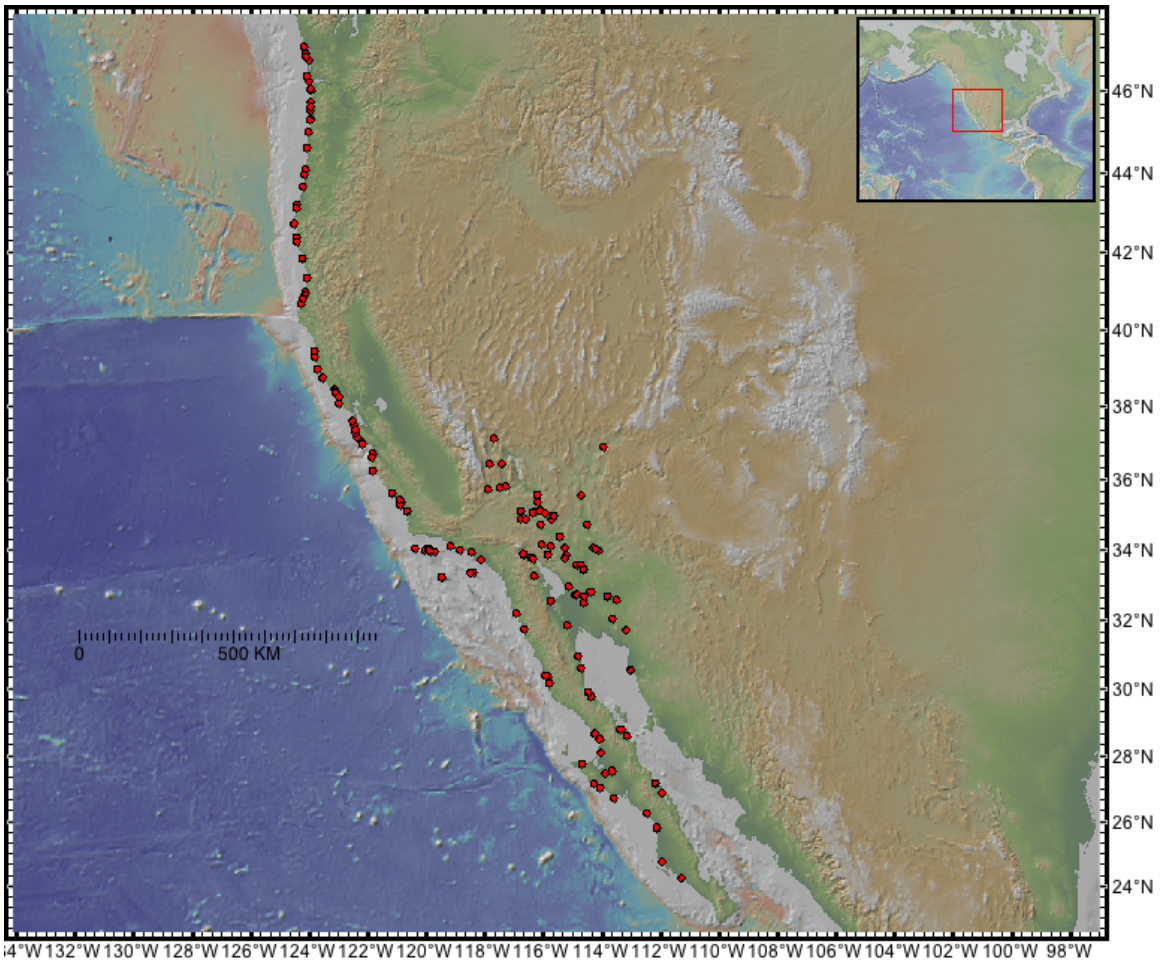

Fig. 1. Map of locations sampled for molecular analyses.

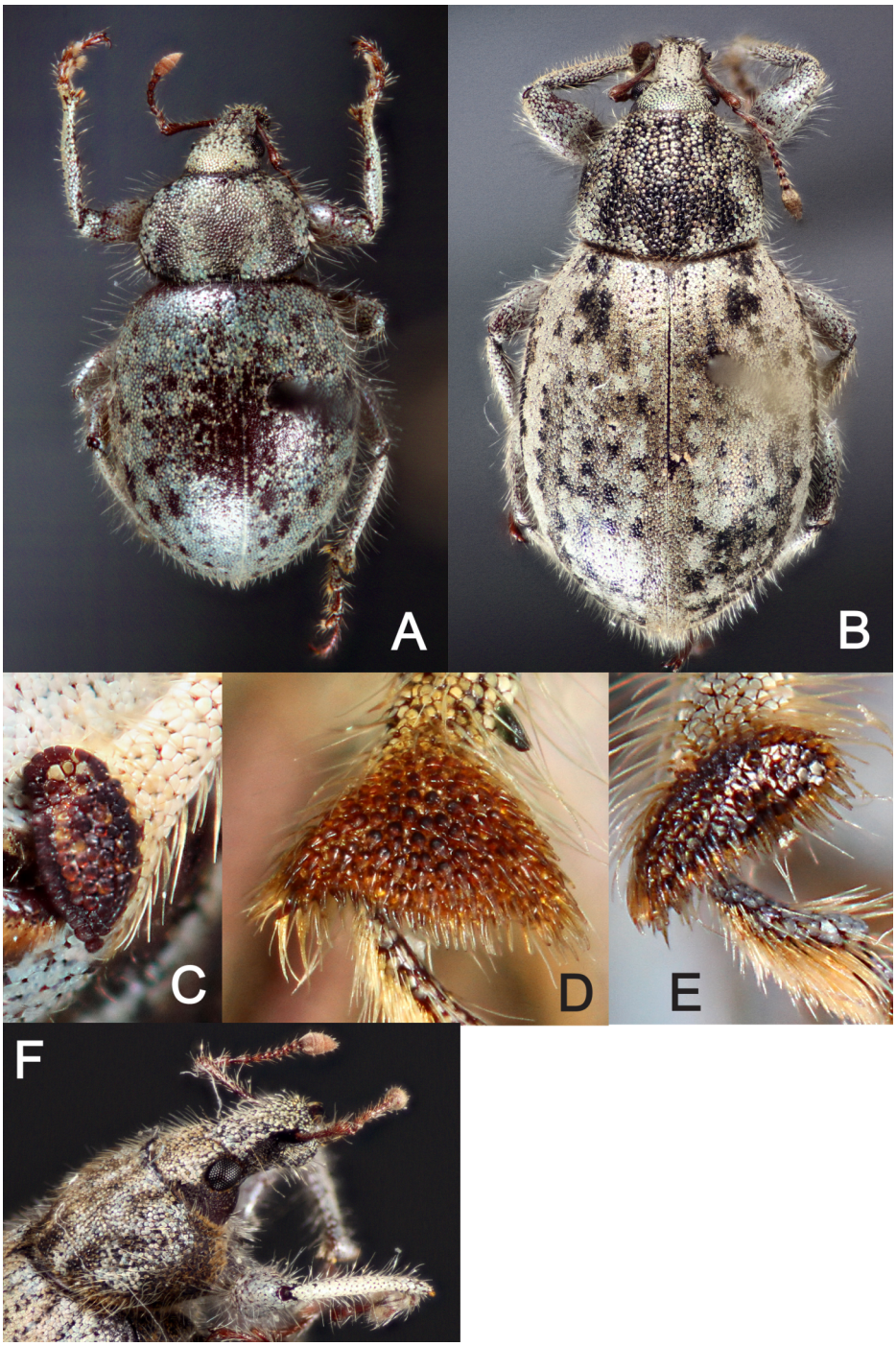

Fig. 2 External morphology of *Trigonoscuta*: **A.** *T.sp.* "Guerrero Negro", dorsal habitus. **B.** *T. sanclemetiensis*, dorsal habitus. **C.** *T. dalei*, hind tibia corbel. **D.** *Plenaschopsis pilosisquama*, hind tibia corbel. **E.** *T. cronies*, hind tibia corbel. **F.** T. sp. coast, lateral profile head and pronotum.

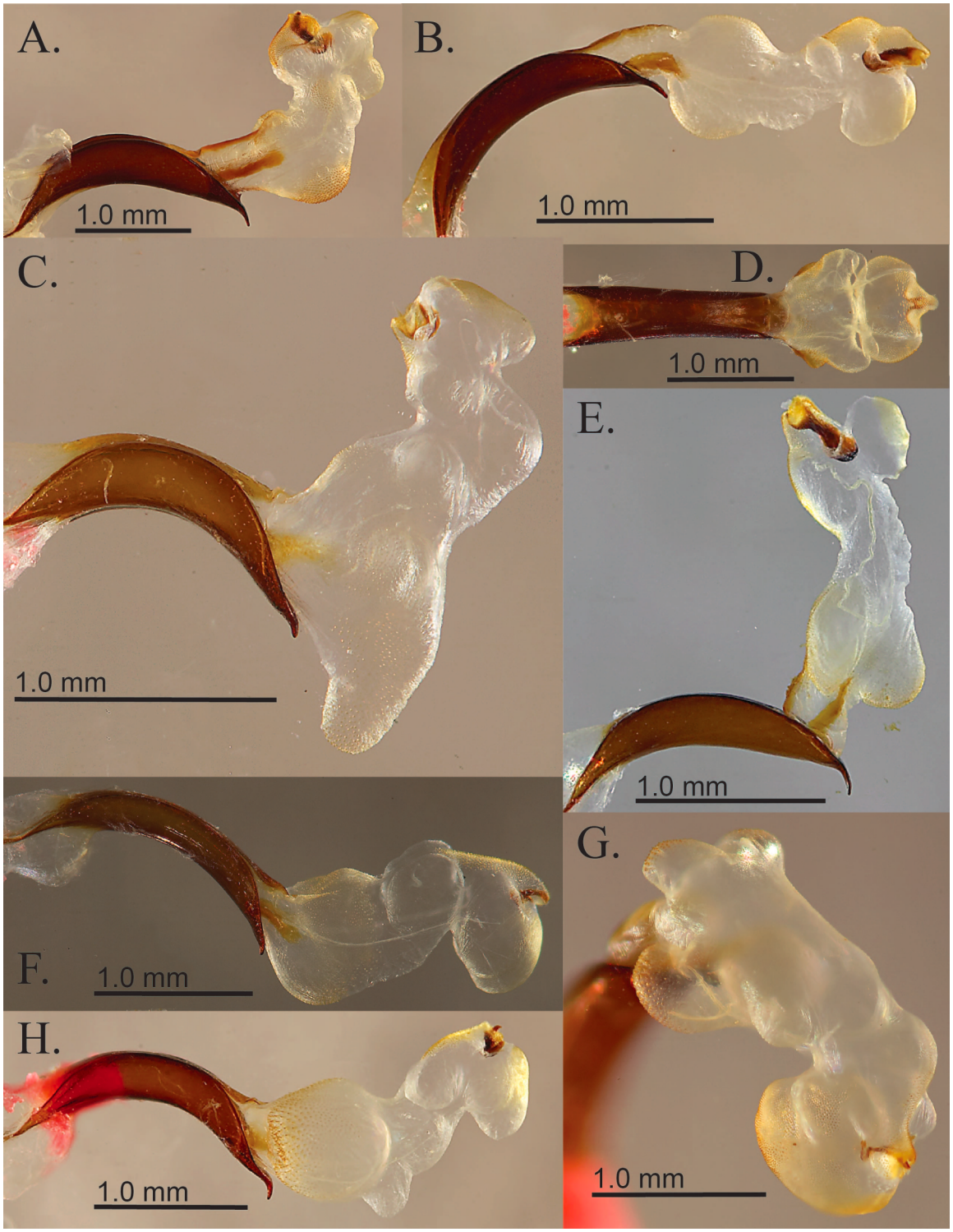

Fig. 3 Endophalli of *Trigonoscuta*. **A.** *T. dalei* Pierce 1975, lateral view **B.** *T. sp.* "Panamint Valley", lateral view **C.** *T.* c.f. *holtvillei* Pierce 1975, lateral view **D.** *T. sp.* "La Poza Grande", dorsal view **E.** *T. sp.* "Rice Dunes", lateral view **F.** *T. sp.* "San Bruno", lateral view **G.** *T. stantoni* Sleeper 1975, dorsolateral view **H.** *T.* c.f. *sanluisi* Pierce 1975, lateral view.

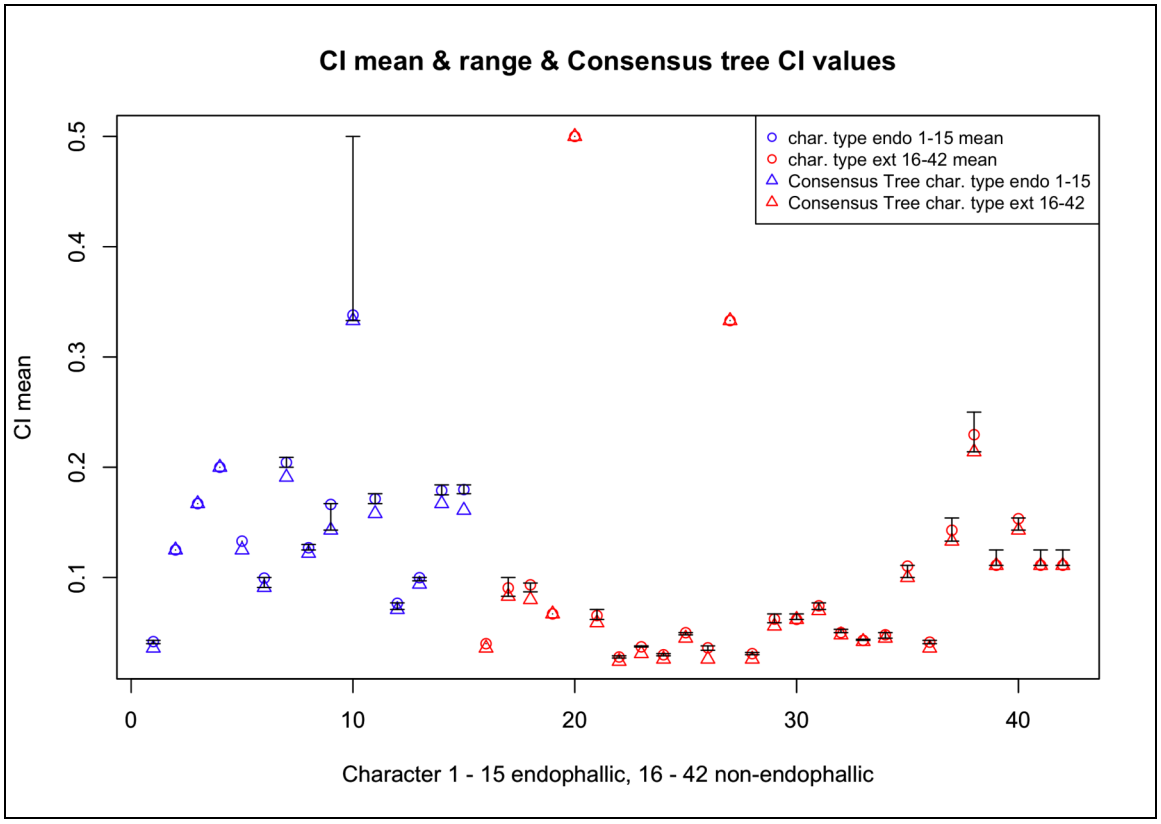
CI mean & range & Consensus tree CI values
char. type endo 1-15 mean
char. type ext 16-42 mean
Consensus Tree char. type endo 1-15
Consensus Tree char. type ext 16-42
CI mean
0.1
0.2
0.3
0.4
0.5
0
10
20
30
40
Character 1 - 15 endophallic, 16 - 42 non-endophallic

Fig. 4

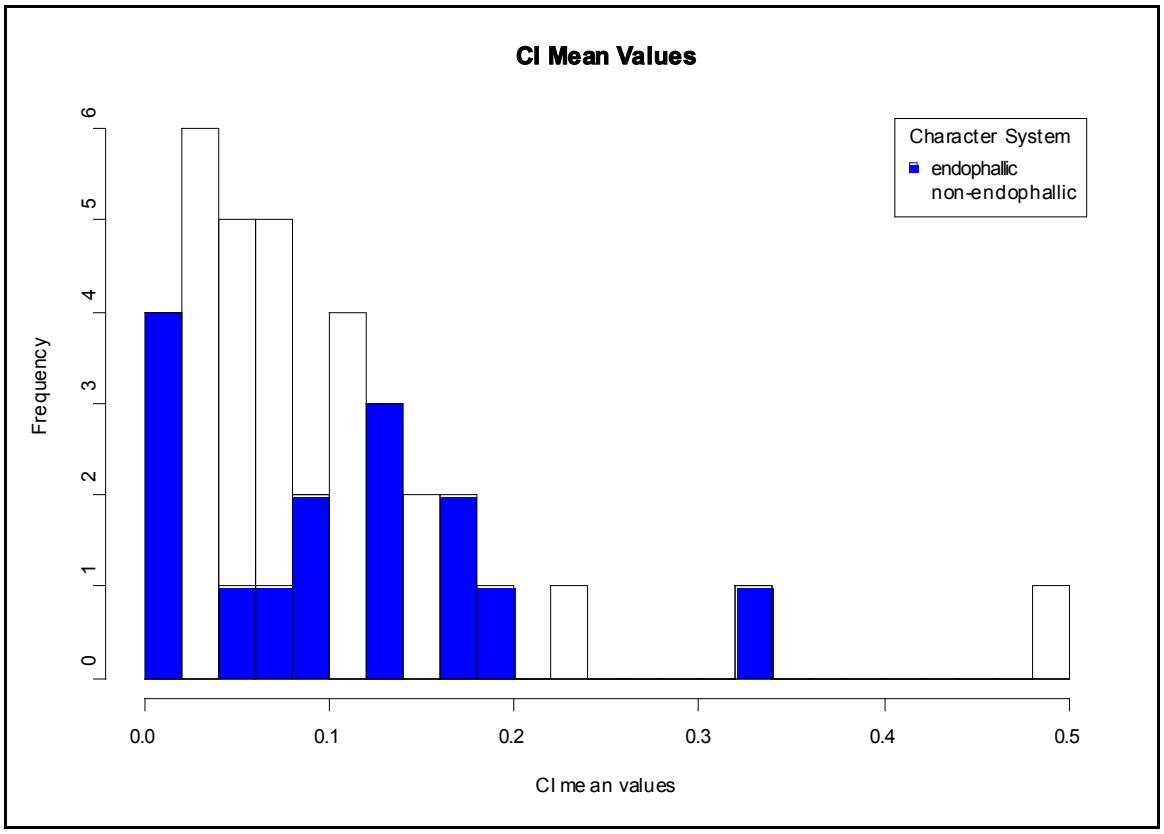
CI Mean Values
Character System
endophallic
non-endophallic
Frequency
0
1
2
3
4
5
6
0.0
0.1
0.2
0.3
0.4
0.5
CI mean values
Fig. 5

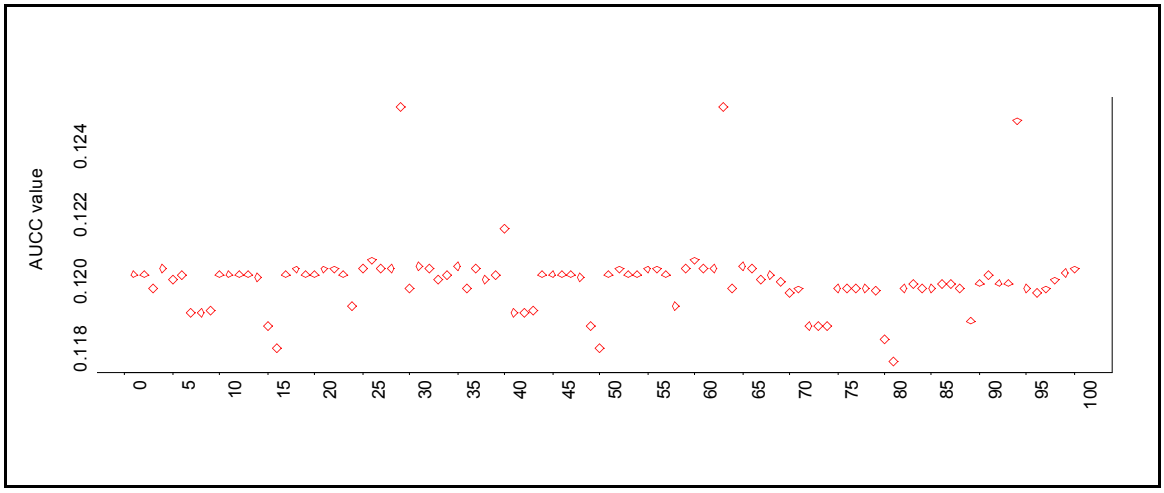
AUCC value
0.118
0.120
0.122
0.124
0
5
10
15
20
25
30
35
40
45
50
55
60
65
70
75
80
85
90
95
100
Fig. 6

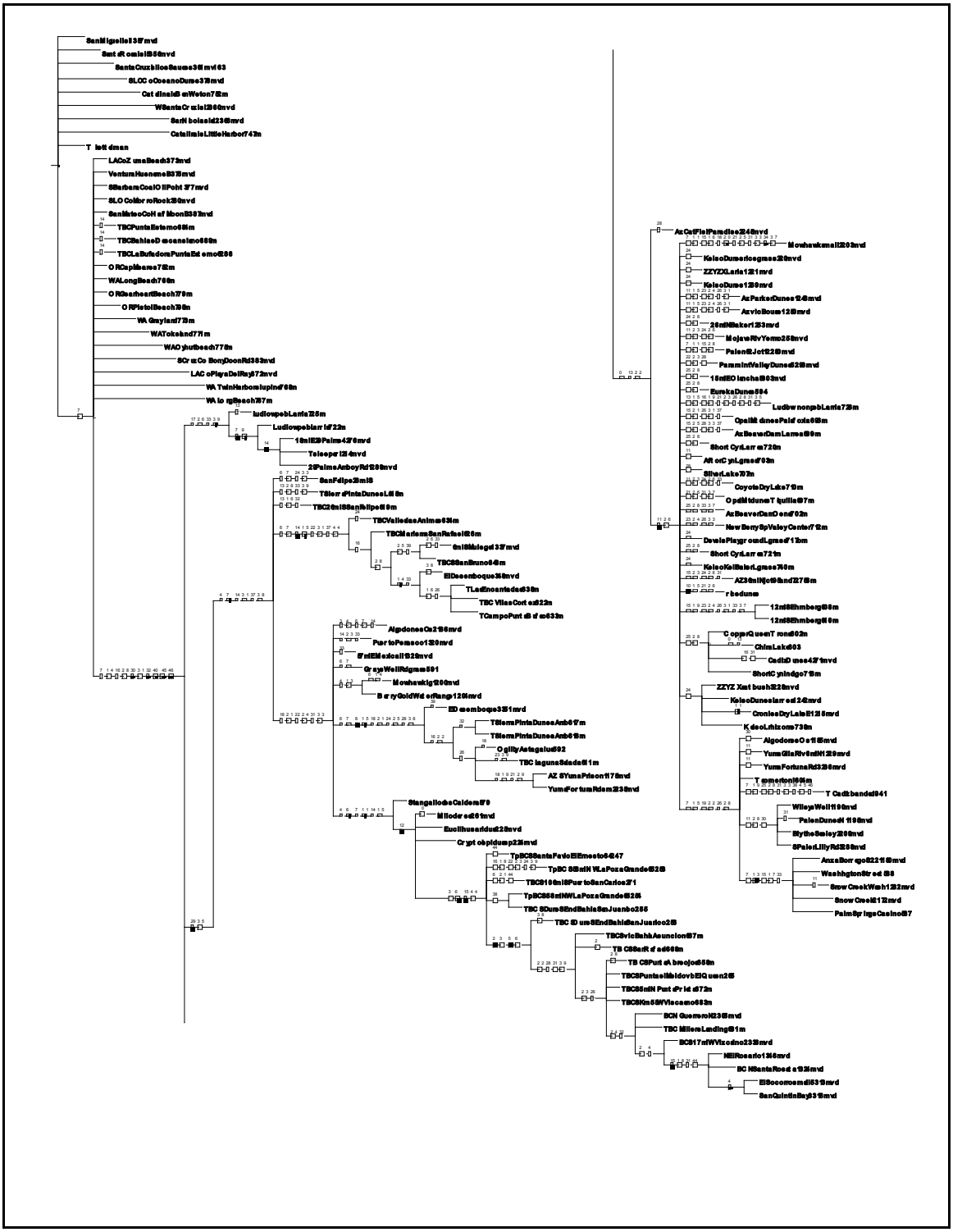

Fig. 7 Strict-consensus tree of morphological characters

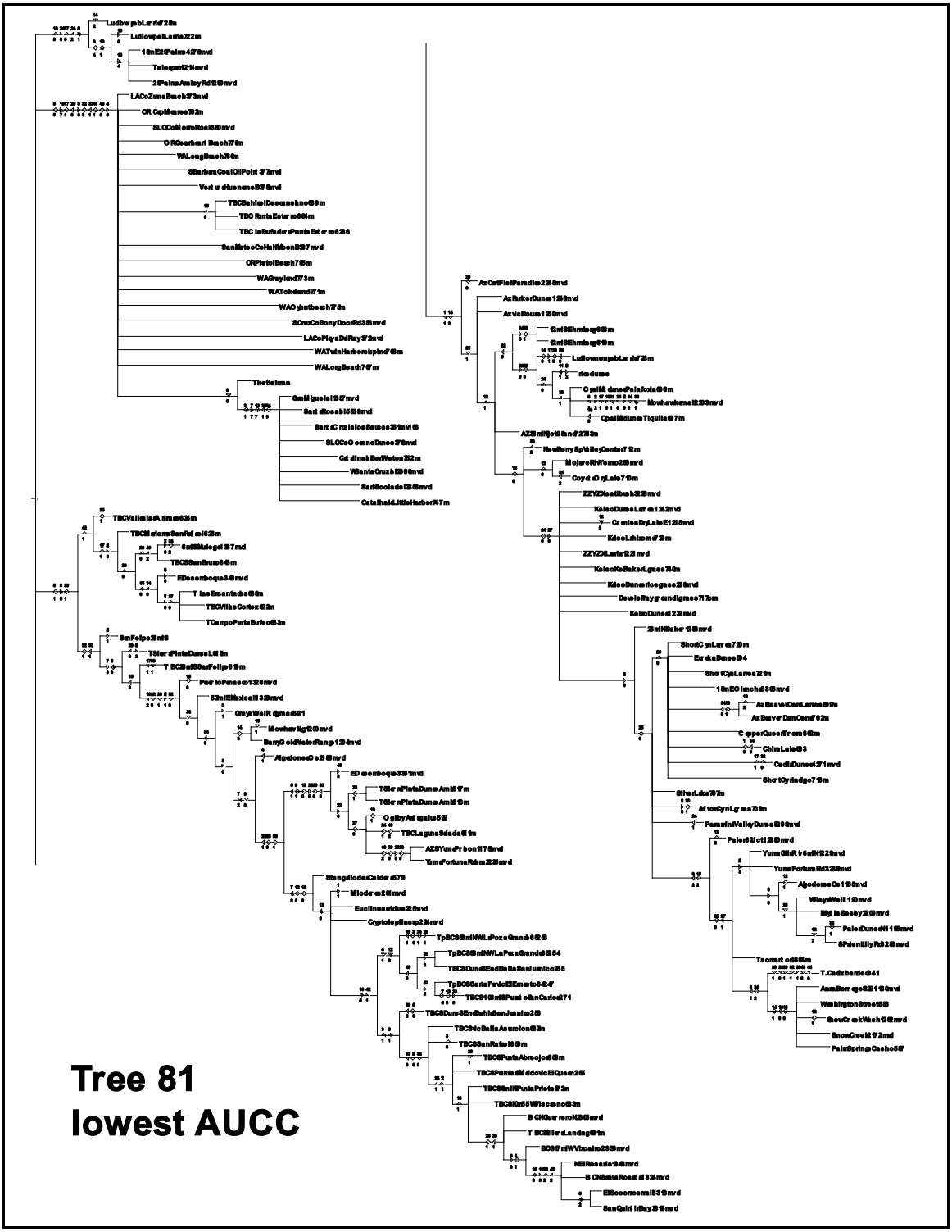

Fig. 8

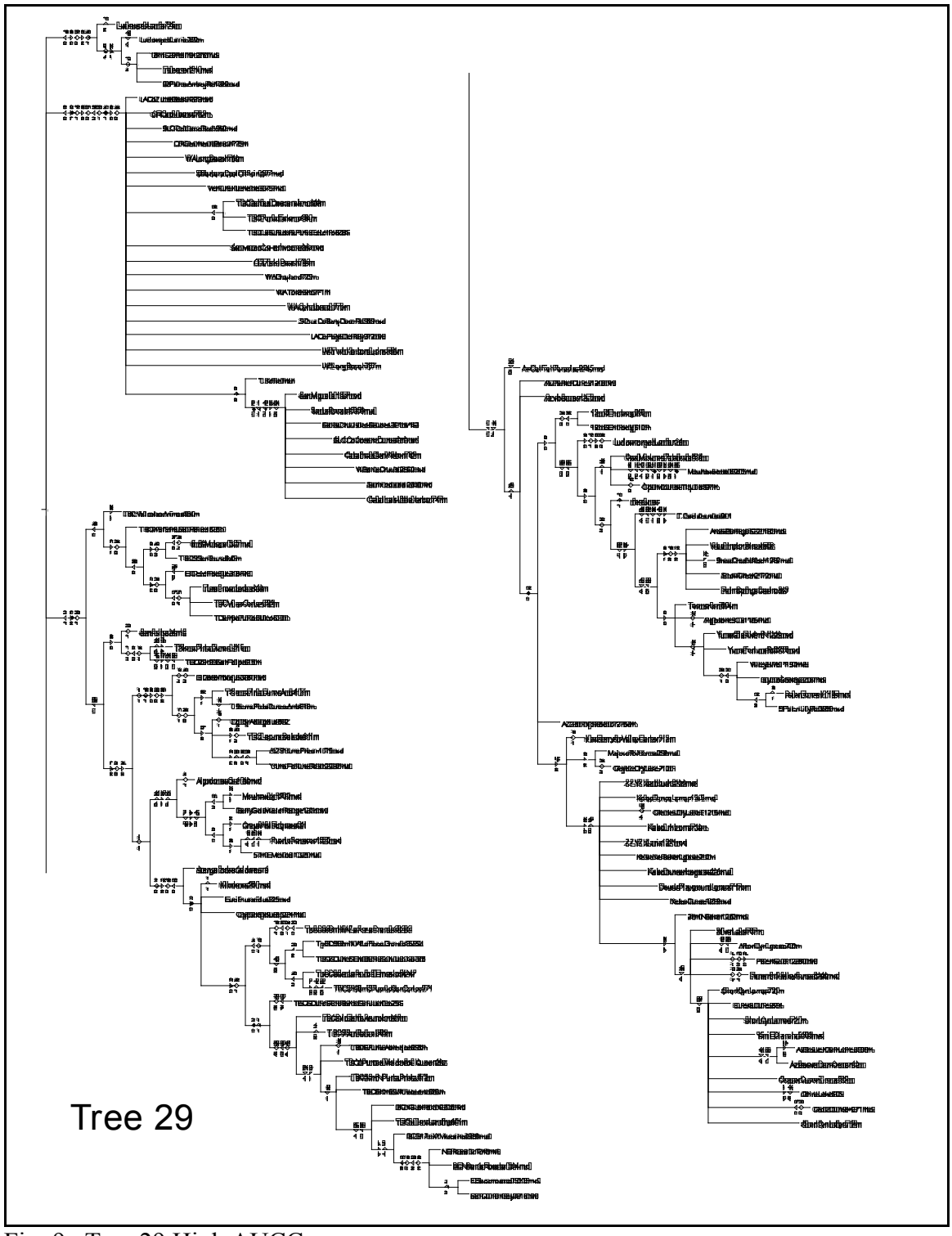

Fig. 9. Tree 29 High AUCC

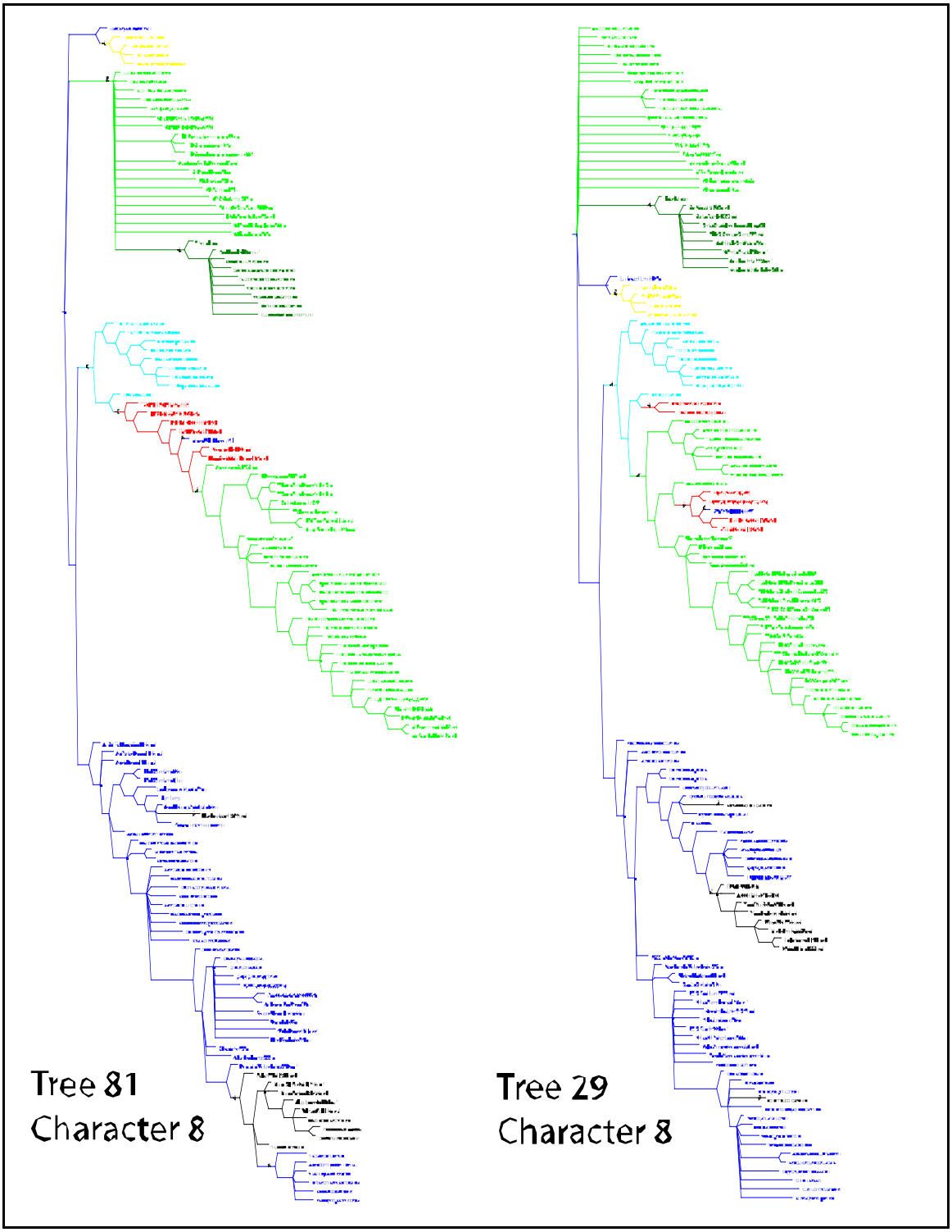

Fig. 10

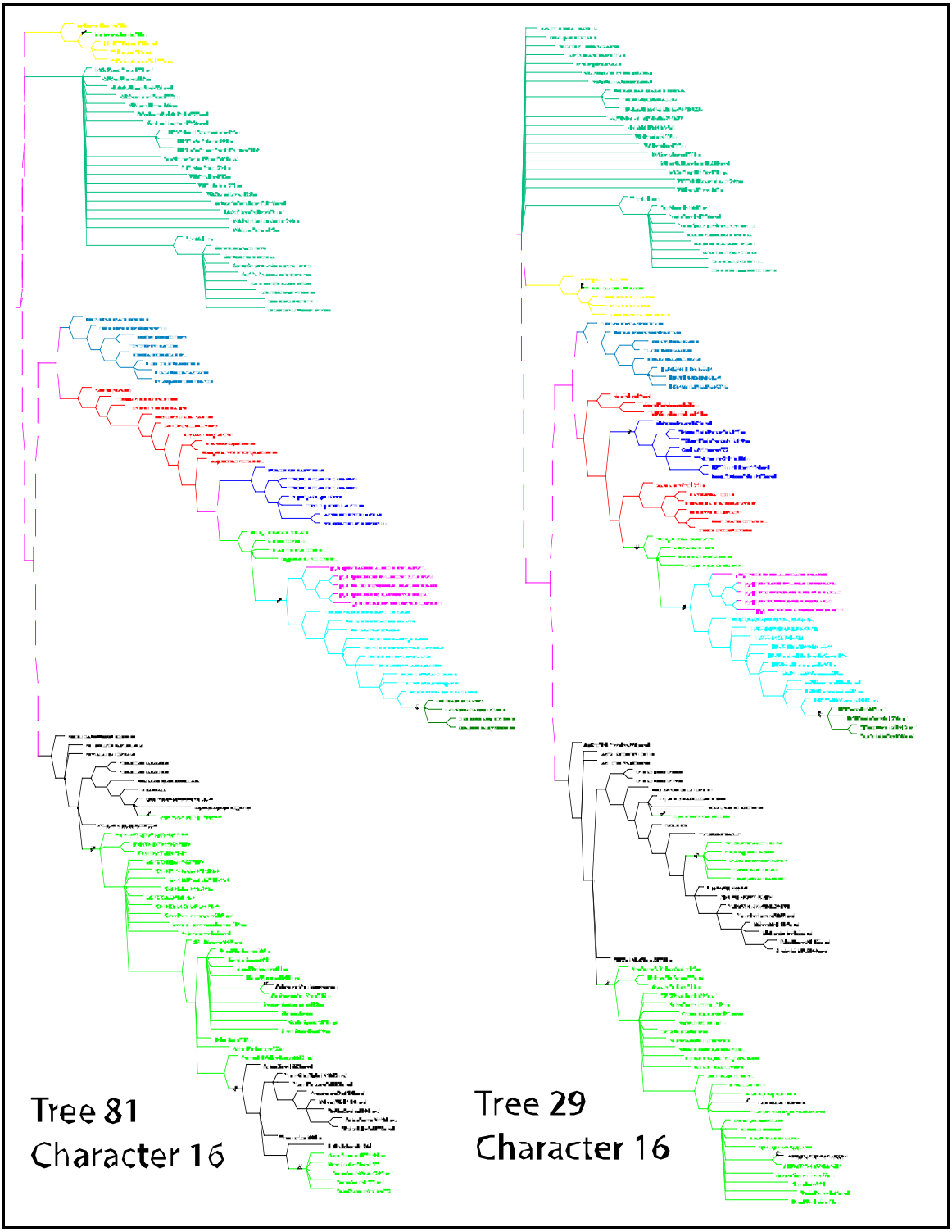

Fig. 11

Fig. 12

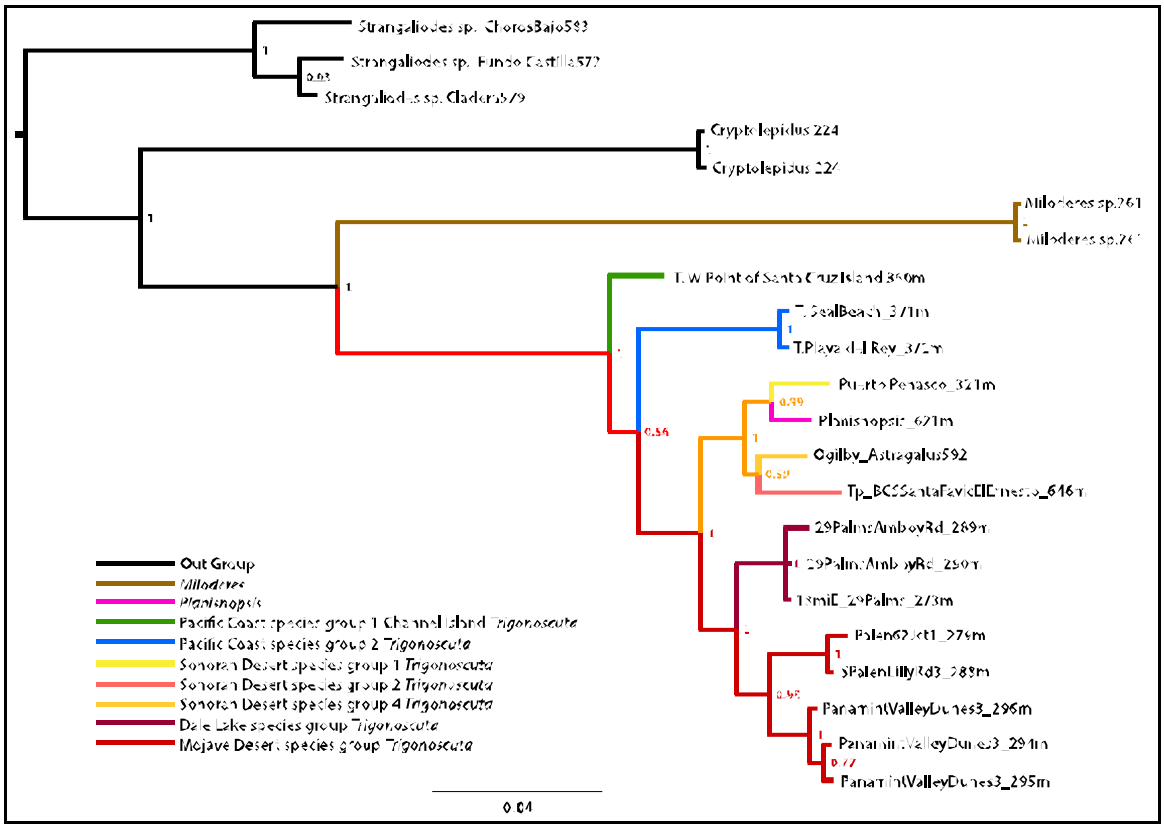

Fig. 13, EF1alpha gene tree for *Trigonoscuta* species groups. Numbers at nodes are posterior probability values.

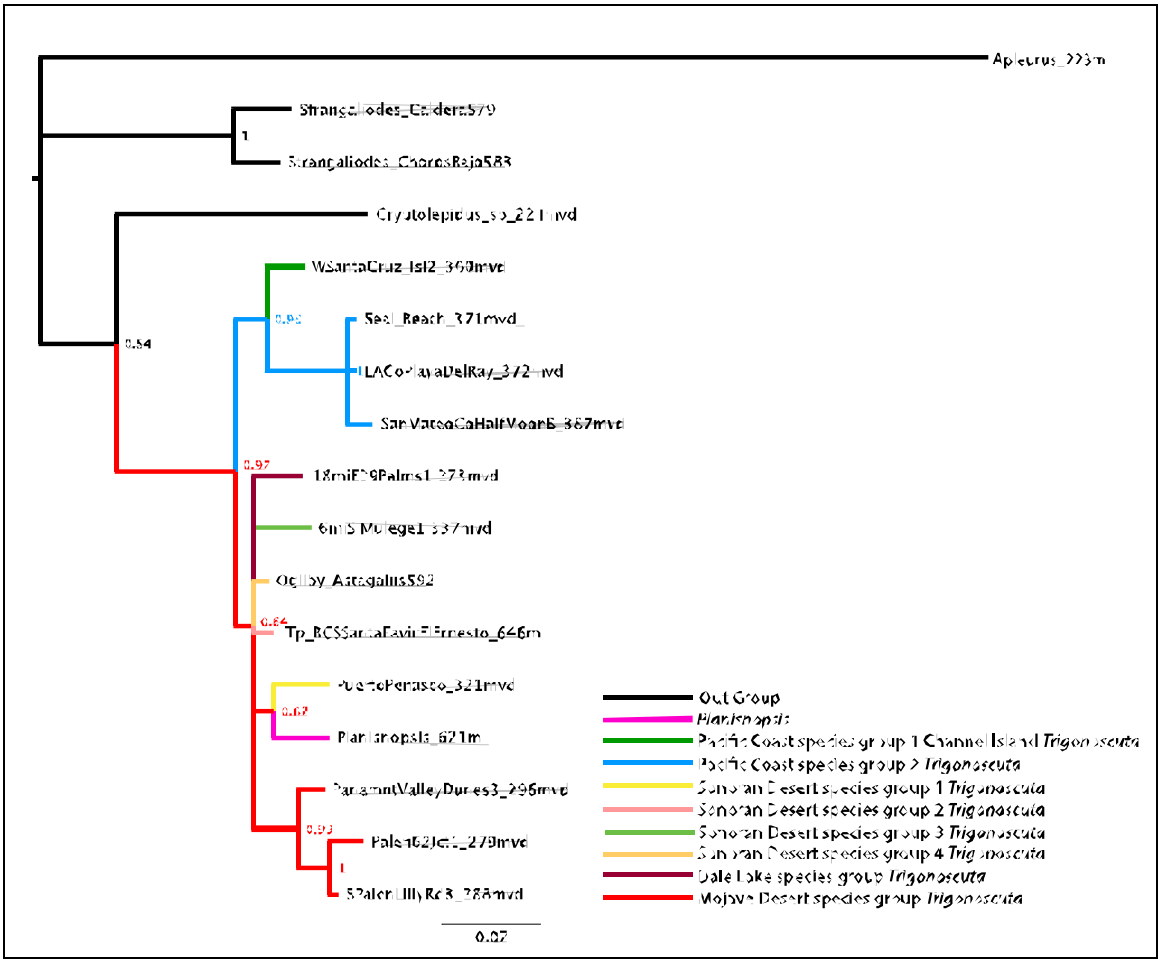

Fig. 14, Argenine Kinase gene tree for *Trigonoscuta* species groups. Numbers at nodes are posterior probability values.

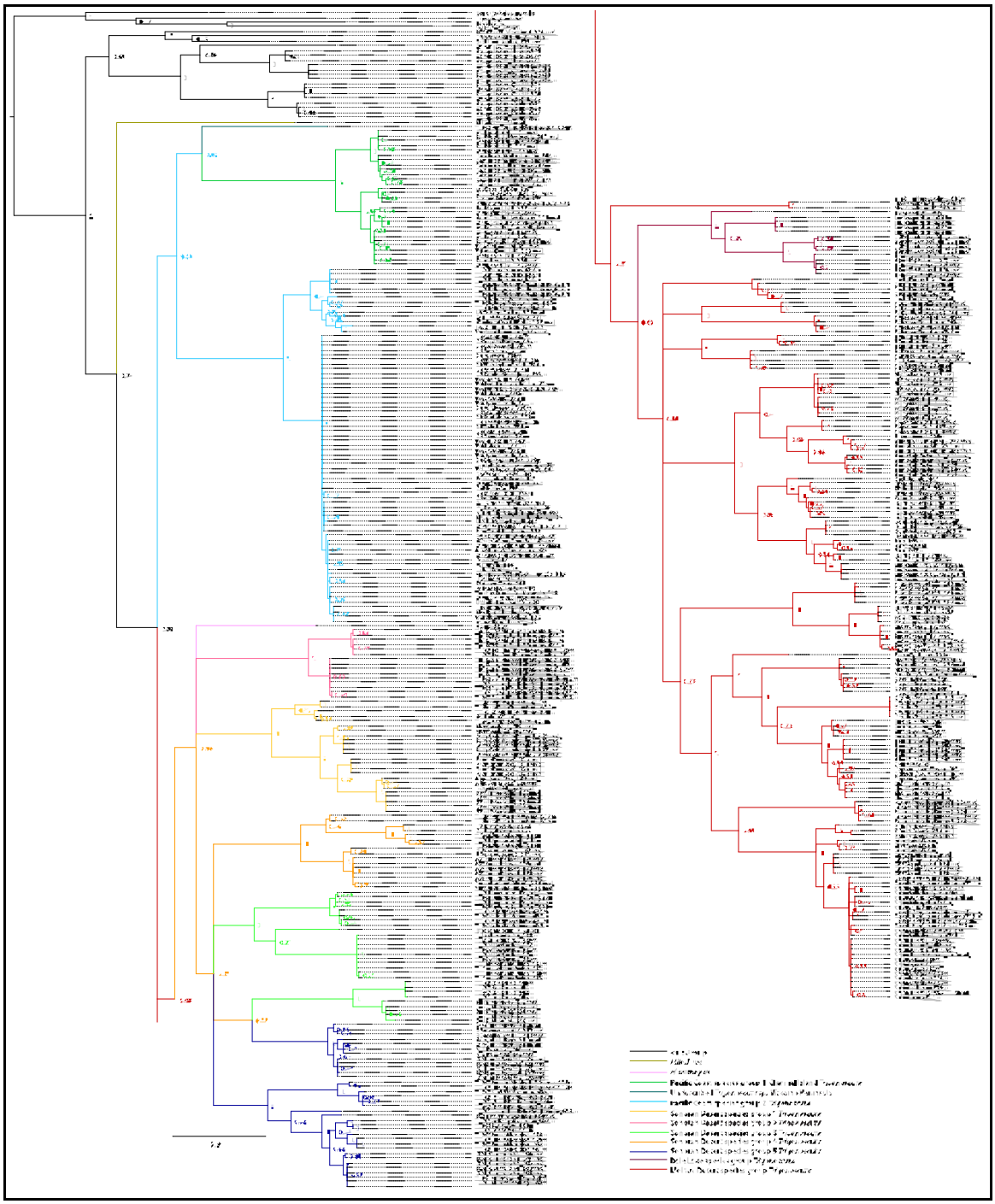

Fig 15. All samples unconstrained

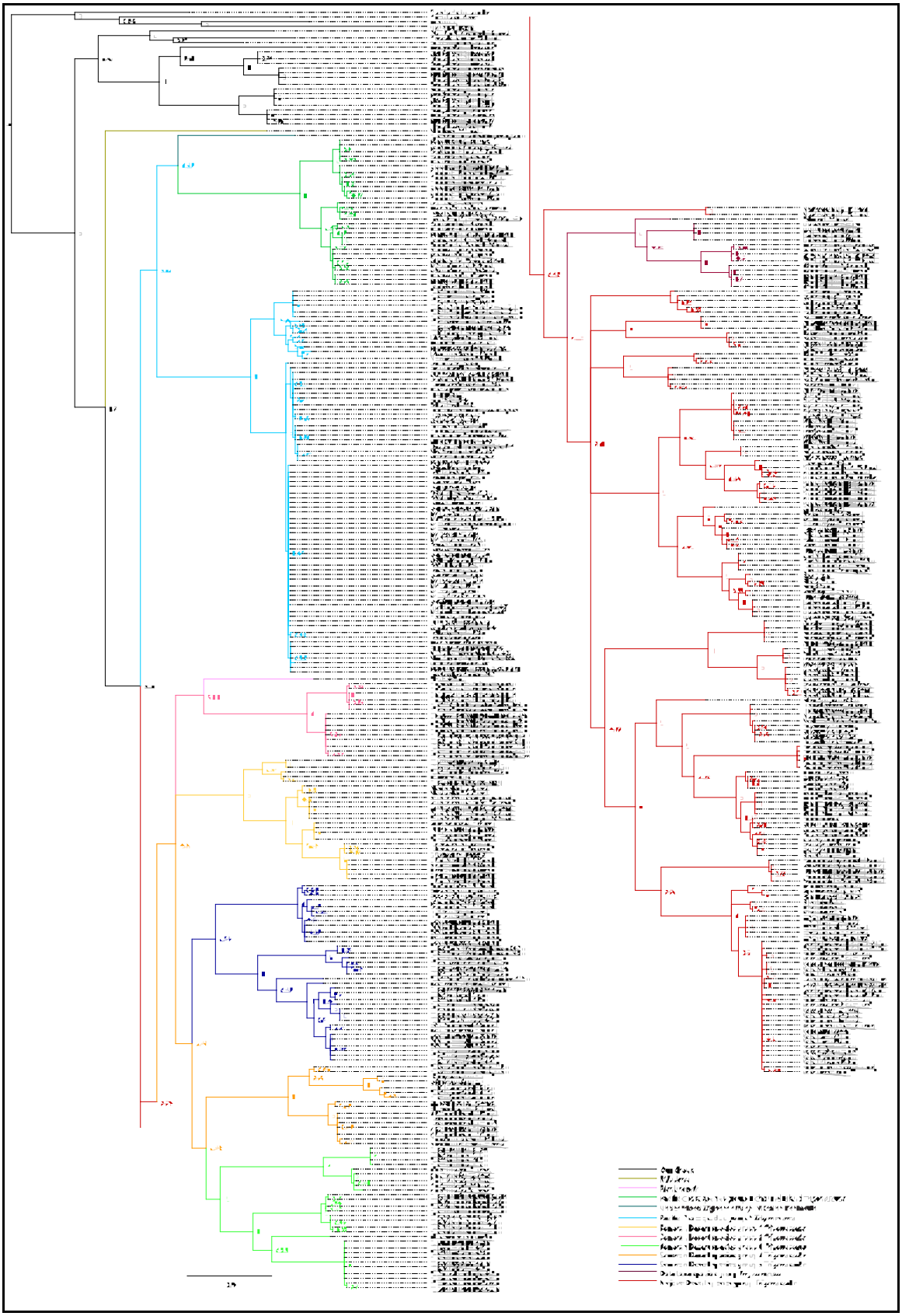

Fig. 16. All samples constrained

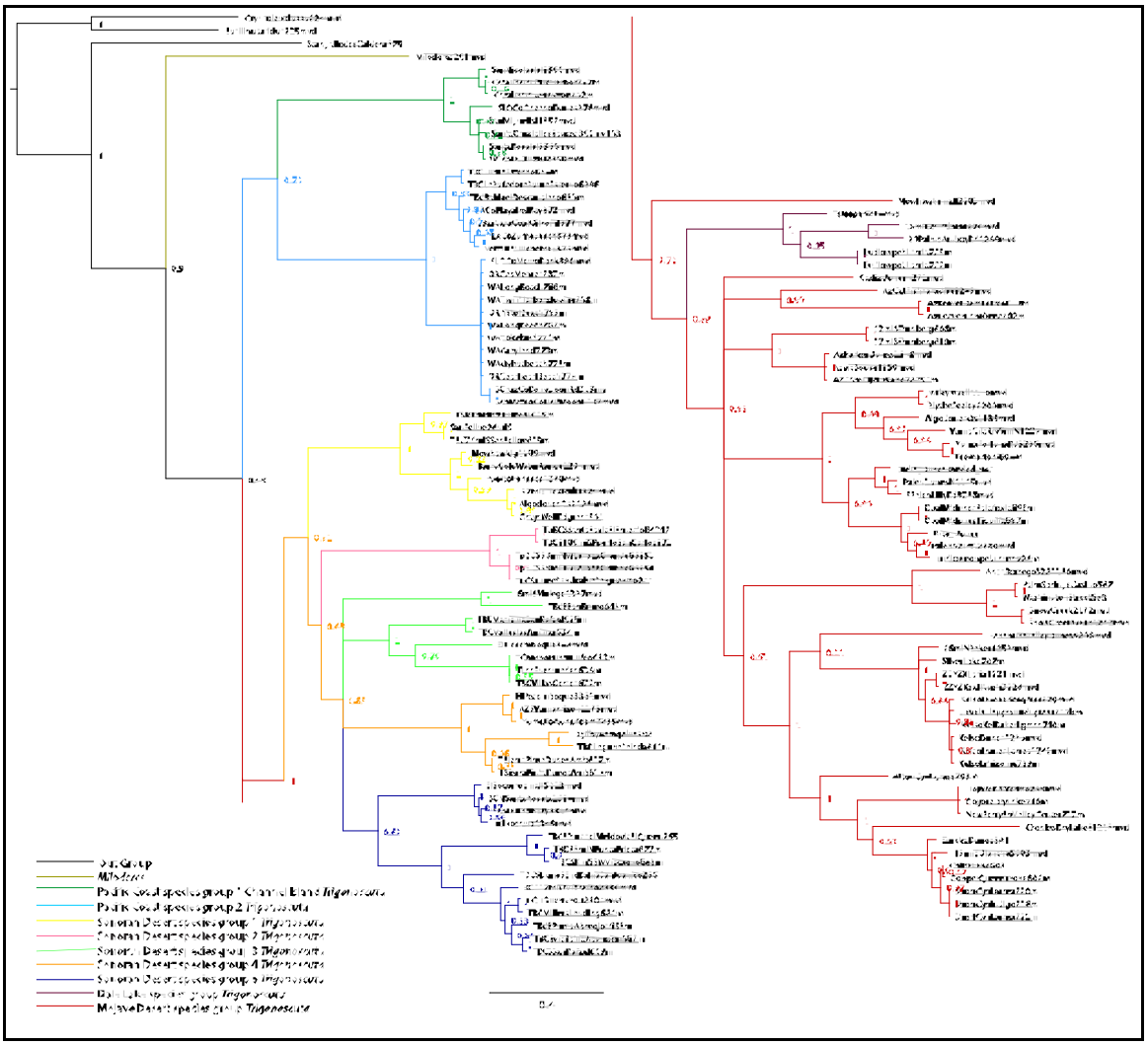

Fig. 17. Unconstrained just molecular data.

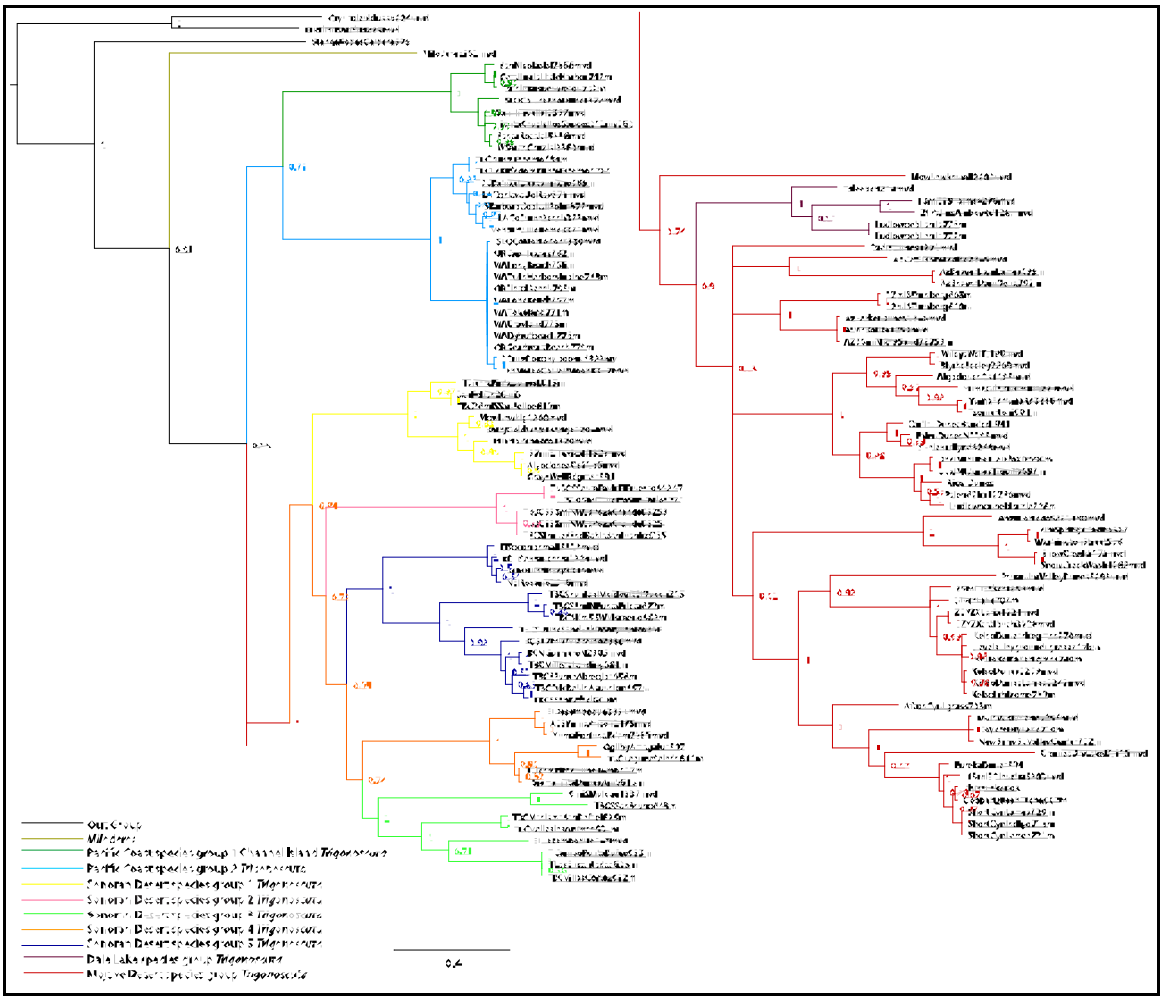

Fig. 18. Constrained just molecular data.

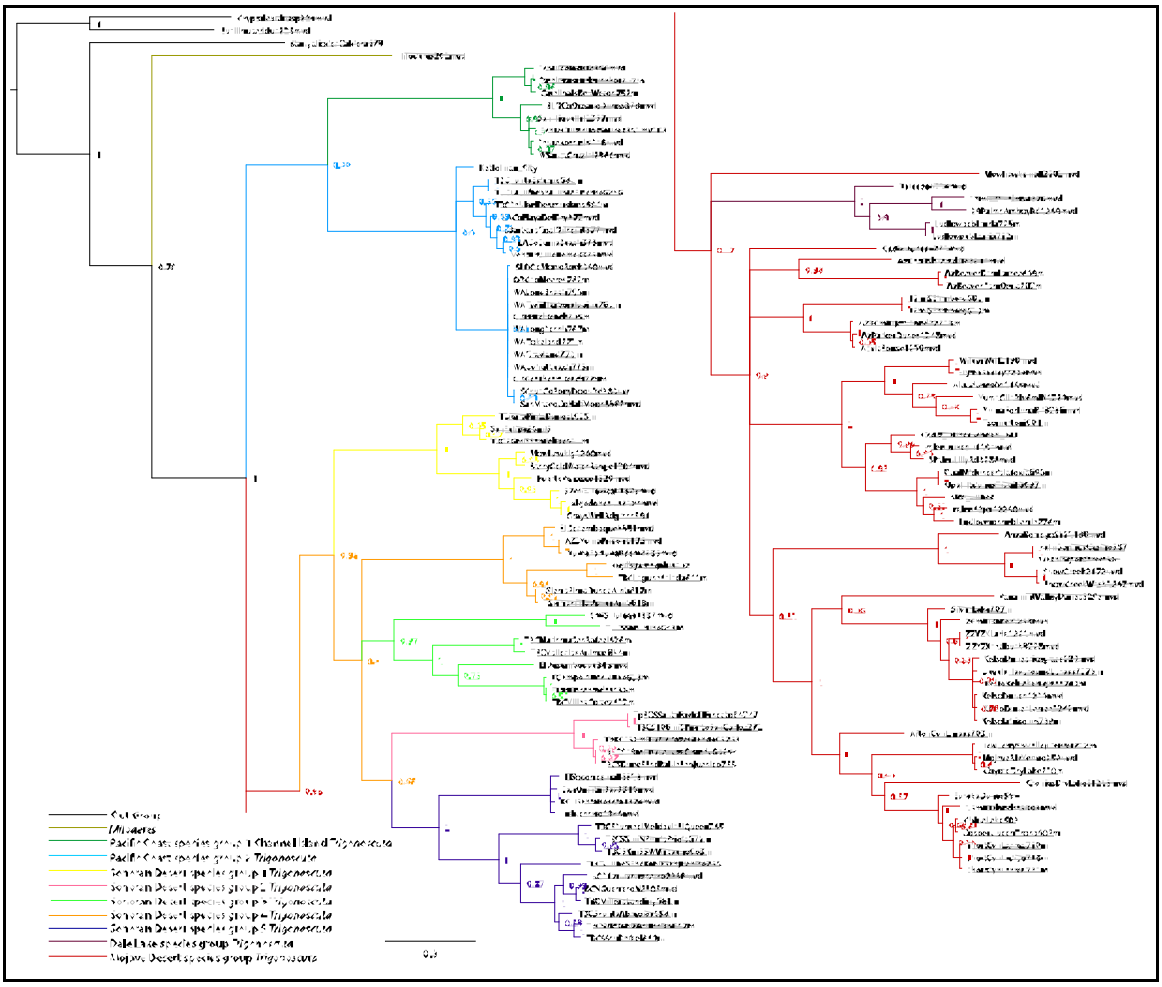

Fig. 19. Unconstrained mol morph

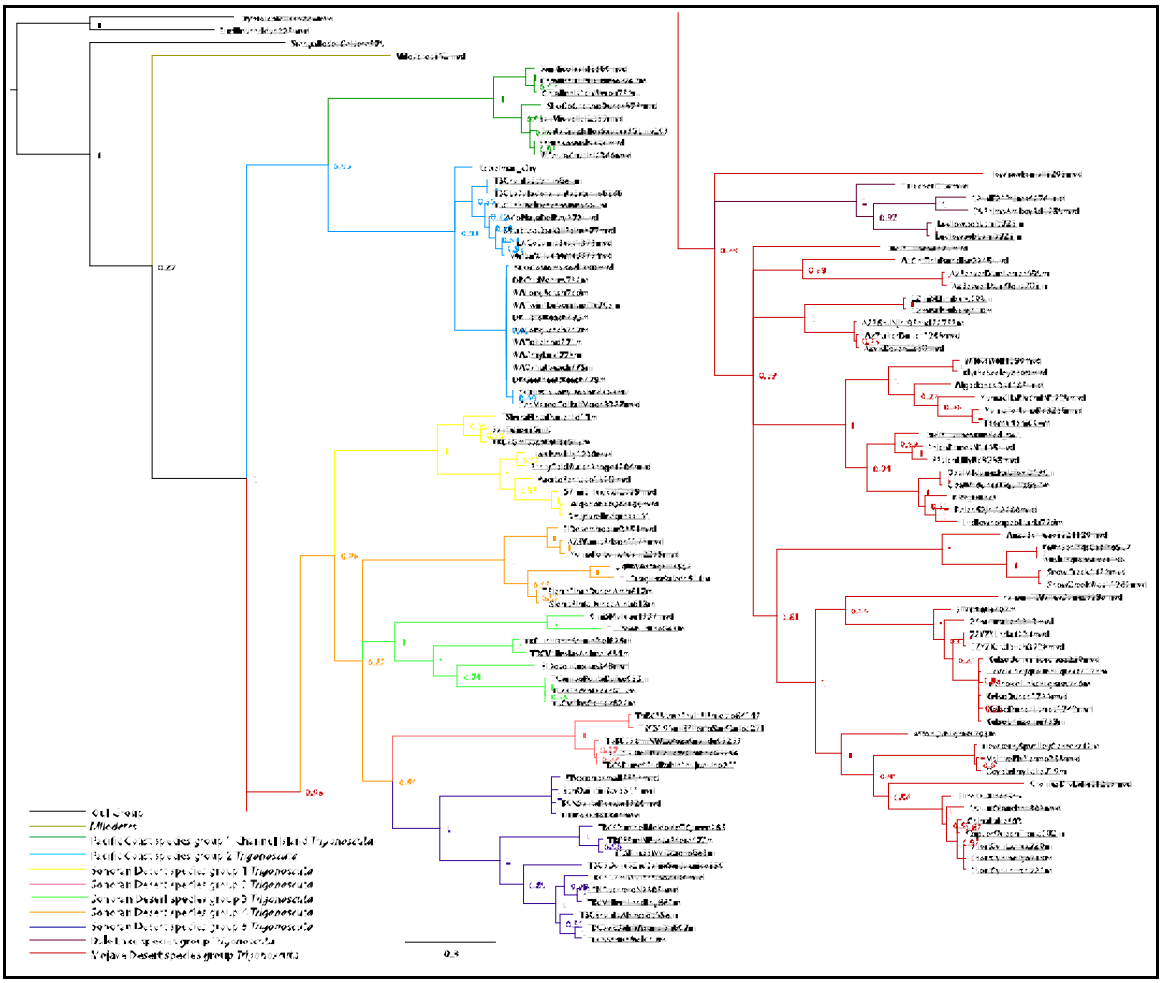

Fig. 20. Constrained mol morph

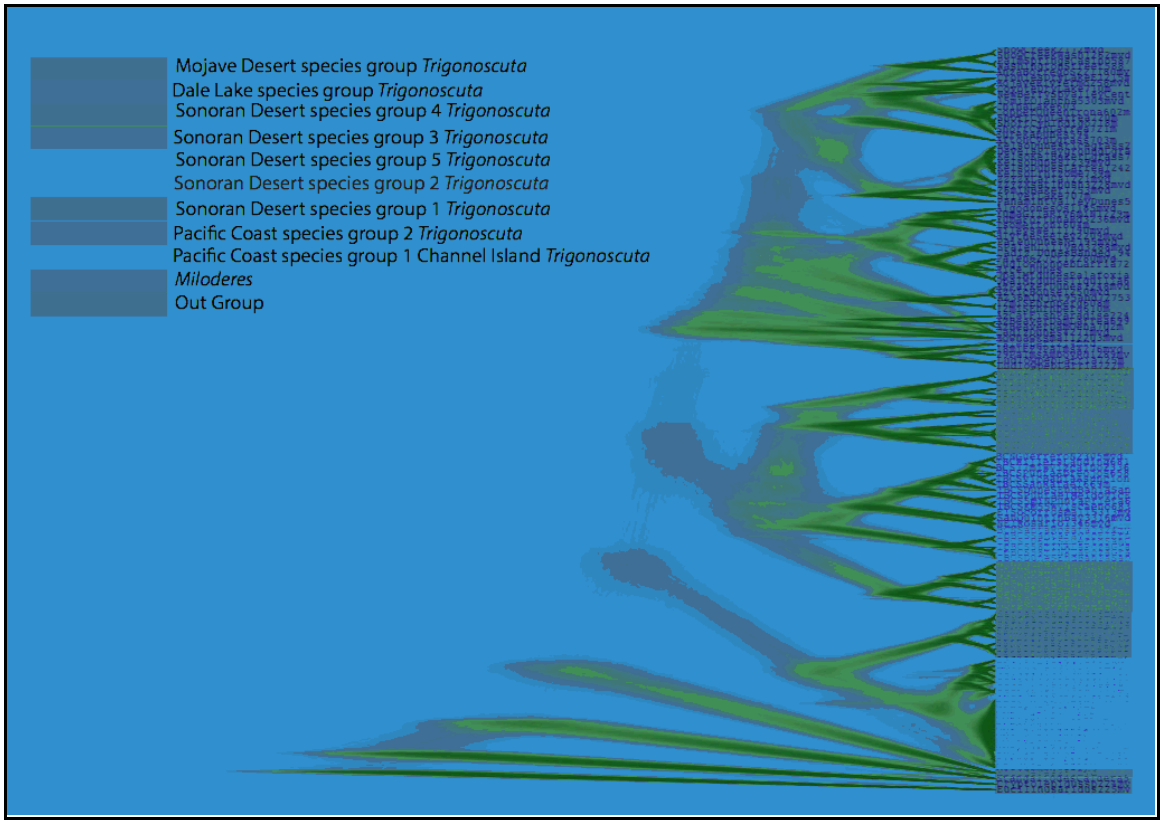

Fig. 21. Densitre visualization of Bayesian unconstrained molecular and morphological data. Visualization of the posterior 10,000 trees.

Table 1.

Character number	min-steps	max-steps	mean number steps	mean CI	mean RI	mean RCI
1	1	50	24.02	0.04186	0.53048	0.02196
2	1	8	8	0.125	0	0
3	1	8	6	0.167	0.286	0.048
4	1	6	5	0.2	0.2	0.04
5	2	26	15	0.133	0.458	0.061
6	1	14	10.06	0.09946	0.30338	0.0304
7	9	78	44.13	0.2043	0.491	0.10035
8	6	81	47.33	0.12698	0.44874	0.05701
9	1	7	6.03	0.16628	0.16199	0.02716
10	1	4	2.97	0.33801	0.34302	0.11769
11	9	96	52.54	0.17138	0.49956	0.08588
12	1	23	13.06	0.07664	0.45224	0.03464
13	3	54	30.05	0.09985	0.47	0.04685
14	7	77	39.03	0.17891	0.54258	0.09691
15	9	95	50.06	0.17976	0.52243	0.09376
16	1	60	25	0.04	0.593	0.024
17	1	14	11.06	0.09058	0.22638	0.02064
18	2	30	21.41	0.09336	0.30663	0.02836
19	1	22	15	0.067	0.333	0.022
20	2	5	4	0.5	0.333	0.166
21	1	18	15.29	0.06551	0.15922	0.01055
22	1	57	36.1	0.0279	0.3732	0.01002
23	1	56	26.86	0.03714	0.52952	0.01928
24	1	42	33.07	0.02993	0.21818	0.00693
25	1	24	20.03	0.04994	0.17268	0.00891
26	1	50	27.66	0.03625	0.45583	0.01637
27	1	4	3	0.333	0.333	0.111
28	1	51	32.04	0.03096	0.3792	0.01196
29	1	39	15.99	0.06229	0.60539	0.03804
30	1	37	15.99	0.06205	0.58328	0.03605
31	3	68	40.32	0.07436	0.42585	0.03136
32	1	41	19.99	0.05003	0.52525	0.02603
33	2	66	46.12	0.04303	0.31023	0.01303
34	1	43	20.92	0.04804	0.52592	0.02504
35	1	19	9.06	0.11034	0.55264	0.06128
36	1	42	24.29	0.04138	0.43204	0.01775
37	2	35	14.02	0.14284	0.63544	0.09088
38	3	15	13.09	0.22953	0.15941	0.03717
39	1	28	8.99	0.11114	0.70437	0.07815
40	2	27	13.06	0.15334	0.5576	0.08528
41	1	28	8.99	0.11114	0.70437	0.07815
42	1	28	8.99	0.11114	0.70437	0.07815

Table 2.

Character number	sd number of steps	sd CI	sd RI	sd RCI
1	0.470975776	0.00075237	0.009673958	0.000941952
2	0	0	0	0
3	0	0	0	0
4	0	0	0	0
5	0	0	0	0
6	0.238683257	0.002148149	0.018378611	0.002386833
7	0.46395315	0.00220422	0.00683869	0.002319766
8	0.532859638	0.001530696	0.007004501	0.001598579
9	0.171446608	0.004114719	0.028631584	0.004800505
10	0.171446608	0.028631584	0.057263167	0.038232594
11	0.673000218	0.002019001	0.007856439	0.002479329
12	0.238683257	0.0014321	0.01097943	0.0014321
13	0.219042914	0.000657129	0.004380858	0.000657129
14	0.3	0.001311141	0.0042	0.001311141
15	0.488659267	0.001954637	0.005576384	0.001954637
16	0	0	0	0
17	0.422115882	0.003533905	0.032502923	0.003699631
18	0.533617349	0.002134469	0.018737234	0.002134469
19	0	0	0	0
20	0	0	0	0
21	0.537389876	0.002595626	0.031266072	0.002686949
22	0.362371538	0.000362372	0.006522688	0.000140705
23	0.348735088	0.000348735	0.006277232	0.00069747
24	0.455161199	0.000455161	0.011214511	0.000455161
25	0.171446608	0.000342893	0.007543651	0.00051434
26	0.684902116	0.000891883	0.013772359	0.00077401
27	0	0	0	0
28	0.315268044	0.000315268	0.006305361	0.000315268
29	0.502418394	0.002070939	0.013323402	0.002009674
30	0.1	5.00E-04	0.0028	5.00E-04
31	0.566399224	0.001132798	0.008940177	0.001132798
32	0.1	3.00E-04	0.0025	3.00E-04
33	0.408989887	0.000171447	0.006219641	0.000171447
34	0.562821177	0.001377452	0.013507708	0.001377452
35	0.238683257	0.002625516	0.013366262	0.002864199
36	0.537389876	0.000992701	0.012897357	0.000657129
37	0.317184584	0.003305092	0.009646604	0.003444451
38	0.37859389	0.006617172	0.031714985	0.008130321
39	0.1	0.0014	0.0037	0.0015
40	0.238683257	0.002625516	0.00954733	0.002864199
41	0.1	0.0014	0.0037	0.0015
42	0.1	0.0014	0.0037	0.0015

Table 3.

Analyses	*Harmonic mean of likelihood scores*	*Bayes factors*
unconstrained molecular and morphological data	-16095.8	0.43
constrained molecular and morphological data	-16095.37	
unconstrained molecular data 131 taxa	-14593.43	14.16
constrained molecular data 131 taxa	-14579.27	
unconstrained molecular data 418 taxa	-19827.98	-27.11
constrained molecular data 418 taxa	-19855.09	

Table 4.

Partition Type Morphological data, endophallic- nonendophallic	*SS Marginal likelihood (ln)*	*Bayes Factor HM2-all equal*	*Bayes Factor HM2-all gamma*
		all equal	all gamma
all equal	-1607.07	NA	NA
all gamma	-1559.69	NA	NA
equal-equal	-1662.71	-55.64	-103.02
gamma-gamma	-1808.83	-201.76	-249.14
equal-gamma	-1787.53	-180.46	-227.84
gamma-equal	-1847.74	-240.67	-288.05

References:

Allen R. T. 1972. A revision of the genus Loxandrus LeConte (Coleoptera: Carabidae) in North America. Entomologica Americana 46:1-184.

Alonso-Zarazaga M., and C. Lyal. 1999. A world catalogue of families and genera of Curculionoidea dentification of South American weevils (Insecta: Coleoptera)(Excepting Scolytidae and Platypodidae). Entomopraxis, Barcelona, Spain .

Anderson R. S. 2002. Chapter 131. Curculionidae. Pp. 722 *in* R. H. J. Arnett, Thomas. M.C. and P. Skelley, eds. American Beetles Volume 2. CRC Press, s, Boca Raton, Florida,.

Anderson R. S. 1987. Systematics Phylogeny and Biogeography of New World Weevils Traditionally of the Tribe Cleonini Coleoptera Curculionidae Cleoninae. Quaestiones Entomologicae 23.

Angus R., R. Brown, and L. Bryant. 2000. Chromosomes and identification of the sibling species Pterostichus nigrita (Paykull) and P. rhaeticus Heer (Coleoptera: Carabidae). Syst. Entomol. 25:325-337.

Arnqvist G., and L. Rowe. 2002. Correlated evolution of male and female morphologies in water striders. Evolution 56:936-947.

Berlov O. 1992. Dry permanent preparation of the endophallus in the genus *Carabus* L. (Coleoptera Carabidae). Boll. Soc. Entomol. Ital. 124.

Brandley M. C., A. Schmitz, and T. W. Reeder. 2005. Partitioned Bayesian analyses, partition choice, and the phylogenetic relationships of scincid lizards. Syst. Biol. 54:373-390.

Brown J. M., and A. R. Lemmon. 2007. The importance of data partitioning and the utility of Bayes factors in Bayesian phylogenetics. Syst. Biol. 56:643-655.

Coyne J. A., and H. A. Orr. 2004. Speciation. Sinauer Associates Sunderland, MA, .

Düngelhoef S., and M. Schmitt. 2010. Genital feelers: the putative role of parameres and aedeagal sensilla in Coleoptera Phytophaga (Insecta). Genetica 138:45-57.

Dybas L. K., and H. S. Dybas. 1981. Coadaptation and taxonomic differentiation of sperm and spermathecae in featherwing beetles. Evolution :168-174.

Eberhard W. 1993. Copulatory courtship and morphology of genitalic coupling in seven *Phyllophaga* species (Coleoptera: Melolonthidae). J. Nat. Hist. 27:683-717.

Eberhard W. G. 1993. Evaluating models of sexual selection: genitalia as a test case. Am. Nat. 142:564-571.

--- 1992. Species isolation, genital mechanics, and the evolution of species-specific genitalia in three species of Macrodactylus beetles (Coleoptera, Scarabeidae, Melolonthinae). Evolution :1774-1783.

--- 1985. Sexual selection and animal genitalia. Harvard University Press, .

Evans A. V., and J. N. Hogue. 2006. Field guide to beetles of California. Univ of California Press, .

Fyler C., T. Reeder, A. Berta, G. Antonelis, A. Aguilar, and E. Androukaki. 2005. Historical biogeography and phylogeny of monachine seals (Pinnipedia: Phocidae) based on mitochondrial and nuclear DNA data. J. Biogeogr. 32:1267-1279.

Gilbert E. E. 1964. The genus *Baris* Germar in California (Coleoptera, Curculionidae). University of California Publications in Entomology 34.
Goloboff P. A., J. S. Farris, M. Källersjö, B. Oxelman, M. J. Ramıŕez, and C. A. Szumik. 2003. Improvements to resampling measures of group support. Cladistics 19:324-332.
Higginson D. M., K. B. Miller, K. A. Segraves, and S. Pitnick. 2012. Female reproductive tract form drives the evolution of complex sperm morphology. Proceedings of the National Academy of Sciences 109:4538-4543.
Holman L., R. P. Freckleton, and R. R. Snook. 2007. What Use is an infertile Sperm?A Comparative Study of Sperm-Heteromorphic *Drosophila*. Evolution 62:374-385.
Howden A. T. 1982. Revision of the New World genus *Hadromeropsis* Pierce (Coleoptera, Curculionidae, Tanymecini). Contrib. Am. Entomol. Inst. 19.
Jeannel R. 1911. Révision des Bathysciinae (Coléopteres silphidés): morphologie, distribution géographique, systématique. Librairie Albert Schulz, .
Kissinger D. G. 1964. Curculionidae of America north of Mexico: a key to the genera. Taxonomic Publications South Lancaster, MA, .
Kluge A. G., and J. S. Farris. 1969. Quantitative phyletics and the evolution of anurans. Syst. Biol. 18:1-32.
Kuschel G. 1995. A phylogenetic classification of Curculionoidea to families and subfamilies. Mem. Entomol. Soc. Wash. 14:5-33.
Lewis P. O. 2001. A likelihood approach to estimating phylogeny from discrete morphological character data. Syst. Biol. 50:913-925.
Liebherr J. K. 1994. Biogeographic patterns of montane mexican and Central American Carabidae (Coleoptera). The Canadian Entomologist 126:841-860.
Maddison W., and D. Maddison. 2010. Mesquite: a modular system for evolutionary analysis. Version 2.6. 2009. Mesquite website.Available at mesquiteproject.org/mesquite/mesquite.html.Accessed March 23.
Marvaldi A. E. 1998. Larvae of Entiminae (Coleoptera: Curculionidae): tribal diagnoses and phylogenetic key, with a proposal about natural groups within Entimini. Insect Syst. Evol. 29:89-98.
--- 1997. Higher Level Phylogeny of Curculionidae (Coleoptera: Curculionoidea) based mainly on Larval Characters, with Special Reference to Broad-Nosed Weevils. Cladistics 13:285-312.
Matsumura Y., and K. Yoshizawa. 2012. Homology of the internal sac components in the leaf beetle subfamily criocerinae and evolutionary novelties related to the extremely elongated flagellum. J. Morphol. 273:507-518.
Minder A., D. Hosken, and P. Ward. 2005. Co-evolution of male and female reproductive characters across the Scathophagidae (Diptera). J. Evol. Biol. 18:60-69.
Nylander J. 2002. MrModeltest v1. 0b. Program distributed by the author.Department of Systematic Zoology, Uppsala University .
O'Brien C. W. 2009. New Notiodes semiaquatic weevil (Curculionidae) from sporocarps of Marsilea mollis (Marsileaceae) in southern Arizona, USA. West. N. Am. Nat. 69:421-425.
O'Brien C. W., and G. J. Wibmer. 1982. Annotated checklist of the weevils (Curculionidae sensu lato) of North America, Central America, and the West Indies (Coleoptera: Curculionoidea).
Paradis E., J. Claude, and K. Strimmer. 2004. APE: analyses of phylogenetics and evolution in R language. Bioinformatics 20:289-290.
Pierce W. D. 1975. The Sand Dune Weevils of the Genus Trigonoscuta, with a Correlation of Their Anatomy to the Geological History of Our Coast Lines. Natural History Museum of Los Angeles County, .
Pitnick S., T. Markow, and G. S. Spicer. 1999. Evolution of multiple kinds of female sperm-storage organs in *Drosophila*. Evolution :1804-1822.
Presgraves D. C., R. H. Baker, and G. S. Wilkinson. 1999. Coevolution of sperm and female reproductive tract morphology in stalk–eyed flies. Proceedings of the Royal Society of London.Series B: Biological Sciences 266:1041-1047.
Puniamoorthy N., M. Kotrba, and R. Meier. 2010. Unlocking the "Black box": internal female genitalia in Sepsidae (Diptera) evolve fast and are species-specific. BMC evolutionary biology 10:275.
R Development Core Team. 2011. R: A Language and Environment for Statistical Computing.R Foundation for Statistical Computing, Vienna, Austria, .
Rambaut A., and A. Drummond. 2008. FigTree: Tree figure drawing tool, version 1.2. 2. Institute of Evolutionary Biology, University of Edinburgh .
Rönn J., M. Katvala, and G. Arnqvist. 2007. Coevolution between harmful male genitalia and female resistance in seed beetles. Proceedings of the National Academy of Sciences 104:10921-10925.
Ronquist F., M. Teslenko, P. van der Mark, D. L. Ayres, A. Darling, S. Höhna, B. Larget, L. Liu, M. A. Suchard, and J. P. Huelsenbeck. 2012. MrBayes 3.2: efficient Bayesian phylogenetic inference and model choice across a large model space. Syst. Biol. 61:539-542.
Rugman-Jones P. F., and P. E. Eady. 2008. Co-evolution of male and female reproductive traits across the Bruchidae (Coleoptera). Funct. Ecol. 22:880-886.
Sang T. 1995. New measurements of distribution of homoplasy and reliability of parsimonious cladograms. Taxon :77-82.

Sasakawa K., and K. Kubota. 2007. Phylogeny and genital evolution of carabid beetles in the genus Pterostichus and its allied genera (Coleoptera: Carabidae) inferred from two nuclear gene sequences. Ann. Entomol. Soc. Am. 100:100-109.
Schliep K. P. 2011. phangorn: Phylogenetic analysis in R. Bioinformatics 27:592-593.
Schoof H. F. 1942. The genus *Conotrachelus* Dejean (Coleoptera, Curculionidae) in the North Central United States. Illinois Biol Monogr 19:1-170.
Seago A. E., J. A. Giorgi, J. Li, and A. Ślipiński. 2011. Phylogeny, classification and evolution of ladybird beetles (Coleoptera: Coccinellidae) based on simultaneous analysis of molecular and morphological data. Mol. Phylogenet. Evol. 60:137-151.
Shapiro A. M., and A. H. Porter. 1989. The lock-and-key hypothesis: evolutionary and biosystematic interpretation of insect genitalia. Annu. Rev. Entomol. 34:231-245.
Sharp D., and F. Muir. 2009. The comparative anatomy of the male genital tube in Coleoptera. Transactions of the Royal Entomological Society of London 60:477-642.
Sharp D. 1918. Studies in Rhynchophora. iv. A preliminary note on the male genitalia. Transactions of the Entomological Society of London 1918.
Silfverberg H. 1974. The west Palaearctic species of *Galerucella* Crotch and related genera (Coleoptera, Chrysomelidae). Not. Entomol. 54:1-11.
Sota T., and K. Kubota. 1998. Genital lock-and-key as a selective agent against hybridization. Evolution :1507-1513.
Takami Y., and T. Sota. 2007. Rapid diversification of male genitalia and mating strategies in Ohomopterus ground beetles. J. Evol. Biol. 20:1385-1395.
Takami Y. 2002. Mating behavior, insemination and sperm transfer in the ground beetle Carabus insulicola. Zool. Sci. 19:1067-1073.
Takami Y., and T. Sota. 2007. Sperm competition promotes diversity of sperm bundles in Ohomopterus ground beetles. Naturwissenschaften 94:543-550.
Tanabe T., and T. Sota. 2008. Complex copulatory behavior and the proximate effect of genital and body size differences on mechanical reproductive isolation in the millipede genus Parafontaria. Am. Nat. 171:692-699.
Tarasov S. I., and A. Y. Solodovnikov. 2011. Phylogenetic analyses reveal reliable morphological markers to classify mega-diversity in Onthophagini dung beetles (Coleoptera: Scarabaeidae: Scarabaeinae). Cladistics 27:490-528.
Thompson R. T. 1992. Observations on the morphology and classification of weevils (Coleoptera, Curculionoidea) with a key to major groups. J. Nat. Hist. 26:835-891.
Thompson R. T. 1988. Revision of the weevil genus Leptostethus Waterhouse, 1853 (Coleoptera: Curculionidae: Entiminae). Cimbebasia Memoir 7.
Tracy J. L., and T. O. Robbins. 2009. Taxonomic revision and biogeography of the Tamarix-feeding Diorhabda elongata (Brulle, 1832) species group (Coleoptera: Chrysomelidae: Galerucinae: Galerucini) and analysis of their potential in biological control of Tamarisk. Zootaxa .
Verhoeff C. 1895. Vergleichend-morphologische Untersuchungen uber das Abdomen der Endomychiden, Erotyliden und Languriiden (im alten Sinne) und uber die Muskulatur des Copulationsapparates von Triplax. Archiv fuer Naturgeschichte lxi:.213-287.
Whitehead D. R., and G. E. Ball. 1997. The middle American genus *Onypterygia* Dejean (Insecta: Coleoptera: Carabidae: Platynini): A taxonomic revision of the species, with notes about their way of life and geographical distribution. Annals of Carnegie Museum 66.
Will K. 2002. Revision of the new world abariform genera Neotalus n. gen. and Abaris Dejean (Coleoptera: Carabidae: Pterostichini (Auctorum)). ANNALS-CARNEGIE MUSEUM PITTSBURGH 71:143-214.
Wood H. M., N. J. Matzke, R. G. Gillespie, and C. E. Griswold. 2013. Treating Fossils as Terminal Taxa in Divergence Time Estimation Reveals Ancient Vicariance Patterns in the Palpimanoid Spiders. Syst. Biol. 62:264-284.

SUPPLEMENTARY DOCUMENTS

Table 1.

Primer region		Reference
COI	2183: 5' CAACATTTATTTTGATTTTTTGG 3' 3041: 5' TYCATTGCACTAATCTGCCATATTAG 3'	Simon et al. (1994)
COI trig	F: 5' CAATTGGCTTATTAGGCTTCGT 3' R: 5' CTCAGCTGGCGGAAAGAAT 3'	This study
Arginine kinase	AK183F: 5' GATTCTGGAGTCGGNATYTAYGCNCCYGAY 3' AK939R: 5' GCCNCCYTCRGCYTCRGTG 3'	Wild and Maddison (2008)
EF1-Alpha	efs149: 5′ ATCGAGAAGTTCGAGAAGGAGGCYCARGAAATGGG 3′ efa1043: 5′ GTATATCCATTGGAAATTTGACCNGGRTGRTT 3′	Normark et al. (1999)

BIOGEOGRAPHY OF DUNE-RESTRICTED ANIMALS IN THE DESERT SOUTH WEST OF NORTH AMERICA

Abstract

Historical biogeography aspires to explain why organisms have their particular distribution patterns, but lacks model-based approaches to test the perceived patterns. Here we present a new approach, explicitly testing several models that give different probabilities to dispersal and vicariance, as well as the influence of connectivity and distance on an organism's dispersal ability. We do so in a continental habitat island setting, using the sand dunes of the North American Deserts. Our aim is to identify the effect that three major geologic events may have had on the sand dune fauna. We use four clades of dune-restricted taxa as well as four clades of aquatic desert taxa that may have been affected by the same geologic events. The geologic events hypothesized to influence biogeographic patterns are the uplift of the Sierra Madre Occidental, the formation of lakes in the Bouse Embayment, and the production of modern dune fields from Pleistocene lacustrine sediments via sand transport pathways. Our results indicate that divergence times varied across taxa, with some diversifying in the last million years, whereas others have diversified over the past 70 million. Some taxa were affected by all the events, whereas others show only the influence of the most recent events. The results from analyses testing a vicariance-only model versus one that includes founder event speciation (jump dispersal) are decidedly in favor of jump dispersal, with only a single taxon showing support for the vicariance-only model. The inclusion of a constrained dispersal matrix to explicitly test the hypothesized dispersal pathways was favored only by three of the eight taxa examined. Additionally, some taxa were not affected by the distance of dispersal events, whereas others were less likely to disperse over long distance. Our results do not show support for any one event shaping the overall biogeographic patterns of theses desert taxa. Instead, we find that, though taxa share some common responses, they are largely shaped by idiosyncratic events differentially affecting specific lineages.

Introduction

The use of islands as natural laboratories to study evolution dates back to Wallace and Darwin. Island systems have been indispensable for understanding the processes generating biodiversity. Examples from the Galapagos, Caribbean, and Hawaiian archipelagos demonstrate the utility of islands for the study of adaptation, community assembly, and speciation (Grant & Grant 2002; Losos *et al.* 2003; Gillespie 2004). In addition to true islands, habitat islands are also of great interest to evolutionary biologists studying many of the same questions (Wake 1987; Masta 2000; Knowles & Carstens 2007). Unlike true oceanic islands, habitat islands are discrete patches of habitat surrounded by a contrasting habitat (Whittaker & Fernandez-Palacios 2007). Barriers between the different habitats may be more or less stringent for any given taxon. This is a notable difference relative to oceanic islands, as the nature of terrestrial habitat islands means that the rules governing dispersal and vicariance may not be the same between

oceanic islands and habitat islands. Here, we examine the question of vicariance or dispersal via a study of a habitat island system – the sand dunes of the southwest deserts of North America. The sand dune-restricted taxa in this study are specialists on this substrate, and are never found more than one-hundred meters from sand dunes (Norris 1958; Pierce 1975; Hardy & Andrews 1976; Cazier 1985). This highly specialized habitat preference combined with their isolated and disjunct distributions leads to the question of how these animals came to occupy their current distributions. Norris (1958), first proposed for the fringe toed lizard genus *Uma*, that they may have used the sandy river corridors and sand-transport pathways as a means of dispersal during Pleistocene climate fluctuations, when sandy sediments would periodically become available. Here we test this hypothesis as well as other major geologic events (Bouse Lakes Formation and uplift of the Sierra Madre Occidental) that may have shaped the distributions of dune-restricted taxa. We use a new approach to test the hypothesized connectivity between areas, as well as the effect that distance has on the ability of a particular taxon to disperse. Our methodology is implemented in the R package BioGeoBEARS (Matzke 2013).

Background: biogeography of the southwestern desert

The formation of desert fauna has received considerable study. Axelrod (1979, 1983) theorized that the Sonoran desert flora formed during the drying of the Tertiary from surrounding non-arid adapted flora. Other hypotheses have focused on climatic fluctuations, emphasizing vicariance events during the Pleistocene as a driver of diversification (Orr 1960; Savage 1960; Hubbard 1973; Morafka 1977; Knowles & Carstens 2007). Studies stressing vicariance have proposed a role for the Neogene uplift of the Sierra Madre Occidental and Mexican Plateau (Morafka 1977; Ortega-Gutiérrez & Guerrero-Garcia 1982; Riddle 1995; Wilson & Pitts 2010). Other major geologic events proposed to be important for diversification during the Neogene include the opening of the Gulf of California (Murphy 1983; Grismer 1994; Upton & Murphy 1997; Murphy & Aguirre-León 2002) as well as the "Bouse Embayment" (Turner 1983; Jones 1995; Orange *et al.* 1999; Riddle *et al.* 2000; Murphy *et al.* 2006; Douglas *et al.* 2006; Devitt 2006; Castoe *et al.* 2007; Smith & Pellmyr 2007; Wood *et al.* 2008; Wilson *et al.* 2012). Other studies have suggested that both of these events have played a role in the diversification of desert taxa (Riddle & Hafner 2006). Here we expand on previous work by devising and conducting a statistical test of major geologic hypotheses that may have contributed to the distribution of dune-restricted organisms.

We propose three events that may have driven biogeogarphical outcomes for the dune-restricted taxa under study. The first of these events is the uplift of the Sierra Madre Occidental occurring between ~34-15 Ma (Ferrari *et al.* 1999; Nieto-Samaniego 1999). This event is believed to be one of the major factors responsible for dividing the Sonoran and Chihuahuan deserts. The second major event is the "Bouse Embayment" (Lucchitta 1979, 2001; Turak 2000), which was not actually an embayment of the Gulf of California but a series of paleo-lakes of relatively high salinity, created by high rates of evaporation relative to input from the proto-Colorado River (Spencer & Jonathan Patchett 1997; Poulson & John 2003; House *et al.* 2005, 2008; Roskowski *et al.* 2010; Spencer *et al.* 2013) This will be referred to herein as the Bouse Lakes Formation (BLFs). The BFLs were believed to have covered a large area of the Mojave and upper Sonoran

Deserts ~10,000 km^2 in area. The lakes are thought to have filled this area from 4.83 Ma to 4.80 Ma. When the BLFs drained, the Colorado River was connected to the early Pliocene Gulf of California by ca. 4.80 Ma (Spencer *et al.* 2013). This 30,000-year period may have been a formative time for the biogeographic pattern seen in today's dune-restricted taxa. The connection of the Colorado River to the Gulf created a divide between the western and eastern Mojave Deserts 4.80 Ma as the BLFs drained (Spencer *et al.* 2013). Finally, the last geologic events occurred more recently, namely the extension and retreat of lakes and rivers in the desert southwest during the glacial-interglacial cycles of the Pleistocene (Muhs & Bettis 2003). We hypothesize that dune-restricted taxa followed the sandy corridors of the Pleistocene lakes and rivers. If the dune-restricted fauna did in fact use river corridors as dispersal pathways, then they should exhibit biogeographic patterns similar to those observed for aquatic organisms of the North American Deserts. This hypothesis is based on the premise that the river corridors initially provided aquatic habitat connections required by fish and other aquatic organisms, and subsequently, as they began to dry, exposed sandy sediments that were utilized by dune-restricted taxa to traverse the same pathways. To test this hypothesis, we included four different aquatic taxa that are found in desert regions adjacent to many of our focal sand dunes. Additionally, we were able to test if dispersal or vicariance was the predominant type of event driving current distributions. Past comparative biogeographic studies (Riddle & Hafner 2006) were not able to include the timing of the vicariance events, nor were they able to distinguish between dispersal and vicariance. Here we utilize dated phylogenies and additionally test between vicariance and dispersal using a model-based approach.

Dune formation

Dune formation is associated with climate change. For example, the climate of the Mojave in cooler, wetter periods resulted in the formation of lakes (Bacon *et al.* 2006). During cool climate periods sediments are eroded and moved into lakes. As the climate becomes more arid, the lakes and rivers dry and the deposits of lake sand and silt are moved by wind to form dunes. These sediments are transported from their source (lake beds and rivers) to the point of deposition to form dunes. Sand transport pathways follow the wind patterns and deposit sand along these pathways. Muhs (2003), Lancaster (1994) Clarke and Rendell (1998), Zimbelman et al. (1995), and others have used geological evidence to investigate aeolian sand transport pathways between dune systems in the Mojave and other deserts. Sand transport pathways are the paths that sand takes from a source (such as lake playas) to areas of deposition where it forms dunes (Muhs & Bettis 2003). Other than climate, vegetation is the main factor that stabilizes dunes. During relatively wet periods, sediment transport is inhibited by vegetation, but as the climate dries and vegetation diminishes, sediments are easily transported by wind. Many of these dune systems have also been dated through the process of luminescence dating (Stokes 1999). The dunes of the southwest are geologically recent formations (Clarke & Rendell 1998). For example, the Gran Desierto, North America's largest active dune system, is at most only ~25 ka (Beveridge *et al.* 2006). The first to recognize the potential for how dune organisms might be using these systems was Norris (1958), with his seminal work on *Uma*, desert fringe-toed lizards. He illustrated dispersal pathways along Pleistocene

river and lake corridors that *Uma* may have used to explain the disjunct populations of this highly dune-restricted genus.

Focal Taxa

We selected our focal taxa based on shared distributions across the sand dunes of North America. The fly genus *Rhaphiomidas*, consists of 23 described species and 5 subspecies (Van Dam 2010) endemic to the deserts of North America. The adult flies are active in spring and fall, when they feed on floral nectar. *Rhaphiomidas terminatus abdominalis* is the only species of U.S. Diptera federally listed as Endangered under the U.S. Endangered Species Act. Three other listed taxa – *Rhaphiomidas terminatus terminatus*, *R. trochilus*, and *R. moapa* –are also threatened with extinction (Rogers & Van Dam 2007). For example, *Rhaphiomidas terminatus terminatus* is known only from a 20 ha region in the middle of a golf course on the Palos Verdes Peninsula (George & Mattoni 2006).

Beetles of the genus *Trigonoscuta* (Coleoptera: Curculionidae) include 65 species and 90 subspecies (Pierce 1975). *Trigonoscuta* has a distribution which covers the Californian coastal dunes as well as dunes of the Mojave and Sonoran Deserts. In addition, each of the California Channel Islands has endemic species. *Trigonoscuta* is highly restricted to sand dunes, feeding on a variety of dune plants. All members of this genus are entirely flightless. Adults bury themselves under sand during the day and are surface-active on sand and sand-inhabiting plants during the night. Most *Trigonoscuta* taxa are known from only a single sand dune system, and most species are allopatric (Pierce 1975). Some authors have questioned the validity of many species described by Pierce (1975), especially sympatric species exhibiting little if any external morphological variation (Anderson 2002; Evans & Hogue 2006).

The group commonly known as sand treader crickets (Rhaphidophoridae: Ceuthophilinae) is comprised of five different genera representing 13 species. All members of this family are entirely apterous. They are so-called sand treaders because of their enlarged tibial spines (sand-basket), which they use to dig into the sand to avoid desiccation during the day. Sand treader crickets are of interest not only for their biogeography, but also as exemplars of the process of adaptation to dune life. It appears that there have been several independent cases of adaptation to life in sand within this group. In this study, we are focusing on a monophyletic clade composed of five genera, all of which are sand dune-restricted or found on sandy soils and dunes (in the case of *Daihinia*).

METHODS

Background: biogeographic methods

Phylogeography and historical biogeography examine the diversification of lineages in a temporal and spatial framework, with the main difference being the depth of time considered. Although the terminology is sometimes confused (Lawing and Matzke 2013), historical biogeography operates at the scale of phylogenetics, and phylogeography operates at the scale of population genetics (Zink 2002). Combining

these two approaches is perhaps the most powerful way to examine biogeographic questions. Comparison of multiple lineages and species will yield a more detailed picture of the historic process involved in the distribution and diversification of a group.

Pattern-based historical biogeography tries to find congruent phylogenetic patterns between multiple clades (Platnick & Nelson 1978; Rosen 1978; Nelson & Platnick 1981; Riddle & Hafner 2006). This congruence is interpreted as the splitting of ancestral populations/species due to vicariance events (Avise 2000; Zink 2002). The comparison of multiple taxa in comparative phylogeography allows for inferences on the historic stability of populations (Lapointe & Rissler 2005). In addition to the different ways in which studies have been categorized, there have been many different ways in which comparative biogeographic studies have been performed. Other than simply comparing the pattern seen in clades by eye (Castoe *et al.* 2009), Brooks Parsimony Analysis (BPA; Brooks, Van Veller, & McLennan, 2002) has been used to estimate consensus area relationships. One of the main problems with this method is that it does not require divergence dates between taxa (Donoghue & Moore 2003), so the conclusions drawn from these analyses regarding the underlying process are tenuous at best.

Event-based historical biogeography methods estimate ancestral areas by assuming some model of how geographic range evolves on a phylogeny. These include Dispersal-Vicariance Analysis (DIVA; Ronquist 1996, 1997) – a parsimony-based method that assigns costs to events of dispersal and extinction, but zero cost to vicariance of a widespread ancestor. The LAGRANGE program (Ree *et al.* 2005; Ree & Smith 2008) pioneered the use of maximum likelihood in inferring biogeographic history, using a DEC (dispersal-extinction cladogenesis) model. Here, "dispersal" means range expansion; and "extinction" means local extirpation, or range contraction. Recently the DEC model was expanded to include founder event speciation, referred to herein as "jump dispersal" the DEC+J model at speciation events (Matzke 2013). This model is included in the R package BioGeoBEARS (Matzke 2013).

An innovation of LAGRANGE was the ability to include a user-specified dispersal matrix, which altered the transition matrix between states depending on the relative probability of dispersal between areas. However, the construction of the dispersal probability matrix was usually rather subjective. Recent methods such as SHIBA (Webb & Ree 2012) allow for these rates to be calculated as a function of adjacency and distance, but the SHIBA method employs an approximate Bayesian approach, which is computationally slow, restricting analyses to a small number of areas. SHIBA also does not contain explicit model selection capability, making comparisons between models much more difficult. Here we implement a similar method in BioGeoBEARS, allowing the use of connectivity and distance matrices in the biogeographical models. As the likelihood of geographic range data can be calculated under each model, standard model selection can be performed. To the best of our knowledge, this is the first time a study has taken into account and tested the effects of both connectivity and distance. For a detailed review of the different biogeographic methods please see (Matzke 2013)

Taxon Sampling

Traditionally, comparative biogeography has focused on the biogeographic

relationships between different species, whereas comparative phylogeography compares the patterns seen within individual species. Although these terms may fit particular study systems, it is difficult to apply these boundaries across broad taxa sets. For instance, a species in one higher taxon may not be evolutionarily equivalent to a species in another. This non-uniformity is due to the different evolutionary processes generating biodiversity (de Queiroz 1999). We therefore refrain from defining our study as strictly biogeographic or phylogeographic. Instead, we will examine monophyletic clades as they pertain to our area of interest, whether these clades have been taxonomically designated as species, subspecies, or populations. This is not to say that recognizing the distinctiveness of separate lineages or species is not important, but to try and fit into one category or another when the process of speciation is non-uniform, is an arbitrary way of dividing up the natural world. Here we will use the more inclusive term comparative biogeography for comparing among different clades of historically independent organisms.

Specimens were collected from 2006-2011 and included the published range of *Trigonoscuta*, *Rhaphiomidas* and the sand treader crickets, as well as samples from Baja California and Sonora, Mexico that were well outside the documented ranges of many of these groups. The total number of locations is over 200. Specimens were preserved in 95% ethanol stored on ice in the field and then transferred to a -20°C. *Trigonoscuta* outgroups were selected from the putative sister taxa to *Trigonoscuta* (Pierce 1975), as well as other North American dune-restricted weevils (*Miloderes*). The ingroup taxa were selected from each of the known populations described in Pierce (1975), as well as localities from museum specimens (CAS, CDFA, COB, EMEC, LACM, UCD, UCR). For *Rhaphiomidas* flies, outgroups included members of four separate subfamilies of Mydidae, Apioceridae, and a single Asilidae. The outgroups for the Ceuthophilinae subfamily of crickets were sampled from the Pristoceuthophilini (*Pristoceuthophilus*), Argytini (*Argyrtes*), and Macropathinae (Macropathini, *Heteromallaus*). For each location (isolated sand dunes), individual specimens were treated as separate taxa so as not to bias the sampling by imposing previous taxonomic concepts. A maximum of 12 individuals were sampled per population, with an average of four for all but the US coastal species of *Trigonoscuta*. This sampling regime was used to assess levels of incomplete lineage sorting between samples, or instances of mitochondrial introgression. We also included another group of sand-restricted taxa, the fringe-toed lizard genus *Uma*, as well as four different lineages of aquatic taxa found in the desert Southwest, including three genera of Gastropods (*Pyrgulopsis*, *Tryonia* and *Assiminea*) and the desert pupfish, *Cyprinodon*. For the references to the sources of sequences not generated in this study please see supplementary documents.

Extraction, PCR, sequencing and alignment

Trigonoscuta DNA extractions were performed by dissecting the male genitalia and or pulling a hind leg. DNA extractions for sand treader crickets were obtained from muscle tissue dissected from the hind femur. Tissue of *Rhaphiomidas* was dissected from the thoracic muscle or an entire leg was used. Each tissue specimen was soaked in DNAEasy(r) tissue kit extraction buffer (with proteinase K) overnight, followed by completion of the manufacturer's DNA extraction protocol for animal tissue. The specimens and their associated parts were vouchered and used in subsequent

morphological studies. For primers and genes used in this study, please see Table 2. PCR was performed by using 12.5 ul GoTaq Master Mix (including DNTPs, buffer, taq and dye; Promega Corporation, Madison, WI), 1.25 ul 10lM forward and reverse primer, 7.0 ul water, and 1.0 ul template DNA yielding a 25ul reaction. PCR products were purified with Exosap-IT (US Biochemical Corporation, Cleveland, OH). Sanger sequencing was performed at UC Berkeley's DNA Sequencing Facility. Contigs were assembled and edited in Geneious Pro v. 4.6.4 (Biomatters Ltd.). Sequences were aligned using ClustalW-2.0.10 (Larkin *et al.* 2007) with settings set to GAPOPEN=90.0, GAPEXT=10. Sequences were color-coded by amino acid in Mesquite version 2.71 (Build 514) (Maddison & Maddison 2009) and checked by eye for stop codons.

Phylogenetic Analyses

For analyses of DNA data, each sequence was partitioned by codon position. This partitioning strategy was selected because it has been demonstrated repeatedly that incorporating different rates of DNA evolution for each codon position outperforms single partitioning strategies (Brandley *et al.* 2005; Fyler *et al.* 2005; Seago *et al.* 2011). Model selection was performed in MrModeltest2 (Nylander 2002). The models for different partitions were selected using Akaike information criterion (AIC). For phylogenetic reconstruction, BEAST version 1.7.5 (Drummond *et al.* 2012) was used. For prior parameters see Table 3. Phylogenetic trees were dated using relaxed clock methods (Drummond *et al.* 2006; and see Table 3). Each of the Markov chain Monte Carlo (MCMC) analyses were run for sufficient generations to reach stationarity, with trees and model parameters sampled from the stationary posterior distribution. Stationarity was assessed using the program Tracer version 1.5.3 (Drummond 2007). Trees were calibrated using a variety of calibration points included fossil and biogeographic calibration points; if none were available then a relaxed clock rate was used (Table 3).

Biogeographic Analyses

For biogeographic analyses, we used the R package BioGeoBEARS (Matzke 2013). BioGeoBEARS requires as inputs (1) a dated phylogeny, (2) a file of geographic ranges indicating presence/absence of each species or coalescing population in each discrete area in the analysis, and (3) constraint matrices indicating connectivity and/or distance between the discrete areas. In order to test the hypothesis that sand dune taxa used Pleistocene rivers and sand transport pathways, the different sampling locations were separated into the following discrete areas: Mojave River watershed, Owens Valley River, Bristol Trough and Clarks Path sand transport pathway, Parker Dunes, Colorado River Dunes, Sonoran Desert, Chihuahuan Desert, Great Basin Desert and Great Plains (Fig 1). We allowed for a maximum of four areas at each node, therefore a total of 562 possible states (geographic ranges) per node. We could not include larger numbers of areas per node due to computational limitations. Areas and distances between the areas were defined in ArcGIS software, distance measured in kilometers (Fig 1), these distances were used in the constrained-distance-dependent dispersal matrix. The boundaries between the sand transport pathways (Clarks, Bristol, Parker, and Mojave

River) were set as defined by Muhs et al. 2003. The Colorado River pathway was traced as the area adjacent to the river, as this was one of the hypothesized dispersal corridors of Norris (1958). For the distances and shapes of the Great Basin, Sonoran, and Chihuahuan deserts, we set the perimeters of these areas to encompass the most peripheral dunes of each region. The area in between that did not contain any sand dunes was included in the distance measurements, even though these desert regions encompass lager areas. The resulting shape-files were imported into R to construct distance and connectivity matrices between regions.

The specimen-level phylogenies were pruned so that a single OTU was left per species/coalescing monophyletic population. This was done because the dispersal-extinction-cladogenesis (DEC) models, including the DEC+J model, explicitly assume that a lineage can possibly inhabit more than one area. If a specimen-level tree is used in a DEC analysis, biased results will be obtained if the individual specimens themselves are used as OTUs because a specimen by definition can only inhabit a single area. Phylogenies in which all OTUs inhabit single areas will tend to strongly prefer "+J" models, which include jump dispersal (Matzke 2013). This is acceptable if each species/monophyletic population really is restricted to a single area, but not if this is due to the OTUs being specimens. An additional reason to prune the specimen-level phylogenies down to species/coalescing population OTUs is that we are interested in identifying models that best explain the present geographic ranges of species/monophyletic populations. The geographic structure of gene trees *within* species/coalescing populations also is interesting, but is not the topic of this study. One additional advantage of pruning the specimen-level trees is substantially improved computation time.

We implemented six different models in BioGeoBEARS and then tested amongst them using the AIC and AICc (AIC corrected for finite sample size) to assess the support that geographic range data lend to each model. The six models are: (1) the DEC model, (2) the DEC+J (which adds founder event speciation i.e., jump dispersal), (3) DEC model with the constraint on dispersal only to adjacent areas, (4) the DEC+J model with the constraint on dispersal only to adjacent areas, (5) the DEC+x model, where dispersal is limited to adjacent areas dependent on the exponent of distance, and (6) the DEC+J+x model, in which dispersal is limited to adjacent areas dependent on the exponent of distance.

Comparison of the DEC and DEC+J models for each dataset tests whether or not adding jump dispersal yields a better explanation of the geographic range data than the traditional DEC model, which relies on processes such as range expansion followed by vicariance of widespread ancestors. Comparison of these models with models that only allow dispersal between adjacent areas, or models in which dispersal probability is a function of distance, allows us to test if these models are improvements over the DEC+J model. If the DEC+J+x model receives higher support from the data then this would tend to favor the sand transport/river corridor model over one in which jump dispersal was equally likely between connected areas. If distance does not have an effect, this would favor a scenario in which taxa were free to follow sand transport or river corridors once they formed, regardless of distance. If distance is found to have an effect, then the length of a corridor affects the ability of a taxon to move between areas. Interpretation of the parameter x (exponent on distance) are as follows. If we find an improvement in the

likelihood with adjacency but we find distance had no effect (x=~0), then the taxa were able to use the rivers/sand pathways freely. If x equals a negative number, then this would be interpreted as dispersal probability declining as distance increases. One interpretation is that when rivers or sand pathways connected these populations, the organisms moved freely between areas, but longer corridors provide a stronger filter than shorter corridors, decreasing the probability of dispersal.

Results

Molecular Data

Sequence data were obtained for total of 411 *Trigonoscuta* individuals (855bp mtDNA COI), 227 sand treader crickets individuals ([1536bp mtDNA COI], [353bp nDNA H3]), and 219 *Rhaphiomidas* individuals ([2904bp mtDNA; COI, COII, 16S], [3720bp nDNA; EF1alpha, PGD, snf, Wg, CAD]).

Phylogenetic Analyses and results of DEC vs. DEC+J analyses

Results from the time calibrated phylogenetic analyses varied greatly depending on the group. For example *Rhaphiomidas* diverged from the rest of the Mydidae during the early Cretaceous (see supplementary documents for trees). Other genera were much more recent, such as *Assiminea* which is less than 10 million years old, with many recent species dating into the Pleistocene. BEAST trees are presented in supplementary documents. The results of the biogeographic analyses and model selection are listed in Table 1. The DEC+J model was selected over the DEC model in all but two of the taxa (*Uma* and *Assiminea*). In the case of *Assiminea,* the DEC+J model was rejected with the constrained dispersal matrix. The constrained dispersal matrix was preferred over the unconstrained dispersal matrix in only two of the eight groups (*Cyprinodon* and the Ceuthophilinae). In one of the groups (*Trigonoscuta*), the constrained and unconstrained matrices produced similar likelihoods, separated only by 0.2 -lnLikelihood units. The DEC+J+x model was a slight improvement (by 1.1-lnLikelihood units) relative to the DEC+J unconstrained model.. For the individual taxon-specific biogeographic reconstructions, please see supplementary documents.

Biogeographic Results

Aquatic Taxa

Cyprinodon has two main biogeographic clades in North America, the Chihuahuan Desert clade consisting of only Chihuahuan Desert species, and a clade containing species found in the Sonoran, Chihuahuan, and Great Basin Deserts, and the Mojave River Drainage system. The Owens Valley pupfish, *C. radulosus,* is sister to the rest of the pupfish found in the latter clade. The 95% confidence interval around its divergence time falls just outside of the age of the drainage of the Bouse Lakes Formation (BLFs), suggesting that this colonization event happened after the drainage of the BLFs and was probably unrelated to that event. There are two separate colonization events out of the Chihuahuan desert, one a dispersal event to the Sonoran desert, and the

second a dispersal to the Great Basin Desert; both occurred approximately 2 Ma. Echelle (2008) also found this in his analyses of the western pupfish, and suggested a yet undiscovered geologic connection between the Guzman Basin and the Death Valley region through the connection of the Gila and Colorado River at this time period. The results from previous allozyme studies also support the recent divergence within this clade of the western pupfish (Echelle & Echelle 1993).

The divergence between Chihuahuan desert *Assiminea* and the remaining members of this clade occurred roughly 2 Ma ago. However, most of this genus' diversification occurred during the last 500,000 years. *Assiminia californica*, which occupies the California coast estuaries, was the next species to diverge and is the sister to the remaining desert taxa. The majority of the remaining species occupy the Mojave River drainage. There is one sister taxa pair that shares a disjunct distribution between the Mojave River drainage and the Sonoran desert.

Tryonia underwent rapid diversification within the last 2 Ma. The basal nodes support two separate vicariant events between the Chihuahuan and Great Basin deserts. Similar to *Cyprinidon* and *Assiminea,* there are several separate jump dispersal events between the Chihuahuan Desert and Mojave River Drainage and the Great Basin Desert. The events occurred roughly within the last 1 Ma. Most species are only known from a single area with the exception of *Tryonia porrecta* species, which is widely distributed.

The large genus of spring snails *Pyrgulopsis* diversified throughout the last 10 Ma. The splits between the Sonoran and Chihuahuan deserts postdate the uplift of the Sierra Madre Occidental. There are several splits between Sonoran and Great Basin Desert/Mojave River drainage taxa that coincide with the BLFs formation and drainage events. There are three separate events in which Chihuahuan desert taxa are sister to either Great Basin or Mojave River taxa. In one of these events, the procession of biogeographic divergences proceeds from a Chihuahuan clade, with the divergence of a Sonoran desert species (*Pyrgulopsis mimbres*). Later in the Chihuahuan clade there is a divergence between species found along the Colorado River, *Pyrgulopsis deserta* and Chihuahuan desert species, *Pyrgulopsis chupaderae*. This is unusual for the genus because most clades are only found in a single region with almost no range shifts in the last 2 Ma. The vicariance and dispersal events occur primarily at the deeper nodes in the tree.

Dune-Restricted Taxa

The results for the dune-restricted taxa favored the DEC+J model, except for *Uma*. When looking at the constrained dispersal matrix the improvements in the likelihoods between the DEC+J unconstrained and DEC+J constrained were marginally different.

Rhaphiomidas is the oldest taxon examined with a basal divergence occurring at 70 Ma. However much of the diversification of the lineage occurred in the last 15 Ma. The two Chihuahuan and Sonoran Desert divergence events both occurred at roughly the time of the Sierra Madre Occidental uplift. The divergence events within the *R. acton* clade coincide with the BLFs, as does the *R. aitkeni* and *R. trochilus* divergence, but they are unlikely to have been affected by these large bodies of water as they are well outside of the range of the BLFs. Several species are restricted to a single drainage/sand transport system and may have extended their ranges as the BLFs drained and exposed

sediments that they colonized. The results of the BiogeoBEARS analyses of *Rhaphiomidas,* the likelihood was considerably lower for the constrained model. As with the gastropods, *Rhaphiomidas* has highly disjunct distributions such as those between the Colorado River Dunes and Sonoran desert, and between the Mojave River drainage and the Parker Dunes. These disjunctions are likely the result of the age of the *Rhaphiomidas* lineage. *Rhaphiomidas* is sister to all the remaining Mydidae. Fossil taxa of the Mydidae from the mid-Cretaceous are placed into the derived subfamily of the Mydinae (Dikow, personal comm.). This establishes the minimum age of the monotypic subfamily Rhaphiomidinae, allowing for the processes of extinction and vicariance events to fracture this genus across the southwest of North America. In addition, when we look at the population-level tree for *R. arenagena*, (see supplementary figure), most of the sand dune locations form monophyletic clades, indicating perhaps that they are not inclined to long distance dispersal.

Trigonoscuta is the most widely distributed taxon latitudinally, with a range that extends from Baja California Sur to the Canadian-US border. The diversification of this group occurred after the uplift of the Sierra Madre Occidental. There are no divergence events that coincide with the BLFs. The species on either side of the Colorado River split well before the BLFs event. In a more recent time frame, there is all but one divergence event that occurs within the Pleistocene in desert systems. There was a significant improvement in the likelihood with the inclusion of the jump dispersal parameter (J). A small improvement was seen in the likelihood for the constrained hypotheses, indicating some support for the overall fit of the dispersal constraints. An improvement was seen again in the DEC+J+x model with distance having a negative effect on dispersal ability. This may indicate that the dispersal paths chosen may in fact have some biological reality.

The sand treader crickets are composed of five separate genera (Fig. 2), and have a distribution that covers all the desert regions of North America. The genera *Daihinia* and *Utabaenetes* are sister taxa that occupy only the dunes and sandy river deposits of the Great Plains and the San Rafael Desert of the Great Basin, respectively. The genus *Daihinibaenetes* occupies the Great Basin desert as well as the northern portions of the Sonoran Desert. *Daihiniodes*, which was not sampled in this study, is restricted to the Chihuahuan and Great Basin Deserts and may be a member of *Daihinibaenetes* based on morphology. *Ammobaenetes* is found throughout North America with representative species in all of the desert regions. One species in particular is found from the Mojave Desert through the Great Basin and into the Chihuahuan Desert. The other species are restricted to the Mojave and Sonoran deserts and are endemic to only a few dune systems. *Macrobaenetes* is found in the Mojave and Sonoran deserts and its species are narrowly restricted to a single sand transport pathway or a single set of dunes. The divergence times vary throughout this group and do not seem to be tied to any of our hypothesized events. The results of the BioGeoBEARS analyses favored the constrained DEC+J very marginally over the unconstrained DEC+J hypothesis (Table 1). This finding indicates there is weak support for the constrained dispersal pathways. The constrained DEC+J model was preferred over the DEC+J+x model marginally again. This is likely due to the disjunct distributions in *Ammobaenetes* increasing the likelihood for an unconstrained model.

Uma is composed of five species, two in the Chihuahuan Desert and two in the

Sonoran desert and one primarily in the Mojave Desert. The divergence between the Mojave and Sonoran species and the Chihuahuan species occurred at roughly the same time as the Sierra Madre uplift. The divergence between the Sonoran and Mojave species occurred in the time frame of the BLFs event. *Uma* favored the constrained DEC+x model rejecting the DEC+J and DEC+J+x models. This result should however be taken with some caution. *Uma scoparia* is broadly distributed and would likely favor a different model if populations were defined as OTUs as each dune sampled came out as a monophyletic clade. In addition there are very few nodes in the tree (9 including tips), so there are probably insufficient samples for the evaluation of the parameters *J* and *x*.

Discussion

There is little overall consensus in the biogeographic pattern and timing among our study taxa. The one event that did seem to receive support from *Uma,* and two clades in *Rhaphiomidas* was the uplift of the Sierra Madre Occidental. The implications from the DEC and DEC+J analyses show that without jump dispersal the likelihood that species were once more broadly distributed and then broken up by vicariance alone is highly unlikely. This implication points to identifying possible scenarios that may have allowed taxa to take advantage of dispersal events. For example we find little to no evidence for the BLFs, suggesting that this event may not have played a role in the divergence of taxa but perhaps we should shift our focus to examining the formation of river corridors that would have allowed for dispersal to take place after its drainage. This highlights one of the difficulties of continental island systems, if dispersal is the primary means by which speciation happens through chance founder events when areas were connected briefly there is not likely to be a strong geologic record of such events. The longer persisting vicariance events such as mountain uplifts are much easier to detect because of their broad geographic range and time interval and so have received much more attention even though their role in the diversification of desert biota is not tremendously large, as we have demonstrated.

What we can also see in our data is that the recent Pleistocene river connections are likely to have played a role in how species diversified in sand dune and aquatic desert fauna. In particular recent *Cyprinodon* species occupying Death Valley and other northern extensions of the Mojave River Drainage Basin and Trigonoscuta species both share the pattern and timing in this basin. *Trigonoscuta'*s pattern and timing show that they did in fact use the Mojave River to disperse. Both of these clades patterns seem to indicate local dispersal during the Pleistocene time scale with long period of isolation between dispersal events as indicated at deeper nodes. However we were not able to capitalize fully on these more recent and fine scale patterns due to computation limitations in the number of areas. Further fine scale study of these systems will give more evidence as to what effect the Pleistocene river corridors have has on shaping desert communities. The speciation pattern may be one of escape and radiate as seen in oceanic island systems but here there are not any new niches to fill just small isolated patched of habitat that are briefly connected and rapidly colonized then isolated for long periods of time.

Overall there was little evidence that the Bouse Lakes Formation (BLFs) were a barrier to the different clades examined. In the case of the aquatic taxa, it may have even

allowed for animals to disperse. However only a few nodes in the *Pyrgulopsis* phylogeny showed congruence with this event and these may be coincidental, just by random chance. The uplift of the Sierra Madre Occidental coincided with the divergence between several taxa in *Rhaphiomidas* and *Uma*. The recent time frame of the sand transport pathways is consistent with taxa using these corridors to disperse locally within drainage systems. However there is not a clear pattern of how they moved between the different drainage systems. The divergence events between the different drainage basins and sand transport pathways occurred at a much deeper time than the Pleistocene production of modern dune systems.

Jump dispersal seems to have played a significant role in the biogeography of taxa inhabiting sand dune systems. This does not eliminate vicariance as an important factor, but without the inclusion of jump dispersal, the biogeographic reconstructions receive much lower likelihoods. In all but two of the taxa (*Uma* and *Assiminea*) the DEC model was rejected in favor of the DEC+J model. However, if *Uma* were to be broken down by populations, it is likely that a jump dispersal mode of range expansion would be best-fitting, as the populations have a similar biogeographic pattern as for *Trigonoscuta,* for which jump dispersal was the preferred model. With *Assiminea,* the DEC model was rejected in favor of the DEC+J model, but when a connectivity matrix between areas was included, the DEC+J and DEC+J+x were rejected in favor of the DEC model. One interpretation of this could be that because several of the disjunct distributions between sister taxa were not allowed in the dispersal connectivity matrix, it conferred a higher likelihood to a more broadly distributed ancestor thereby favoring events found in the DEC model. The biological interpretation of these disjunct sister taxa relationships could be explained as a result of bird-mediated dispersal. Other authors have hypothesized such an explanation for snails (Hershler & Liu 2008). In addition, there is some biological evidence for the possibility of birds distributing snail larvae (van Leeuwen *et al.* 2012). The recent time frame of the taxa is too young to support older vicariance events such as the Colorado River draining out to the Coast of California as opposed to the Gulf of California. DEC+J being the overall preferred model suggests that founder event speciation is an important process for the formation of the biogeographic ranges in this continental island system.

The inclusion of the dispersal connectivity matrix seemed to have a negative effect with regard to aquatic taxa except in the case of *Cyprinodon*. For *Assiminia,* the likelihood decreased between the unconstrained and constrained dispersal analyses, most likely for the reasons explained above. We also find support for the unconstrained analyses in *Tryonia* and *Pyrgulopsis*. *Tryonia* have larvae that develop inside the snail's female genitalic track (Hershler 2001) unlike the other genera of snails in this study, and this may contribute to why, with one exception, each species is confined to a single locality. *Tryonia porrecta* is the only member of this genus that is parthenogenetic, which may explain why this species has a relatively broad distribution (Hershler *et al.* 2005). The comparison between the unconstrained and constrained models supports the unconstrained dispersal matrix, which may be due to the observed distribution having sister taxa in areas that are not allowed in the dispersal matrix, such as between the Mojave River Drainage and Sonoran Desert. *Pyrgulopsis* also has several sister taxa with distributions not allowed by the connectivity matrix, likely explaining the preference for the unconstrained matrix. In the case of *Cyprinodon* (pupfish), there was a marginal

improvement in the likelihood with the inclusion of the constrained dispersal matrix. This finding is consistent with hypothesized riverine transport between areas.

Conclusions

Only three of the eight genera showed a preference for the constrained model. Although these do show support for the proposed transport paths, the other genera do not support these models. As explained above, the often disjunct distributions were not allowed by the adjacency matrix. This raises the larger issue of how one determines the areas and connectivity between the areas. Here we used the geologic information provided by sand transport pathways or looked for the nearest distance between sand dunes of an area e.g., Coast and Mojave River. It would be far better to have a more complete geologic picture of past drainages to derive the adjacency matrix. The complexity of continental geology is one of the major hindrances to continental historical biogeography. More refined geologic models going back beyond the Pleistocene, further into the Neogene, would be very useful for testing some of the older disjunct distributions that were observed in our study taxa. In this study, we also demonstrated the utility of incorporating GIS for making explicit measurements for which parameter values such as x were calculated. Further we found that the addition of this parameter allowed us to distinguish the effect of distance on our focal taxa and allowed for further interpretation, such as distance not affecting dispersal for *Cyprinodon* supporting fast transport by river corridors, and inhibiting dispersal for highly dispersal limited taxa such as flightless weevils *Trigonoscuta*. It is our hope that this approach of explicitly testing biogeographic models in a hierarchical fashion, e.g., dispersal constraints vs. unconstrained will be more widely adopted. Finally we also hope that researchers will utilize more geologically and biologically meaningful measurements for computing the effect of distance as we have done here.

References Cited

Anderson RS (2002) Curculionidae. In: *American Beetles, Vol. 2: Polyphaga. Scarabaeoidea through Curculionoidea* (eds Arnett RH, Thomas MC, Skelley PE, Frank JH), pp. 722–815. CRC Press., Boca Raton, FL.
Avise JC (2000) *Phylogeography: The History and Formation of Species*. Harvard University Press.
Axelrod D (1979) Age and origin of Sonoran Desert vegetation. *Occas. Pap. Calif. Acad. Sci*, **132**, 1–74.
Axelrod D (1983) Biogeography of oaks in the Arcto-Tertiary province. *Annals of the Missouri Botanical Garden*, **70**, 629–657.
Bacon SN, Burke RM, Pezzopane SK, Jayko AS (2006) Last glacial maximum and Holocene lake levels of Owens Lake, eastern California, USA. *Quaternary Science Reviews*, **25**, 1264–1282.
Beveridge C, Kocurek G, Ewing RC *et al.* (2006) Development of spatially diverse and complex dune-field patterns: Gran Desierto Dune Field, Sonora, Mexico. *Sedimentology*, **53**, 1391–1409.
Brandley MC, Schmitz A, Reeder TW (2005) Partitioned Bayesian analyses, partition choice, and the phylogenetic relationships of scincid lizards. *Systematic biology*, **54**, 373–90.
Brooks DR, Van Veller MGP, McLennan DA (2002) How to do BPA, really. *Journal of Biogeography*, **28**, 345–358.
Castoe TA, Daza JM, Smith EN *et al.* (2009) Comparative phylogeography of pitvipers suggests a consensus of ancient Middle American highland biogeography. *Journal of Biogeography*, **36**, 88–103.
Castoe TA, Spencer CL, Parkinson CL (2007) Phylogeographic structure and historical demography of the western diamondback rattlesnake (Crotalus atrox): A perspective on North American desert biogeography. *Molecular Phylogenetics and Evolution*, **42**, 193–212.
Cazier MA (1985) A revision of the North American flies belonging to the genus Rhaphiomidas (Diptera, Apioceridae). *Bulletin of the AMNH*, **182**, 182–263.
Clarke ML, Rendell HM (1998) Climate change impacts on sand supply and the formation of desert sand dunes in the south-west U.S.A. *Journal of Arid Environments*, **39**, 517–531.
Van Dam MH (2010) A new species and key for Rhaphiomidas Osten Sacken (Diptera: Mydidae). *Zootaxa*, **2622**, 49–60.
DeQueiroz K (1999) The general lineage concept of species and the defining properties of the species category. In: *Species: New interdisciplinary essays* (ed Wilson AR), pp. 49–89. MIT Press, Cambridge, Massachusetts.
Devitt TJ (2006) Phylogeography of the Western Lyresnake (Trimorphodon biscutatus): testing aridland biogeographical hypotheses across the Nearctic-Neotropical transition. *Molecular ecology*, **15**, 4387–407.
Donoghue MJ, Moore BR (2003) Toward an integrative historical biogeography. *Integrative and comparative biology*, **43**, 261–70.
Douglas ME, Douglas MR, Schuett GW, Porras LW (2006) Evolution of rattlesnakes (Viperidae; Crotalus) in the warm deserts of western North America

shaped by Neogene vicariance and Quaternary climate change. *Molecular ecology*, **15**, 3353–74.
Drummond A (2007) Tracer v1. 5.3.
Drummond AJ, Ho SYW, Phillips MJ, Rambaut A (2006) Relaxed phylogenetics and dating with confidence. (D Penny, Ed,). *PLoS biology*, **4**, e88.
Drummond AJ, Suchard MA, Xie D, Rambaut A (2012) Bayesian phylogenetics with BEAUti and the BEAST 1.7. *Molecular biology and evolution*, **29**, 1969–73.
Echelle A (2008) The western North American pupfish clade (Cyprinodontidae: Cyprinodon): mitochondrial DNA divergence and drainage history. In: *Late Cenozoic Drainage History of the Southwestern Great Basin and Lower Colorado River Region: Geologic and Biotic Perspectives* (eds Reheis MC, Hershler R, Miller DM), pp. 27–38. Geological Society Am Special Paper of Americal Special Paper.
Echelle A, Echelle A (1993) Allozyme perspective on mitochondrial DNA variation and evolution of the Death Valley pupfishes (Cyprinodontidae: Cyprinodon). *Copeia*, 275–287.
Evans A V., Hogue JN (2006) *Field Guide to Beetles of California*. University of California Press, Berkeley.
Ferrari L, López-martínez M, Aguirre-díaz G *et al.* (1999) Space-time patterns of Cenozoic arc volcanism in central Mexico: From the Sierra Madre Occidental to the Mexican Volcanic Belt. *Geology*, **27**, 303–306.
Fyler CA, Reeder TW, Berta A *et al.* (2005) Historical biogeography and phylogeny of monachine seals (Pinnipedia: Phocidae) based on mitochondrial and nuclear DNA data. *Journal of Biogeography*, **32**, 1267–1279.
George J, Mattoni R (2006) Rhaphiomidas terminatus terminatus Cazier, 1985 (Diptera: Mydidae): notes on the rediscovery and conservation biology of a presumed extinct species. *Pan-Pacific entomologist*, **82**, 32–35.
Gillespie R (2004) Community assembly through adaptive radiation in Hawaiian spiders. *Science (New York, N.Y.)*, **303**, 356–359.
Grant PR, Grant BR (2002) Unpredictable evolution in a 30-year study of Darwin's finches. *Science (New York, N.Y.)*, **296**, 707–711.
Grismer LLL (1994) The origin and evolution of the peninsular herpetofauna of Baja California, Mexico. *Herpetological Natural History*, **2**, 51–106.
Hardy A, Andrews F (1976) *A final report to the Office of Endangered Species on contract 14-16-0008-966*. Insect Taxonomy Laboratory, Division of Plant Industry, California Dept. of Food and Agriculture, Sacramento, CA.
Hershler R (2001) Systematics of the North and Central American aquatic snail genus Tryonia (Rissooidea: Hydrobiidae). *Smithsonian Contributions to Zoology*, **612**, 1–53.
Hershler R, Liu H (2008) Ancient vicariance and recent dispersal of springsnails (Hydrobiidae: Pyrgulopsis) in the Death Valley system, California-Nevada. *Special Papers- Geological Society of America*, **439**.
Hershler R, Mulvey M, Liu H-P (2005) Genetic variation in the Desert Springsnail (Tryonia porrecta): implications for reproductive mode and dispersal. *Molecular ecology*, **14**, 1755–65.
House PK, Pearthree PA, Howard KA *et al.* (2005) Birth of the lower Colorado River—Stratigraphic and geomorphic evidence for its inception near the conjunction

of Nevada, Arizona, and California. In: *Geological Society of America Field Guide 6* (eds Pederson JL, Dehler C.), pp. 357–387. Geological Society of America, Interior Western United States: Boulder, Colorado,.
House P, Pearthree PA, Perkins ME (2008) Stratigraphic evidence for the role of lake spillover in the inception of the lower Colorado River in southern Nevada and western Arizona. *Geological Society of Ametica Special Paper 4*, **439**.
Hubbard J (1973) Avian evolution in the aridlands of North America. *Living Bird*, **12**, 155–196.
Jones K (1995) Phylogeography of the desert horned lizard (Phrynosoma platyrhinos) and the short-horned lizard (Phrynosoma douglassi): patterns of divergence and diversity. University of Nevada, Las Vegas.
Knowles LL, Carstens BC (2007) Delimiting species without monophyletic gene trees. *Systematic biology*, **56**, 887–895.
Lancaster N (1994) Arid geomorphology - progress report. *Progress in Physical Geography*, **23**, 97–102.
Lapointe F-J, Rissler LJ (2005) Congruence, consensus, and the comparative phylogeography of codistributed species in California. *The American naturalist*, **166**, 290–9.
Larkin MA, Blackshields G, Brown NP *et al.* (2007) Clustal W and Clustal X version 2.0. *Bioinformatics*, **23**, 2947–2948.
Van Leeuwen CH a, van der Velde G, van Lith B, Klaassen M (2012) Experimental quantification of long distance dispersal potential of aquatic snails in the gut of migratory birds. *PloS one*, **7**, e32292.
Losos JB, Leal M, Glor RE *et al.* (2003) Niche lability in the evolution of a Caribbean lizard community. *Nature*, **424**, 542–545.
Lucchitta I (1979) Late Cenozoic uplift of the southwestern Colorado Plateau and adjacent lower Colorado River region. *Tectonophysics*.
Lucchitta I (2001) The Bouse formation and post-Miocene uplift of the Colorado Plateau. In: *The Colorado River: Origin and Evolution* (eds Young R., Spamer E.), pp. 173–178. Grand Canyon Association, Grand Canyon, AZ.
Maddison W, Maddison D (2009) Mesquite: a modular system for evolutionary analysis Version 2.6. *Bioinformatics*.
Masta SE (2000) Phylogeography of the jumping spider Habronattus pugillis (araneae: salticidae): recent vicariance of sky island populations? *Evolution; international journal of organic evolution*, **54**, 1699–1711.
Matzke N (2013) Probabilistic Historical Biogeography: New Models for Founder-Event Speciation, Imperfect Detection, and Fossils Allow Improved Accuracy and Model-Testing. *Ph.D. thesis, Department Integrative Biology and Designated Emphasis in Computational and Genomic Biology, University of California, Berkeley*, 1–240.
Morafka D (1977) A biogeographical analysis of the Chihuahuan Desert through its herpetofauna.
Muhs D, Bettis E (2003) Quaternary loess-paleosol sequences as examples of climate-driven sedimentary extremes. *Geological Society of America*.
Murphy R (1983) The Reptiles: Origins and Evolution. *Island Biogeography in the Sea of Cortâez*.

Murphy R, Aguirre-León G (2002) The nonavian reptiles. ... *island biogeography …*.
Murphy RW, Trépanier TL, Morafka DJ (2006) Conservation genetics, evolution and distinct population segments of the Mojave fringe-toed lizard, Uma scoparia. *Journal of Arid Environments*, **67**, 226–247.
Nelson G, Platnick N (1981) *Systematics and biogeography: cladistics and vicariance*. Columbia University Press, New York.
Nieto-Samaniego Á (1999) Variation of Cenozoic extension and volcanism across the southern Sierra Madre Occidental volcanic province, Mexico. ... *Society of America …*.
Norris KS (1958) The evolution and systematics of the iguanid genus Uma and its relation to the evolution of other North American desert reptiles. *Bulletin of the American Museum of Natural History*, **114**, 251.
Nylander J (2002) MrModeltest 2.2.
Orange D, Riddle B, Nickle D (1999) Phylogeography of a wide-ranging desert lizard, Gambelia wislizenii (Crotaphytidae). *Copeia*.
Orr RT (1960) An Analysis of the Recent Land Mammals. *Systematic Zoology*, **9**, 171.
Ortega-Gutiérrez F, Guerrero-Garcia J (1982) The geologic regions of Mexico. ... *in regional geological synthesis. D–NAG …*.
Pierce WD (1975) *The sand dune weevils of the genus Trigonoscuta, with a correlation of their anatomy to the geological history of our coast lines* (G John, Ed,). Natural History Museum of Los Angeles County, Los Angeles.
Platnick NI, Nelson G (1978) A Method of Analysis for Historical Biogeography. *Systematic Zoology*, **27**, 1.
Poulson SR, John BE (2003) Stable isotope and trace element geochemistry of the basal Bouse Formation carbonate, southwestern United States: Implications for the Pliocene uplift history of the Colorado Plateau. *Geological Society of America Bulletin*, **115**, 434–444.
Ree RH, Moore BR, Webb CO, Donoghue MJ (2005) A likelihood framework for inferring the evolution of geographic range on phylogenetic trees. *Evolution; international journal of organic evolution*, **59**, 2299–311.
Ree RH, Smith S a (2008) Maximum likelihood inference of geographic range evolution by dispersal, local extinction, and cladogenesis. *Systematic biology*, **57**, 4–14.
Riddle B (1995) Molecular biogeography in the pocket mice (Perognathus and Chaetodipus) and grasshopper mice (Onychomys): the late Cenozoic development of a North American. *Journal of Mammalogy*.
Riddle BR, Hafner DJ (2006) A step-wise approach to integrating phylogeographic and phylogenetic biogeographic perspectives on the history of a core North American warm deserts biota. *Journal of Arid Environments*, **66**, 435–461.
Riddle BR, Hafner DJ, Alexander LF, Jaeger JR (2000) Cryptic vicariance in the historical assembly of a Baja California peninsular desert biota. *Proceedings of the National Academy of Sciences of the United States of America*, **97**, 14438–14443.
Rogers R, Van Dam MH (2007) Two new species of Rhaphiomidas (Diptera: Mydidae). *Zootaxa*, **68**, 61–68.

Ronquist F (1996) DIVA v. 1.1. Computer program for MacOS and Win32.
Ronquist F (1997) Dispersal-Vicariance Analysis: A New Approach to the Quantification of Historical Biogeography. *Systematic Biology*, **46**, 195–203.
Rosen DE (1978) Vicariant Patterns and Historical Explanation in Biogeography. *Systematic Zoology*, **27**, 159.
Roskowski J a., Patchett PJ, Spencer JE *et al.* (2010) A late Miocene-early Pliocene chain of lakes fed by the Colorado River: Evidence from Sr, C, and O isotopes of the Bouse Formation and related units between Grand Canyon and the Gulf of California. *Geological Society of America Bulletin*, **122**, 1625–1636.
Savage JM (1960) Evolution of a Peninsular Herpetofauna. *Systematic Zoology*, **9**, 184.
Seago AE, Giorgi JA, Li J, Ślipiński A (2011) Phylogeny, classification and evolution of ladybird beetles (Coleoptera: Coccinellidae) based on simultaneous analysis of molecular and morphological data. *Molecular Phylogenetics and Evolution*, **60**, 137–151.
Smith CI, Pellmyr O (2007) Population structure in Joshua Trees and their pollinating moths testing the Bouse Embayment vicariance hypothesis. In:. Portland, OR.
Spencer JE, Jonathan Patchett P (1997) Sr isotope evidence for a lacustrine origin for the upper Miocene to Pliocene Bouse Formation, lower Colorado River trough, and implications for timing of Colorado Plateau uplift. *Geological Society of America Bulletin*, **109**, 767–778.
Spencer JE, Patchett PJ, Pearthree P a. *et al.* (2013) Review and analysis of the age and origin of the Pliocene Bouse Formation, lower Colorado River Valley, southwestern USA. *Geosphere*, **9**, 444–459.
Stokes S (1999) Luminescence dating applications in geomorphological research. *Geomorphology*, **29**, 153–171.
Turak J (2000) *Revaluation of the Miocene/ Pliocene depositional history of the Bouse Formation, Colorado River trough, southern Basin and Range(CA, NV, and AZ)(MS thesis)*. University of Wyoming, Laramie.
Turner B (1983) Genic variation and differentiation of remnant natural populations of the desert pupfish, Cyprinodon macularius. *Evolution*.
Upton DE, Murphy RW (1997) Phylogeny of the Side-Blotched Lizards (Phrynosomatidae:Uta) Based on mtDNA Sequences: Support for a Midpeninsular Seaway in Baja California. *Molecular Phylogenetics and Evolution*, **8**, 104–113.
Wake DB (1987) Adaptive Radiation of Salamanders in Middle American Cloud Forests. *Annals of the Missouri Botanical Garden*, **72**, 242–264.
Webb CO, Ree R (2012) *Biotic Evolution and Environmental Change in Southeast Asia* (D Gower, K Johnson, J Richardson, *et al.*, Eds,). Cambridge University Press, Cambridge.
Whittaker RJ, Fernandez-Palacios JM (2007) *Island Biogeography: Ecology, Evolution, and Conservation*. Oxford University Press.
Wilson JS, Clark SL, Williams K a., Pitts JP (2012) Historical biogeography of the arid-adapted velvet ant Sphaeropthalma arota (Hymenoptera: Mutillidae) reveals cryptic species. *Journal of Biogeography*, **39**, 336–352.
Wilson J, Pitts J (2010) Phylogeographic analysis of the nocturnal velvet ant genus

Dilophotopsis (Hymenoptera: Mutillidae) provides insights into diversification in the Nearctic deserts. *Biological journal of the Linnean Society*.
Wood DA, Fisher RN, Reeder TW (2008) Novel patterns of historical isolation, dispersal, and secondary contact across Baja California in the Rosy Boa (Lichanura trivirgata). *Molecular phylogenetics and evolution*, **46**, 484–502.
Zimbelman J, Williams S, Tchakerian V (1995) Sand transport paths in the Mojave Desert, southwestern United States. In: *Desert Aeolian Processes* (ed Tchakerian VP). Chapman & Hall, New York.
Zink RM (2002) Methods in comparative phylogeography, and their application to studying evolution in the north american aridlands. *Integrative and comparative biology*, **42**, 953–9.

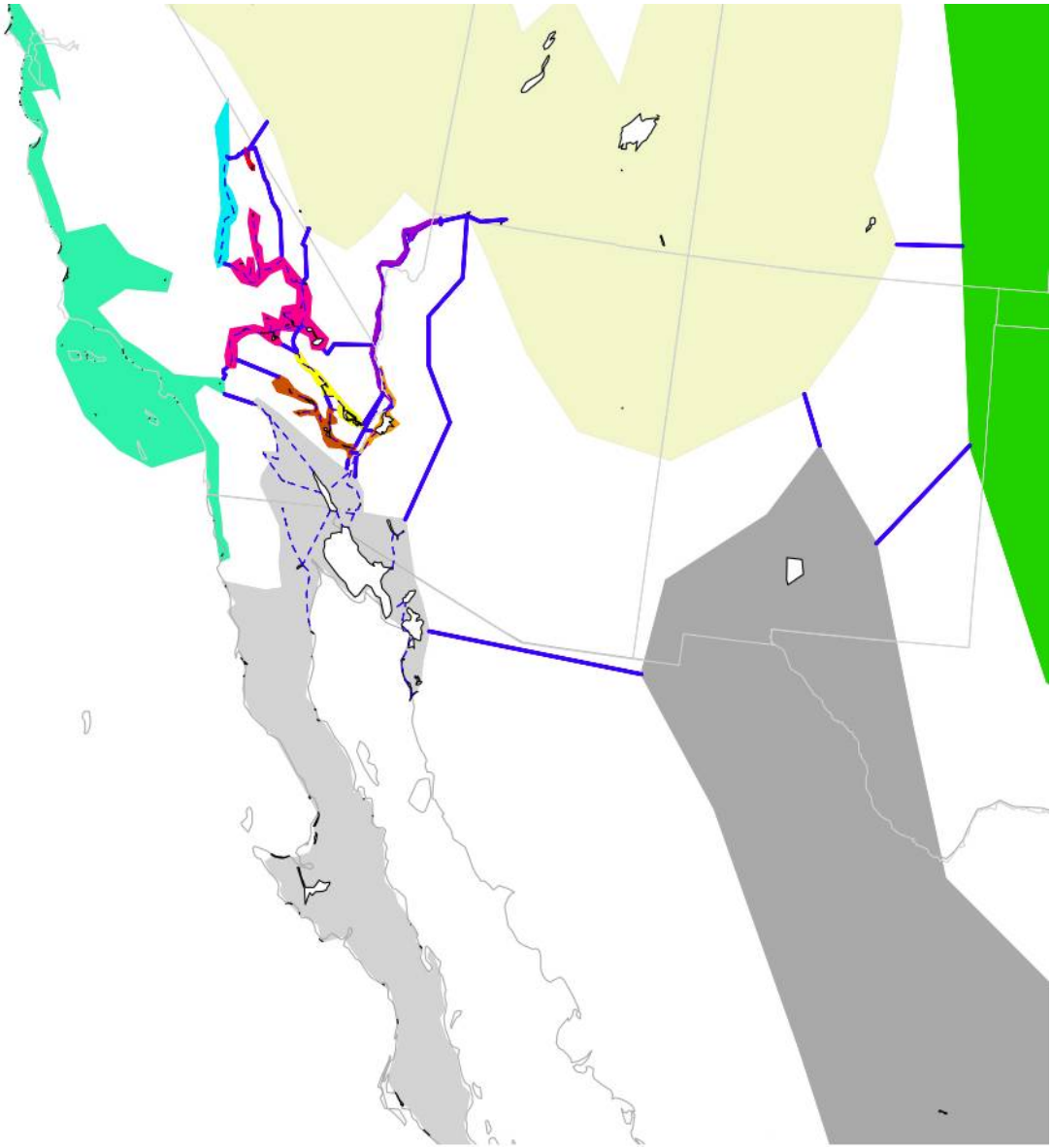

Fig. 1 Map of North American Desert Regions. Solid blue lines indicate paths that were calculated between areas. Colors represent biogeographic areas tested in analyses.

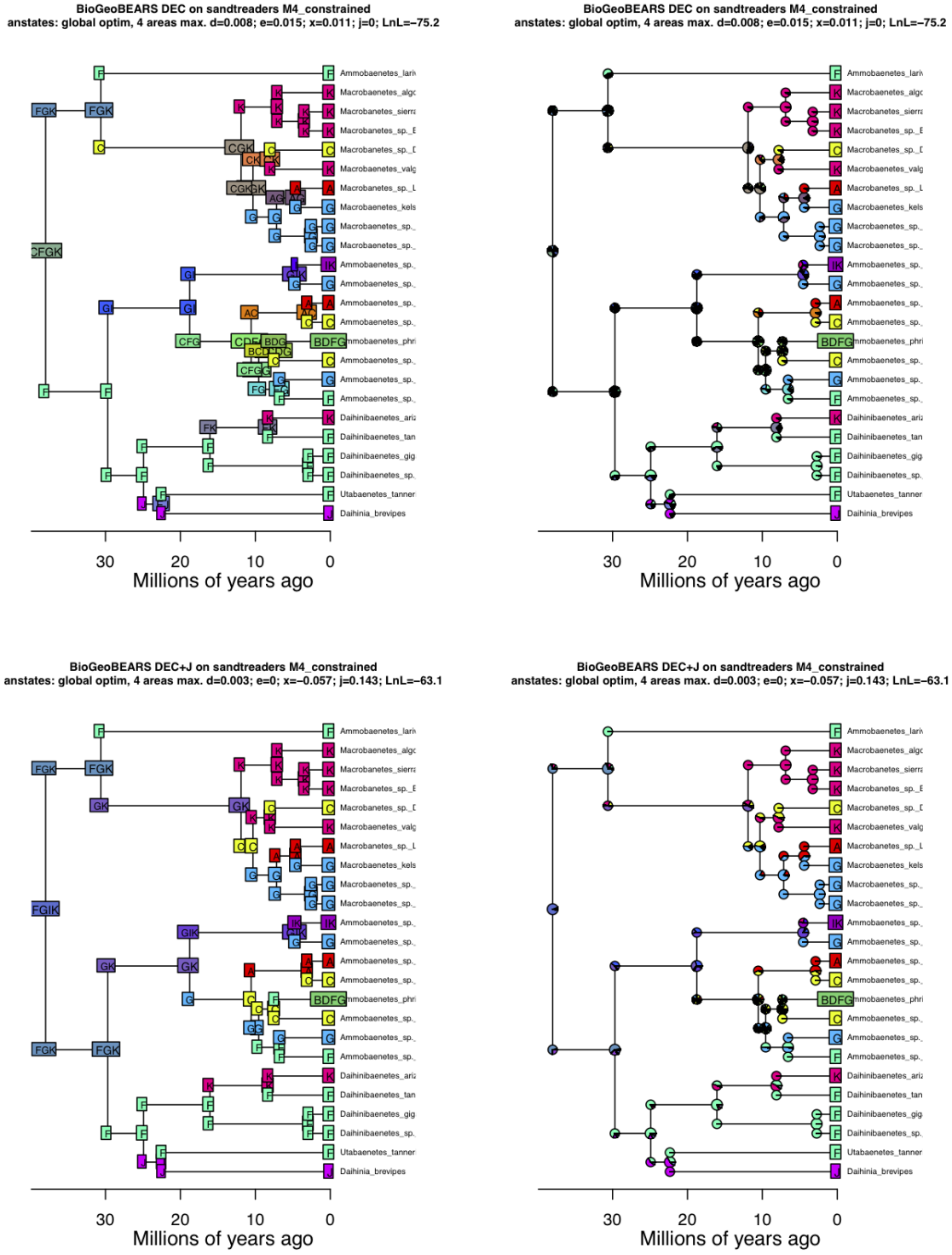

Fig. 2, BioGeoBEARS biogeographic reconstruction for sandtreader crickets. State Codes for biogeographic reconstructions: Bristol Trough A, Chihuahuan Desert B, Clarks Pass C, Colorado River Dunes D, Pacific Coast E, Great Basin F, Mojave River Drainage G, Owens Valley H, Parker Dunes I, Great Plains J, Sonoran Desert K.

BioGeoBEARS DEC on Rhaphiomidas M0
anstates: global optim, 4 areas max. d=0.004; e=0.02; j=0; LnL=–106.9

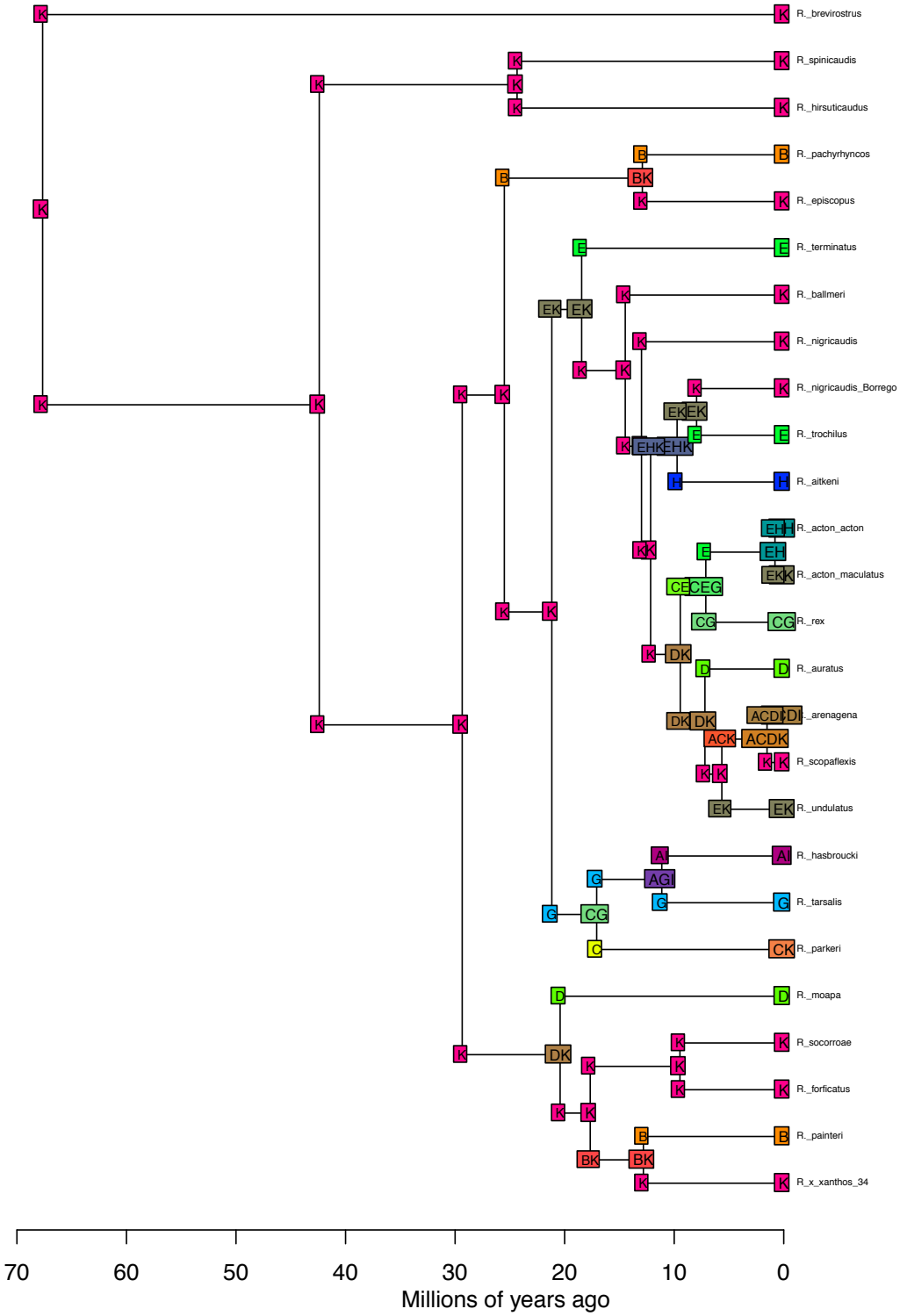

BioGeoBEARS DEC on Rhaphiomidas M0
anstates: global optim, 4 areas max. d=0.004; e=0.02; j=0; LnL=–106.9

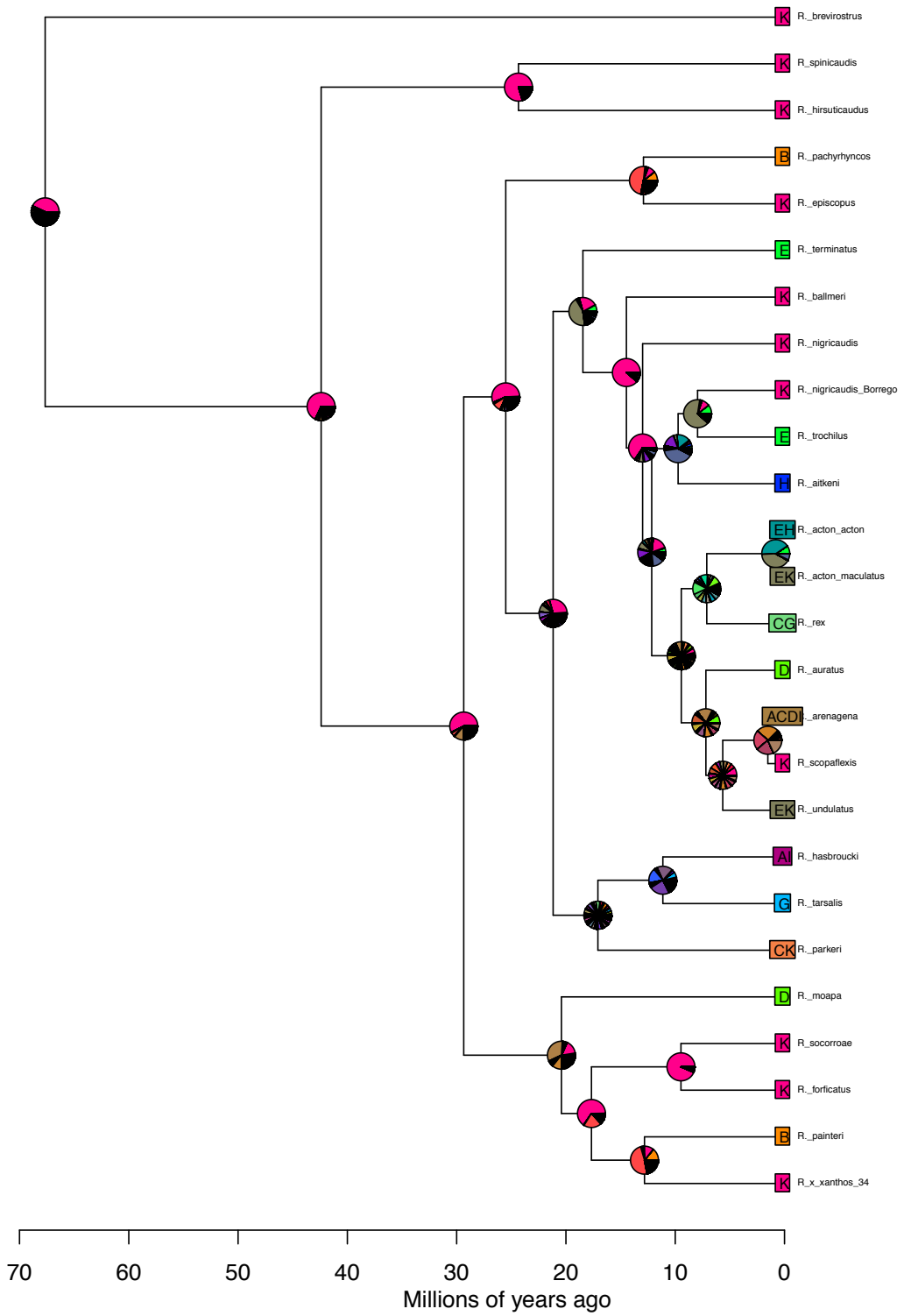

BioGeoBEARS DEC+J on Rhaphiomidas M0
anstates: global optim, 4 areas max. d=0.002; e=0; j=0.053; lnL=–96.5

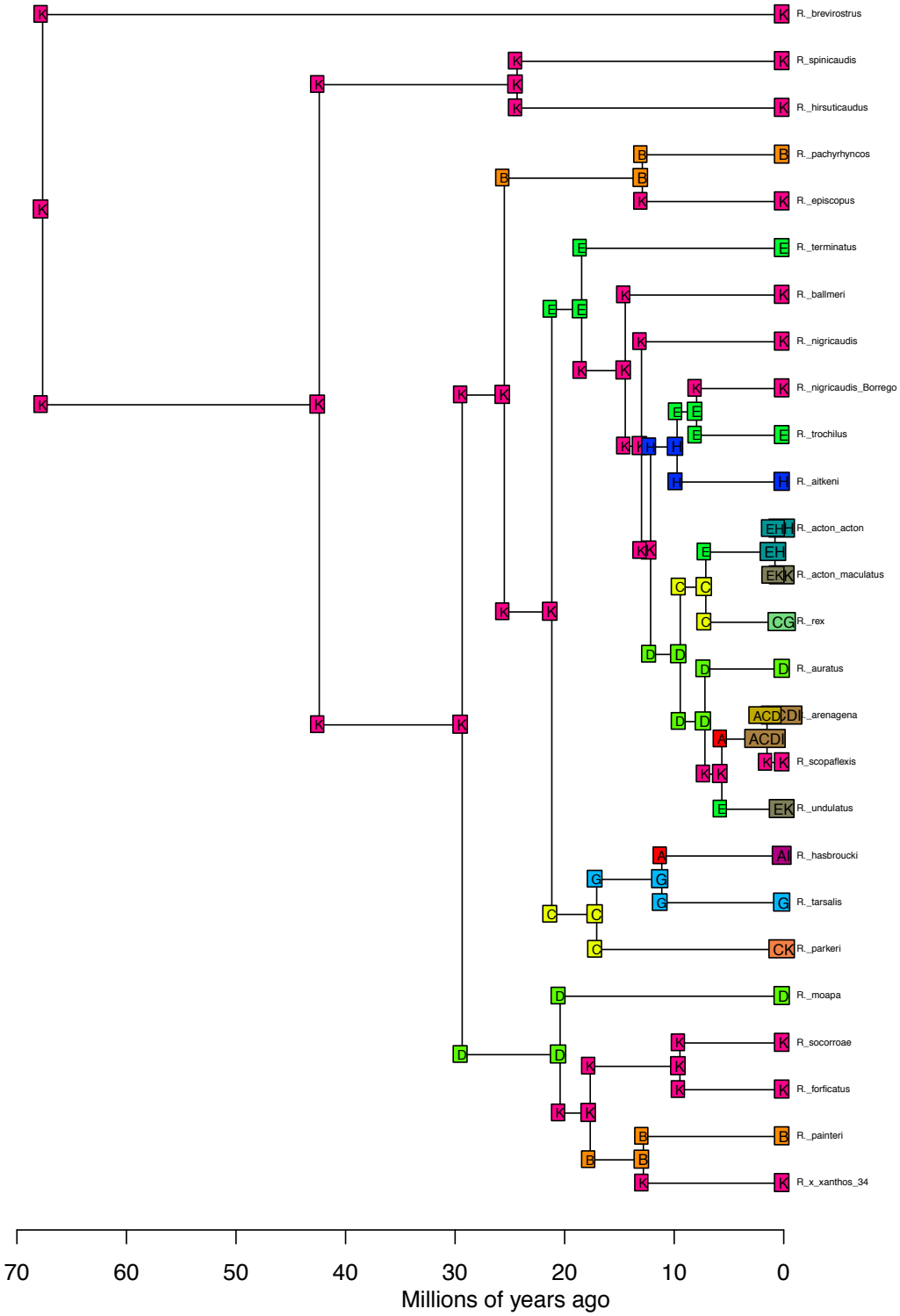

BioGeoBEARS DEC+J on Rhaphiomidas M0
anstates: global optim, 4 areas max. d=0.002; e=0; j=0.053; LnL=–96.5

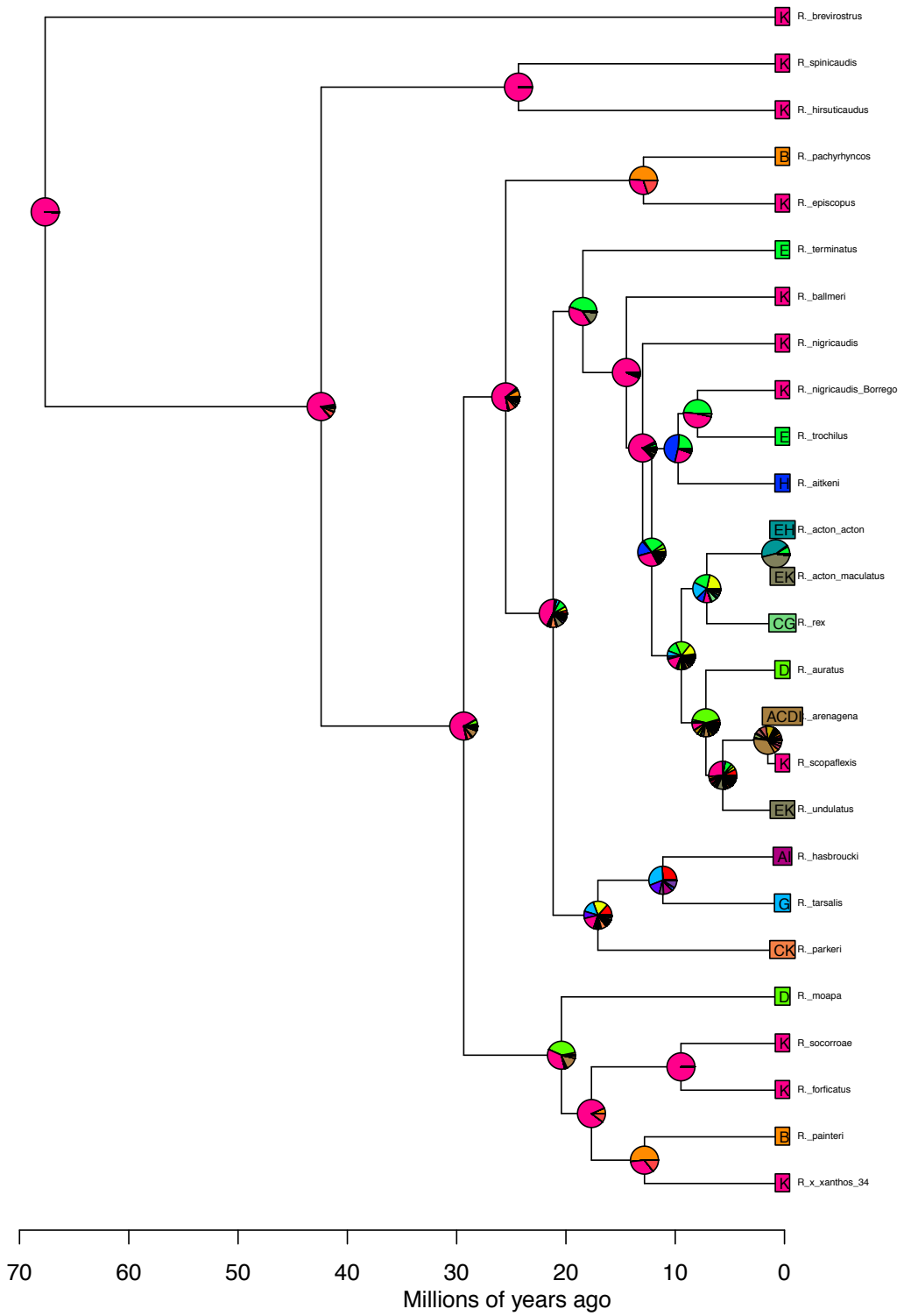

BioGeoBEARS DEC on Rhaphiomidas M3
anstates: global optim, 4 areas max. d=0.013; e=0.029; j=0; LnL=–110.5

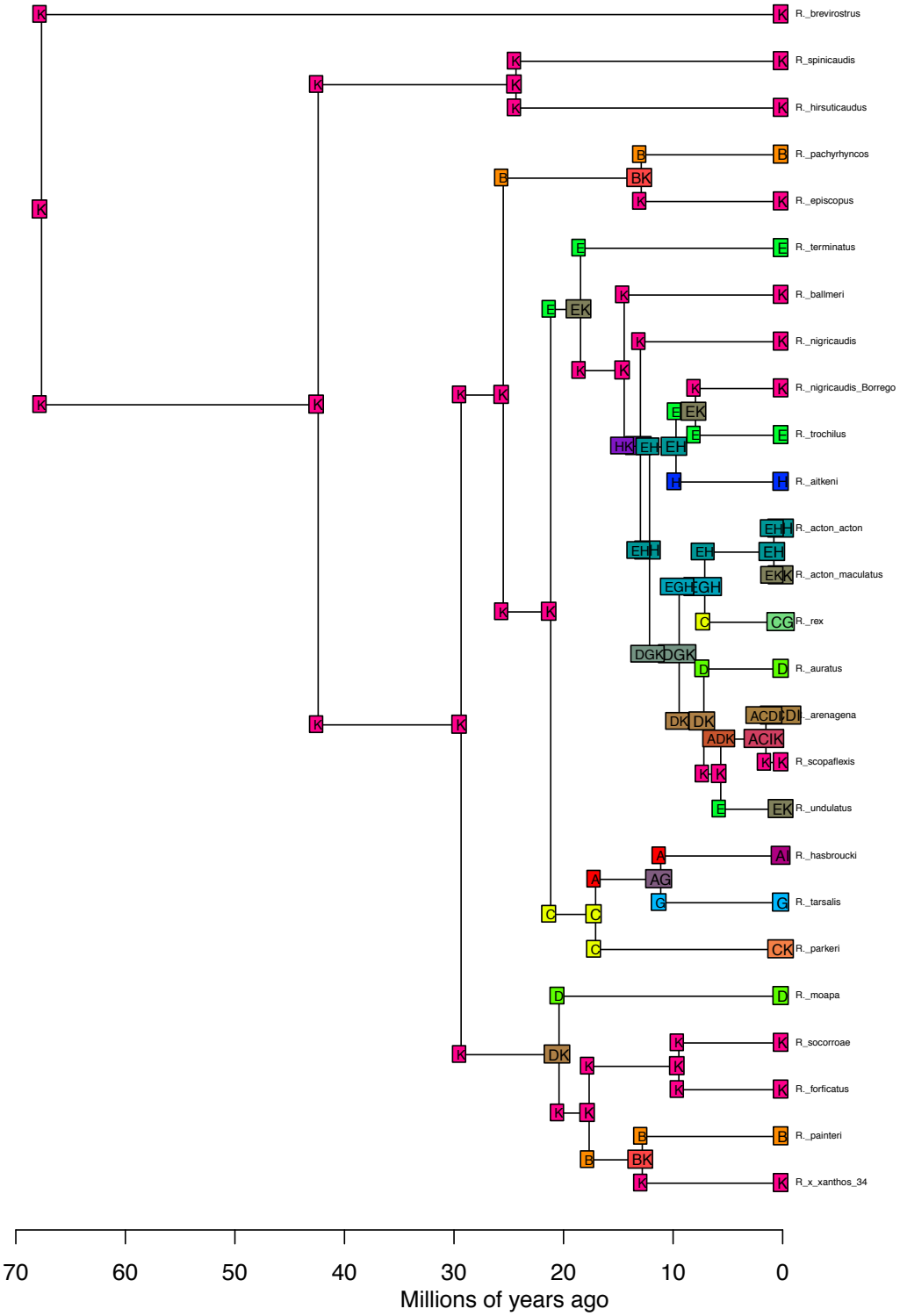

BioGeoBEARS DEC on Rhaphiomidas M3
anstates: global optim, 4 areas max. d=0.013; e=0.029; j=0; LnL=–110.5

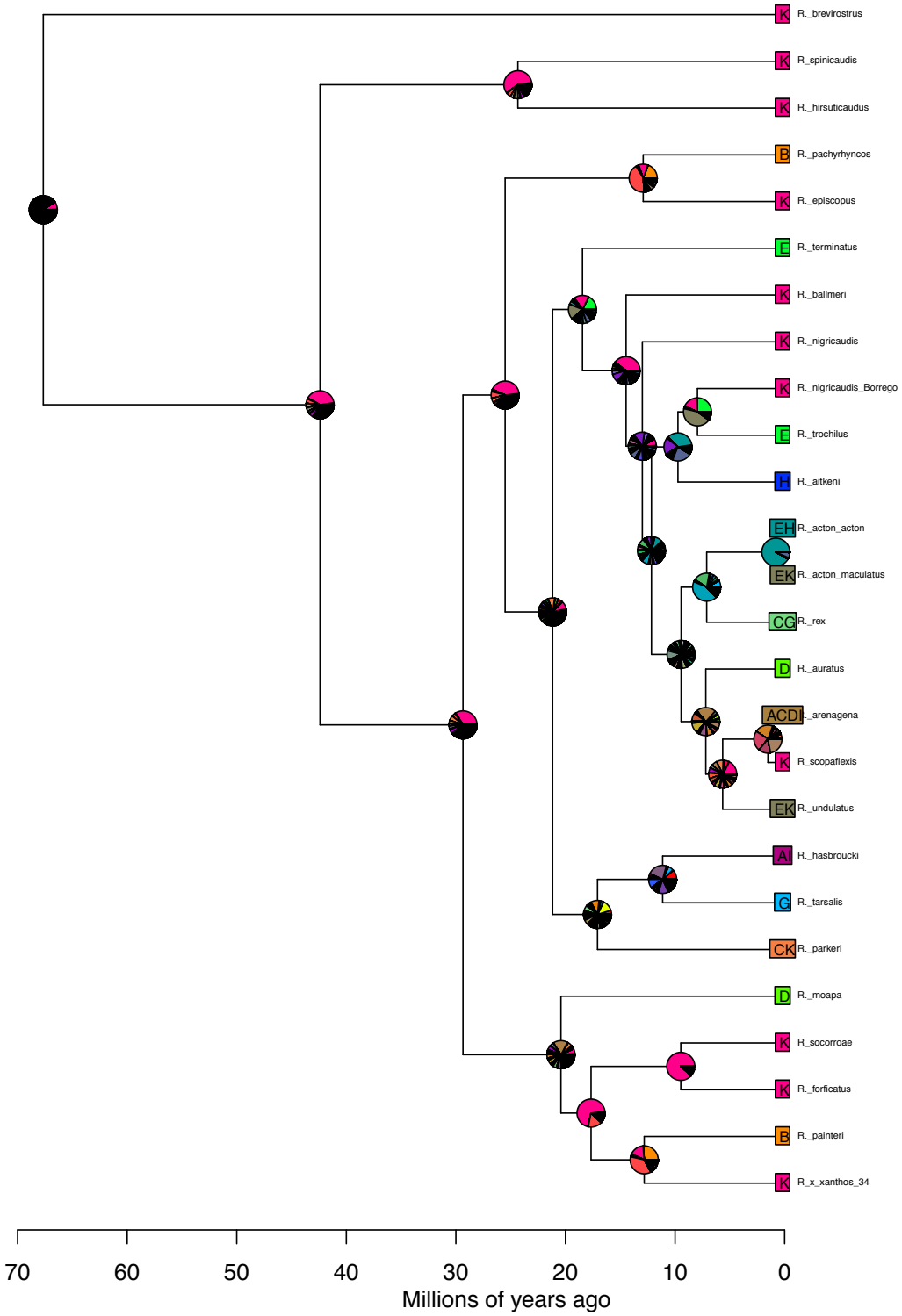

BioGeoBEARS DEC+J on Rhaphiomidas M3
anstates: global optim, 4 areas max. d=0.007; e=0.013; j=0.279; LnL=–101.5

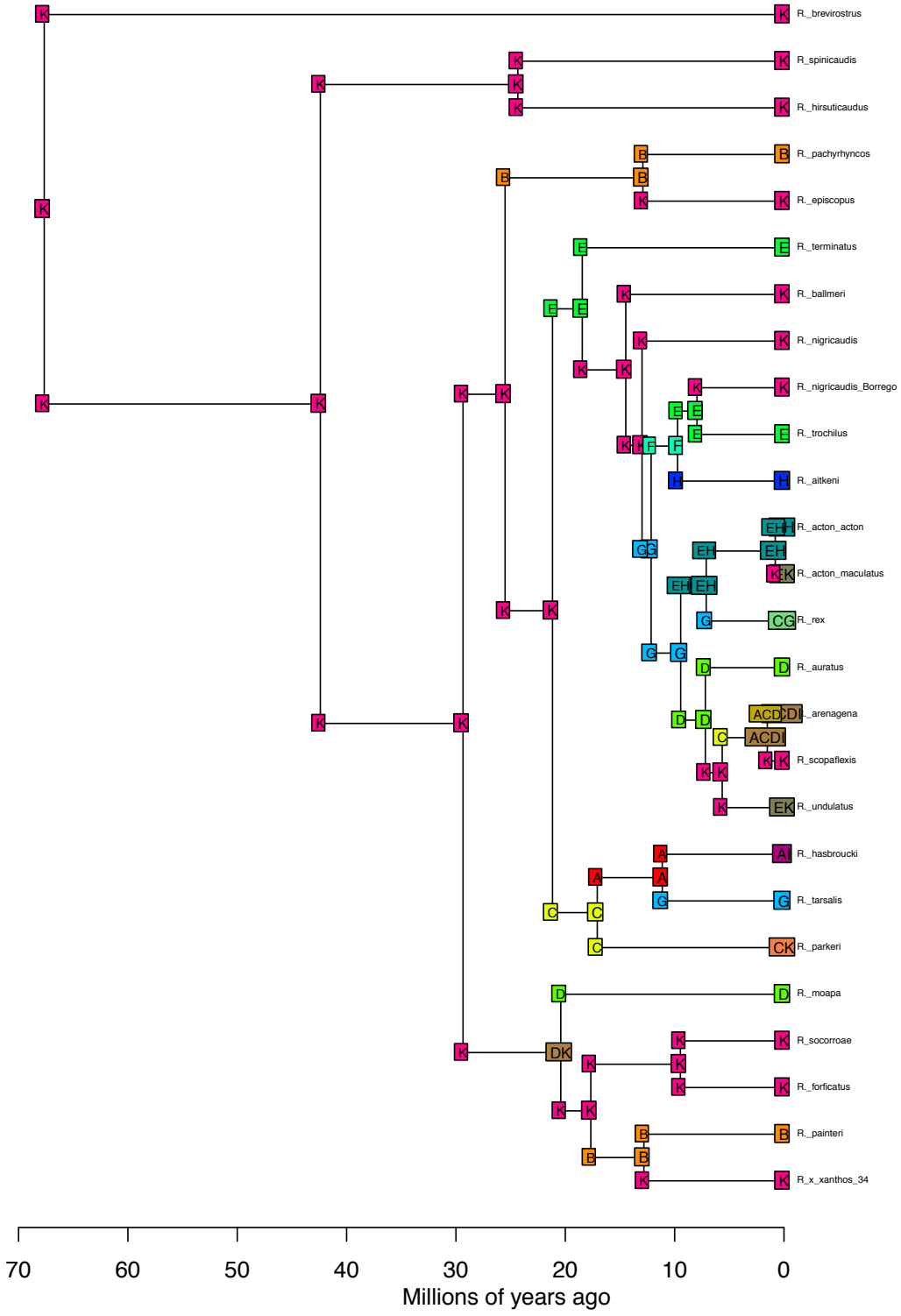

BioGeoBEARS DEC+J on Rhaphiomidas M3
anstates: global optim, 4 areas max. d=0.007; e=0.013; j=0.279; LnL=−101.5

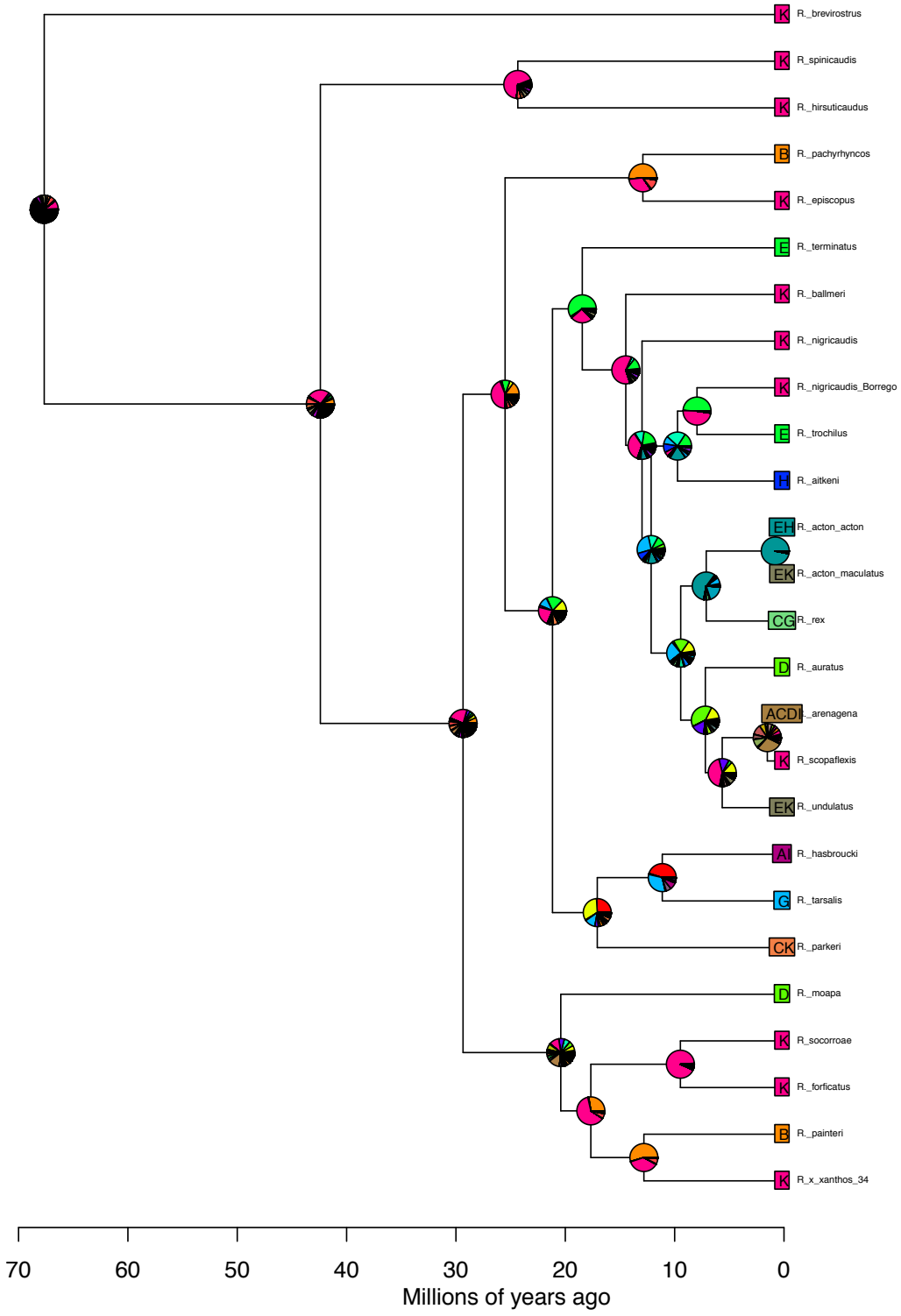

BioGeoBEARS DEC on Rhaphiomidas M4
anstates: global optim, 4 areas max. d=0.048; e=0.028; x=−0.342; j=0; LnL=−108.6

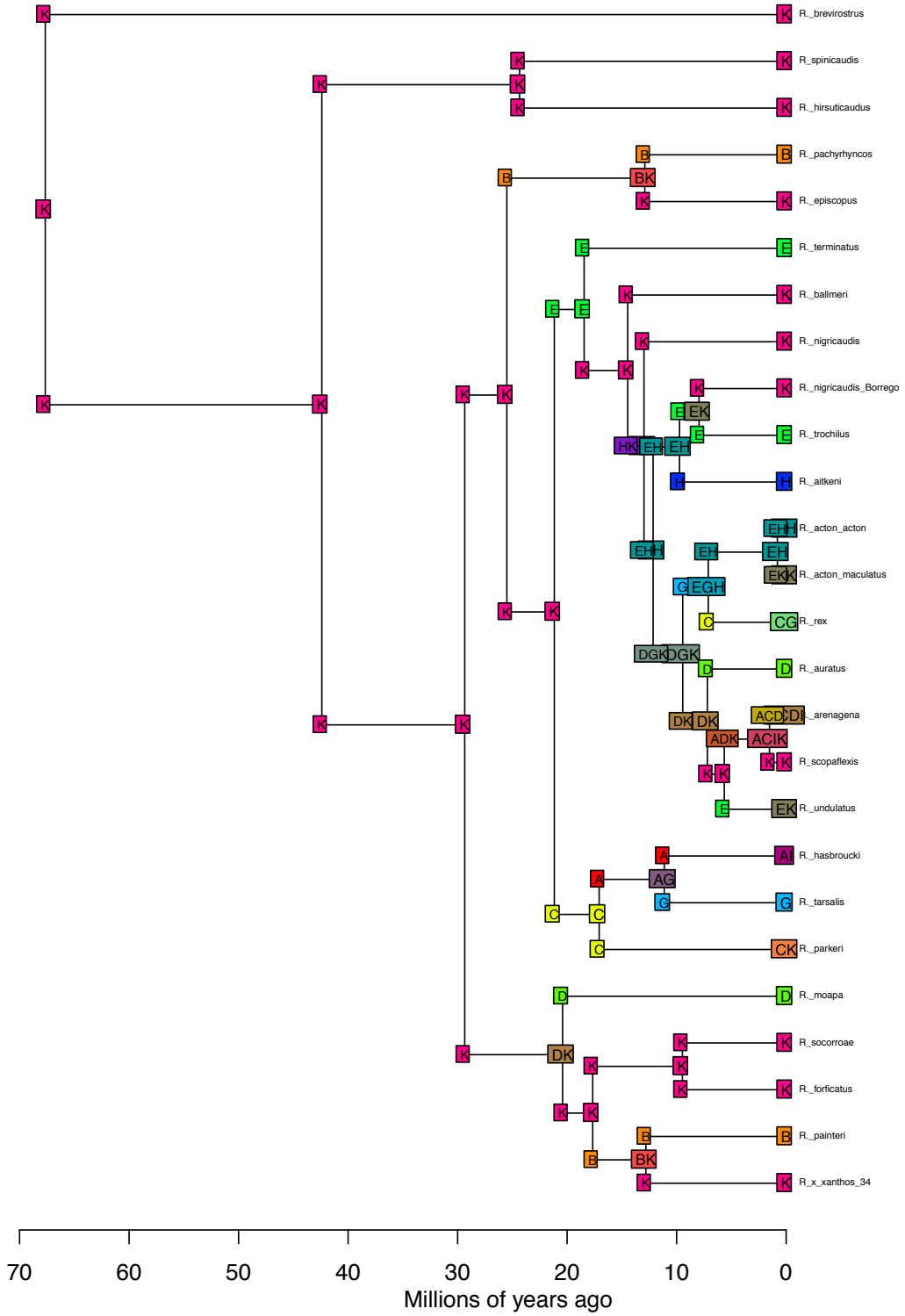

BioGeoBEARS DEC on Rhaphiomidas M4
anstates: global optim, 4 areas max. d=0.048; e=0.028; x=−0.342; j=0; LnL=−108.6

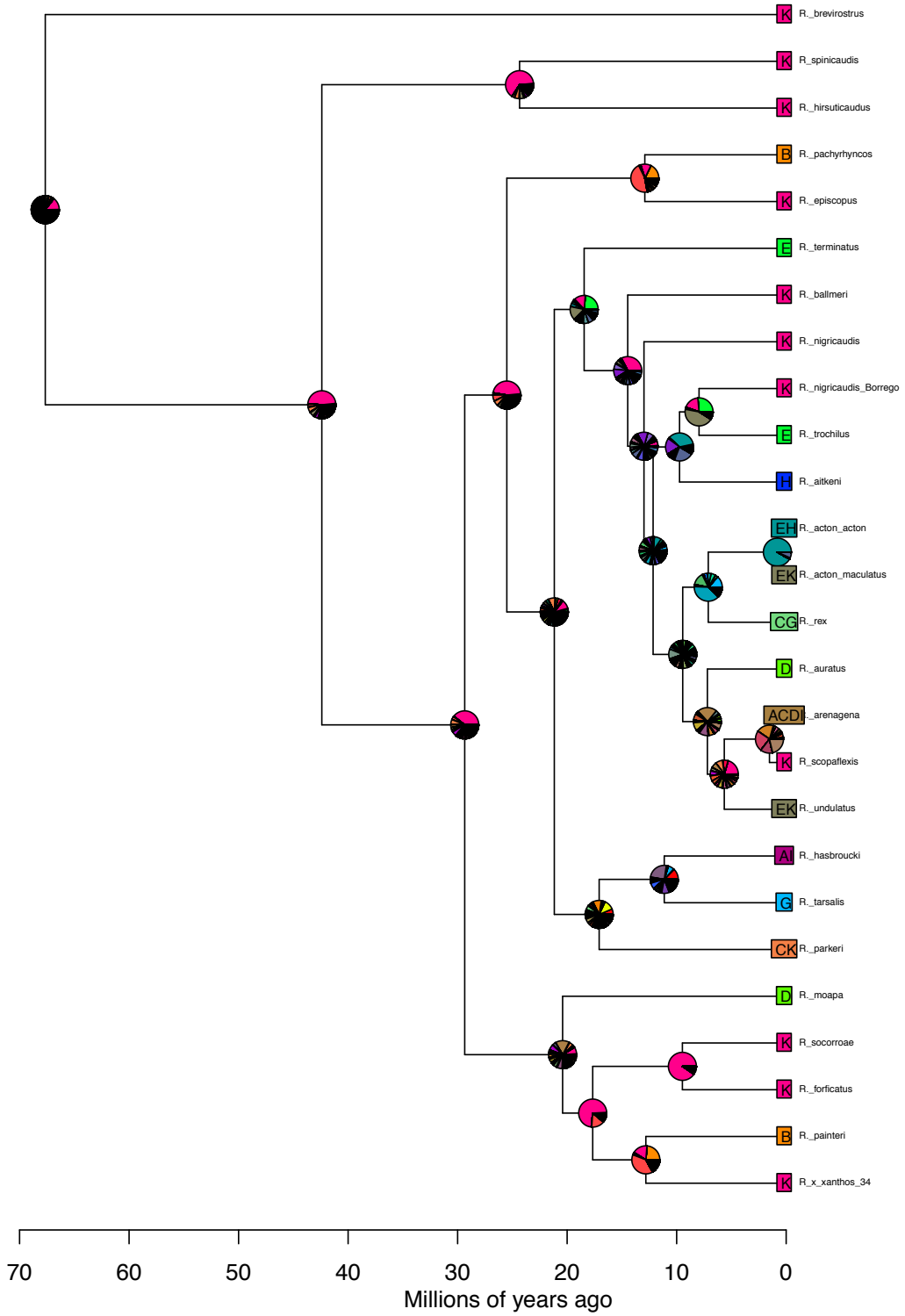

BioGeoBEARS DEC+J on Rhaphiomidas M4
anstates: global optim, 4 areas max. d=0.007; e=0.012; x=–0.103; j=0.514; LnL=–100.8

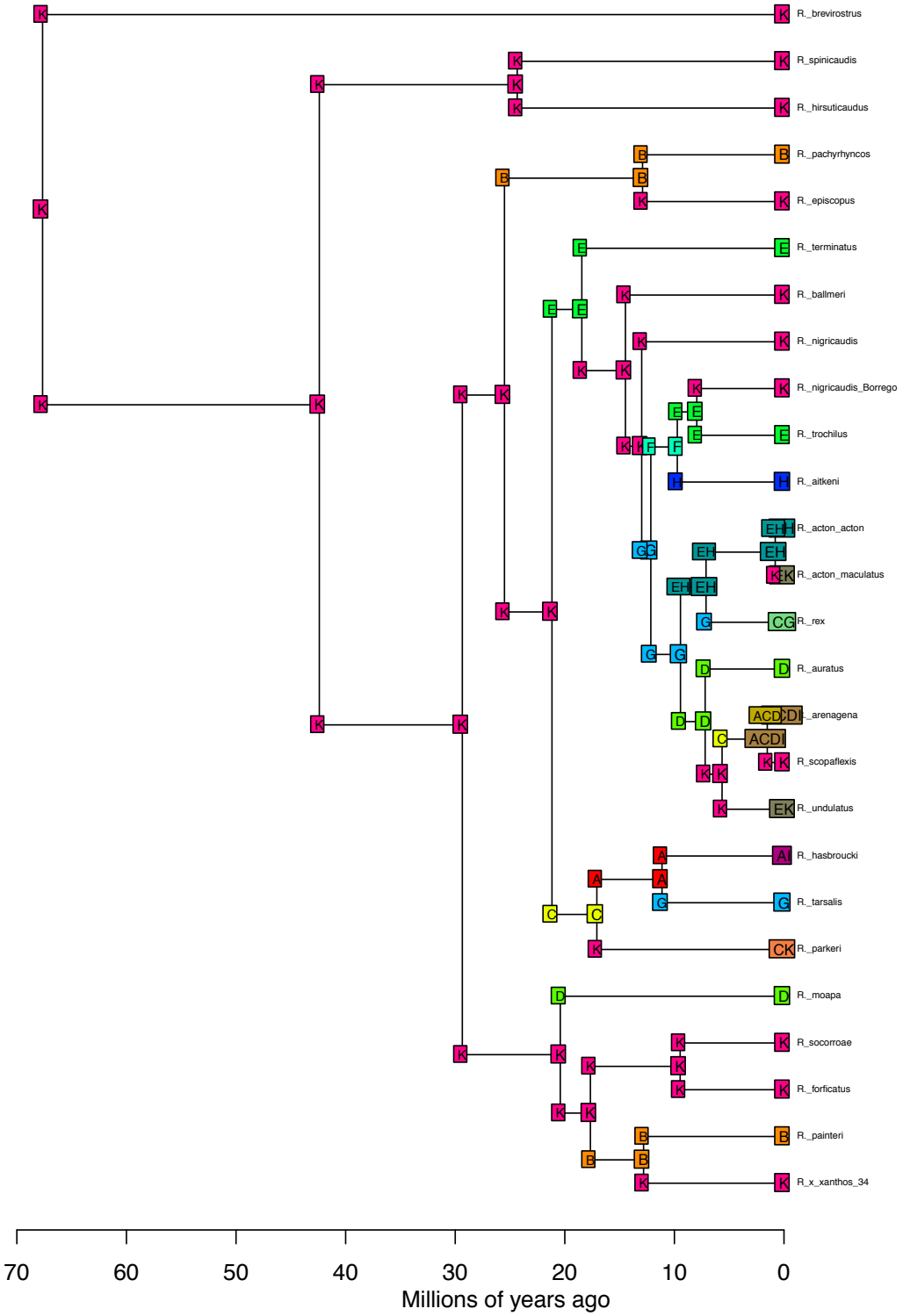

BioGeoBEARS DEC+J on Rhaphiomidas M4
anstates: global optim, 4 areas max. d=0.007; e=0.012; x=–0.103; j=0.514; LnL=–100.8

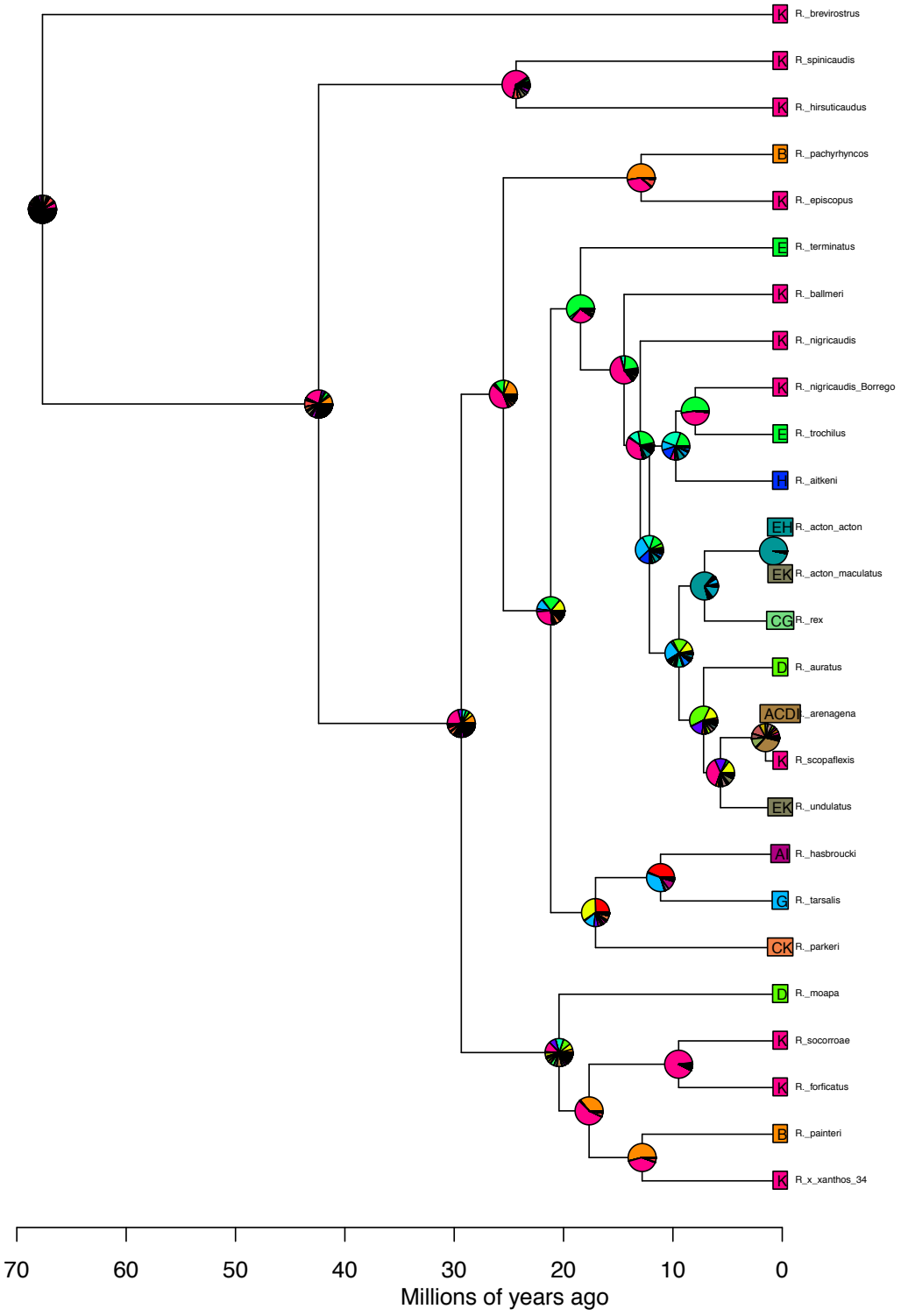

BioGeoBEARS DEC on sandtreaders M0_unconstrai
lobal optim, 4 areas max. d=0.003; e=0; x=−0.057; j=0.

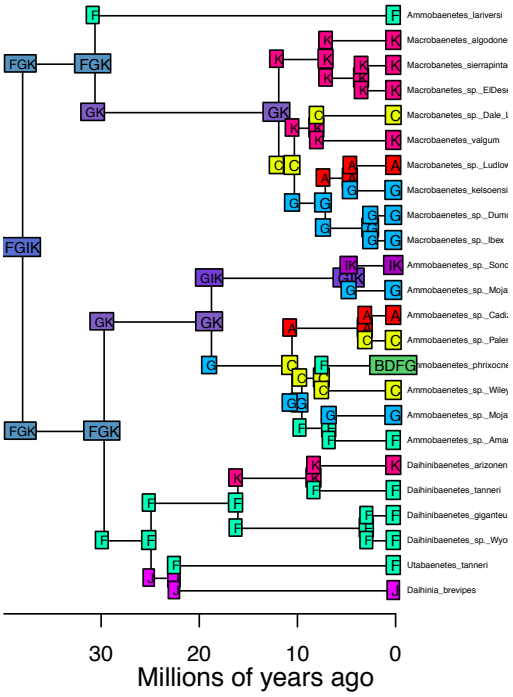

BioGeoBEARS DEC on sandtreaders M0_unconstrai
lobal optim, 4 areas max. d=0.003; e=0; x=−0.057; j=0.

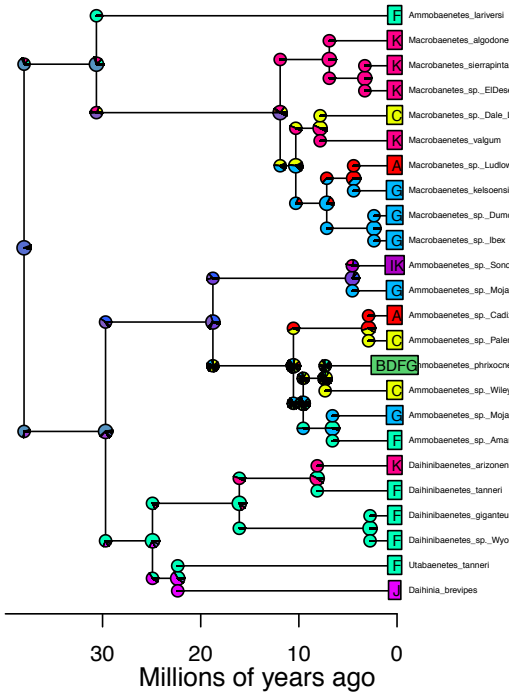

BioGeoBEARS DEC+J on sandtreaders M0_unconstra
tes: global optim, 4 areas max. d=0.001; e=0; j=0.066;

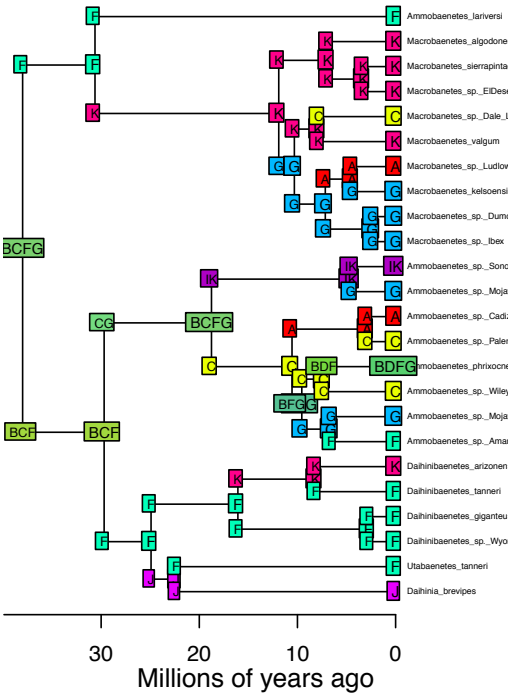

BioGeoBEARS DEC+J on sandtreaders M0_unconstra
tes: global optim, 4 areas max. d=0.001; e=0; j=0.066; l

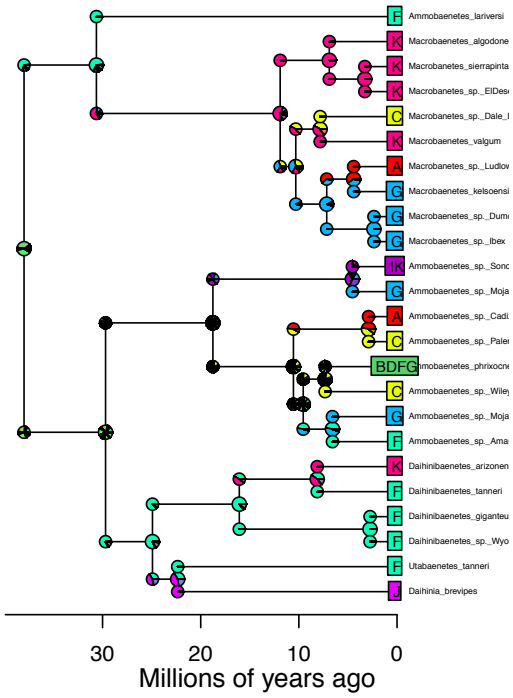

BioGeoBEARS DEC on sandtreaders M3_constraine
tes: global optim, 4 areas max. d=0.008; e=0.015; j=0;

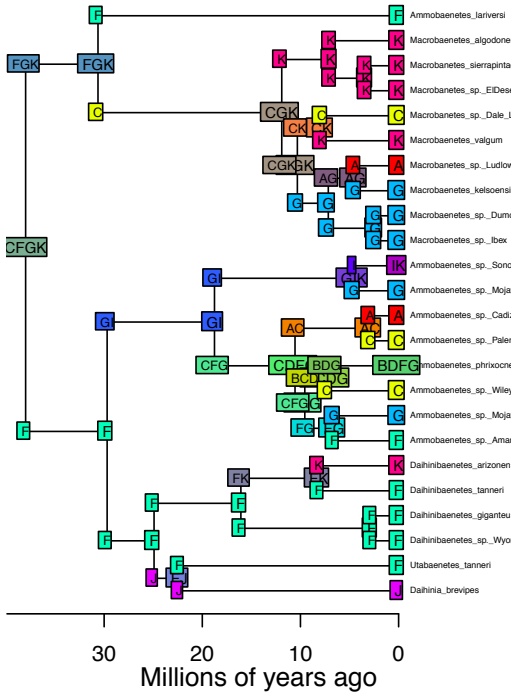

BioGeoBEARS DEC on sandtreaders M3_constraine
tes: global optim, 4 areas max. d=0.008; e=0.015; j=0; l

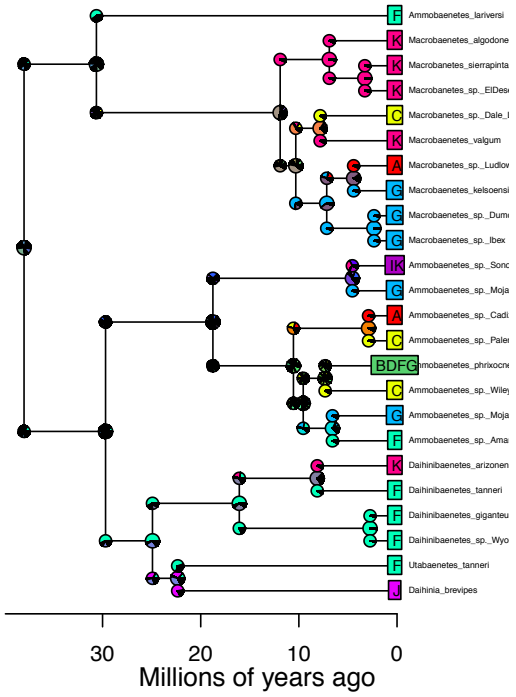

BioGeoBEARS DEC+J on sandtreaders M3_constrair
tes: global optim, 4 areas max. d=0.002; e=0; j=0.133;

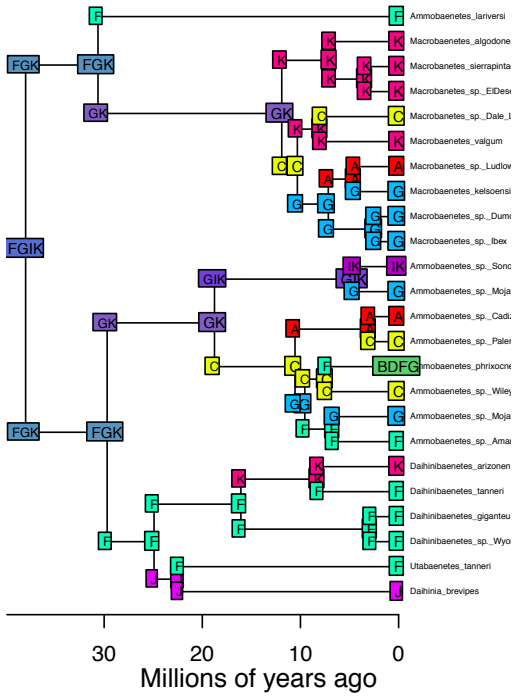

BioGeoBEARS DEC+J on sandtreaders M3_constrair
tes: global optim, 4 areas max. d=0.002; e=0; j=0.133; l

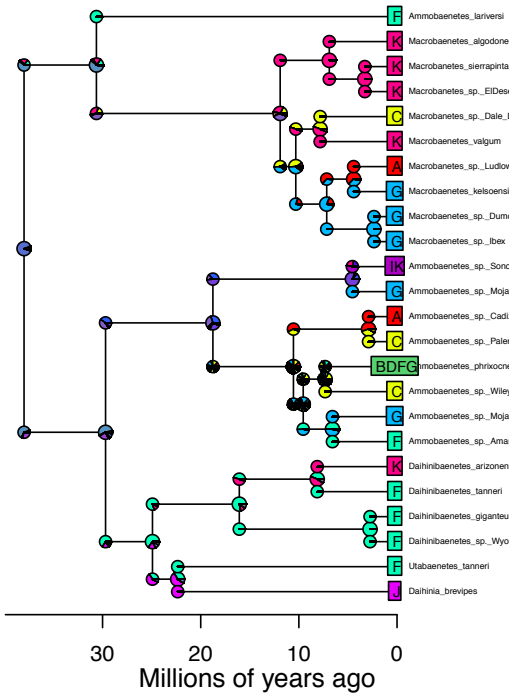

BioGeoBEARS DEC on sandtreaders M4_constrained
anstates: global optim, 4 areas max. d=0.008; e=0.015; x=0.011; j=0; LnL=−75.2

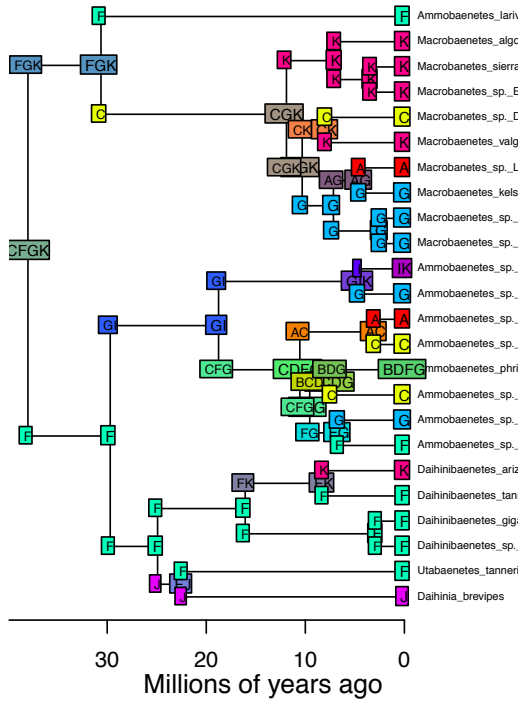

BioGeoBEARS DEC on sandtreaders M4_constrained
anstates: global optim, 4 areas max. d=0.008; e=0.015; x=0.011; j=0; LnL=−75.2

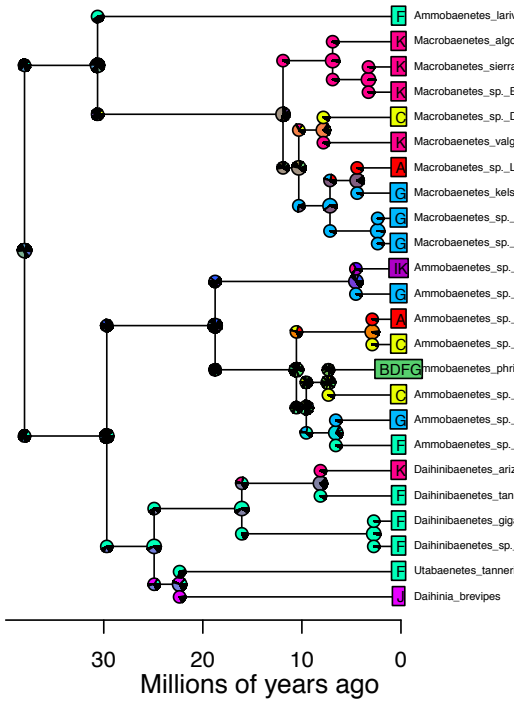

BioGeoBEARS DEC+J on sandtreaders M4_constrained
anstates: global optim, 4 areas max. d=0.003; e=0; x=−0.057; j=0.143; LnL=−63.1

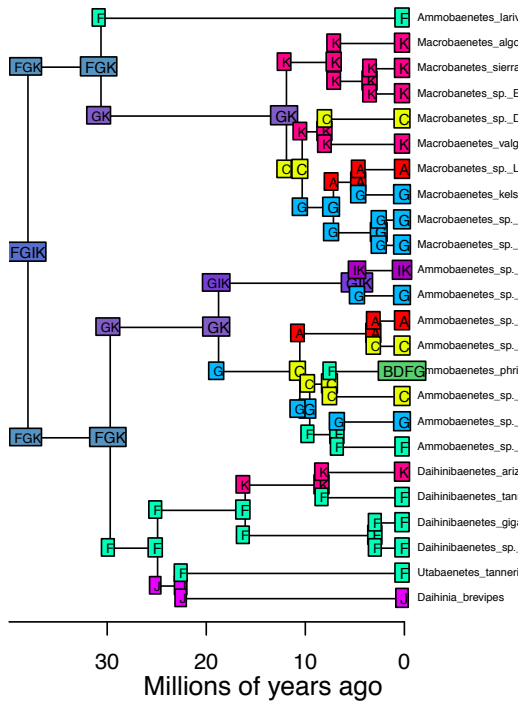

BioGeoBEARS DEC+J on sandtreaders M4_constrained
anstates: global optim, 4 areas max. d=0.003; e=0; x=−0.057; j=0.143; LnL=−63.1

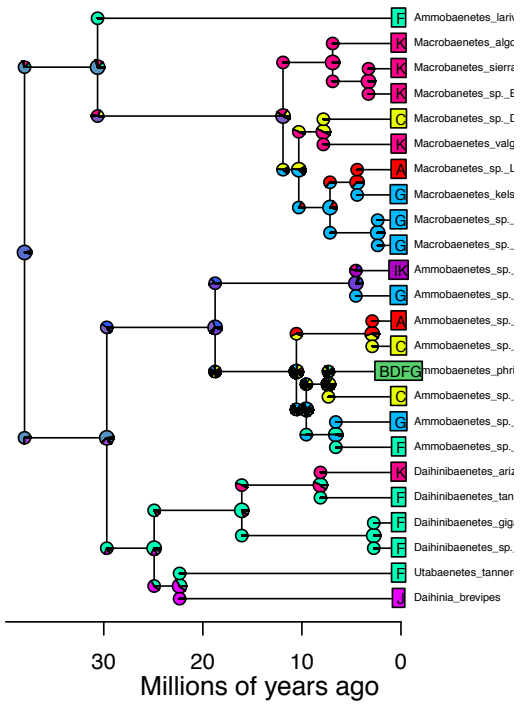

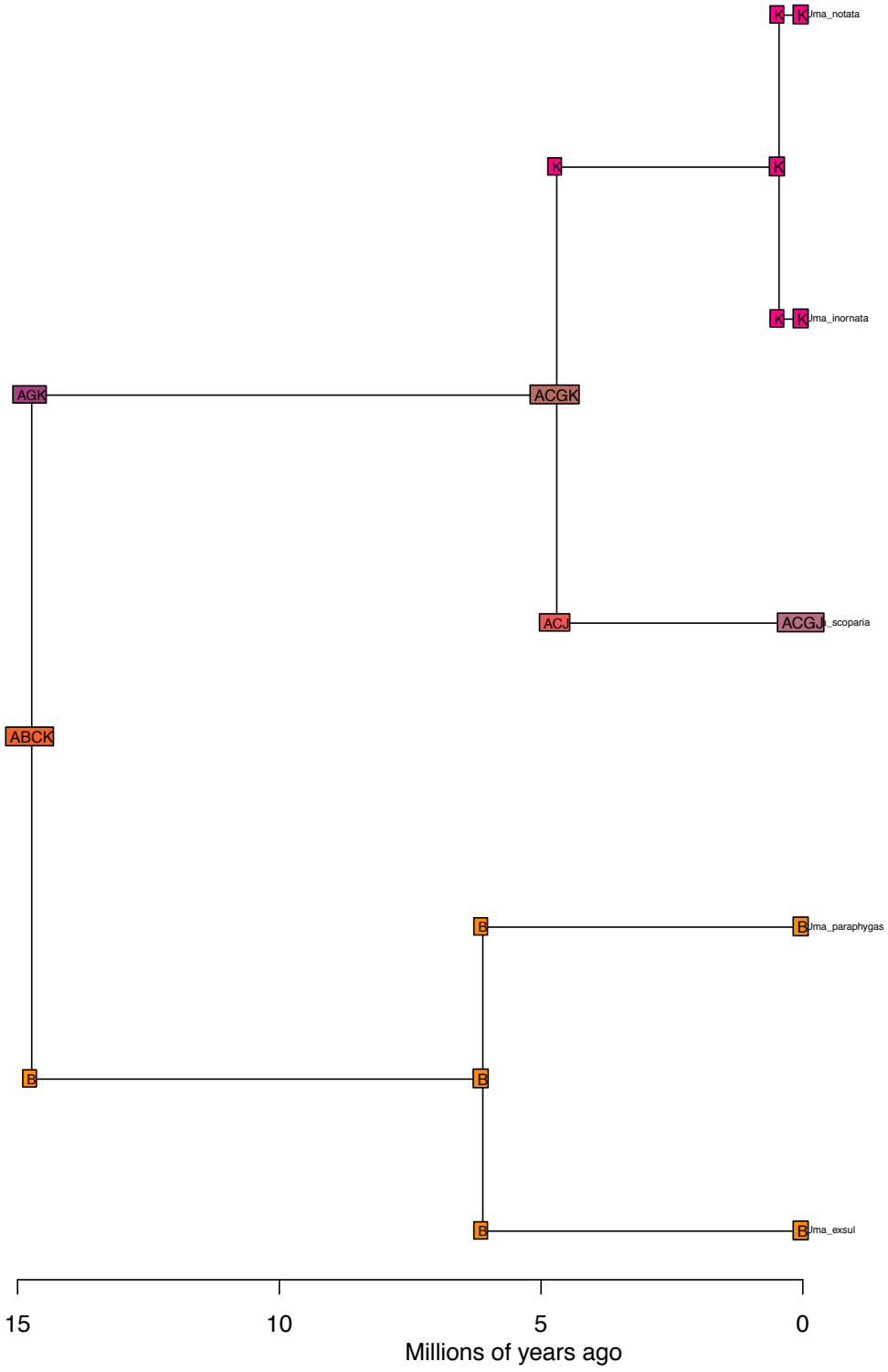
BioGeoBEARS DEC on Uma M0
anstates: global optim, 4 areas max. d=0.005; e=0; j=0; LnL=-9.2
K
K
Uma_notata
K
K
K
K
Uma_inornata
AGK
ACGK
ACJ
ACGJ
_scoparia
ABCK
B
B
Uma_paraphygas
B
B
B
Uma_exsul
15
10
5
0
Millions of years ago

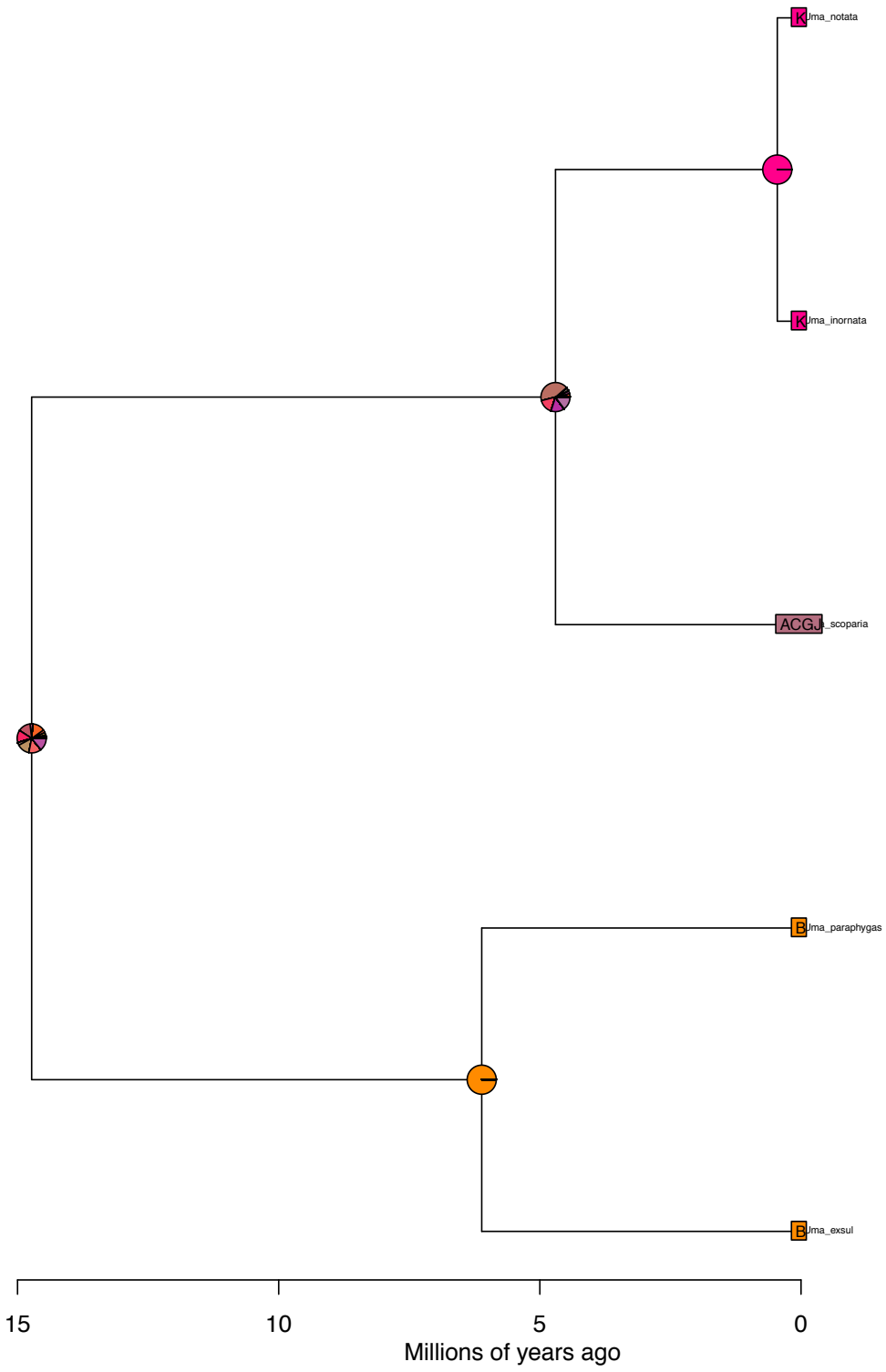
BioGeoBEARS DEC on Uma M0
anstates: global optim, 4 areas max. d=0.005; e=0; j=0; LnL=−9.2
Uma_notata
Uma_inornata
Uma_scoparia
Uma_paraphygas
Uma_exsul
15
10
5
0
Millions of years ago

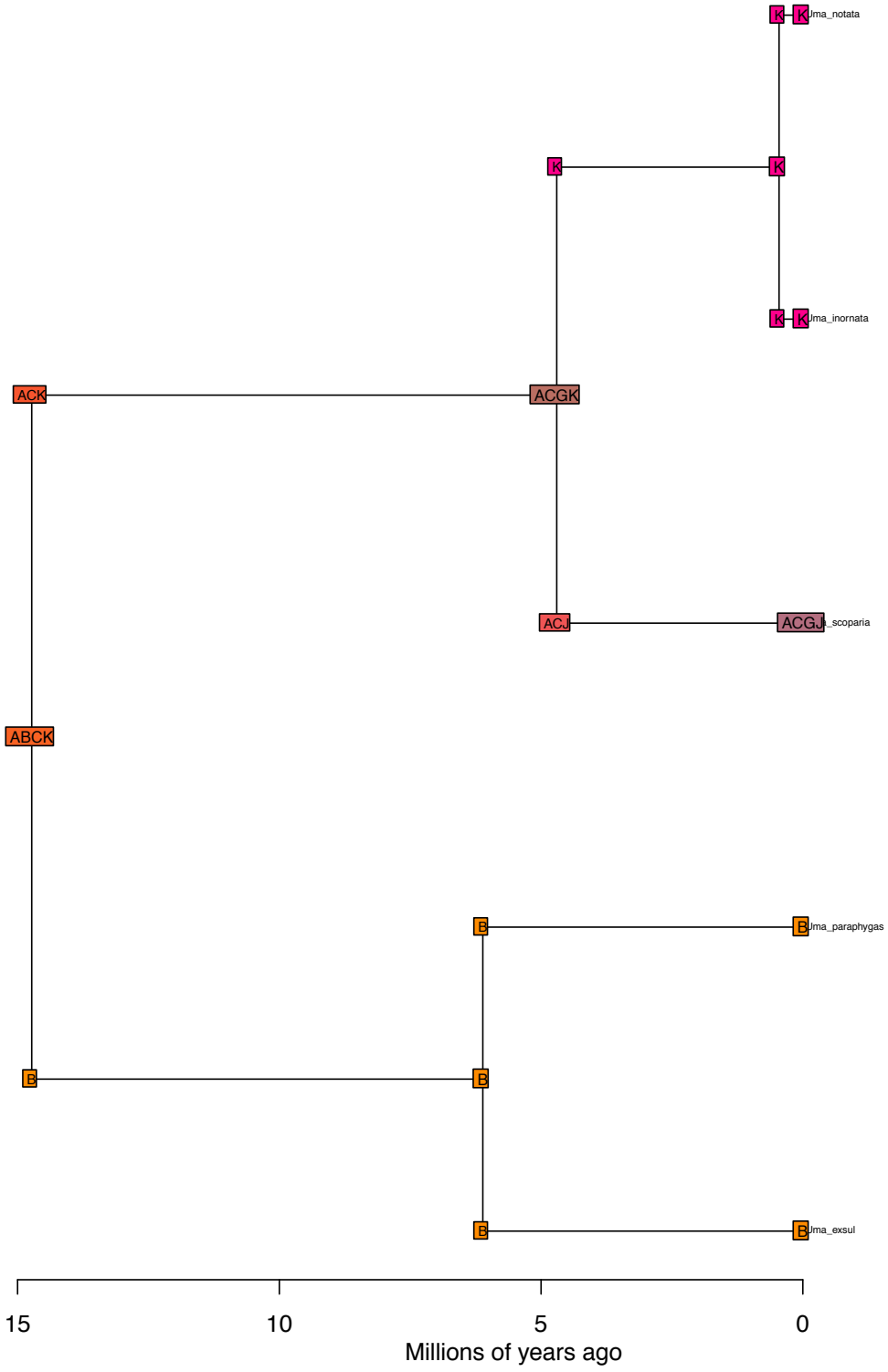
BioGeoBEARS DEC+J on Uma M0
anstates: global optim, 4 areas max. d=0.005; e=0; j=0; LnL=-9.2
K
K
Uma_notata
K
K
K
K
Uma_inornata
ACK
ACGK
ACJ
ACGJ
_scoparia
ABCK
B
B
Uma_paraphygas
B
B
Uma_exsul
15
10
5
0
Millions of years ago

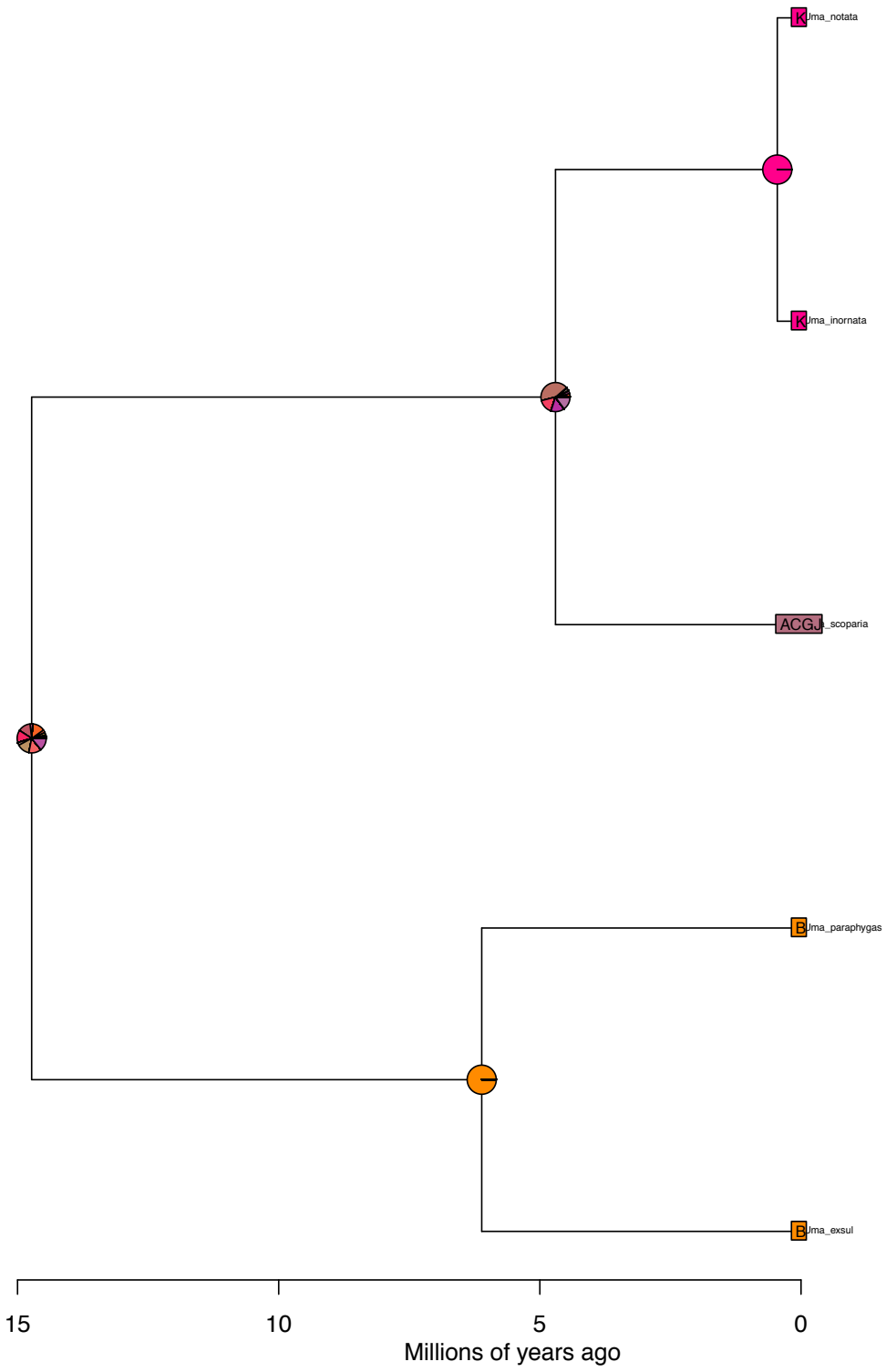
BioGeoBEARS DEC+J on Uma M0
anstates: global optim, 4 areas max. d=0.005; e=0; j=0; LnL=-9.2
K
Uma_notata
K
Uma_inornata
ACGJ
_scoparia
B
Uma_paraphygas
B
Uma_exsul
15
10
5
0
Millions of years ago

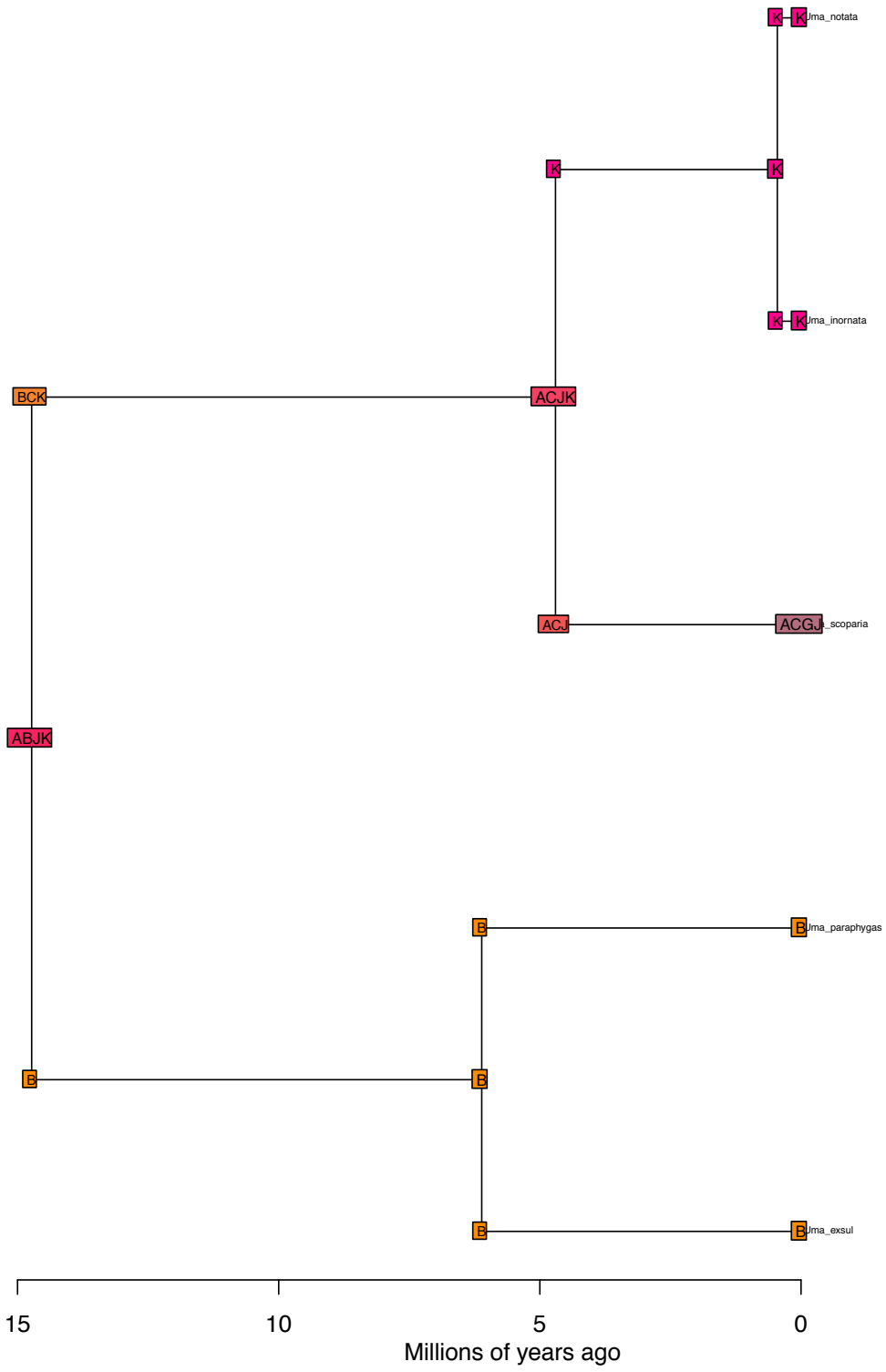
BioGeoBEARS DEC_constrained on Uma M3
anstates: global optim, 4 areas max. d=0.013; e=0; j=0; LnL=-9.3
K
K
Uma_notata
K
K
K
K
Uma_inornata
BCK
ACJK
ACJ
ACGJ
_scoparia
ABJK
B
B
Uma_paraphygas
B
B
B
B
Uma_exsul
15
10
5
0
Millions of years ago

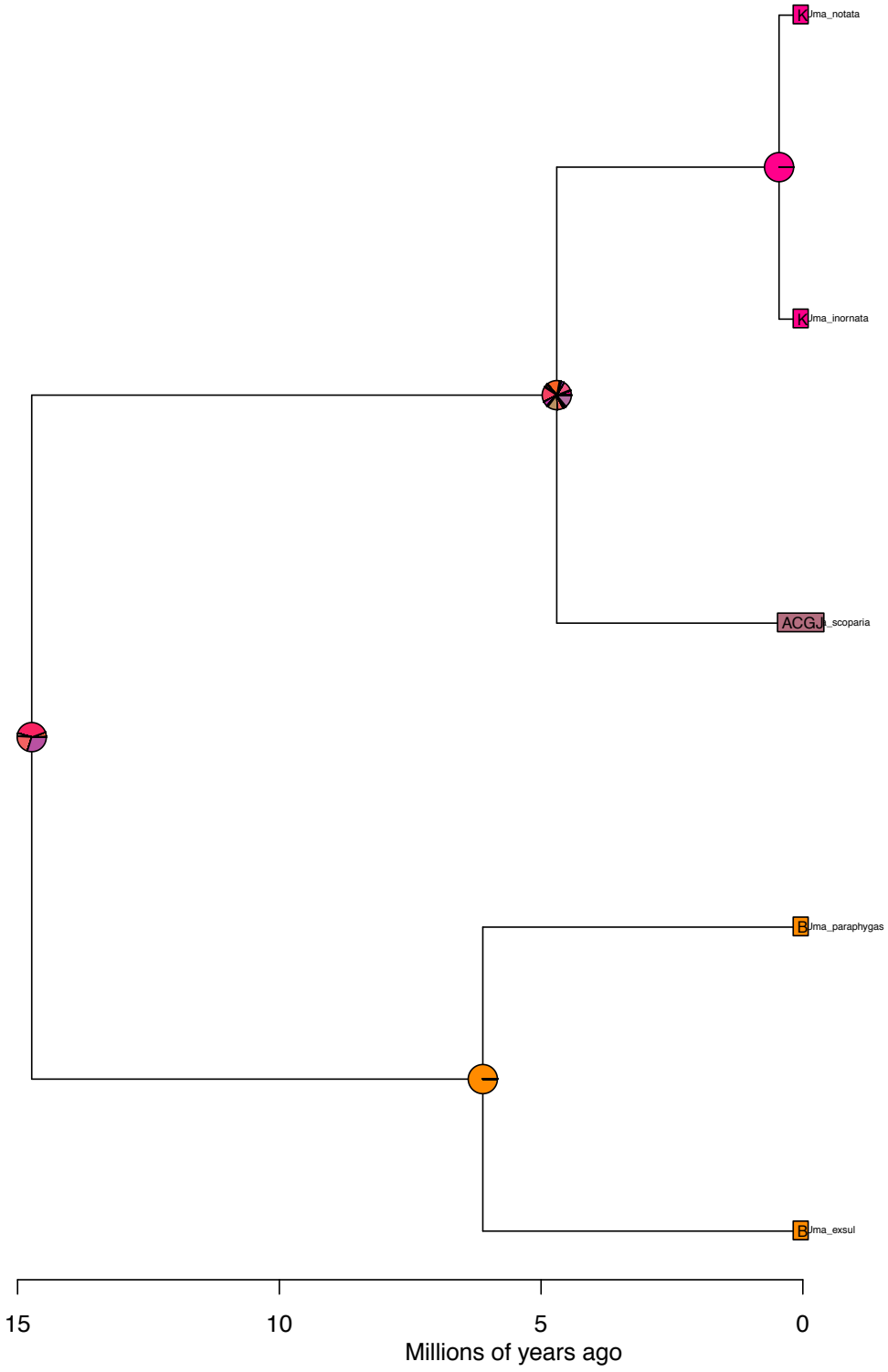
BioGeoBEARS DEC_constrained on Uma M3
anstates: global optim, 4 areas max. d=0.013; e=0; j=0; LnL=-9.3
Kuma_notata
Kuma_inornata
ACGJa_scoparia
Buma_paraphygas
Buma_exsul
15
10
5
0
Millions of years ago

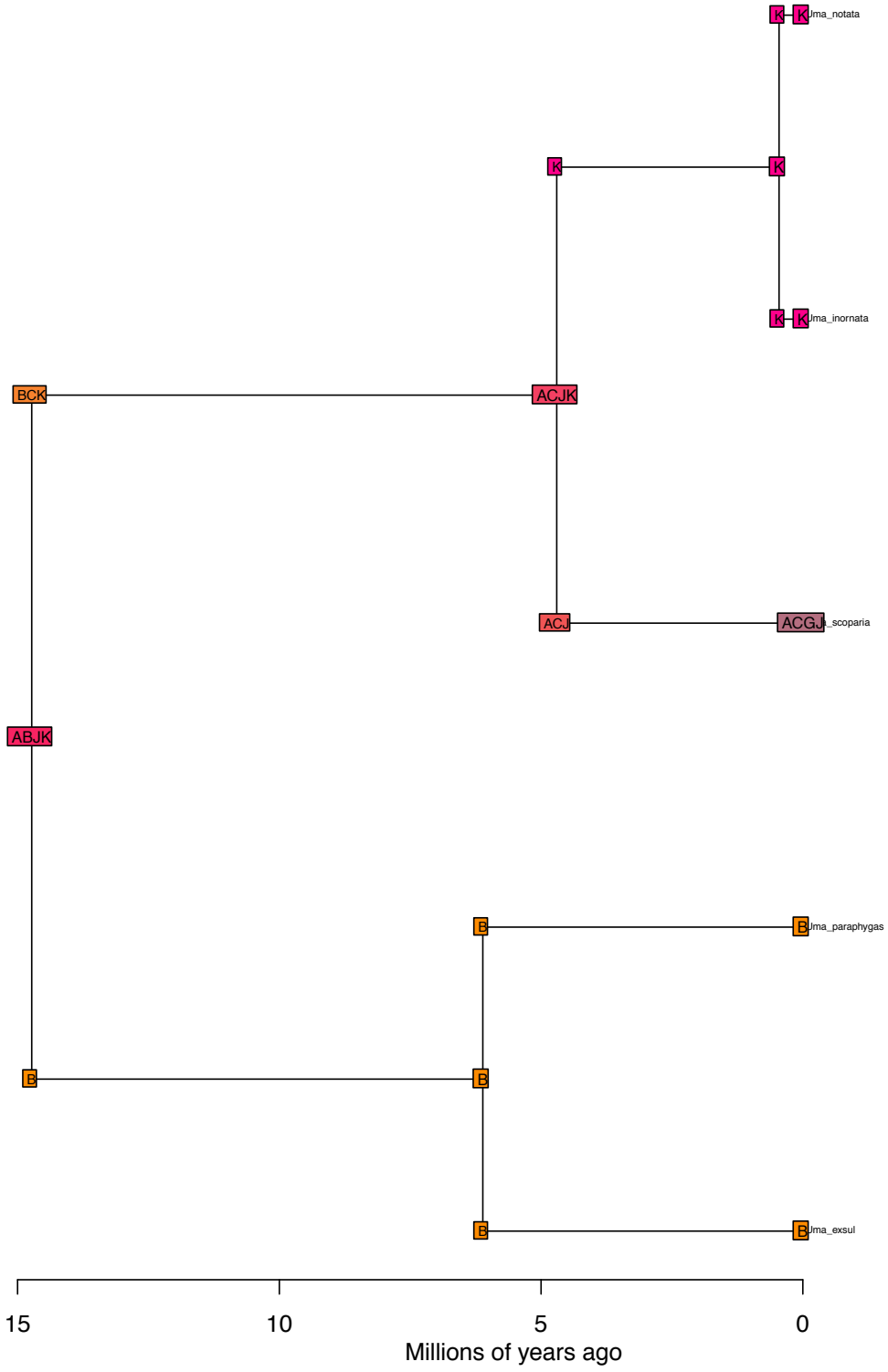
BioGeoBEARS DEC+J_constrained on Uma M3
anstates: global optim, 4 areas max. d=0.013; e=0; j=0; LnL=-9.3
K
K
Uma_notata
K
K
K
K
Uma_inornata
BCK
ACJK
ACJ
ACGJ
_scoparia
ABJK
B
B
Uma_paraphygas
B
B
B
B
Uma_exsul
15
10
5
0
Millions of years ago

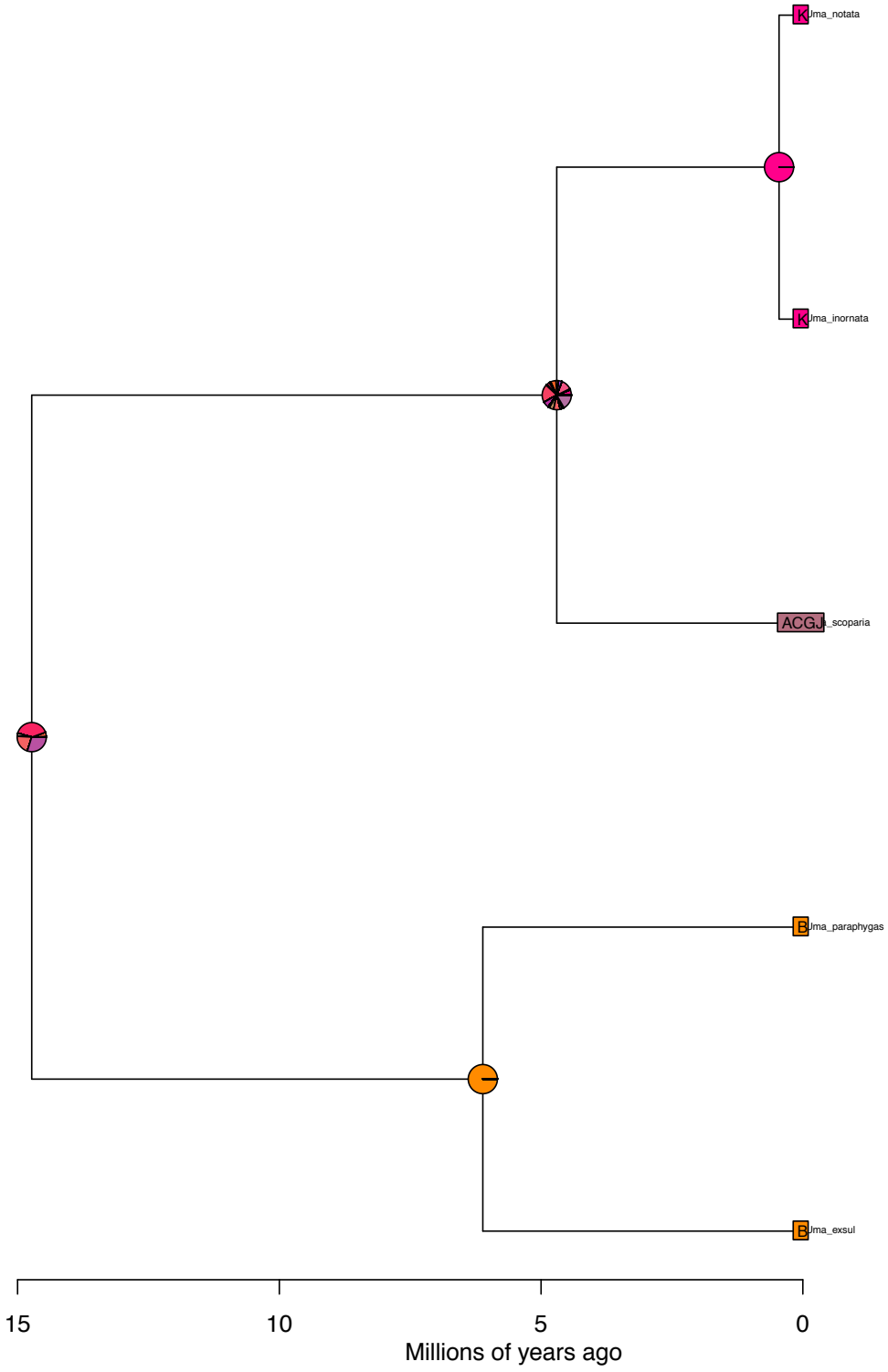
BioGeoBEARS DEC+J_constrained on Uma M3
anstates: global optim, 4 areas max. d=0.013; e=0; j=0; LnL=-9.3
Kuma_notata
Kuma_inornata
ACGJuma_scoparia
Buma_paraphygas
Buma_exsul
15
10
5
0
Millions of years ago

BioGeoBEARS DEC_distances on Uma M4
anstates: global optim, 4 areas max. d=0.452; e=0; x=–0.901; j=0; LnL=–8.1

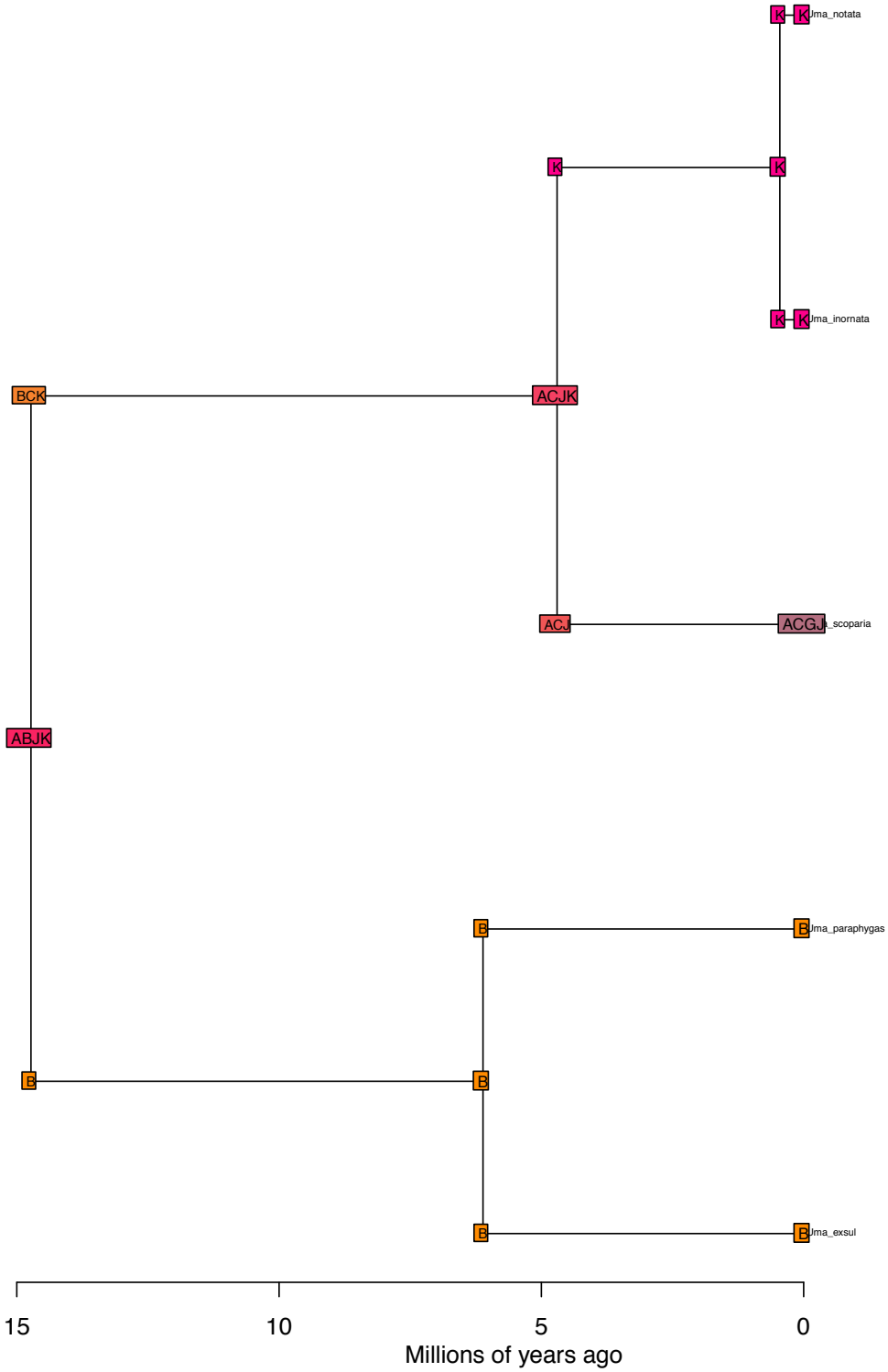

BioGeoBEARS DEC_distances on Uma M4
anstates: global optim, 4 areas max. d=0.452; e=0; x=–0.901; j=0; LnL=–8.1

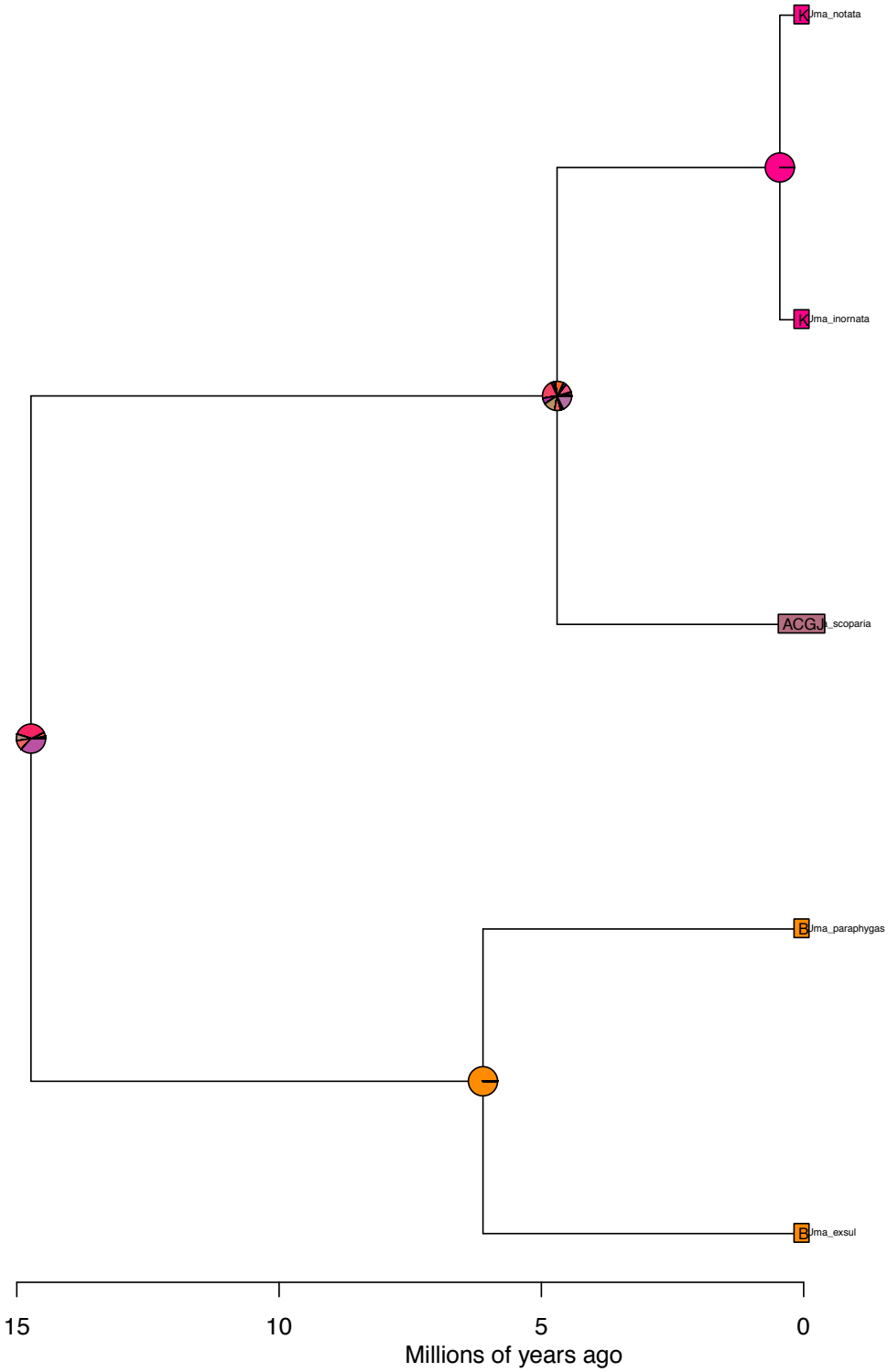

BioGeoBEARS DEC+J_distances on Uma M4
anstates: global optim, 4 areas max. d=0.013; e=0; x=0.003; j=0; LnL=–9.3

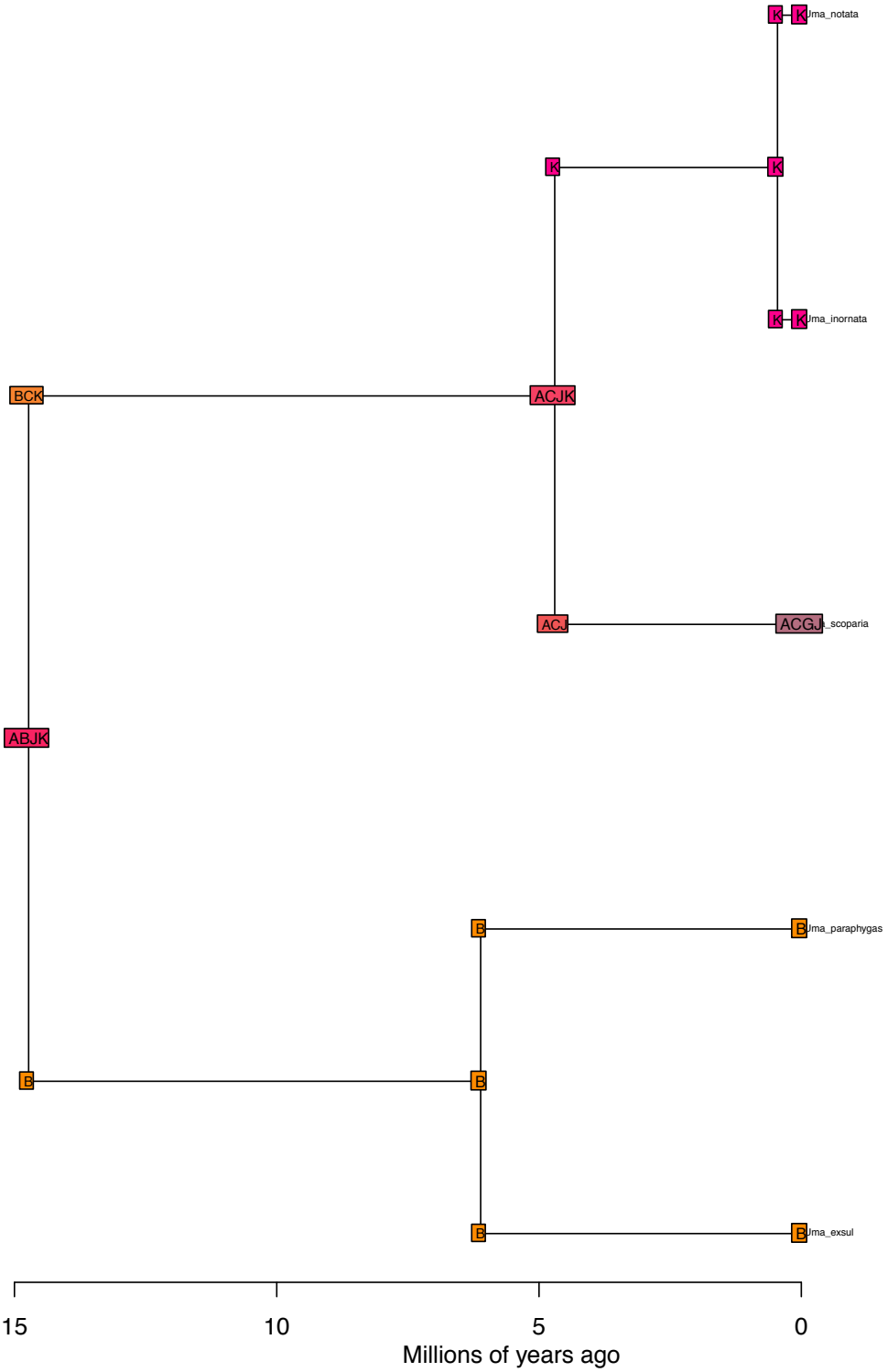

BioGeoBEARS DEC+J_distances on Uma M4
anstates: global optim, 4 areas max. d=0.013; e=0; x=0.003; j=0; LnL=–9.3

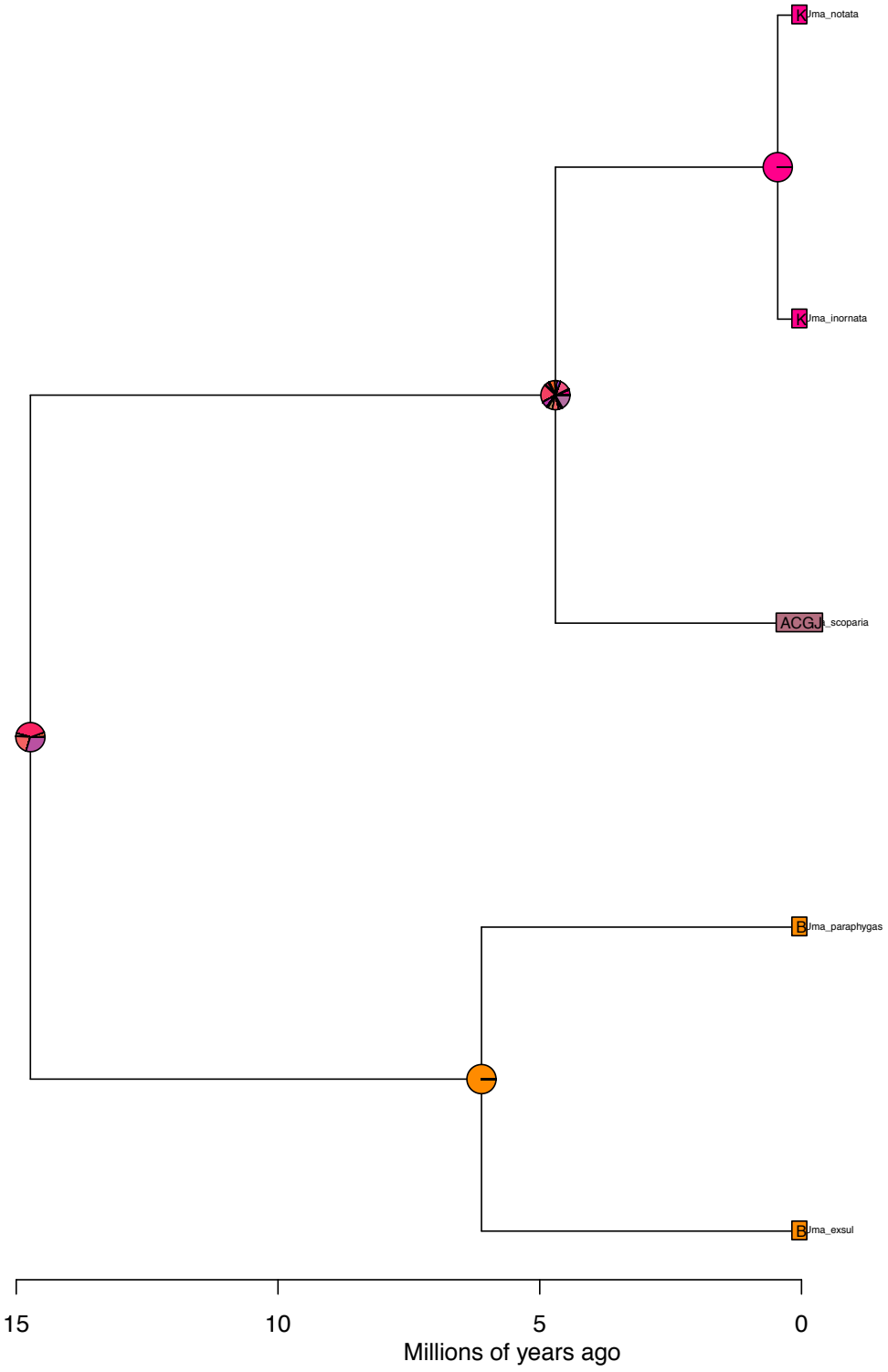

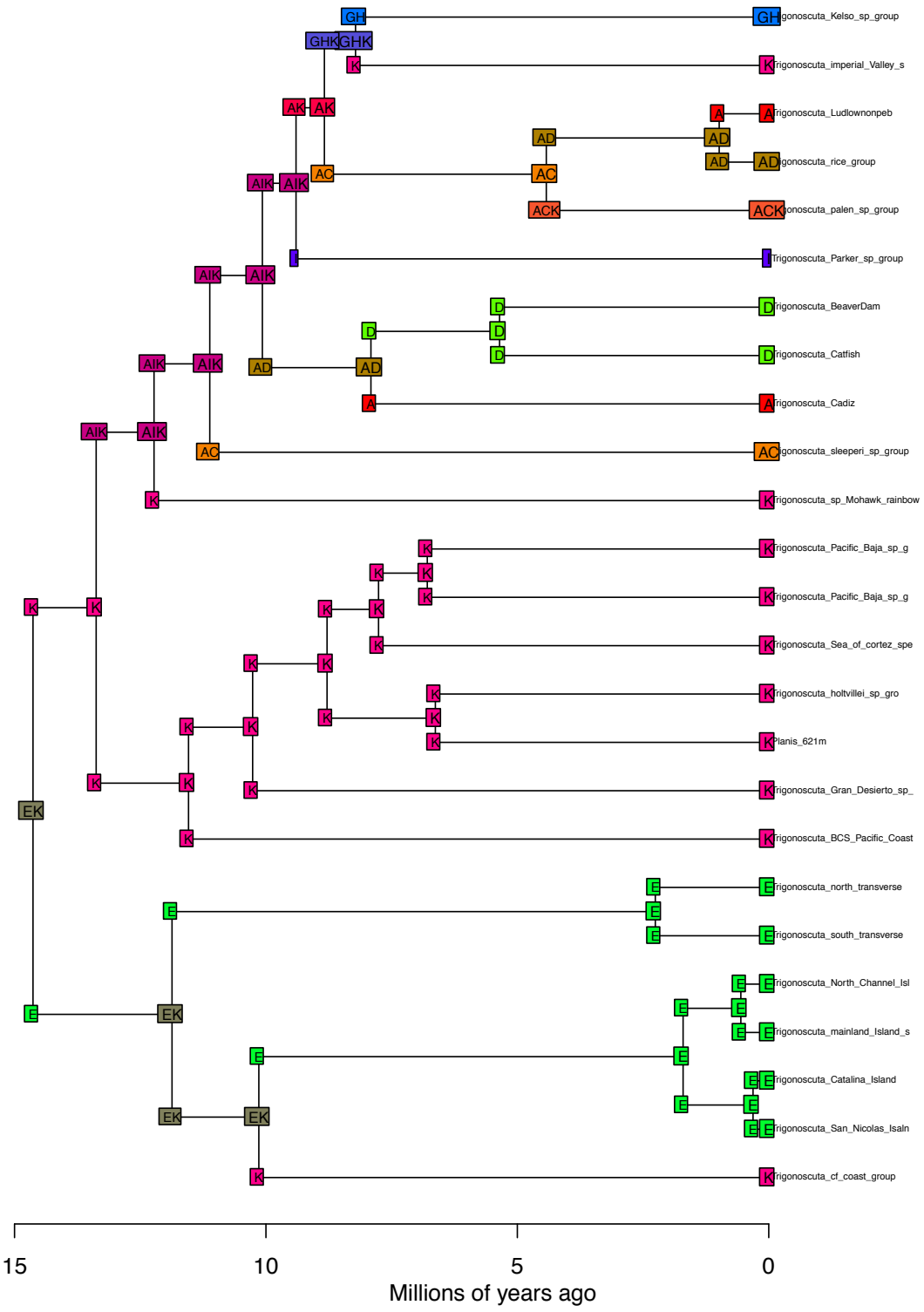
BioGeoBEARS DEC on Trigonoscuta M0
anstates: global optim, 4 areas max. d=0.004; e=0.008; j=0; LnL=–59
Trigonoscuta_Kelso_sp_group
Trigonoscuta_imperial_Valley_s
Trigonoscuta_Ludlownonpeb
Trigonoscuta_rice_group
Trigonoscuta_palen_sp_group
Trigonoscuta_Parker_sp_group
Trigonoscuta_BeaverDam
Trigonoscuta_Catfish
Trigonoscuta_Cadiz
Trigonoscuta_sleeperi_sp_group
Trigonoscuta_sp_Mohawk_rainbow
Trigonoscuta_Pacific_Baja_sp_g
Trigonoscuta_Pacific_Baja_sp_g
Trigonoscuta_Sea_of_cortez_spe
Trigonoscuta_holtvillei_sp_gro
Planis_621m
Trigonoscuta_Gran_Desierto_sp_
Trigonoscuta_BCS_Pacific_Coast
Trigonoscuta_north_transverse
Trigonoscuta_south_transverse
Trigonoscuta_North_Channel_Isl
Trigonoscuta_mainland_Island_s
Trigonoscuta_Catalina_Island
Trigonoscuta_San_Nicolas_Isaln
Trigonoscuta_cf_coast_group
15
10
5
0
Millions of years ago

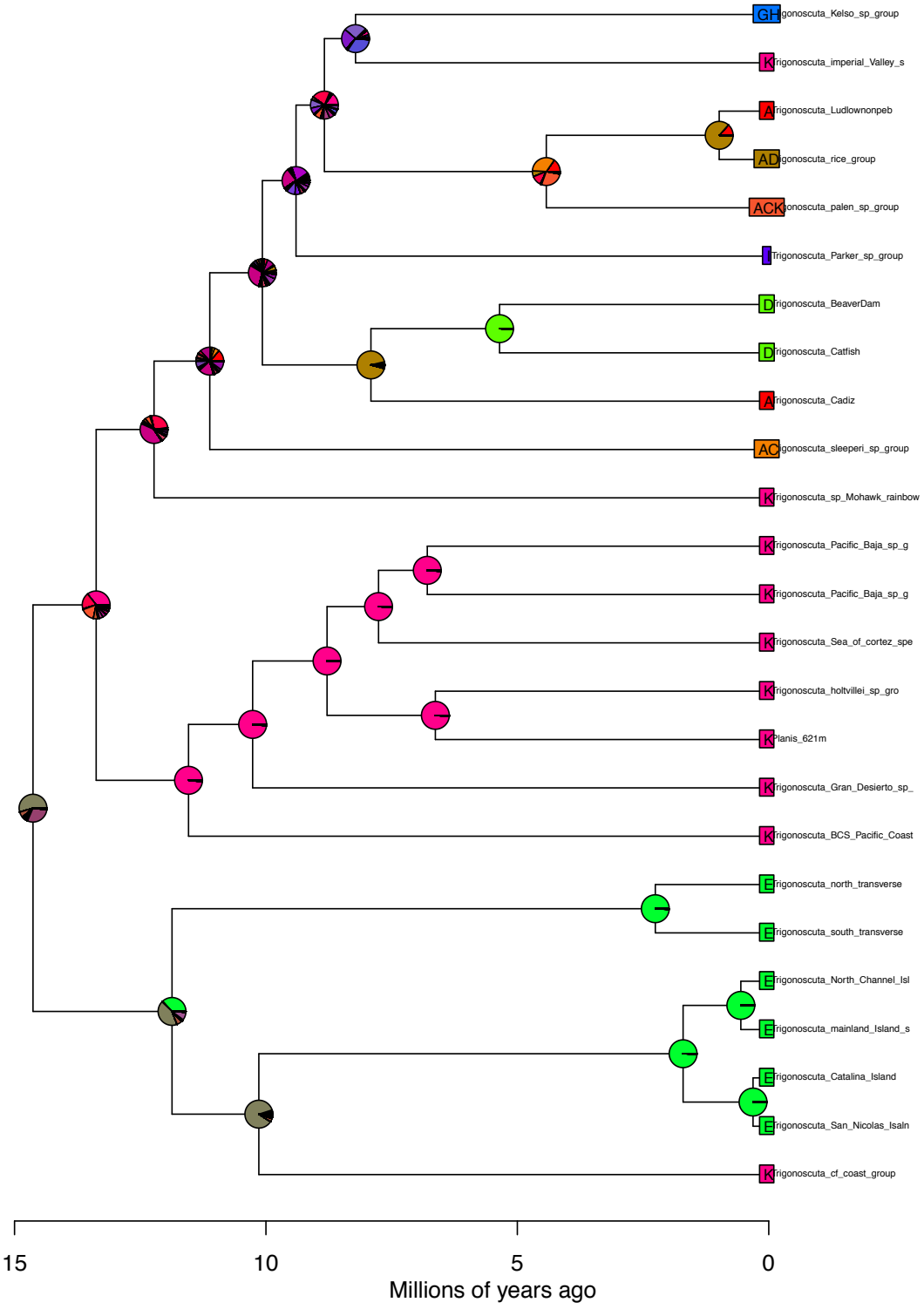
BioGeoBEARS DEC on Trigonoscuta M0
anstates: global optim, 4 areas max. d=0.004; e=0.008; j=0; LnL=–59
GHrigonoscuta_Kelso_sp_group
Krigonoscuta_imperial_Valley_s
Arigonoscuta_Ludlownonpeb
ADigonoscuta_rice_group
ACKonoscuta_palen_sp_group
Trigonoscuta_Parker_sp_group
Drigonoscuta_BeaverDam
Drigonoscuta_Catfish
Arigonoscuta_Cadiz
ACgonoscuta_sleeperi_sp_group
Krigonoscuta_sp_Mohawk_rainbow
Krigonoscuta_Pacific_Baja_sp_g
Krigonoscuta_Pacific_Baja_sp_g
Krigonoscuta_Sea_of_cortez_spe
Krigonoscuta_holtvillei_sp_gro
Kplanis_621m
Krigonoscuta_Gran_Desierto_sp_
Krigonoscuta_BCS_Pacific_Coast
Erigonoscuta_north_transverse
Erigonoscuta_south_transverse
Erigonoscuta_North_Channel_Isl
Erigonoscuta_mainland_Island_s
Erigonoscuta_Catalina_Island
Erigonoscuta_San_Nicolas_Isaln
Krigonoscuta_cf_coast_group
15
10
5
0
Millions of years ago

BioGeoBEARS DEC+J on Trigonoscuta M0
anstates: global optim, 4 areas max. d=0.002; e=0; j=0.015; LnL=–54.1

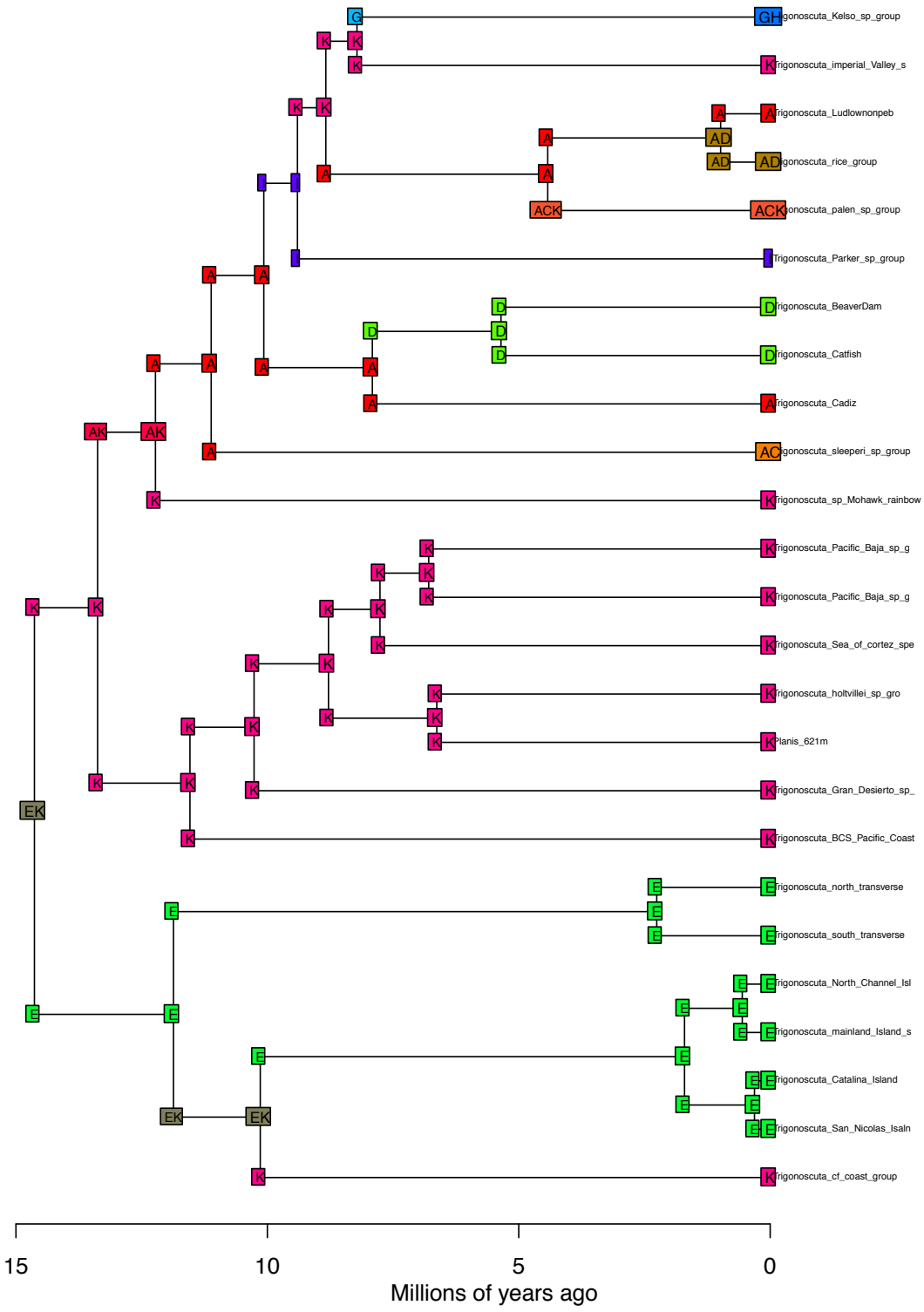

BioGeoBEARS DEC+J on Trigonoscuta M0
anstates: global optim, 4 areas max. d=0.002; e=0; j=0.015; lnL=–54.1

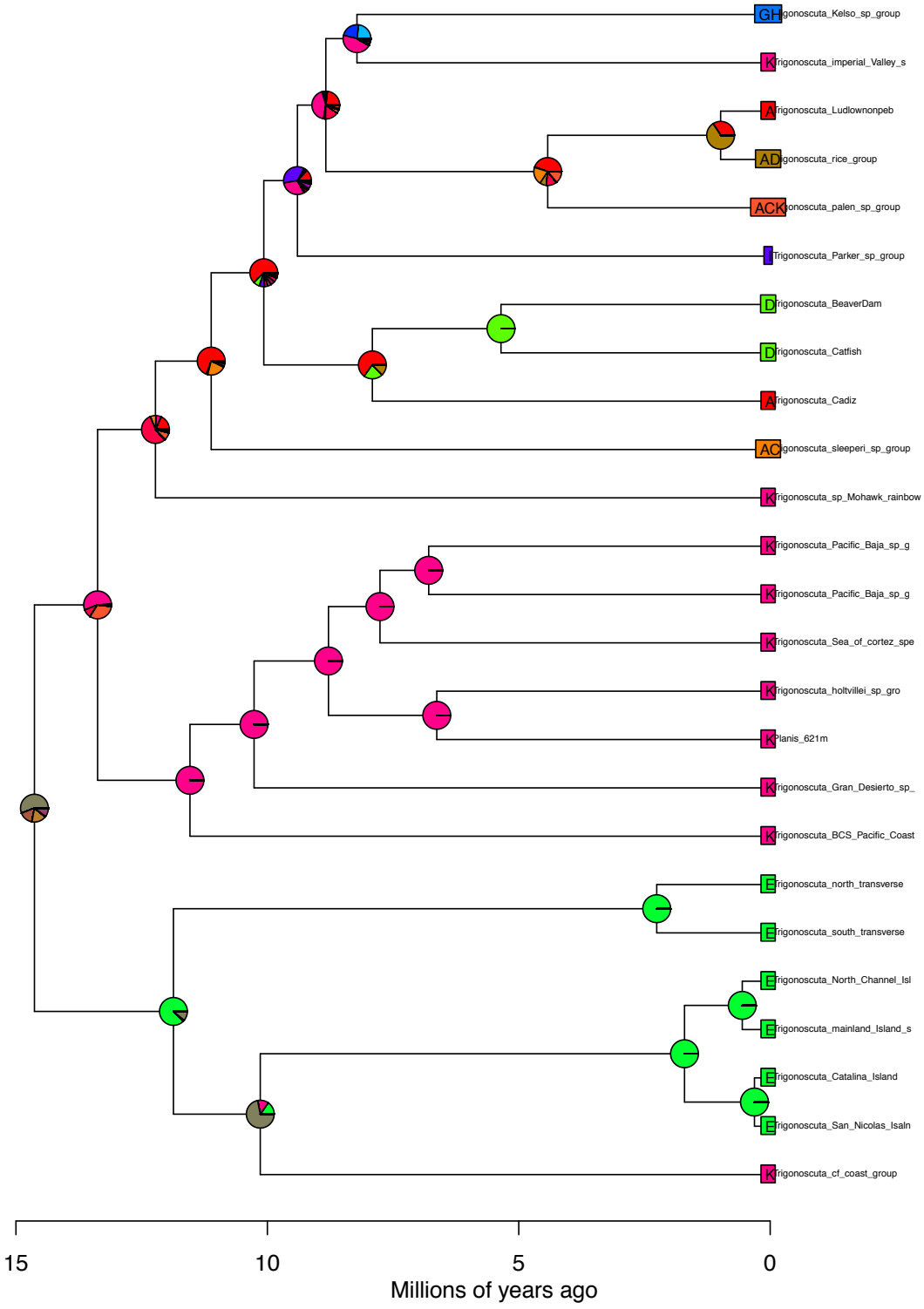

BioGeoBEARS DEC on Trigonoscuta M4
anstates: global optim, 4 areas max. d=0.026; e=0; x=–0.317; j=0; LnL=–54.9

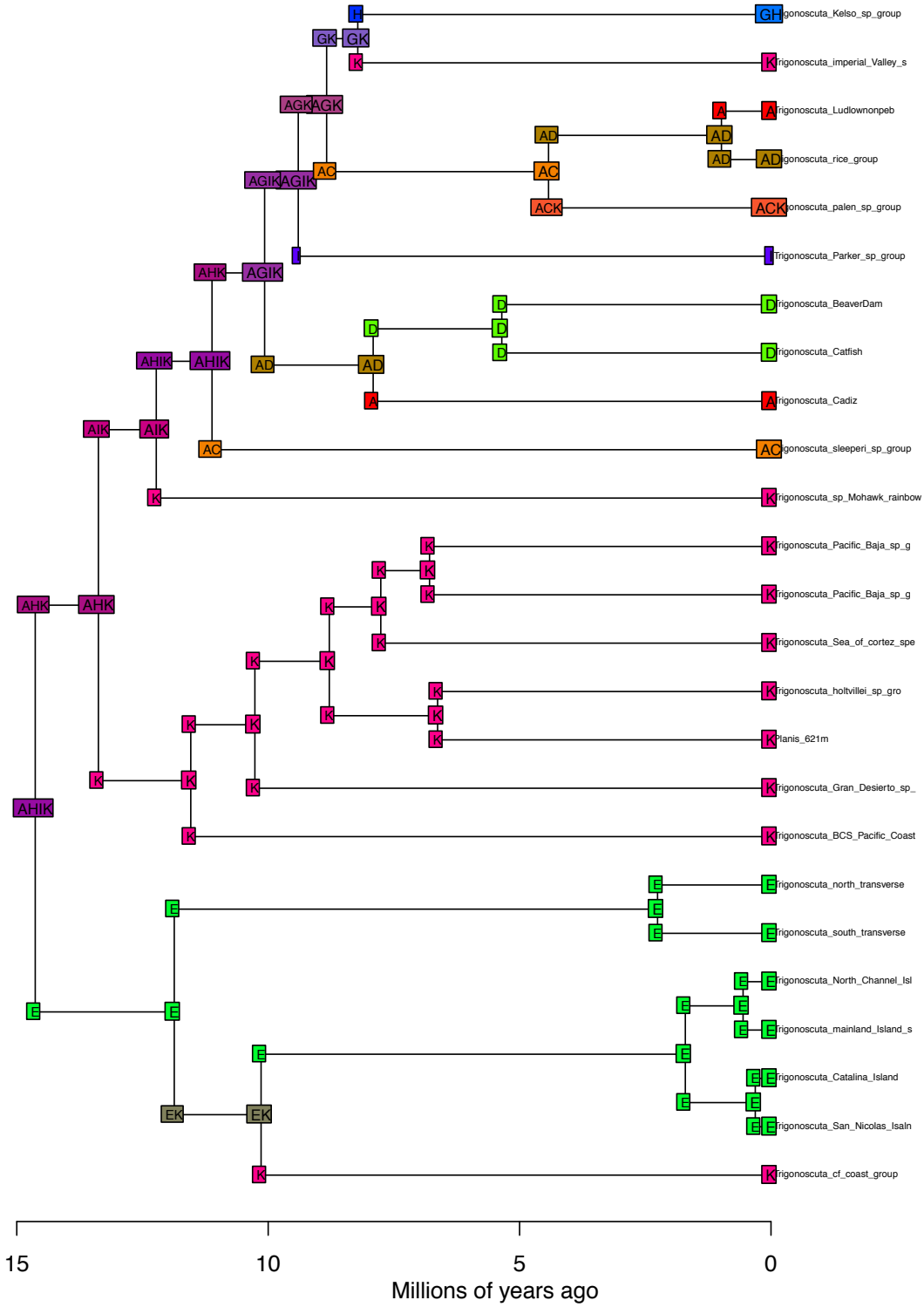

BioGeoBEARS DEC on Trigonoscuta M4
anstates: global optim, 4 areas max. d=0.026; e=0; x=–0.317; j=0; LnL=–54.9

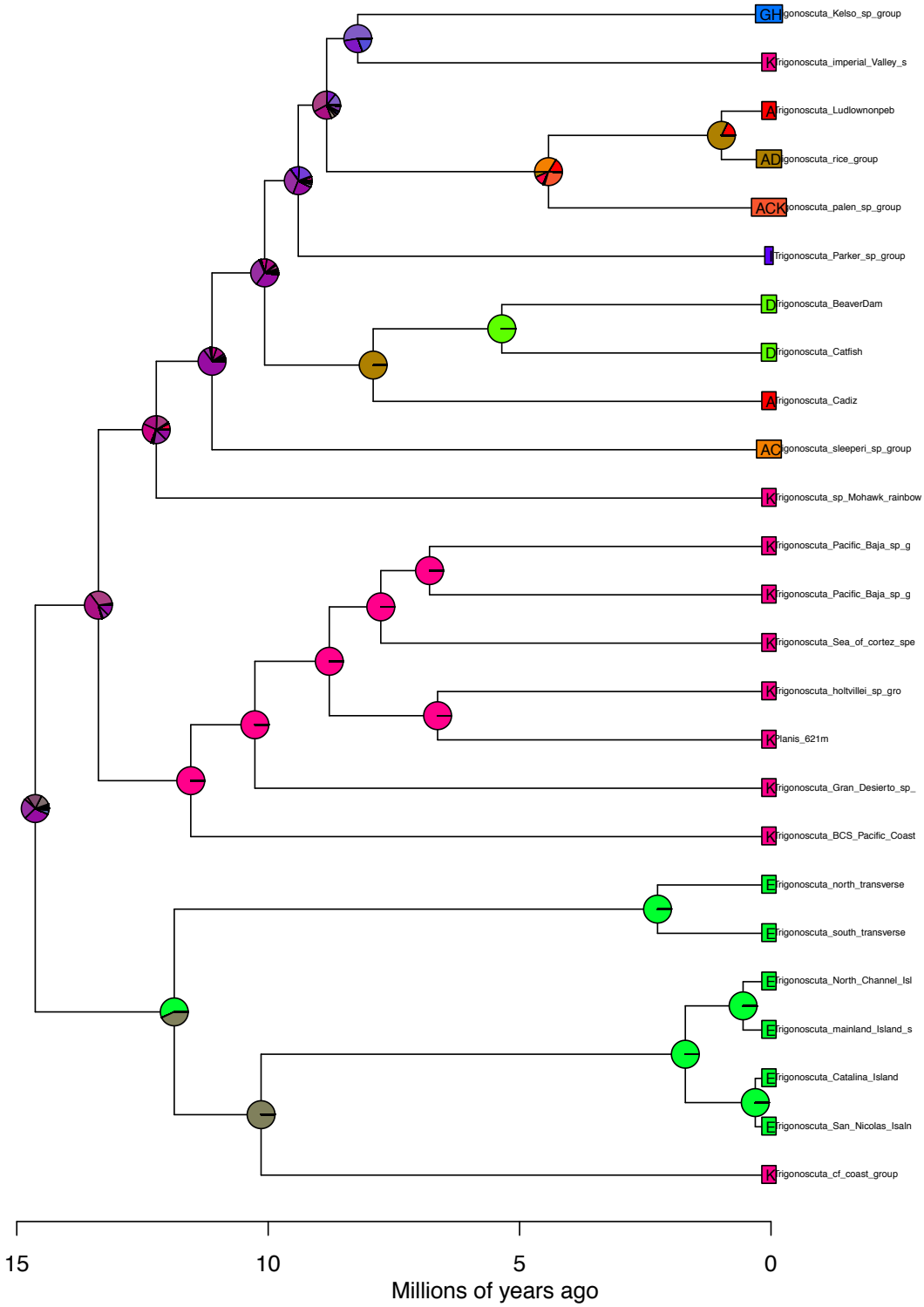

BioGeoBEARS DEC+J on Trigonoscuta M4
anstates: global optim, 4 areas max. d=0.021; e=0; x=–0.327; j=0.057; LnL=–53

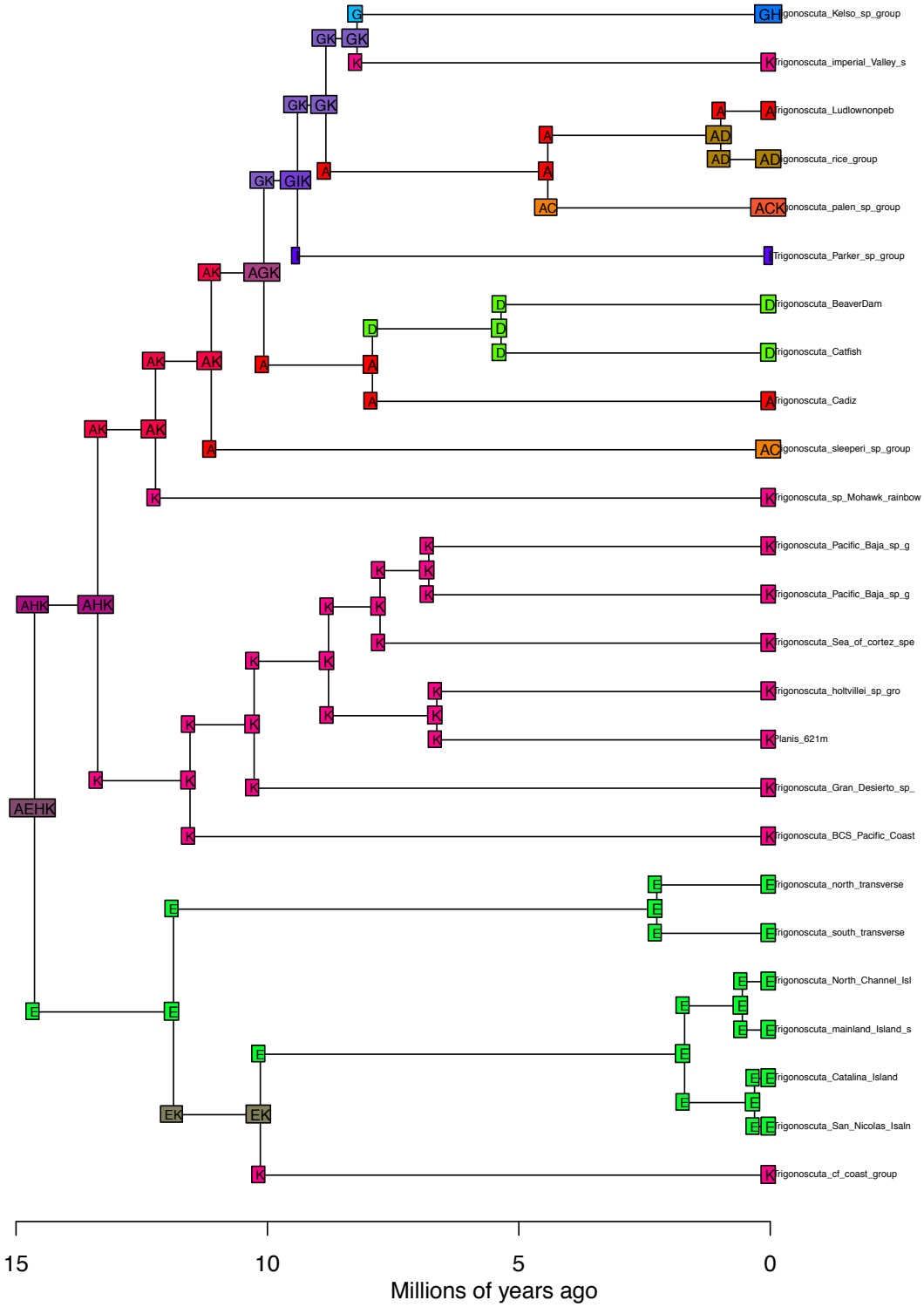

BioGeoBEARS DEC+J on Trigonoscuta M4
anstates: global optim, 4 areas max. d=0.021; e=0; x=–0.327; j=0.057; LnL=–53

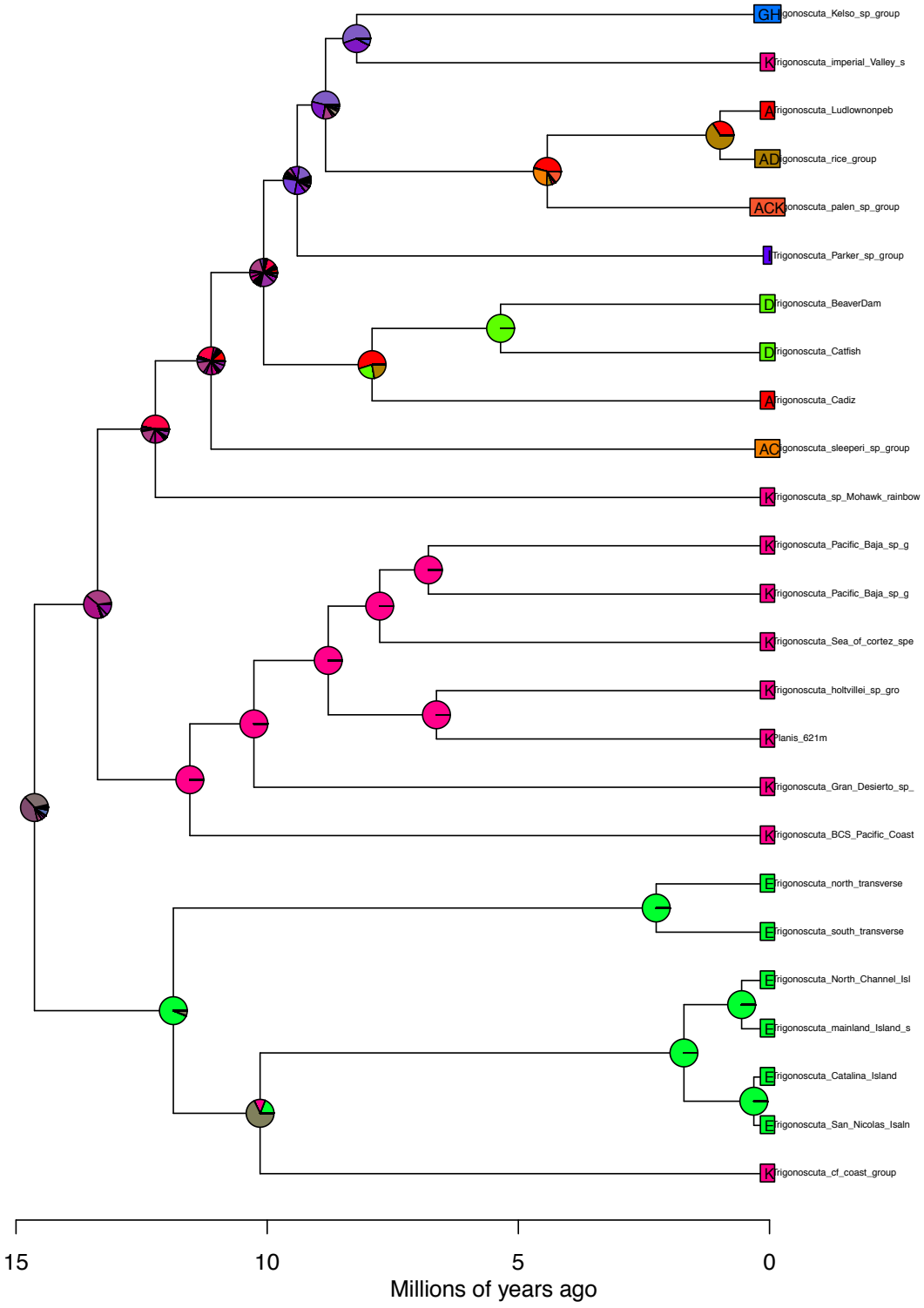

BioGeoBEARS DEC on Cyprinodon M0
anstates: global optim, 4 areas max. d=0.005; e=0; j=0; LnL=–34.3

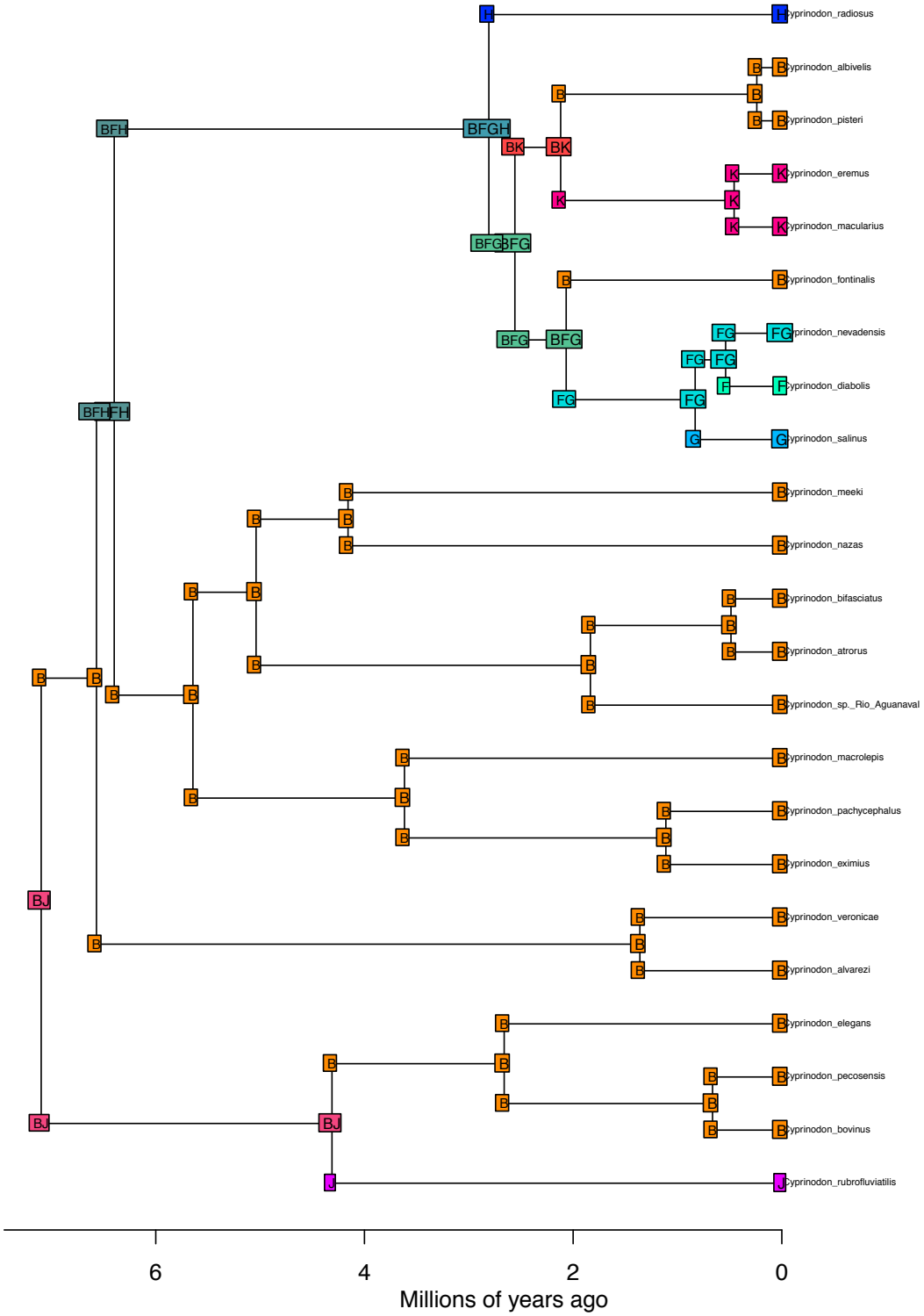

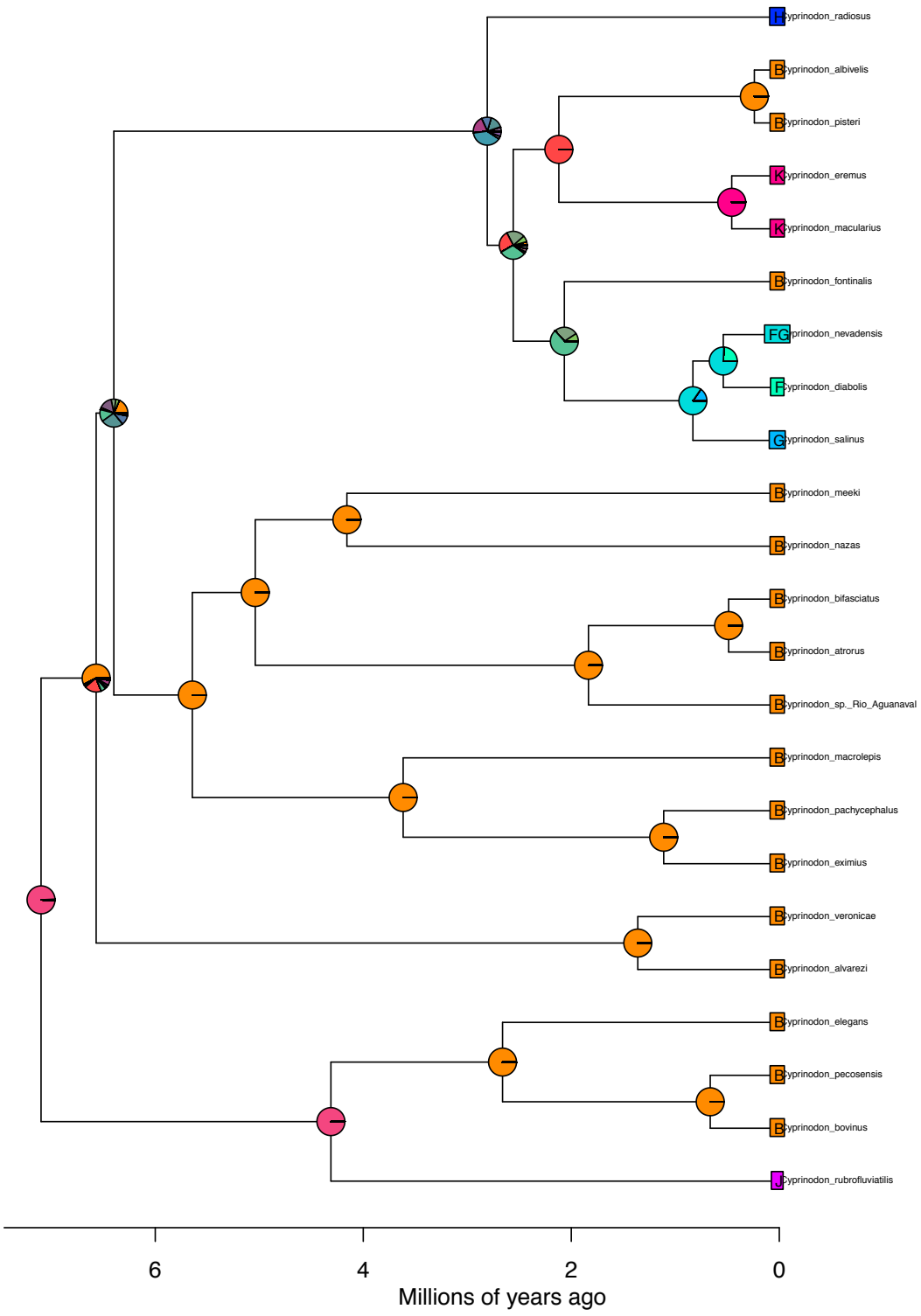
BioGeoBEARS DEC on Cyprinodon M0
anstates: global optim, 4 areas max. d=0.005; e=0; j=0; LnL=–34.3
Cyprinodon_radiosus
Cyprinodon_albivelis
Cyprinodon_pisteri
Cyprinodon_eremus
Cyprinodon_macularius
Cyprinodon_fontinalis
Cyprinodon_nevadensis
Cyprinodon_diabolis
Cyprinodon_salinus
Cyprinodon_meeki
Cyprinodon_nazas
Cyprinodon_bifasciatus
Cyprinodon_atrorus
Cyprinodon_sp._Rio_Aguanaval
Cyprinodon_macrolepis
Cyprinodon_pachycephalus
Cyprinodon_eximius
Cyprinodon_veronicae
Cyprinodon_alvarezi
Cyprinodon_elegans
Cyprinodon_pecosensis
Cyprinodon_bovinus
Cyprinodon_rubrofluviatilis
6
4
2
0
Millions of years ago

BioGeoBEARS DEC+J on Cyprinodon M0
anstates: global optim, 4 areas max. d=0.001; e=0; j=0.01; LnL=–29.8

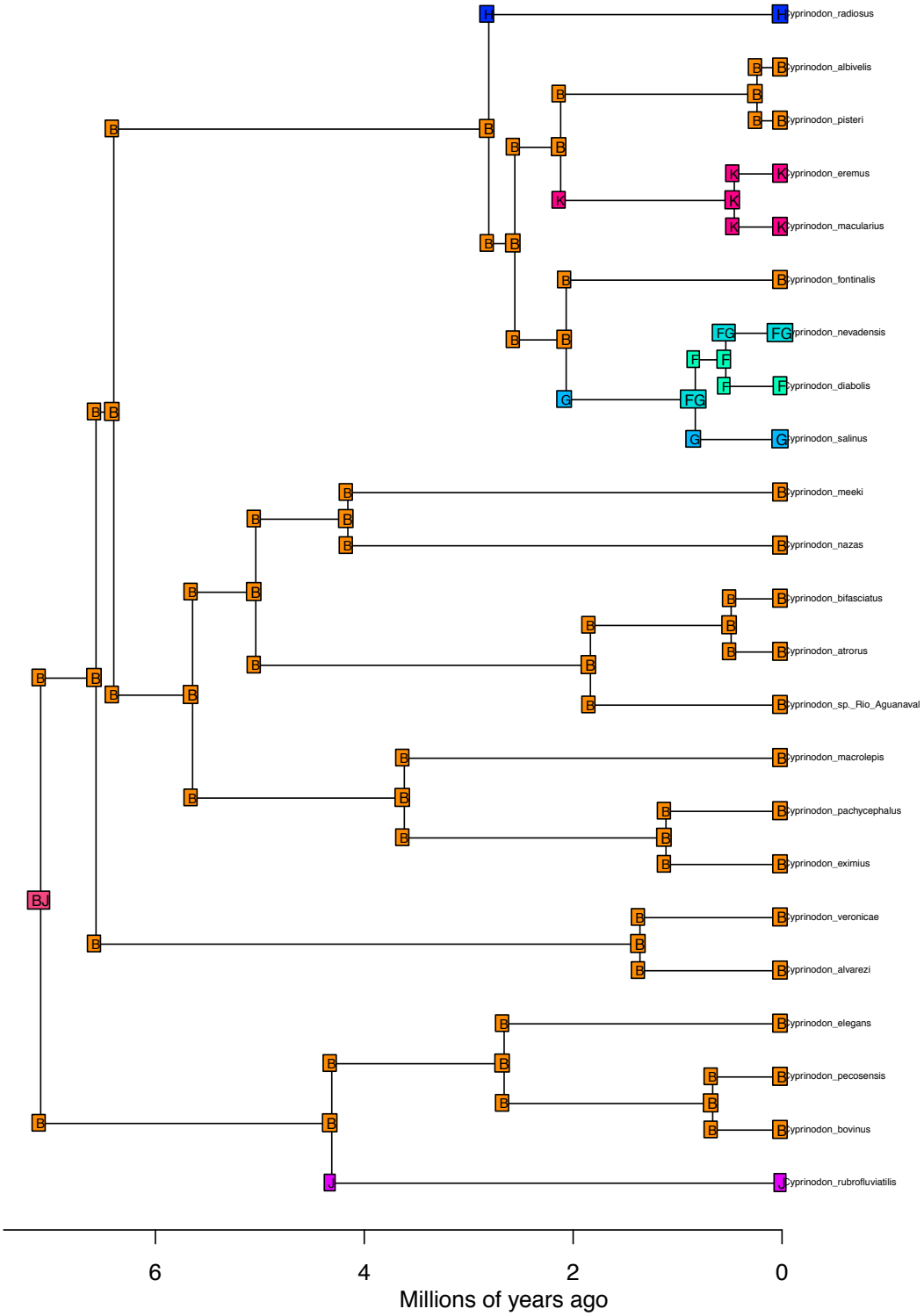

BioGeoBEARS DEC+J on Cyprinodon M0
anstates: global optim, 4 areas max. d=0.001; e=0; j=0.01; LnL=–29.8

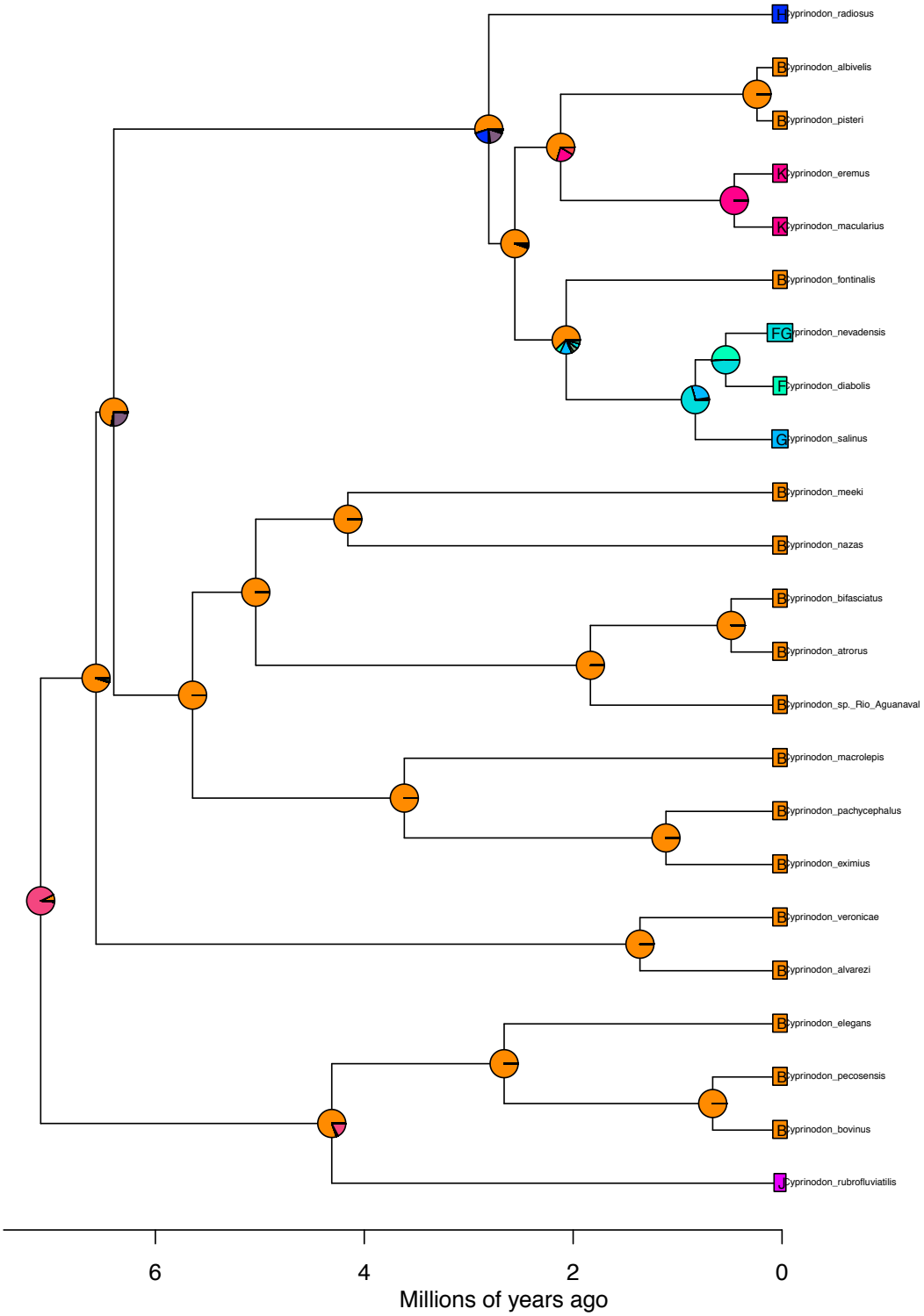

BioGeoBEARS DEC_constrained on Cyprinodon M3
anstates: global optim, 4 areas max. d=0.016; e=0; j=0; LnL=–32.3

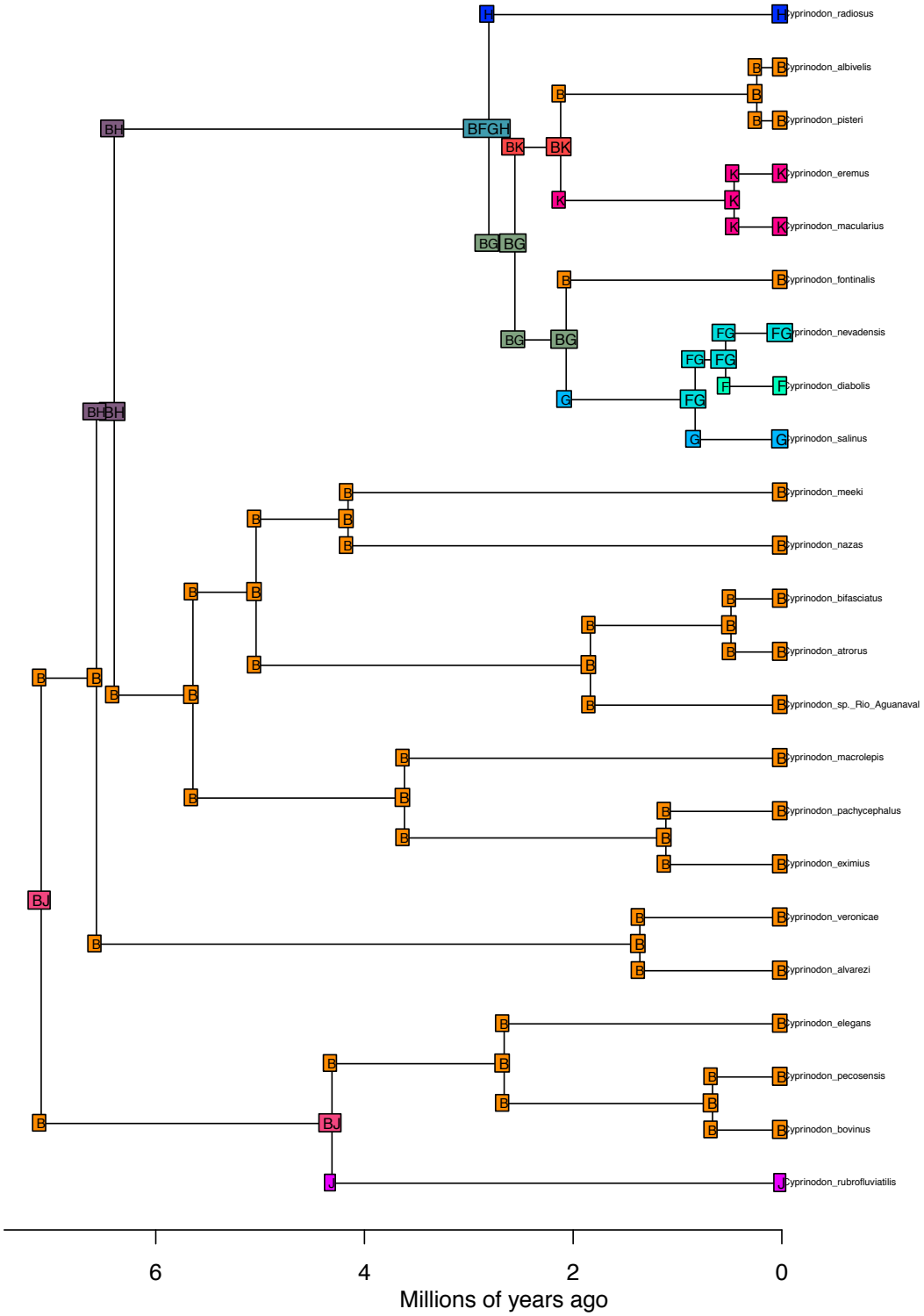

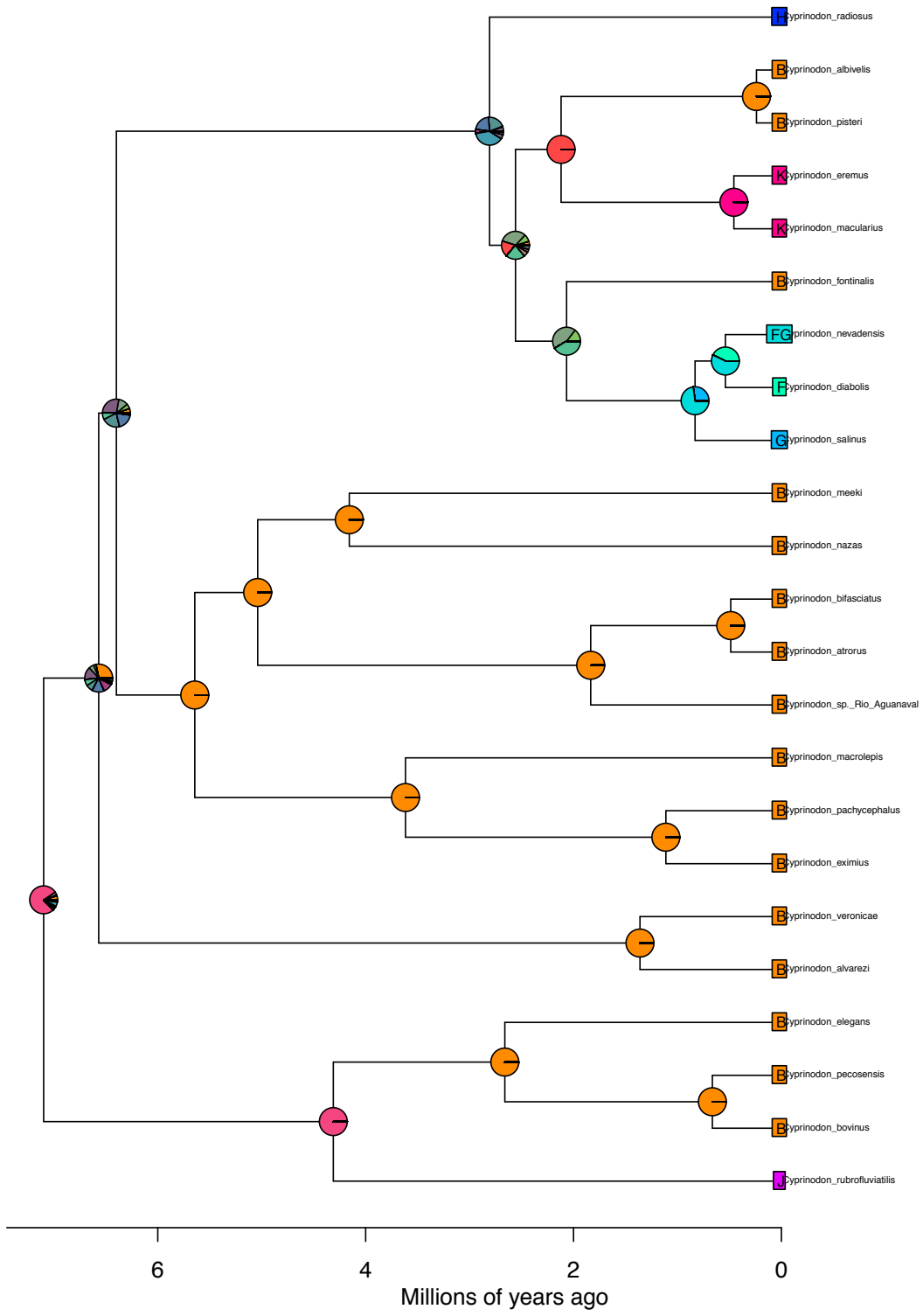
BioGeoBEARS DEC_constrained on Cyprinodon M3
anstates: global optim, 4 areas max. d=0.016; e=0; j=0; lnL=–32.3
Cyprinodon_radiosus
Cyprinodon_albivelis
Cyprinodon_pisteri
Cyprinodon_eremus
Cyprinodon_macularius
Cyprinodon_fontinalis
Cyprinodon_nevadensis
Cyprinodon_diabolis
Cyprinodon_salinus
Cyprinodon_meeki
Cyprinodon_nazas
Cyprinodon_bifasciatus
Cyprinodon_atrorus
Cyprinodon_sp._Rio_Aguanaval
Cyprinodon_macrolepis
Cyprinodon_pachycephalus
Cyprinodon_eximius
Cyprinodon_veronicae
Cyprinodon_alvarezi
Cyprinodon_elegans
Cyprinodon_pecosensis
Cyprinodon_bovinus
Cyprinodon_rubrofluviatilis
6
4
2
0
Millions of years ago

BioGeoBEARS DEC+J_constrained on Cyprinodon M3
anstates: global optim, 4 areas max. d=0.004; e=0; j=0.03; LnL=−28.5

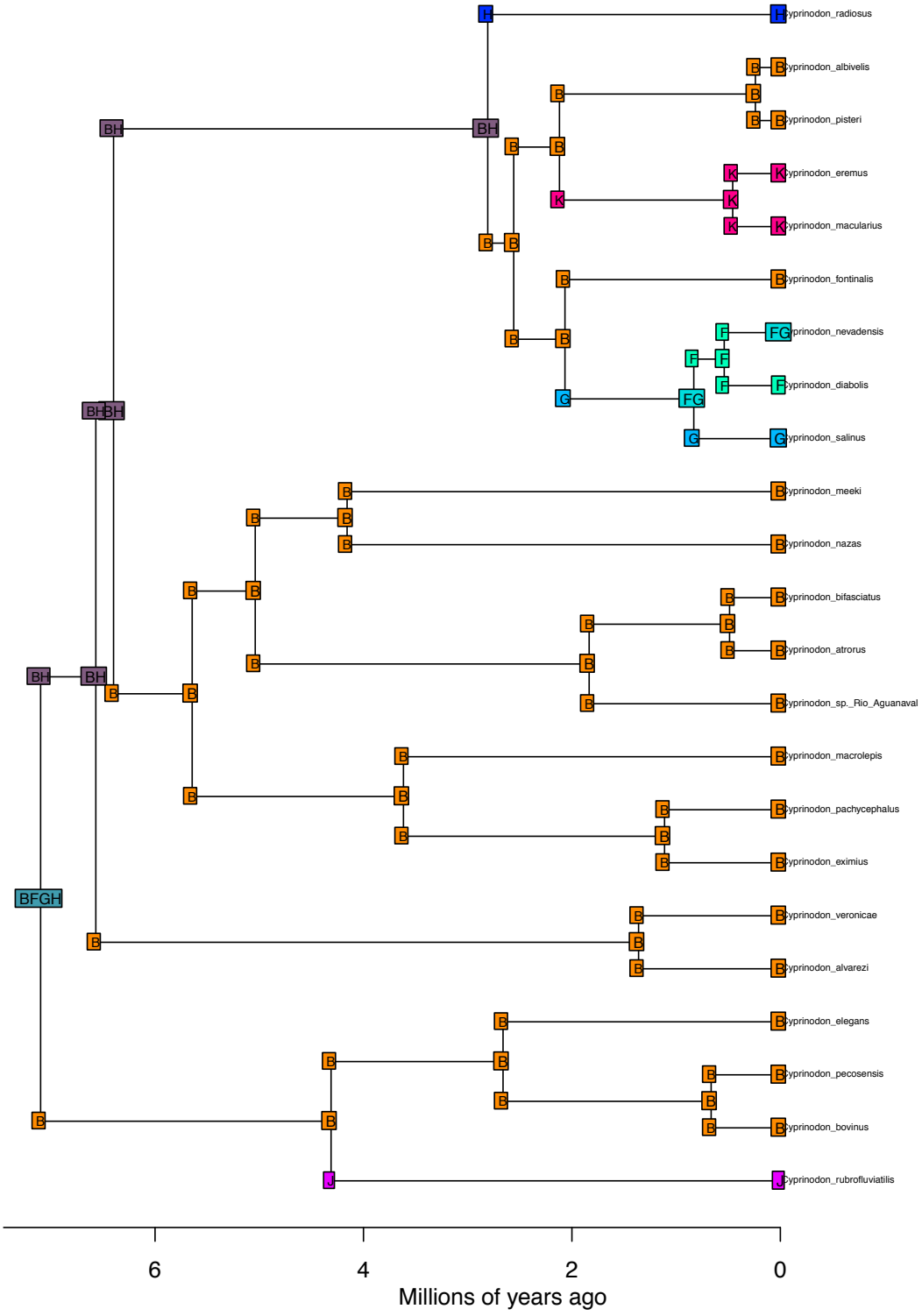

BioGeoBEARS DEC+J_constrained on Cyprinodon M3
anstates: global optim, 4 areas max. d=0.004; e=0; j=0.03; LnL=–28.5

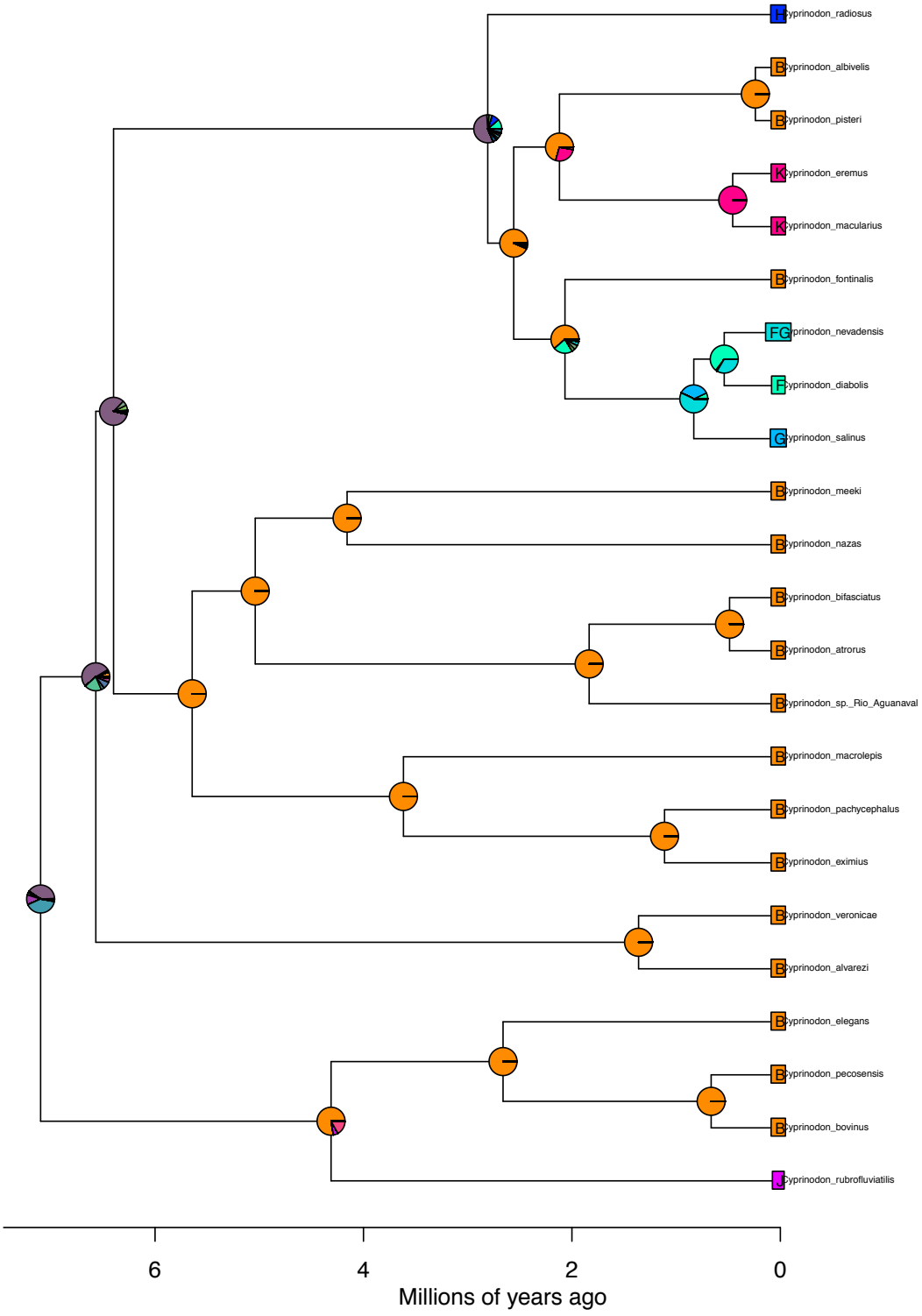

BioGeoBEARS DEC_distances on Cyprinodon M4
anstates: global optim, 4 areas max. d=0.037; e=0; x=–0.174; j=0; LnL=–32.2

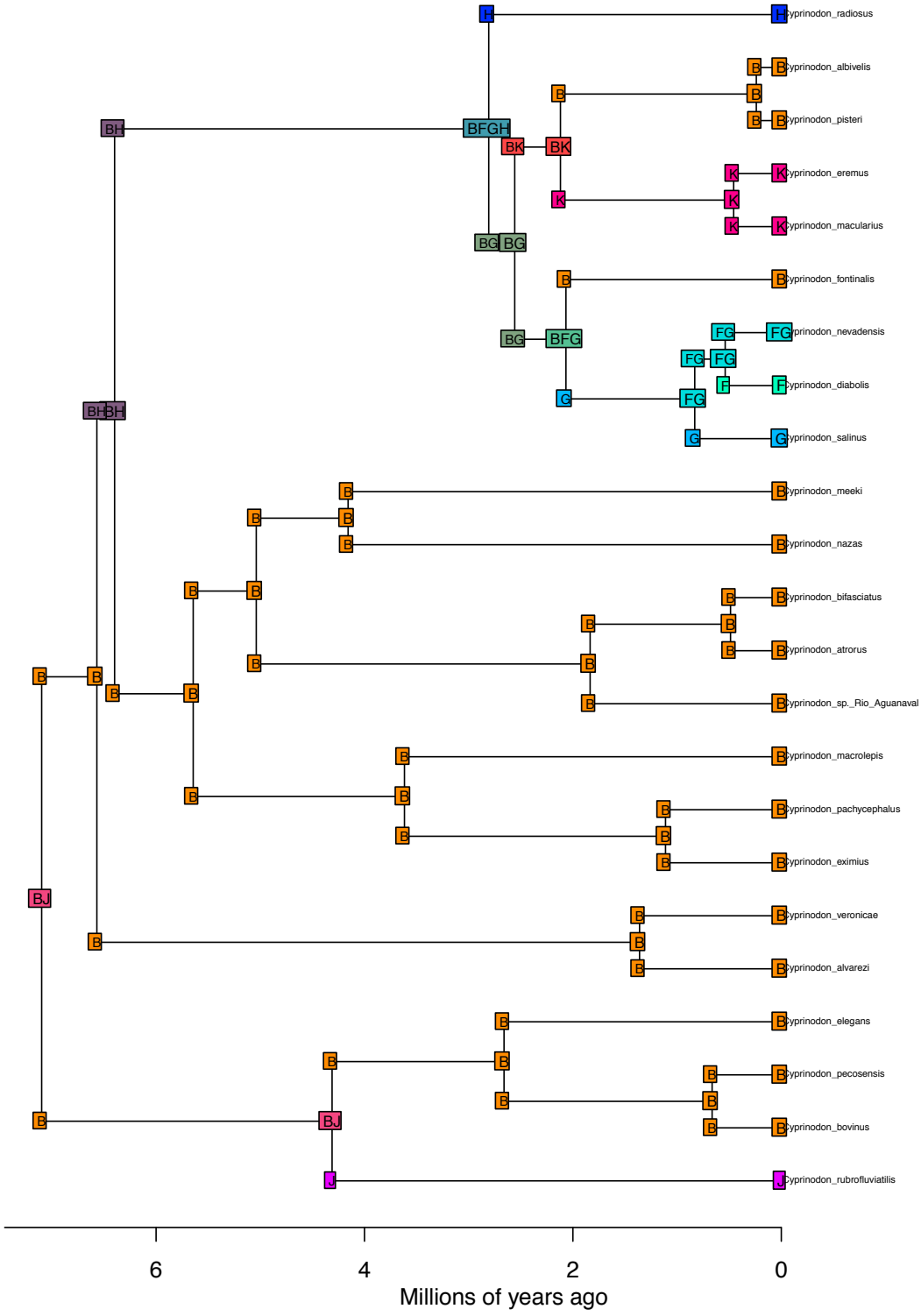

BioGeoBEARS DEC_distances on Cyprinodon M4
anstates: global optim, 4 areas max. d=0.037; e=0; x=–0.174; j=0; LnL=–32.2

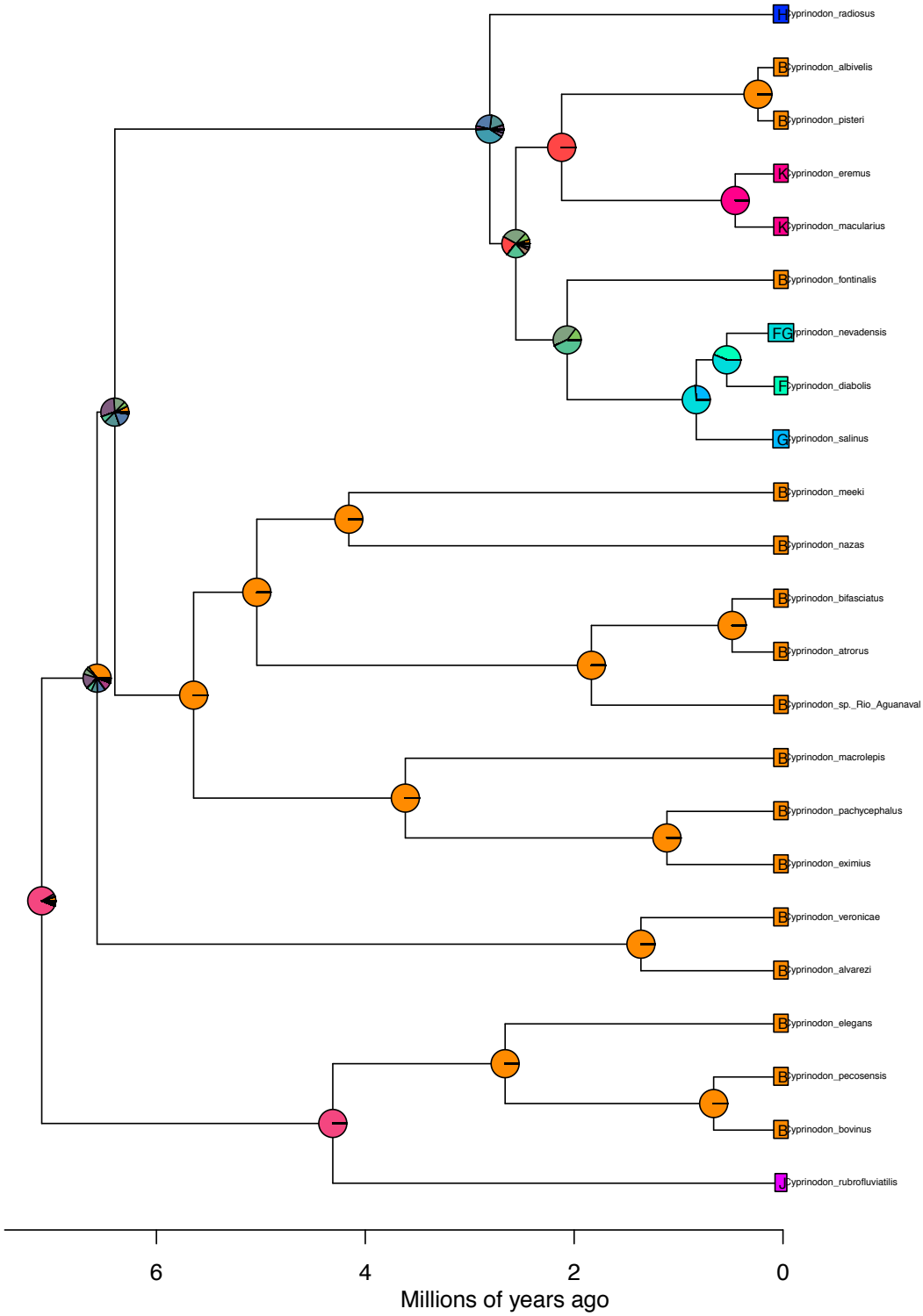

BioGeoBEARS DEC+J_distances on Cyprinodon M4
anstates: global optim, 4 areas max. d=0.004; e=0; x=0.011; j=0.03; LnL=−28.5

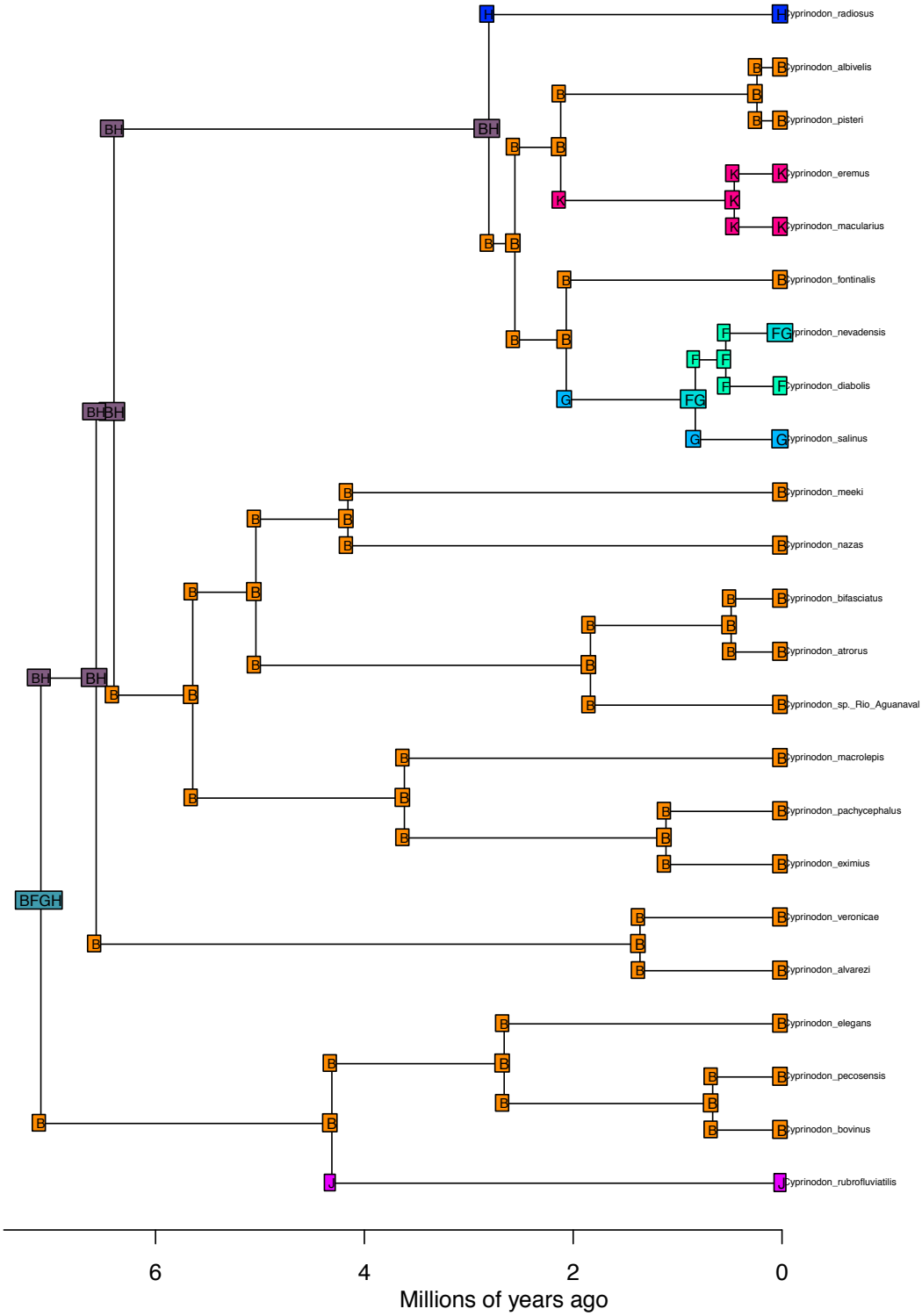

BioGeoBEARS DEC+J_distances on Cyprinodon M4
anstates: global optim, 4 areas max. d=0.004; e=0; x=0.011; j=0.03; LnL=−28.5

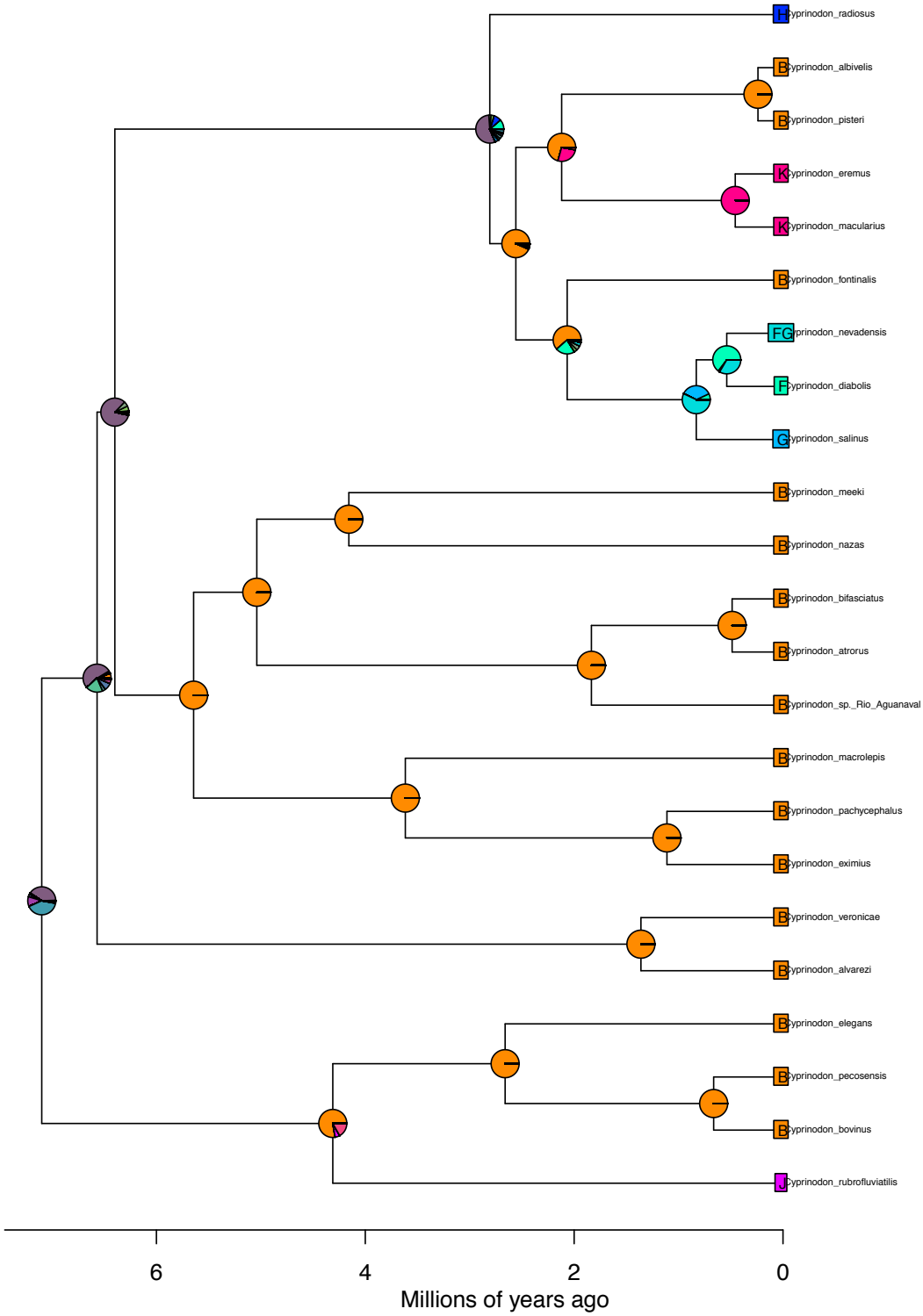

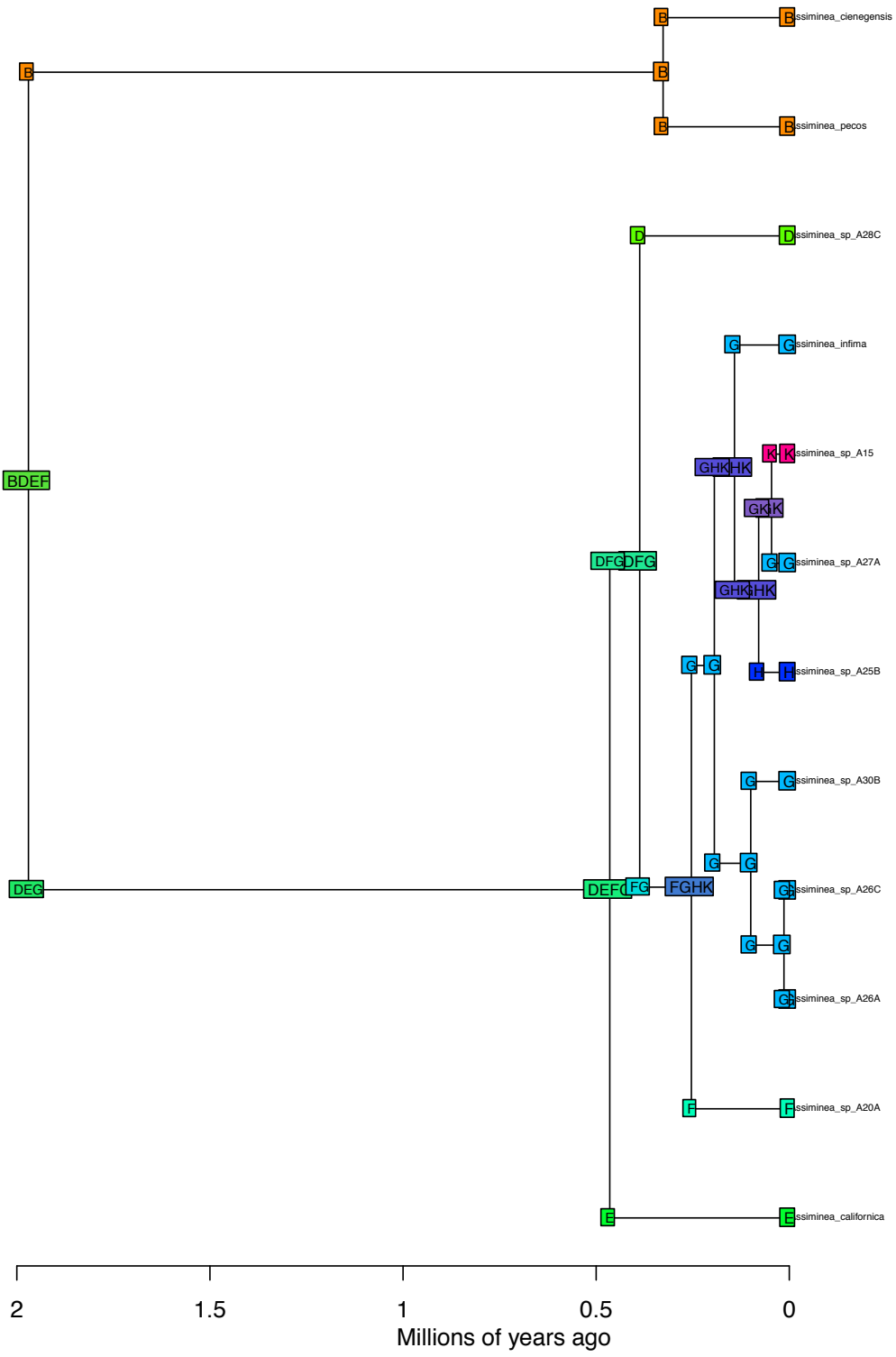
BioGeoBEARS DEC on Assiminia M0
anstates: global optim, 4 areas max. d=0.052; e=0; j=0; LnL=−26.5
Assiminea_cienegensis
Assiminea_pecos
Assiminea_sp_A28C
Assiminea_infima
Assiminea_sp_A15
Assiminea_sp_A27A
Assiminea_sp_A25B
Assiminea_sp_A30B
Assiminea_sp_A26C
Assiminea_sp_A26A
Assiminea_sp_A20A
Assiminea_californica
BDEF
DEG
2
1.5
1
0.5
0
Millions of years ago

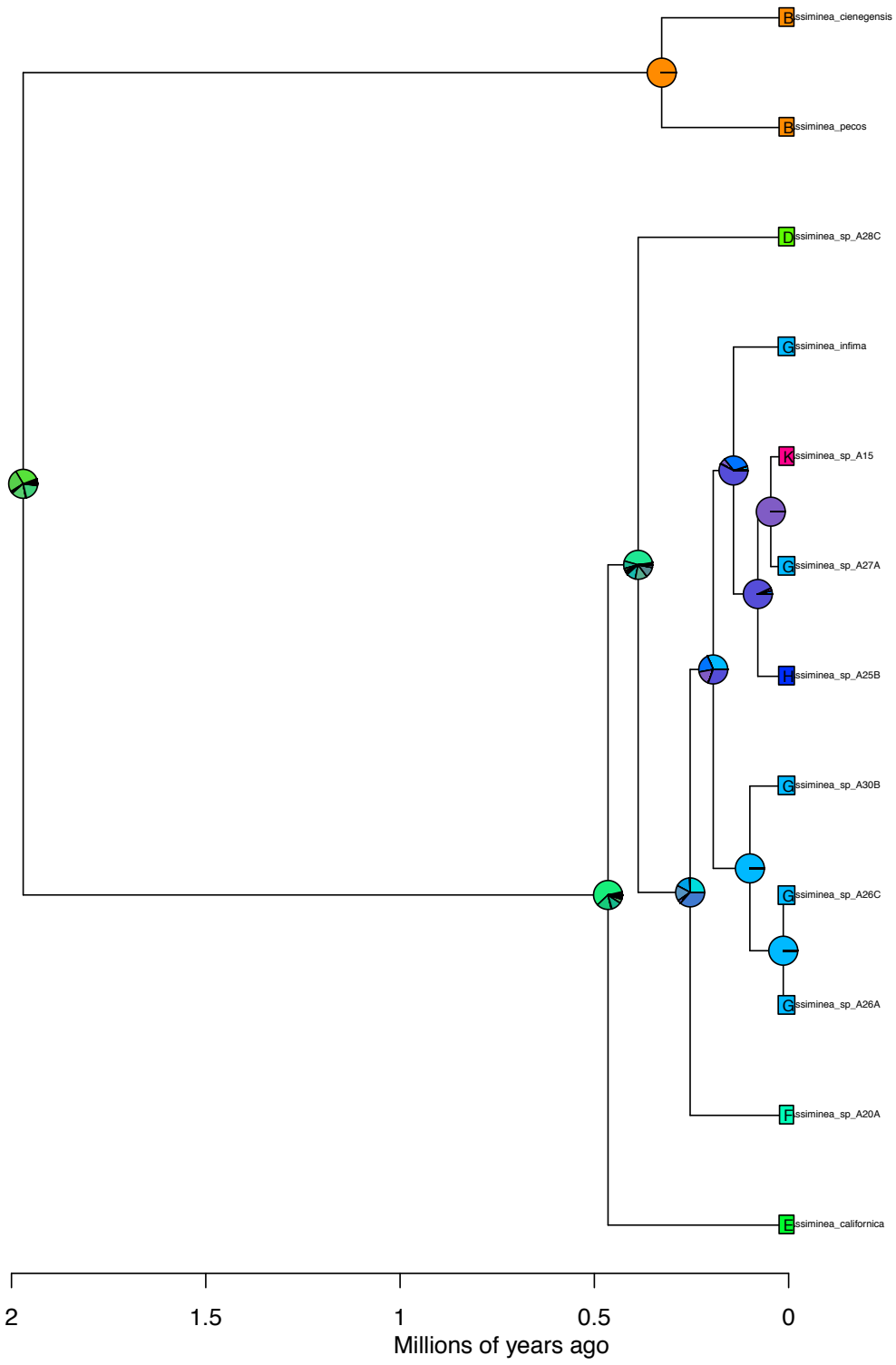
BioGeoBEARS DEC on Assiminia M0
anstates: global optim, 4 areas max. d=0.052; e=0; j=0; LnL=−26.5
Bassiminea_cienegensis
Bassiminea_pecos
Dassiminea_sp_A28C
Gassiminea_infima
Kassiminea_sp_A15
Gassiminea_sp_A27A
Hassiminea_sp_A25B
Gassiminea_sp_A30B
Gassiminea_sp_A26C
Gassiminea_sp_A26A
Fassiminea_sp_A20A
Eassiminea_californica
2
1.5
1
0.5
0
Millions of years ago

BioGeoBEARS DEC+J on Assiminia M0
anstates: global optim, 4 areas max. d=0; e=0.045; j=0.041; LnL=–19.8

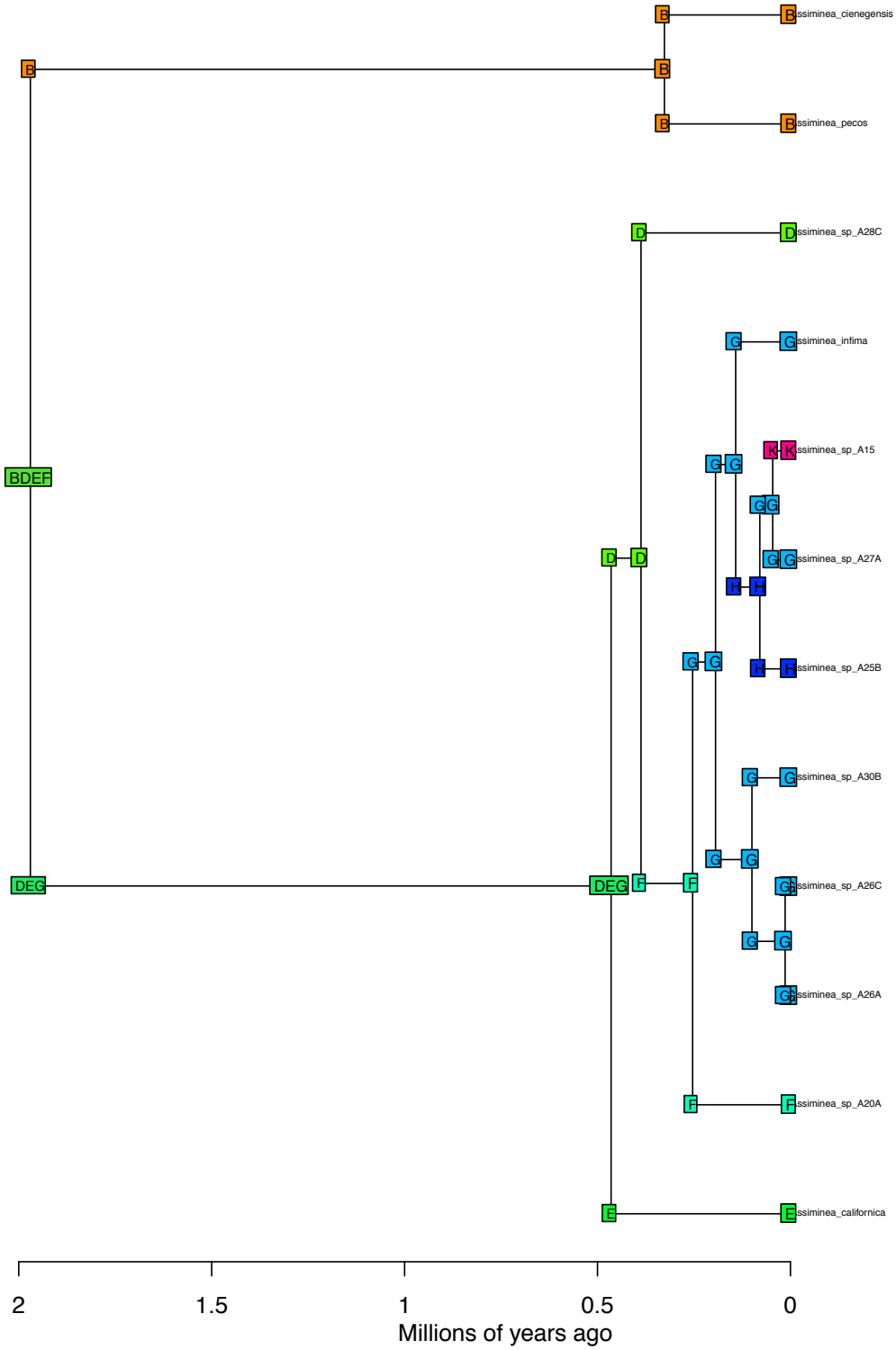

BioGeoBEARS DEC+J on Assiminia M0
anstates: global optim, 4 areas max. d=0; e=0.045; j=0.041; LnL=–19.8

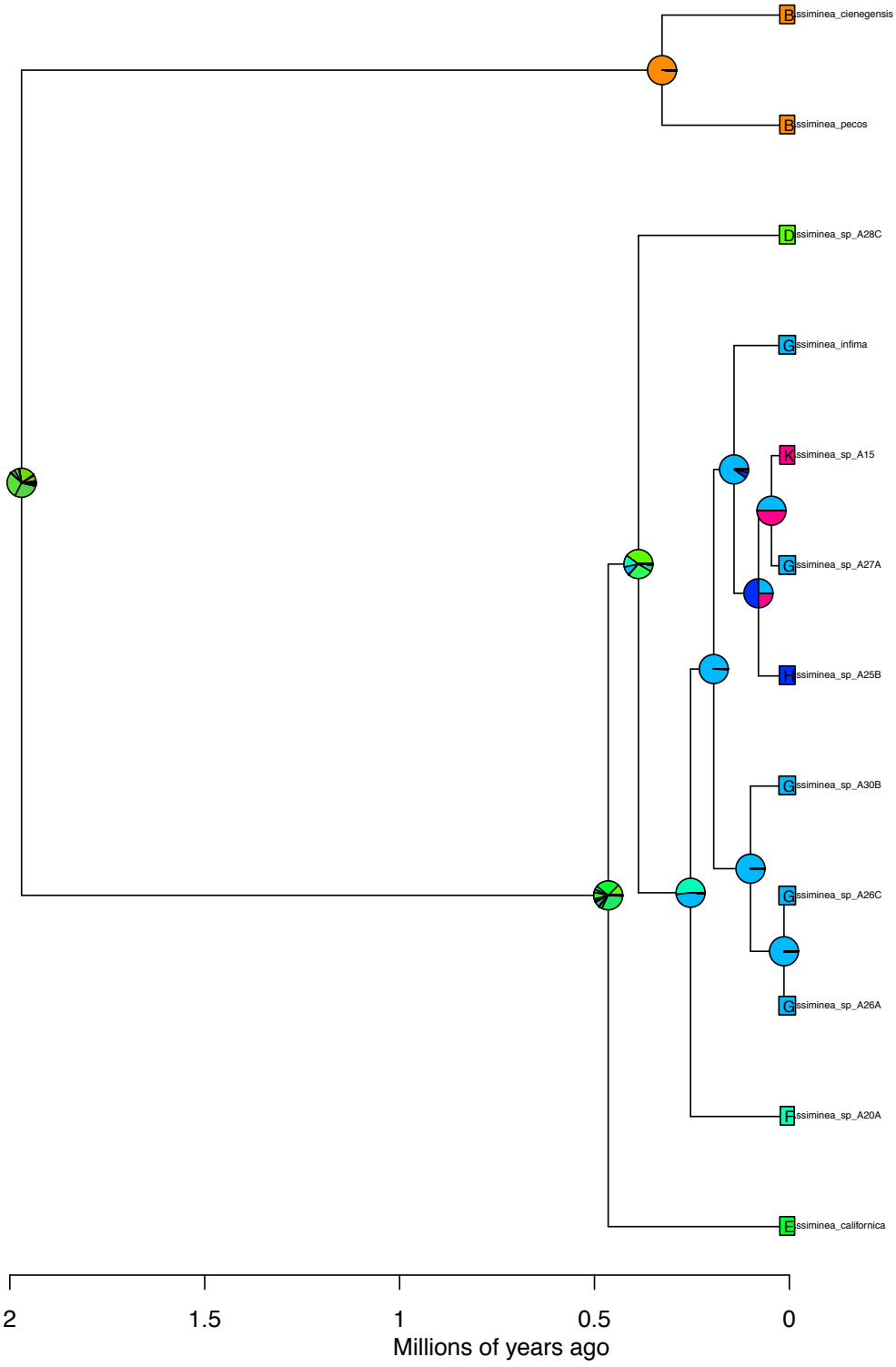

BioGeoBEARS DEC_constrained on Assiminia M3
anstates: global optim, 4 areas max. d=0.129; e=0; j=0; LnL=−26.7

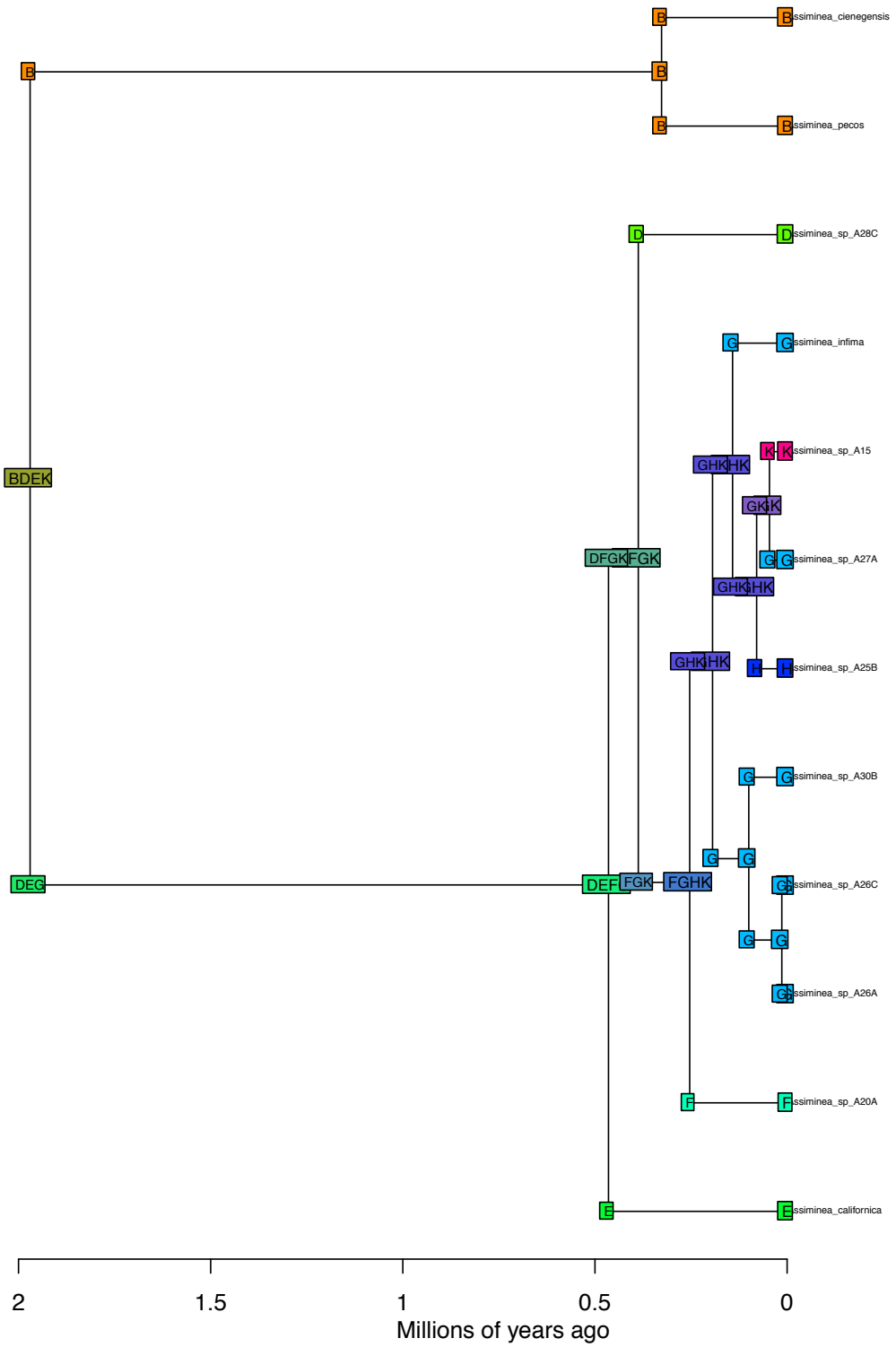

BioGeoBEARS DEC_constrained on Assiminia M3
anstates: global optim, 4 areas max. d=0.129; e=0; j=0; LnL=−26.7

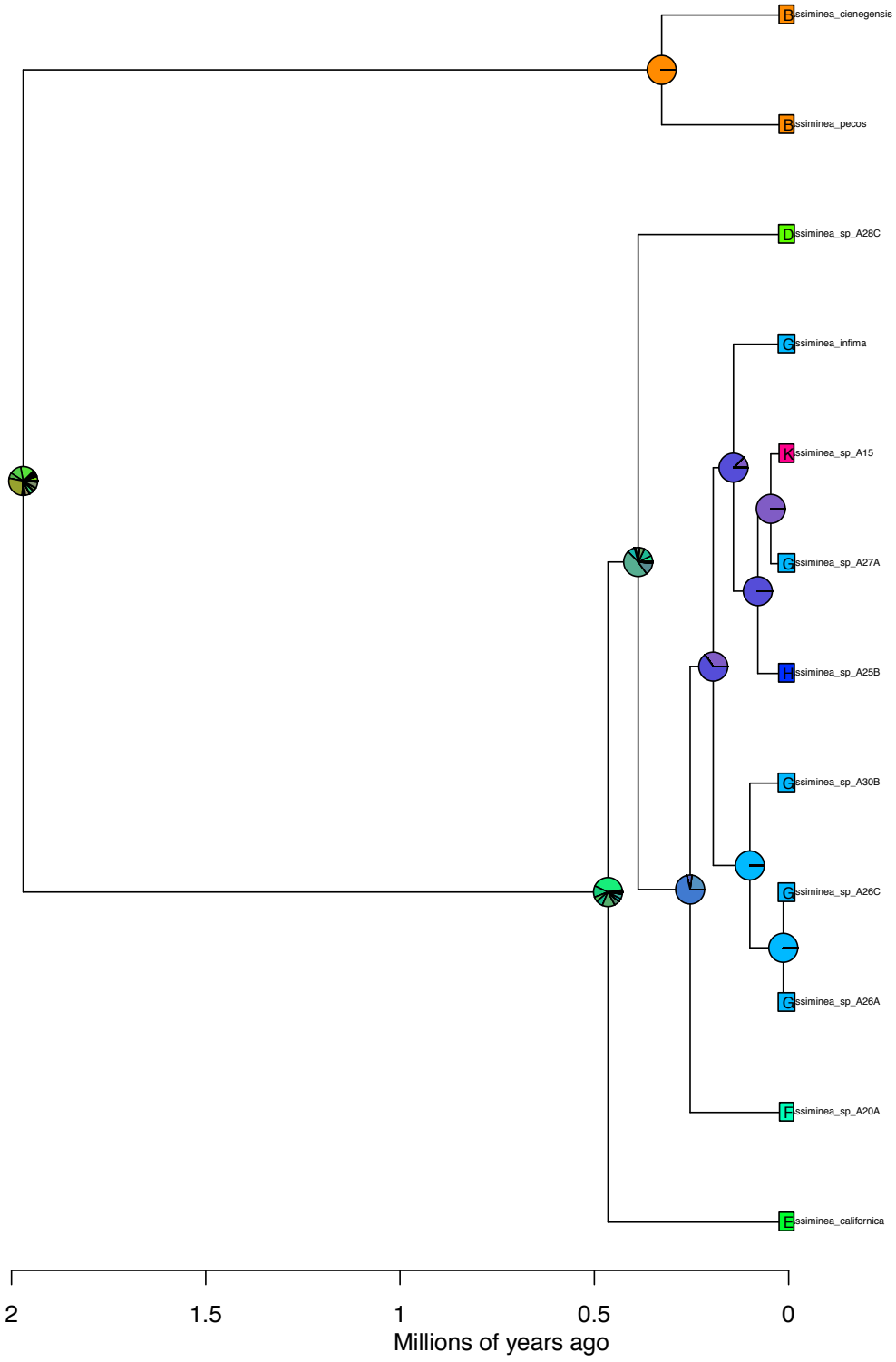

BioGeoBEARS DEC+J_constrained on Assiminia M3
anstates: global optim, 4 areas max. d=0.039; e=0; j=0.081; LnL=–25.9

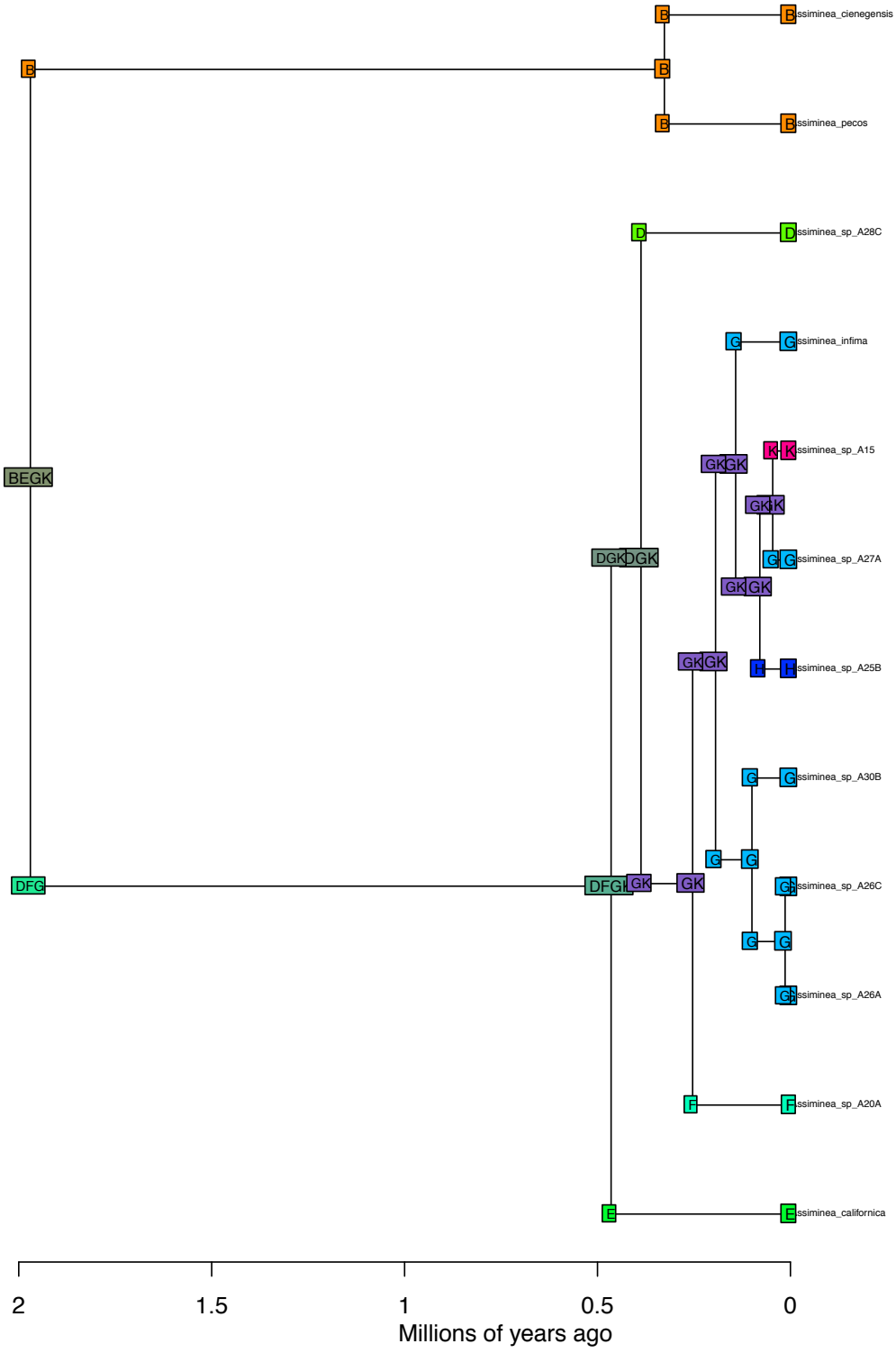

BioGeoBEARS DEC+J_constrained on Assiminia M3
anstates: global optim, 4 areas max. d=0.039; e=0; j=0.081; LnL=–25.9

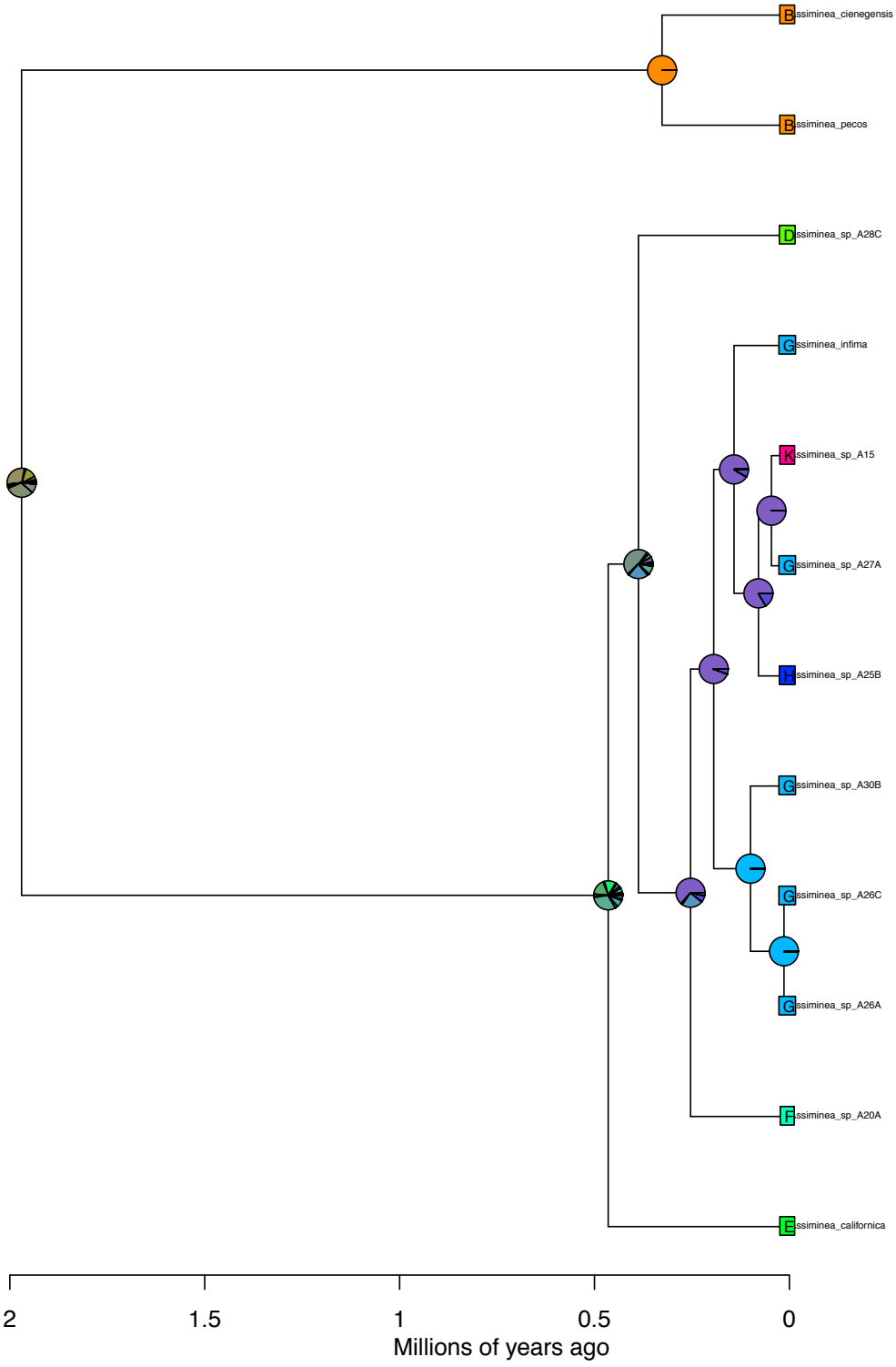

BioGeoBEARS DEC_distances on Assiminia M4
anstates: global optim, 4 areas max. d=0.132; e=0; x=–0.023; j=0; LnL=–26.7

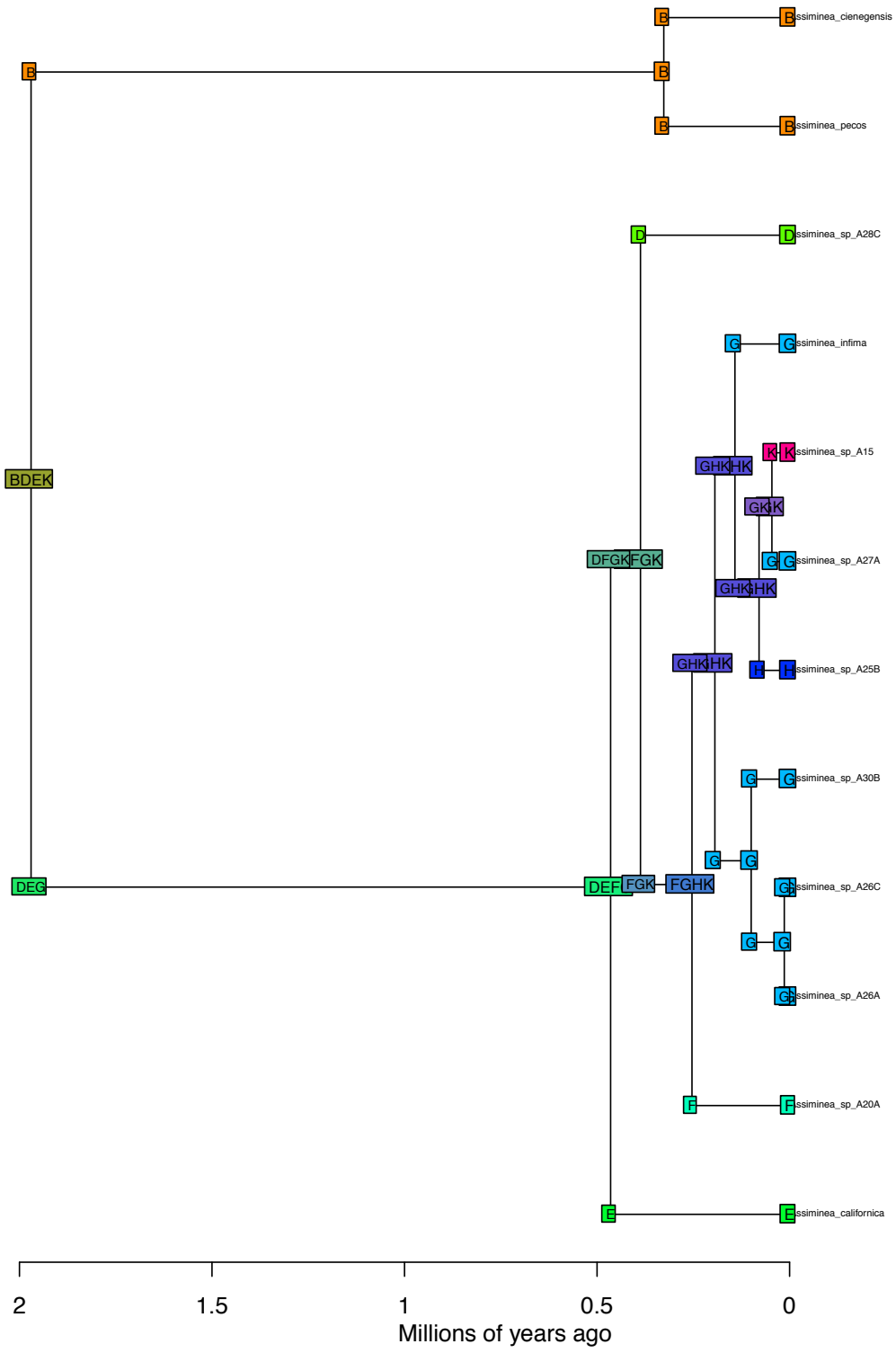

BioGeoBEARS DEC_distances on Assiminia M4
anstates: global optim, 4 areas max. d=0.132; e=0; x=–0.023; j=0; LnL=–26.7

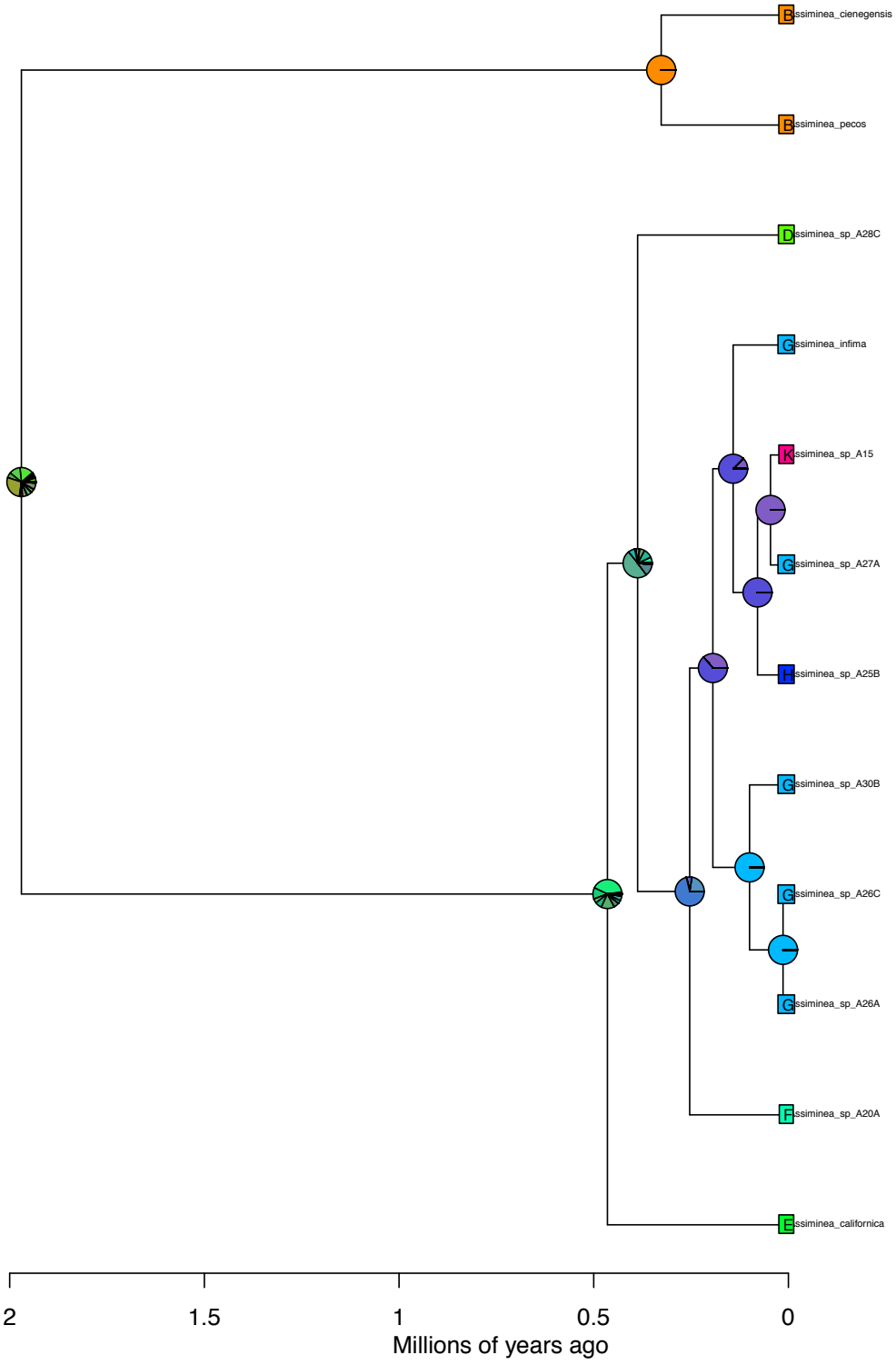

BioGeoBEARS DEC+J_distances on Assiminia M4
anstates: global optim, 4 areas max. d=0.034; e=0; x=–0.141; j=0.082; LnL=–25.9

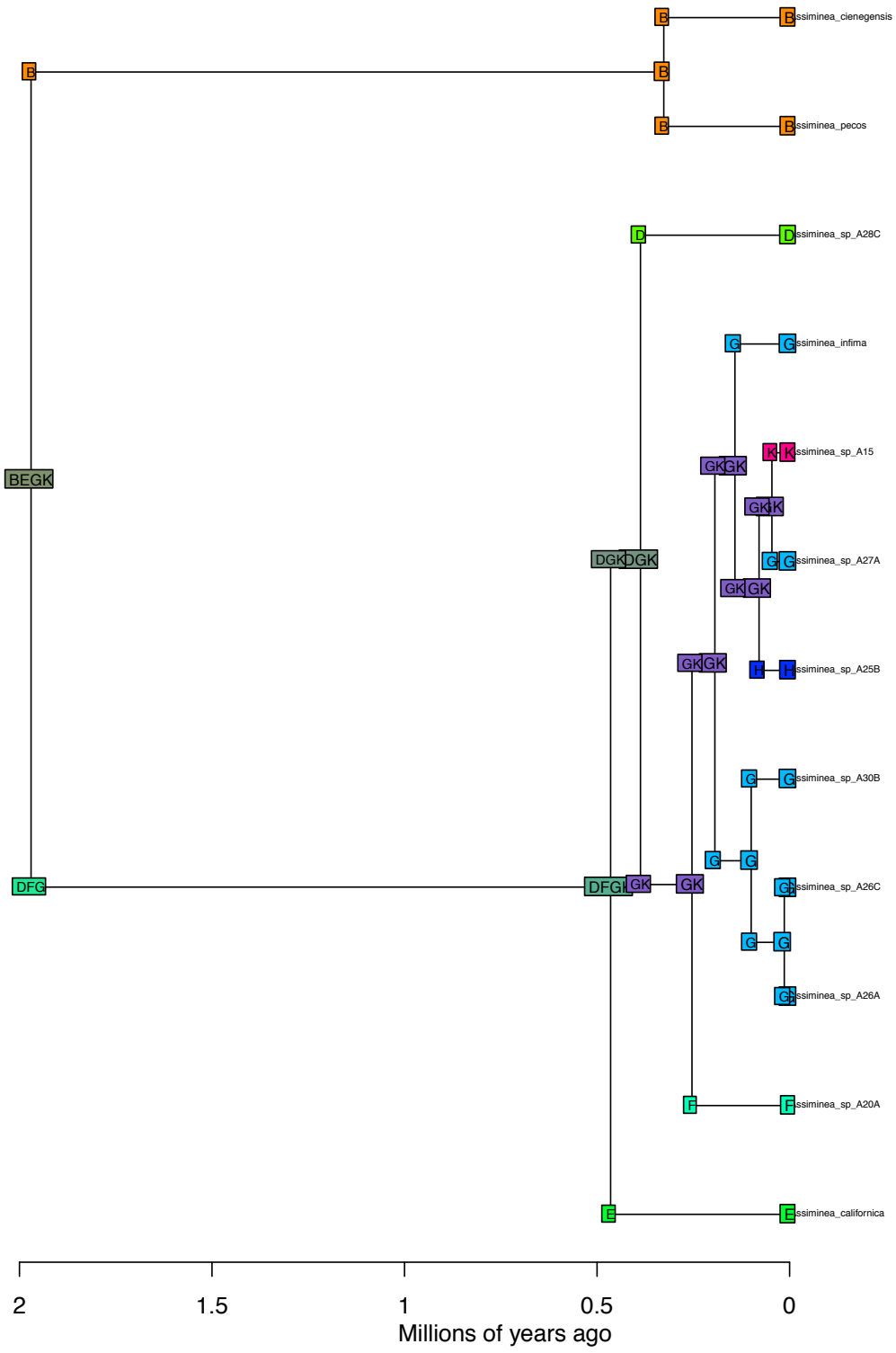

BioGeoBEARS DEC+J_distances on Assiminia M4
anstates: global optim, 4 areas max. d=0.034; e=0; x=–0.141; j=0.082; LnL=–25.9

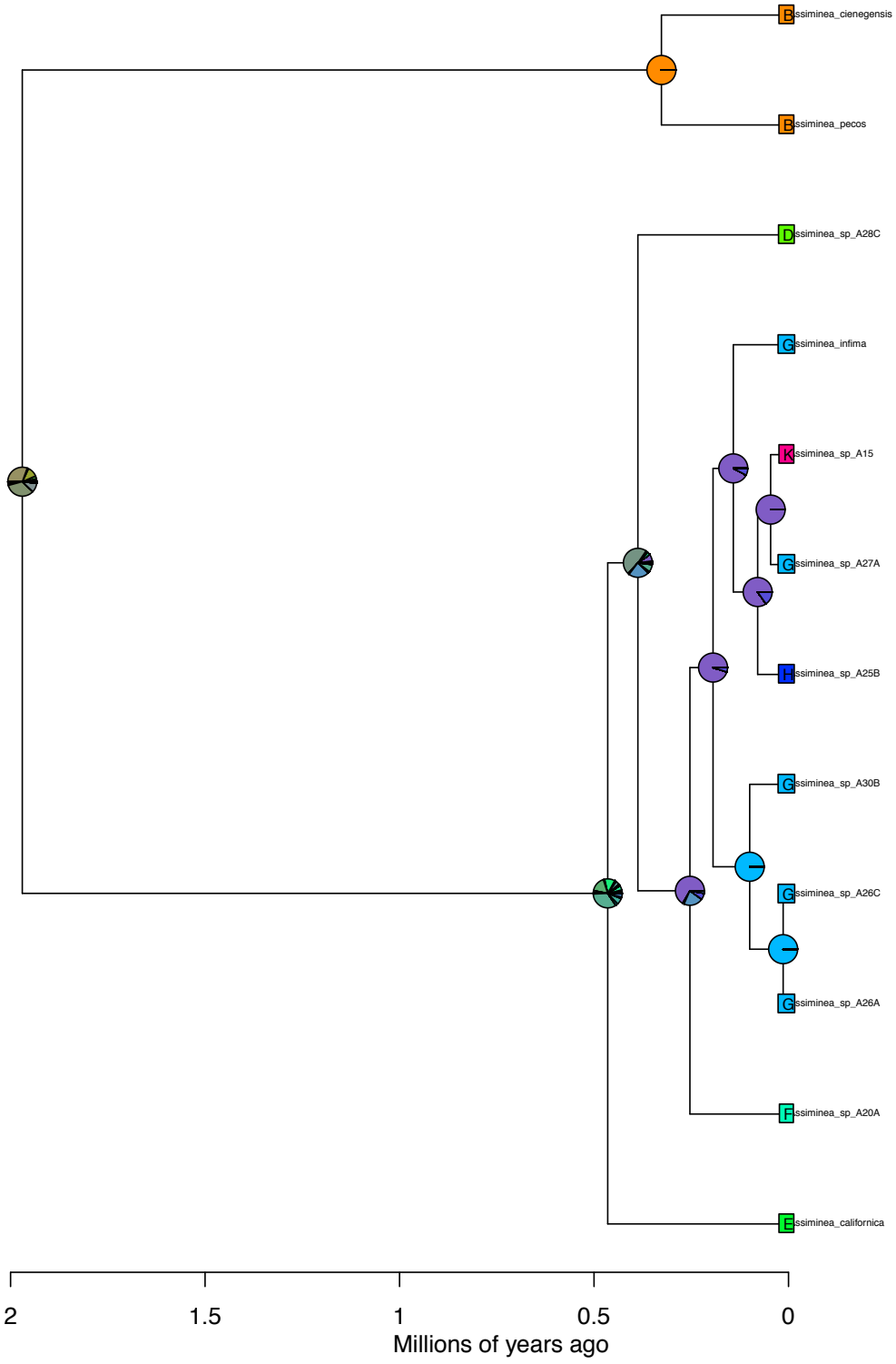

BioGeoBEARS DEC on Pyrgulopsis M0
anstates: global optim, 4 areas max. d=0.008; e=0.033; j=0; LnL=−210.7

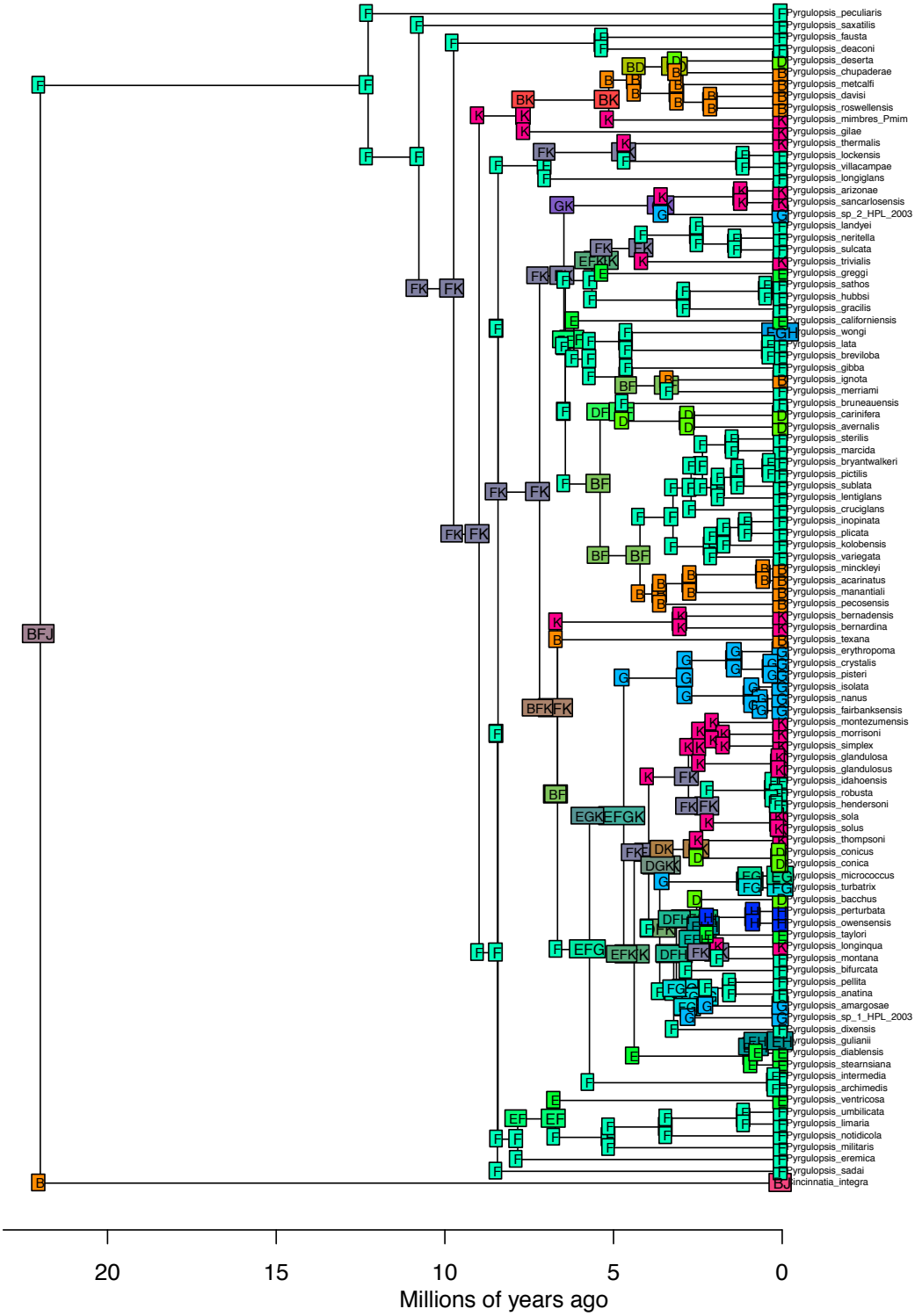

BioGeoBEARS DEC on Pyrgulopsis M0
anstates: global optim, 4 areas max. d=0.008; e=0.033; j=0; LnL=−210.7

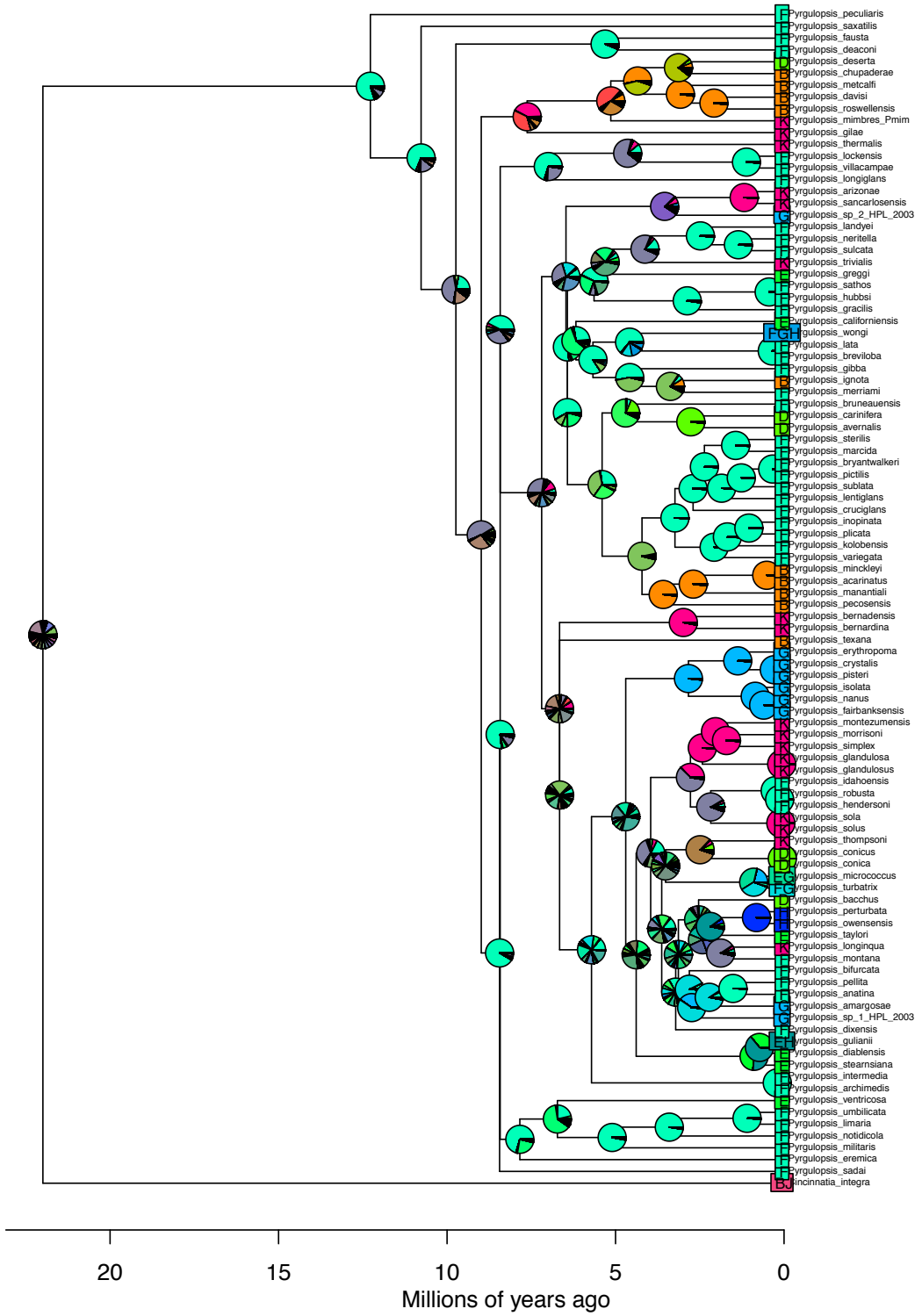

BioGeoBEARS DEC+J on Pyrgulopsis M0
anstates: global optim, 4 areas max. d=0.001; e=0; j=0.02; LnL=−171.1

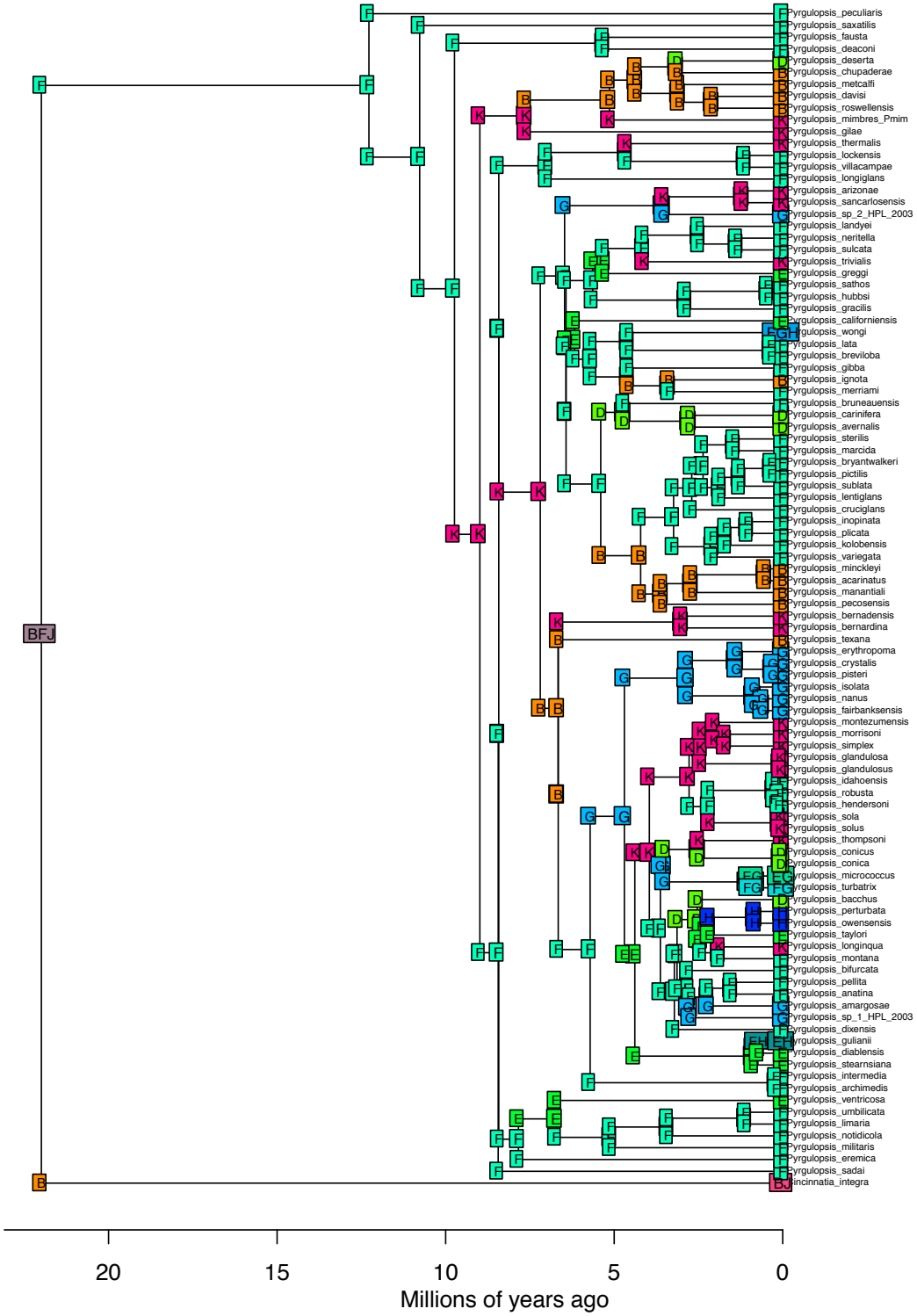

BioGeoBEARS DEC+J on Pyrgulopsis M0
anstates: global optim, 4 areas max. d=0.001; e=0; j=0.02; LnL=−171.1

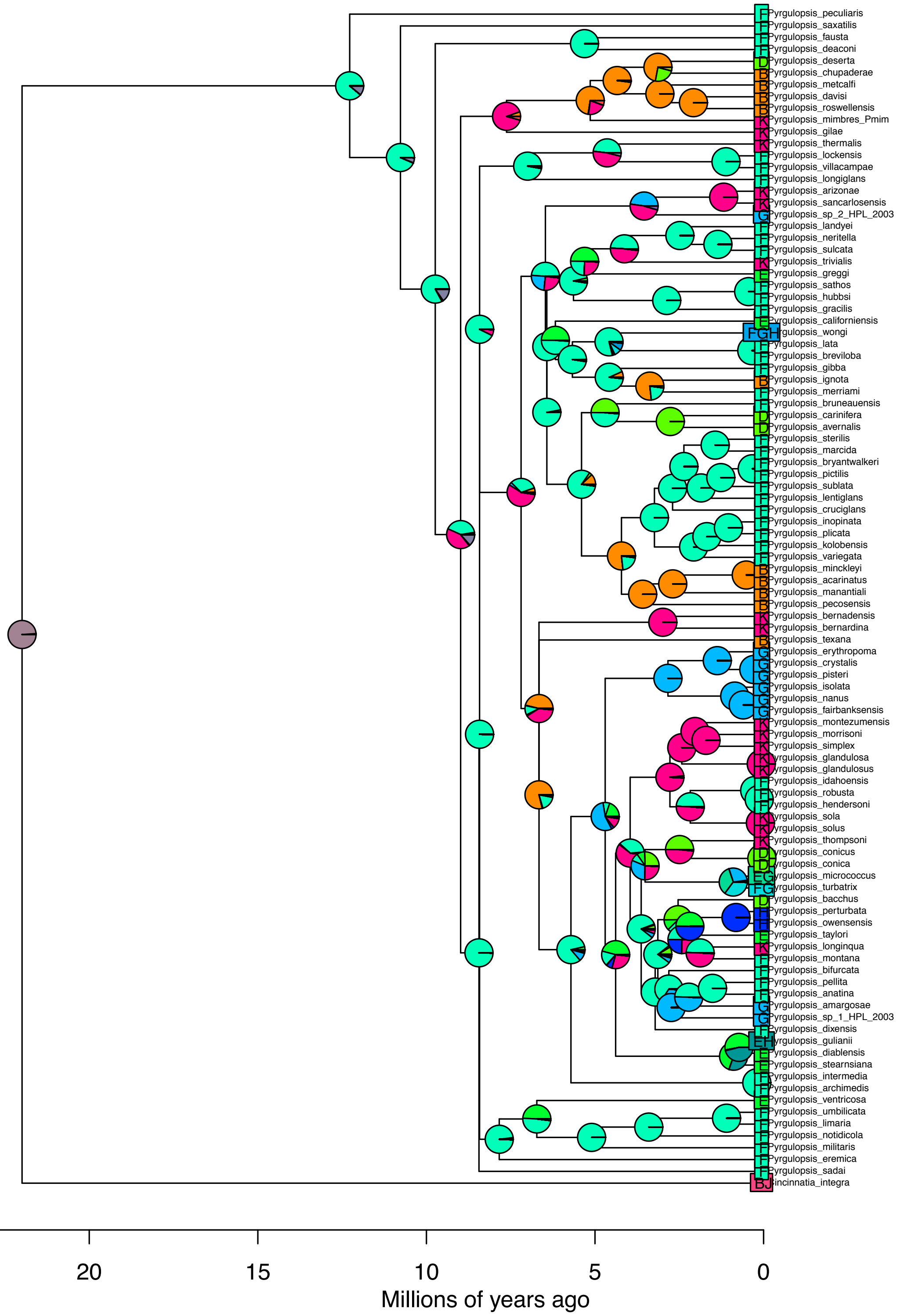

BioGeoBEARS DEC_constrained on Pyrgulopsis M3
anstates: global optim, 4 areas max. d=0.015; e=0.043; j=0; LnL=−204.3

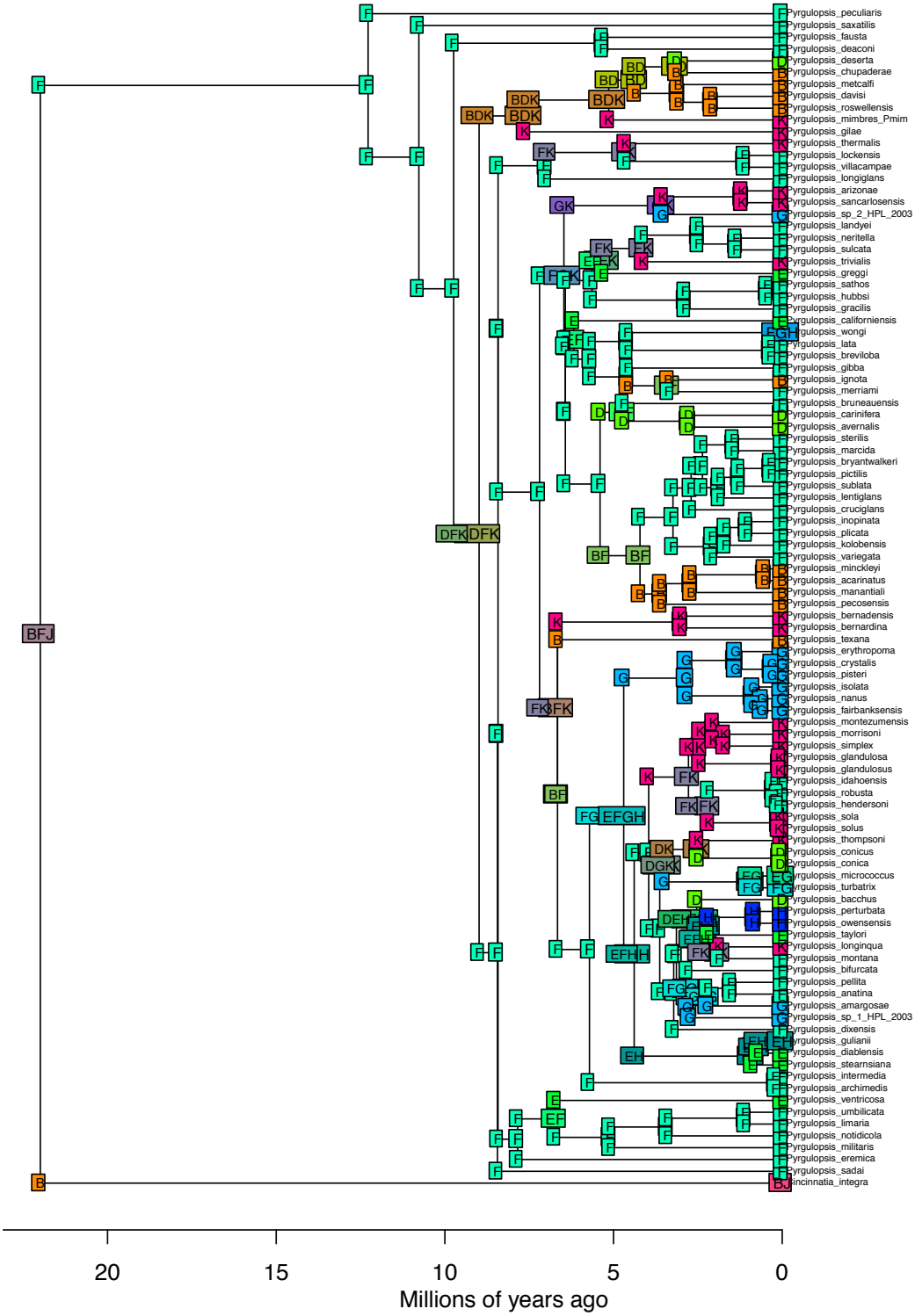

BioGeoBEARS DEC_constrained on Pyrgulopsis M3
anstates: global optim, 4 areas max. d=0.015; e=0.043; j=0; LnL=−204.3

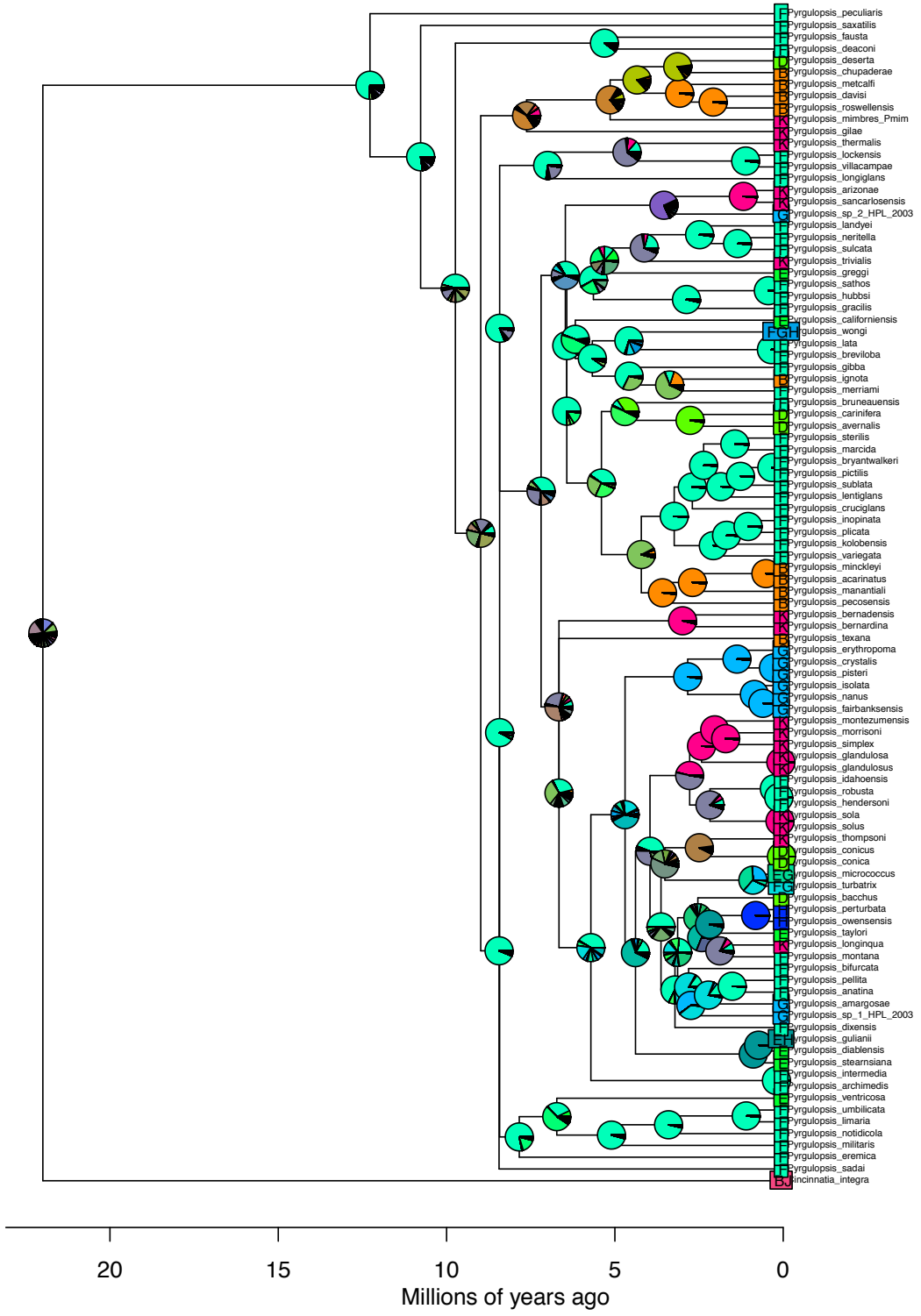

BioGeoBEARS DEC+J_constrained on Pyrgulopsis M3
anstates: global optim, 4 areas max. d=0.006; e=0.016; j=0.024; LnL=−187.7

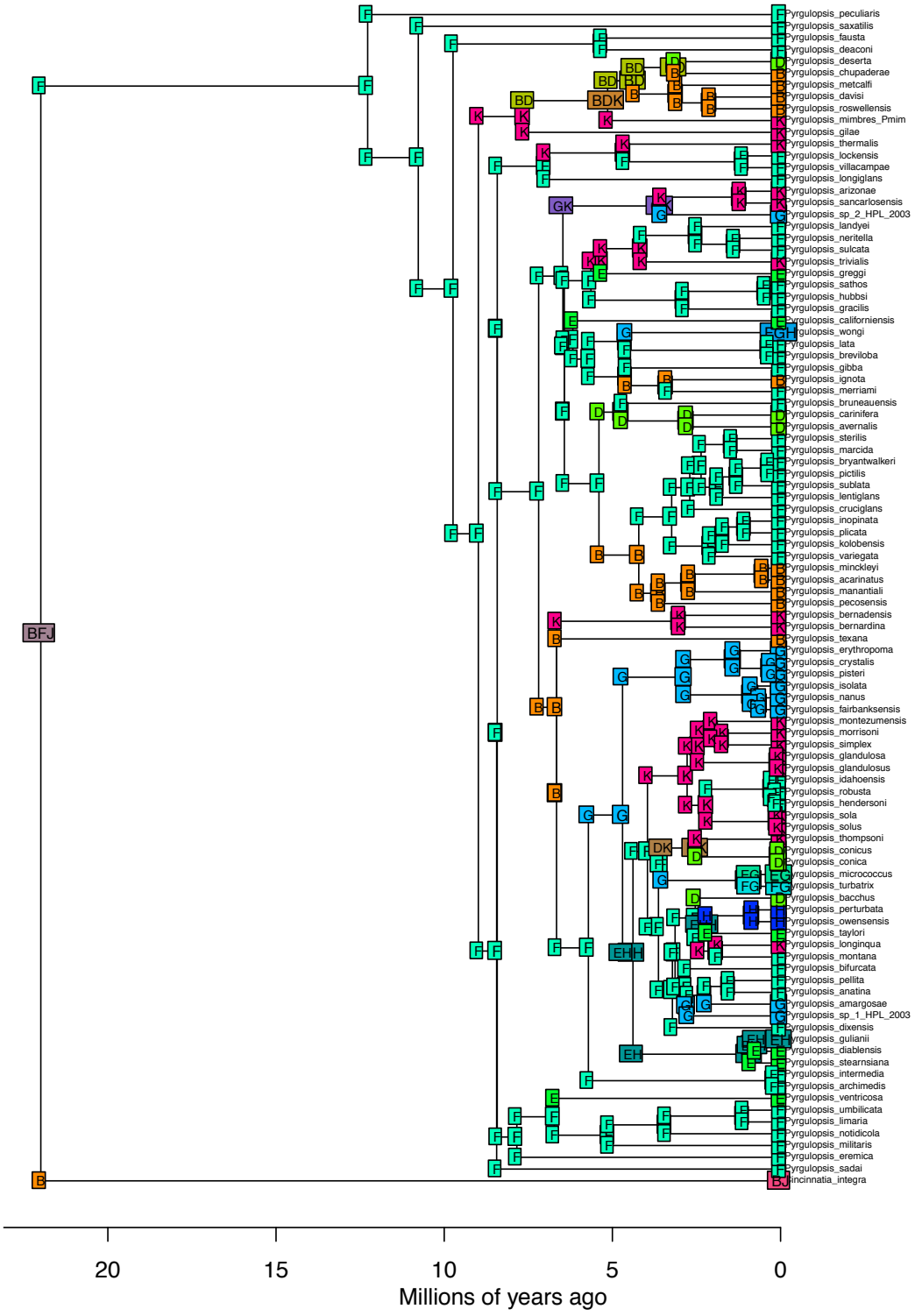

BioGeoBEARS DEC+J_constrained on Pyrgulopsis M3
anstates: global optim, 4 areas max. d=0.006; e=0.016; j=0.024; LnL=−187.7

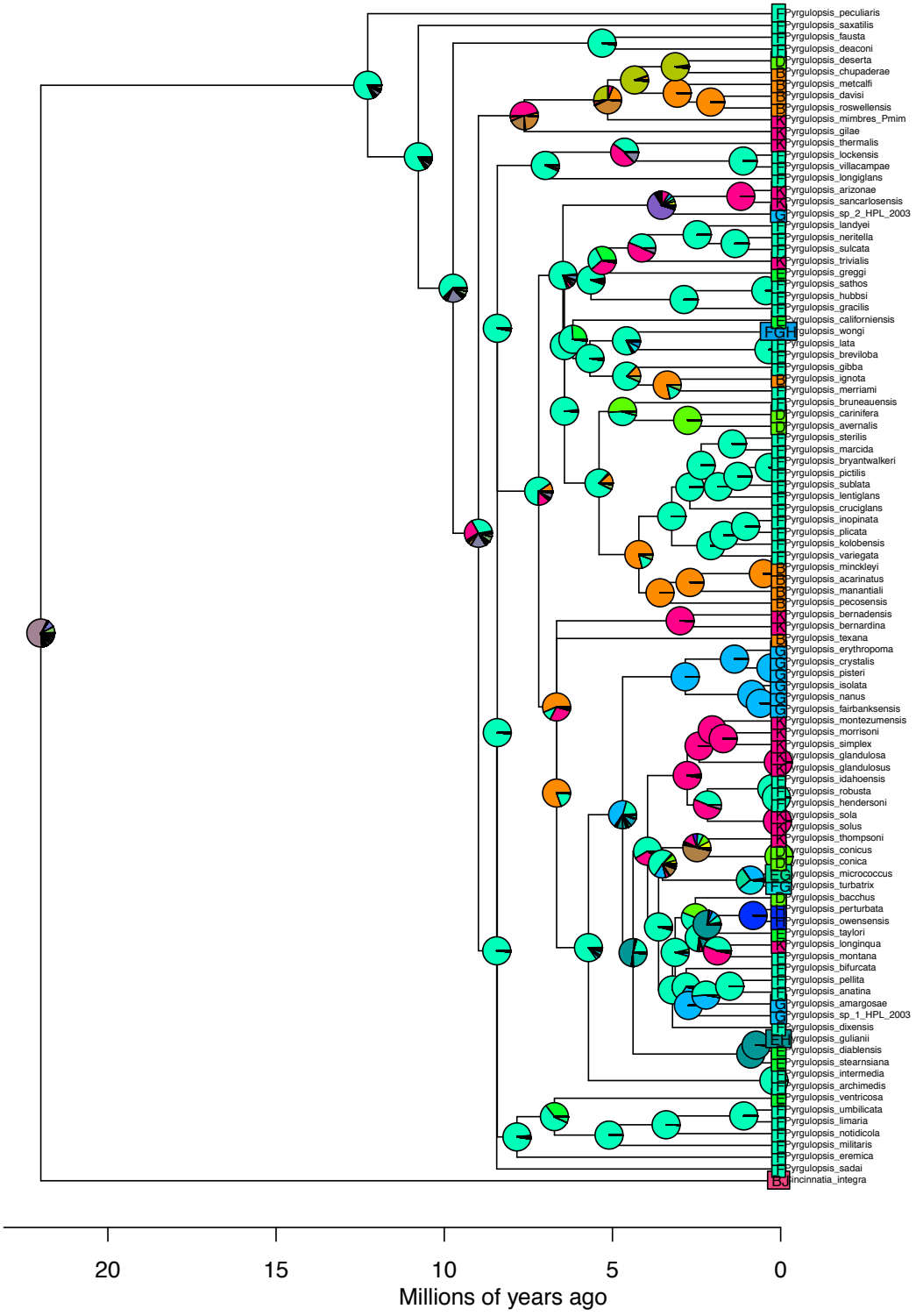

BioGeoBEARS DEC_distances on Pyrgulopsis M4
anstates: global optim, 4 areas max. d=0.009; e=0.042; x=0.116; j=0; LnL=−203.4

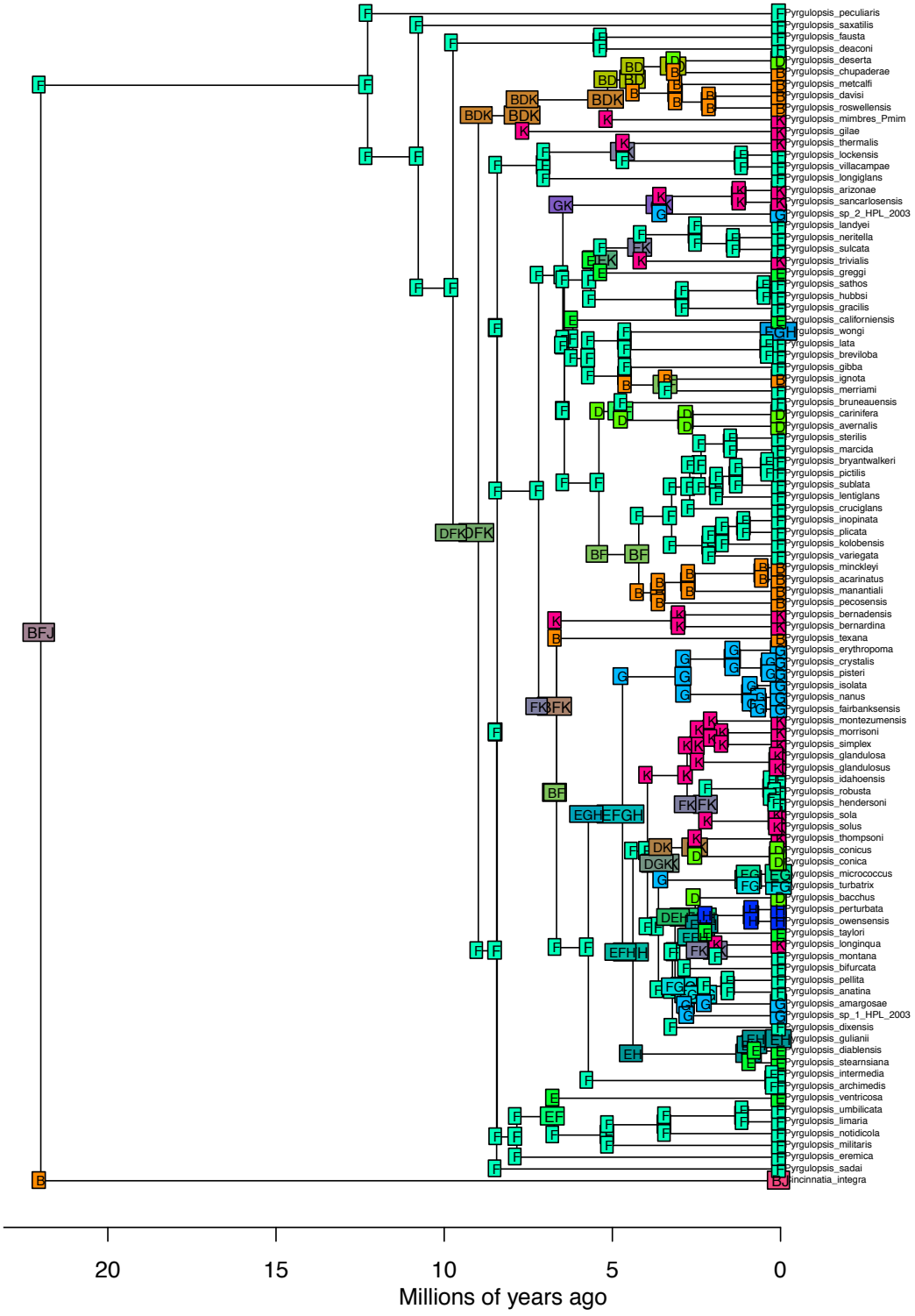

BioGeoBEARS DEC_distances on Pyrgulopsis M4
anstates: global optim, 4 areas max. d=0.009; e=0.042; x=0.116; j=0; LnL=−203.4

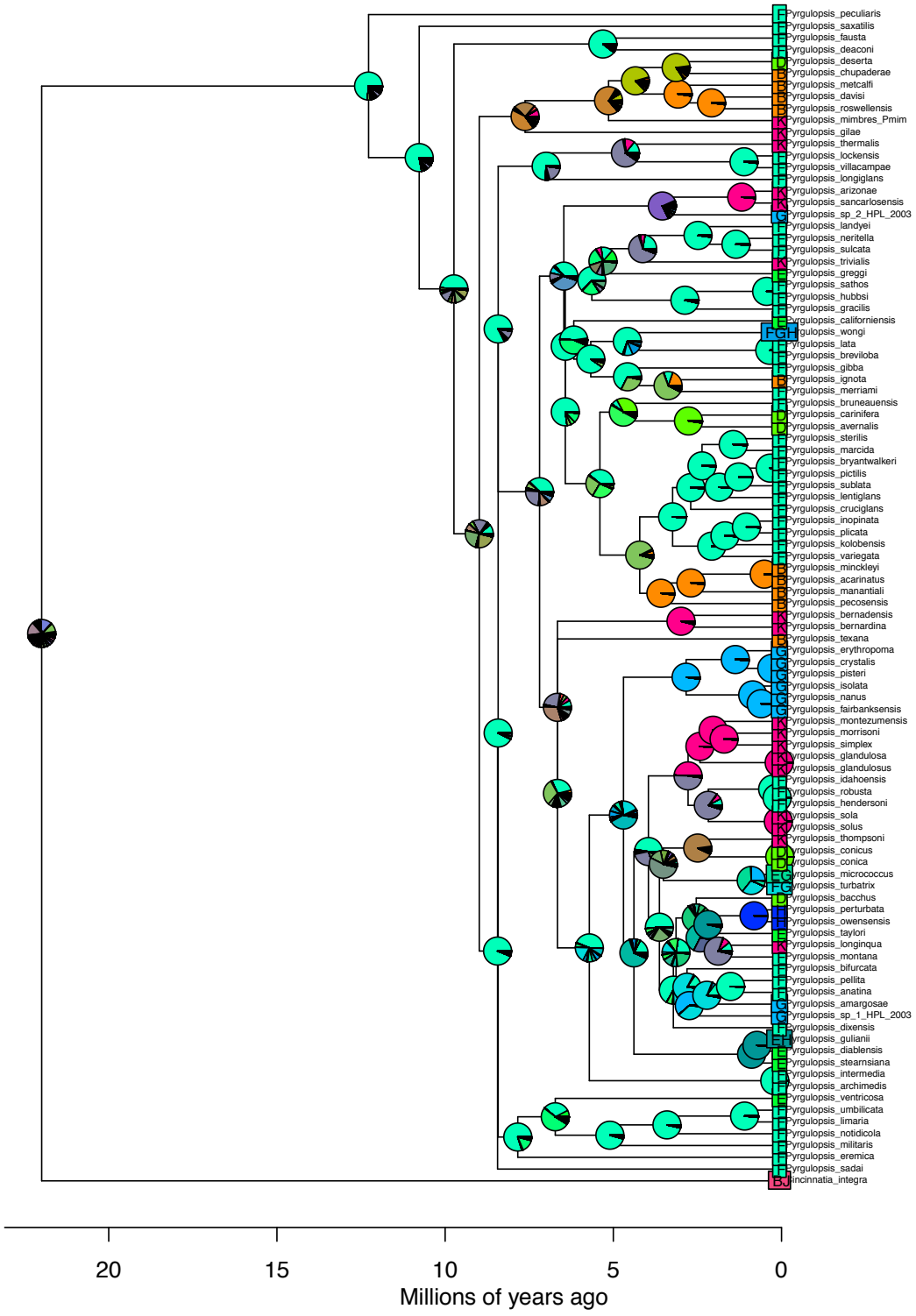

BioGeoBEARS DEC+J_distances on Pyrgulopsis M4
anstates: global optim, 4 areas max. d=0.006; e=0.016; x=0.003; j=0.024; LnL=−187.7

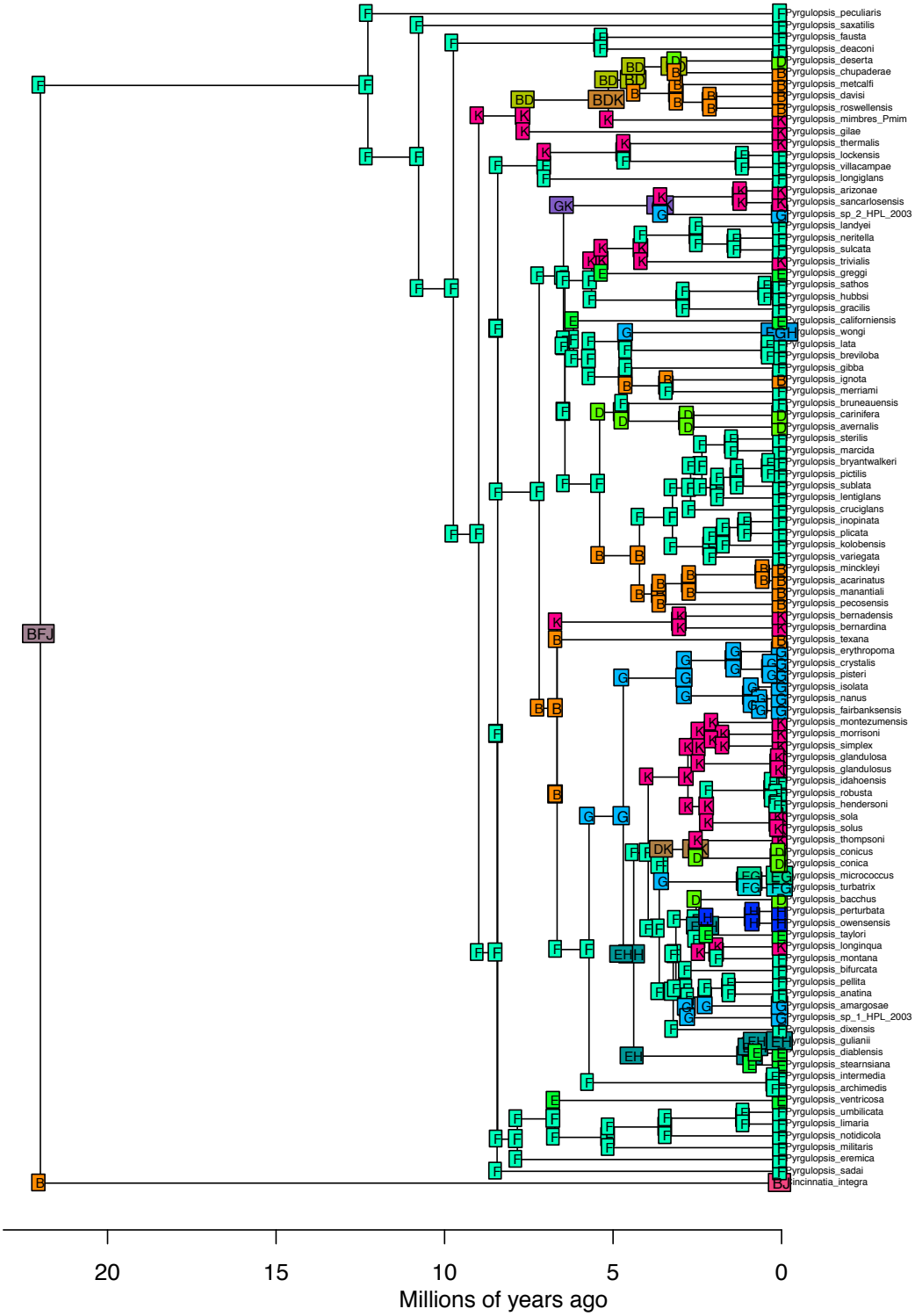

BioGeoBEARS DEC+J_distances on Pyrgulopsis M4
anstates: global optim, 4 areas max. d=0.006; e=0.016; x=0.003; j=0.024; LnL=−187.7

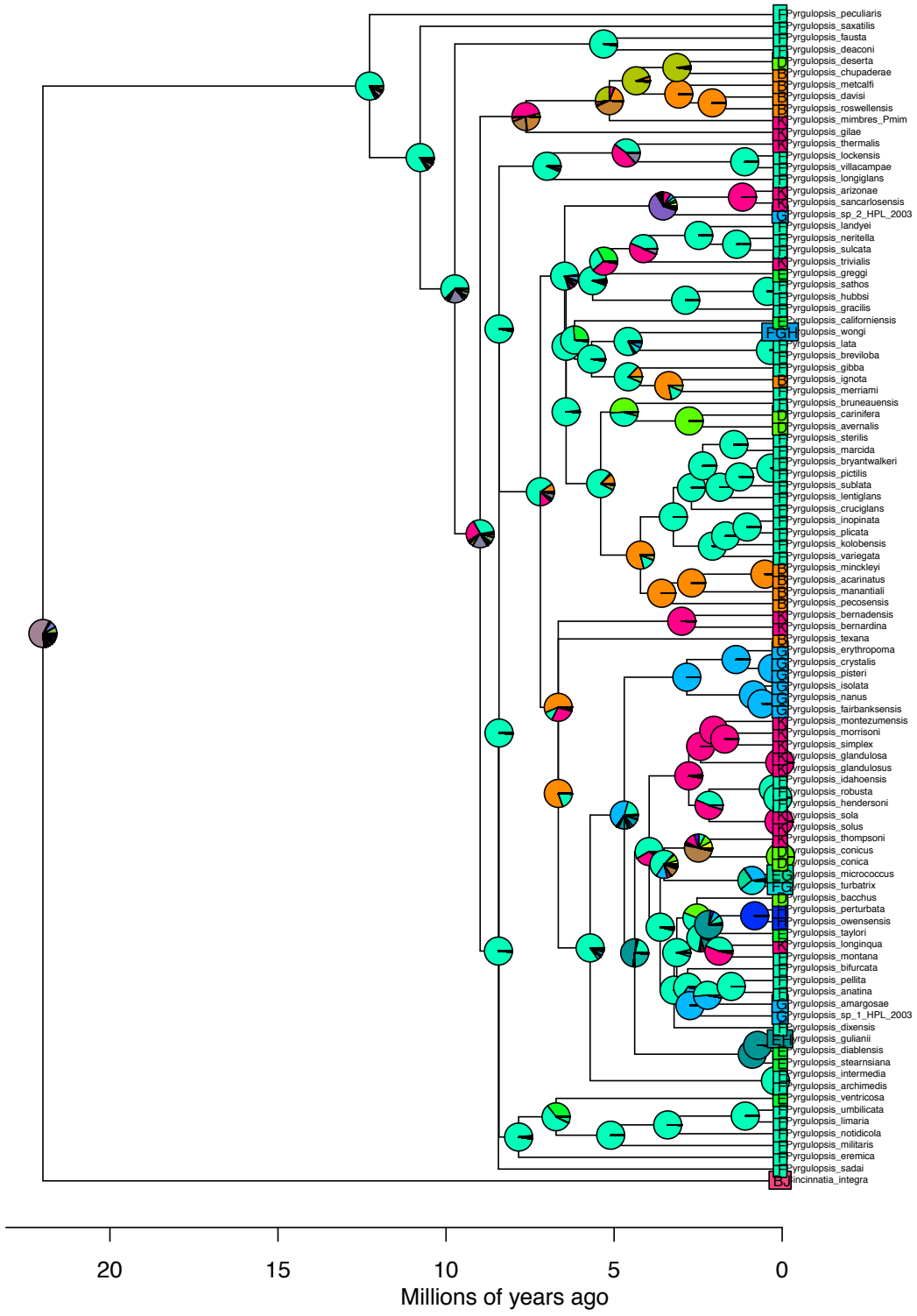

BioGeoBEARS DEC on Tyronia M3
anstates: global optim, 4 areas max. d=0.078; e=0.19; j=0; LnL=–105

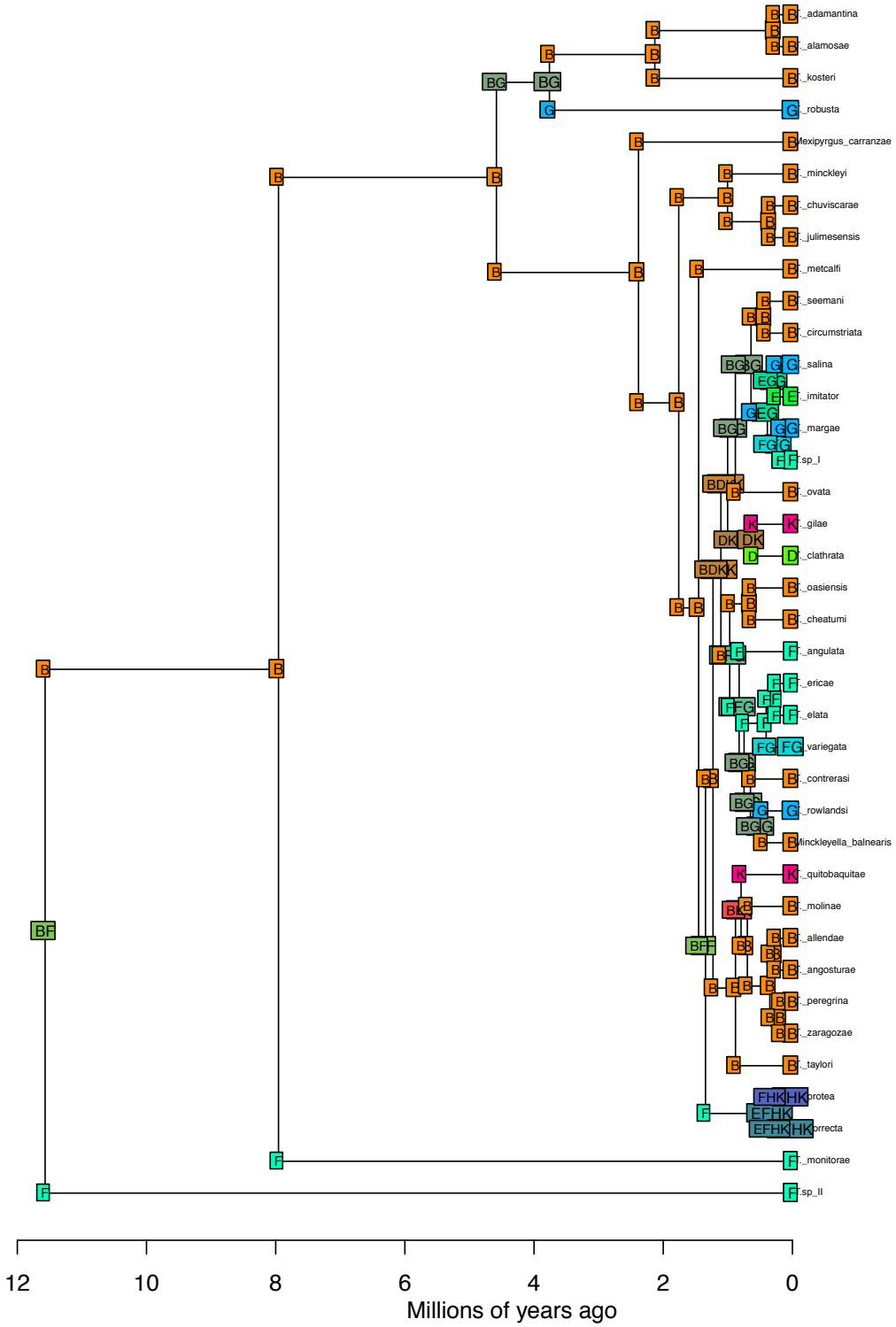

BioGeoBEARS DEC on Tyronia M3
anstates: global optim, 4 areas max. d=0.078; e=0.19; j=0; LnL=−105

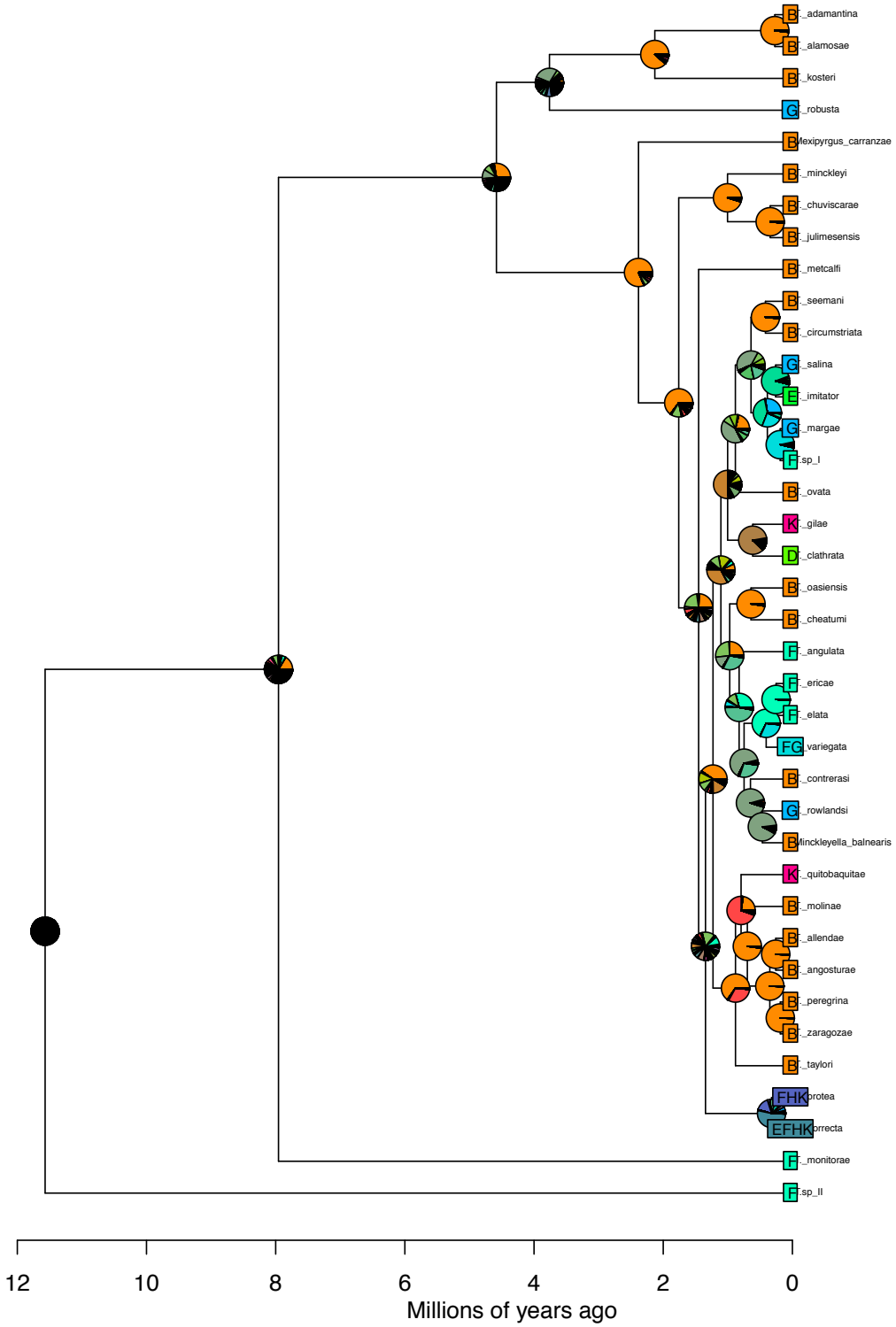

BioGeoBEARS DEC+J on Tyronia M3
anstates: global optim, 4 areas max. d=0.049; e=0.112; j=0.068; LnL=–95.5

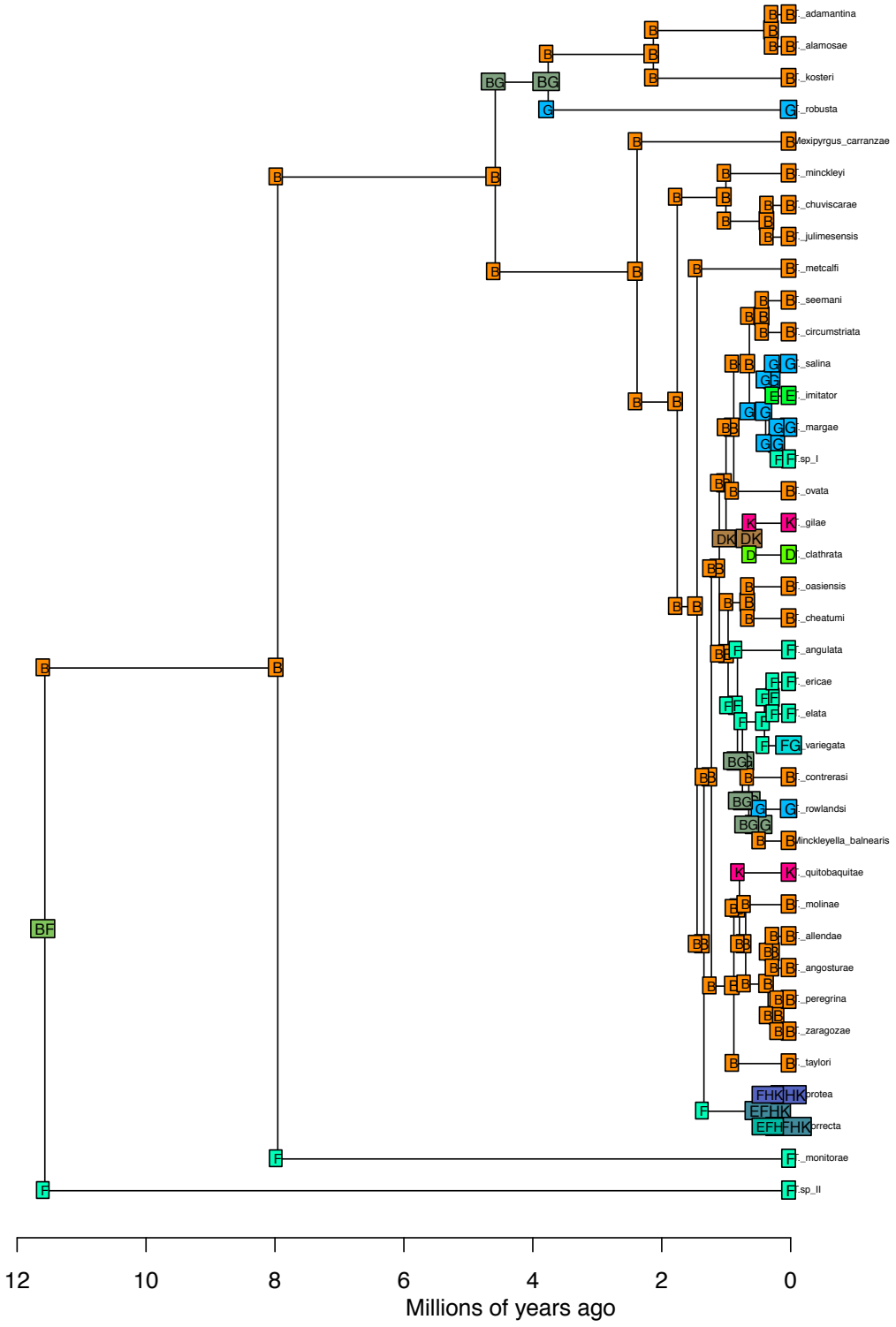

BioGeoBEARS DEC+J on Tyronia M3
anstates: global optim, 4 areas max. d=0.049; e=0.112; j=0.068; LnL=–95.5

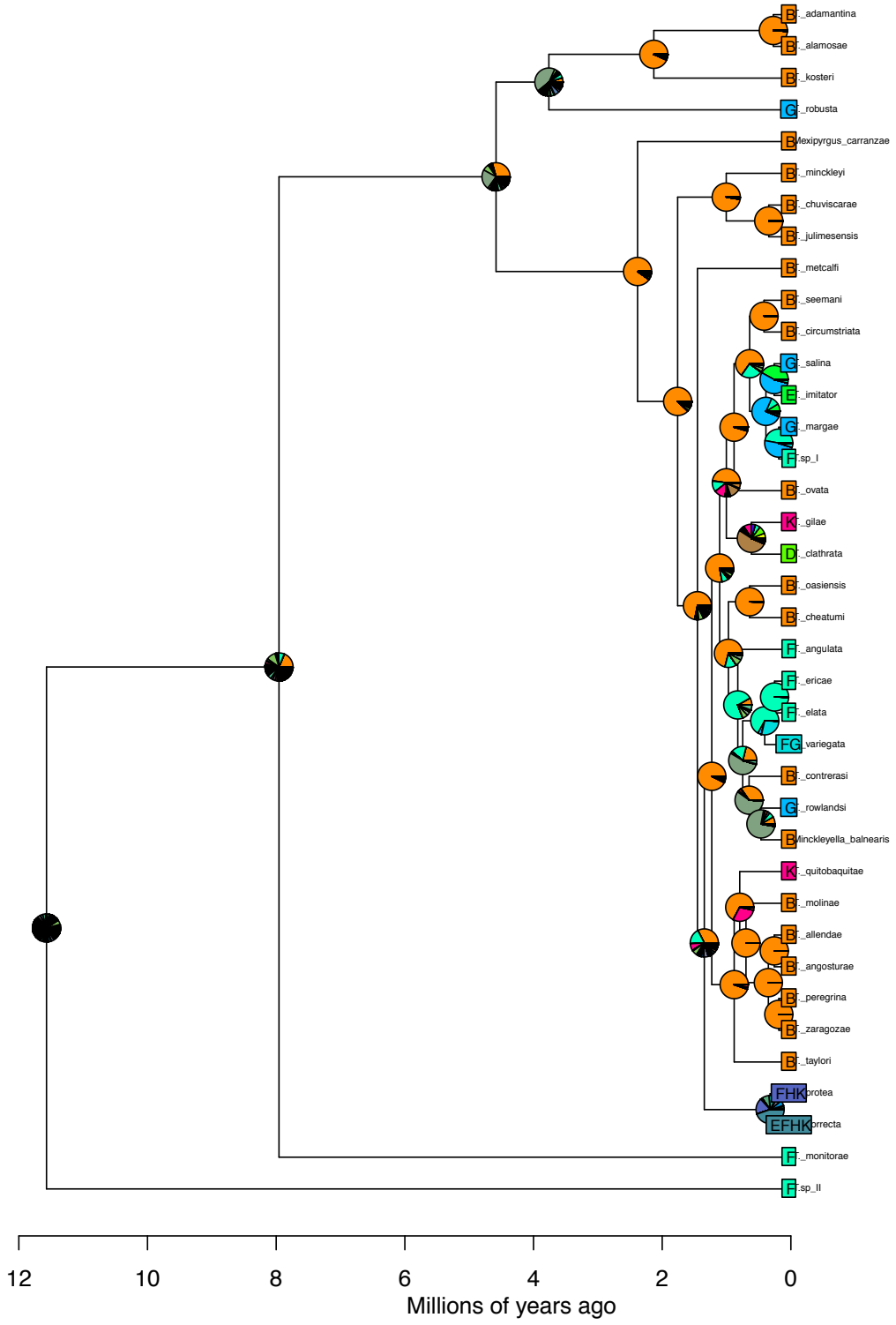

BioGeoBEARS DEC_constrained on Tyronia M3
anstates: global optim, 4 areas max. d=0.078; e=0.19; j=0; LnL=−105

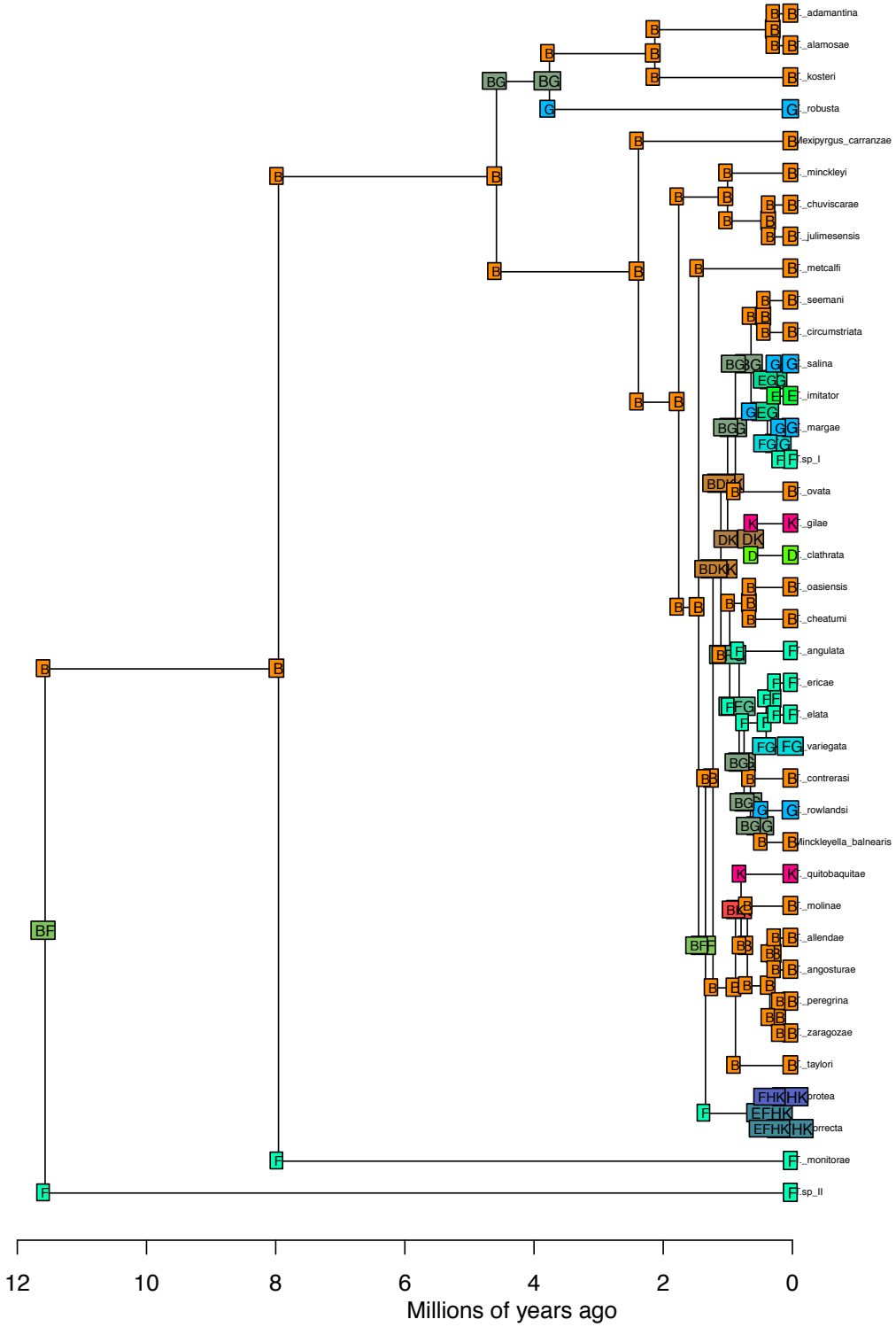

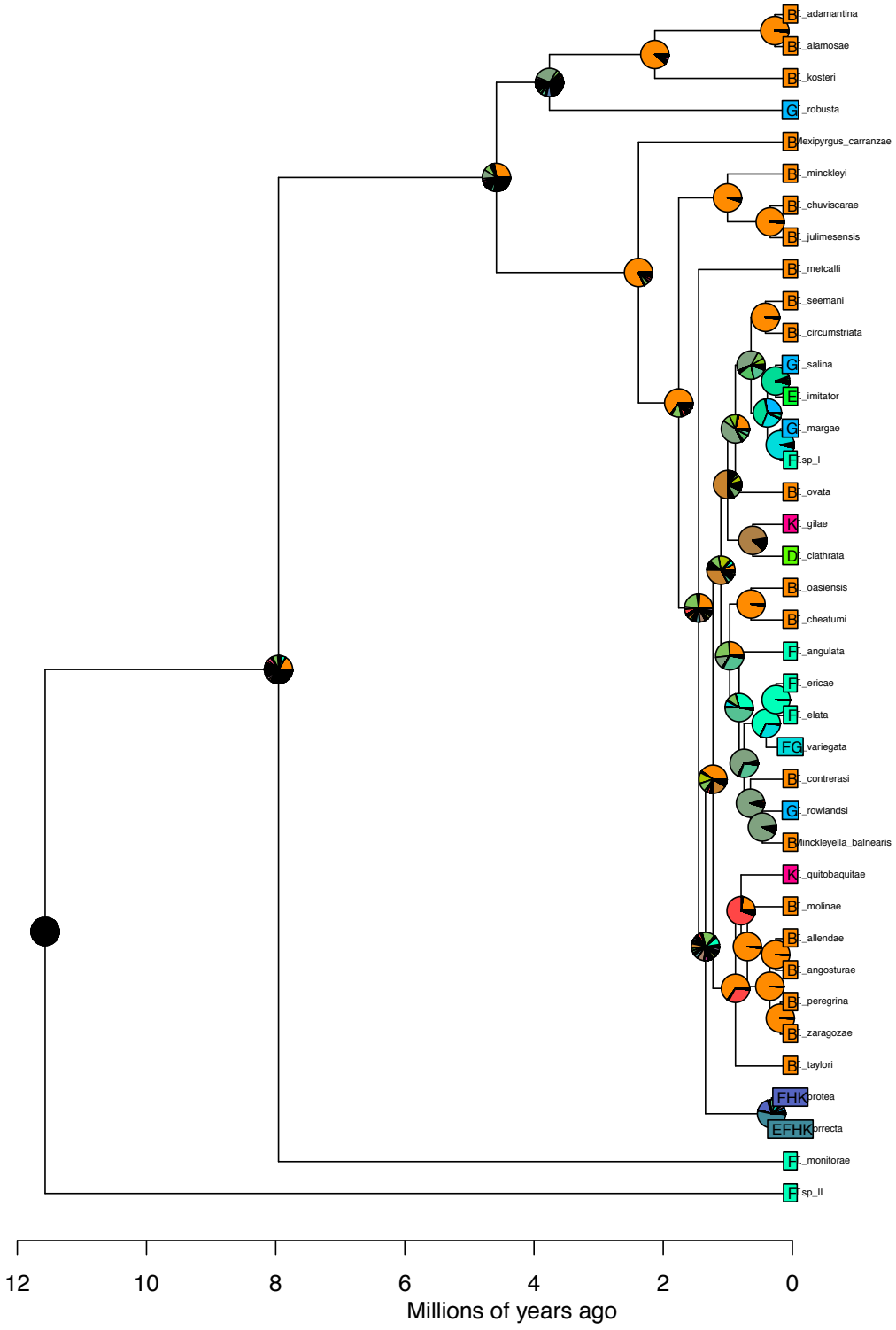
BioGeoBEARS DEC_constrained on Tyronia M3
anstates: global optim, 4 areas max. d=0.078; e=0.19; j=0; LnL=-105
B_adamantina
B_alamosae
B_kosteri
G_robusta
Bmexipyrgus_carranzae
B_minckleyi
B_chuviscarae
B_julimesensis
B_metcalfi
B_seemani
B_circumstriata
G_salina
E_imitator
G_margae
F_sp_I
B_ovata
K_gilae
D_clathrata
B_oasiensis
B_cheatumi
F_angulata
F_ericae
F_elata
FG_variegata
B_contrerasi
G_rowlandsi
Bminckleyella_balnearis
K_quitobaquitae
B_molinae
B_allendae
B_angosturae
B_peregrina
B_zaragozae
B_taylori
FHKprotea
EFHKbrrecta
F_monitorae
F_sp_II
12
10
8
6
4
2
0
Millions of years ago

BioGeoBEARS DEC+J_constrained on Tyronia M3
anstates: global optim, 4 areas max. d=0.049; e=0.112; j=0.068; LnL=–95.5

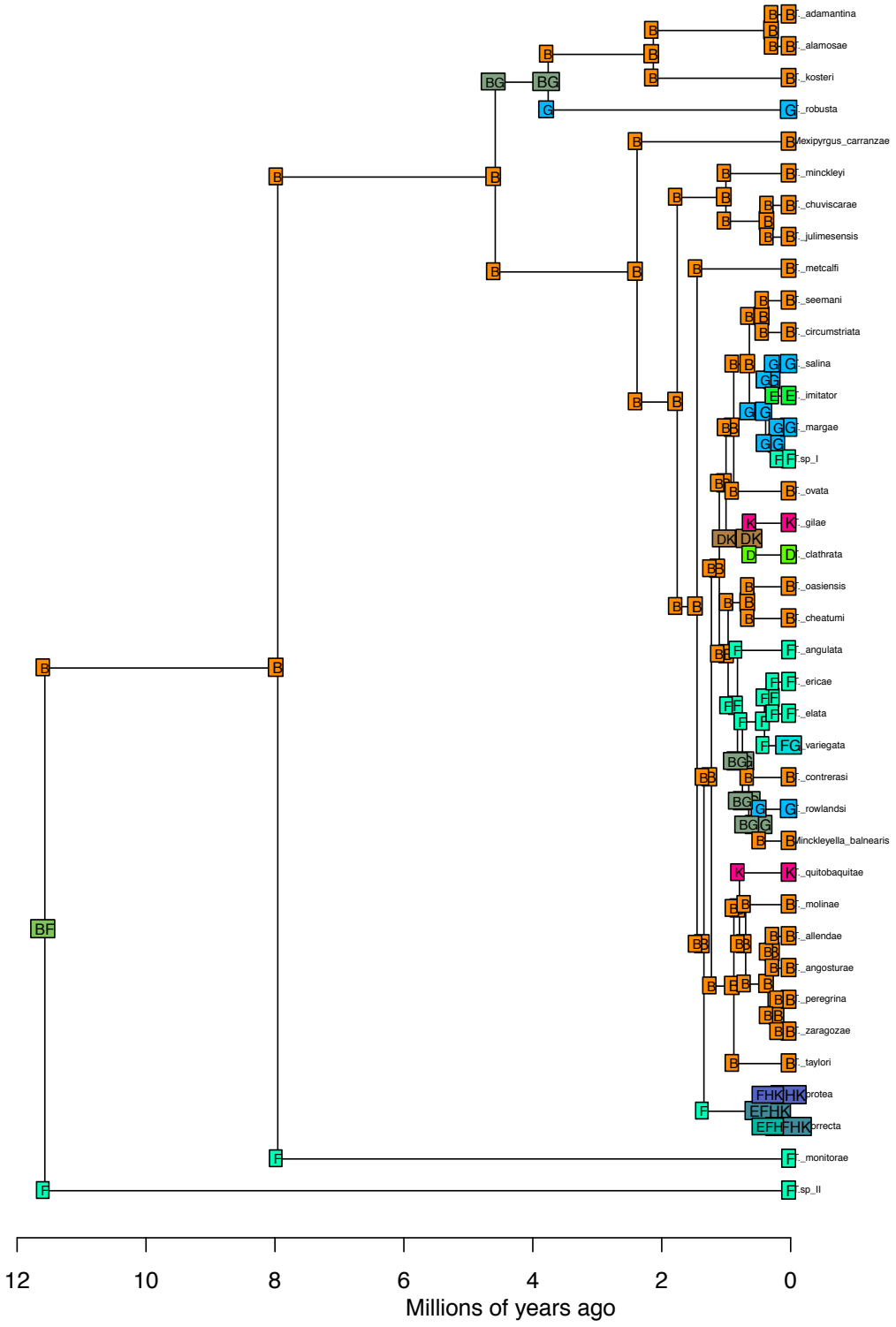

BioGeoBEARS DEC+J_constrained on Tyronia M3
anstates: global optim, 4 areas max. d=0.049; e=0.112; j=0.068; LnL=–95.5

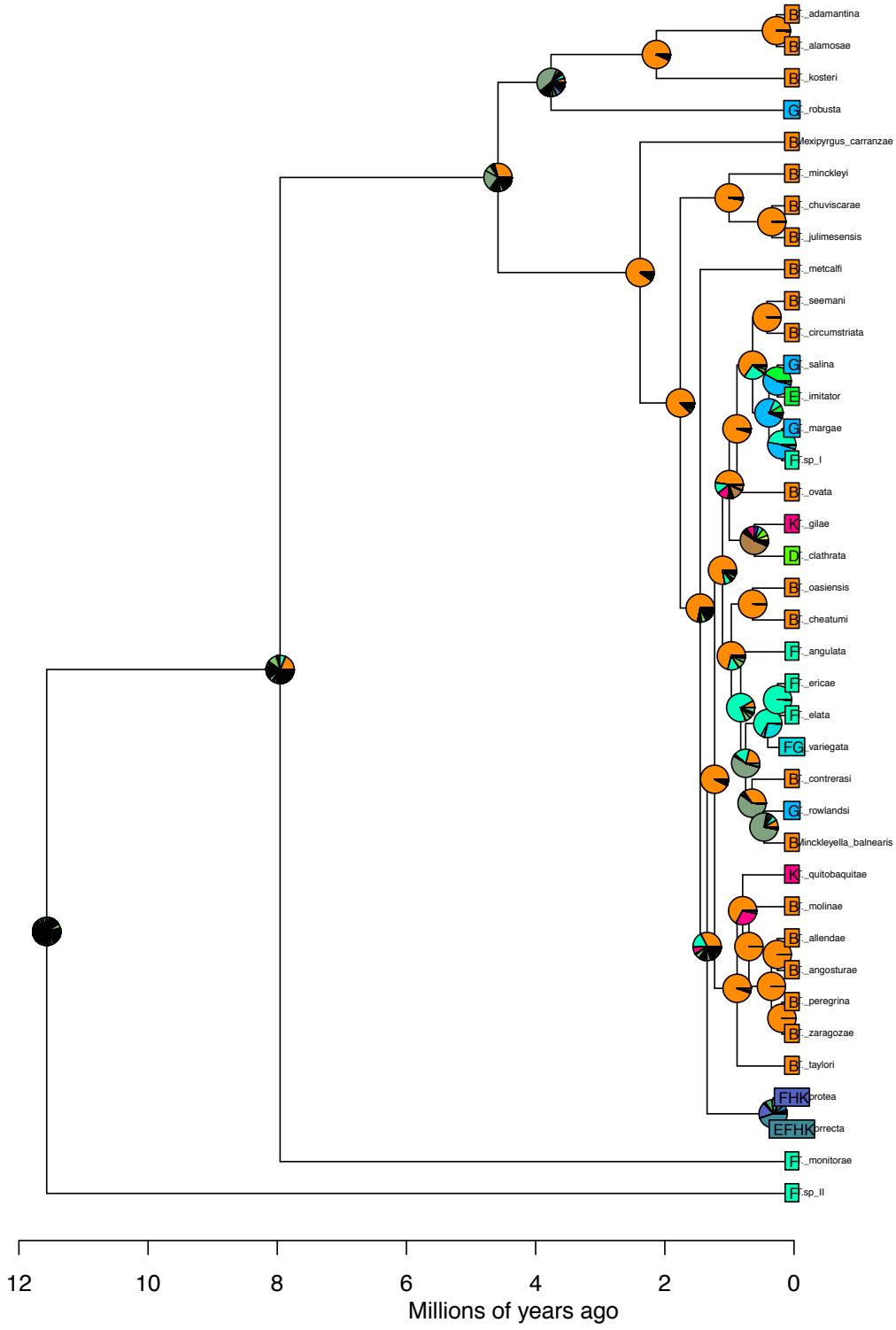

BioGeoBEARS DEC_distances on Tyronia M4
anstates: global optim, 4 areas max. d=0.049; e=0.193; x=0.15; j=0; LnL=−104.7

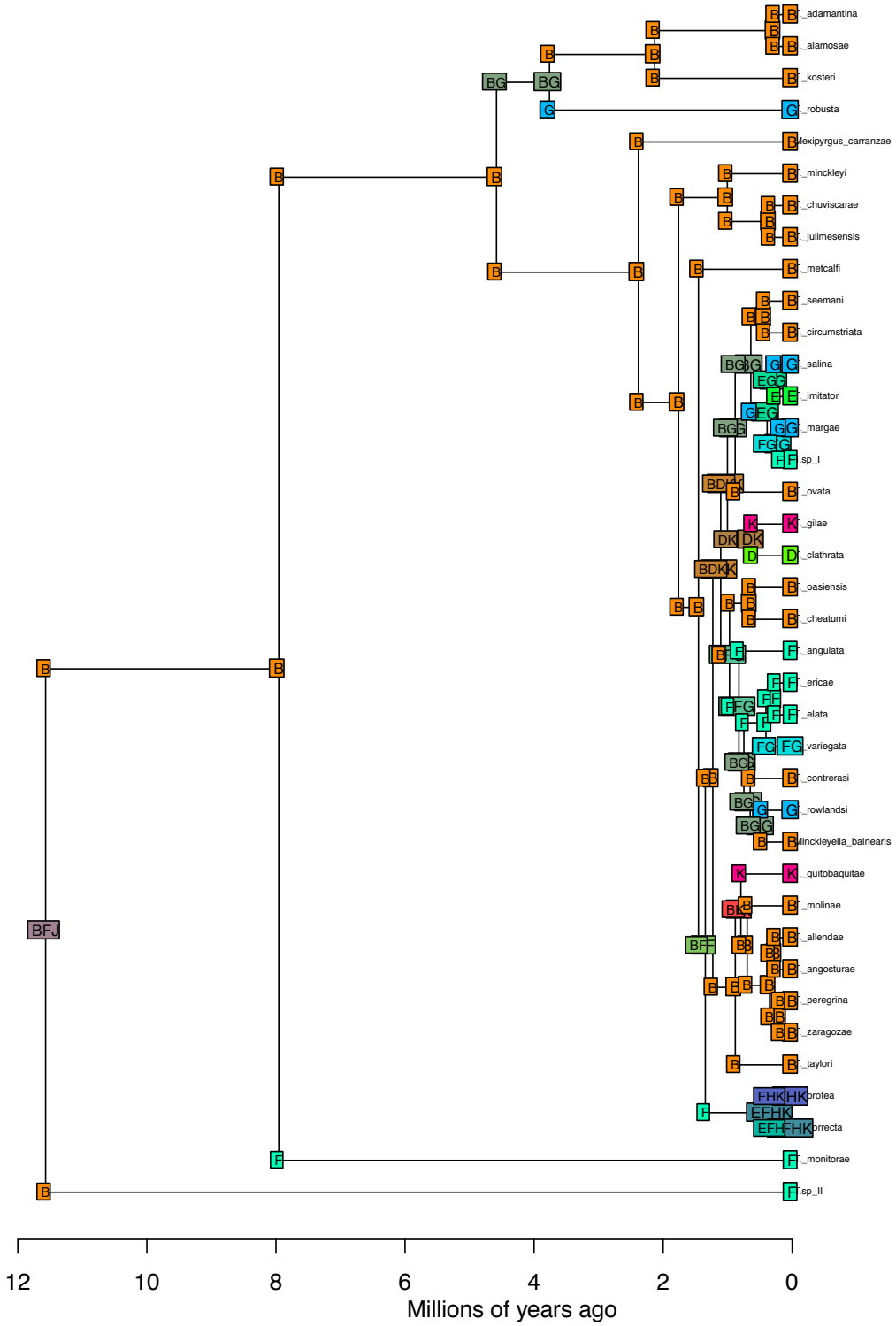

BioGeoBEARS DEC_distances on Tyronia M4
anstates: global optim, 4 areas max. d=0.049; e=0.193; x=0.15; j=0; LnL=−104.7

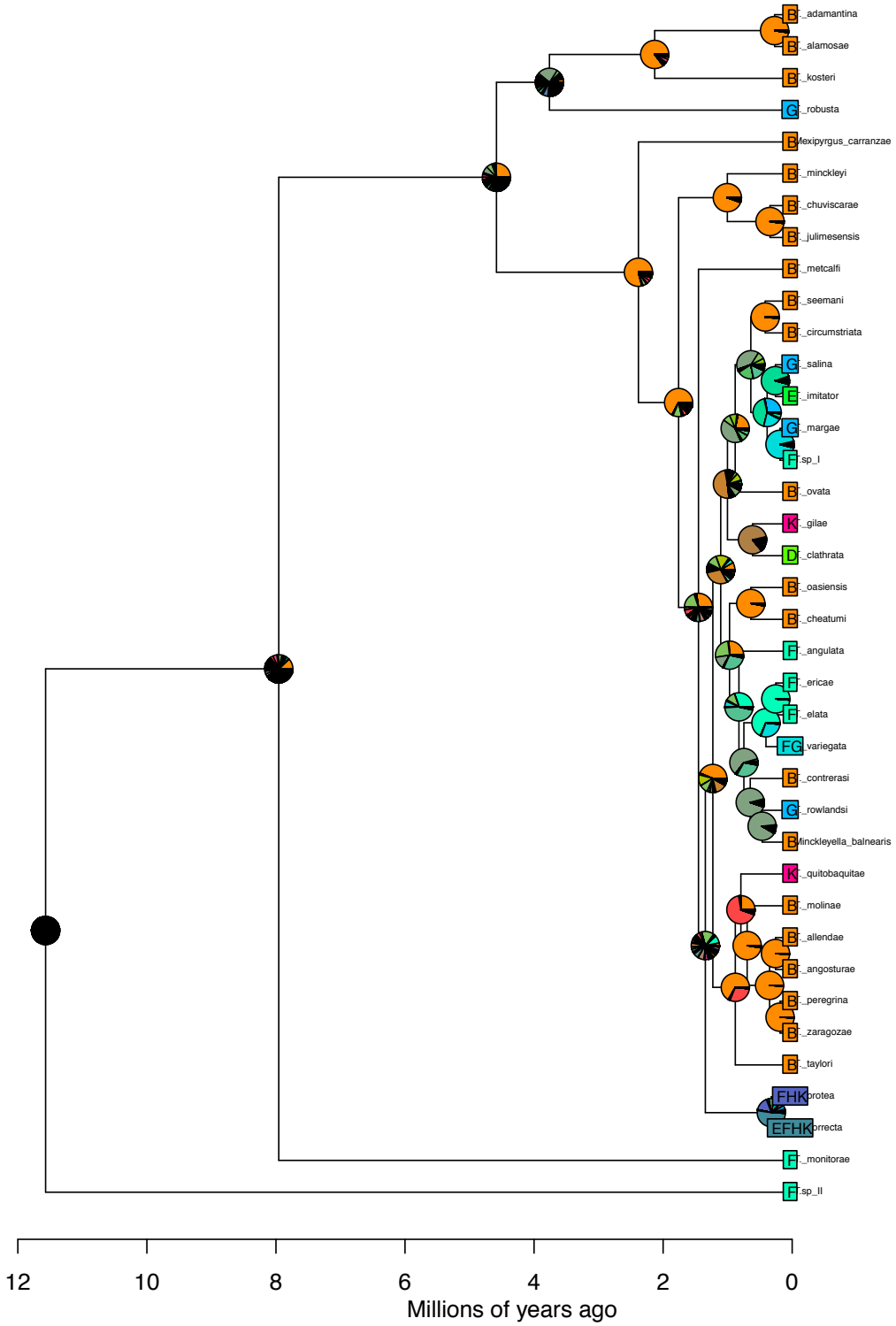

BioGeoBEARS DEC+J_distances on Tyronia M4
anstates: global optim, 4 areas max. d=0.048; e=0.104; x=0.083; j=0.067; LnL=–95.5

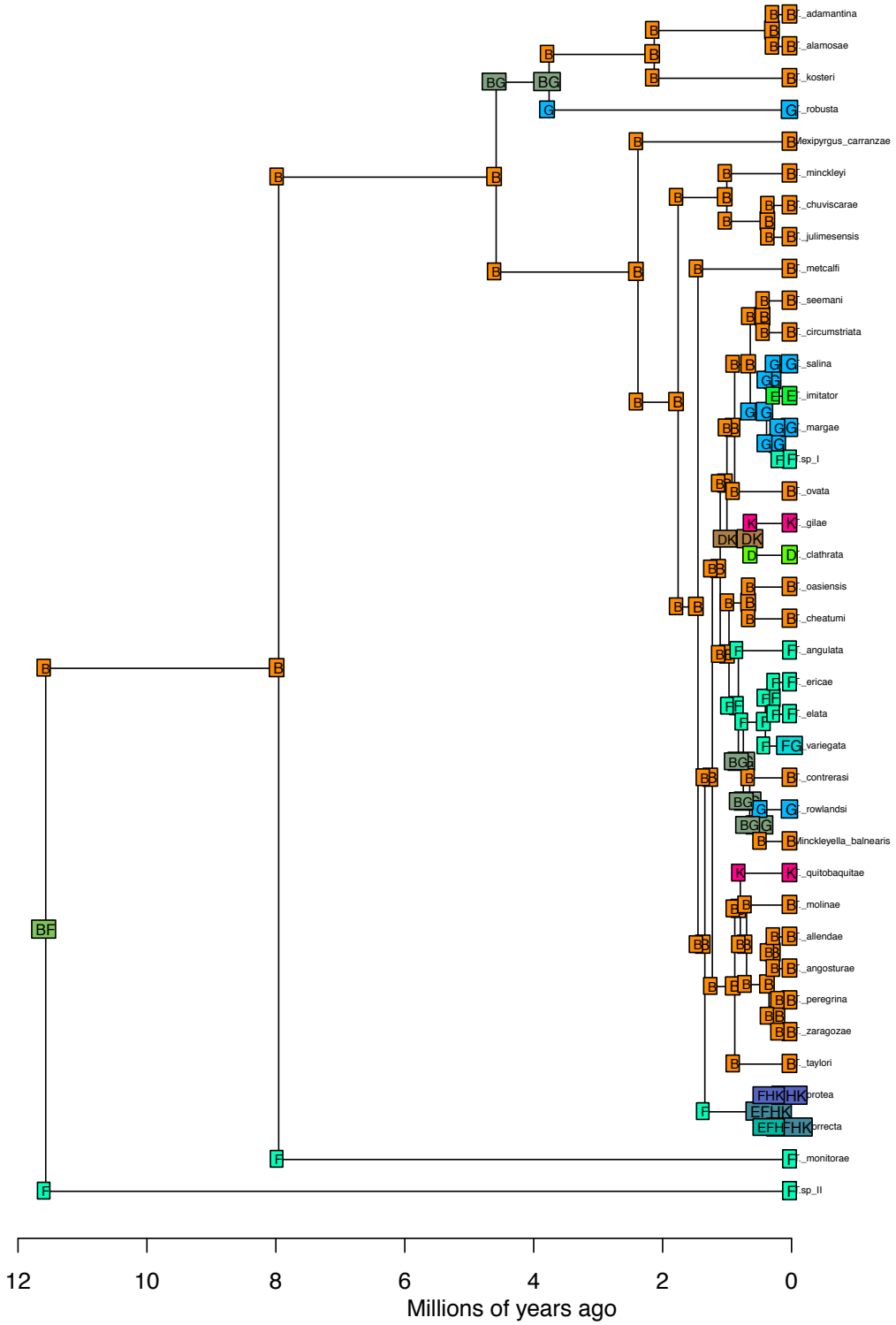

BioGeoBEARS DEC+J_distances on Tyronia M4
anstates: global optim, 4 areas max. d=0.048; e=0.104; x=0.083; j=0.067; LnL=–95.5

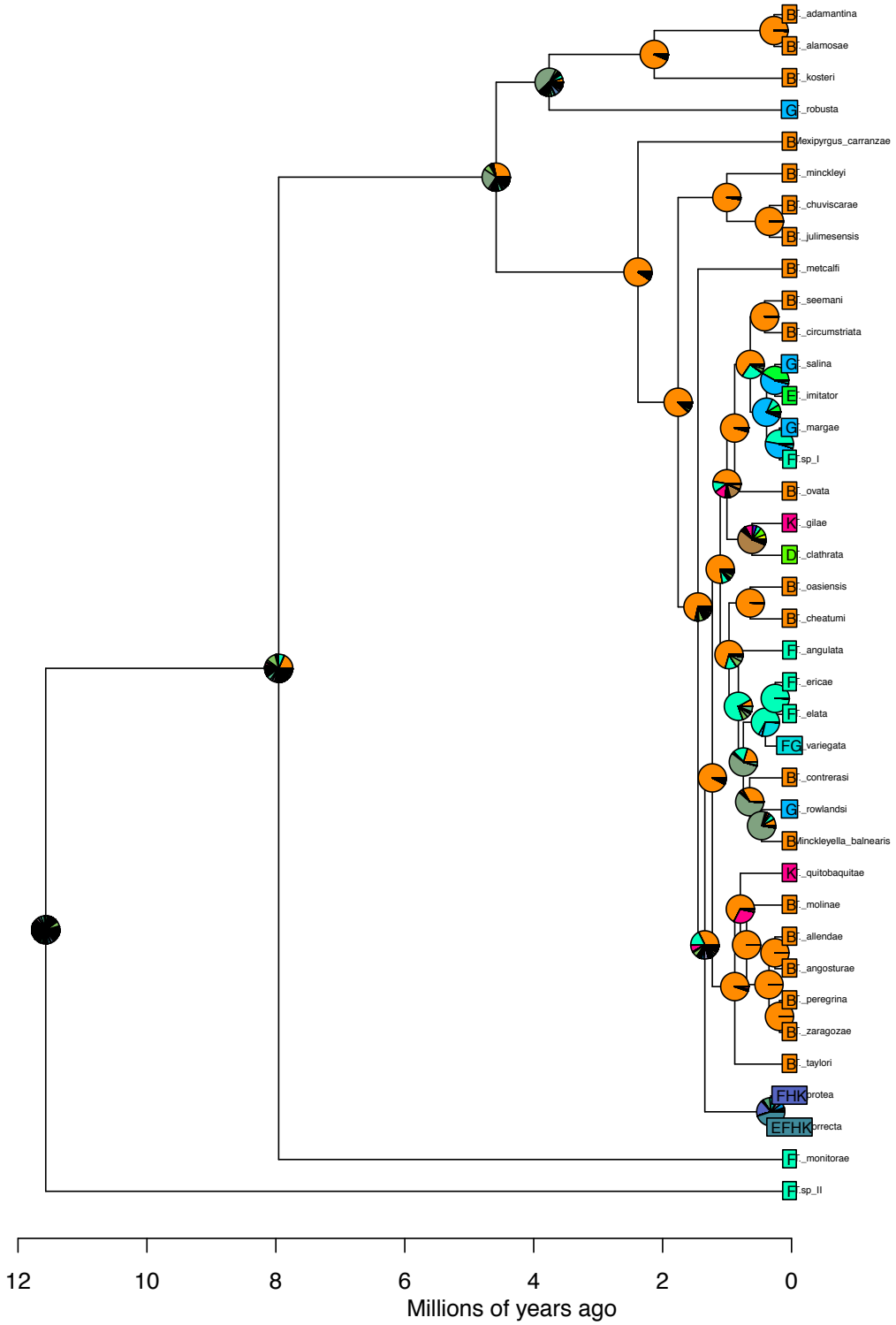

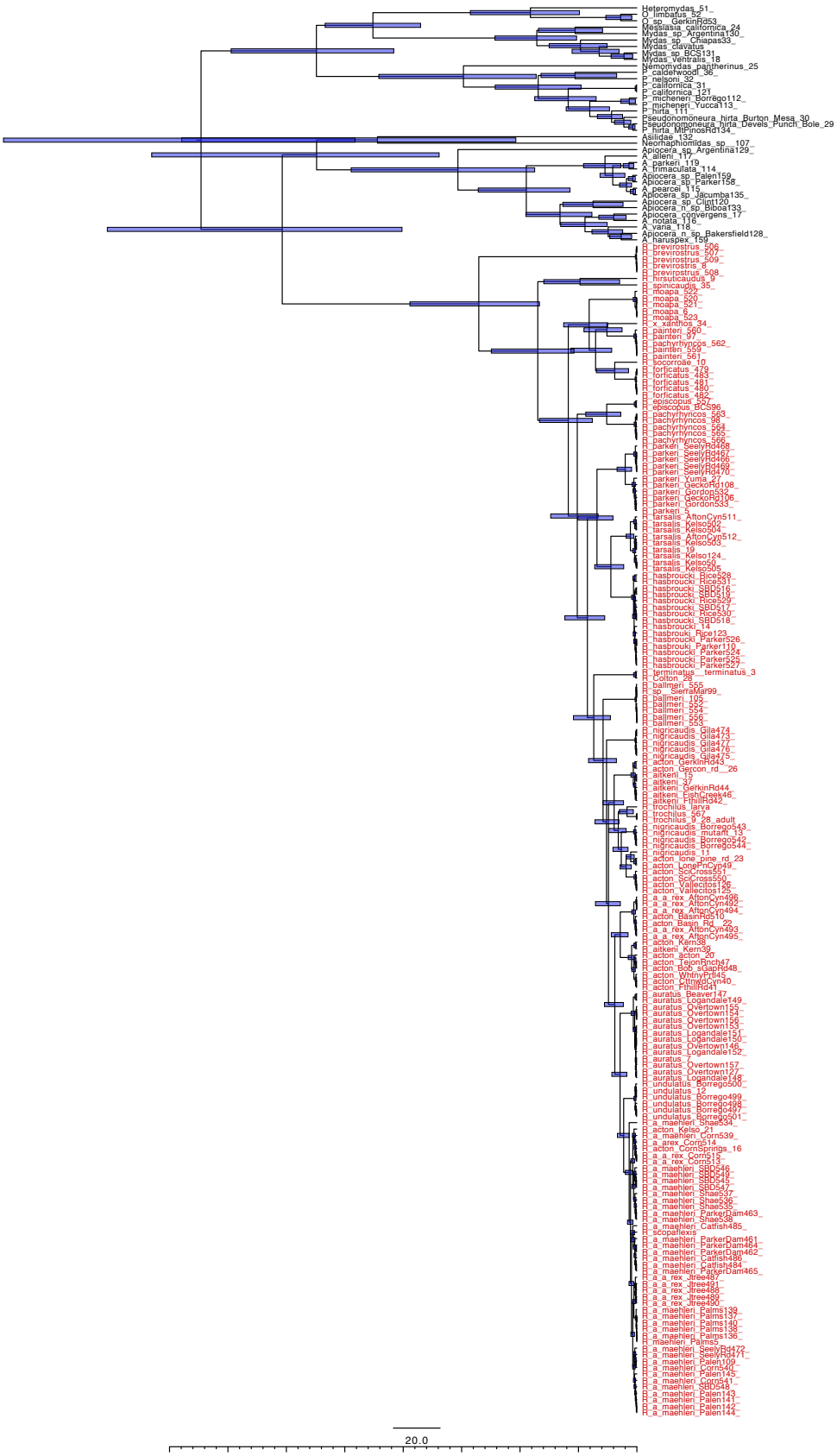
Heteromydas_51_
O_limbatus_52_
O_sp._GerkinRd53_
Nesiasia_californica_24_
Mydas_sp._Argentina130_
Mydas_sp._Chiapas33_
Mydas_clavatus_
Mydas_sp._BCS131_
Mydas_Ventralis_18_
Nemomydas_pantherinus_25_
P._caldelwoodi_36_
P._heljoni_32_
P._californica_31_
P._californica_121_
P._micheneri_Borrego112_
P._micheneri_Yucca113_
P._hirta_111_
Pseudonomoneura_hirta_Burton_Mesa_30_
Pseudonomoneura_hirta_Devels_Punch_Bole_29_
P._hirta_MtPinosRd134_
Asilidae_132_
Neorhaphiomitidas_sp._107_
Apiocera_sp._Argentina129_
A._alieni_117_
A._parkeri_119_
A._trimaculata_114_
Apiocera_sp._Palen159_
Apiocera_sp._Parker158_
A._pearcei_115_
Apiocera_sp._Jacumba135_
Apiocera_sp._Clint120_
Apiocera_n._sp._Biboa133_
Apiocera_convergens_17_
A._notata_116_
A._varia_118_
Apiocera_n._sp._Bakersfield128_
A._haruspex_139_
R._brevirostrus_506_
R._brevirostrus_507_
R._brevirostrus_509_
R._brevirostris_6_
R._brevirostrus_508_
R._hirsuticaudus_9_
R._spinicaudis_35_
R._moapa_522_
R._moapa_520_
R._moapa_521_
R._moapa_6_
R._moapa_523_
R._x_xanthos_34_
R._painteri_560_
R._painteri_97_
R._pachyrhynchos_562_
R._painteri_559_
R._painteri_561_
R._socorroae_10_
R._torficatus_479_
R._torficatus_483_
R._torficatus_481_
R._torficatus_480_
R._torficatus_482_
R._episcopus_567_
R._episcopus_BCS96_
R._pachyrhynchos_563_
R._pachyrhynchos_98_
R._pachyrhynchos_564_
R._pachyrhynchos_565_
R._pachyrhynchos_566_
R._parkeri_SeelyRd468_
R._parkeri_SeelyRd467_
R._parkeri_SeelyRd466_
R._parkeri_SeelyRd469_
R._parkeri_SeelyRd470_
R._parkeri_Yuma_27_
R._parkeri_GeckoRd108_
R._parkeri_Gordon532_
R._parkeri_GeckoRd106_
R._parkeri_Gordon533_
R._parkeri_5_
R._tarsalis_AftonCyn511_
R._tarsalis_Kelso502_
R._tarsalis_Kelso504_
R._tarsalis_AftonCyn512_
R._tarsalis_Kelso503_
R._tarsalis_19_
R._tarsalis_Kelso124_
R._tarsalis_Kelso502_
R._tarsalis_Kelso505_
R._hasbroucki_Rice528_
R._hasbroucki_Rice531_
R._hasbroucki_SBD516_
R._hasbroucki_SBD519_
R._hasbroucki_Rice529_
R._hasbroucki_SBD517_
R._hasbroucki_Rice530_
R._hasbroucki_SBD518_
R._hasbroucki_14_
R._hasbroucki_Rice123_
R._hasbroucki_Parker526_
R._hasbroucki_Parker110_
R._hasbroucki_Parker524_
R._hasbroucki_Parker525_
R._hasbroucki_Parker527_
R._terminatus_terminatus_3_
R._Colton_28_
R._ballmeri_555_
R._sp._SierraMar99_
R._ballmeri_105_
R._ballmeri_552_
R._ballmeri_554_
R._ballmeri_556_
R._ballmeri_553_
R._nigricaudis_Gila474_
R._nigricaudis_Gila473_
R._nigricaudis_Gila477_
R._nigricaudis_Gila476_
R._nigricaudis_Gila475_
R._acton_GerkinRd43_
R._acton_Gercon_rd__26_
R._aitkeni_15_
R._aitkeni_37_
R._aitkeni_GerkinRd44_
R._aitkeni_FishCreek46_
R._aitkeni_PhillRd42_
R._trochilus_larva_
R._trochilus_561_
R._trochilus_9_28_adult_
R._nigricaudis_Borrego543_
R._nigricaudis_mutant_13_
R._nigricaudis_Borrego542_
R._nigricaudis_Borrego544_
R._nigricaudis_11_
R._acton_lone_pine_rd_23_
R._acton_LonePnCyn549_
R._acton_SciCross551_
R._acton_SciCross550_
R._acton_Vallecitos126_
R._acton_Vallecitos125_
R._a_a_rex_AftonCyn496_
R._a_a_rex_AftonCyn492_
R._a_a_rex_AftonCyn494_
R._acton_BasinRd510_
R._acton_Basin_Rd__22_
R._a_a_rex_AftonCyn493_
R._a_a_rex_AftonCyn495_
R._acton_Kern38_
R._aitkeni_Kern39_
R._acton_acton_20_
R._acton_TejonRnch47_
R._acton_Bob_sGapRd48_
R._acton_WhitnyPt45_
R._acton_DuttonCyn40_
R._acton_PhillRd41_
R._auratus_Beaver147_
R._auratus_Logandale149_
R._auratus_Overtown152_
R._auratus_Overtown154_
R._auratus_Overtown156_
R._auratus_Overtown153_
R._auratus_Logandale151_
R._auratus_Logandale150_
R._auratus_Overtown146_
R._auratus_Logandale152_
R._auratus_2_
R._auratus_Overtown157_
R._auratus_Overtown127_
R._auratus_Logandale148_
R._undulatus_Borrego500_
R._undulatus_12_
R._undulatus_Borrego499_
R._undulatus_Borrego498_
R._undulatus_Borrego497_
R._undulatus_Borrego501_
R._a_maehleri_Shae534_
R._acton_Kelso_21_
R._a_maehleri_Corn539_
R._a_a_rex_Corn514_
R._acton_ComSprings_16_
R._a_a_rex_Corn515_
R._a_a_rex_Corn513_
R._a_maehleri_SBD546_
R._a_maehleri_SBD549_
R._a_maehleri_SBD545_
R._a_maehleri_SBD547_
R._a_maehleri_Shae537_
R._a_maehleri_Shae536_
R._a_maehleri_Shae535_
R._a_maehleri_ParkerDam463_
R._a_maehleri_Shae538_
R._a_maehleri_Catfish485_
R._scopaflexis_
R._a_maehleri_ParkerDam461_
R._a_maehleri_ParkerDam464_
R._a_maehleri_ParkerDam462_
R._a_maehleri_Catfish486_
R._a_maehleri_Catfish484_
R._a_maehleri_ParkerDam465_
R._a_a_rex__tree487_
R._a_a_rex_tree491_
R._a_a_rex_tree488_
R._a_a_rex_tree489_
R._a_a_rex_tree490_
R._a_maehleri_Palms139_
R._a_maehleri_Palms137_
R._a_maehleri_Palms140_
R._a_maehleri_Palms138_
R._a_maehleri_Palms136_
R._maehleri_Palms141_
R._a_maehleri_SeelyRd472_
R._a_maehleri_SeelyRd471_
R._a_maehleri_Palen109_
R._a_maehleri_Corn540_
R._a_maehleri_Palen145_
R._a_maehleri_Corn541_
R._a_maehleri_SBD548_
R._a_maehleri_Palen143_
R._a_maehleri_Palen141_
R._a_maehleri_Palen142_
R._a_maehleri_Palen144_
20.0
200.0
175.0
150.0
125.0
100.0
75.0
50.0
25.0
0.0

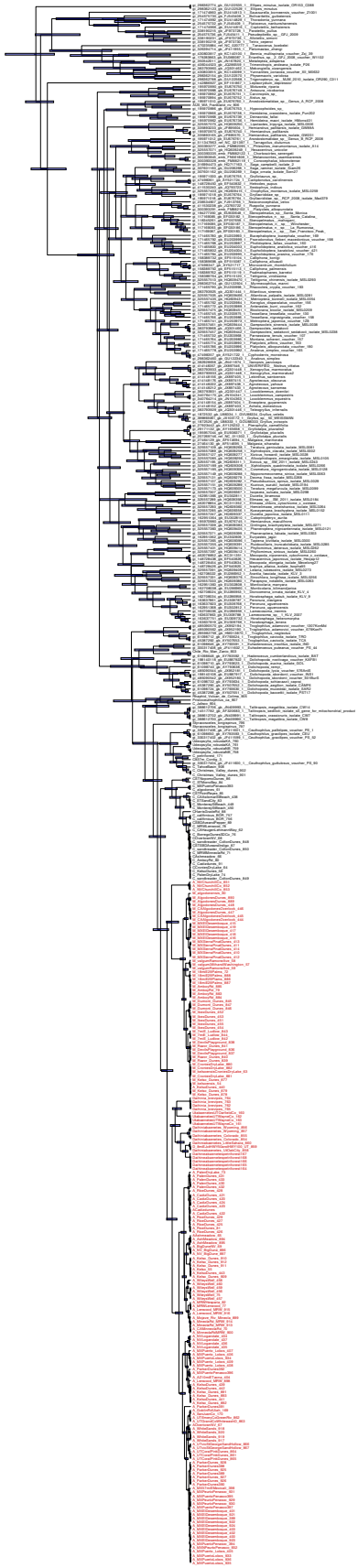

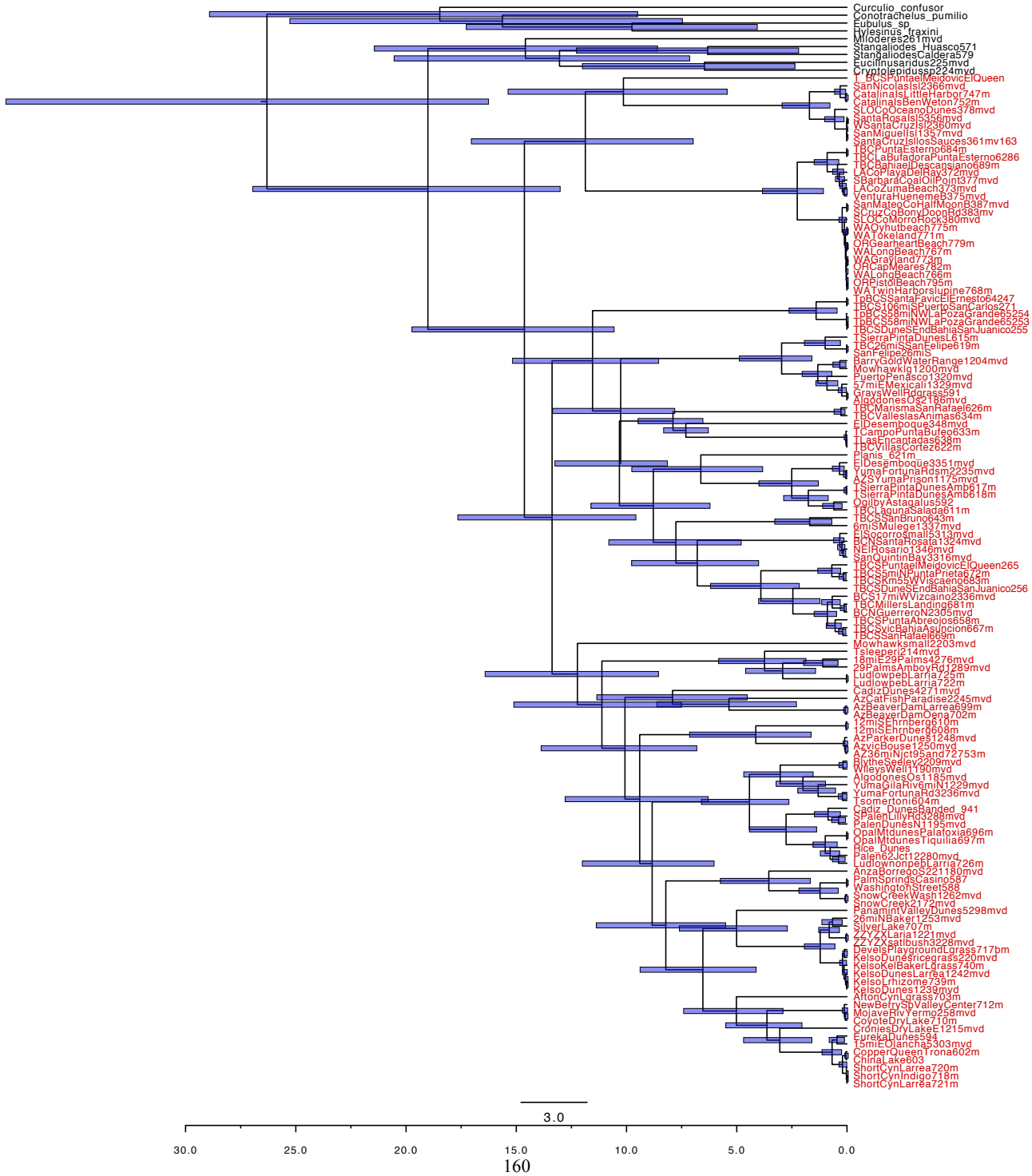
Curculio_confusor
Conotrachelus_pumilio
Eubulus_sp
Hylesinus_fraxini
Miloderes261mvd
Stangaliodes_Huasco571
StangaliodesCaldera579
Eucilinusaridus225mvd
Cryptolepidussp224mvd
1_BCSPuntaElMeidovicElQueen
SanNicolasIsl2366mvd
CatalinaIsLittleHarbor747m
CatalinaIsBenWeton752m
SLOCoOceanoDunes378mvd
SantaRosaIsl5356mvd
WSantaCruzIsl2360mvd
SanMiguelIsl1357mvd
SantaCruzIsIlosSauces361mv163
TBCPuntaEsterno684m
TBCLaBufadoraPuntaEsterno6286
TBCBahiaElDescansiano689m
LACoPlayaDelRay372mvd
SBarbaraCoalOilPoint377mvd
LACoZumaBeach373mvd
VenturaHuenemeB375mvd
SanMateoCoHalfMoonB387mvd
SCruzCoBonyDoonRd383mv
SLOCoMorroRock380mvd
WAOyhutbeach775m
WATokeland771m
ORGearheartBeach779m
WALongBeach767m
WAGrayland773m
ORCapMeares782m
WALongBeach766m
ORPistolBeach795m
WATwinHarborslupine768m
TBCSSantaFavicElErnesto64247
TBCS106miSPuertoSanCarlos271
TBCS58miNWLaPozaGrande65254
TBCS58miNWLaPozaGrande65253
TBCSDuneSEndBahiaSanJuanico255
TSierraPintaDunesL615m
TBC28miSSanFelipe619m
SanFelipe26miS
BarryGoldWaterRange1204mvd
Mowhawkig1200mvd
PuertoPenasco1320mvd
57miEMexicali1329mvd
GraysWellRdgrass591
AlgodonesOs2186mvd
TBCMarismaSanRafael626m
TBCValleslasAnimas634m
ElDesemboque348mvd
TCampoPuntaBufe633m
TLasEncantadas638m
TBCVillasCortez622m
Planis_621m
ElDesemboque3351mvd
YumaFortunaRdsm2235mvd
AZSYumaPrison1175mvd
TSierraPintaDunesAmp617m
TSierraPintaDunesAmb618m
OgilbyAstagalus592
TBCLagunaSalada611m
TBCSSanBruno643m
6miSMulege1337mvd
ElSocorro8mall5313mvd
BCNSantaRosata1324mvd
NElRosario1346mvd
SanQuintinBay3316mvd
TBCSPuntaElMeidovicElQueen265
TBCS5miNPuntaPrieta672m
TBCSKm55WVizcaeno663m
TBCSDuneSEndBahiaSanJuanico256
BCS17miWVizcaino2336mvd
TBCMillersLanding681m
BCNGuerreroN2305mvd
TBCSPuntaAbreojos658m
TBCSvicBahiaAsuncion667m
TBCSSanRafael669m
Mowhawksmall2203mvd
Tsleeperi214mvd
18miE29Palms4276mvd
29PalmsAmboyRd1289mvd
LudlowpebLarria725m
LudlowpebLarria722m
CadizDunes4271mvd
AzCatFishParadise2245mvd
AzBeaverDamLarrea699m
AzBeaverDamOena702m
12miSEhrnberg610m
12miSEhrnberg608m
AzParkerDune51248mvd
AzvicBouse1250mvd
AZ36miNJct95and72753m
BlytheSeeley2209mvd
WileysWell1190mvd
AlgodonesOs1185mvd
YumaGilaRiv6miN1229mvd
YumaFortunaRd3236mvd
Tsometoni604m
Cadiz_DunesBanded_941
SPalenLillyRd3288mvd
PalenDunesN1195mvd
OpalMtdunesPalafoxia696m
OpalMtdunesTiquilia697m
Rice_Dunes
Palen62Jct12280mvd
LudlownonpebLarria726m
AnzaBorregoS2211180mvd
PalmSpringsCasino597
WashingtonStreet568
SnowCreekWash1262mvd
SnowCreek2172mvd
PanamintValleyDunes5298mvd
26miNBaker1253mvd
SilverLake707m
ZZYZXLaria1221mvd
ZZYZXsatbush3228mvd
DevelsPlaygroundLgrass717bm
KelsoDunesGrassgrass220mvd
KelsoKelBakerLgrass740m
KelsoDunesLarrea1242mvd
KelsoLrhizome739m
KelsoDunes1239mvd
AftonCynLgrass703m
NewBerrySpValleyCenter712m
MojaveRivYermo258mvd
CoyoteDryLake710m
CroniesDryLakeE1215mvd
EurekaDunes594
15miEOlancha5303mvd
CopperQueenTrona602m
ChiriaLake603
ShortCynLarrea720m
ShortCynIndigo718m
ShortCynLarrea721m
3.0
30.0
25.0
20.0
15.0
10.0
5.0
0.0

160

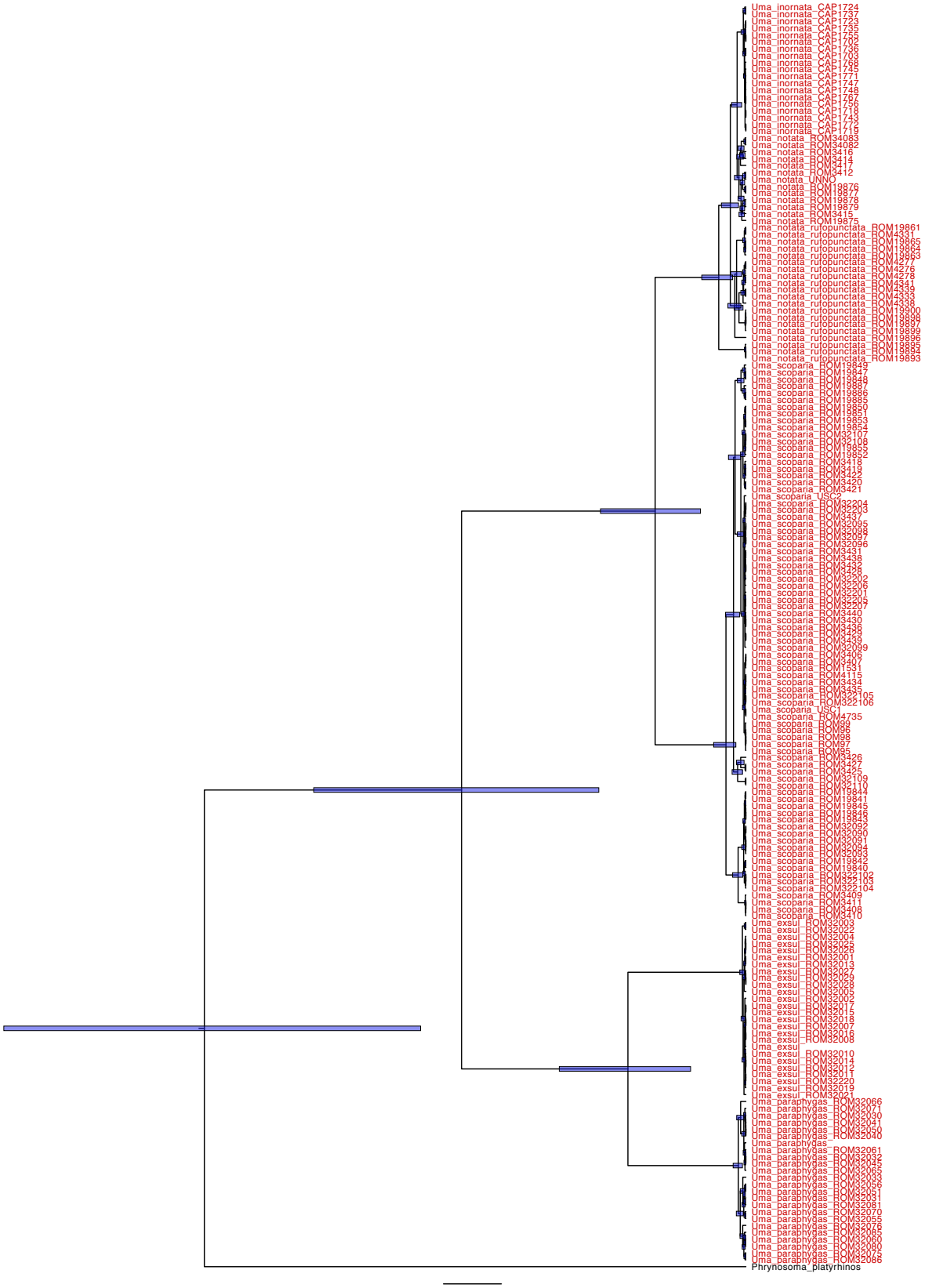
Uma_inornata_CAP1724
Uma_inornata_CAP1737
Uma_inornata_CAP1739
Uma_inornata_CAP1735
Uma_inornata_CAP1755
Uma_inornata_CAP1702
Uma_inornata_CAP1736
Uma_inornata_CAP1703
Uma_inornata_CAP1768
Uma_inornata_CAP1745
Uma_inornata_CAP1771
Uma_inornata_CAP1747
Uma_inornata_CAP1748
Uma_inornata_CAP1767
Uma_inornata_CAP1756
Uma_inornata_CAP1718
Uma_inornata_CAP1743
Uma_inornata_CAP1772
Uma_inornata_CAP1719
Uma_notata_ROM34083
Uma_notata_ROM34082
Uma_notata_ROM3416
Uma_notata_ROM3414
Uma_notata_ROM3417
Uma_notata_ROM3412
Uma_notata_UNNO
Uma_notata_ROM19876
Uma_notata_ROM19877
Uma_notata_ROM19878
Uma_notata_ROM19879
Uma_notata_ROM3415
Uma_notata_ROM19875
Uma_notata_rufopunctata_ROM19861
Uma_notata_rufopunctata_ROM4331
Uma_notata_rufopunctata_ROM19865
Uma_notata_rufopunctata_ROM19864
Uma_notata_rufopunctata_ROM19863
Uma_notata_rufopunctata_ROM4277
Uma_notata_rufopunctata_ROM4276
Uma_notata_rufopunctata_ROM4278
Uma_notata_rufopunctata_ROM4341
Uma_notata_rufopunctata_ROM4339
Uma_notata_rufopunctata_ROM4333
Uma_notata_rufopunctata_ROM4338
Uma_notata_rufopunctata_ROM19900
Uma_notata_rufopunctata_ROM19898
Uma_notata_rufopunctata_ROM19897
Uma_notata_rufopunctata_ROM19899
Uma_notata_rufopunctata_ROM19896
Uma_notata_rufopunctata_ROM19895
Uma_notata_rufopunctata_ROM19894
Uma_notata_rufopunctata_ROM19893
Uma_scoparia_ROM19849
Uma_scoparia_ROM19847
Uma_scoparia_ROM19848
Uma_scoparia_ROM19887
Uma_scoparia_ROM19886
Uma_scoparia_ROM19885
Uma_scoparia_ROM19850
Uma_scoparia_ROM19851
Uma_scoparia_ROM19853
Uma_scoparia_ROM19854
Uma_scoparia_ROM32107
Uma_scoparia_ROM32108
Uma_scoparia_ROM19855
Uma_scoparia_ROM19852
Uma_scoparia_ROM3418
Uma_scoparia_ROM3419
Uma_scoparia_ROM3422
Uma_scoparia_ROM3420
Uma_scoparia_ROM3421
Uma_scoparia_USC2
Uma_scoparia_ROM32204
Uma_scoparia_ROM32203
Uma_scoparia_ROM3437
Uma_scoparia_ROM32095
Uma_scoparia_ROM32098
Uma_scoparia_ROM32097
Uma_scoparia_ROM32096
Uma_scoparia_ROM3431
Uma_scoparia_ROM3438
Uma_scoparia_ROM3439
Uma_scoparia_ROM3432
Uma_scoparia_ROM3428
Uma_scoparia_ROM32202
Uma_scoparia_ROM32206
Uma_scoparia_ROM32201
Uma_scoparia_ROM32205
Uma_scoparia_ROM32207
Uma_scoparia_ROM3440
Uma_scoparia_ROM3430
Uma_scoparia_ROM3436
Uma_scoparia_ROM3429
Uma_scoparia_ROM3433
Uma_scoparia_ROM32099
Uma_scoparia_ROM3406
Uma_scoparia_ROM3407
Uma_scoparia_ROM1531
Uma_scoparia_ROM4115
Uma_scoparia_ROM3434
Uma_scoparia_ROM3435
Uma_scoparia_ROM322105
Uma_scoparia_ROM322106
Uma_scoparia_USC1
Uma_scoparia_ROM4735
Uma_scoparia_ROM99
Uma_scoparia_ROM96
Uma_scoparia_ROM98
Uma_scoparia_ROM97
Uma_scoparia_ROM95
Uma_scoparia_ROM3426
Uma_scoparia_ROM3427
Uma_scoparia_ROM3425
Uma_scoparia_ROM32109
Uma_scoparia_ROM32110
Uma_scoparia_ROM19844
Uma_scoparia_ROM19841
Uma_scoparia_ROM19845
Uma_scoparia_ROM19846
Uma_scoparia_ROM19843
Uma_scoparia_ROM32092
Uma_scoparia_ROM32090
Uma_scoparia_ROM32091
Uma_scoparia_ROM32084
Uma_scoparia_ROM32083
Uma_scoparia_ROM19842
Uma_scoparia_ROM19840
Uma_scoparia_ROM322102
Uma_scoparia_ROM322103
Uma_scoparia_ROM322104
Uma_scoparia_ROM3409
Uma_scoparia_ROM3411
Uma_scoparia_ROM3408
Uma_scoparia_ROM3410
Uma_exsul_ROM32003
Uma_exsul_ROM32022
Uma_exsul_ROM32004
Uma_exsul_ROM32023
Uma_exsul_ROM32026
Uma_exsul_ROM32001
Uma_exsul_ROM32013
Uma_exsul_ROM32024
Uma_exsul_ROM32029
Uma_exsul_ROM32028
Uma_exsul_ROM32005
Uma_exsul_ROM32002
Uma_exsul_ROM32017
Uma_exsul_ROM32015
Uma_exsul_ROM32018
Uma_exsul_ROM32007
Uma_exsul_ROM32016
Uma_exsul_ROM32008
Uma_exsul_
Uma_exsul_ROM32010
Uma_exsul_ROM32014
Uma_exsul_ROM32012
Uma_exsul_ROM32011
Uma_exsul_ROM32220
Uma_exsul_ROM32019
Uma_exsul_ROM32021
Uma_paraphygas_ROM32066
Uma_paraphygas_ROM32071
Uma_paraphygas_ROM32030
Uma_paraphygas_ROM32041
Uma_paraphygas_ROM32040
Uma_paraphygas_ROM32042
Uma_paraphygas_
Uma_paraphygas_ROM32061
Uma_paraphygas_ROM32032
Uma_paraphygas_ROM32045
Uma_paraphygas_ROM32065
Uma_paraphygas_ROM32033
Uma_paraphygas_ROM32056
Uma_paraphygas_ROM32052
Uma_paraphygas_ROM32031
Uma_paraphygas_ROM32081
Uma_paraphygas_ROM32070
Uma_paraphygas_ROM32055
Uma_paraphygas_ROM32076
Uma_paraphygas_ROM32085
Uma_paraphygas_ROM32060
Uma_paraphygas_ROM32080
Uma_paraphygas_ROM32075
Uma_paraphygas_ROM32086
Phrynosoma_platyrhinos
3.0
30.0
25.0
20.0
15.0
10.0
5.0
0.0

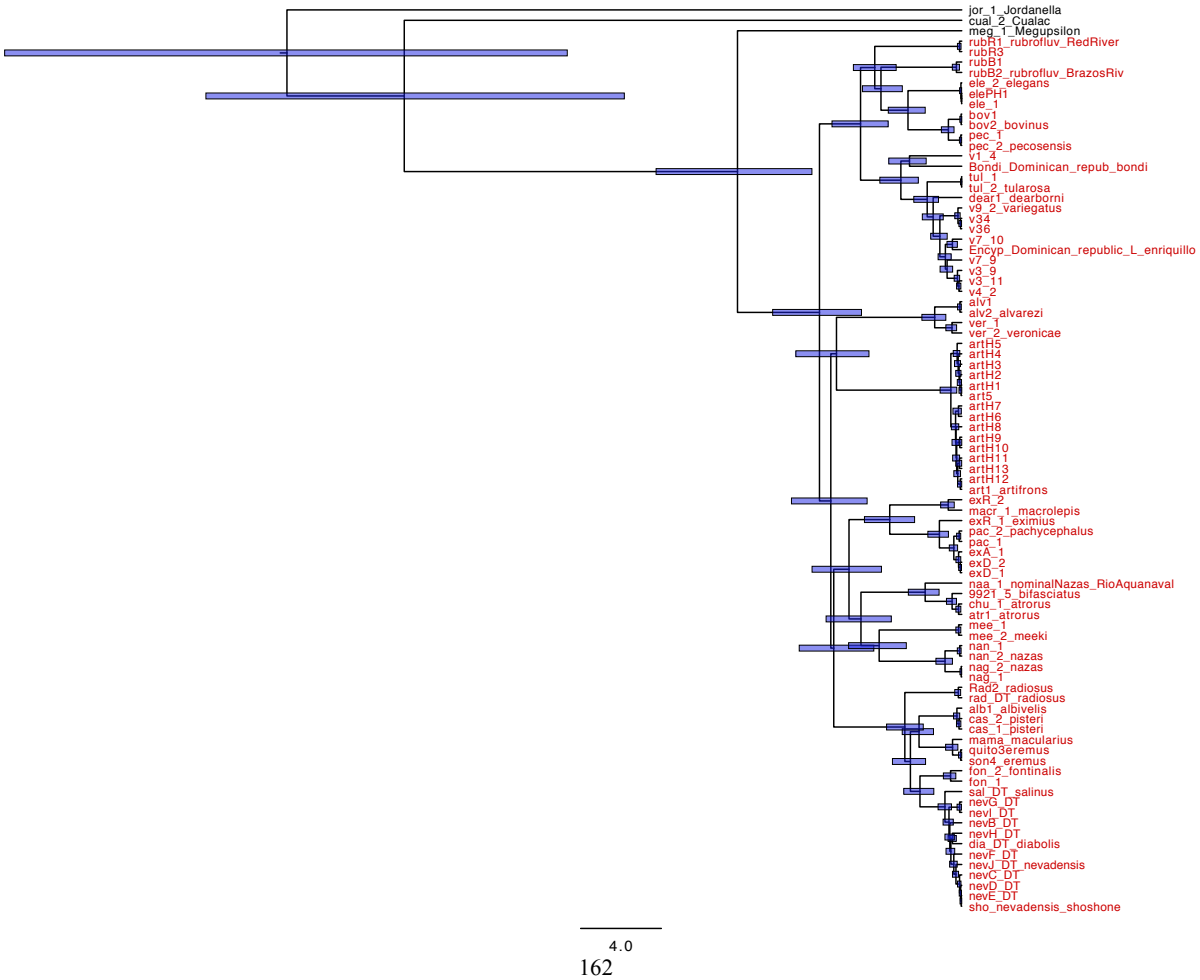
jor_1_Jordanella
cual_2_Cualac
meg_1_Megupsilon
rubR1_rubrofluv_RedRiver
rubR3
rubB1
rubB2_rubrofluv_BrazosRiv
ele_2_elegans
elePH1
ele_1
bov1
bov2_bovinus
pec_1
pec_2_pecosensis
v1_4
Bondi_Dominican_repub_bondi
tul_1
tul_2_tularosa
dear1_dearborni
v9_2_variegatus
v34
v36
v7_10
Encyp_Dominican_republic_L_enriquillo
v7_9
v3_9
v3_11
v4_2
alv1
alv2_alvarezi
ver_1
ver_2_veronicae
artH5
artH4
artH3
artH2
artH1
art5
artH7
artH6
artH8
artH9
artH10
artH11
artH13
artH12
art1_artifrons
exR_2
macr_1_macrolepis
exR_1_eximius
pac_2_pachycephalus
pac_1
exA_1
exD_2
exD_1
naa_1_nominalNazas_RioAquanaval
9921_5_bifasciatus
chu_1_atrorus
atr1_atrorus
mee_1
mee_2_meeki
nan_1
nan_2_nazas
nag_2_nazas
nag_1
Rad2_radiosus
rad_DT_radiosus
alb1_albivelis
cas_2_pisteri
cas_1_pisteri
mama_macularius
quito3eremus
son4_eremus
fon_2_fontinalis
fon_1
sal_DT_salinus
nevG_DT
nevI_DT
nevB_DT
nevH_DT
dia_DT_diabolis
nevF_DT
nevJ_DT_nevadensis
nevC_DT
nevD_DT
nevE_DT
sho_nevadensis_shoshone
4.0

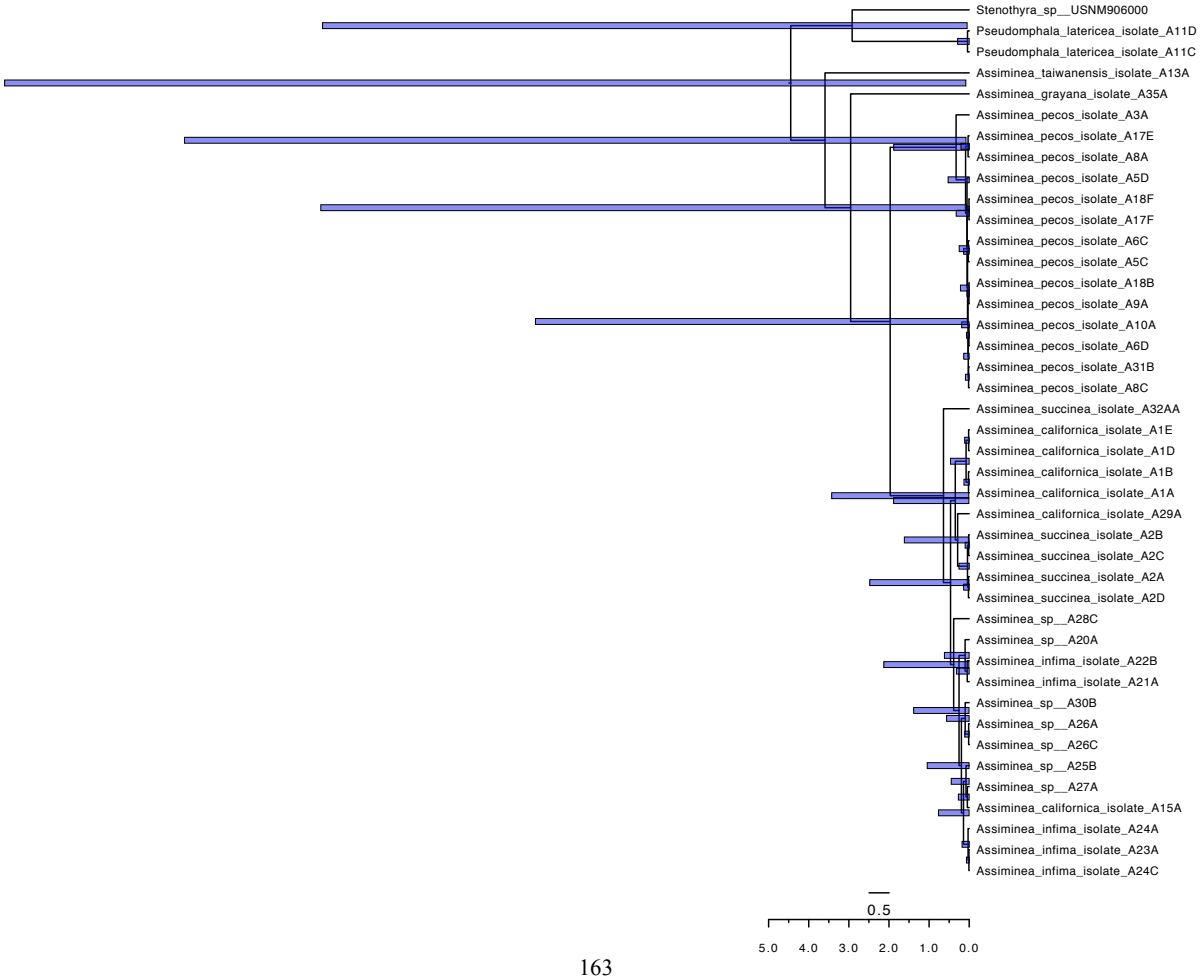
Stenothyra_sp__USNM906000
Pseudomphala_latericea_isolate_A11D
Pseudomphala_latericea_isolate_A11C
Assiminea_taiwanensis_isolate_A13A
Assiminea_grayana_isolate_A35A
Assiminea_pecos_isolate_A3A
Assiminea_pecos_isolate_A17E
Assiminea_pecos_isolate_A8A
Assiminea_pecos_isolate_A5D
Assiminea_pecos_isolate_A18F
Assiminea_pecos_isolate_A17F
Assiminea_pecos_isolate_A6C
Assiminea_pecos_isolate_A5C
Assiminea_pecos_isolate_A18B
Assiminea_pecos_isolate_A9A
Assiminea_pecos_isolate_A10A
Assiminea_pecos_isolate_A6D
Assiminea_pecos_isolate_A31B
Assiminea_pecos_isolate_A8C
Assiminea_succinea_isolate_A32AA
Assiminea_californica_isolate_A1E
Assiminea_californica_isolate_A1D
Assiminea_californica_isolate_A1B
Assiminea_californica_isolate_A1A
Assiminea_californica_isolate_A29A
Assiminea_succinea_isolate_A2B
Assiminea_succinea_isolate_A2C
Assiminea_succinea_isolate_A2A
Assiminea_succinea_isolate_A2D
Assiminea_sp__A28C
Assiminea_sp__A20A
Assiminea_infima_isolate_A22B
Assiminea_infima_isolate_A21A
Assiminea_sp__A30B
Assiminea_sp__A26A
Assiminea_sp__A26C
Assiminea_sp__A25B
Assiminea_sp__A27A
Assiminea_californica_isolate_A15A
Assiminea_infima_isolate_A24A
Assiminea_infima_isolate_A23A
Assiminea_infima_isolate_A24C
0.5
5.0
4.0
3.0
2.0
1.0
0.0

163

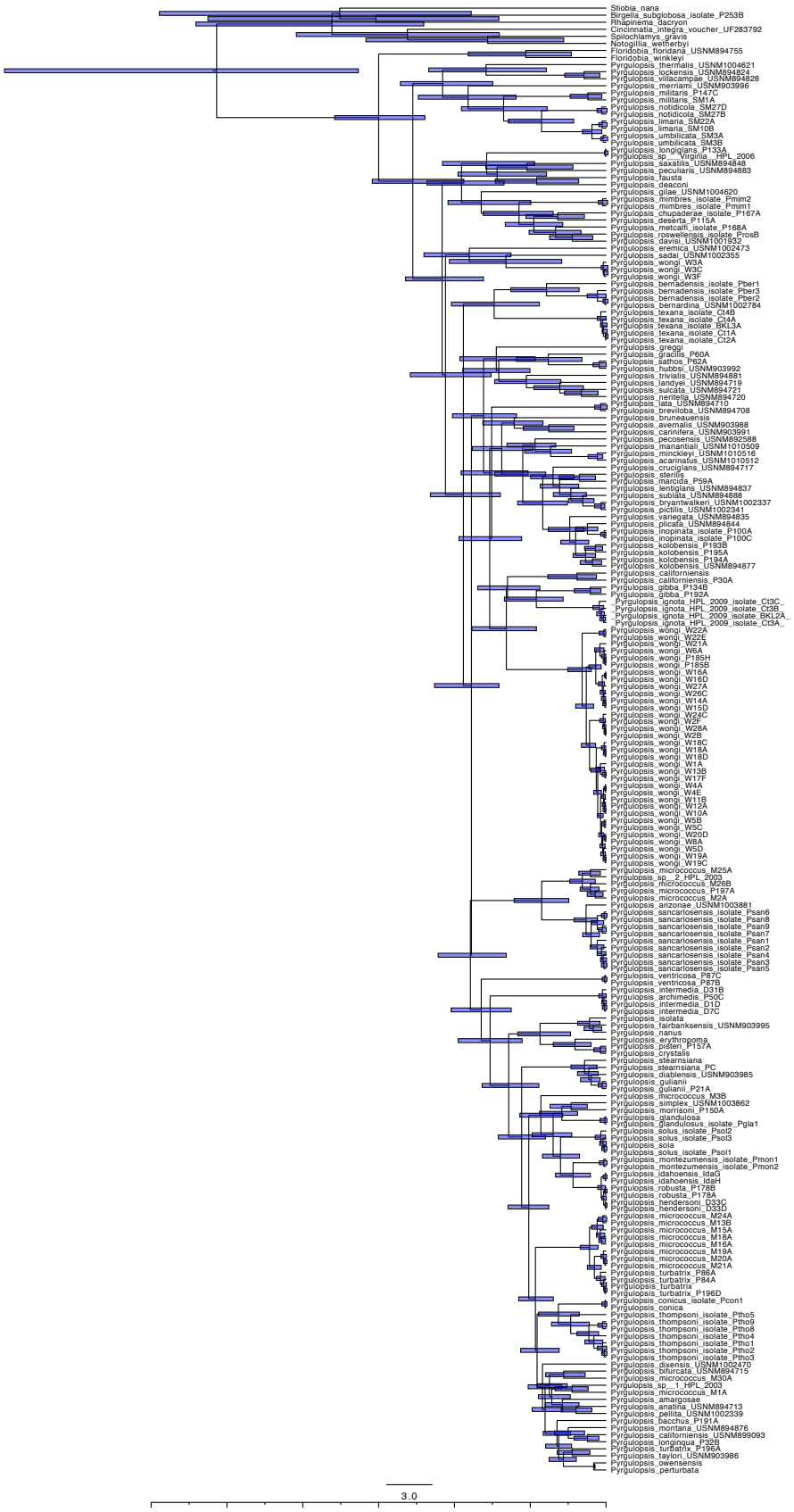
Stiobia_nana
Birgella_subglobosa_isolate_P253B
Rhapinema_dacryon
Cincinnatia_integra_voucher_UF283792
Spilochlamys_gravis
Notogillia_wetherbyi
Floridobia_floridana_USNM894755
Floridobia_winkleyi
Pyrgulopsis_thermalis_USNM1004621
Pyrgulopsis_lockensis_USNM894824
Pyrgulopsis_villacampae_USNM894828
Pyrgulopsis_merriami_USNM903996
Pyrgulopsis_militaris_P147C
Pyrgulopsis_militaris_SM1A
Pyrgulopsis_notidicola_SM27D
Pyrgulopsis_notidicola_SM27B
Pyrgulopsis_limaria_SM22A
Pyrgulopsis_limaria_SM10B
Pyrgulopsis_umbilicata_SM3A
Pyrgulopsis_umbilicata_SM3B
Pyrgulopsis_longiglans_P133A
Pyrgulopsis_sp._Virginia_HPL_2006
Pyrgulopsis_saxatilis_USNM894848
Pyrgulopsis_peculiaris_USNM894883
Pyrgulopsis_lausta
Pyrgulopsis_deaconi
Pyrgulopsis_gilae_USNM1004620
Pyrgulopsis_mimbres_isolate_Pmim2
Pyrgulopsis_mimbres_isolate_Pmim1
Pyrgulopsis_chupaderae_isolate_P167A
Pyrgulopsis_deserta_P115A
Pyrgulopsis_metcalfi_isolate_P168A
Pyrgulopsis_roswellensis_isolate_ProsB
Pyrgulopsis_davisi_USNM1001932
Pyrgulopsis_eremica_USNM1002473
Pyrgulopsis_sadai_USNM1002355
Pyrgulopsis_wongi_W3A
Pyrgulopsis_wongi_W3C
Pyrgulopsis_wongi_W3F
Pyrgulopsis_bernadensis_isolate_Pber1
Pyrgulopsis_bernadensis_isolate_Pber3
Pyrgulopsis_bernadensis_isolate_Pber2
Pyrgulopsis_bernardina_USNM1002784
Pyrgulopsis_texana_isolate_Ct4B
Pyrgulopsis_texana_isolate_Ct4A
Pyrgulopsis_texana_isolate_BKL3A
Pyrgulopsis_texana_isolate_Ct1A
Pyrgulopsis_texana_isolate_Ct2A
Pyrgulopsis_greggi
Pyrgulopsis_gracilis_P60A
Pyrgulopsis_sathos_P62A
Pyrgulopsis_hubbsi_USNM903992
Pyrgulopsis_trivialis_USNM894881
Pyrgulopsis_landyei_USNM894719
Pyrgulopsis_sulcata_USNM894721
Pyrgulopsis_neritella_USNM894720
Pyrgulopsis_lata_USNM894710
Pyrgulopsis_breviloba_USNM894708
Pyrgulopsis_bruneauensis
Pyrgulopsis_avernalis_USNM903988
Pyrgulopsis_carinifera_USNM903991
Pyrgulopsis_pecosensis_USNM892588
Pyrgulopsis_manantialis_USNM1010509
Pyrgulopsis_minckleyi_USNM1010516
Pyrgulopsis_acarinatus_USNM1010512
Pyrgulopsis_crucilglans_USNM894717
Pyrgulopsis_sterilis
Pyrgulopsis_marcida_P59A
Pyrgulopsis_lentiglans_USNM894837
Pyrgulopsis_sublata_USNM894888
Pyrgulopsis_bryantwalkeri_USNM1002337
Pyrgulopsis_pictilis_USNM1002341
Pyrgulopsis_variegata_USNM894835
Pyrgulopsis_plicata_USNM894844
Pyrgulopsis_inopinata_isolate_P100A
Pyrgulopsis_inopinata_isolate_P100C
Pyrgulopsis_kolobensis_P193B
Pyrgulopsis_kolobensis_P195A
Pyrgulopsis_kolobensis_P194A
Pyrgulopsis_kolobensis_USNM894877
Pyrgulopsis_californiensis
Pyrgulopsis_californiensis_P30A
Pyrgulopsis_gibba_P134B
Pyrgulopsis_gibba_P192A
Pyrgulopsis_ignota_HPL_2009_isolate_Ct3C
Pyrgulopsis_ignota_HPL_2009_isolate_Ct3B
Pyrgulopsis_ignota_HPL_2009_isolate_BKL2A
Pyrgulopsis_ignota_HPL_2009_isolate_Ct3A
Pyrgulopsis_wongi_W22A
Pyrgulopsis_wongi_W22E
Pyrgulopsis_wongi_W21A
Pyrgulopsis_wongi_W6A
Pyrgulopsis_wongi_P185H
Pyrgulopsis_wongi_P185B
Pyrgulopsis_wongi_W16A
Pyrgulopsis_wongi_W16D
Pyrgulopsis_wongi_W27A
Pyrgulopsis_wongi_W26C
Pyrgulopsis_wongi_W14A
Pyrgulopsis_wongi_W15D
Pyrgulopsis_wongi_W24C
Pyrgulopsis_wongi_W2F
Pyrgulopsis_wongi_W28A
Pyrgulopsis_wongi_W26
Pyrgulopsis_wongi_W18C
Pyrgulopsis_wongi_W18A
Pyrgulopsis_wongi_W18D
Pyrgulopsis_wongi_W1A
Pyrgulopsis_wongi_W13B
Pyrgulopsis_wongi_W17F
Pyrgulopsis_wongi_W4A
Pyrgulopsis_wongi_W4E
Pyrgulopsis_wongi_W11B
Pyrgulopsis_wongi_W12A
Pyrgulopsis_wongi_W10A
Pyrgulopsis_wongi_W5B
Pyrgulopsis_wongi_W5C
Pyrgulopsis_wongi_W20D
Pyrgulopsis_wongi_W8A
Pyrgulopsis_wongi_W5D
Pyrgulopsis_wongi_W19A
Pyrgulopsis_wongi_W19C
Pyrgulopsis_micrococcus_M25A
Pyrgulopsis_sp._2_HPL_2003
Pyrgulopsis_micrococcus_M26B
Pyrgulopsis_micrococcus_P197A
Pyrgulopsis_micrococcus_M2A
Pyrgulopsis_arizonae_USNM1003881
Pyrgulopsis_sancarlosensis_isolate_Psan6
Pyrgulopsis_sancarlosensis_isolate_Psan8
Pyrgulopsis_sancarlosensis_isolate_Psan9
Pyrgulopsis_sancarlosensis_isolate_Psan7
Pyrgulopsis_sancarlosensis_isolate_Psan1
Pyrgulopsis_sancarlosensis_isolate_Psan2
Pyrgulopsis_sancarlosensis_isolate_Psan4
Pyrgulopsis_sancarlosensis_isolate_Psan3
Pyrgulopsis_sancarlosensis_isolate_Psan5
Pyrgulopsis_ventricosa_P87C
Pyrgulopsis_ventricosa_P87B
Pyrgulopsis_intermedia_D31B
Pyrgulopsis_archimedis_P50C
Pyrgulopsis_intermedia_D1D
Pyrgulopsis_intermedia_D7C
Pyrgulopsis_isolata
Pyrgulopsis_fairbanksensis_USNM903995
Pyrgulopsis_nanus
Pyrgulopsis_erythropoma
Pyrgulopsis_pilsbri_P157A
Pyrgulopsis_crystalis
Pyrgulopsis_stearnsiana
Pyrgulopsis_stearnsiana_PC
Pyrgulopsis_diablensis_USNM903985
Pyrgulopsis_gulianii
Pyrgulopsis_gulianii_P21A
Pyrgulopsis_micrococcus_M3B
Pyrgulopsis_simplex_USNM1003862
Pyrgulopsis_morrisoni_P150A
Pyrgulopsis_glandulosa
Pyrgulopsis_glandulosus_isolate_Pgla1
Pyrgulopsis_solus_isolate_Psol2
Pyrgulopsis_solus_isolate_Psol3
Pyrgulopsis_sola
Pyrgulopsis_solus_isolate_Psol1
Pyrgulopsis_montezumensis_isolate_Pmon1
Pyrgulopsis_montezumensis_isolate_Pmon2
Pyrgulopsis_idahoensis_IdaG
Pyrgulopsis_idahoensis_IdaH
Pyrgulopsis_robusta_P178B
Pyrgulopsis_robusta_P178A
Pyrgulopsis_hendersoni_D33C
Pyrgulopsis_hendersoni_D33D
Pyrgulopsis_micrococcus_M24A
Pyrgulopsis_micrococcus_M13B
Pyrgulopsis_micrococcus_M15A
Pyrgulopsis_micrococcus_M18A
Pyrgulopsis_micrococcus_M16A
Pyrgulopsis_micrococcus_M19A
Pyrgulopsis_micrococcus_M20A
Pyrgulopsis_micrococcus_M21A
Pyrgulopsis_turbatrix_P86A
Pyrgulopsis_turbatrix_P84A
Pyrgulopsis_turbatrix
Pyrgulopsis_turbatrix_P196D
Pyrgulopsis_conicus_isolate_Pcon1
Pyrgulopsis_conica
Pyrgulopsis_thompsoni_isolate_Ptho5
Pyrgulopsis_thompsoni_isolate_Ptho9
Pyrgulopsis_thompsoni_isolate_Ptho8
Pyrgulopsis_thompsoni_isolate_Ptho4
Pyrgulopsis_thompsoni_isolate_Ptho1
Pyrgulopsis_thompsoni_isolate_Ptho2
Pyrgulopsis_thompsoni_isolate_Ptho3
Pyrgulopsis_dixensis_USNM1002470
Pyrgulopsis_bifurcata_USNM894715
Pyrgulopsis_micrococcus_M30A
Pyrgulopsis_sp._1_HPL_2003
Pyrgulopsis_micrococcus_M1A
Pyrgulopsis_amargosae
Pyrgulopsis_anatina_USNM894713
Pyrgulopsis_pellita_USNM1002339
Pyrgulopsis_bacchus_P191A
Pyrgulopsis_montana_USNM894876
Pyrgulopsis_californiensis_USNM899093
Pyrgulopsis_longinqua_P32B
Pyrgulopsis_turbatrix_P196A
Pyrgulopsis_taylori_USNM903986
Pyrgulopsis_owensensis
Pyrgulopsis_perturbata
3.0
30.0
25.0
20.0
15.0
10.0
5.0
0.0

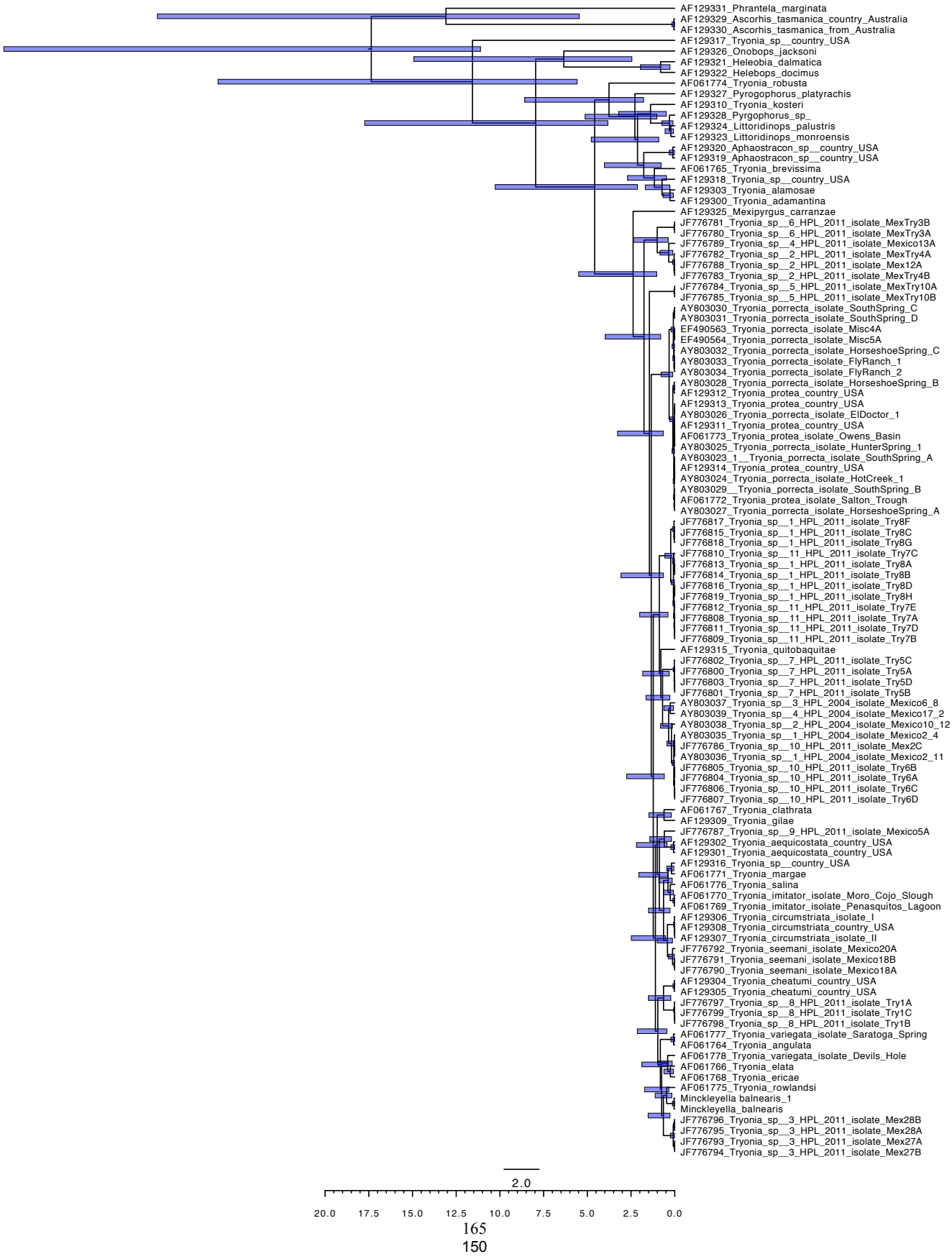
AF129331_Phrantela_marginata
AF129329_Ascorhis_tasmanica_country_Australia
AF129330_Ascorhis_tasmanica_from_Australia
AF129317_Tryonia_sp__country_USA
AF129326_Onobops_jacksoni
AF129321_Heleobia_dalmatica
AF129322_Helebops_docimus
AF061774_Tryonia_robusta
AF129327_Pyrogophorus_platyrachis
AF129310_Tryonia_kosteri
AF129328_Pyrgophorus_sp_
AF129324_Littoridinops_palustris
AF129323_Littoridinops_monroensis
AF129320_Aphaostracon_sp__country_USA
AF129319_Aphaostracon_sp__country_USA
AF061765_Tryonia_brevissima
AF129318_Tryonia_sp__country_USA
AF129303_Tryonia_alamosae
AF129300_Tryonia_adamantina
AF129325_Mexipyrgus_carranzae
JF776781_Tryonia_sp__6_HPL_2011_isolate_MexTry3B
JF776780_Tryonia_sp__6_HPL_2011_isolate_MexTry3A
JF776789_Tryonia_sp__4_HPL_2011_isolate_Mexico13A
JF776782_Tryonia_sp__2_HPL_2011_isolate_MexTry4A
JF776788_Tryonia_sp__2_HPL_2011_isolate_Mex12A
JF776783_Tryonia_sp__2_HPL_2011_isolate_MexTry4B
JF776784_Tryonia_sp__5_HPL_2011_isolate_MexTry10A
JF776785_Tryonia_sp__5_HPL_2011_isolate_MexTry10B
AY803030_Tryonia_porrecta_isolate_SouthSpring_C
AY803031_Tryonia_porrecta_isolate_SouthSpring_D
EF490563_Tryonia_porrecta_isolate_Misc4A
EF490564_Tryonia_porrecta_isolate_Misc5A
AY803032_Tryonia_porrecta_isolate_HorseshoeSpring_C
AY803033_Tryonia_porrecta_isolate_FlyRanch_1
AY803034_Tryonia_porrecta_isolate_FlyRanch_2
AY803028_Tryonia_porrecta_isolate_HorseshoeSpring_B
AF129312_Tryonia_protea_country_USA
AF129313_Tryonia_protea_country_USA
AY803026_Tryonia_porrecta_isolate_ElDoctor_1
AF129311_Tryonia_protea_country_USA
AF061773_Tryonia_protea_isolate_Owens_Basin
AY803025_Tryonia_porrecta_isolate_HunterSpring_1
AY803023_1__Tryonia_porrecta_isolate_SouthSpring_A
AF129314_Tryonia_protea_country_USA
AY803024_Tryonia_porrecta_isolate_HotCreek_1
AY803029__Tryonia_porrecta_isolate_SouthSpring_B
AF061772_Tryonia_protea_isolate_Salton_Trough
AY803027_Tryonia_porrecta_isolate_HorseshoeSpring_A
JF776817_Tryonia_sp__1_HPL_2011_isolate_Try8F
JF776815_Tryonia_sp__1_HPL_2011_isolate_Try8C
JF776818_Tryonia_sp__1_HPL_2011_isolate_Try8G
JF776810_Tryonia_sp__11_HPL_2011_isolate_Try7C
JF776813_Tryonia_sp__1_HPL_2011_isolate_Try8A
JF776814_Tryonia_sp__1_HPL_2011_isolate_Try8B
JF776816_Tryonia_sp__1_HPL_2011_isolate_Try8D
JF776819_Tryonia_sp__1_HPL_2011_isolate_Try8H
JF776812_Tryonia_sp__11_HPL_2011_isolate_Try7E
JF776808_Tryonia_sp__11_HPL_2011_isolate_Try7A
JF776811_Tryonia_sp__11_HPL_2011_isolate_Try7D
JF776809_Tryonia_sp__11_HPL_2011_isolate_Try7B
AF129315_Tryonia_quitobaquitae
JF776802_Tryonia_sp__7_HPL_2011_isolate_Try5C
JF776800_Tryonia_sp__7_HPL_2011_isolate_Try5A
JF776803_Tryonia_sp__7_HPL_2011_isolate_Try5D
JF776801_Tryonia_sp__7_HPL_2011_isolate_Try5B
AY803037_Tryonia_sp__3_HPL_2004_isolate_Mexico6_8
AY803039_Tryonia_sp__4_HPL_2004_isolate_Mexico17_2
AY803038_Tryonia_sp__2_HPL_2004_isolate_Mexico10_12
AY803035_Tryonia_sp__1_HPL_2004_isolate_Mexico2_4
JF776786_Tryonia_sp__10_HPL_2011_isolate_Mex2C
AY803036_Tryonia_sp__1_HPL_2004_isolate_Mexico2_11
JF776805_Tryonia_sp__10_HPL_2011_isolate_Try6B
JF776804_Tryonia_sp__10_HPL_2011_isolate_Try6A
JF776806_Tryonia_sp__10_HPL_2011_isolate_Try6C
JF776807_Tryonia_sp__10_HPL_2011_isolate_Try6D
AF061767_Tryonia_clathrata
AF129309_Tryonia_gilae
JF776787_Tryonia_sp__9_HPL_2011_isolate_Mexico5A
AF129302_Tryonia_aequicostata_country_USA
AF129301_Tryonia_aequicostata_country_USA
AF129316_Tryonia_sp__country_USA
AF061771_Tryonia_margae
AF061776_Tryonia_salina
AF061770_Tryonia_imitator_isolate_Moro_Cojo_Slough
AF061769_Tryonia_imitator_isolate_Penasquitos_Lagoon
AF129306_Tryonia_circumstriata_isolate_I
AF129308_Tryonia_circumstriata_country_USA
AF129307_Tryonia_circumstriata_isolate_II
JF776792_Tryonia_seemani_isolate_Mexico20A
JF776791_Tryonia_seemani_isolate_Mexico18B
JF776790_Tryonia_seemani_isolate_Mexico18A
AF129304_Tryonia_cheatumi_country_USA
AF129305_Tryonia_cheatumi_country_USA
JF776797_Tryonia_sp__8_HPL_2011_isolate_Try1A
JF776799_Tryonia_sp__8_HPL_2011_isolate_Try1C
JF776798_Tryonia_sp__8_HPL_2011_isolate_Try1B
AF061777_Tryonia_variegata_isolate_Saratoga_Spring
AF061764_Tryonia_angulata
AF061778_Tryonia_variegata_isolate_Devils_Hole
AF061766_Tryonia_elata
AF061768_Tryonia_ericae
AF061775_Tryonia_rowlandsi
Minckleyella balnearis_1
Minckleyella_balnearis
JF776796_Tryonia_sp__3_HPL_2011_isolate_Mex28B
JF776795_Tryonia_sp__3_HPL_2011_isolate_Mex28A
JF776793_Tryonia_sp__3_HPL_2011_isolate_Mex27A
JF776794_Tryonia_sp__3_HPL_2011_isolate_Mex27B
2.0
20.0
17.5
15.0
12.5
10.0
7.5
5.0
2.5
0.0

NATURAL HISTORY MATTERS IN CLIMATE NICHE MODELING

ABSTRACT: We explored how partitioning climate data by day (Daymet data) influences niche model predictions, estimated by the MaxEnt machine learning algorithm, for taxa with constrained phenologies. We compared the results with WorldClim data that is partitioned by month to examine what effect using more precise data has on species distribution models. We also compared life history strategies related to climate change within *Rhaphiomidas*. We examined how phylogenetic signal in phenotypic traits and climate tolerances can tell us about how they adapt to different climates. Quantitative information about adaptation can be used to better inform projected range shifts and local extirpations. The findings show that the standard Bioclim variables are misleading as to the real climate space that a focal taxon may occupy. In addition, the use of the Daymet data also allowed for the detection of phylogenetic signal of thermal preferences. We used a Bayesian threshold model to test the hypothesis that darker maculation of some *Rhaphiomidas* is an adaptation to cooler daytime temperatures, as they may be a means for more rapidly warming their bodies when basking, leading to more efficient flight. We found that there was a correlation between these two variables, indicating that the dark coloration of *Rhaphiomidas* species is an adaptation for dealing with suboptimal temperatures, allowing them to expand their ecological niche from inland desert to coastal habitats.

INTRODUCTION

Evaluating an organism's response to climate change has become an important research area as global warming is anticipated to change many ecosystems. Examining response to climate change and predicting future distributions is of concern to a wide array of ecologists and evolutionary biologists. In addition, identifying whether a particular species or population adapts to climate change by adjusting its phenology or morphological/physiological traits as opposed to changing its range through dispersal, is key to predicting future distributions. These responses can be identified and tested through long-term ecological studies and through phylogenetic analyses. Most studies attempting to predict future ranges or assessing a species' climate preferences have relied upon the Worldclim database (Hijmans *et al.* 2005) and the standard 19 Bioclim variables. Although we believe these data are appropriate for capturing realized niches based on abiotic environmental factors experienced year around, as for perennial plants and some mammals, we believe reliance on these variable will likely lead to biased predictions for an entire suite of organisms that have discrete phenologies (e.g. are subterranean or dormant part of the year), as the key bioclimatic features influencing activity cycles in these species are unlikely to be captured by the 19 Bioclim variables. The variables themselves are based on monthly averages that have their own limitations for capturing the niche of an organism that may be active for a month or less or that straddles two calendar months, only. In this paper we present a novel way of capturing the niches for organisms with discrete phenologies and discuss the implications for further downstream analyses of periods of activity, reconstructions of ancestral climate

variable states, and future niche forecasting in the presence of global environmental change.

The idea of a fundamental niche extends back to Hutchinson (1957), and is broadly used to describe where a species would live without interspecific competition. This is what is being modeled in part when we reconstruct the environmental niche of an organism. Although our information about species is based on the realized niche we are still able to make perditions in areas where species are likely to occur but do not due to any number of historic biogeographic or ecological factors. Environmental niche modeling attempts to describe a probability surface of where an organism is likely to occur based on known occurrence data and the environmental variables related to those sites. The resulting niche models are the joint product of the occurrence data and the environmental variables read into the modeling mechanisms, whether they are climate niche envelope models or maximum entropy machine learning algorithms. The current approach is to take the occurrence data and let these algorithms identify the factors separating the known occurrence environmental variables from the surrounding regions not having a similar profile. Few authors actually try to evaluate if these variables are actually realistic in capturing what is important for their organisms of concern. Monthly averages are a human construct and are not natural, and binning these further may create problems in addressing a species/population fundamental niche and response to climate change, especially for animals and plants with discrete phenologies. No amount of binning of these time slices in further ways will solve this potential problem because the initial averages based on months, constrain all further attempts at capturing salient niche factors. To get around this fundamental issue we utilized climate data that was averaged by day at a 1km square scale from Daymet (Thornton *et al.* 2012).

One of the current goals of environmental niche modeling is to help forecast the biogeographic ranges organisms will occupy in the near future, however we need to be aware that natural selection is an ongoing process and how organisms adapt to climate change is likely to be the result of lineage specific effects. To try and identify the ways in which organisms adapt to climate change, for instance do they change their phenologies to match the climate (tracking a niche) or do they adapt in a physiological/morphological manner to the current conditions? There are several ways to answer these questions by either long-term ecological studies or by looking at their phylogenetic history. We chose the phylogenetic approach because it allows us to make correlations between species environmental variables that are statistically independent. We can then address the strategies taken by our study organisms that are not confounded by relatedness. It also allow for us to identify how rapidly changes tend to occur.

Daymet variables are recorded on a daily basis over a 31-year period. This gives the user the ability to define the precise phenology of the study organism. This is a more accurate way of representing the environmental variables that an animal or plant is in contact with than currently implemented. The ability to accurately define the environmental niche is likely to affect the outcome of the niche models and further outcomes of analyses they are used in. We expect that using the Daymet data will have significantly different outcomes, than the standard Bioclim variables for organisms with discrete phenologies.

We test the effects discrete phenology on niche reconstruction for flies of the genus *Rhaphiomidas* (Mydidae) (Fig. 1). We also wanted to test the hypothesis that they

adapt to their niche by modifying their external morphology specifically their color. Temperature has been shown to be an important constraint on activity, and we consequently hypothesize that more darkly-colored species of *Rhaphiomidas* evolved this coloration as a response to cooler climates and times of year. We propose that dark coloration is an adaptation facilitating absorption of more solar energy, thereby allowing greater activity in cooler conditions and climates.

Rhaphiomidas consists of 23 described species and 5 subspecies (Van Dam 2010). *Rhaphiomidas* is distributed throughout the deserts of the Southwestern United States and Northern Mexico (Cazier 1985; Van Dam 2010). Many species of *Rhaphiomidas* feed on floral nectar as adults. *Rhaphiomidas* adults fly in the spring and fall and are most active during spring and fall blooms. Multiple studies have been conducted on adult behavior, making note of their activity and the temperatures required for adult activity (Toft & Kimsey 1982; Rogers & Mattoni 1993; Ballmer *et al.* 1994; Kingsley 1996; Steinberg *et al.* 1998).

Fig. 1 *Rhaphiomidas acton,* G.Ballmer

Rhaphiomidas terminatus abdominalis is the only species of Diptera federally listed as endangered in the mainland US. The species is endangered because of dwindling habitat resulting from urban development (U. S. Fish & Wildlife Service 1997). Three other taxa that are also of threatened status are *Rhaphiomidas terminatus terminates, R. trochilus*, and *R. moapa* (Rogers & Van Dam 2007). *Rhaphiomidas terminatus terminatus* is known only from a 20 ha area within a golf course on the Palos Verdes Peninsula (George & Mattoni 2006). The study of related species of *Rhaphiomidas,* as well as other sympatric insect species, will aide in developing a better understanding of the habitat and climatic conditions most crucial for their survival.

Larvae and pupae of *Rhaphiomidas* are entirely subterranean. Little is known of the feeding habits of *Rhaphiomidas* as larvae, except that they feed on soft-bodied insect larvae in captivity. In a study (Van Dam in prep) examining where the larvae reside, final instar *Rhaphiomidas trochilus* larvae were found at soil depths from 3.5-6ft (Fig 2).

Fig. 2 Left: Excavation of *Rhaphiomidas trochilus* larval habitat (M. H. Van Dam and G. Ballmer 2006). Right: *R. trochilus,* mature larva ~5cm in length. (Photos Ken Osborne)

METHODS

Extraction, PCR, sequencing and alignment

DNA extraction was performed by dissecting thoracic muscle and a leg, each specimen was soaked in the DNAEasy(r) tissue kit's extraction buffer (with proteinase K) overnight, followed by completion of the manufacturer's DNA extraction protocol for animal tissue. The specimens and their associated parts were vouchered and used in subsequent morphological studies. Primers and genes used in this study are listed in Table 1. PCR was performed by using 12.5 ul GoTaq Master Mix (including DNTPs, buffer, taq and dye; Promega Corporation, Madison, WI), 1.25 ul 10lM forward and reverse primer, 7.0 ul water, and 1.0 ul template DNA yielding a 25ul reaction. PCR products were purified with Exosap-IT (US Biochemical Corporation, Cleveland, OH). Sanger sequenced was performed at UC Berkeley's DNA Sequencing Facility. Contigs were assembled and edited in Geneious Pro v. 4.6.4 (Biomatters Ltd.). Sequences were aligned by ClustalW-2.0.10 (Larkin *et al.* 2007) with settings set to GAPOPEN=90.0, GAPEXT=10. Sequences were colored by Amino acid in Mesquite version 2.71 (Build 514) (Maddison & Maddison 2009) and checked by eye for stop codons.

Phylogenetic Analyses

I sequenced 219 individuals, including 183 *Rhaphiomidas* exemplars and 36 outgroup samples. These data comprised 2904bp of mtDNA (COI, COII, and 16S genes), and 3720bp of nDNA (EF1alpha, PGD, snf, Wg, and CAD). For the analysis of DNA data, each coding sequence was partitioned by codon position, and non-coding regions were treated as a separate single partition. This partitioning strategy was selected because it has been demonstrated repeatedly that incorporating different rates of DNA evolution for each codon position outperforms single partitioning strategies This partitioning strategy was selected because of repeated demonstration that incorporating different rates of DNA evolution outperforms single partitioning strategies (Brandley *et al.* 2005; Fyler *et al.* 2005; Seago *et al.* 2011). Model selection was performed in MrModeltest2.2 (Nylander 2004). The models for different partitions were selected using Akaike information criterion (AIC). For phylogenetic reconstruction, BEAST version 1.7.5 (Drummond *et al.* 2012) was employed. Phylogenetic trees were dated using the relaxed clock methods with a birth death tree prior (Drummond *et al.* 2006). The Markov chain Monte Carlo (MCMC) process was run for $20x10^6$ generations sampling every 1000. Stationary was assessed using the program Tracer version 1.5 3 (Rambaut & Drummond 2007). We used lognormal relaxed clock prior parameters to estimate rates of nucleotide change. The tree was calibrated using a fossil calibration point for the origin of the Mydinae in the late Cretaceous using a normal distribution with a mean of 120Ma and a standard deviation of ±10 Ma.

Data acquisition/Niche Modeling

Specimen data for *Rhaphiomidas* was acquired from museum collections (EMEC, CAS, LACM) and previously published literature (Cazier 1985; Rogers & Mattoni 1993; Rogers & Van Dam 2007; Van Dam 2010), as well as from personal collection of M. H. Van Dam, as part of his thesis work. Locations were georeferenced in ArcGIS (ESRI 2011) and were recorded in both WGS_84 degrees minutes seconds and Lambert Conformal Conic projection required for Daymet georeferencing (http://daymet.ornl.gov/datasupport). A total of 409 occurrence points were used for the

genus with an average of 15 per species and a range of 10-40. The Worldclim database (Hijmans *et al.* 2005) and the 19 Bioclim variables were also downloaded at a 1km by 1km scale and the same set of analyses were undertaken using these bioclimatic variables except where noted. A minimum of 10 georeference points were used for each species. As several of the species are only known from a single dune system, points were randomly scattered across such dune fields. A list of the Daymet tiles is provided in supplementary documents Table 1. The 1km by 1km resolution tiles were downloaded from years 1980-2011. A total of seven variables were used from the Daymet database (vapor pressure *vp*, day length *dayl*, precipitation *prcp*, snow water equivalent *swe*, solar radiation *srad*, temperature max *tmax* and temperature min *tmin*). The data totaled just over 2-terabites of information. The first and last occurrence times were recoded from the specimen data and used to define the time slices to extract from the Daymet climate data. Data for the first and last occurrence dates (Fig. 3) were used as the time slices and environmental variables averaged over the 30 years. For precipitation and snow water equivalent, data were summed by year and then averaged. Each occurrence time slice was saved in the ASCraterII format (Fig. 4). This was done in R statistical software with a custom script (see supplementary information). We utilized the R packages ncdf4, raster, maps and dismo for this process (Hijmans & Etten 2010; Hijmans 2012; Hijmans and van Etten 2010, Brownrigg 2013, Hijmans et al. 2012). Niche models were constructed in MaxEnt (Phillips *et al.* 2006) using the R program *dismo*.

Ancestral state reconstructions and niche overlap

In order to identify the way *Rhaphiomidas* adapts to climate change in different climates regimens, we surveyed historical evidence using ancestral state reconstructions. Ancestral niche states were reconstructed as in Evans *et al* (2009). Predicted niche occupancy (PNO) profiles were first constructed in *phyloclim*, and 100 random samples were then drawn from the PNO profile. PNOs are an interpretation between the niche model produced by MaxEnt and the raster layers from which the models were produced to give a probability of occupancy across an environmental gradient (for a single variable) calculated for each taxon. Calculations of the PNOs from the Daymet data were performed in a different way than for the Bioclim data. Because each one of our time slices were unique to each taxon this could not be performed as for the Bioclim data set because all environmental layers are shared among taxa with Bioclim variables. In contrast, we calculated the range across all taxa layers for a variable, and then calculated the probability of occupancy for each species across its range. Ancestral states were reconstructed under a Brownian motion model using generalized least squares approach (GLS; Martins & Hansen 1997; Cunningham *et al.* 1998). The morphological disparity index (Harmon *et al.* 2003) using the R package *geiger* was computed using the average Manhattan distance between tip state means calculated from PNOs in *phyloclim*. In order to address our hypothesis of niche evolution the morphological disparity index (MDI), was calculated to examine if there was significantly more disparity seen within clades than between clades than expected under Brownian motion. Disparity through time was plotted against the median value calculated from 1000 simulations of the environmental variables under the Brownian motion model. The MDI was calculated as the average difference between subclades, the mean of the observed disparity and median of the simulated data sets (Harmon *et al.* 2003). A positive MDI indicates that there is more

disparity distributed within subclades, whereas a negative value indicates that there is more disparity distributed between subclades than within. A negative value is more indicative of niche conservatism within clades than expected under Brownian motion. Niche overlap was computed in *phyloclim* using PNO profiles, and summary statistics (Schoener's *D* (1968) and Hellinger Distances *I* ;Van der Vaart, 1998) were calculated for overlap as in Warren et al. (2008).

We also wanted to look at how niche overlap changes through time using another metric to measure how *Rhaphiomidas* has changed its niche in a phylogenetic context. One way to examine the relative disparity through time is to look at the age range correlation (ARC; Fitzpatrick & Turelli 2006). This also gives an estimate of the relative conservatism of a niche over time. Niche overlap was calculated in the R program *phyloclim* from the niche overlap values for Schoeners *D*. The age range correlations were also calculated and tested against 1000 simulated randomized data sets for a particular variable. The significance is assessed via the slopes and intercepts when a linear model is fitted to the age range correlations. The ARC was assessed for all of the environmental variables individually.

In order test if *Rhaphiomidas* showed evidence of tracking a particular environmental variable range (e.g. low or high precipitation) or was locally adapting to the environment, we quantified the amount of phylogenetic clustering or overdispersion (Cavender-Bares *et al.* 2004) for a particular environmental variable. Calculations for Blomberg's *K* statistic (Blomberg & Garland 2002; Blomberg *et al.* 2003) and P values were calculated in the R package *picante* 1.6 (Kembel *et al.* 2010).

Evaluating correlation between temperature and body color of Rhaphiomidas

In order to examine whether colder daytime temperatures (when the adult flies are active) are correlated with a darker maculation on the body of the flies, we conducted a Bayesian quantitative genetics threshold model (Wright ,1934); Felsenstein 2012) using MCMC to estimate the liabilities (the point at which the discrete trait changes by way of an unobserved factor the 'liability' at a given threshold, under a continuous time Markov process). We used the R package *phytools* 0.3-72 (Revell 2012), which implements this model in the function *threshBayes*. We ran the MCMC chain for $2x10^6$ generations sampling every 1,000 generations with a burn-in of 2500 samples. We were then able to measure the correlation between the two characters and assess if the correlation coefficients differ significantly from 0.

RESULTS

Molecular data and phylogenetics

Our phylogenetic analysis found that *Rhaphiomidas* is sister to the remaining Mydidae, and these groups together are sister to the Apioceridae (see supplementary Figures). This result is consistent with the phylogeny proposed by Yeates and Irwin (1996) based on morphological data. The basal node of *Rhaphiomidas* is estimated to have diverged 70 ± 42 Ma (node height 95% HPD), but with most of the species diversifying in the last 18.5 ± 11 Ma. There is evidence for considerable incomplete lineage sorting or introgression between some of the more recent species of *Rhaphiomidas*. This pattern was observed between *R. acton acton* and *R. aitkeni,* where

the two species were found in sympatry. In another case, *R. arenagena* and *R. rex* showed a similar pattern where the two species were sympatric. However, in this case, the sympatric populations of the two species are allochronically isolated and *R. acton acton* and *R. aitkeni* are synchronic. When pruning the tree to include single exemplars per species for comparative analyses, these findings were taken into consideration and care was taken to ensure that the genetic data for included exemplars did not reflect introgressed haplotypes (introgressed terminals were removed leaving a topology that was also congruent with a tree constructed from morphological characters of the male epandria).

Niche Modeling Results

Niche models using Daymet and Bioclim variables produced range estimations that were in some cases in agreement, and in other cases strikingly different. The contribution of the seven bioclimatic variables in the Daymet data set showed a pattern in which the snow water equivalent contributed 0% to the bioclimatic models. This was to be expected as the flies are only active in the late spring and summer months at relatively low elevations. Other variables, such as precipitation, contributed consistent and large percentages of the model probability – 90% in the case of *R. undulatus*. Other variables such as DayLength contributed modestly to the model predictions, ranging up to 30% for *R. xanthos*. For Bioclim analyses, precipitation variables also came out as relevant predictors, in addition to temperature in the driest quarter. The distributions predicted by the Bioclim data tended to give more restricted probable distributions, where as the Daymet data tended to give broader range predictions.

Predicted niche occupancy profiles and ancestral state reconstructions

The predicted niche occupancy profiles for the Daymet data show that the niches of most of the *Rhaphiomidas* species are broadly overlapping for precipitation, solar radiation, and vapor pressure. Vapor pressure and precipitation both indicate that the fall-active species experience more rain and humidity. Solar radiation may decrease as part of the increase in vapor pressure, but the species found in areas that have the highest vapor pressure are also found at the lowest elevations. Maximum and minimum temperature both seemed to converge on a zone of preferred temperature for the inland desert species, but the coastal species varied the greatest from near the root average. This may indicate that transitions between climate types, cool coastal to hot inland, may be sharp as there are no species occupying intermediate climate types within clades. This can be seen when looking at the chronograms with the tips plotted to the mean of these variables (Fig. 7). Similar trends are seen in the Bioclim variables where the coastal- and fall-active species varied greatly from the inland desert species.

Niche Overlap and Disparity Through Time

The results from the niche overlap test also highlight how the Daymet data is more sensitive to differences in niche overlap as derived from the PNO data. An average of niche overlap was taken across all the environmental variables. The average species niche overlap also differs between Daymet and Bioclim variables (Fig. 6).

Since we are interested in how *Rhaphiomidas* has partitioned its strategies as a means of adapting to different climate regimes, we wanted to look at the MDI to see if

more change was seen within subclades or between subclades. The morphological disparity of each clade (sister taxa or single taxon and weighted averages of the sister clade) was calculated (Fig. 9) and then these were used to calculate the disparity through time. Simulations of the data as in Garland *et al.* (1993) and Harmon *et al.* (2003) were conducted to produce a null distribution. The MDI was calculated from these null distributions. The results of the MDI show that the precipitation layer of the Daymet data is equivalent in terms of disparity to the Bioclim precipitation warmest quarter layer (Fig. 10). Day length also showed a weak signal of varying more within than between clades. The remaining variables all showed relatively strong signal for more within clade disparity. In addition the disparity through time plots also show that most of the disparity is near the tips of the trees.

Age Range Correlation

The age range correlation (ARC) takes into account the phylogenetic structure of the data when calculating ranges of overlap between clades. When these values are plotted against time and a linear regression fitted to the data, the intercept and slope can be used to estimate phylogenetic signal. Randomly permuting the niche overlap matrix via Monte Carlo simulation, and then calculating the ARC will create a null distribution (Fig. 13). Significance is assessed by determining if the slope and intercept fall outside the null distribution. Differences from the null were seen primarily in the Daymet data (Fig. 14), with all but day length and the slope of precipitation showing significant differences. All of the Bioclim variables failed to reject the null of no phylogenetic signal.

Phylogenetic Signal, Blomberg's K

Calculations for Blomberg's *K* statistic and P values are listed in the Table 1.

Variable	K	PIC.variance.obs	PIC.variance.rnd.mean	PIC.variance.P	PIC.variance.Z	P-value
DAYMET						
tmin	0.41052493	0.750469367	2.469622224	0.013	-1.365531375	0.015015015
tmax	0.147161142	2.125293825	2.10592177	0.602	0.017049197	0.499499499
vp	0.498317445	6151.410904	25815.8969	0.023	-0.950286133	0.068068068
srad	0.448740199	41.80997336	157.1321028	0.008	-1.238997633	0.032032032
prcp	0.471503062	61.03407937	242.7489913	0.067	-0.842329433	0.131131131
dayl	0.247864757	797261.2121	1697478.577	0.103	-1.185963873	0.149149149
BIO CLIM						
Annual Mean Temperature	0.279339193	97.46817329	208.4304018	0.141	-0.94745174	0.116116116
Mean Diurnal Range	0.060542276	0.997934641	0.459377	0.905	1.591381311	0.920920921
Isothermality	0.277041675	0.000458225	0.001049347	0.063	-1.19478555	0.123123123
Temperature Seasonality	0.179635205	376468.0301	571657.1105	0.271	-0.730826519	0.382382382
Maximun Temperature Warmest Month	0.15962036	218.200109	282.3719385	0.379	-0.468998239	0.628628629
Minimum Temperature Warmest Month	0.160644959	233.9285537	305.836055	0.412	-0.445232268	0.491491491
Temperature Annual Range	0.102689356	732.5288211	662.6736681	0.66	0.204835144	0.666666667
Mean Temperatuer Wettest Quarter	0.37694939	495.5144256	1248.446709	0.045	-1.294201278	0.026026026
Mean Temperature Driest Quarter	0.154141161	117.9773157	161.4336817	0.43	-0.437750421	0.516516517
Mean Temperature Warmest Quarter	0.309017862	107.4975317	255.6073112	0.065	-1.211212855	0.076076076
Mean Temperature Coldest Quarter	0.18386955	234.7478391	326.8652502	0.363	-0.553072307	0.23023023
Annual Precipitation	0.294392555	1037.34982	2038.396001	0.157	-0.99056061	0.162162162
Precipitation Wettest Month	0.306089262	51.16300319	108.8715968	0.102	-1.101619614	0.256256256
Precipitation Driest Month	0.230610879	0.875826662	1.659092462	0.406	-0.490337337	0.393393393
Precipitation Seasonality	0.231042585	38.56825589	77.41439467	0.121	-0.988995802	0.282282282
Precipitation Wettest Quarter	0.371251943	302.1812615	749.0976519	0.045	-1.298336423	0.018018018
Precipitation Driest Quarter	0.267934459	7.006673131	14.21346974	0.21	-0.729800228	0.384384384
Precipitation Warmest Quarter	0.434417166	113.5896318	421.5135823	0.019	-1.229907211	0.049049049
Precipitation Coldest Quarter	0.308210187	247.0845255	502.5096138	0.198	-0.927930846	0.138138138

Table 1. Blomberg's *K* statistic and P values by variable.

Two of the Daymet variables (temperature minimum and solar radiation) showed significant phylogenetic signal according to this metric. Among the Bioclim variables, only 3 showed significant phylogenetic signal (Precipitation Wettest Quarter and Mean

Temperature Wettest Quarter), Precipitation Warmest Quarter was marginally significant with a P-value of 0.049.

Evaluating the correlation between temperature and body color of Rhaphiomidas

In order to see if dark body coloration was associated with cooler temperatures, we ran a Bayesian threshold analysis that models the binary color data as a threshold realization of an underlying Brownian motion and evaluates its phylogenetically independent correlation with temperature. The correlation coefficient between color and temperature is -0.7562854, indicating that, as temperature decreases there is a trait change from pale 0 to dark 1 along the tree. A plot of the posterior distribution of the correlation is in Fig. 15. The 95% HPD varied from -0.9718621 to -0.4401001. The correlation coefficient between the color and temperature is -0.7562854. Because this is a Bayesian analysis significance is assessed through the 95% credible interval and its over lap with 0. Our 95% credible interval does not over lap with zero (Fig. 15), so we can say there is a significant correlation between temperature and color.

DISCUSSION

The niche models that were produced from the Daymet data tended to have slightly larger projected niches when compared to those estimated using Bioclim niche models. The Bioclim models seem to show that most of the species of *Rhaphiomidas* are micro-endemics. In some cases this is true, such as for *R. moapa,* which is only known from a single wash. That the Daymet models indicated larger range projections, such as for *R. undulatus,* leads to the question of why the species has not been found in the wider predicted range. One variable we did not include was soil type (sand dune or not), and we suspect that inclusion of this variable or others such as vegetation cover might help to explain why some species have such restricted ranges relative to the predicted environmental conditions suitable for them.

The question as to which environmental layers best capture the conditions that the flies are actually experiencing is best answered by looking at the PNO profiles (Fig. 5). If we look at a set of species that occur in partial sympatry but are separated in time, the Bioclim data does not show any difference between the peaks of highest probable occupancy, whereas the Daymet data does. In parallel with the PNO profiles, we also see marked differences when we look at the niche overlap statistics *D* and *I* (Fig. 6). We would contend that this does in fact demonstrate that the partitioned Daymet data does a better job of capturing the conditions that the flies are experiencing in the adult phase of their life cycle. For example, *R. arenagena* (aka *R. acton maehleri* as labeled in the niche models) is active earlier in the year compared to *R. rex*, and the Bioclim shows their profiles to be overlapping in temperature, whereas they are not overlapping in the Daymet inference. This is seen with all the species that are partially sympatric but separated in time, as well as for some of the allopatric species that are also separated in time.

The ancestral state reconstructions yield some interesting results for *Rhaphiomidas*. The root node could be interpreted as a maximum likelihood reconstruction for the clade *Rhaphiomidas,* as a mean of suitability around which species deviate. This reconstruction does a fair job of quantifying the average suitable

environmental conditions for *Rhaphiomidas*, as a clade that prefers hot temperatures during the day and cool nights, with relatively low humidity and almost no precipitation – a desert taxon. In terms of phylogenetic signal, the minimum temperature (night time) may have more influence on where the flies can live, as this was identified to be an important factor in the niche reconstructions and it shows evidence of phylogenetic signal. We interpret this to mean that clades have certain preferred minimum temperatures that they can withstand during the night, but during the day they are more labile as to what they can adapt to. As this trait showed no significant phylogenetic signal, the response to differences in climates are not tightly bound within a clade and they adapt to local conditions. This inference is also echoed in the disparity through time plots where we can see that for temperature maxima there was significant deviation away from the 95% credible interval indicated in gray, whereas the minimum temperature showed almost no deviation from this and tracked the mean (dashed line) closely (Fig. 11). The MDI also tells us that most of the disparity is seen within clades, suggesting that most of the disparity is seen between sister taxa.

The results from the age range correlations (ARC) suggest that the negative correlation between age and niche overlap. This implies that more recent derived species have greater overlap while older lineages have less. We think the interpretations of the ARC showing phylogenetic signal for more recent species being more similar in trait values than older ones, may have some standing as to the over all trend of the data. However it does not capture the variance of the data, by looking at the regressions significance alone. For example the slope and intercept for tmax both were significant (different from random (i.e. high signal)), however when we look at the disparity through time plot and the Blomberg's *K* value it shows the opposite trend, that there is no over-all signal, and that disparity increases sharply near the tips at several nodes. Further a Mantel test conducted between the overall niche overlap (Schoeners *D*) and phylogenetic distance showed a non-significant negative correlation of -0.1036915 (P-val=0.7869). A similar result also came from the Hellinger Distances *I* and phylogenetic distance (r=-0.1148381, P-val=0.8023).

Finally, in order to see if dark body coloration was associated with cooler temperatures we conducted a Bayesian threshold model. This indicates that there is evidence that the darker coloration of *Rhaphiomidas* is a response to the colder temperatures. This is expected, as *Rhaphiomidas* adults are usually only active above 26.6 ºC (Kingsley 1996, 2002) . The dark coloration allows them to warm themselves adequately, which is necessary to take flight. This is probably especially important for larger flies such as *Rhaphiomidas* species as their larger mass would require more time and energy to heat up.

CONCLUSIONS

There are two main observations that this study demonstrates. One that partitioning climate data to match the environmental conditions works better at describing the environmental niches than does the traditional Bioclim variables. This is seen in the PNO plots as well as in niche overlap values. Understanding the basic life history of an organism can go a long way to producing more realistic niche models. Many animals, especially desert-adapted species, partition their life histories in response to local conditions and so share similar phenologies. For example desert tortoises,

Gopherus agassizii, spend the majority of their life underground during the winter and summer months primarily active in the spring. Modeling the effect of phenology on such species' perceived niches will be critical for better predictions of how these species might respond in the face of future climate change.

The other major finding of this study was the identification of how *Rhaphiomidas* species adapts to different environments. They appear to adapt to cooler conditions by evolving larger areas of maculation (i.e. becoming darker), allowing them to emerge in times when the conditions would otherwise be too cool for them to fly efficiently, or at all. With the evidence from the threshBayes analyses and the phylogenetic disparity through time studies, we can say that the dark coloration of the cooler temperature species is an adaptation for cooler daytime temperatures. The results from the phylogenetic signal test using the *K* statistic also confirms this observation. As there was phylogenetic signal for dealing with the minimum temperatures of the nighttime conditions but this pattern of phylogenetic signal disappeared when looking at the maximal daytime temperatures. This adaptation for dealing with the cooler temperatures has allowed *Rhaphiomidas* to deviate from their thermal mean seen in the ancestral state reconstructions and allowed them to expand to new habitats.

References Cited

Ballmer G, Cazier MA, Osborne K. (1994) Delhi Sands flower-loving fly. In: *Life on the edge: a guide to California's endangered natural resources: wildlife* (eds Helander CG, Crabtree M), pp. 416–417. BioSystems Books.

Blomberg SP, Garland T (2002) Tempo and mode in evolution: phylogenetic inertia, adaptation and comparative methods. *Journal of Evolutionary Biology*, **15**, 899–910.

Blomberg SP, Garland T, Ives AR (2003) Testing for phylogenetic signal in comparative data: behavioral traits are more labile. *Evolution*, **57**, 717–745.

Brandley MC, Schmitz A, Reeder TW (2005) Partitioned Bayesian analyses, partition choice, and the phylogenetic relationships of scincid lizards. *Systematic biology*, **54**, 373–90.

Cavender-Bares J, Ackerly DD, Baum DA, Bazzaz FA (2004) Phylogenetic overdispersion in Floridian oak communities. *The American naturalist*, **163**, 823–43.

Cazier MA (1985) A revision of the North American flies belonging to the genus Rhaphiomidas (Diptera, Apioceridae). *Bulletin of the AMNH*, **182**, 182–263.

Cunningham CW, Omland KE, Oakley TH (1998) Reconstructing ancestral character states: a critical reappraisal. *Trends in Ecology & Evolution*, **13**, 361–366.

Drummond AJ, Ho SYW, Phillips MJ, Rambaut A (2006) Relaxed phylogenetics and dating with confidence. (D Penny, Ed,). *PLoS biology*, **4**, e88.

Drummond AJ, Suchard MA, Xie D, Rambaut A (2012) Bayesian phylogenetics with BEAUti and the BEAST 1.7. *Molecular biology and evolution*, **29**, 1969–73.

ESRI (2011) ArcGIS Desktop: Release 10. *Redlands, CA: Environmental Systems Research ….*

Evans MEK, Smith SA, Flynn RS, Donoghue MJ (2009) Climate, niche evolution, and diversification of the "bird-cage" evening primroses (Oenothera, sections Anogra and Kleinia). *The American naturalist*, **173**, 225–40.

Felsenstein J (2012) A comparative method for both discrete and continuous characters using the threshold model. *The American naturalist*, **179**, 145–56.

Fitzpatrick BM, Turelli M (2006) The geography of mammalian speciation: mixed signals from phylogenies and range maps. *Evolution*, **60**, 601–615.

Fyler CA, Reeder TW, Berta A *et al.* (2005) Historical biogeography and phylogeny of monachine seals (Pinnipedia: Phocidae) based on mitochondrial and nuclear DNA data. *Journal of Biogeography*, **32**, 1267–1279.

Garland T, Dickerman AW, Janis CM, Jones JA (1993) Phylogenetic Analysis of Covariance by Computer Simulation. *Systematic Biology*, **42**, 265–292.

George J, Mattoni R (2006) Rhaphiomidas terminatus terminatus Cazier, 1985 (Diptera: Mydidae): notes on the rediscovery and conservation biology of a presumed extinct species. *Pan-Pacific entomologist*, **82**, 32–35.

Harmon LJ, Schulte JA, Larson A, Losos JB (2003) Tempo and mode of evolutionary radiation in iguanian lizards. *Science (New York, N.Y.)*, **301**, 961–4.

Hijmans RJ (2012) Cross-validation of species distribution models: removing spatial sorting bias and calibration with a null model. *Ecology*, **93**, 679–688.

Hijmans RJ, Cameron SE, Parra JL, Jones PG, Jarvis A (2005) Very high resolution interpolated climate surfaces for global land areas. *International Journal of Climatology*, **25**, 1965–1978.

Hijmans R, Etten J Van (2010) Raster: geographic analysis and modeling with raster data.

Hutchinson GE (1957) Concluding Remarks. *Cold Spring Harbor Symposia on Quantitative Biology*, **22**, 415–427.

Kembel SW, Cowan P, Helmus MR *et al.* (2010) Picante: R tools for integrating phylogenies and ecology. *Bioinformatics*, **26**, 1463–1464.

Kingsley KJ (1996) Behavior of the Delhi Sands Flower-Loving Fly (Diptera: Mydidae), a Little-Known Endangered Species. *Annals of the Entomological Society of America*, **89**, 883–891.

Kingsley KJ (2002) Population Dynamics, Resource Use, and Conservation Needs of the Delhi Sands Flower-loving Fly (Rhaphiomidas Terminatus Abdominalis Cazier) (Diptera: Mydidae), an Endangered Species. *Journal of Insect Conservation*, **6**, 93–101.

Larkin MA, Blackshields G, Brown NP *et al.* (2007) Clustal W and Clustal X version 2.0. *Bioinformatics*, **23**, 2947–2948.

Maddison W, Maddison D (2009) Mesquite: a modular system for evolutionary analysis Version 2.6. *Bioinformatics*.

Martins E, Hansen T (1997) Phylogenies and the comparative method: a general approach to incorporating phylogenetic information into the analysis of interspecific data. *American Naturalist*, 646–667.

Nylander, JAA (2004) MrModeltest v2. Program distributed by the author. Evolutionary Biology Centre, Uppsala University.

Phillips SJ, Anderson RP, Schapire RE (2006) Maximum entropy modeling of species geographic distributions. *Ecological Modelling*, **190**, 231–259.

Rambaut A, Drummond AJ (2007) Tracer v1.4, Available from http://beast.bio.ed.ac.uk/Tracer

Revell LJ (2012) phytools: an R package for phylogenetic comparative biology (and other things). *Methods in Ecology and Evolution*, **3**, 217–223.

Rogers R, Van Dam MH (2007) Two new species of Rhaphiomidas (Diptera : Mydidae). *Zootaxa*, **68**, 61–68.

Rogers R, Mattoni R (1993) Observations on the natural history and conservation biology of the giant flower loving flies, Rhaphiomidas (Diptera: Apioceridae). *Dipterological Research*, **4**, 21–34.

Schoener TW (1968) The Anolis Lizards of Bimini: Resource Partitioning in a Complex Fauna. *Ecology*, **49**, 704.

Seago AE, Giorgi JA, Li J, Ślipiński A (2011) Phylogeny, classification and evolution of ladybird beetles (Coleoptera: Coccinellidae) based on simultaneous analysis of molecular and morphological data. *Molecular Phylogenetics and Evolution*, **60**, 137–151.

Steinberg M, Dorsett D, Shah C, Jones CE, Burk J (1998) Pupal case of Rhaphiomidas acton Coquillett (Diptera: Mydidae) and behavior of newly-emerged adult. *Pan-Pacific Entomologist*, **74**, 178 –180.

Thornton P, Thornton M, Mayer B (2012) DAYMET: Daily Surface Weather on a 1 km Grid for North America. 1980–2008. ... *Center, Oak Ridge, T, N. doi*.

Toft CA, Kimsey LS (1982) Habitat and behavior of selected Apiocera and Rhaphiomidas (Diptera, Apioceridae), and descriptions of the immature stages of A. hispida. *Journal of the Kansas Entomological Society*, **55**, 177–186.

U. S. Fish & Wildlife Service. (1997) *Delhi Sands flower-loving fly (Rhaphiomidas terminatus abdominalis) Recovery Plan*. Portland, Oregon.

Van Dam MH (2010) A new species and key for Rhaphiomidas Osten Sacken (Diptera: Mydidae). *Zootaxa*, **2622**, 49–60.

Van der Vaart A (1998) *Asymptotic statistics. Vol. 3*. Cambridge university press.

Warren DL, Glor RE, Turelli M (2008) Environmental niche equivalency versus conservatism: quantitative approaches to niche evolution. *Evolution; international journal of organic evolution*, **62**, 2868–83.

Wright S (1934) An Analysis of Variability in Number of Digits in an Inbred Strain of Guinea Pigs. *Genetics*, **19**, 506–36.

Yeates DK, Irwin ME (1996) Apioceridae (Insecta: Diptera): cladistic reappraisal and biogeography. *Zoological Journal of the Linnean Society*, **116**, 247–301.

Supplementary Documents: Table 1

List of Daymet Cells: all_cells	rows_N_to_S
12625	1
12626	1
12627	1
12628	1
12629	1
12630	1
12631	1
12632	1
12447	2
12448	2
12449	2
12450	2
12451	2
12452	2
12268	3
12269	3
12270	3
12271	3
12272	3
12088	4
12089	4
12090	4
12091	4
12092	4
11908	5
11909	5
11910	5
11911	5
11912	5
11728	6
11729	6
11730	6
11731	6
11732	6
11733	6
11734	6
11735	6
11736	6
11737	6
11738	6
11739	6
11740	6
11549	7

11550	7
11551	7
11552	7
11553	7
11554	7
11555	7
11556	7
11557	7
11558	7
11559	7
11560	7
11369	8
11370	8
11371	8
11372	8
11373	8
11374	8
11375	8
11376	8
11377	8
11378	8
11379	8
11380	8
11190	9
11191	9
11192	9
11193	9
11194	9
11195	9
11196	9
11197	9
11198	9
11199	9
11200	9
11010	10
11011	10
11012	10
11013	10
11014	10
11015	10
11016	10
11017	10
11018	10
11019	10
11020	10
11021	10

11022	10
10832	11
10833	11
10834	11
10835	11
10836	11
10837	11
10838	11
10839	11
10840	11
10841	11
10842	11
10653	12
10654	12
10655	12
10656	12
10657	12
10658	12
10659	12
10660	12
10661	12
10662	12
10473	13
10474	13
10475	13
10476	13
10477	13
10478	13
10479	13
10480	13
10481	13
10482	13
10294	14
10295	14
10296	14
10297	14
10298	14
10299	14
10300	14
10301	14
10302	14
10115	15
10116	15
10117	15
10118	15
10119	15

10120	15
10121	15
10122	15
9938	16
9939	16
9940	16
9941	16
9942	16

NATURAL HISTORY MATTERS IN CLIMATE NICHE MODELING

ABSTRACT: We explored how partitioning climate data by day (Daymet data) influences niche model predictions, estimated by the MaxEnt machine learning algorithm, of taxa with constrained phenologies. We compared the results with WorldClim data that is partitioned by month to examine what effect using more precise data has on species distribution models. We also compared life history strategies related to climate change, within *Rhaphiomidas*. We examined how phylogenetic signal in both their phenotypic traits and climate tolerances can tell us about how they adapt to different climates. Quantitative information about adaptation can be used to better inform projected range shifts and local extirpations. The findings show that the standard Bioclim variables are misleading as to the real climate space that a focal taxa may occupy. In addition, the use of the Daymet data also allowed for the detection for phylogenetic signal of their thermal preferences. We used a Bayesian threshold model to test the hypothesis that darker maculation of some *Rhaphiomidas* are an adaptation to cooler daytime temperatures, as these may be a means of more rapidly warming their bodies when basking leading to more efficient flight. We found that there was a correlation between these two variables indicating that the dark coloration of *Rhaphiomidas* species is an adaptation for dealing with suboptimal temperatures, allowing them to expand their ecological niche from inland desert to coastal habitats.

INTRODUCTION

Evaluating an organism's response to climate change has become an important research area as global warming is anticipated to change many ecosystems. Examining response to climate change and predicting the future distribution is of concern to a wide array of ecologists and evolutionary biologists. In addition, identifying if a particular species or population adapts to climate change by changing their phenologies or morphological/physiological traits vs changing their range through dispersal, is key to predicting future distributions. These responses can be identified and tested through long-term ecological studies and through phylogenetic analyses. Predicting the future ranges and reconstruction of a species' fundamental niche has relied upon the Worldclim database (Hijmans *et al.* 2005) and the 19 Bioclim variables with ~3722 citations. Although we believe these data are good for capturing the fundamental niches based on abiotic environmental factors experienced year around as in perennial plants and some mammals, it leaves out a whole suite of organisms that have discrete phenologies (e.g. are subterranean or dormant part of the year) that are not captured by the 19 Bioclim variables. The variables themselves are based on monthly averages that have their own limitations for capturing the niche of an organism that may be active for a month or less or that straddles two calendar months, only. In this paper we present a novel way of capturing the niches for organisms with discrete phenologies and discuss the implications for further downstream analyses of periods of activity, reconstructions of ancestral states of climate variables and future niche forecasting in the presence of global environmental change.

The idea of a fundamental niche extends back to Hutchinson (1957), and is broadly used to describe where a species would live without interspecific competition. This is what is being modeled when we reconstruct the environmental niche of an organism. Environmental niche modeling attempts to describe a probability surface of where an organism is likely to occur based on known occurrence data and the environmental variables related to those sites. The resulting niche models are the joint product of the occurrence data and the environmental variables read into the modeling mechanisms whether it is climate niche envelope models or maximum entropy machine learning algorithms. The current approach is to take the occurrence data and let these algorithms identify what factors separate the known occurrence environmental variables from the surrounding regions not having a similar profile. Few authors actually try and evaluate if these variables are actually realistic in capturing what is important for their organisms of concern. Monthly averages are a human construct and are not natural, and binning these further may create problems in addressing a species/population fundamental niche and response to climate change, especially for animals and plants with discrete phenologies. No amount of binning these time slices in further ways will solve this potential problem because the initial averages based on months, constrains all further attempts at capturing salient niche factors. To get around this fundamental issue we utilized climate data that was averaged by day at a 1km square scale from Daymet (Thornton *et al.* 2012).

One possible system to test the effects of having a discrete phenology on niche reconstruction would be in the genus of flies *Rhaphiomidas* (Mydidae). The genus of flies *Rhaphiomidas* (Fig. 1), consists of 23 described species and 5 subspecies (Van Dam 2010). *Rhaphiomidas* is distributed throughout the deserts of the Southwest United States and Northern Mexico (Cazier 1985; Van Dam 2010). Many species of *Rhaphiomidas* feed on floral nectar as adults. *Rhaphiomidas* adults fly in the spring and fall and are most active during spring and fall blooms. Multiple studies have been conducted on the adults' behavior making note of their activity and the temperatures required for the adults to become active (Toft & Kimsey 1982; Rogers & Mattoni 1993; Ballmer *et al.* 1994; Kingsley 1996; Steinberg *et al.* 1998) . This is important because we hypothesize that the darker species of *Rhaphiomidas* evolved this coloration as a response to cooler climates and times of year, and their coloration represents an adaptation to absorb more solar energy and increase their body temperature so they may remain active in cooler climates.

Fig. 1 *Rhaphiomidas acton,* G.Ballmer

Rhaphiomidas terminatus abdominalis is the only species of Diptera federally listed as endangered in the mainland US. The species remains endangered because of dwindling habitat as a result of urban development (U. S. Fish & Wildlife Service 1997). Three other taxa that are also of threatened status are *Rhaphiomidas terminatus terminatus* and *R. trochilus*, and *R. moapa* (Rogers & Van Dam 2007). *Rhaphiomidas terminatus terminatus* is only known from a 20 ha area in the middle of a golf course on the Palos Verdes Peninsula (George & Mattoni 2006). The study of related species of

Rhaphiomidas as well as other sympatric insect species will aide in a better understanding of what habitat is most crucial for their survival.

Larvae and pupa of *Rhaphiomidas* are entirely subterranean. Little is known of the feeding habits of *Rhaphiomidas* as larvae, except that they feed on soft-bodied insect larvae in captivity. In a study (Van Dam in prep) examining where the larvae reside mature *Rhaphiomidas trochilus* larvae (confirmed identity using DNA sequencing) were found at soil depths from 3.5-6ft under the soils surface (Fig 2).

Fig. 2 Left: Excavation of *Rhaphiomidas trochilus* larval habitat (M. H. Van Dam and G. Ballmer 2006). Right: *R. trochilus,* mature larva ~5cm in length. (Photos Ken Osborne)

METHODS

Extraction, PCR, sequencing and alignment

DNA extraction was performed by dissecting thoracic muscle and a leg, each specimen was soaked in the DNAEasy(r) tissue kit's extraction buffer (with proteinase K) overnight, followed by completion of the manufacturer's DNA extraction protocol for animal tissue. The specimens and their associated parts were vouchered and used in subsequent morphological studies. Primers and genes used in this study are listed in Table 1. PCR was performed by using 12.5 ul GoTaq Master Mix (including DNTPs, buffer, taq and dye; Promega Corporation, Madison, WI), 1.25 ul 10lM forward and reverse primer, 7.0 ul water, and 1.0 ul template DNA yielding a 25ul reaction. PCR products were purified with Exosap-IT (US Biochemical Corporation, Cleveland, OH). Sanger sequenced was performed at UC Berkeley's DNA Sequencing Facility. Contigs were assembled and edited in Geneious Pro v. 4.6.4 (Biomatters Ltd.). Sequences were aligned by ClustalW-2.0.10 (Larkin *et al.* 2007) with settings set to GAPOPEN=90.0, GAPEXT=10. Sequences were colored by Amino acid in Mesquite version 2.71 (Build 514) (Maddison & Maddison 2009) and checked by eye for stop codons.

Phylogenetic Analyses

219 individuals (183 *Rhaphiomidas* and 36 outgroups) were sequenced. 2904bp of mtDNA; COI, COII, 16S, and 3720bp of nDNA; EF1alpha, PGD, snf, Wg, CAD, were generated for this study. For the analysis of DNA data, each coding sequence was partitioned by codon position and non-coding regions as singe partition. This partitioning strategy was selected because of repeated demonstration that incorporating different rates of DNA evolution outperforms single partitioning strategies (Brandley *et al.* 2005; Fyler *et al.* 2005; Seago *et al.* 2011). Model selection was performed in MrModeltest2.2 (Nylander 2004). The models for different partitions were

selected using Akaike information criterion (AIC). For phylogenetic reconstruction BEAST version 1.7.5 (Drummond *et al.* 2012) was implemented. Phylogenetic trees were dated using the relaxed clock methods with a birth death tree prior (Drummond *et al.* 2006). The Markov chain Monte Carlo (MCMC) process was run for $20x10^6$ generations sampling every 1000. Stationary was assessed using the program Tracer version 1.5 3 (Rambaut & Drummond 2007). Clock prior parameters used were lognormal relaxed clock to estimate rates of nucleotide change. The tree was calibrated using a fossil calibration point for the origin of the Mydinae in the late Cretaceous using a normal distribution with a mean of 120Ma and a standard deviation of ±10.

Data acquisition/Niche Modeling

Specimen data for *Rhaphiomidas* was acquired from museum collections (EMEC, CAS, LACM) and previously published literature (Cazier 1985; Rogers & Mattoni 1993; Rogers & Van Dam 2007; Van Dam 2010) as well as from personal collection of M. H. Van Dam, as part of his thesis work. Locations were georeferenced in ArcGIS (ESRI 2011) and were recorded in both WGS_84 degrees minutes seconds and Lambert Conformal Conic projection required for Daymet georeferencing (http://daymet.ornl.gov/datasupport). A total of 409 occurrence points were used for the genus with an average of 15 per species and a range of 40 to 10. The Worldclim database (Hijmans *et al.* 2005) and the 19 Bioclim variables were also downloaded at a 1km by 1km scale and underwent all of the same analyses except where noted. A minimum of 10 georeference points was used for a species. As several of the species are only known from a single dune system, points were randomly scattered across such dune fields. A list of the Daymet tiles is provided in supplementary documents Table 1. The 1km by 1km resolution tiles were downloaded from years 1980-2011. A total of seven variables were used from the Daymet database (vapor presser *vp*, day length *dayl*, precipitation *prcp*, snow water equivalent *swe*, solar radiation *srad*, temperature max *tmax* and temperature min *tmin*). The data totaled just over 2-terabites of information. The first and last occurrence times were recoded from the specimen data and used to define the time slices to extract from the Daymet climate data. Data for the first and last occurrence dates (Fig. 3) were used as the time slices and environmental variables averaged over the 30 years. For precipitation and snow water equivalent these were summed by year and then averaged. Each occurrence time slice was saved in the ASCraterII format (Fig. 4). This was done in R statistical software with a script found in the supplementary information. We utilized the R packages ncdf4, raster, maps and dismo for this process (Hijmans & Etten 2010; Hijmans 2012)(Hijmans and van Etten 2010, Brownrigg 2013, Hijmans et al. 2012). Niche models were constructed in MaxEnt (Phillips *et al.* 2006) using the R program *dismo*.

Ancestral state reconstructions and niche overlap

In order to identify the way *Rhaphiomidas* adapts to climate change in different climates regimens, we want to look at historical evidence seen in the ancestral state reconstructions. Ancestral niche states were reconstructed as by Evans *et al* (2009). One hundred random samples were drawn from the predicted niche occupancy (PNO) profile. PNOs were constructed in *phyloclim*. PNOs are an interpretation between the niche model produced by MaxEnt and the raster layers from which the models were produced

to give a probability of occupancy across an environmental gradient (for a single variable) calculated for each taxon. Calculations of the PNOs from the Daymet data were performed in a different way than with the Bioclim data. Because each one of our time slices were unique to each taxon this could not be done as with the Bioclim data set as all environmental layers are shared among taxa in Bioclim. So here we calculated the range across all of the different taxa layers for a variable then given this range calculate the probability of occupancy for each species across their range. Ancestral states were reconstructed under a Brownian motion model using generalized least squares approach (GLS) (Martins & Hansen 1997; Cunningham *et al.* 1998) . The morphological disparity index(Harmon *et al.* 2003) using the R package *geiger* was computed using the average Manhattan distance between tip state means calculated from PNOs in *phyloclim*. The disparity through time plots were plotted against the median value calculated from 1000 simulations of the environmental variables under the Brownian motion model. The morphological disparity index (MDI) was calculated as the average difference between subclades, the mean of the observed disparity and median of the simulated data sets (Harmon *et al.* 2003). A MDI positive indicates that there is more disparity distributed within sublades; when negative the value indicates that there is more disparity distributed between subclades than with in and is more indicative of niche conservatism with in clades. Niche overlap was computed in *phyloclim* using PNO profiles, summary statistics were calculated for overlap as in Warren et al. (2008); Schoeners *D* (1968) and Hellinger Distances *I* (Van der Vaart 1998) .

We also wanted to look at how niche overlap changes through time using another metric to measure how *Rhaphiomidas* has changed its niche in a phylogenetic context. One way to examine the relative disparity through time is to look at the age range correlation (ARC) (Fitzpatrick & Turelli 2006). This also gives an estimate of the relative conservatism of a niche over time. Niche overlap was calculated in the R program *phyloclim* from the niche overlap values Schoeners *D*. The age range correlations were also calculated and tested against 1000 simulated randomized data sets for a particular variable. The significance is assessed via the slopes and intercept when a linear model is fitted to the age range correlations. The ARC was assessed for all of the environmental variables individually.

In order test if *Rhaphiomidas* showed evidence of tracking a particular environmental variable range (e.g. low or high precipitation) or was locally adapting to the environment we quantified the amount of phylogenetic clustering or overdispersion (Cavender-Bares *et al.* 2004) for a particular environmental variable. Calculations for Blomberg's *K* statistic (Blomberg & Garland 2002; Blomberg *et al.* 2003) and P values were calculated in the R package *picante* 1.6 (Kembel *et al.* 2010).

Evaluating correlation between temperature and body color of Rhaphiomidas

Finally in order to examine whether colder daytime temperatures (when the adult flies are active) are correlated with a darker maculation on the body of the flies we conducted a Bayesian quantitative genetics threshold model Wright (1934), Felsenstein (2012)using MCMC to estimate the liabilities. i.e. the point at which the discrete trait changes by way of an unobserved factor the 'liability' at a given threshold, under a continuous time Markov process. We used the R package *phytools* 0.3-72 (Revell 2012), which implements this model in the function *threshBayes*. We ran the MCMC chain for

$2x10^6$ generations sampling every 1,000 generations with a burn-in of 2500 samples. We were then able to measure the correlation between the two characters and assess if the correlation coefficients differ significantly from 0.

RESULTS

Molecular data and phylogenetics

In the results tree (see supplementary Figures), *Rhaphiomidas* is sister to the remaining Mydidae and these in tern are sister to the Apioceridae. This result is consistent with the phylogeny proposed by Yeates and Irwin (1996) based on morphological data. The basal node of *Rhaphiomidas* splits at 70±42Ma (node height 95% HPD) but with most of the species diversifying in the last 18.5±11Ma. There was a considerable amount of incomplete lineage sorting and or introgression in some of the more recent species of *Rhaphiomidas*. This pattern was observed between *R. acotn acton* and *R. aitkeni,* where the two species were found in sympatry. In the other case *R. arenagena* and *R. rex* also showed a similar pattern where the two species were sympatric. However in this case the sympatric populations of the two species are allochronically isolated and *R. acotn acton* and *R. aitkeni* are synchronic. When pruning down the tree into single species for comparative analyses, these patterns were taken into consideration. The introgressed terminals were removed leaving what are believed to be the correct relationships based on morphological evidence from the male epandria.

Niche Modeling Results

Niche models using both Daymet and Bioclim produced distributions that were both similar and different in some striking ways. The contribution of the 7 bioclimatic variables in the Daymet data set showed a pattern where the snow water equivalent contributed 0% to the bioclimatic models. This was to be expected as the flies are only active in the late spring and summer months at relatively low elevations. Other variables such as precipitation contributed consistent and large percentage of the model probability; 90% in the case of *R. undulatus*. Other variables such as DayLength contributed a modestly to the model predictions ranging upwards of 30% in *R. xanthos*. In the case of Bioclim the precipitation variables also came out as a relevant predictor in addition to the temperature in the driest quarter. The distributions predicted by the Bioclim data tended to give more restricted probable distributions, where as the Daymet data tended to give broader predictions.

Predicted niche occupancy profiles and ancestral state reconstructions

The predicted niche occupancy profiles for the Daymet data shows that the niches of most of the *Rhaphiomidas* species are broadly overlapping for precipitation, solar radiation and vapor pressure. Vapor pressure and precipitation both show that the fall active species experience more rain and humidity. Solar radiation may decrease as part of the increase in vapor pressure but the species found in areas that have the highest vapor pressure are also found at the lowest elevations. Maximum and minimum temperature both seemed to converge on a zone of preferred temperature for the inland desert species but the coastal species varied the greatest from this zone. This can be seen when looking at the chronograms with the tips plotted to the mean of these variables (Fig. 7). Similar

trends are seen in the Bioclim variables where the coastal and fall active species varied greatly from the inland desert species.

Niche Overlap and Disparity Through Time

The results from the niche overlap test also highlight how the Daymet data is more sensitive to differences in niche overlap as derived from the PNO data. An average of niche overlap was taken across all the environmental variables. The average species niche overlap also differs between Daymet and Bioclim variables (Fig. 6).

Since we are interested in how *Rhaphiomidas* has partitioned its strategies for adapting to different climate regimes we wanted to look at the MDI to see if more change was seen within subclades or between subclades. The morphological disparity of each clade (sister taxa or single taxon and weighted averages of the sister clade) was calculated (Fig. 9) and then these were used to calculate the disparity through time. Simulations of the data as in (Garland *et al.* 1993; Harmon *et al.* 2003) were conducted to produce a null distribution. The MDI was calculated from these null distributions. The results of the MDI show that the precipitation layer of the Daymet data is equivalent in terms of disparity to the Bioclim precipitation warmest quarter layer (Fig. 10). Day length also showed a weak signal of varying more within than between clades. The remaining variables all showed relatively strong signal for more within clade disparity. In addition the disparity through time plots also show that most of the disparity is near the tips of the trees.

Age Range Correlation

The age range correlation (ARC) takes into account the phylogenetic structure of the data when calculating the range of overlap between clades. When these values are plotted against time and a linear regression fitted to the data the intercept and slope can be used to estimate phylogenetic signal. Randomly permuting the niche overlap matrix via Monte Carlo then calculating the ARC will create a null distribution (Fig. 13). Significance is assessed by seeing if the slope and intercept fall outside the null distribution. Differences from the null were seen primarily in the Daymet data (Fig. 14), with all but day length and the slope of precipitation showing significant difference. All of the Bioclim variables failed to reject the null of no phylogenetic signal.

Phylogenetic Signal, Blomberg's K

Calculations for Blomberg's *K* statistic and P values are listed in the Table 1.

variable	K	PIC.variance.obs	PIC.variance.rnd.mean	PIC.variance.P	PIC.variance.Z	P-value
DAYMET						
tmin	0.41052493	0.750469367	2.469622224	0.013	-1.365531375	0.015015015
tmax	0.147161142	2.125293825	2.10592177	0.602	0.017049197	0.499499499
vp	0.498317445	6151.410904	25815.8969	0.023	-0.950286133	0.068068068
srad	0.448740199	41.80997336	157.1321028	0.008	-1.238997633	0.032032032
prcp	0.471503062	61.03407937	242.7489913	0.067	-0.842329433	0.131131131
dayl	0.247864757	797261.2121	1697478.577	0.103	-1.185963873	0.149149149
BIO CLIM						
Annual Mean Temperature	0.279339193	97.46817329	208.4304018	0.141	-0.94745174	0.116116116
Mean Diurnal Range	0.060542276	0.997934641	0.459377	0.905	1.591381311	0.920920921
Isothermality	0.277041675	0.00045825	0.001049347	0.063	-1.1947855	0.123123123
Temperature Seasonality	0.179635205	376468.0301	571657.1105	0.271	-0.730826519	0.382382382
Maximun Temperature Warmest Month	0.15962036	218.200109	282.3719385	0.379	-0.468998239	0.628628629
Minimum Temperature Warmest Month	0.160644959	233.9285537	305.836055	0.412	-0.445232268	0.491491491
Temperature Annual Range	0.102689356	732.5288211	662.6736681	0.66	0.204835144	0.666666667
Mean Temperatuer Wettest Quarter	0.37694939	495.5144256	1248.446709	0.045	-1.294201278	0.026026026
Mean Temperature Driest Quarter	0.154141161	117.9773157	161.4336817	0.43	-0.437750421	0.516516517
Mean Temperature Warmest Quarter	0.309017862	107.4975317	255.6073112	0.065	-1.211212855	0.076076076
Mean Temperature Coldest Quarter	0.18386955	234.7478391	326.8652502	0.363	-0.553072307	0.23023023
Annual Precipitation	0.294392555	1037.34982	2038.396001	0.157	-0.99056061	0.162162162
Precipitation Wettest Month	0.306089262	51.16300319	108.8715968	0.102	-1.101619614	0.256256256
Precipitation Driest Month	0.230610879	0.875826662	1.659092462	0.406	-0.490337337	0.393393393
Precipitation Seasonality	0.231042585	38.56825589	77.41439467	0.121	-0.988995802	0.282282282
Precipitation Wettest Quarter	0.371251943	302.1812615	749.0976519	0.045	-1.298336423	0.018018018
Precipitation Driest Quarter	0.267934459	7.006673131	14.21346974	0.21	-0.729800228	0.384384384
Precipitation Warmest Quarter	0.434417166	113.5896318	421.5135823	0.019	-1.229907211	0.049049049
Precipitation Coldest Quarter	0.308210187	247.0845255	502.5096138	0.198	-0.927930846	0.138138138

Table 1. Blomberg's *K* statistic and P values by variable.

Two of the Daymet variables (temperature minimum and solar radiation) showed significant phylogenetic signal according to this metric. Among the Bioclim variables only 3 showed significant phylogenetic signal (Precipitation Wettest Quarter and Mean Temperature Wettest Quarter), Precipitation Warmest Quarter was marginally significant with a P-value of 0.049.

Evaluating correlation between temperature and body color of Rhaphiomidas

In order to see if dark body coloration was associated with cooler temperatures we ran a Bayesian threshold analysis that models the binary color data as a thresholded realization of an underlying Brownian motion and evaluates its phylogenetically independent correlation with temperature. The correlation coefficient between color and temperature is -0.7562854, indicating that, as temperature decreases there is a trait change from pale 0 to dark 1 along the tree. A plot of the posterior distribution of the correlation is in (Fig. 15). The 95% HPD varied from -0.9718621 to -0.4401001.

DISCUSSION

The niche models that were produced from the Daymet data tended to have slightly larger projected niches when compared to the to the Bioclim niche models. The Bioclim models seem to show that most of the species of *Rhaphiomidas* are micro-endemics. In some cases this is true, such as in *R. moapa,* which is only known from a single wash. The Daymet models show larger range projections such as in *R. undulatus* leading to the question as to why they have not been found in these wider ranges. One variable we did not include was a binary variable of soil type (sand dune or not) we believe that with the inclusion of this variable or others such as vegetation cover might help to explain why some species have such restricted ranges relative to what environmental conditions are suitable to them.

The question as to which environmental layers best capture the conditions that the flies are actually experiencing is best answered by looking at the PNO profiles (Fig. 5). If we look at a set of species that occur in partial sympatry but are separated in time the

Bioclim data does not show any difference between the peaks of highest probable occupancy, whereas the Daymet data does. In parallel with the PNO profiles we also see marked differences when we look at the niche overlap statistics *D* and *I* (Fig. 6). We would contend that this does in fact demonstrate that the partitioned Daymet data does a better job of capturing the conditions that the flies are experiencing in the adult phase of their life cycle. For example *R. arenagena* (aka *R. acton maehleri* as labeled in the niche models) occurs earlier in the year compared to *R. rex*, and the Bioclim shows their profiles to be overlapping in temperature, whereas they do not in the Daymet data. This is seen with all the species that are partially sympatric but separated in time, as well as some of the allopatric species that are also separated in time.

The ancestral state reconstructions yield some interesting results for *Rhaphiomidas*. The root node could be interpreted as a maximum likelihood reconstruction for the clade *Rhaphiomidas,* as a mean of suitability around which species deviate from. This reconstruction does a fair job of quantifying the average suitable environmental conditions for *Rhaphiomidas*, as a clade that prefers hot temperatures during the day and cool nights with relatively low humidity and almost no precipitation, a desert taxon. In terms of phylogenetic signal the minimum temperature (night time) may have more influence on where the flies can live as this was identified to be an important factor in the niche reconstructions and it shows evidence of phylogenetic signal. The interpretation could be that clades have certain preferred minimum temperatures they can withstand during the night, but during the day they are more labile as to what they can adapt to as this trait showed no significant phylogenetic signal. This inference is also echoed in the disparity through time plots where we can see that for temperature maxima there was significant deviation away from the 95% credible interval indicated in gray, whereas the minimum temperature showed almost no deviation from this and tracked the mean (dashed line) closely (Fig. 11). The MDI also tells us that most of the disparity is seen within clades indicating that most of the disparity is seen between sister taxa.

The results from the age range correlations (ARC) suggest that the negative correlation between age and niche overlap. This implies that more recent derived species have greater overlap while older lineages have less. We think the interpretations as for the ARC showing phylogenetic signal may have some standing as to the over all trend of the data but does not capture the subtleties of the data by looking at the regressions significance alone. For example the slope and intercept for tmax both were significant (different from random (no signal)), however when we look at the disparity through time plot and the Blomberg's *K* value it shows an opposite trend, that there is no over all signal, and that disparity increases sharply near the tips at several nodes. Further a Mantel test conducted between the overall niche overlap Schoeners *D* and phylogenetic distance showed a negative correlation of -0.1036915 between the phylogenetic distance and niche overlap and that the two variables were not significantly correlated P-val=0.7869. A similar result also came from the Hellinger Distances *I* and phylogenetic distance (r=-0.1148381, P-val=0.8023).

Finally in order to see if dark body coloration was associated with cooler temperatures we conducted a Bayesian threshold model. The correlation coefficient between the color and temperature is -0.7562854. This indicates that there is evidence that the darker coloration of *Rhaphiomidas* is a response to the colder temperatures. This is expected, as *Rhaphiomidas* adults are usually only active above 26.6 ºC (Kingsley

1996, 2002) . The dark coloration allows them to warm themselves adequately, which is necessary to take flight. This is probably especially important for larger flies such as *Rhaphiomidas* species as their larger mass would require more time and energy to heat up.

CONCLUSIONS

There are two main observations that this study demonstrates. One that partitioning climate data to match the environmental conditions works better at describing the environmental niches than does the traditional Bioclim variables. This is seen in the PNO plots as well as in niche overlap values. Understanding the basic life history of an organism can go a long way to producing more realistic niche models. Many animals, especially desert-adapted species, partition their life histories in response to local conditions and so share similar phenologies. For example desert tortoises, *Gopherus agassizii,* spend the majority of their life underground during the winter and summer months primarily active in the spring. Modeling the effect of phenology on such species' perceived niches will be critical for better predictions of how these species might respond in the face of future climate change.

The other major finding of this study was the identification of how *Rhaphiomidas* species adapts to different environments. They appear to adapt to cooler conditions by evolving larger areas of maculation (i.e. darker), allowing them to emerge in times when the conditions otherwise may be too cool for them to fly efficiently, or at all. With the evidence from the threshBayes analyses and the phylogenetic disparity through time studies we can say that the dark coloration of the cooler temperature species is an adaptation for cooler daytime temperatures. The results from the phylogenetic signal test using the *K* statistic also confirms this observation. As there was phylogenetic signal for dealing with the minimum temperatures of the nighttime conditions but this pattern of phylogenetic signal disappeared when looking at the maximal daytime temperatures. This adaptation for dealing with the cooler temperatures has allowed *Rhaphiomidas* to deviate from their thermal mean seen in the ancestral state reconstructions and allowed them to expand to new habitats

References Cited

Ballmer G, Cazier MA, Osborne K. (1994) Delhi Sands flower-loving fly. In: *Life on the edge: a guide to California's endangered natural resources: wildlife* (eds Helander CG, Crabtree M), pp. 416–417. BioSystems Books.

Blomberg SP, Garland T (2002) Tempo and mode in evolution: phylogenetic inertia, adaptation and comparative methods. *Journal of Evolutionary Biology*, **15**, 899–910.

Blomberg SP, Garland T, Ives AR (2003) Testing for phylogenetic signal in comparative data: behavioral traits are more labile. *Evolution*, **57**, 717–745.

Brandley MC, Schmitz A, Reeder TW (2005) Partitioned Bayesian analyses, partition choice, and the phylogenetic relationships of scincid lizards. *Systematic biology*, **54**, 373–90.

Cavender-Bares J, Ackerly DD, Baum DA, Bazzaz FA (2004) Phylogenetic overdispersion in Floridian oak communities. *The American naturalist*, **163**, 823–43.

Cazier MA (1985) A revision of the North American flies belonging to the genus Rhaphiomidas (Diptera, Apioceridae). *Bulletin of the AMNH*, **182**, 182–263.

Cunningham CW, Omland KE, Oakley TH (1998) Reconstructing ancestral character states: a critical reappraisal. *Trends in Ecology & Evolution*, **13**, 361–366.

Drummond AJ, Ho SYW, Phillips MJ, Rambaut A (2006) Relaxed phylogenetics and dating with confidence. (D Penny, Ed,). *PLoS biology*, **4**, e88.

Drummond AJ, Suchard MA, Xie D, Rambaut A (2012) Bayesian phylogenetics with BEAUti and the BEAST 1.7. *Molecular biology and evolution*, **29**, 1969–73.

ESRI (2011) ArcGIS Desktop: Release 10. *Redlands, CA: Environmental Systems Research ….*

Evans MEK, Smith SA, Flynn RS, Donoghue MJ (2009) Climate, niche evolution, and diversification of the "bird-cage" evening primroses (Oenothera, sections Anogra and Kleinia). *The American naturalist*, **173**, 225–40.

Felsenstein J (2012) A comparative method for both discrete and continuous characters using the threshold model. *The American naturalist*, **179**, 145–56.

Fitzpatrick BM, Turelli M (2006) The geography of mammalian speciation: mixed signals from phylogenies and range maps. *Evolution*, **60**, 601–615.

Fyler CA, Reeder TW, Berta A *et al.* (2005) Historical biogeography and phylogeny of monachine seals (Pinnipedia: Phocidae) based on mitochondrial and nuclear DNA data. *Journal of Biogeography*, **32**, 1267–1279.

Garland T, Dickerman AW, Janis CM, Jones JA (1993) Phylogenetic Analysis of Covariance by Computer Simulation. *Systematic Biology*, **42**, 265–292.

George J, Mattoni R (2006) Rhaphiomidas terminatus terminatus Cazier, 1985 (Diptera: Mydidae): notes on the rediscovery and conservation biology of a presumed extinct species. *Pan-Pacific entomologist*, **82**, 32–35.

Harmon LJ, Schulte JA, Larson A, Losos JB (2003) Tempo and mode of evolutionary radiation in iguanian lizards. *Science (New York, N.Y.)*, **301**, 961–4.

Hijmans RJ (2012) Cross-validation of species distribution models: removing spatial sorting bias and calibration with a null model. *Ecology*, **93**, 679–688.

Hijmans RJ, Cameron SE, Parra JL, Jones PG, Jarvis A (2005) Very high resolution interpolated climate surfaces for global land areas. *International Journal of Climatology*, **25**, 1965–1978.

Hijmans R, Etten J Van (2010) Raster: geographic analysis and modeling with raster data.
Hutchinson GE (1957) Concluding Remarks. *Cold Spring Harbor Symposia on Quantitative Biology*, **22**, 415–427.
Kembel SW, Cowan P, Helmus MR *et al.* (2010) Picante: R tools for integrating phylogenies and ecology. *Bioinformatics*, **26**, 1463–1464.
Kingsley KJ (1996) Behavior of the Delhi Sands Flower-Loving Fly (Diptera: Mydidae), a Little-Known Endangered Species. *Annals of the Entomological Society of America*, **89**, 883–891.
Kingsley KJ (2002) Population Dynamics, Resource Use, and Conservation Needs of the Delhi Sands Flower-loving Fly (Rhaphiomidas Terminatus Abdominalis Cazier) (Diptera: Mydidae), an Endangered Species. *Journal of Insect Conservation*, **6**, 93–101.
Larkin MA, Blackshields G, Brown NP *et al.* (2007) Clustal W and Clustal X version 2.0. *Bioinformatics*, **23**, 2947–2948.
Maddison W, Maddison D (2009) Mesquite: a modular system for evolutionary analysis Version 2.6. *Bioinformatics*.
Martins E, Hansen T (1997) Phylogenies and the comparative method: a general approach to incorporating phylogenetic information into the analysis of interspecific data. *American Naturalist*, 646–667.
Nylander, JAA (2004) MrModeltest v2. Program distributed by the author. Evolutionary Biology Centre, Uppsala University.
Phillips SJ, Anderson RP, Schapire RE (2006) Maximum entropy modeling of species geographic distributions. *Ecological Modelling*, **190**, 231–259.
Rambaut A, Drummond AJ (2007) Tracer v1.4, Available from http://beast.bio.ed.ac.uk/Tracer
Revell LJ (2012) phytools: an R package for phylogenetic comparative biology (and other things). *Methods in Ecology and Evolution*, **3**, 217–223.
Rogers R, Van Dam MH (2007) Two new species of Rhaphiomidas (Diptera : Mydidae). *Zootaxa*, **68**, 61–68.
Rogers R, Mattoni R (1993) Observations on the natural history and conservation biology of the giant flower loving flies, Rhaphiomidas (Diptera: Apioceridae). *Dipterological Research*, **4**, 21–34.
Schoener TW (1968) The Anolis Lizards of Bimini: Resource Partitioning in a Complex Fauna. *Ecology*, **49**, 704.
Seago AE, Giorgi JA, Li J, Ślipiński A (2011) Phylogeny, classification and evolution of ladybird beetles (Coleoptera: Coccinellidae) based on simultaneous analysis of molecular and morphological data. *Molecular Phylogenetics and Evolution*, **60**, 137–151.
Steinberg M, Dorsett D, Shah C, Jones CE, Burk J (1998) Pupal case of Rhaphiomidas acton Coquillett (Diptera: Mydidae) and behavior of newly-emerged adult. *Pan-Pacific Entomologist*, **74**, 178 –180.
Thornton P, Thornton M, Mayer B (2012) DAYMET: Daily Surface Weather on a 1 km Grid for North America. 1980–2008. ... *Center, Oak Ridge, T, N. doi*.

Toft CA, Kimsey LS (1982) Habitat and behavior of selected Apiocera and Rhaphiomidas (Diptera, Apioceridae), and descriptions of the immature stages of A. hispida. *Journal of the Kansas Entomological Society*, **55**, 177–186.

U. S. Fish & Wildlife Service. (1997) *Delhi Sands flower-loving fly (Rhaphiomidas terminatus abdominalis) Recovery Plan*. Portland, Oregon.

Van Dam MH (2010) A new species and key for Rhaphiomidas Osten Sacken (Diptera: Mydidae). *Zootaxa*, **2622**, 49–60.

Van der Vaart A (1998) *Asymptotic statistics. Vol. 3*. Cambridge university press.

Warren DL, Glor RE, Turelli M (2008) Environmental niche equivalency versus conservatism: quantitative approaches to niche evolution. *Evolution; international journal of organic evolution*, **62**, 2868–83.

Wright S (1934) An Analysis of Variability in Number of Digits in an Inbred Strain of Guinea Pigs. *Genetics*, **19**, 506–36.

Yeates DK, Irwin ME (1996) Apioceridae (Insecta: Diptera): cladistic reappraisal and biogeography. *Zoological Journal of the Linnean Society*, **116**, 247–301.

Supplementary Documents: Table 1

List of Daymet Cells: all_cells	rows_N_to_S
12625	1
12626	1
12627	1
12628	1
12629	1
12630	1
12631	1
12632	1
12447	2
12448	2
12449	2
12450	2
12451	2
12452	2
12268	3
12269	3
12270	3
12271	3
12272	3
12088	4
12089	4
12090	4
12091	4
12092	4
11908	5
11909	5
11910	5
11911	5
11912	5
11728	6
11729	6
11730	6
11731	6
11732	6
11733	6
11734	6
11735	6
11736	6
11737	6
11738	6
11739	6
11740	6
11549	7

11550	7
11551	7
11552	7
11553	7
11554	7
11555	7
11556	7
11557	7
11558	7
11559	7
11560	7
11369	8
11370	8
11371	8
11372	8
11373	8
11374	8
11375	8
11376	8
11377	8
11378	8
11379	8
11380	8
11190	9
11191	9
11192	9
11193	9
11194	9
11195	9
11196	9
11197	9
11198	9
11199	9
11200	9
11010	10
11011	10
11012	10
11013	10
11014	10
11015	10
11016	10
11017	10
11018	10
11019	10
11020	10
11021	10

11022	10
10832	11
10833	11
10834	11
10835	11
10836	11
10837	11
10838	11
10839	11
10840	11
10841	11
10842	11
10653	12
10654	12
10655	12
10656	12
10657	12
10658	12
10659	12
10660	12
10661	12
10662	12
10473	13
10474	13
10475	13
10476	13
10477	13
10478	13
10479	13
10480	13
10481	13
10482	13
10294	14
10295	14
10296	14
10297	14
10298	14
10299	14
10300	14
10301	14
10302	14
10115	15
10116	15
10117	15
10118	15
10119	15

10120	15
10121	15
10122	15
9938	16
9939	16
9940	16
9941	16
9942	16

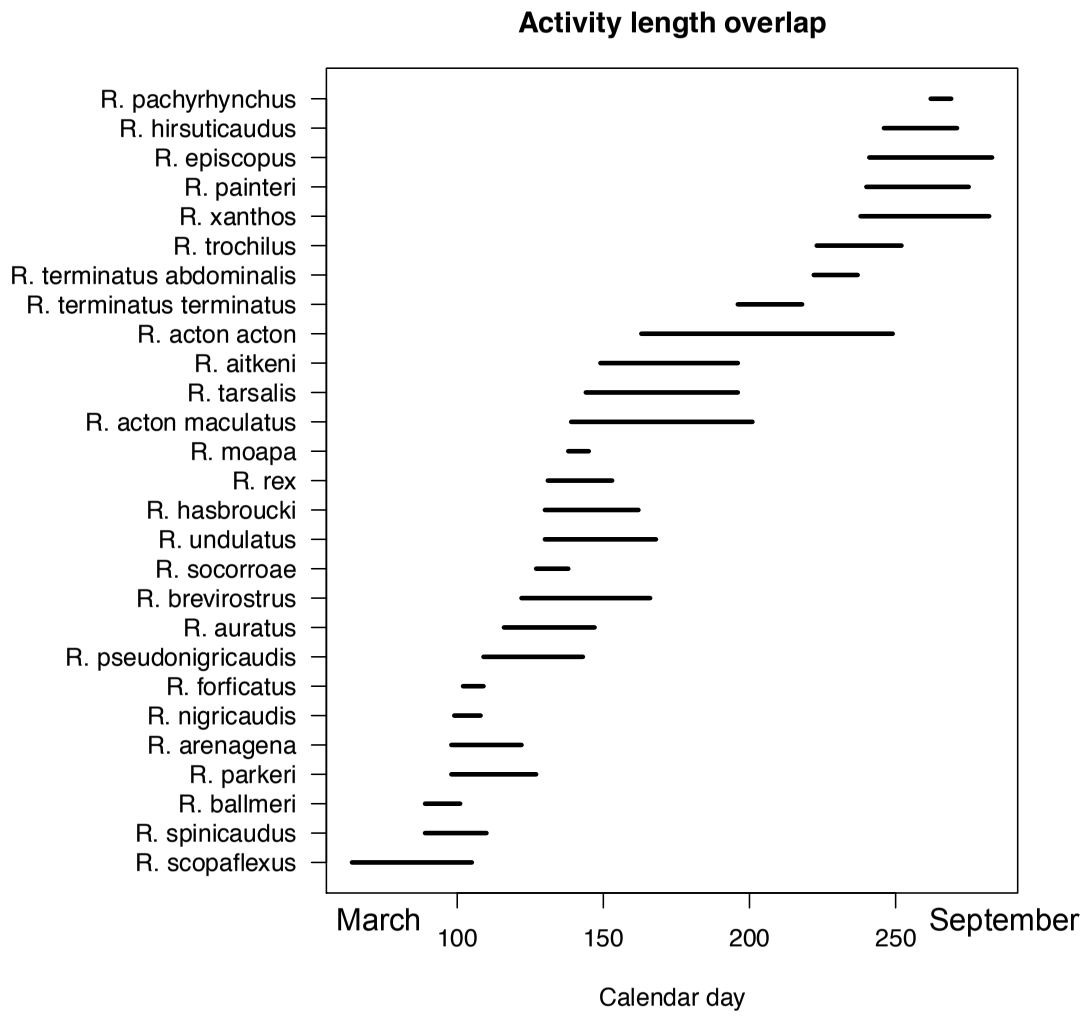

Fig. 3 Activity time and length of *Rhaphiomidas.*

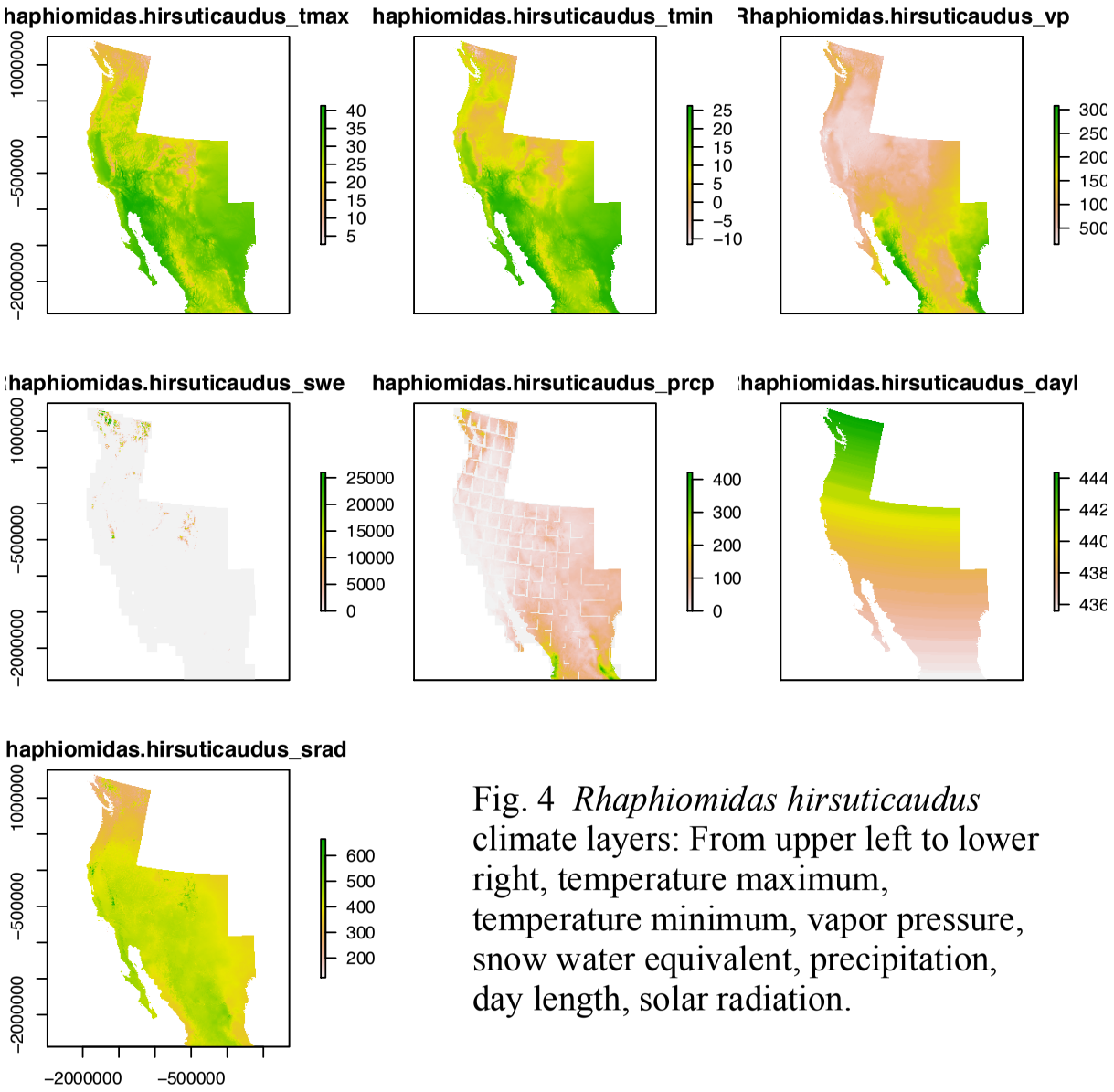

Fig. 4 *Rhaphiomidas hirsuticaudus* climate layers: From upper left to lower right, temperature maximum, temperature minimum, vapor pressure, snow water equivalent, precipitation, day length, solar radiation.

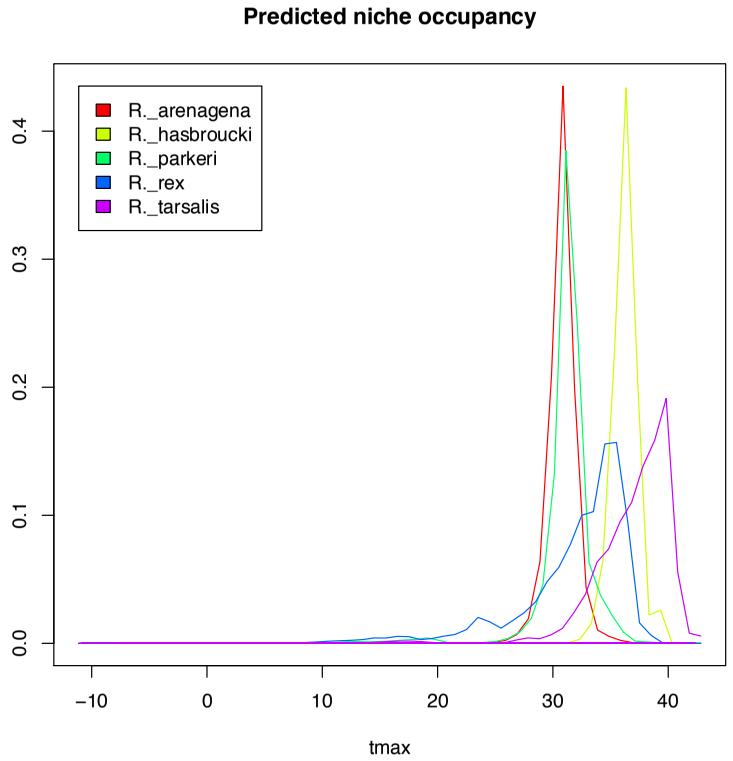

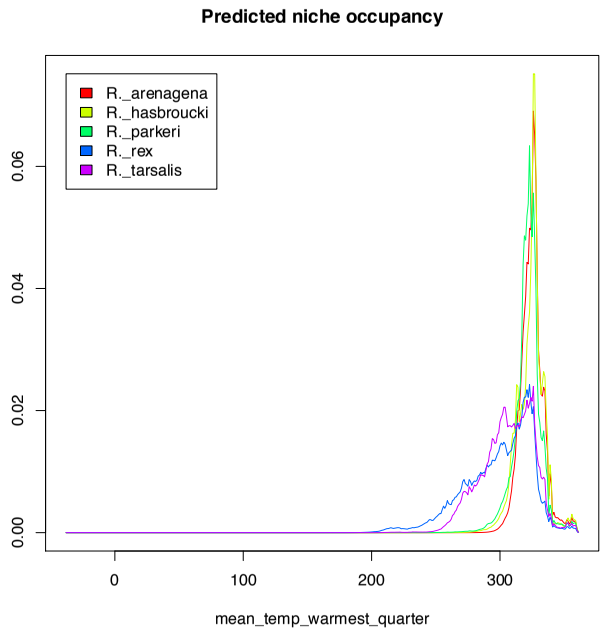

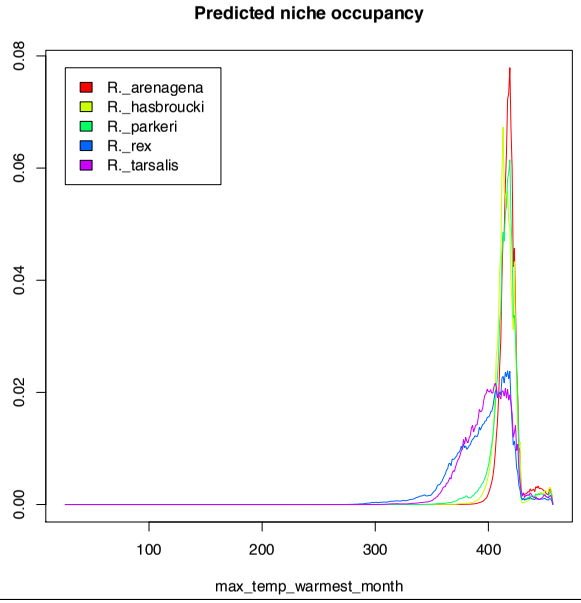

Fig 5. Predicted niche occupancy (PNO), for the sympatrick species of *Rhaphiomidas*. From upper left to lower right: temperature maximum PNO Daymet, mean temperature warmest quarter Bioclim, Maxtemp warmest month.

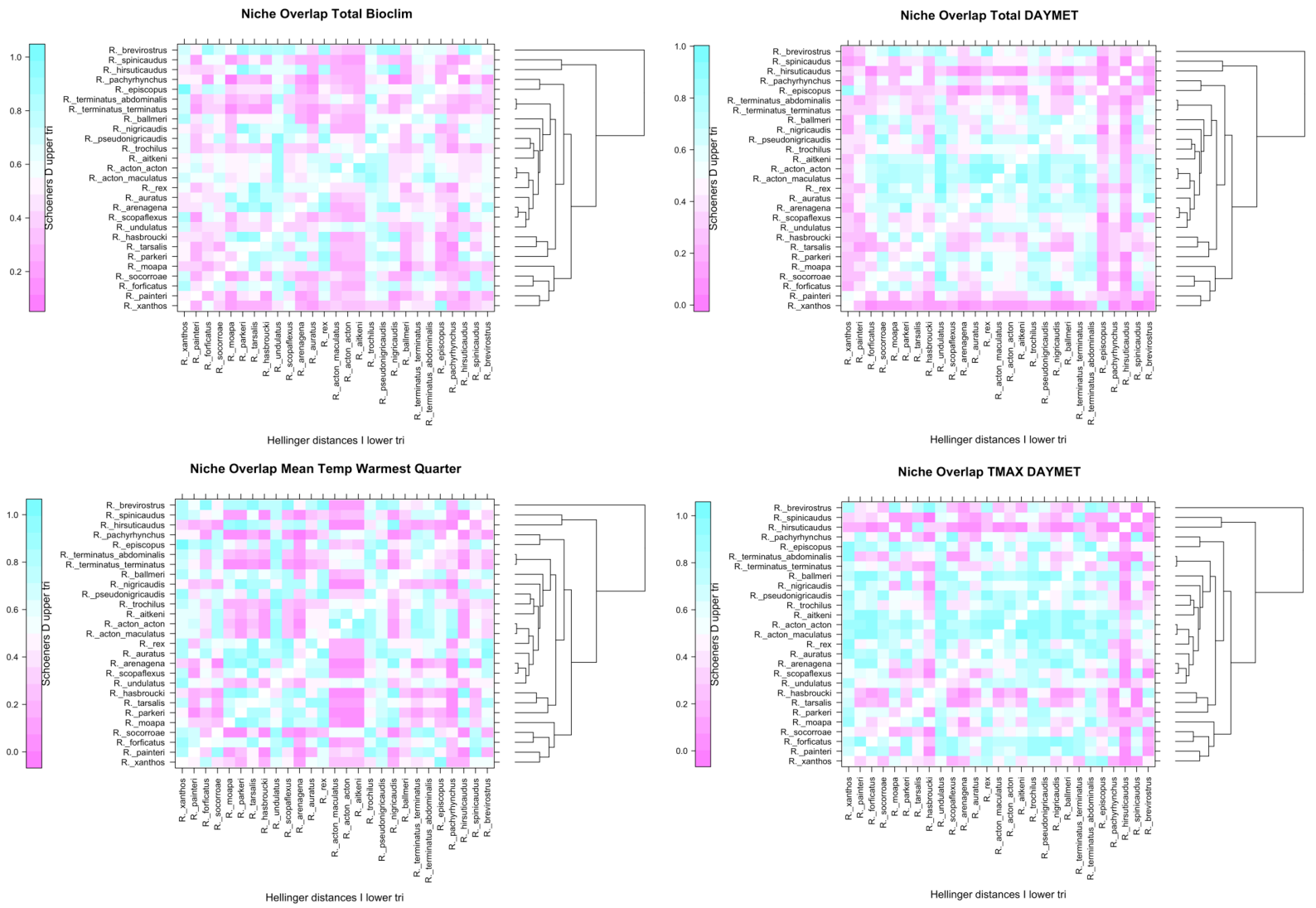

Fig. 6 Niche overlap, phylogeny on right: Upper left to lower right, total overlap Bioclim, total overlap Daymet, niche overlap mean temperature warmest quarter Bioclim, niche overlap temperature maximum Daymet. Upper triangle Schoenhers *D*, lower triangle Hellinger distance *I*.

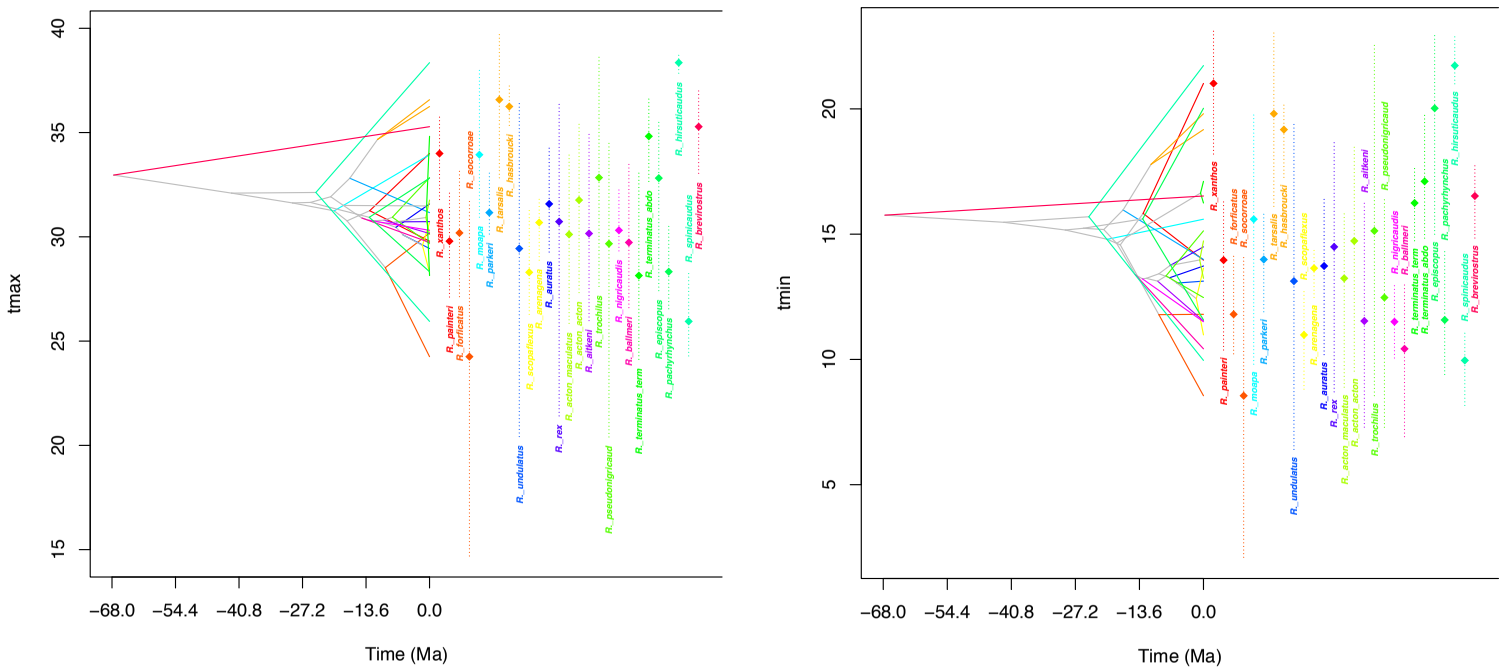

Fig. 7 Ancestral state reconstructions for Daymet environmental variables tmax, tmin. Dashed lines indicate range and diamonds indicate means. Branch tips aligned to mean value.

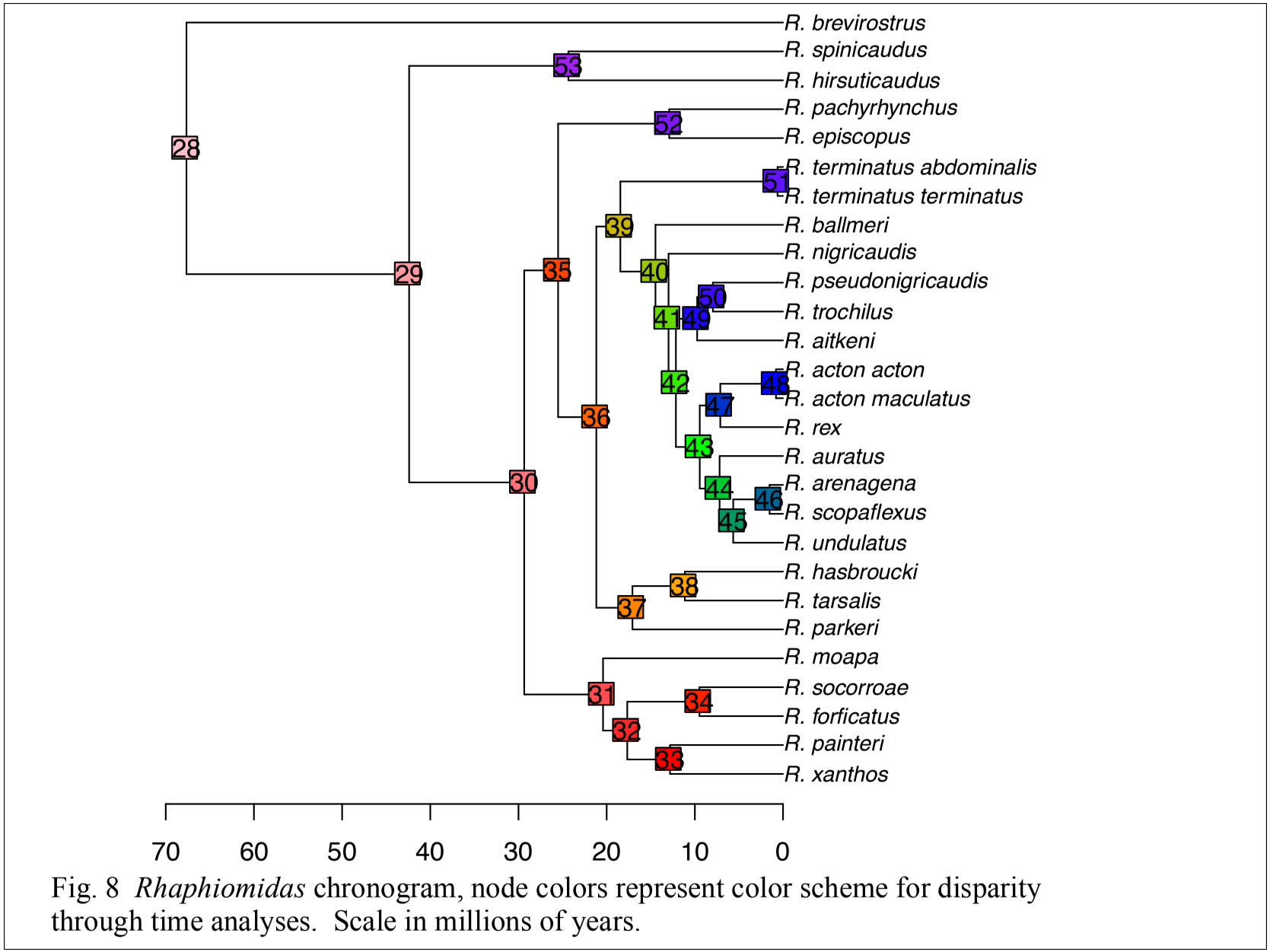

Fig. 8 *Rhaphiomidas* chronogram, node colors represent color scheme for disparity through time analyses. Scale in millions of years.

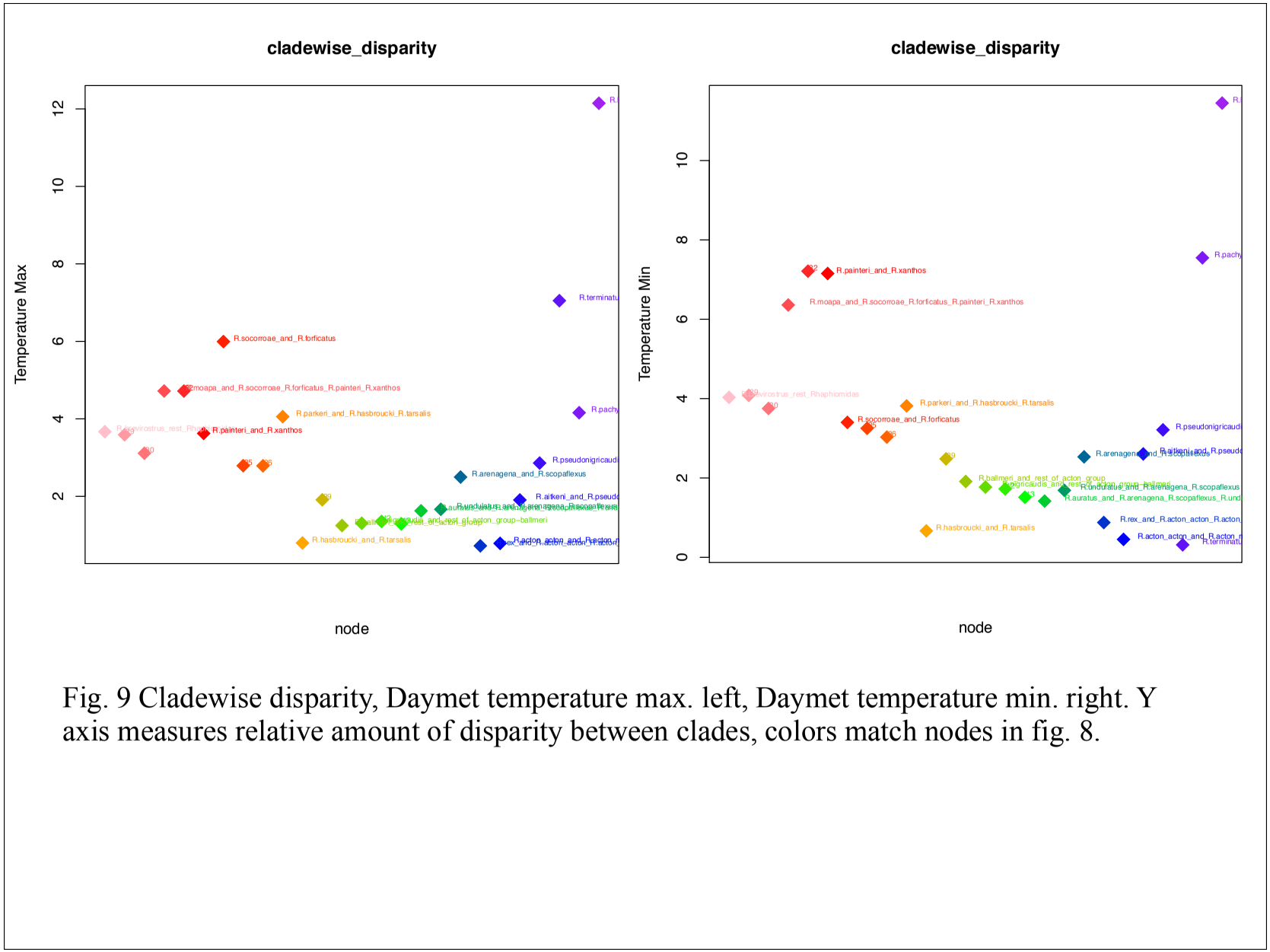

Fig. 9 Cladewise disparity, Daymet temperature max. left, Daymet temperature min. right. Y axis measures relative amount of disparity between clades, colors match nodes in fig. 8.

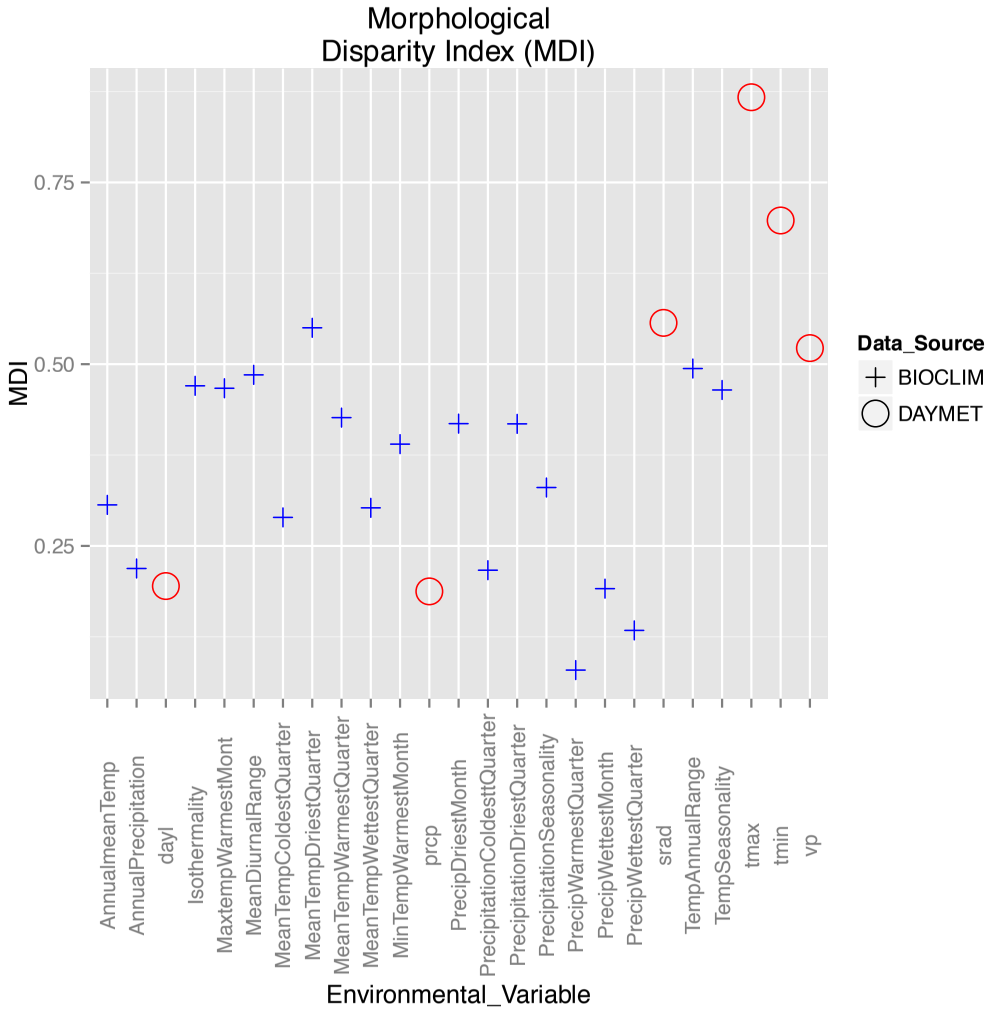

Fig. 10 The results of the morphological disparity index MDI. show that the precipitation layer of the Daymet data is equivalent in terms of disparity to the Bioclim precipitation warmest quarter layer.

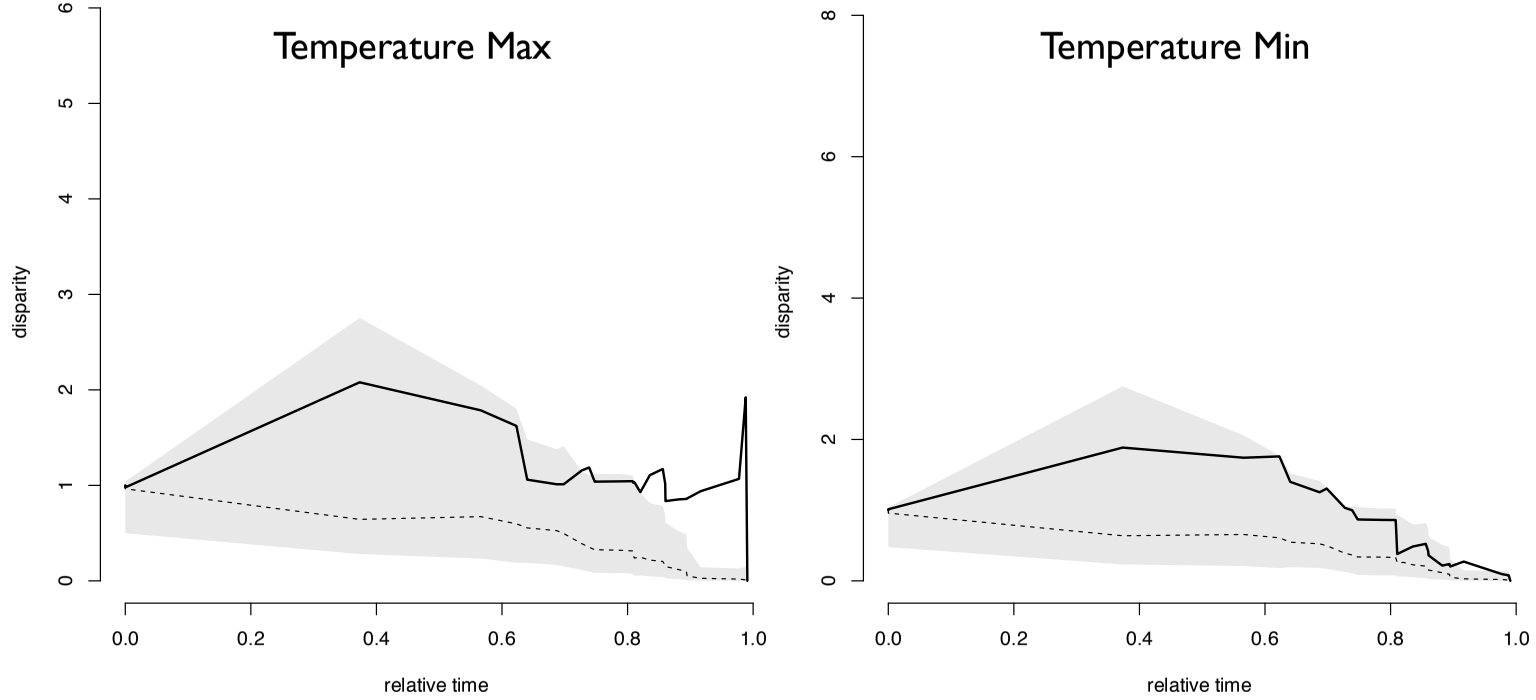

Fig.11 Cladewise disparity through time plots (Daymet data), black lines indicate observed data, dashed mean of simulations and shaded gray area indicate 95% credible interval.

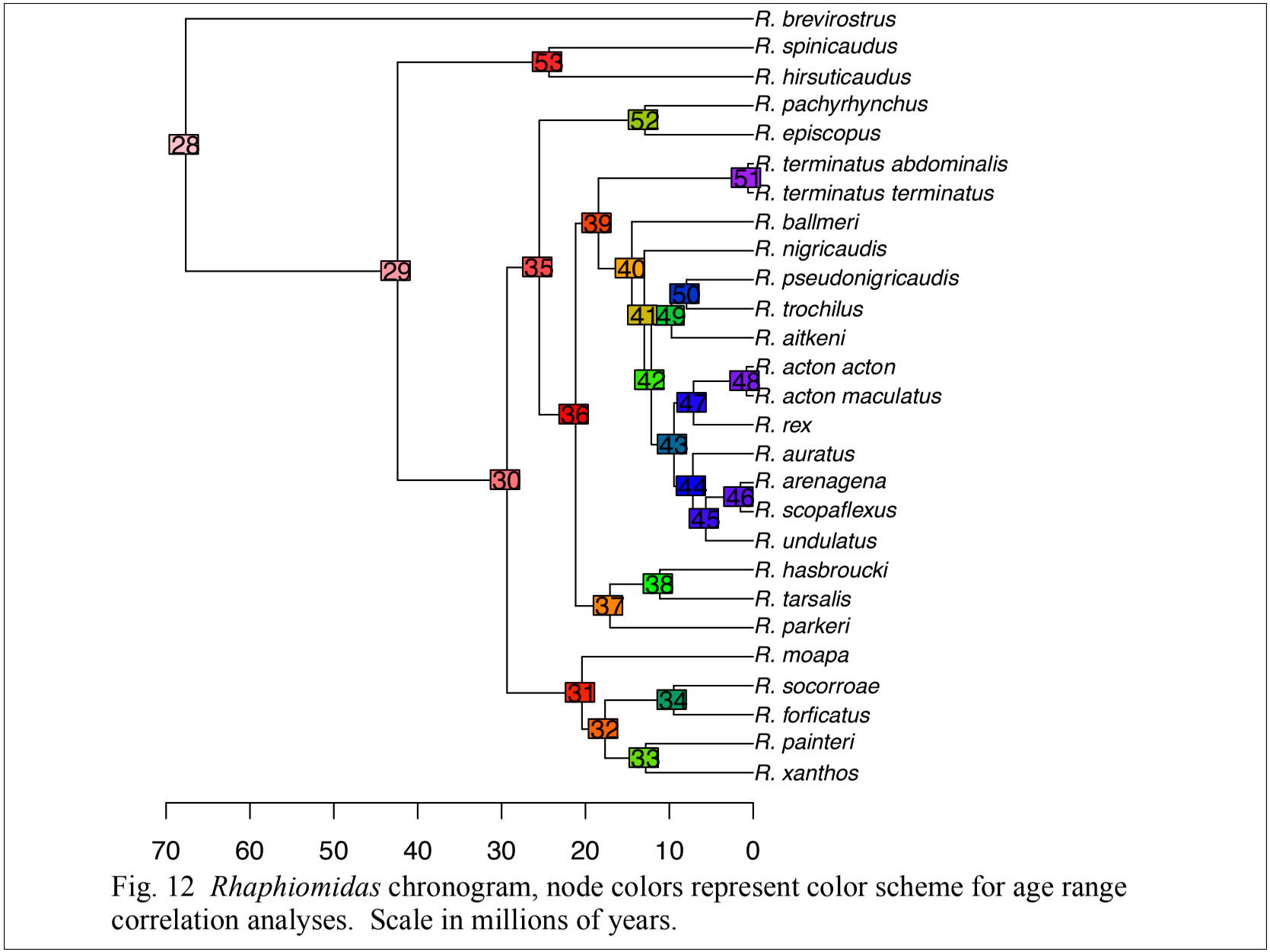

Fig. 12 *Rhaphiomidas* chronogram, node colors represent color scheme for age range correlation analyses. Scale in millions of years.

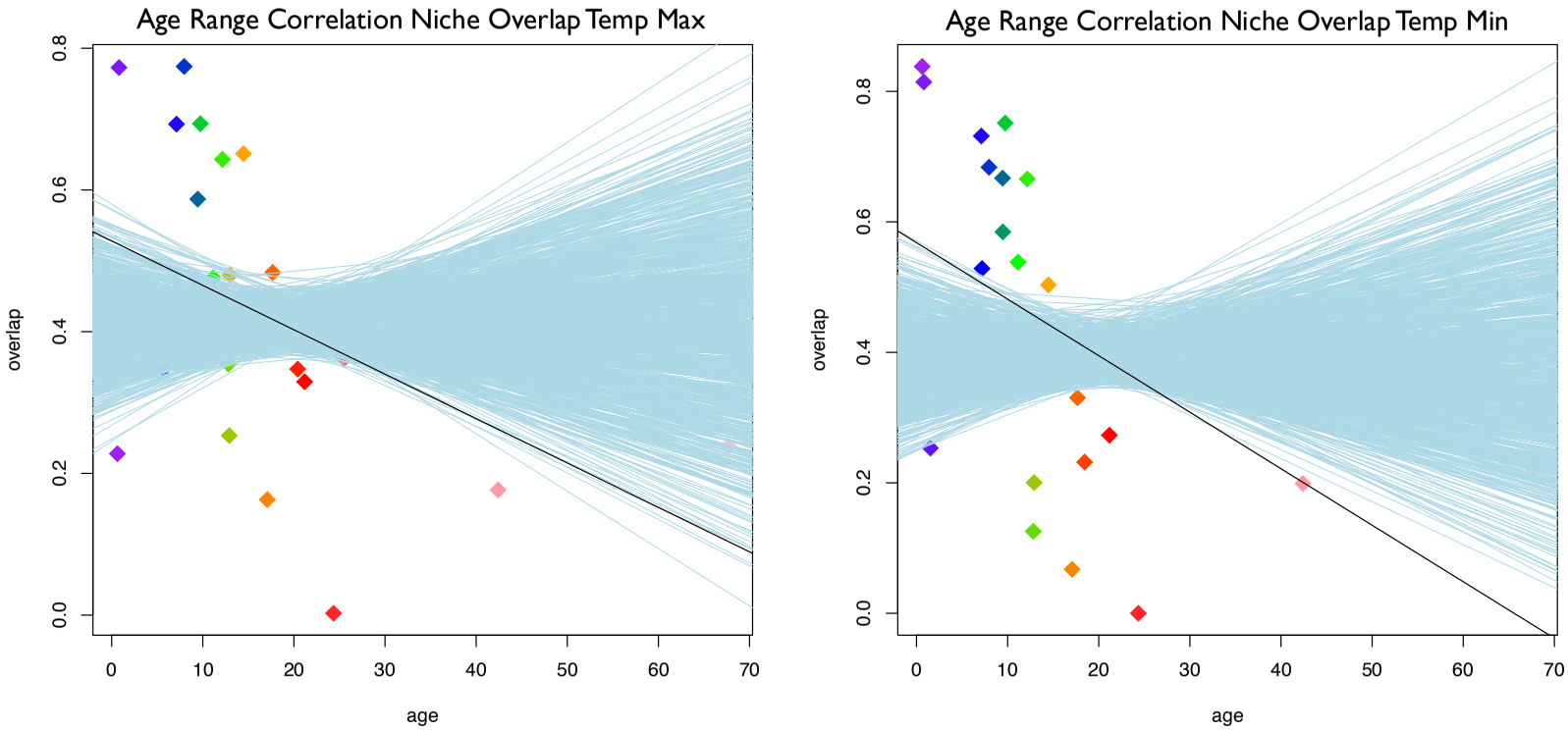

Fig. 13 Age Range Correlation: left temperature max. Daymet, left temperature min. Daymet. Diamonds represent clade (node) comparisons of niche overlap, colors match to nodes in fig. 12. Blue lines represent null distribution of age range correlations. Black line represents observed age range correlation fitted to a linear model. Y axis overlap, X axis age in millions of years.

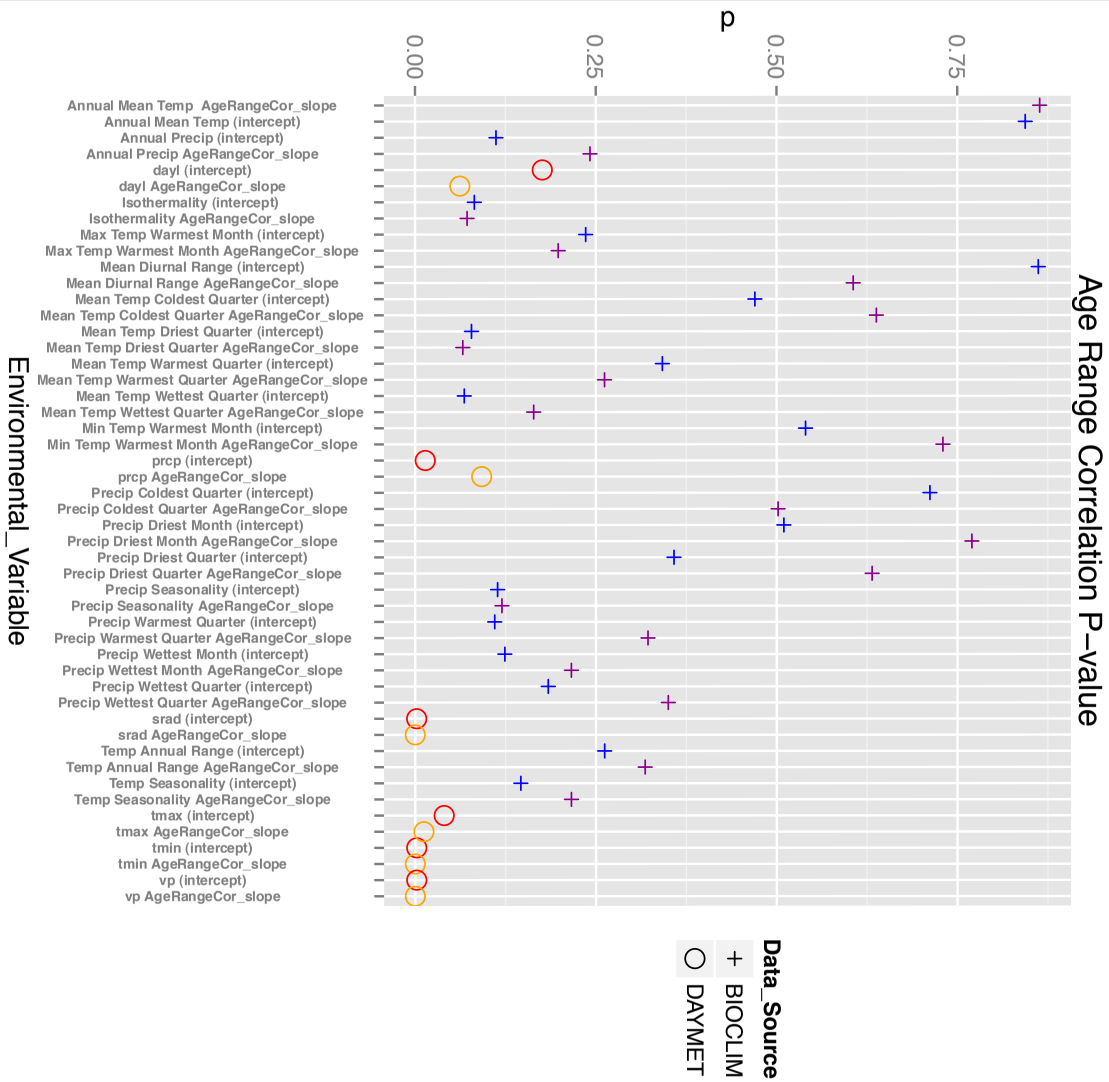

Fig. 14 Age range correlation P-values. Daymet: Red circle P-value slope, Orange circle P-value Y axis intercept of ARC. Bioclim: Purple + P-value slope, Blue + P-value Y axis intercept. Significance assessed by fraction of null values grater than or equal to observed. X axis P-value.

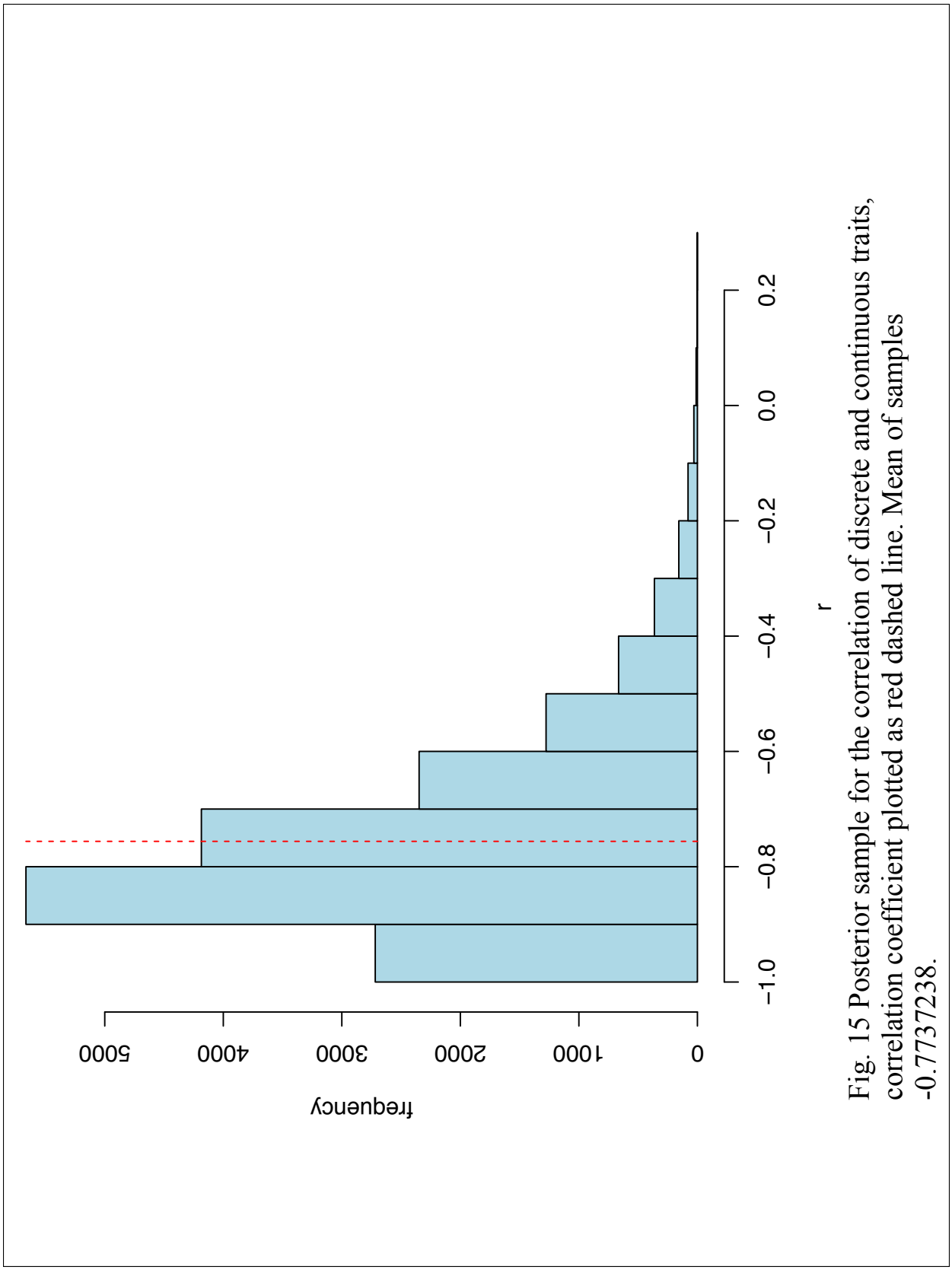

Fig. 15 Posterior sample for the correlation of discrete and continuous traits, correlation coefficient plotted as red dashed line. Mean of samples -0.7737238.

Supplementary Figures: Natural History Matters in Climate Niche Modeling

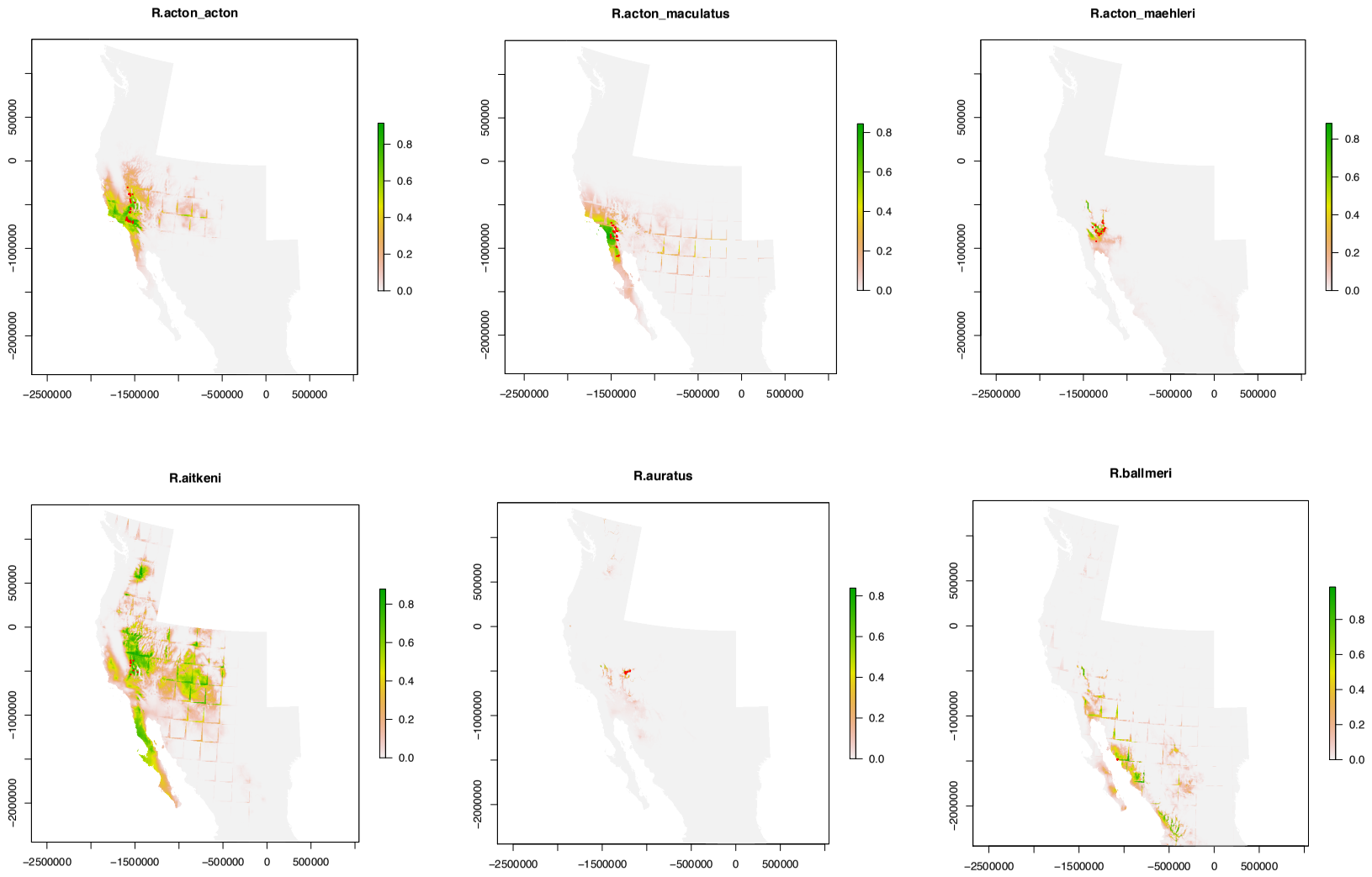

Daymet MaxEnt niche reconstructions

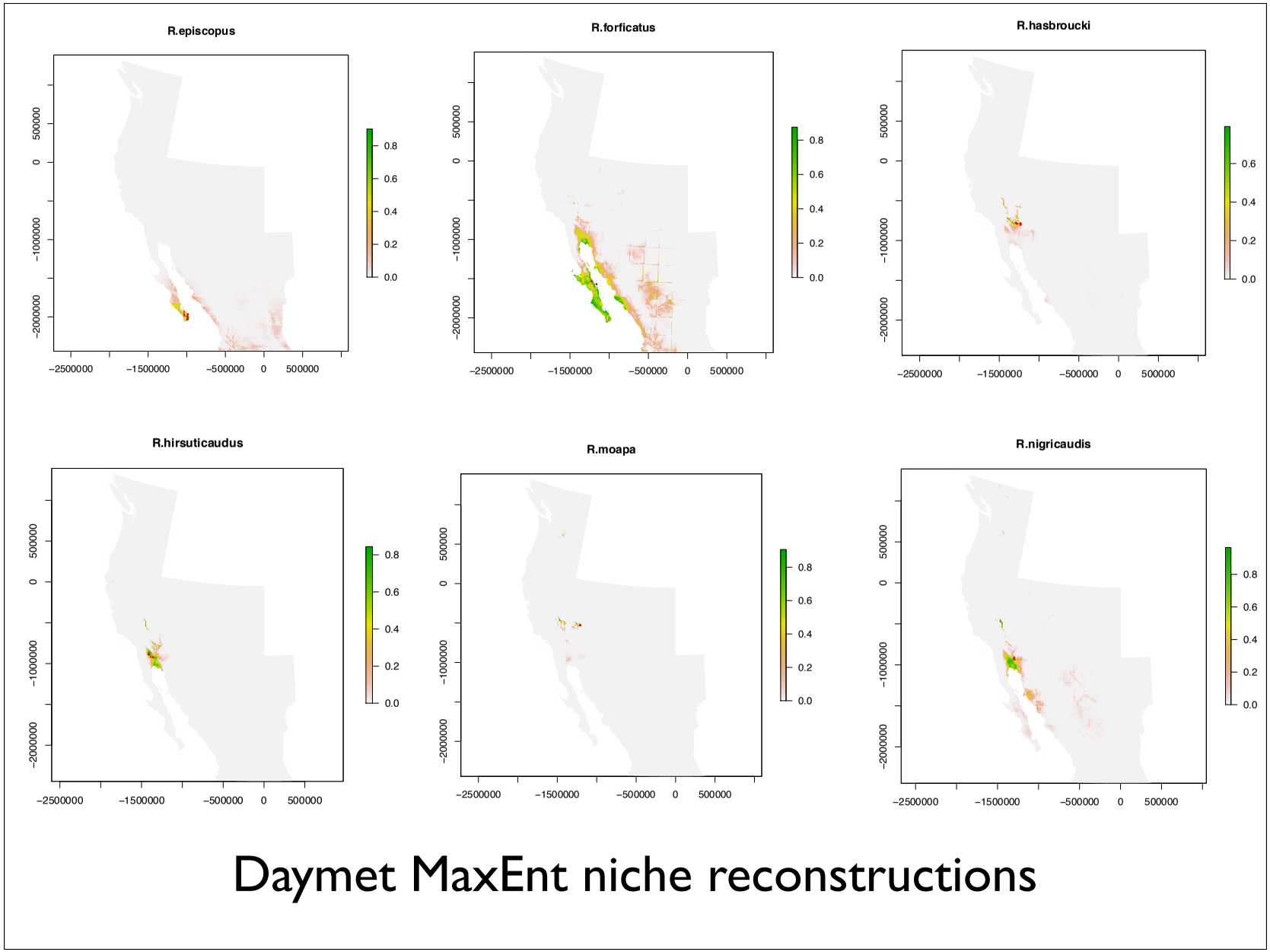

Daymet MaxEnt niche reconstructions

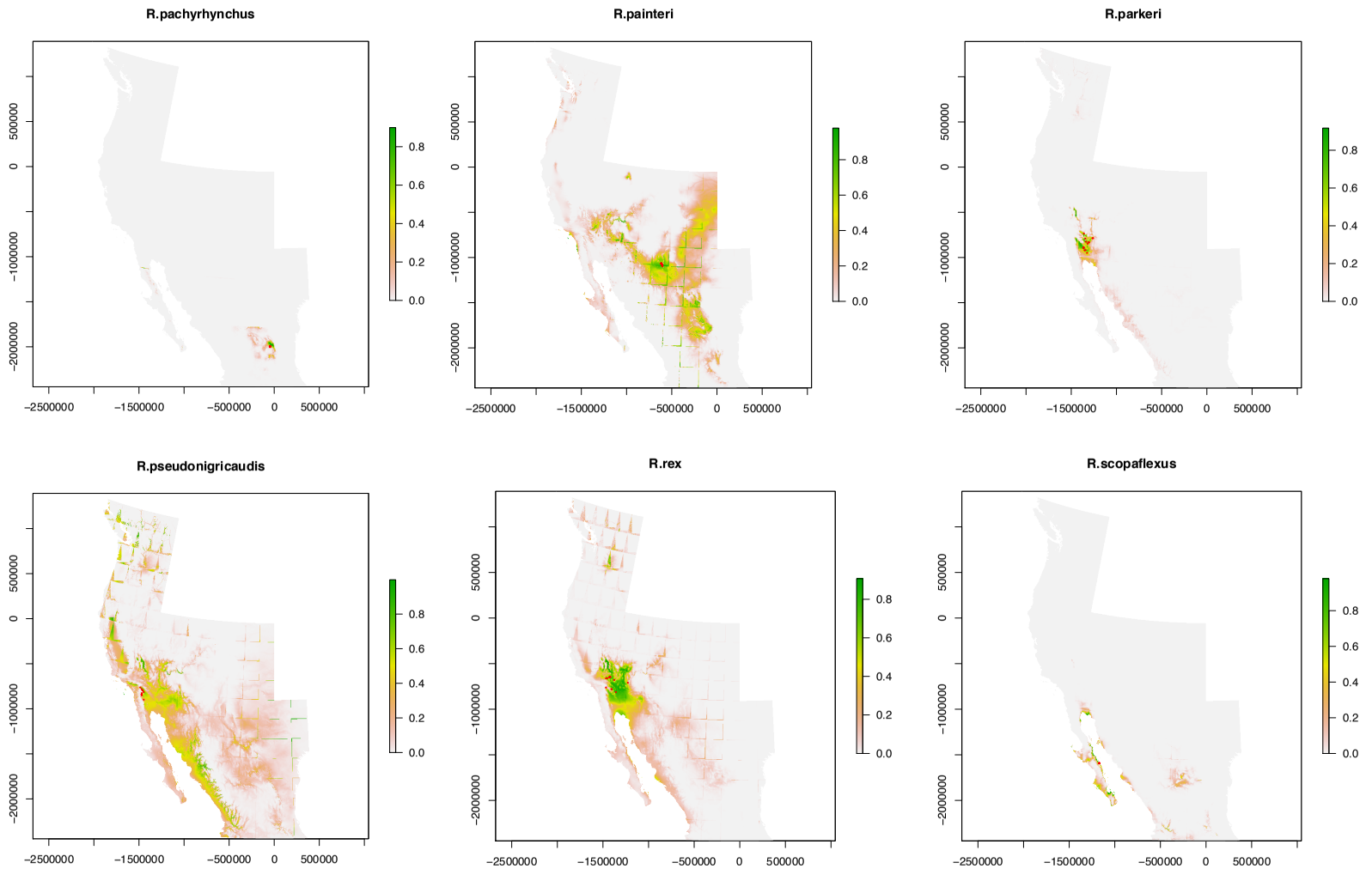

Daymet MaxEnt niche reconstructions

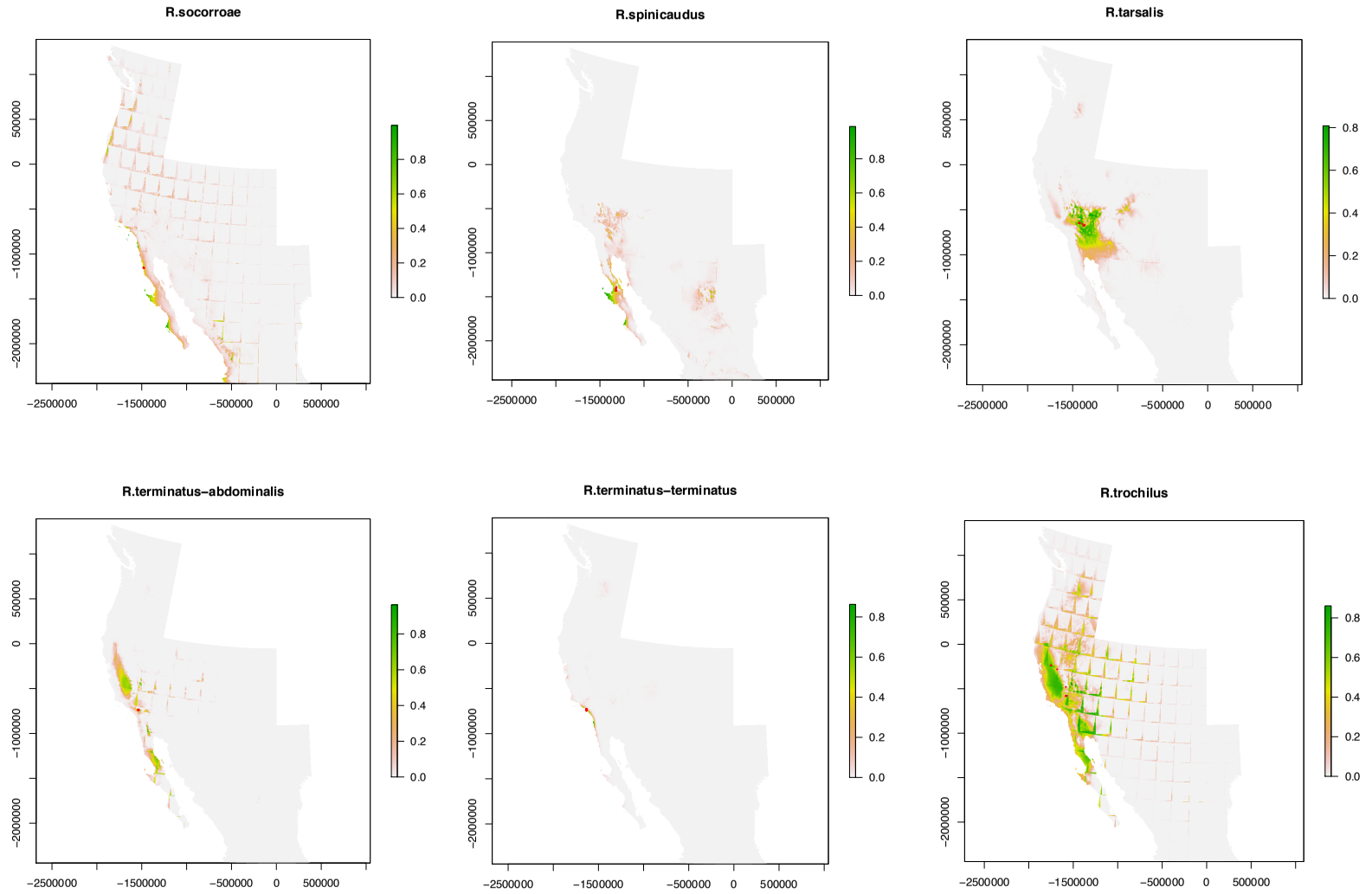

Daymet MaxEnt niche reconstructions

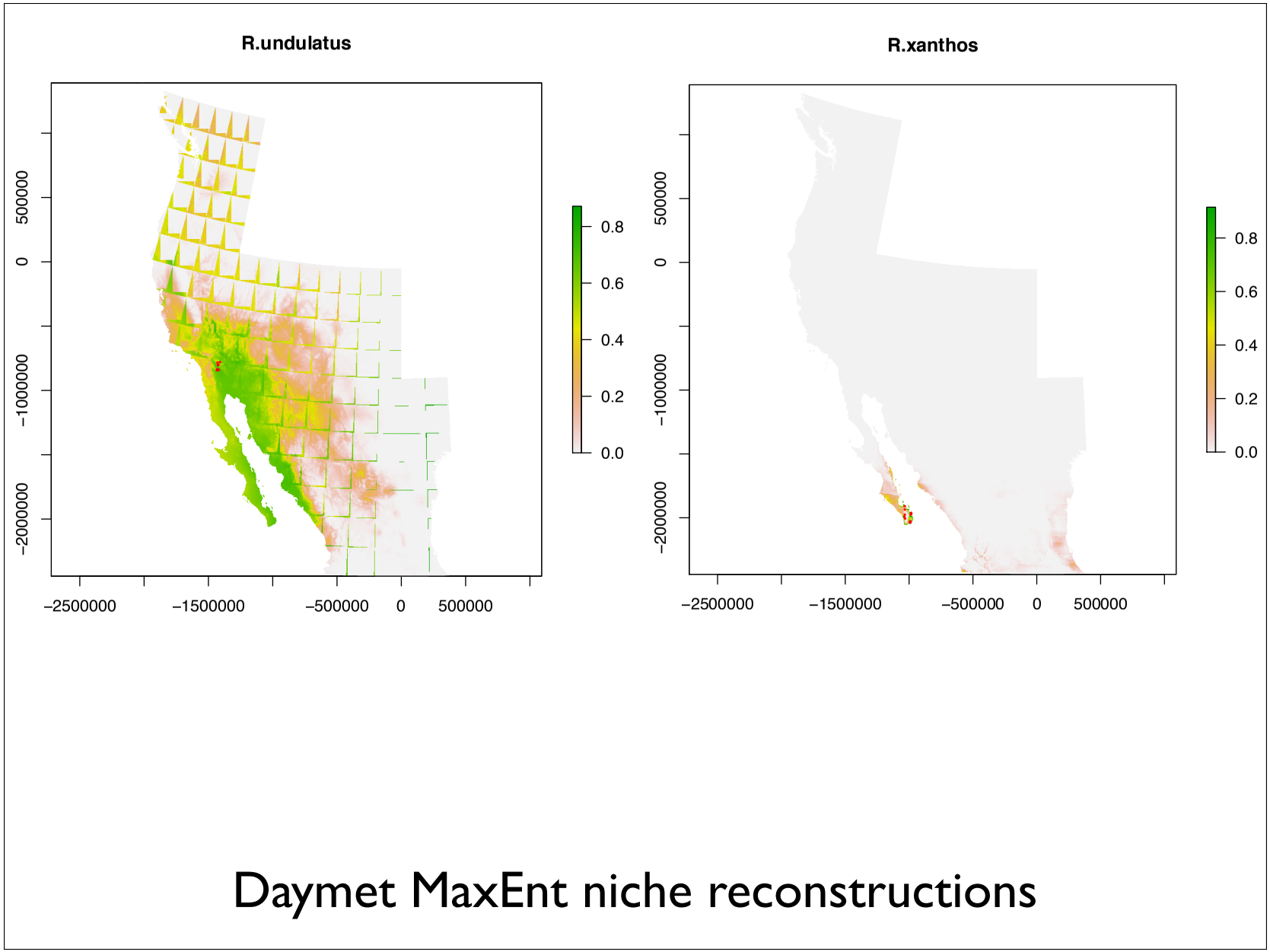

Daymet MaxEnt niche reconstructions

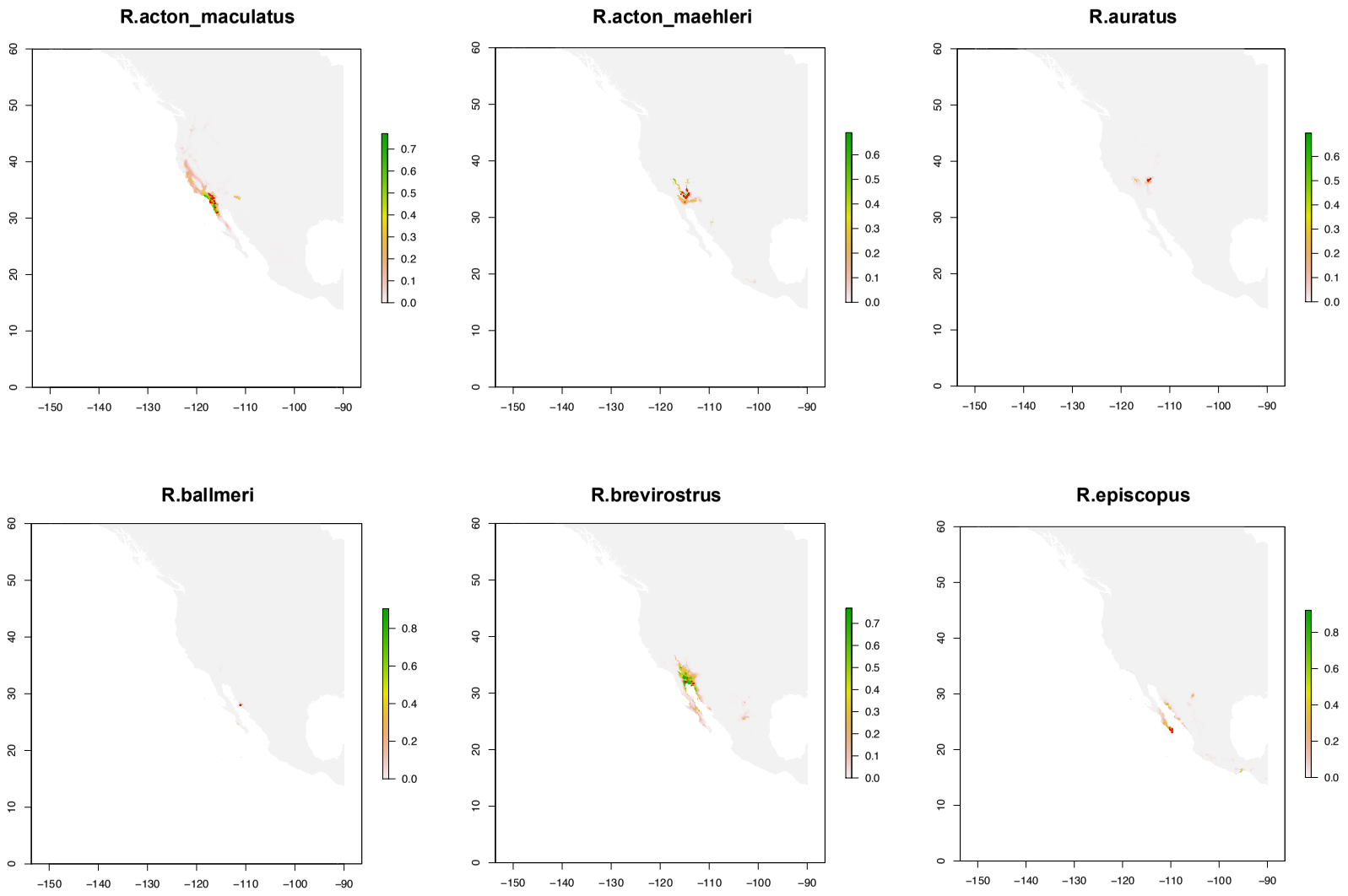

Bioclim MaxEnt niche reconstructions

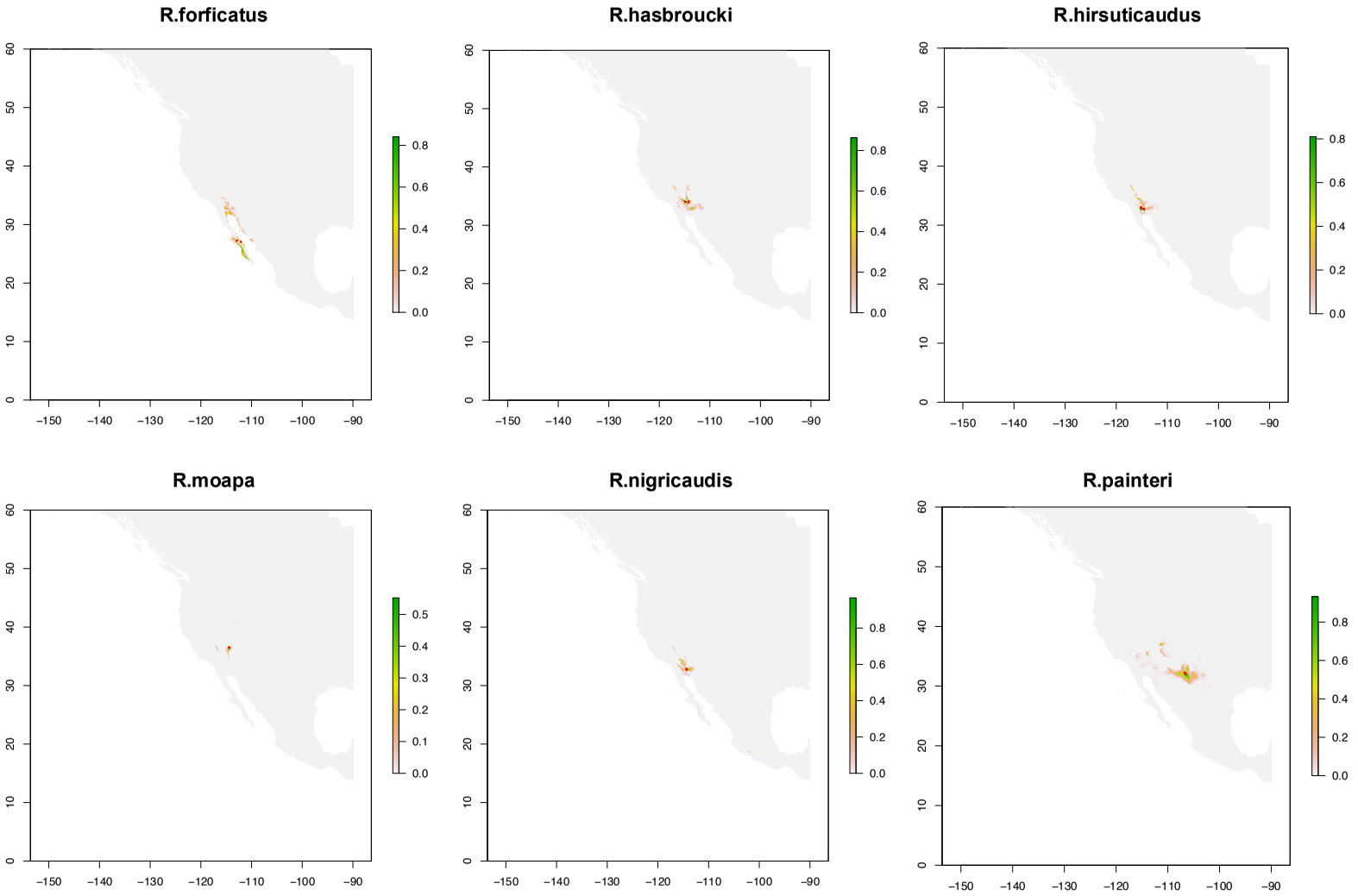

Bioclim MaxEnt niche reconstructions

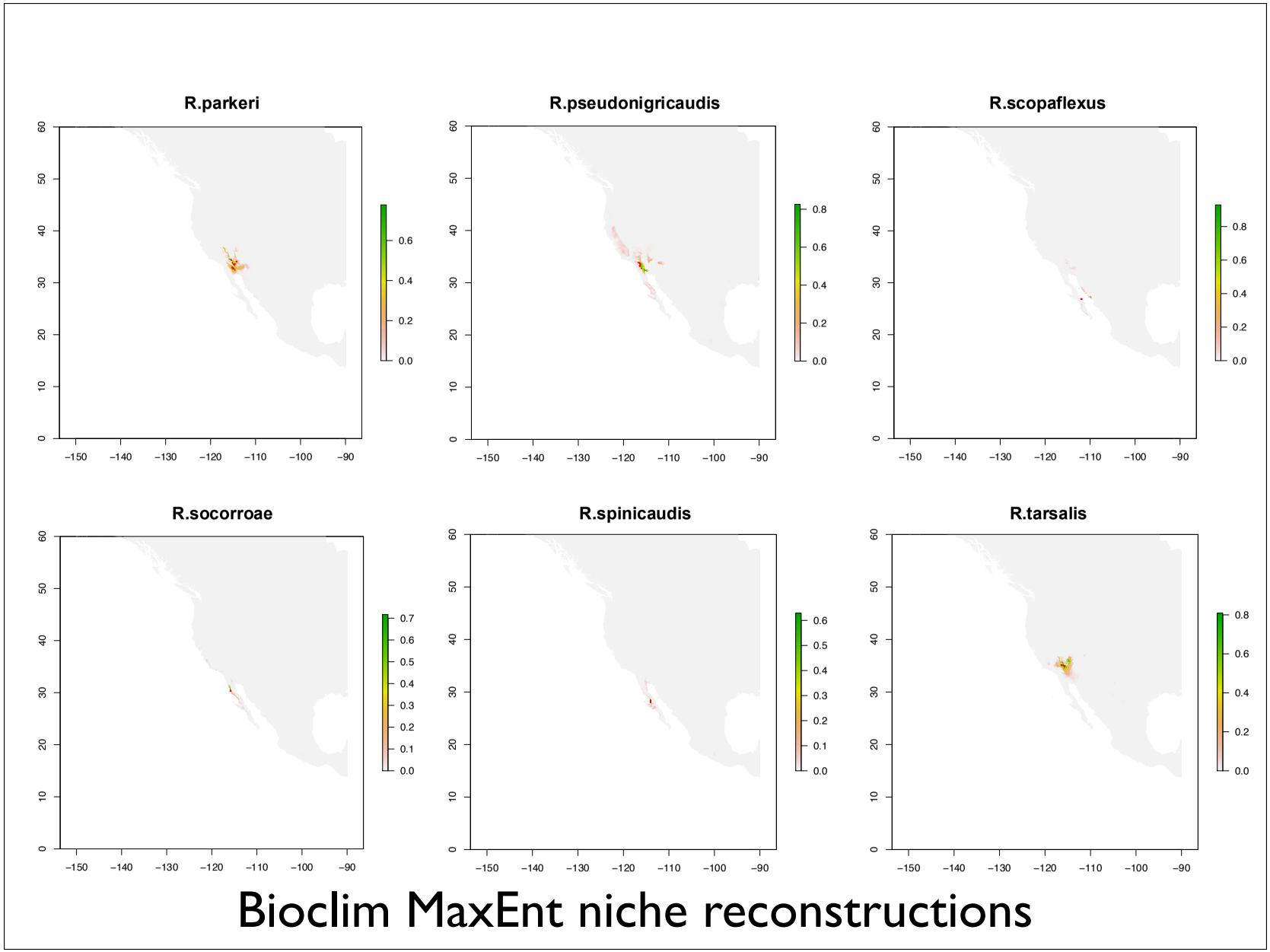

Bioclim MaxEnt niche reconstructions

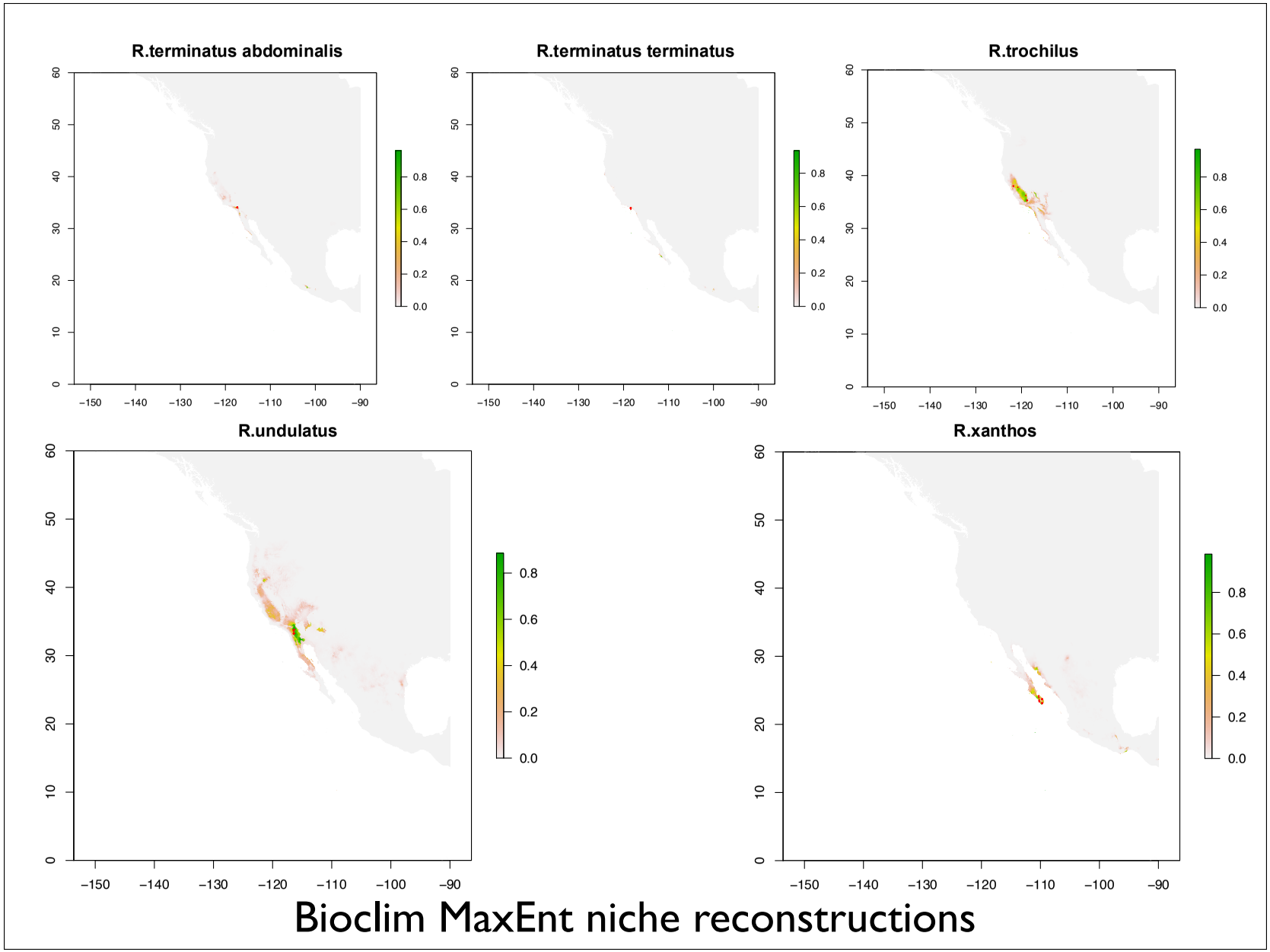

Bioclim MaxEnt niche reconstructions

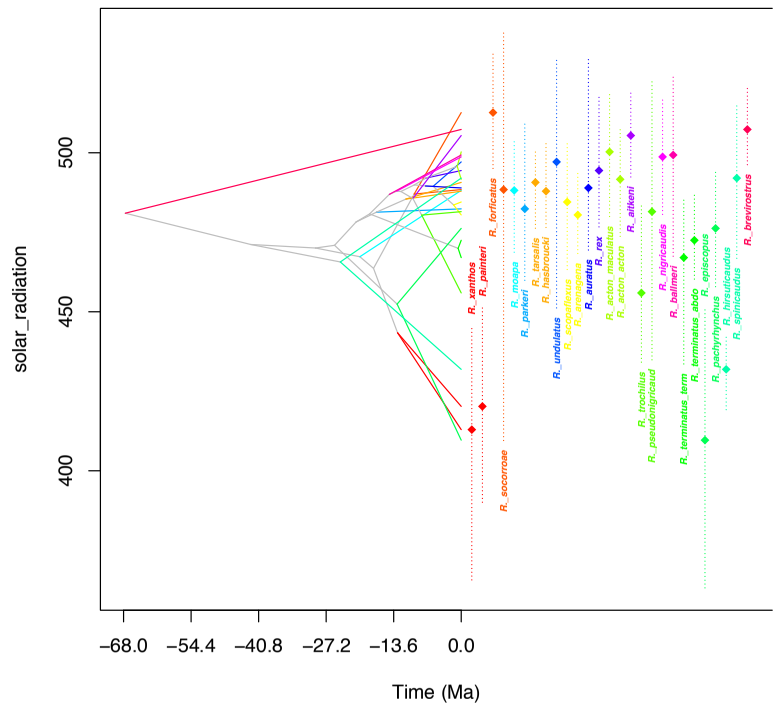

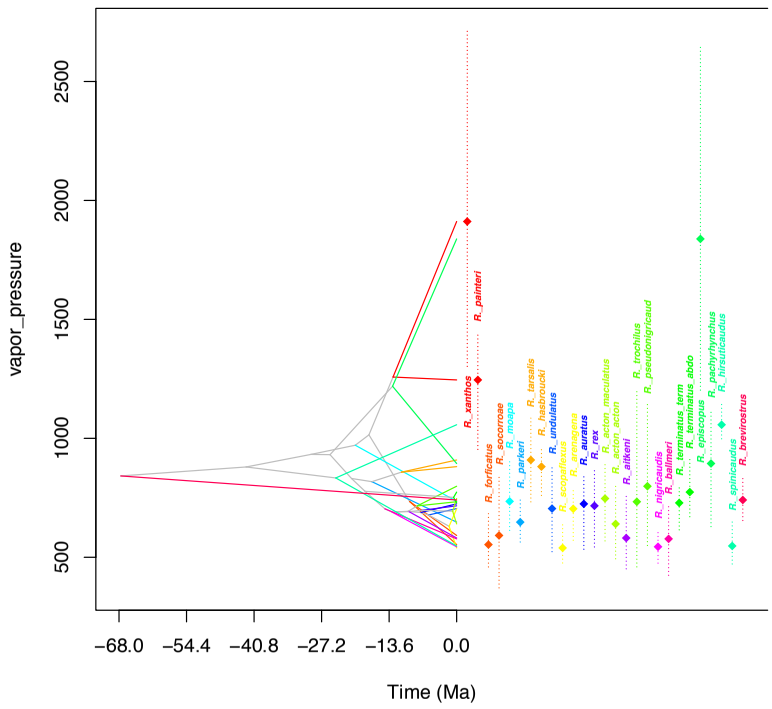

Ancestral state reconstructions for Daymet environmental variables. Dashed lines indicate range and diamonds indicate means

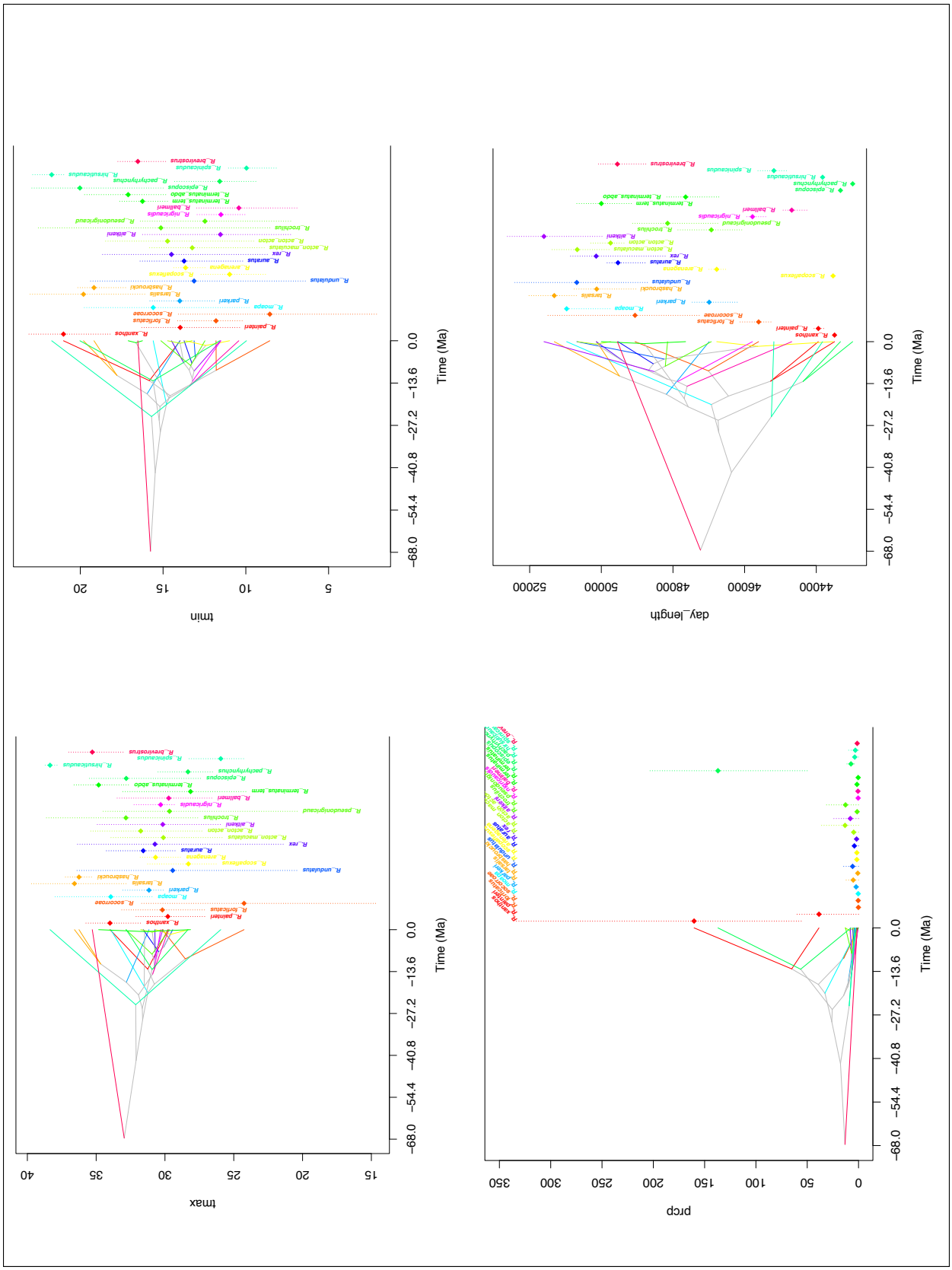
Time (Ma)
0.0
−13.6
−27.2
−40.8
−54.4
−68.0
tmin
5
10
15
20
day_length
44000
46000
48000
50000
52000
prcp
0
50
100
150
200
250
300
350
tmax
15
20
25
30
35
40

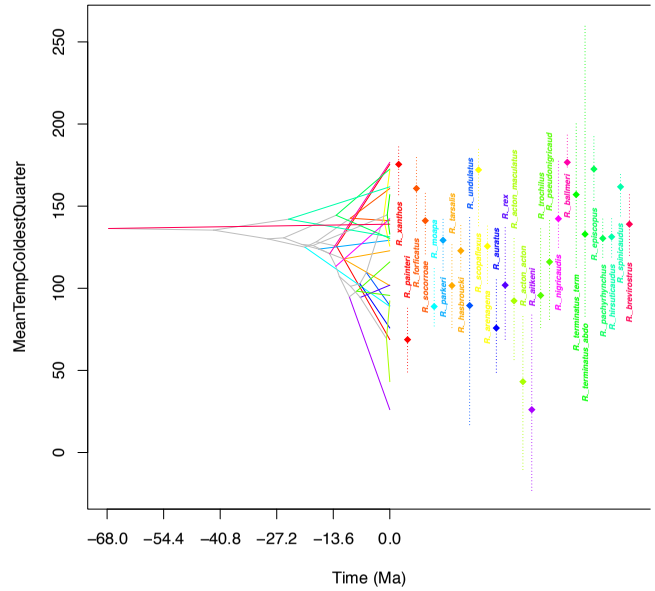

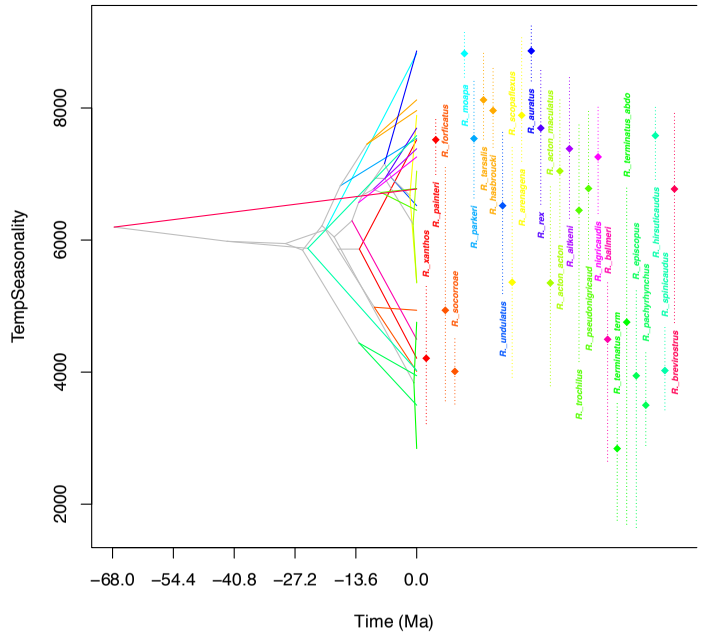

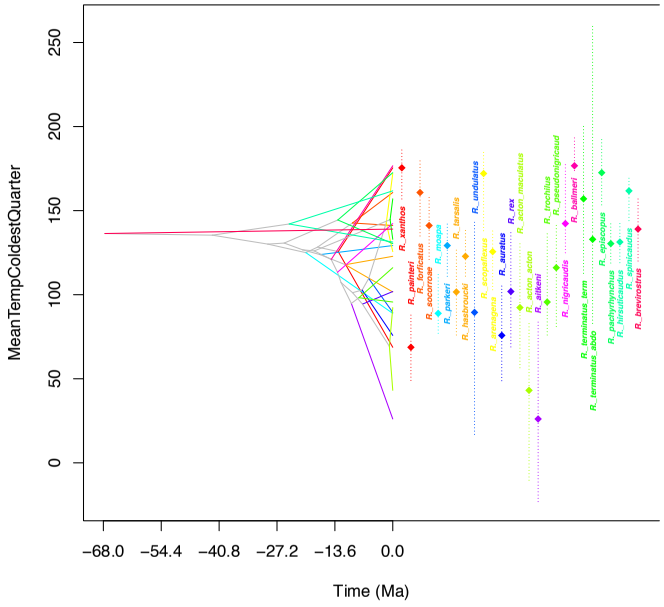

Ancestral state reconstructions for Bioclim environmental variables. Dashed lines indicate range and diamonds indicate means

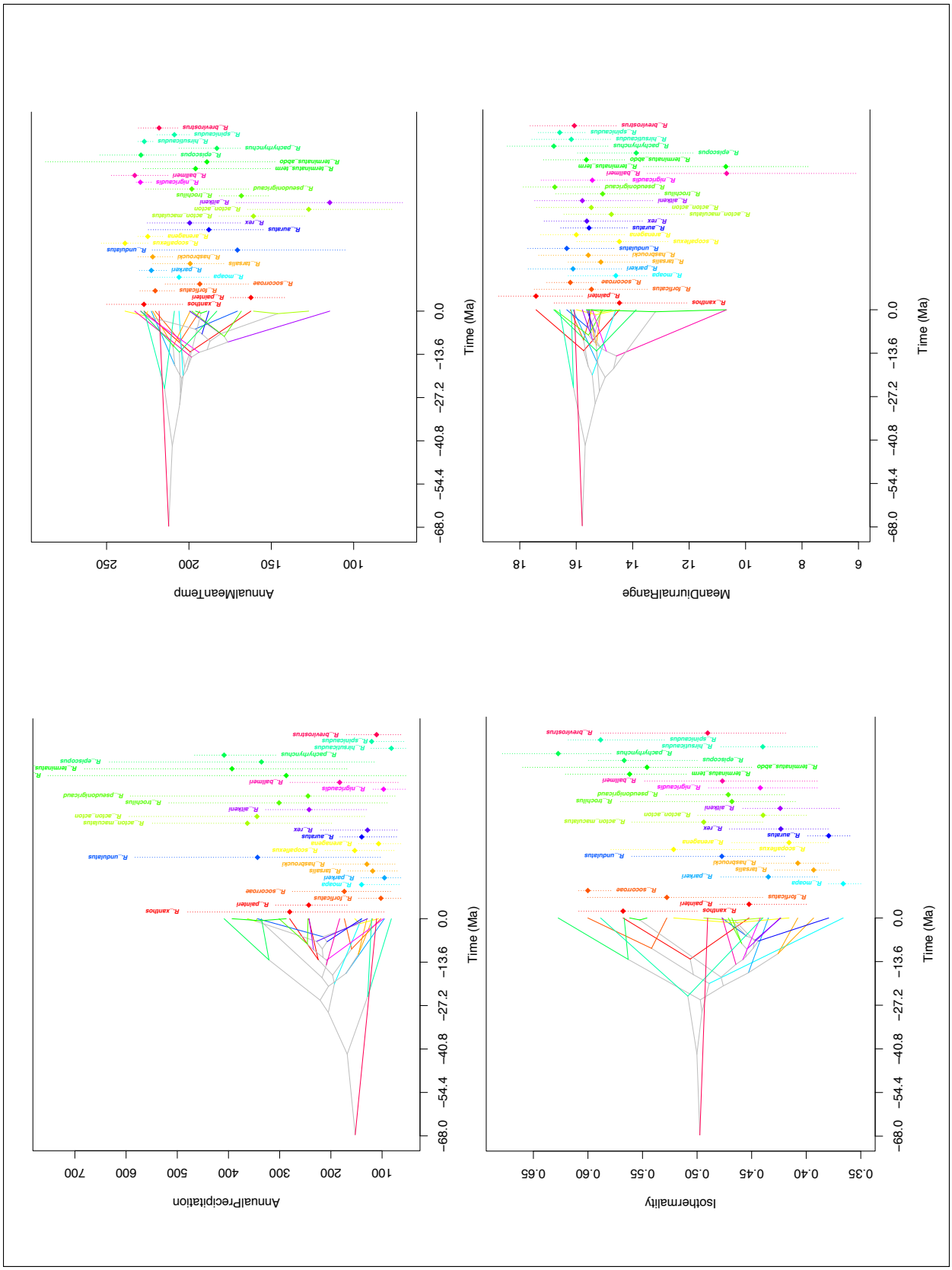
Time (Ma)
−68.0
−54.4
−40.8
−27.2
−13.6
0.0
MeanDiurnalRange
6
8
10
12
14
16
18
AnnualMeanTemp
100
150
200
250
Isothermality
0.35
0.40
0.45
0.50
0.55
0.60
0.65
AnnualPrecipitation
100
200
300
400
500
600
700

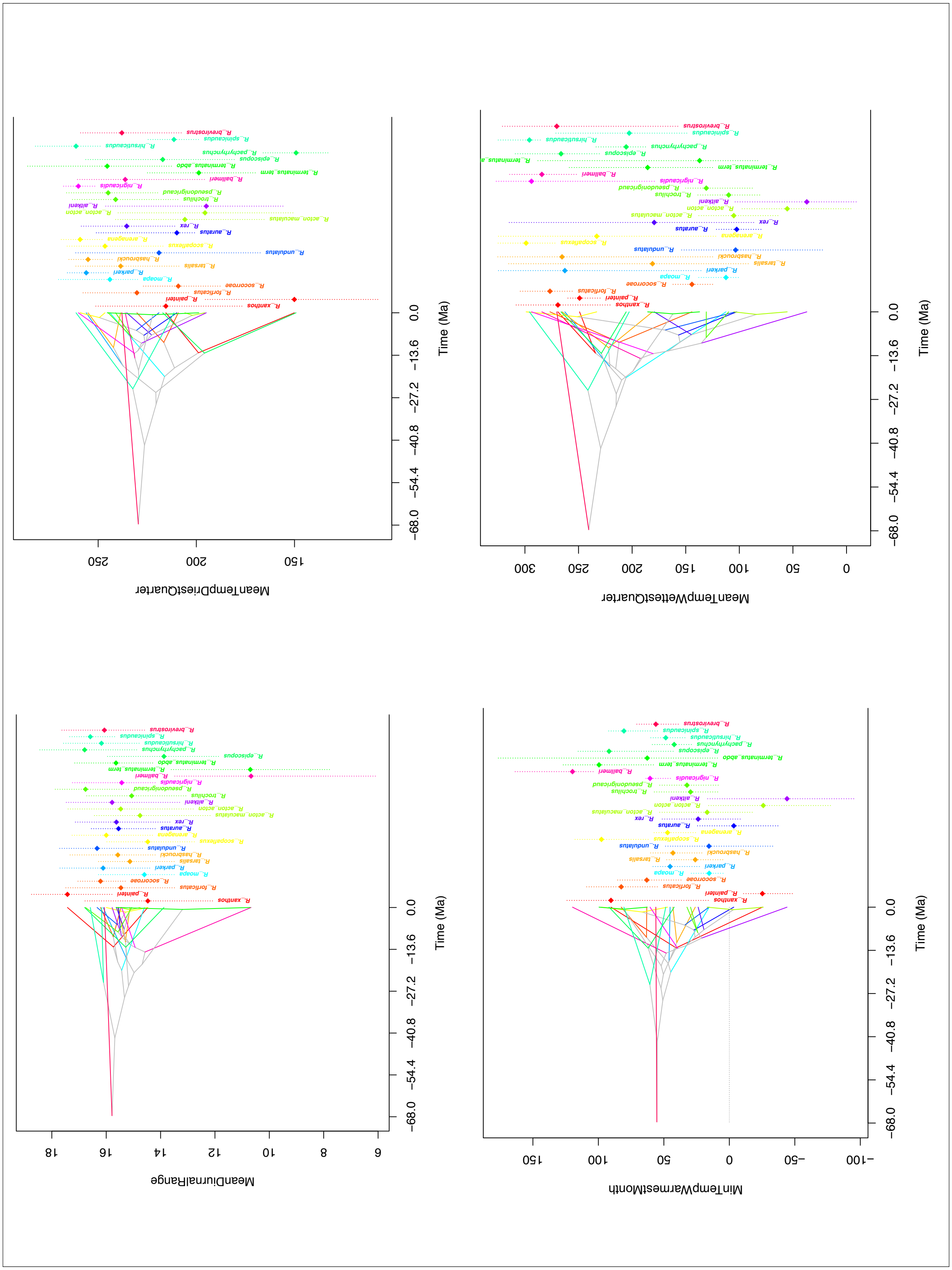
MeanDiurnalRange
MeanTempDriestQuarter
MinTempWarmestMonth
MeanTempWettestQuarter
Time (Ma)

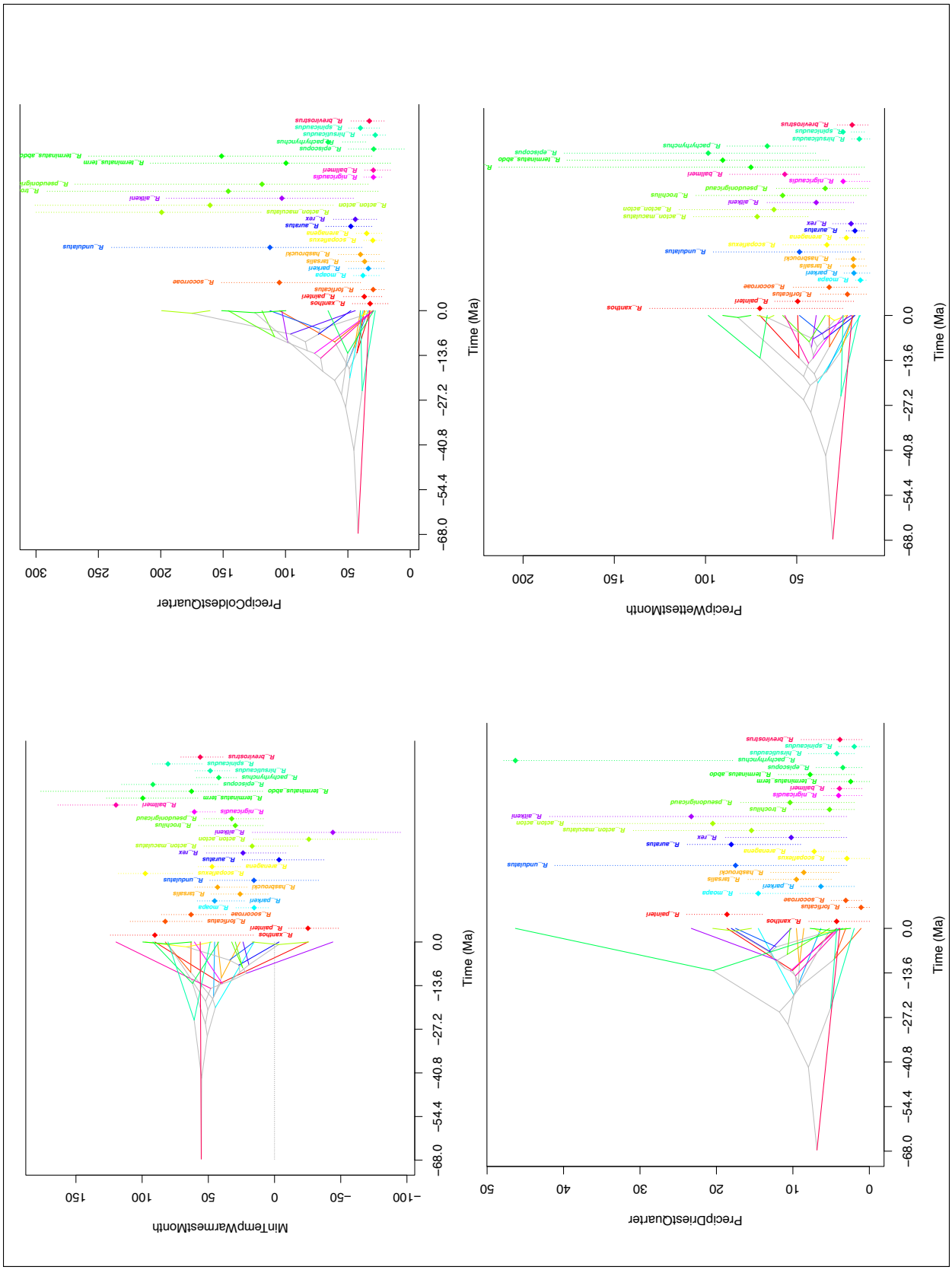
Time (Ma)
0.0
−13.6
−27.2
−40.8
−54.4
−68.0
PrecipColdestQuarter
0
50
100
150
200
250
300
PrecipWettestMonth
50
100
150
200
PrecipDriestQuarter
0
10
20
30
40
50
MinTempWarmestMonth
−100
−50
0
50
100
150

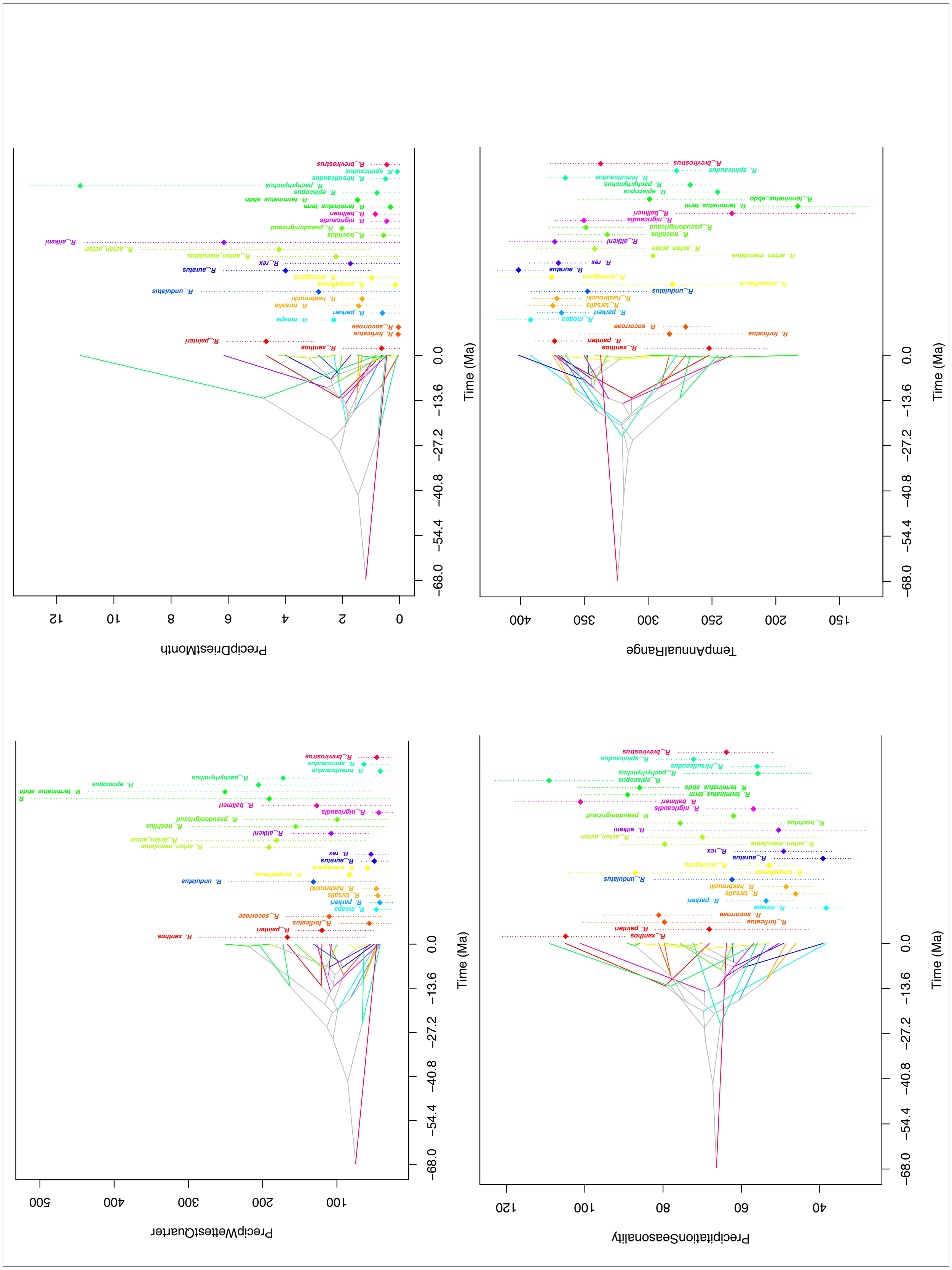
PrecipDriestMonth
PrecipWettestQuarter
TempAnnualRange
PrecipitationSeasonality
Time (Ma)

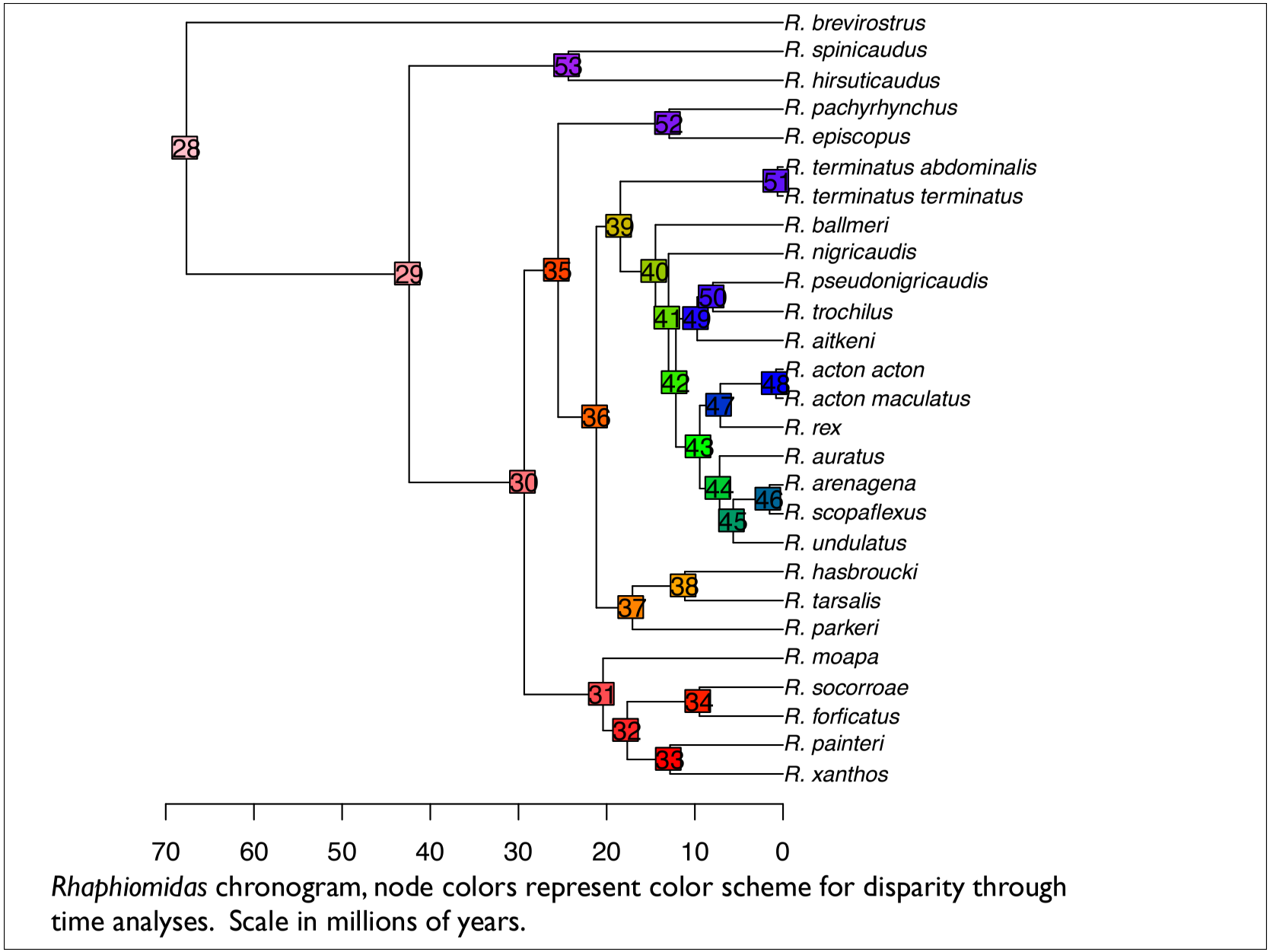

Rhaphiomidas chronogram, node colors represent color scheme for disparity through time analyses. Scale in millions of years.

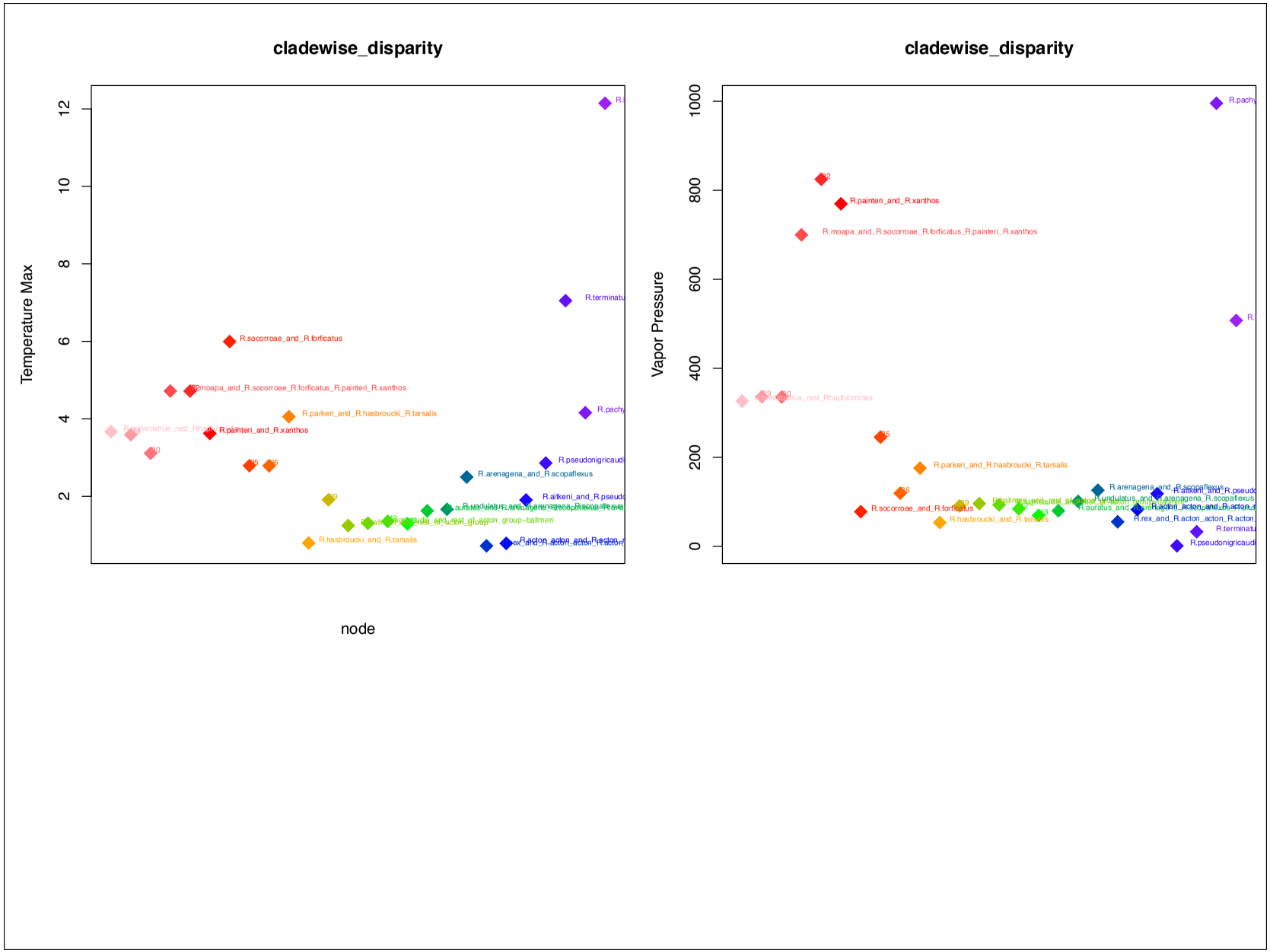
cladewise_disparity
Temperature Max
node
R.socorroae_and_R.forficatus
R.moapa_and_R.socorroae_R.forficatus_R.painteri_R.xanthos
R.parkeri_and_R.hasbroucki_R.tarsalis
R.painteri_and_R.xanthos
R.pachy
R.terminatu
R.pseudonigricaudi
R.arenagena_and_R.scopaflexus
R.aitkeni_and_R.pseudo
R.hasbroucki_and_R.tarsalis
cladewise_disparity
Vapor Pressure
R.pachy
R.painteri_and_R.xanthos
R.moapa_and_R.socorroae_R.forficatus_R.painteri_R.xanthos
R.parkeri_and_R.hasbroucki_R.tarsalis
R.arenagena_and_R.scopaflexus
R.socorroae_and_R.forficatus
R.hasbroucki_and_R.tarsalis
R.rex_and_R.acton_acton_R.acton
R.terminatu
R.pseudonigricaudi

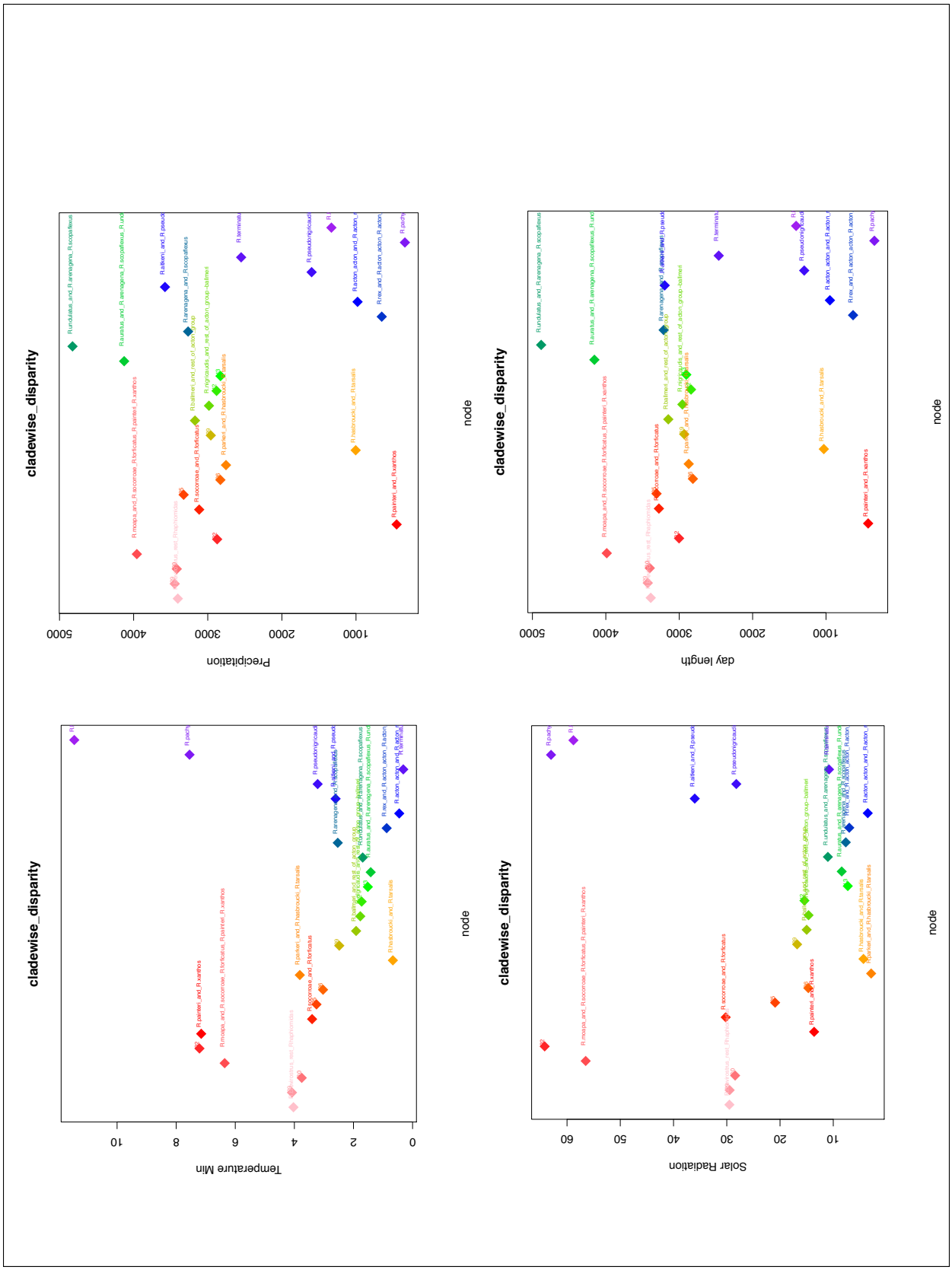
cladewise_disparity
Precipitation
node
cladewise_disparity
day length
node
cladewise_disparity
Temperature Min
node
cladewise_disparity
Solar Radiation
node

cladewise_disparity
annual mean temp
node
cladewise_disparity
mean diurnal range
node
cladewise_disparity
Isothermality
node
cladewise_disparity
Temp Seasonality
node

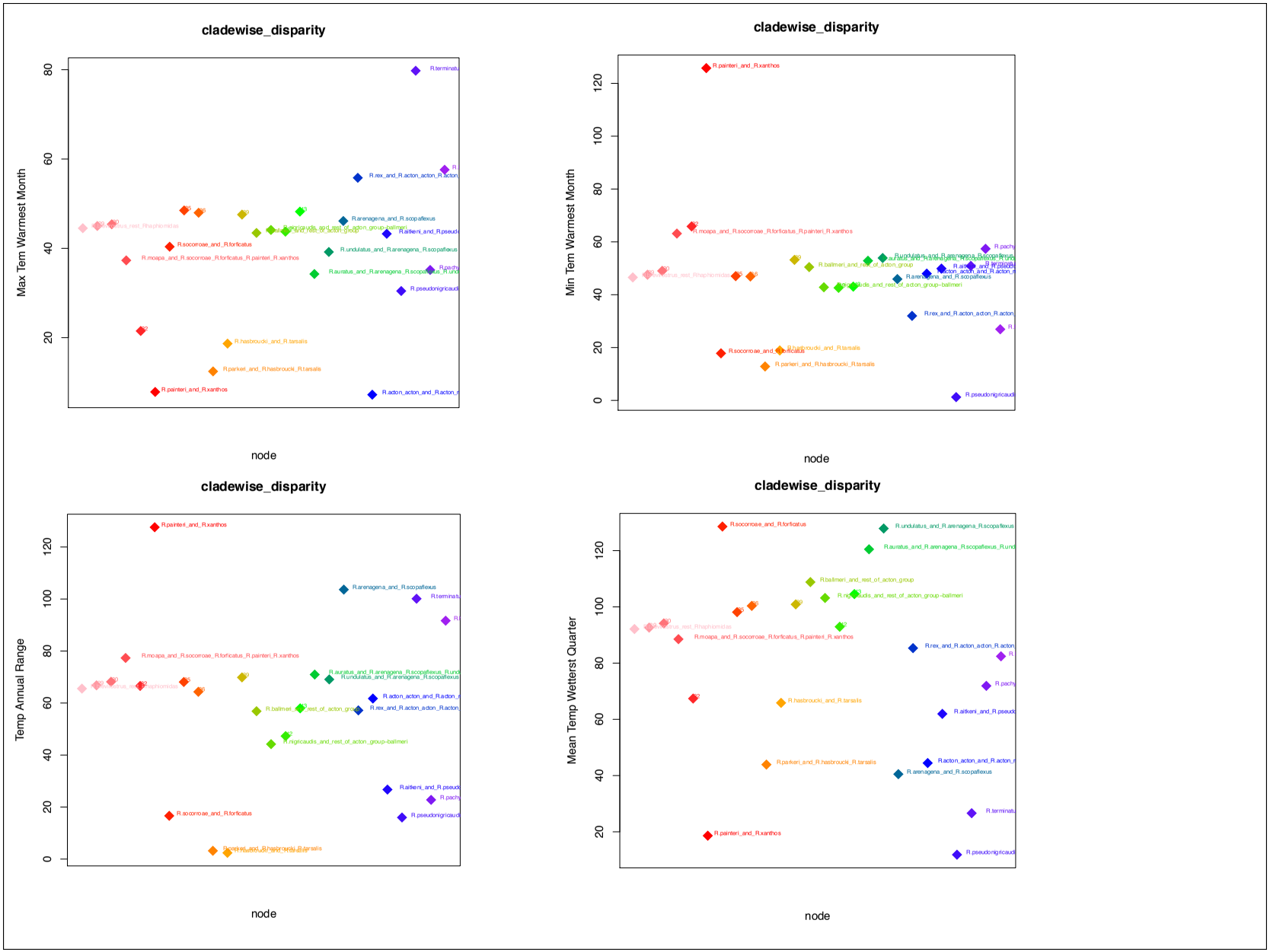
cladewise_disparity
Max Tem Warmest Month
node
cladewise_disparity
Min Tem Warmest Month
node
cladewise_disparity
Temp Annual Range
node
cladewise_disparity
Mean Temp Wettest Quarter
node

cladewise_disparity
Cladewise Disparity Max Temp Warmest Month
node
cladewise_disparity
Cladewise Disparity Mean Temp Coldest Quarter
node
cladewise_disparity
Cladewise Disparity Mean Temp Driest Quarter
node
cladewise_disparity
Cladewise Disparity Mean Temp Warmest Quarter
node

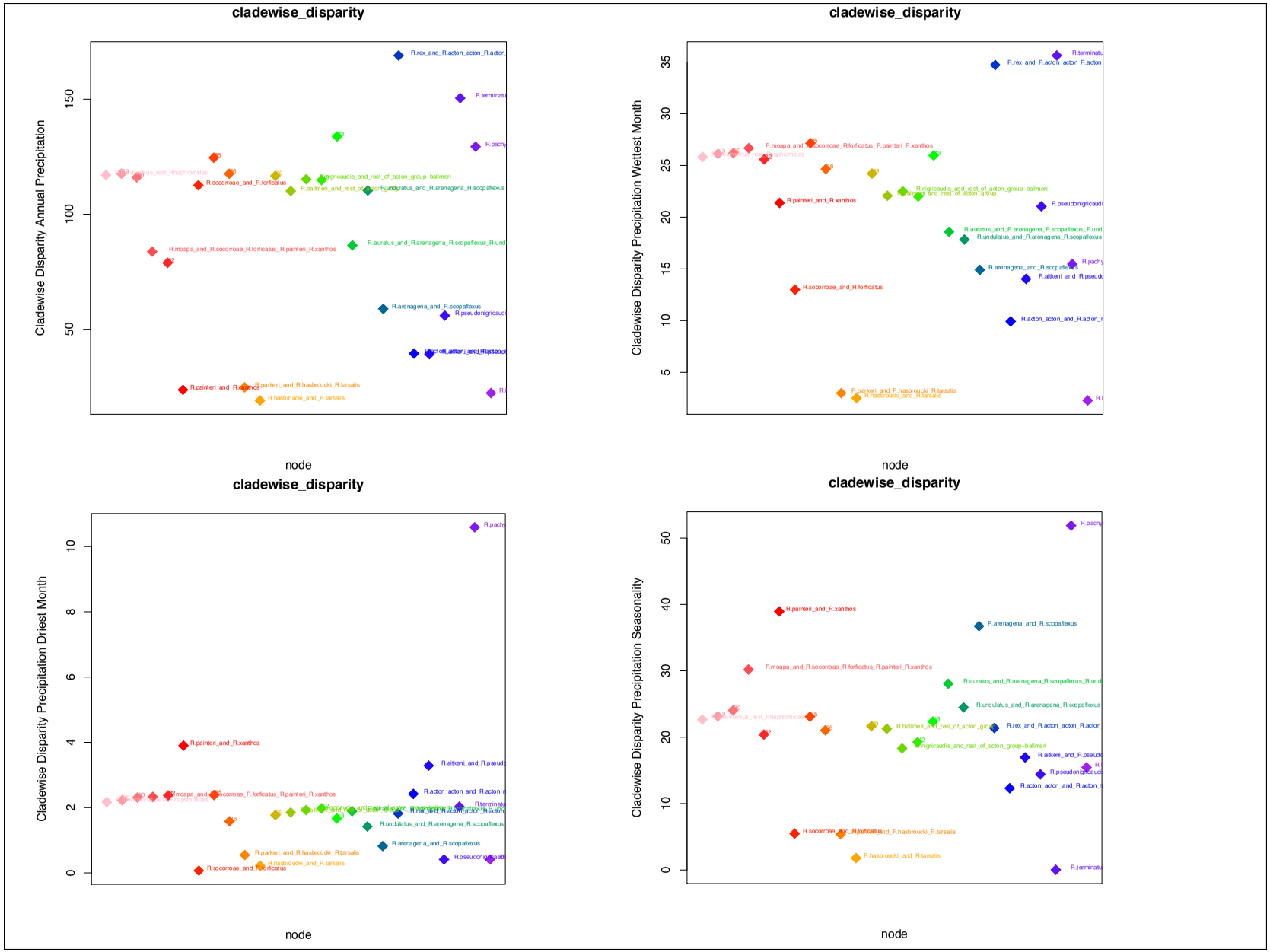
cladewise_disparity
Cladewise Disparity Annual Precipitation
node
cladewise_disparity
Cladewise Disparity Precipitation Wettest Month
node
cladewise_disparity
Cladewise Disparity Precipitation Driest Month
node
cladewise_disparity
Cladewise Disparity Precipitation Seasonality
node

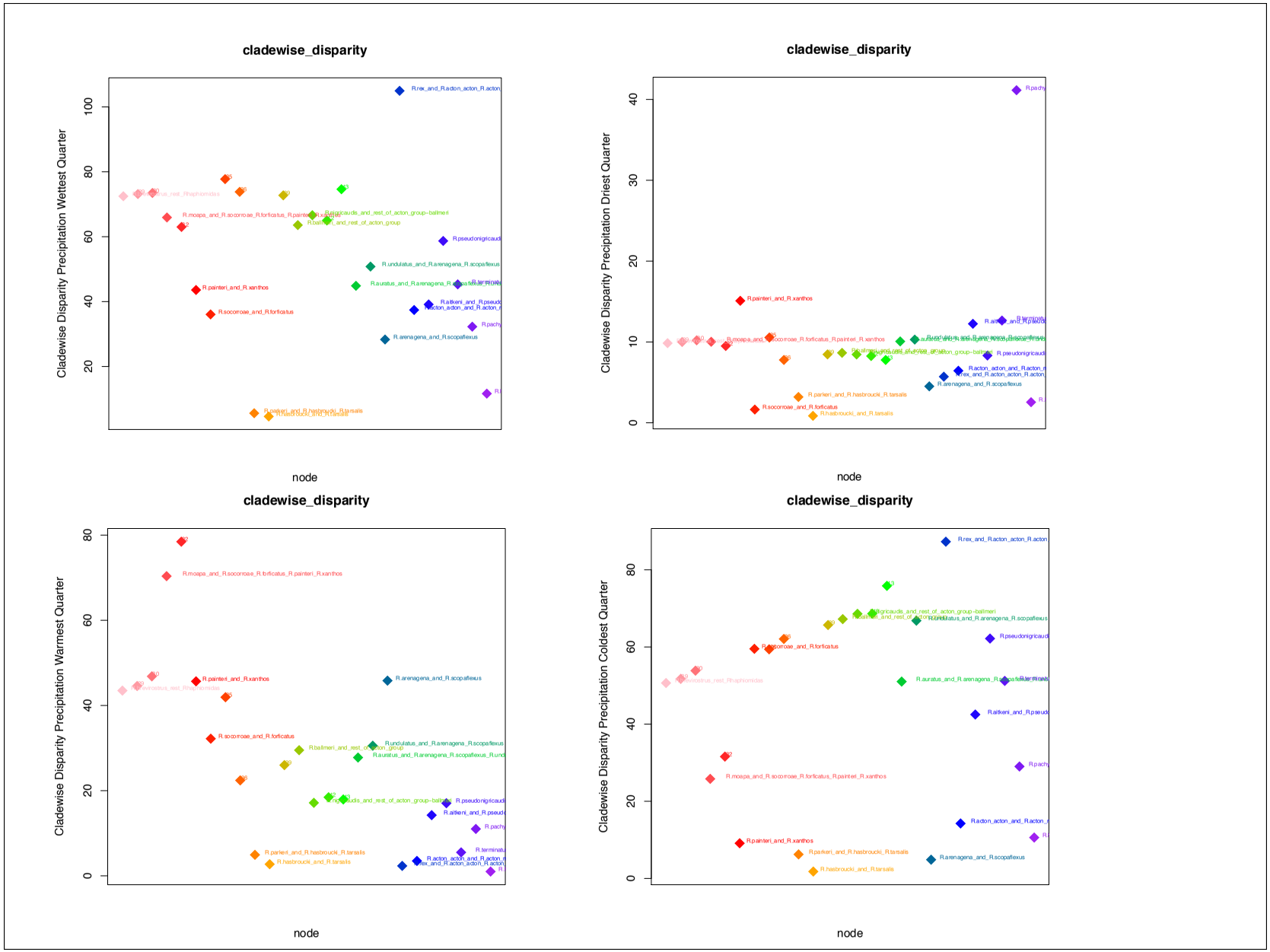
cladewise_disparity
Cladewise Disparity Precipitation Wettest Quarter
node
cladewise_disparity
Cladewise Disparity Precipitation Driest Quarter
node
cladewise_disparity
Cladewise Disparity Precipitation Warmest Quarter
node
cladewise_disparity
Cladewise Disparity Precipitation Coldest Quarter
node

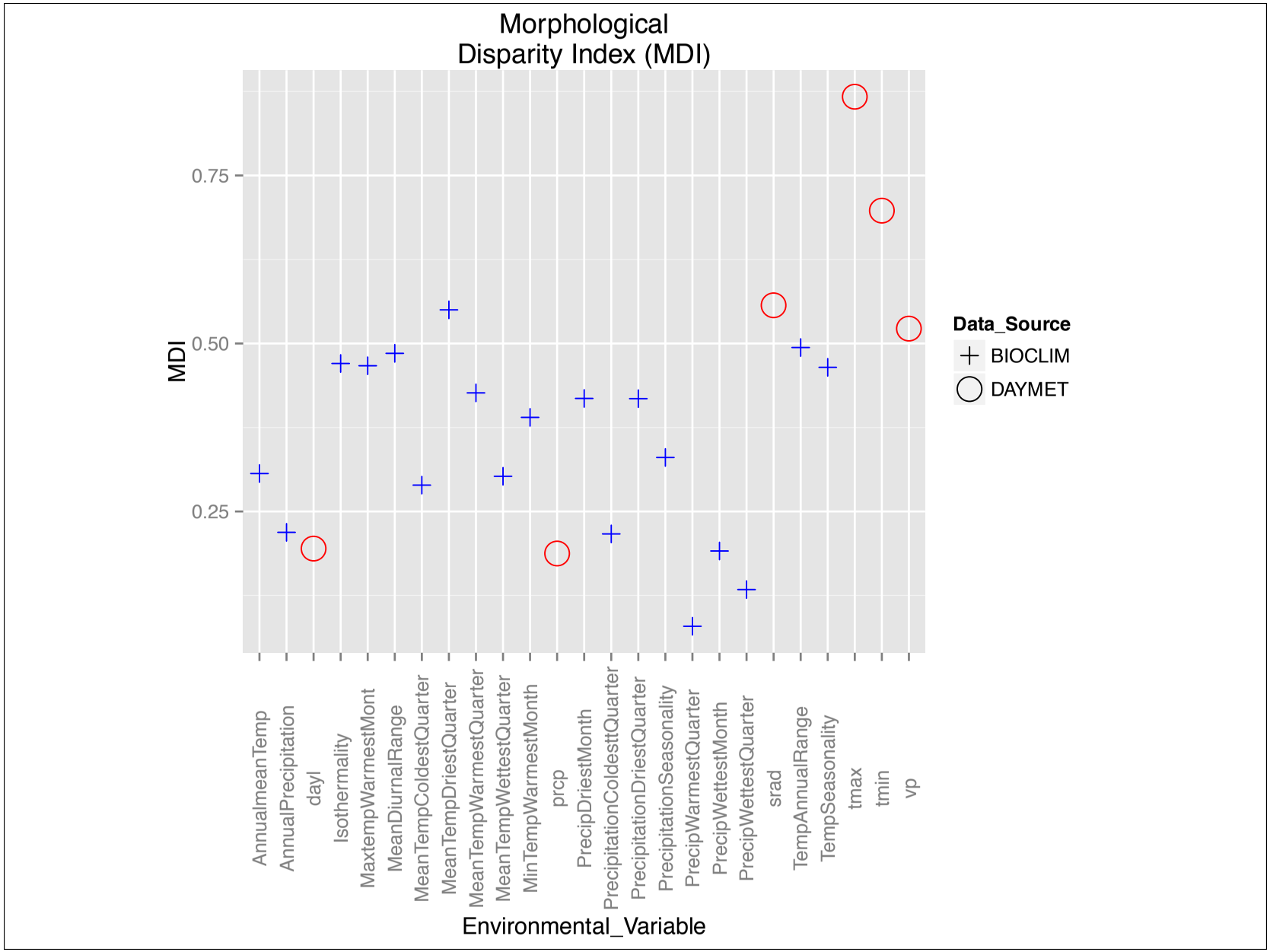
Morphological
Disparity Index (MDI)
MDI
0.75
0.50
0.25
AnnualmeanTemp
AnnualPrecipitation
dayl
Isothermality
MaxtempWarmestMont
MeanDiurnalRange
MeanTempColdestQuarter
MeanTempDriestQuarter
MeanTempWarmestQuarter
MeanTempWettestQuarter
MinTempWarmestMonth
prcp
PrecipDriestMonth
PrecipitationColdesttQuarter
PrecipitationDriestQuarter
PrecipitationSeasonality
PrecipWarmestQuarter
PrecipWettestMonth
PrecipWettestQuarter
srad
TempAnnualRange
TempSeasonality
tmax
tmin
vp
Environmental_Variable
Data_Source
BIOCLIM
DAYMET

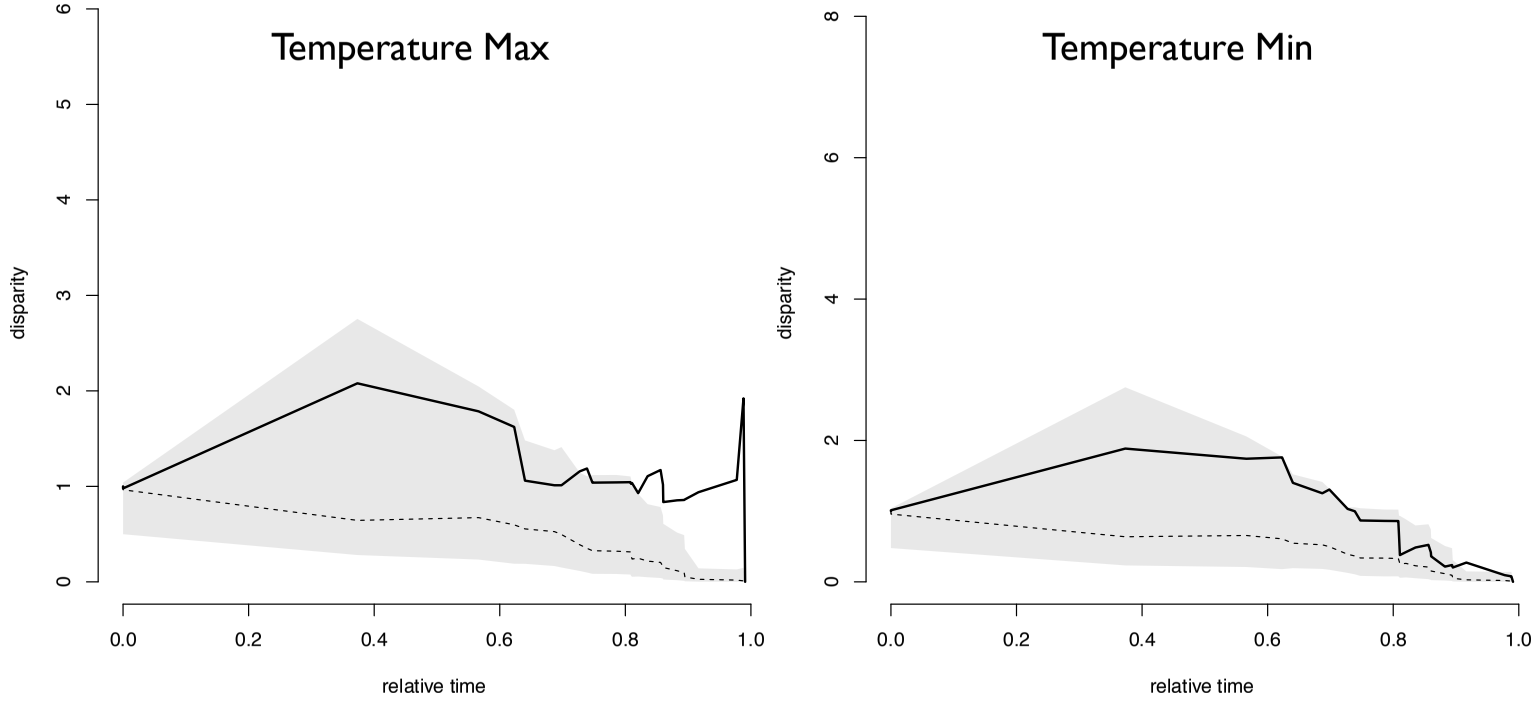

Cladewise disparity through time plots (Daymet data), black lines indicate observed data, dashed mean of simulations and shaded gray area indicate 95% credible interval.

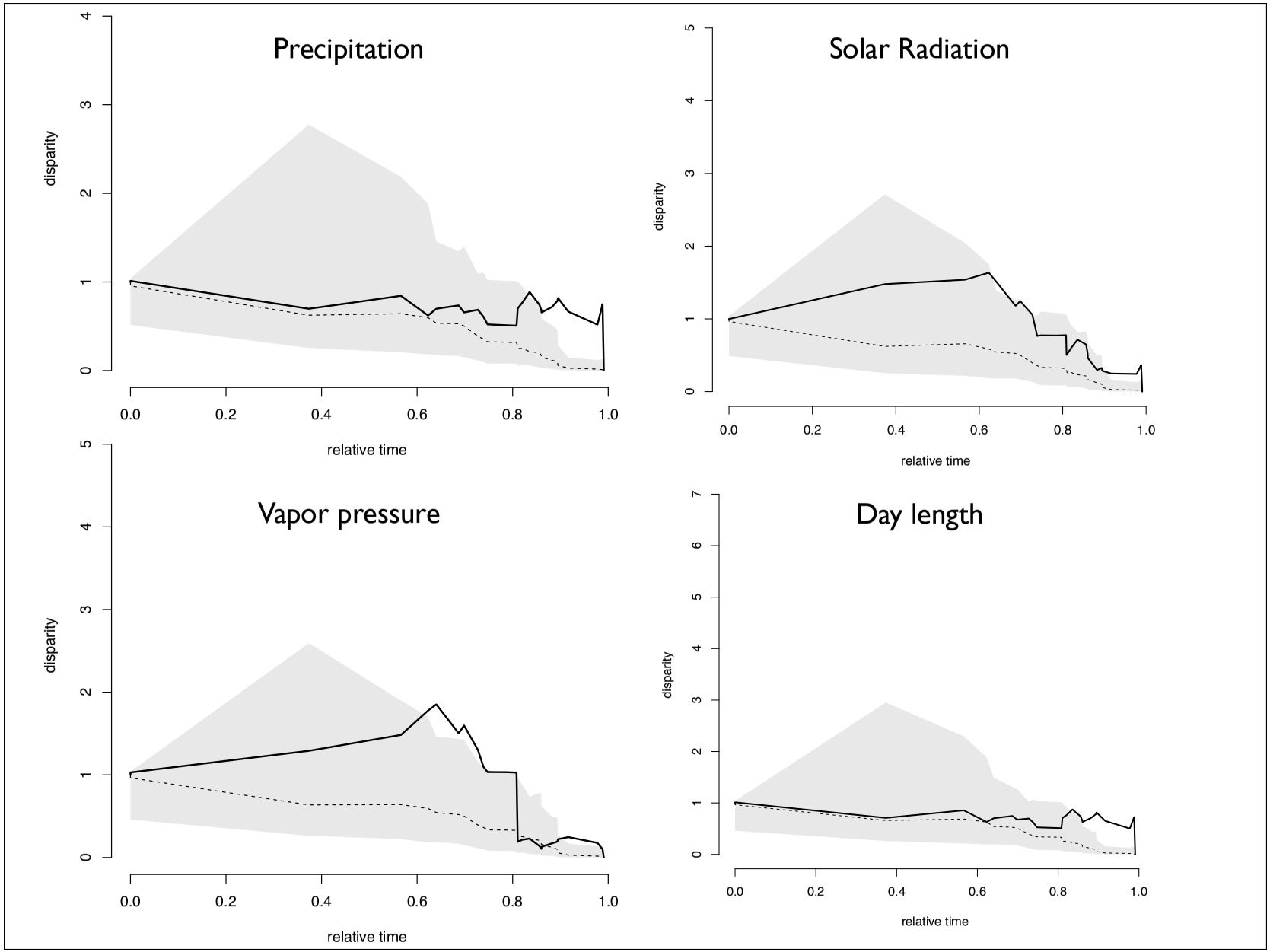
Precipitation
disparity
relative time
Solar Radiation
disparity
relative time
Vapor pressure
disparity
relative time
Day length
disparity
relative time

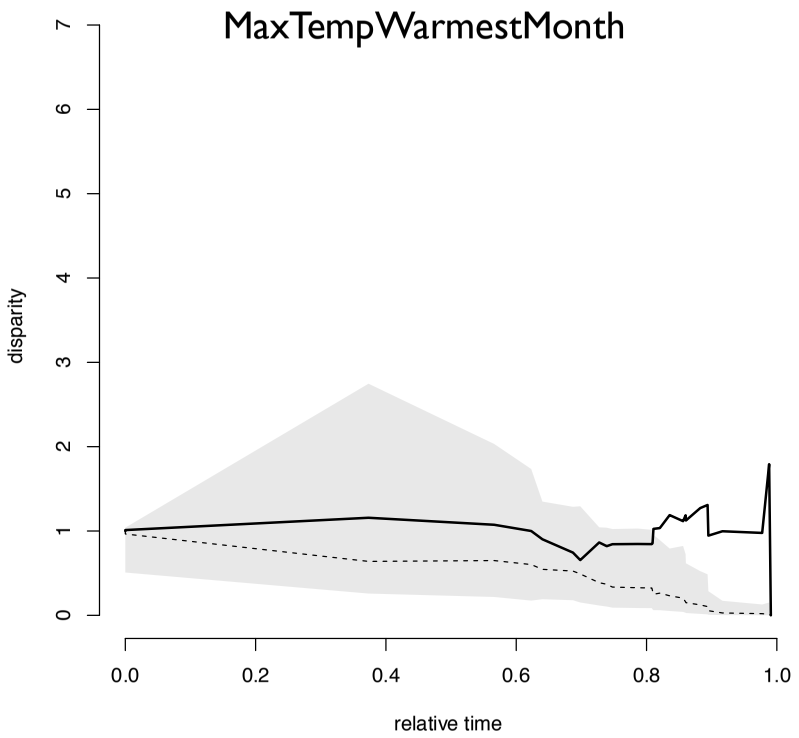

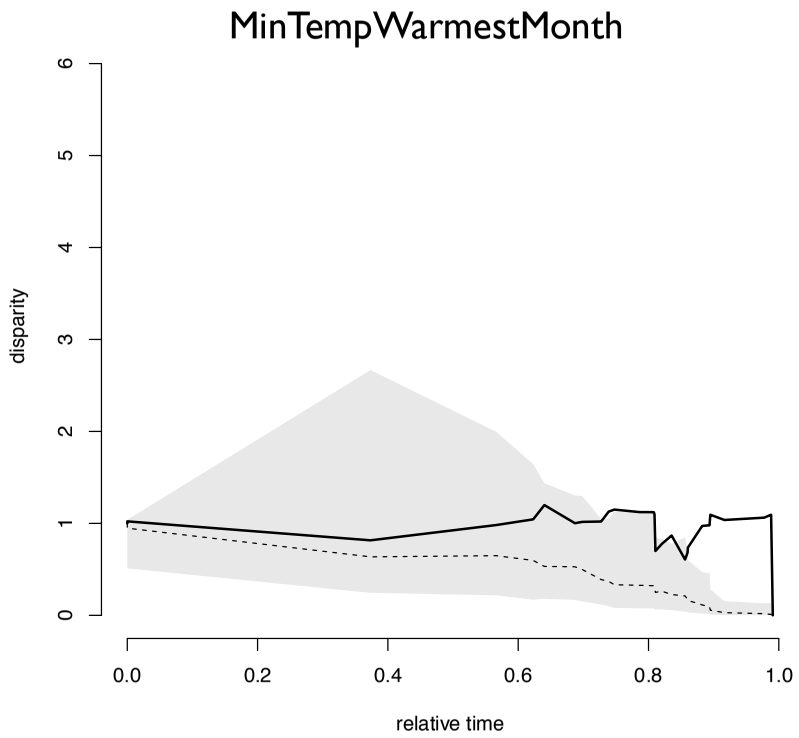

Cladewise disparity through time plots (Bioclim data), black lines indicate observed data, dashed median of simulations and shaded gray area indicate 95% credible interval.

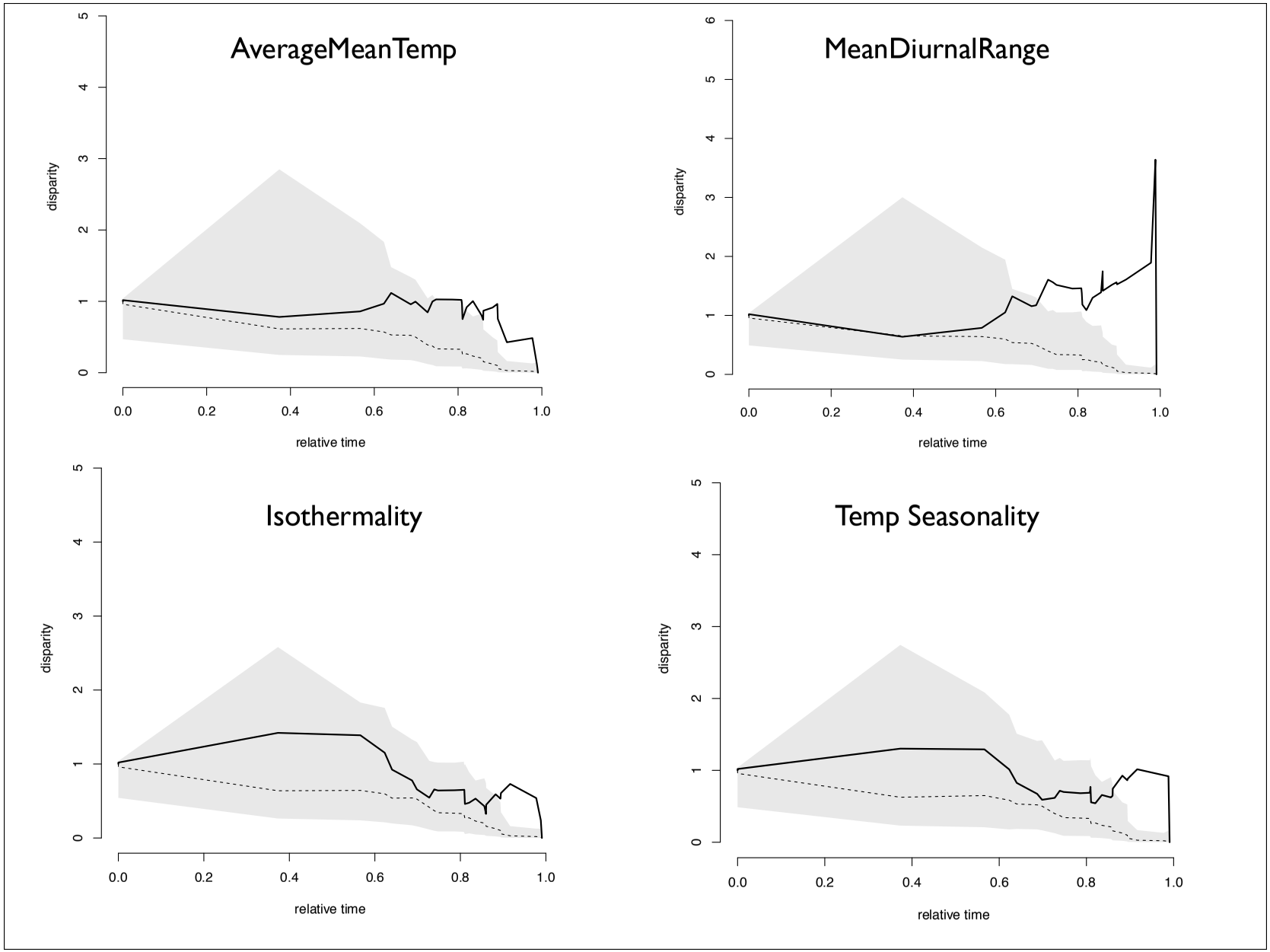
AverageMeanTemp
disparity
relative time
MeanDiurnalRange
disparity
relative time
Isothermality
disparity
relative time
Temp Seasonality
disparity
relative time

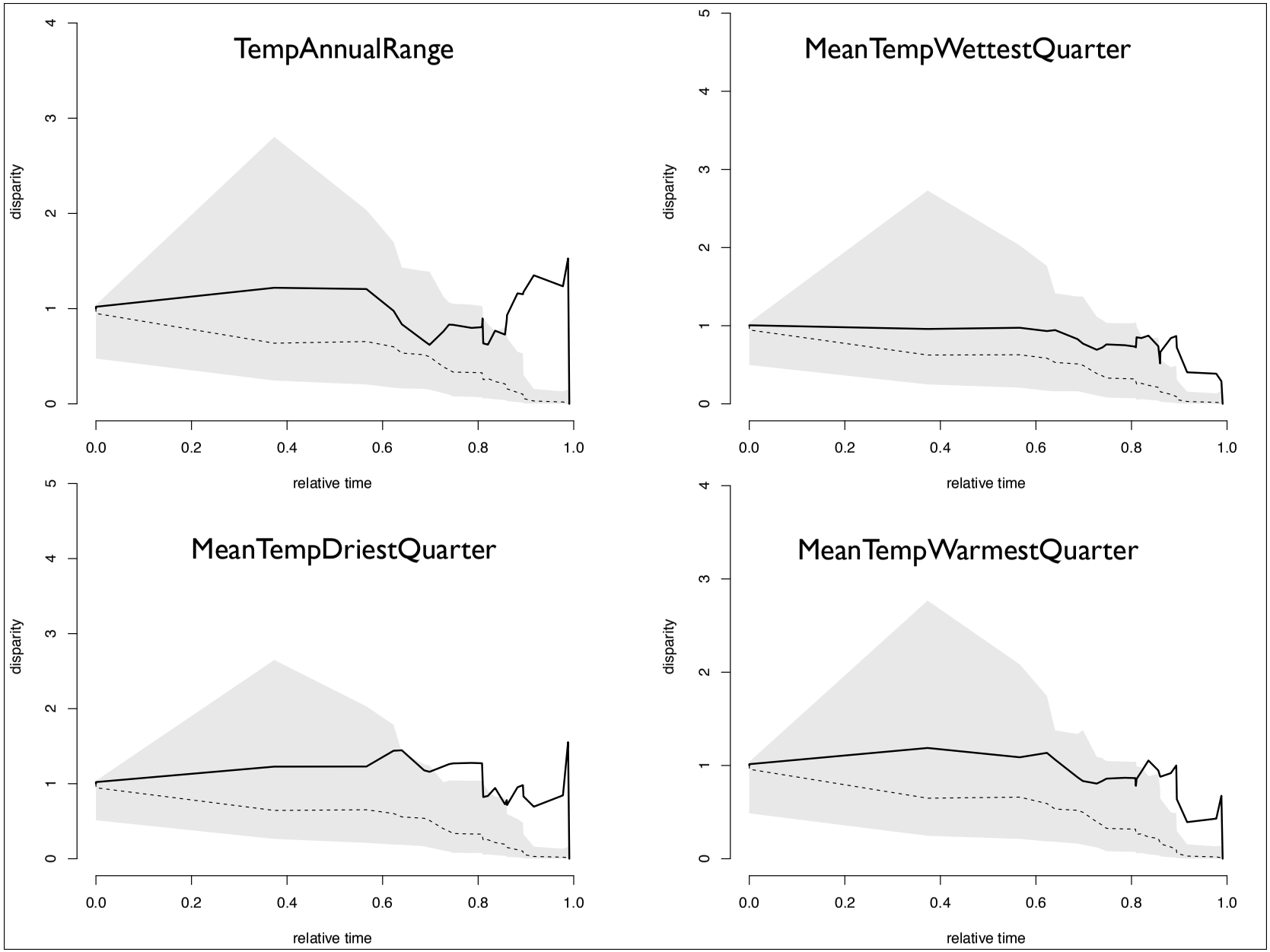
TempAnnualRange
MeanTempWettestQuarter
MeanTempDriestQuarter
MeanTempWarmestQuarter
disparity
relative time
0.0
0.2
0.4
0.6
0.8
1.0

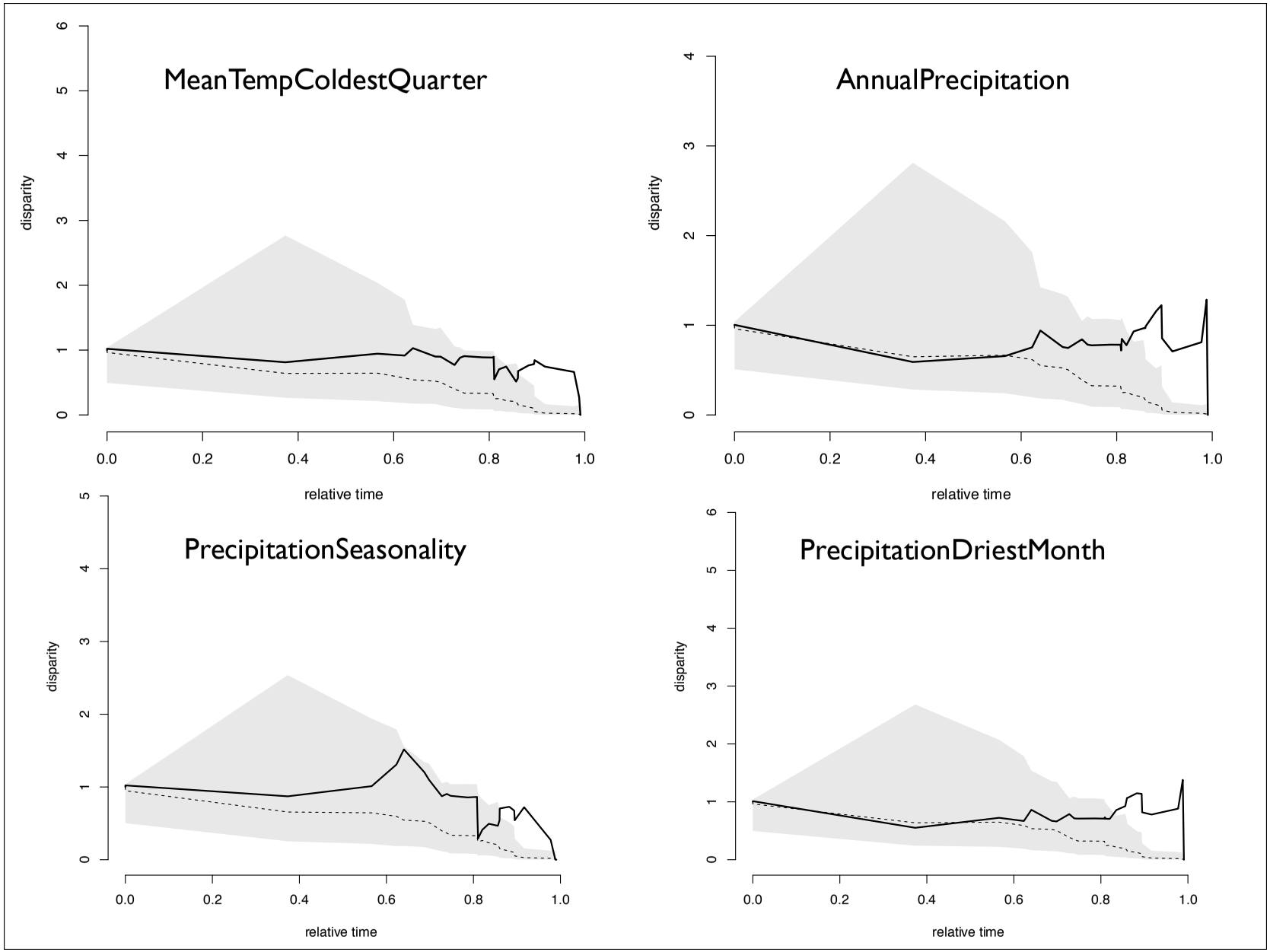
MeanTempColdestQuarter
AnnualPrecipitation
PrecipitationSeasonality
PrecipitationDriestMonth
disparity
relative time
0.0
0.2
0.4
0.6
0.8
1.0

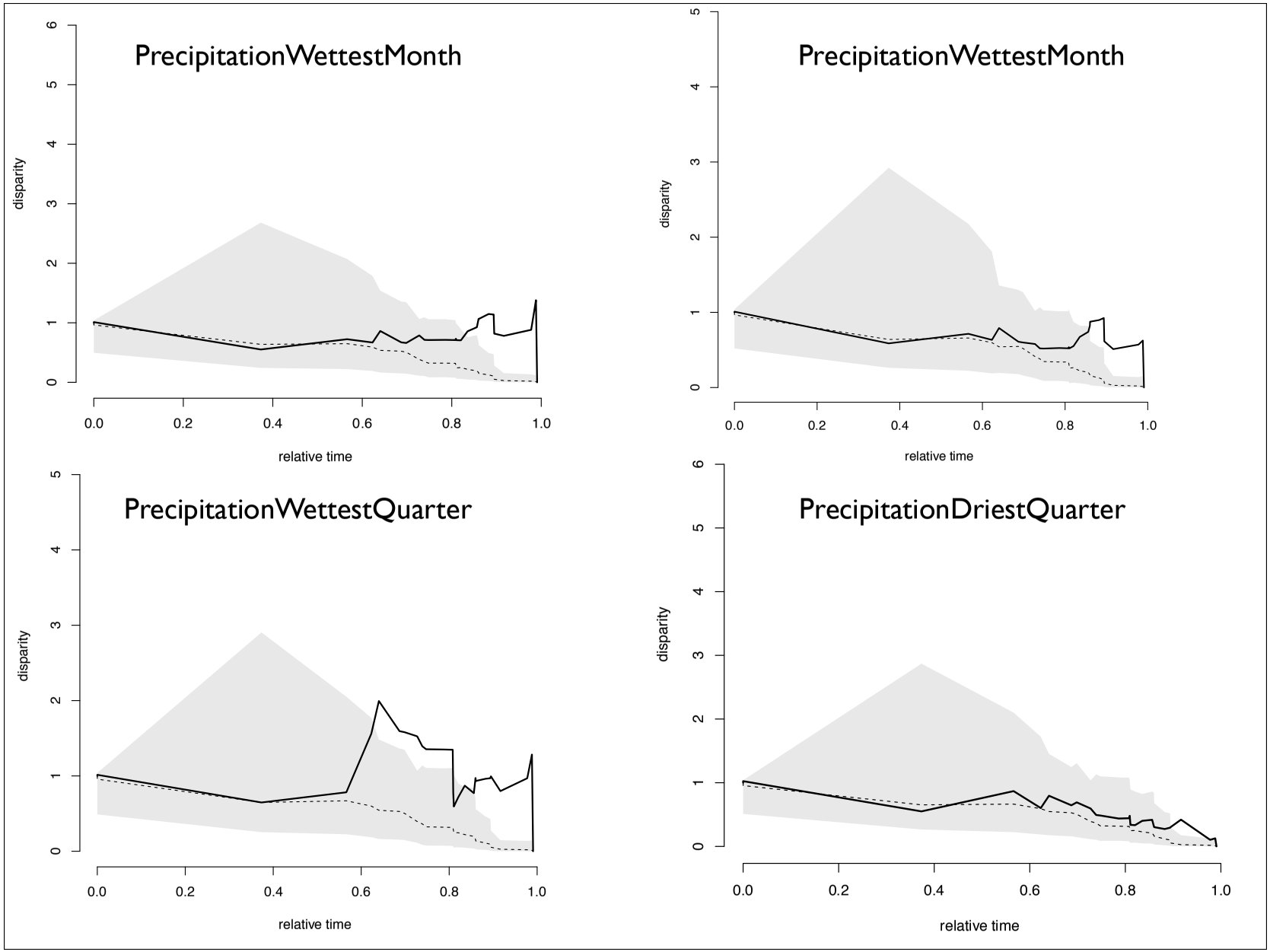
PrecipitationWettestMonth
disparity
relative time
PrecipitationWettestMonth
disparity
relative time
PrecipitationWettestQuarter
disparity
relative time
PrecipitationDriestQuarter
disparity
relative time

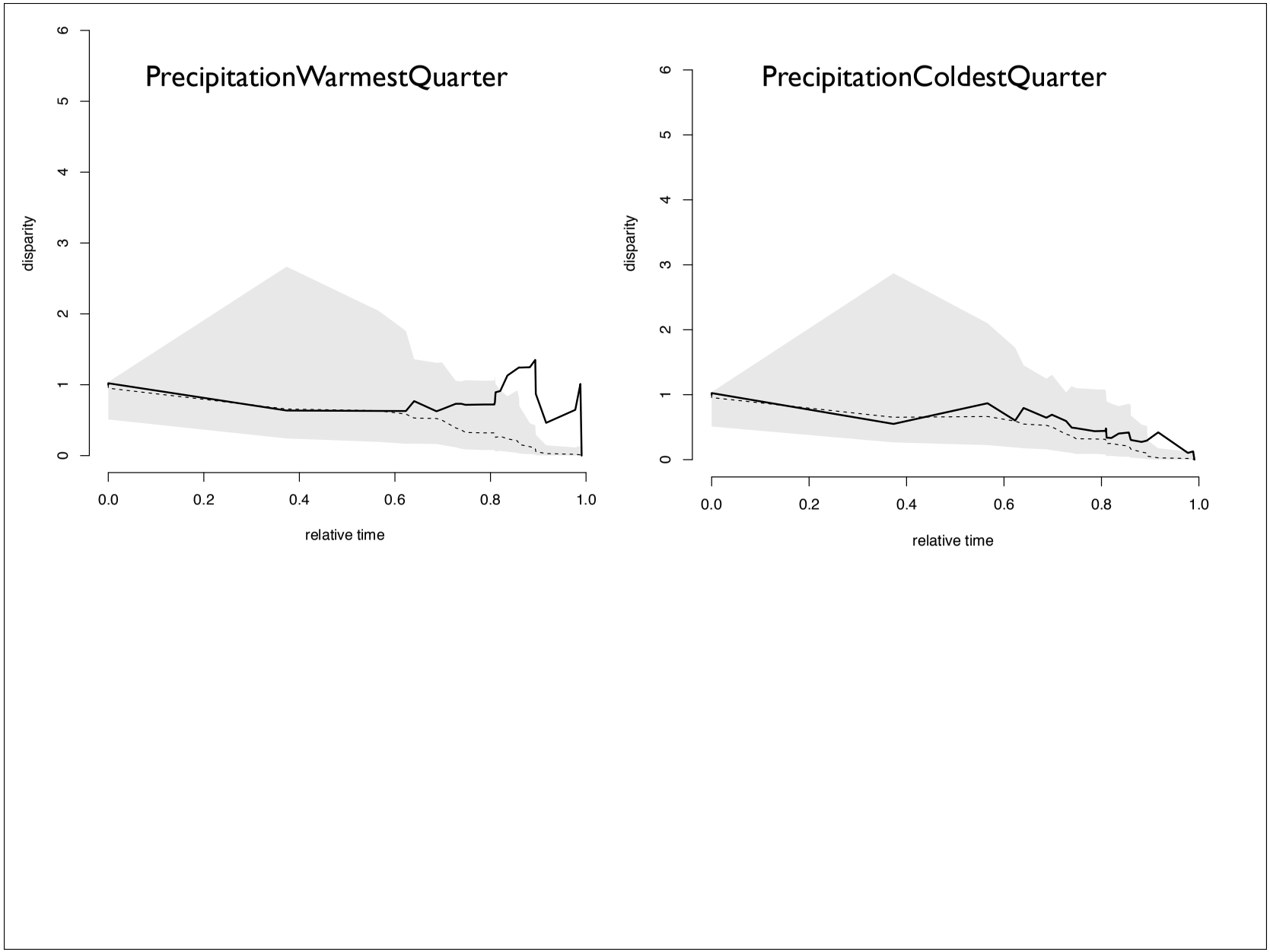
PrecipitationWarmestQuarter
disparity
0
1
2
3
4
5
6
0.0
0.2
0.4
0.6
0.8
1.0
relative time
PrecipitationColdestQuarter
disparity
0
1
2
3
4
5
6
0.0
0.2
0.4
0.6
0.8
1.0
relative time

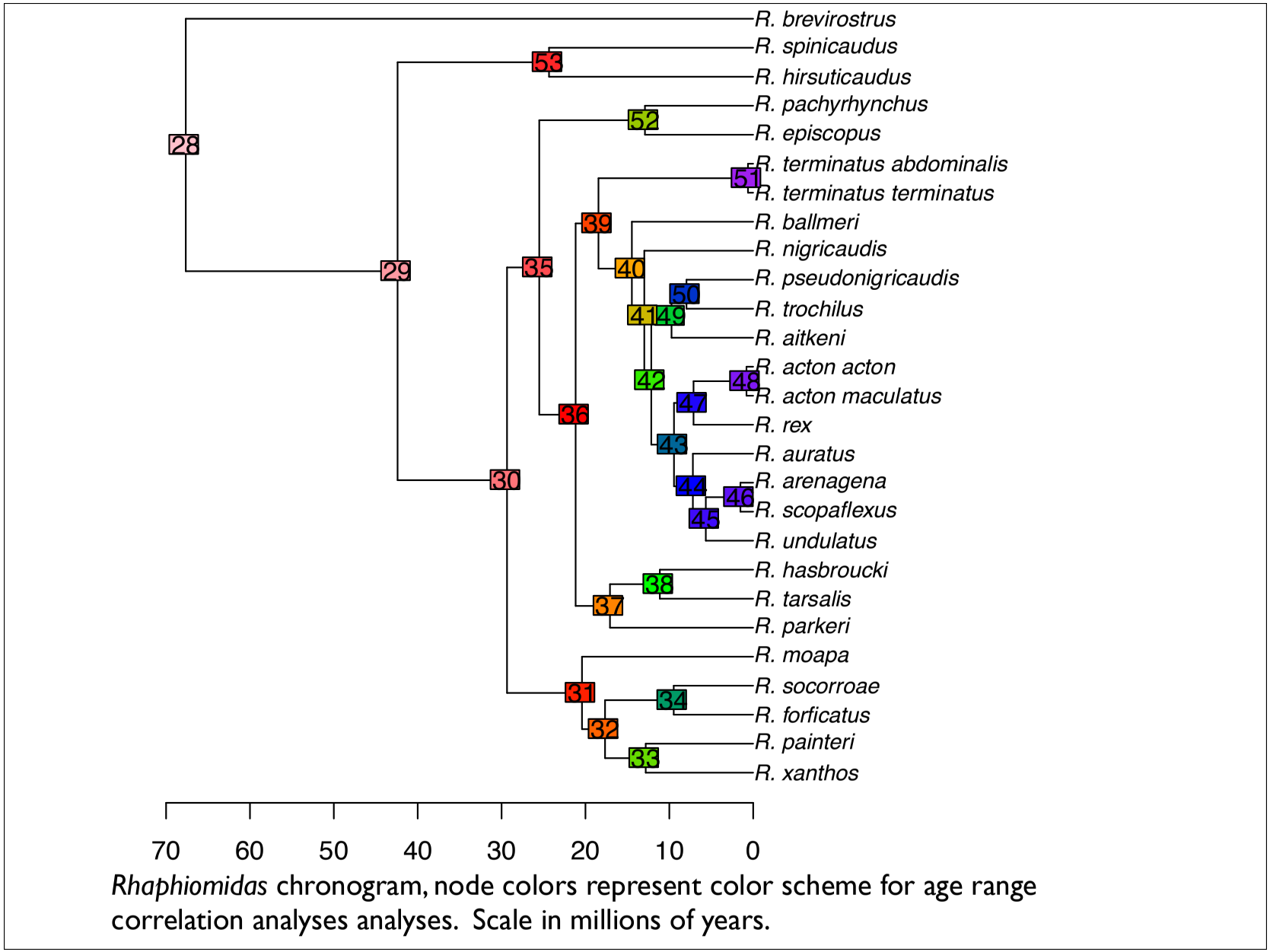

Rhaphiomidas chronogram, node colors represent color scheme for age range correlation analyses analyses. Scale in millions of years.

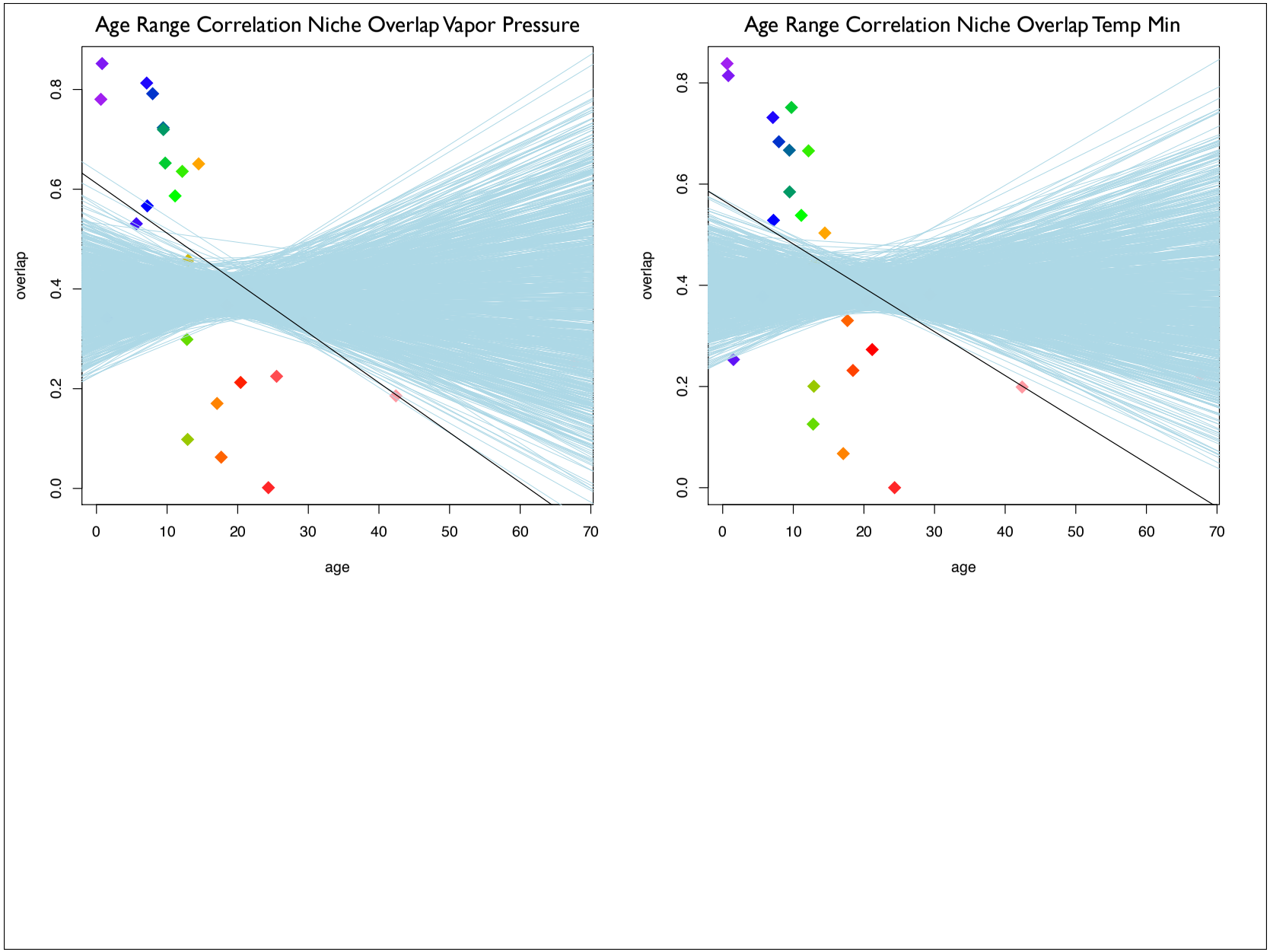
Age Range Correlation Niche Overlap Vapor Pressure
overlap
0.0
0.2
0.4
0.6
0.8
0
10
20
30
40
50
60
70
age
Age Range Correlation Niche Overlap Temp Min
overlap
0.0
0.2
0.4
0.6
0.8
0
10
20
30
40
50
60
70
age

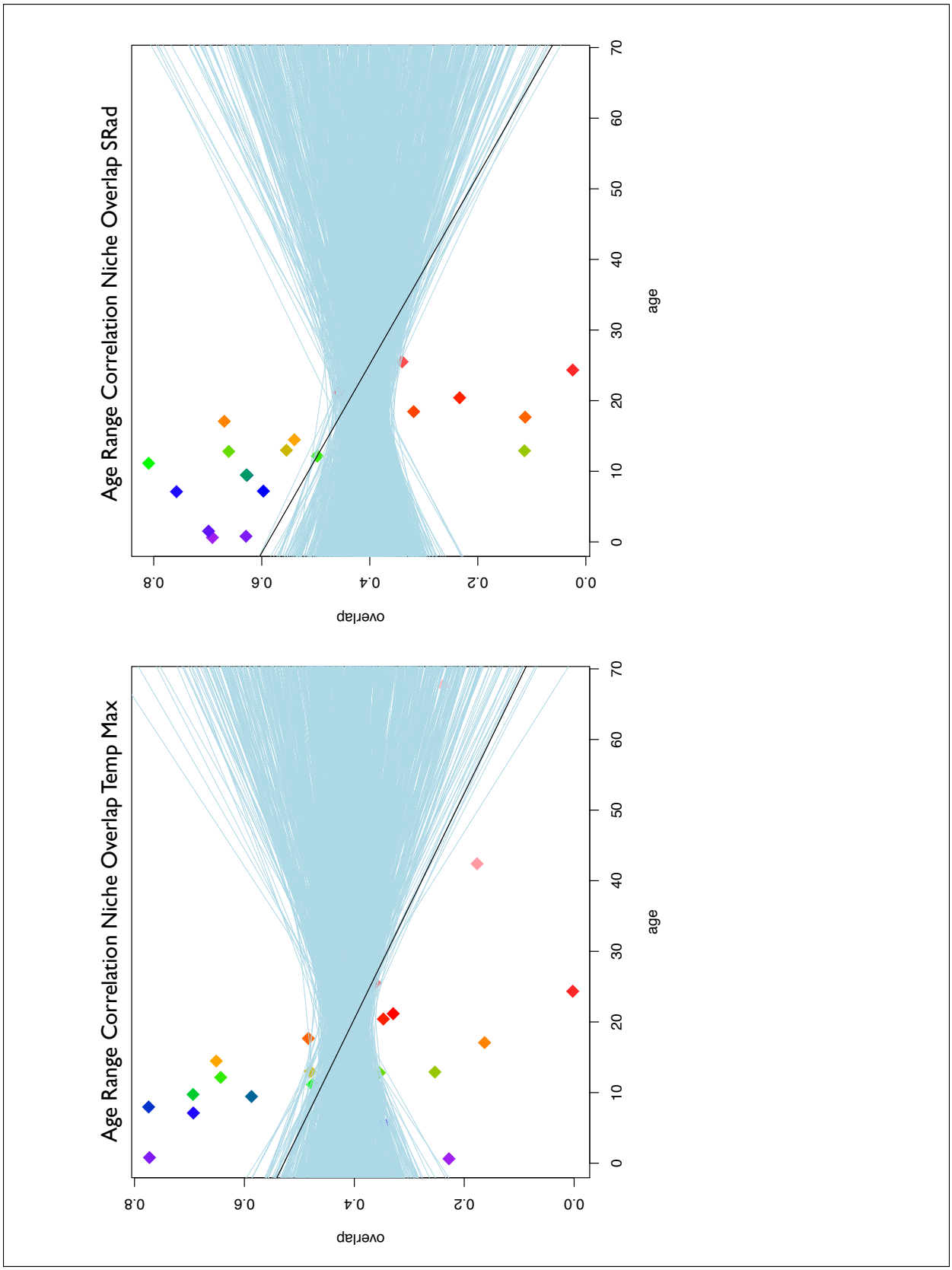
Age Range Correlation Niche Overlap SRad
overlap
0.0
0.2
0.4
0.6
0.8
age
0
10
20
30
40
50
60
70
Age Range Correlation Niche Overlap Temp Max
overlap
0.0
0.2
0.4
0.6
0.8
age
0
10
20
30
40
50
60
70

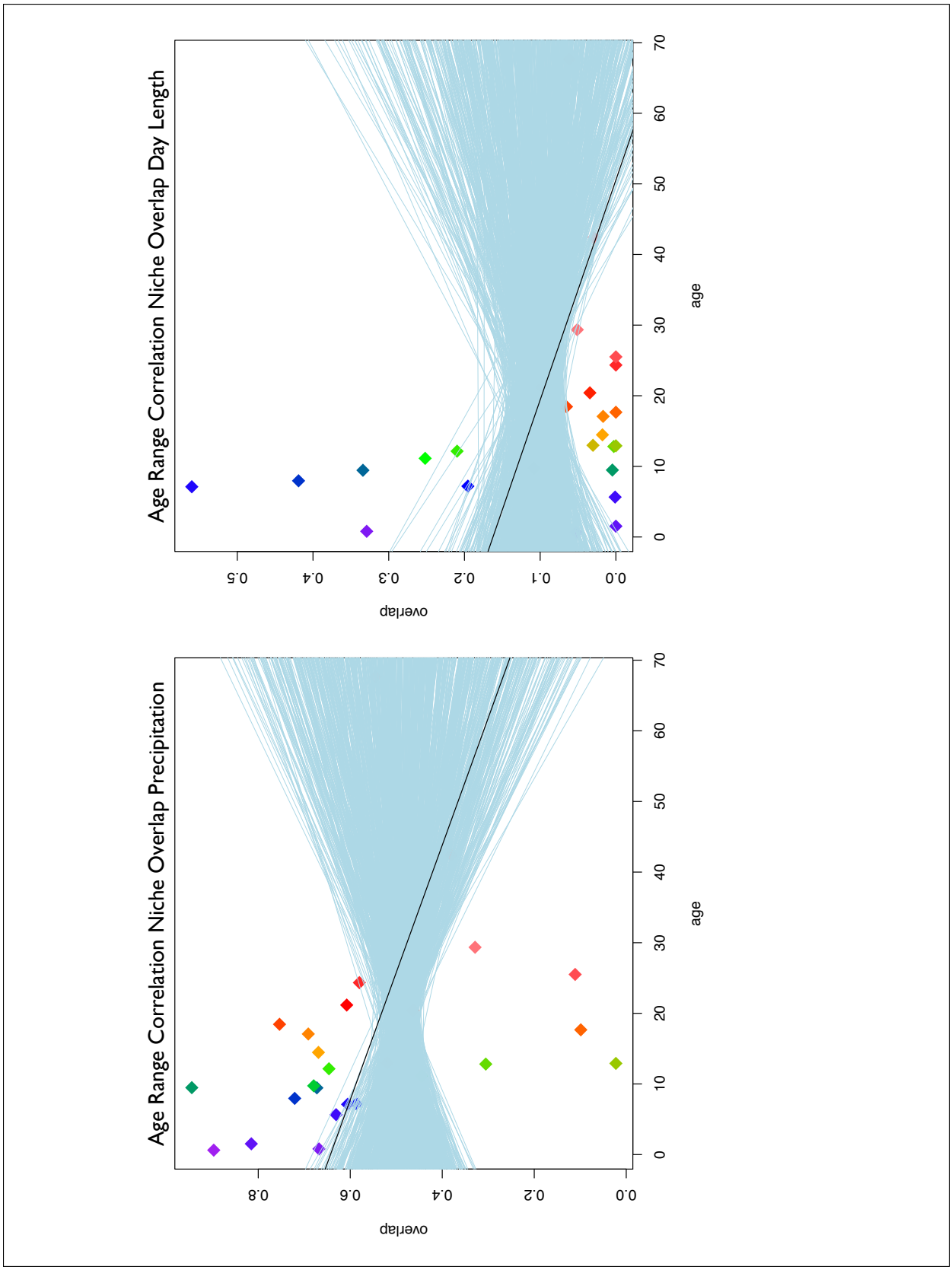
Age Range Correlation Niche Overlap Day Length
overlap
0.0
0.1
0.2
0.3
0.4
0.5
age
0
10
20
30
40
50
60
70
Age Range Correlation Niche Overlap Precipitation
overlap
0.0
0.2
0.4
0.6
0.8
age
0
10
20
30
40
50
60
70

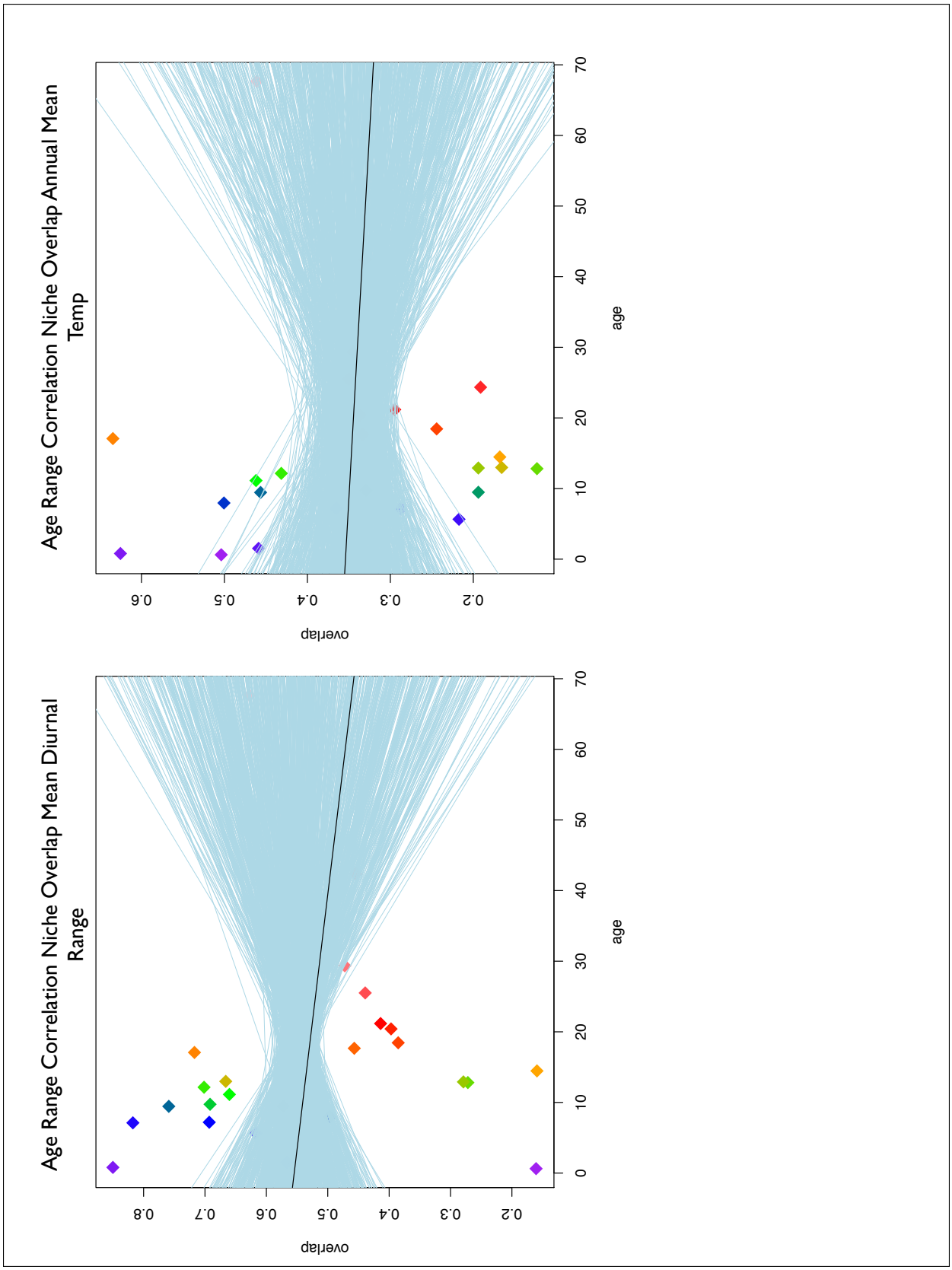
Age Range Correlation Niche Overlap Mean Diurnal Range
overlap
0.2
0.3
0.4
0.5
0.6
0.7
0.8
0
10
20
30
40
50
60
70
age
Age Range Correlation Niche Overlap Annual Mean Temp
overlap
0.2
0.3
0.4
0.5
0.6
0
10
20
30
40
50
60
70
age

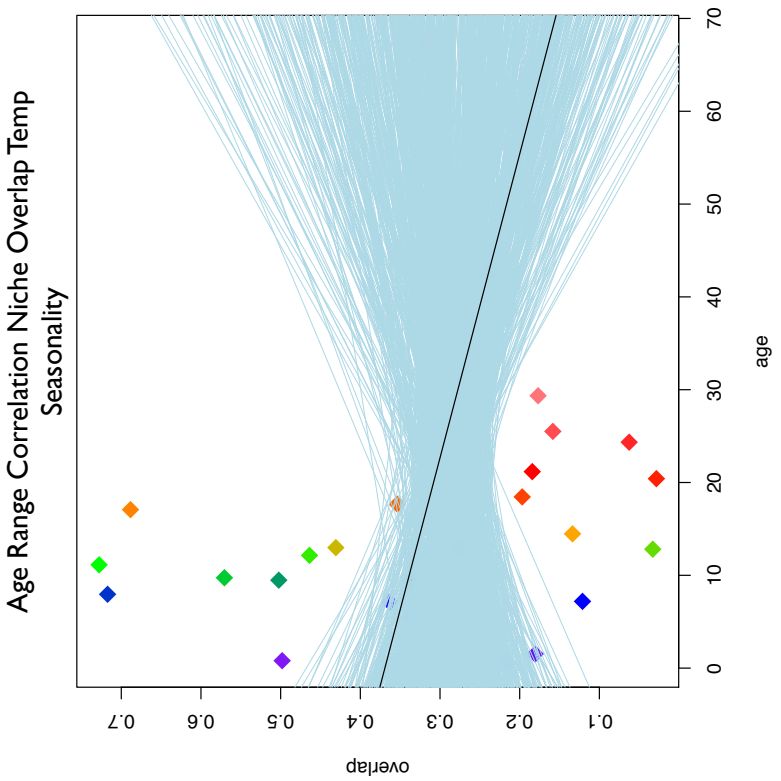
Age Range Correlation Niche Overlap Temp
Seasonality
overlap
0.7
0.6
0.5
0.4
0.3
0.2
0.1
age
0
10
20
30
40
50
60
70

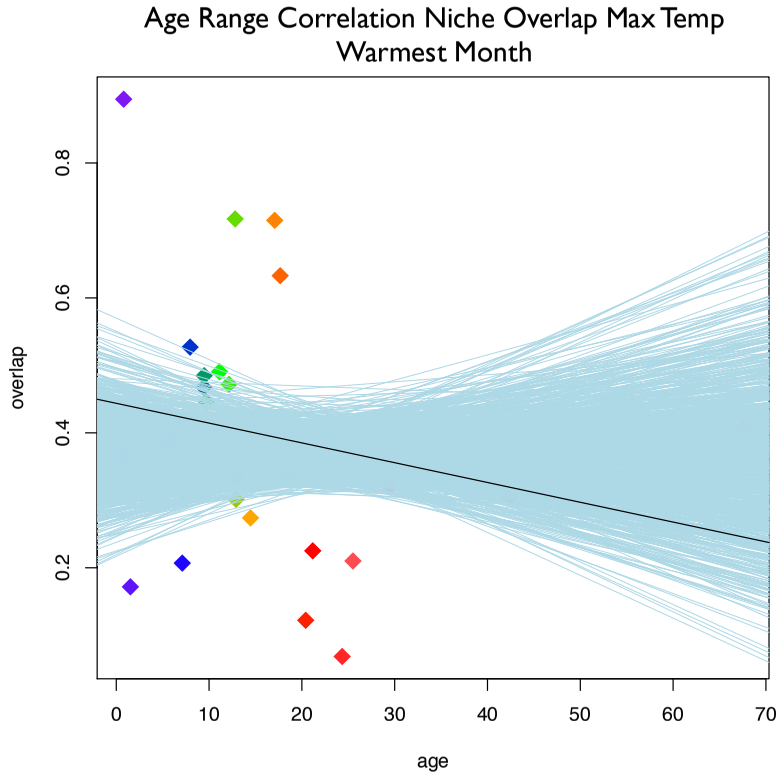
Age Range Correlation Niche Overlap Max Temp Warmest Month
overlap
0.2
0.4
0.6
0.8
0
10
20
30
40
50
60
70
age

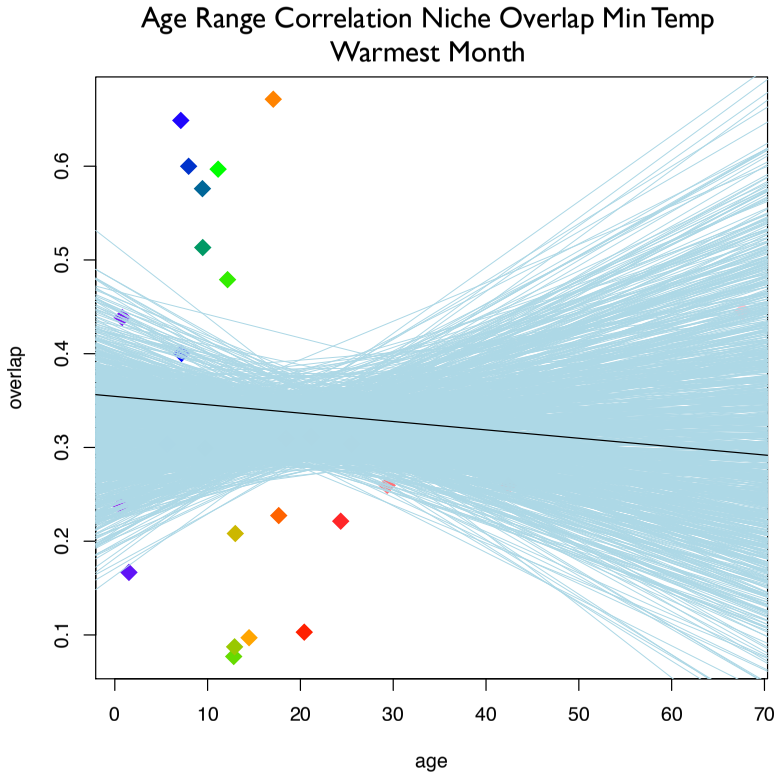
Age Range Correlation Niche Overlap Min Temp Warmest Month
overlap
0.1
0.2
0.3
0.4
0.5
0.6
0
10
20
30
40
50
60
70
age

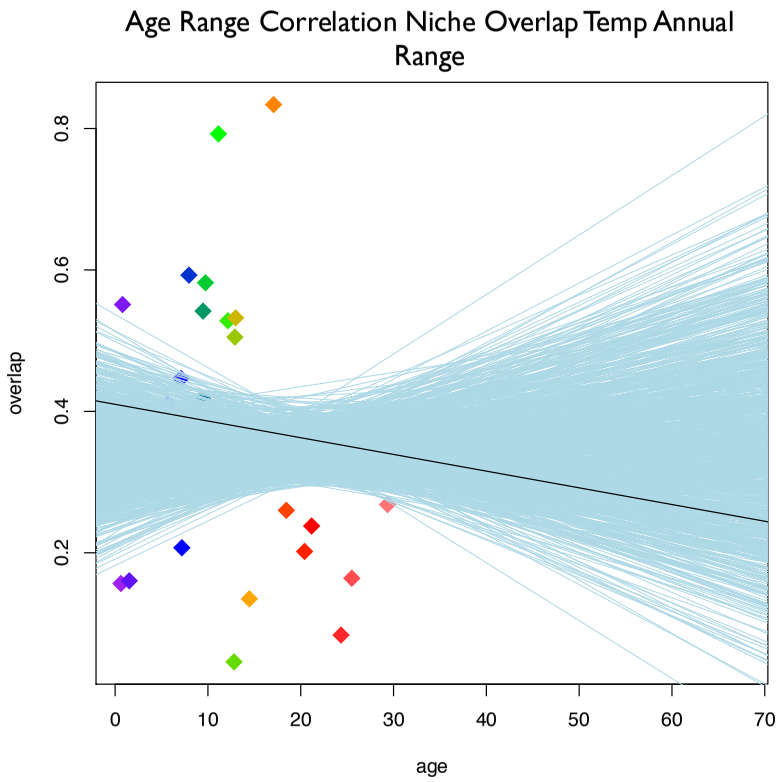
Age Range Correlation Niche Overlap Temp Annual Range
overlap
0.2
0.4
0.6
0.8
0
10
20
30
40
50
60
70
age

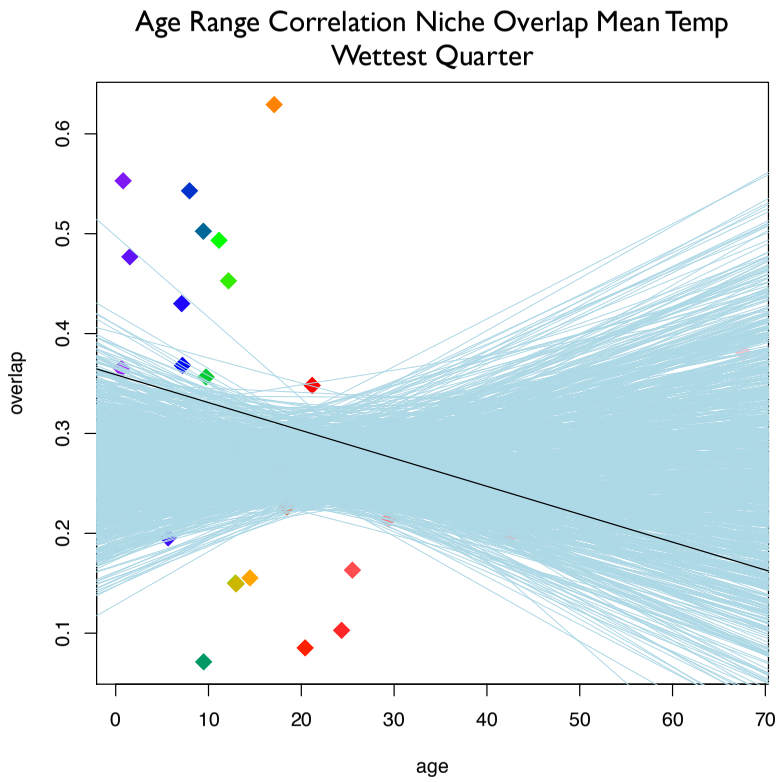
Age Range Correlation Niche Overlap Mean Temp Wettest Quarter
overlap
0.1
0.2
0.3
0.4
0.5
0.6
0
10
20
30
40
50
60
70
age

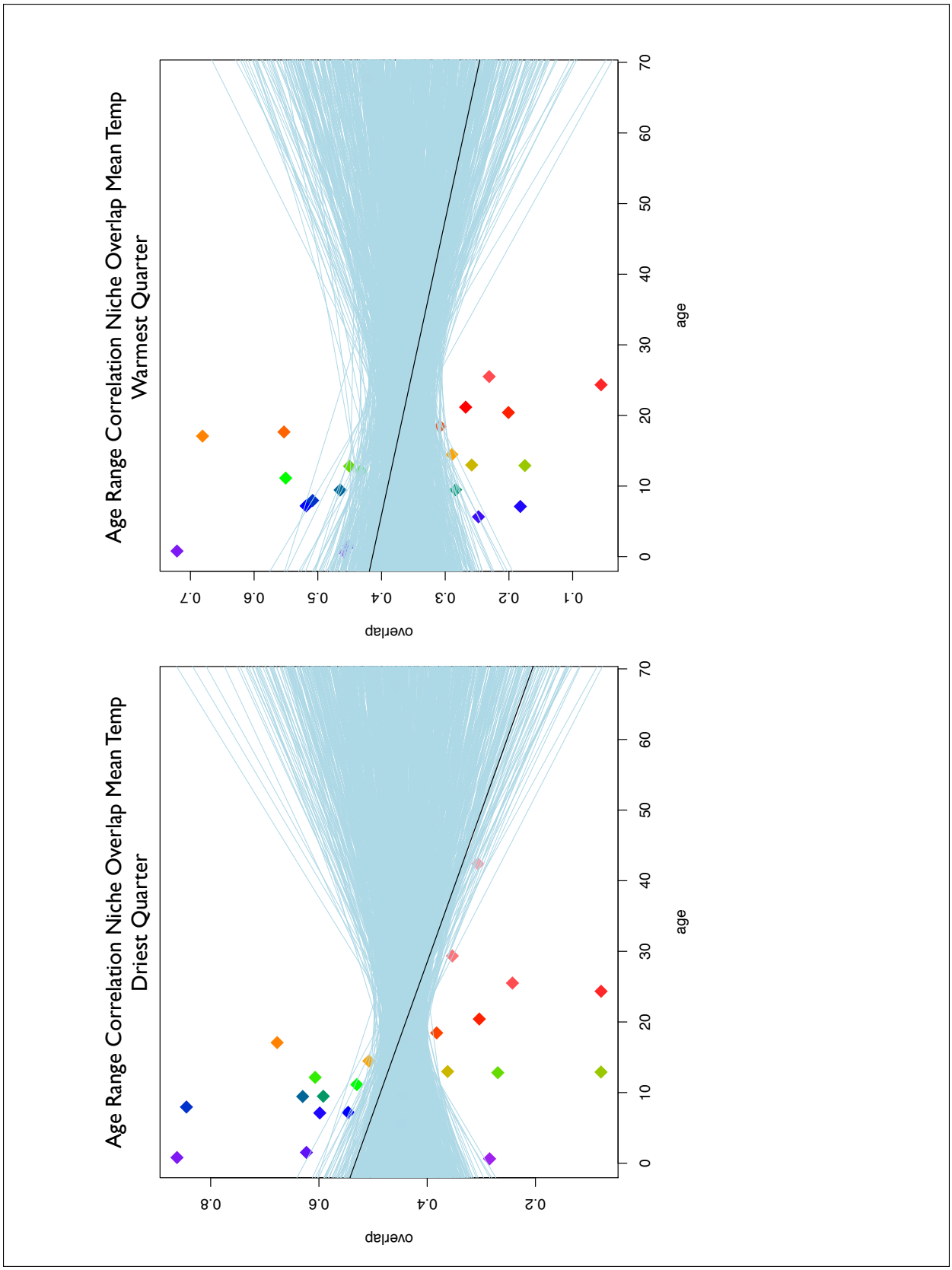
Age Range Correlation Niche Overlap Mean Temp
Warmest Quarter
overlap
0.1
0.2
0.3
0.4
0.5
0.6
0.7
age
0
10
20
30
40
50
60
70
Age Range Correlation Niche Overlap Mean Temp
Driest Quarter
overlap
0.2
0.4
0.6
0.8
age
0
10
20
30
40
50
60
70

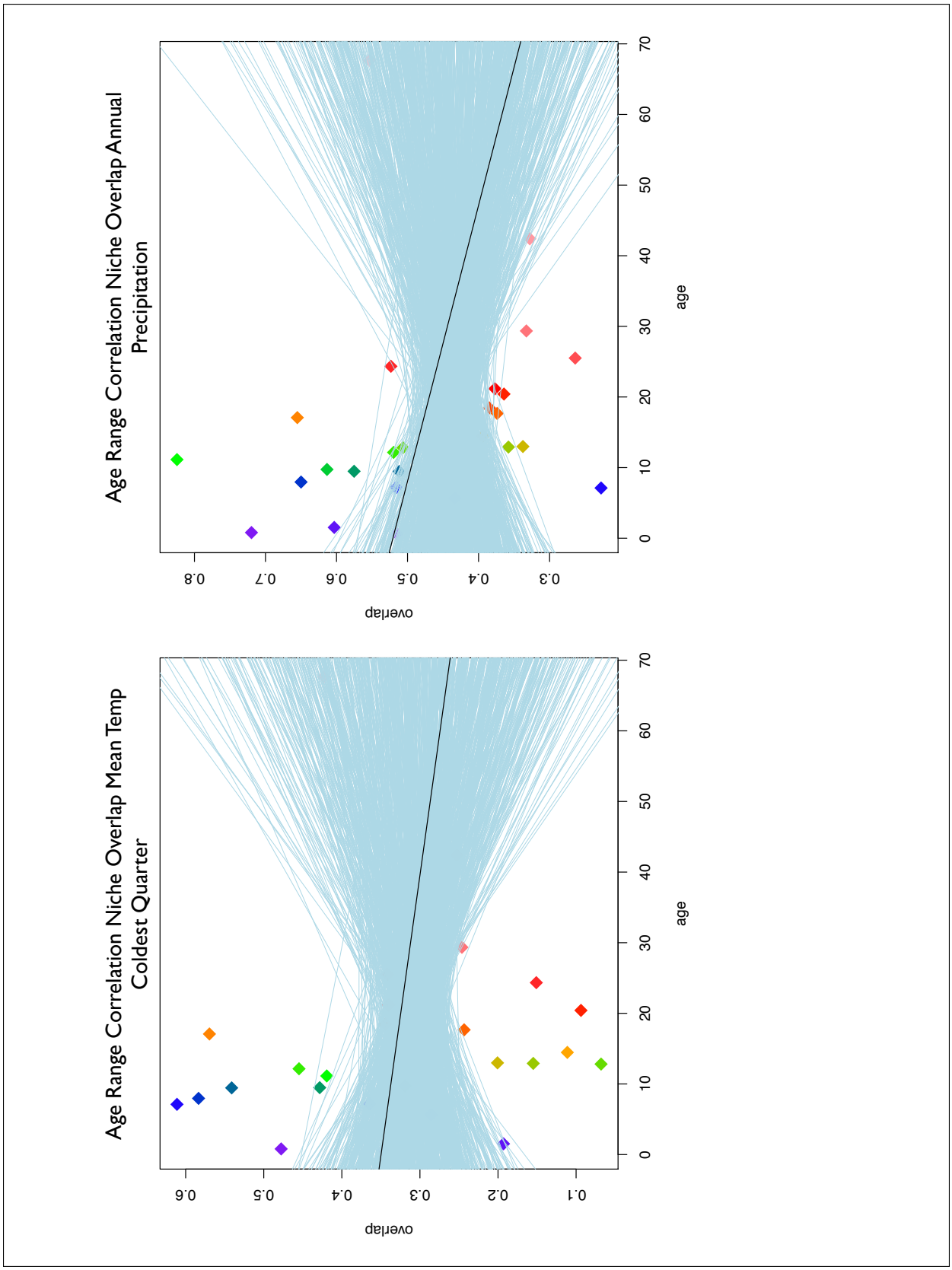
Age Range Correlation Niche Overlap Annual Precipitation
overlap
age
Age Range Correlation Niche Overlap Mean Temp Coldest Quarter
overlap
age

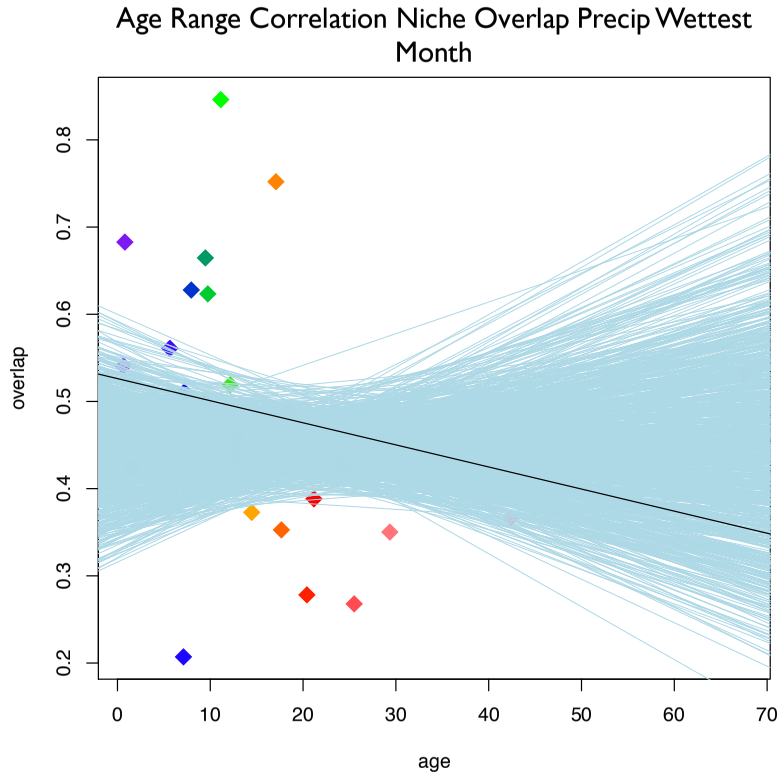
Age Range Correlation Niche Overlap Precip Wettest Month
overlap
age
0.2
0.3
0.4
0.5
0.6
0.7
0.8
0
10
20
30
40
50
60
70

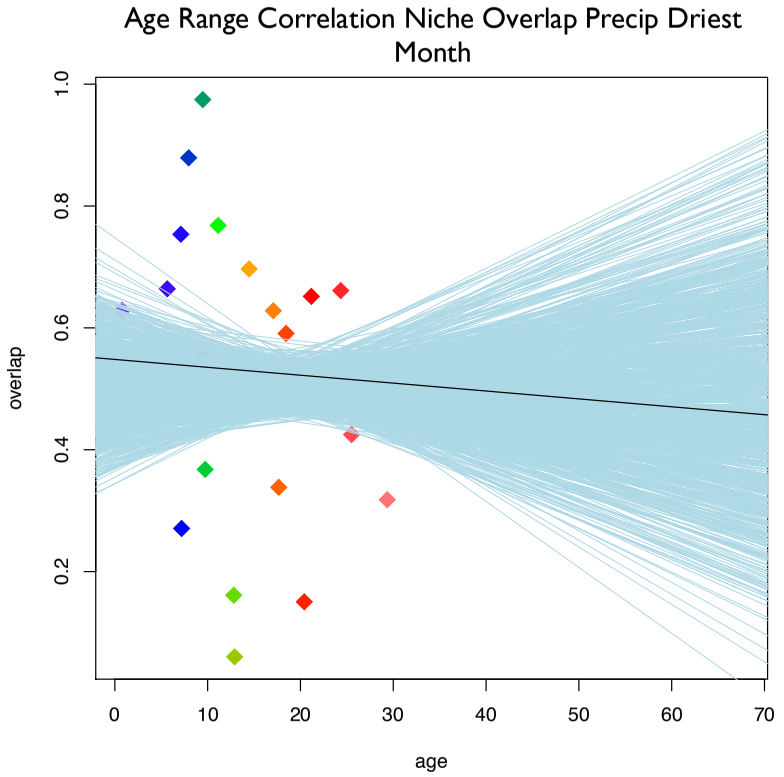
Age Range Correlation Niche Overlap Precip Driest Month
overlap
age
0.2
0.4
0.6
0.8
1.0
0
10
20
30
40
50
60
70

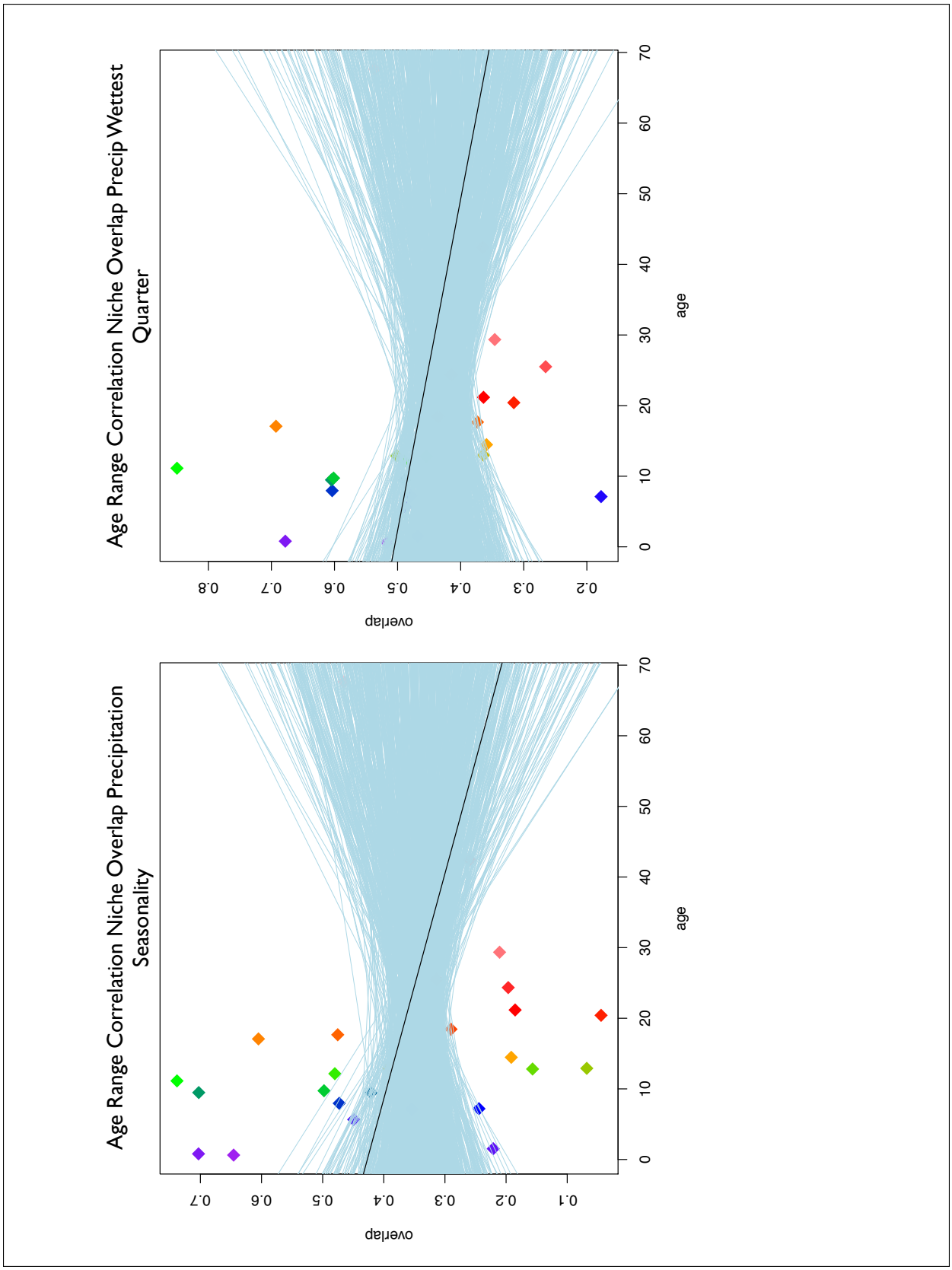
Age Range Correlation Niche Overlap Precip Wettest Quarter
overlap
0.2
0.3
0.4
0.5
0.6
0.7
0.8
age
0
10
20
30
40
50
60
70
Age Range Correlation Niche Overlap Precipitation Seasonality
overlap
0.1
0.2
0.3
0.4
0.5
0.6
0.7
age
0
10
20
30
40
50
60
70

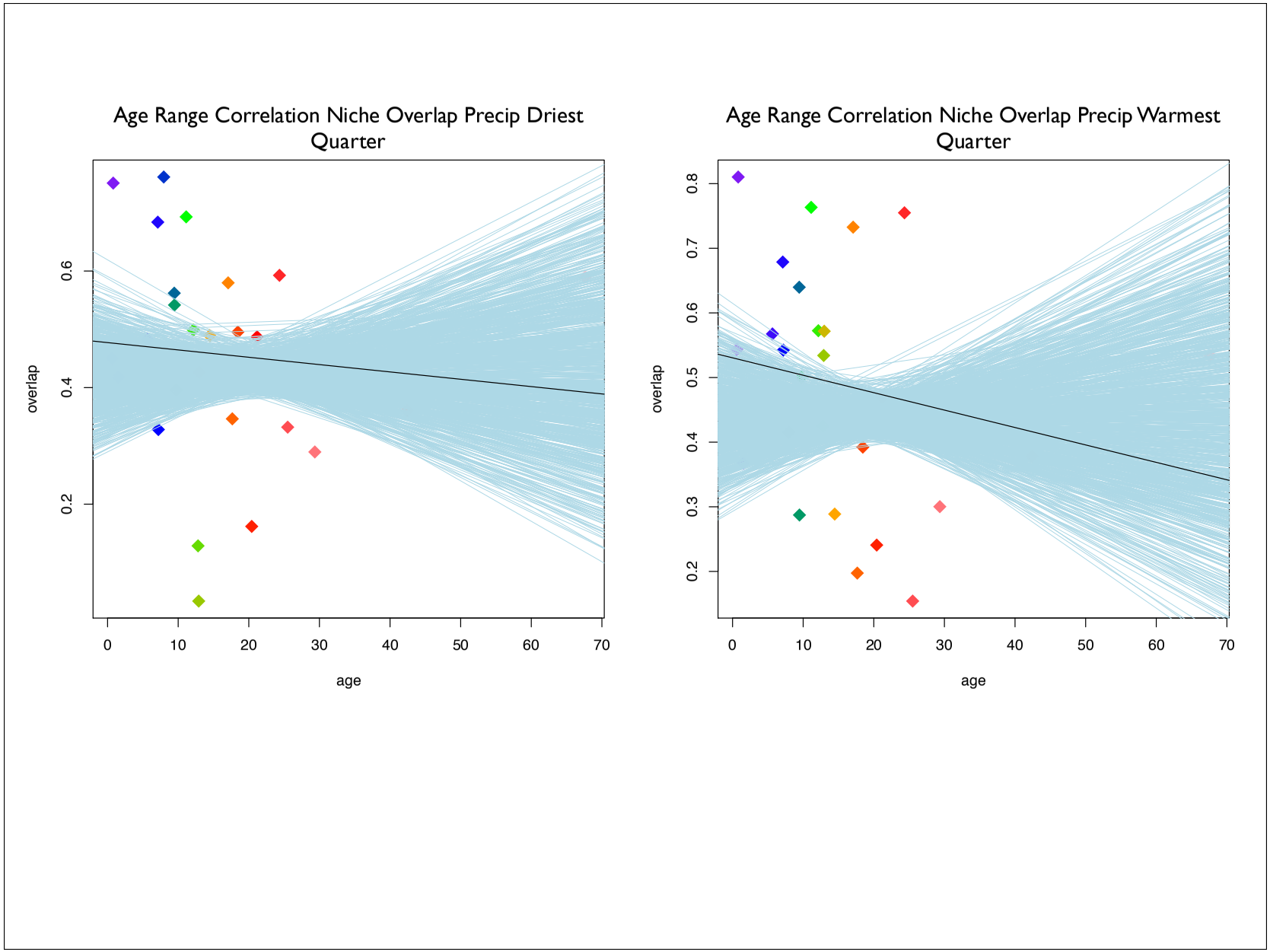
Age Range Correlation Niche Overlap Precip Driest Quarter
overlap
0.2
0.4
0.6
0
10
20
30
40
50
60
70
age
Age Range Correlation Niche Overlap Precip Warmest Quarter
overlap
0.2
0.3
0.4
0.5
0.6
0.7
0.8
0
10
20
30
40
50
60
70
age

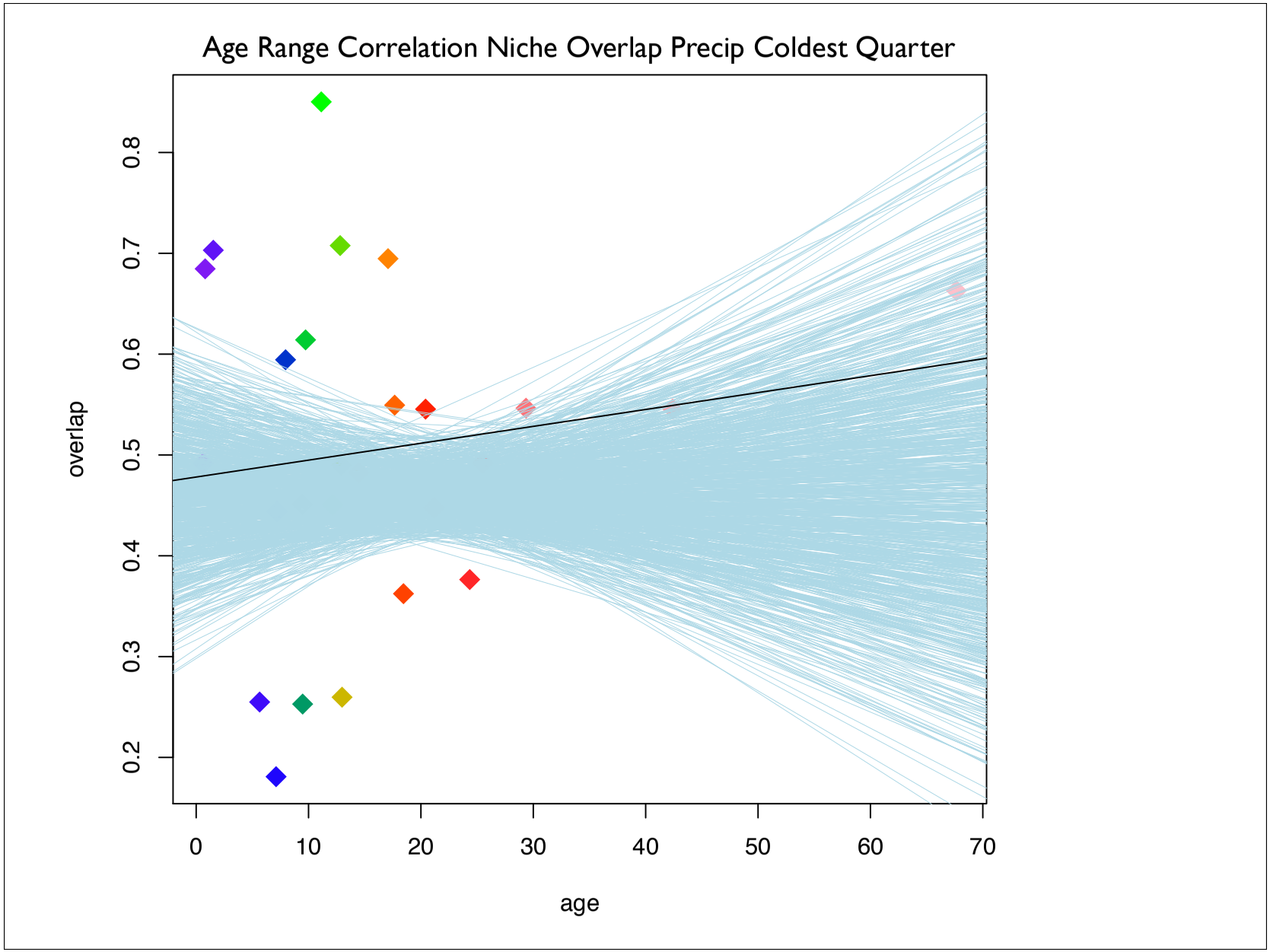
Age Range Correlation Niche Overlap Precip Coldest Quarter
overlap
0.2
0.3
0.4
0.5
0.6
0.7
0.8
0
10
20
30
40
50
60
70
age

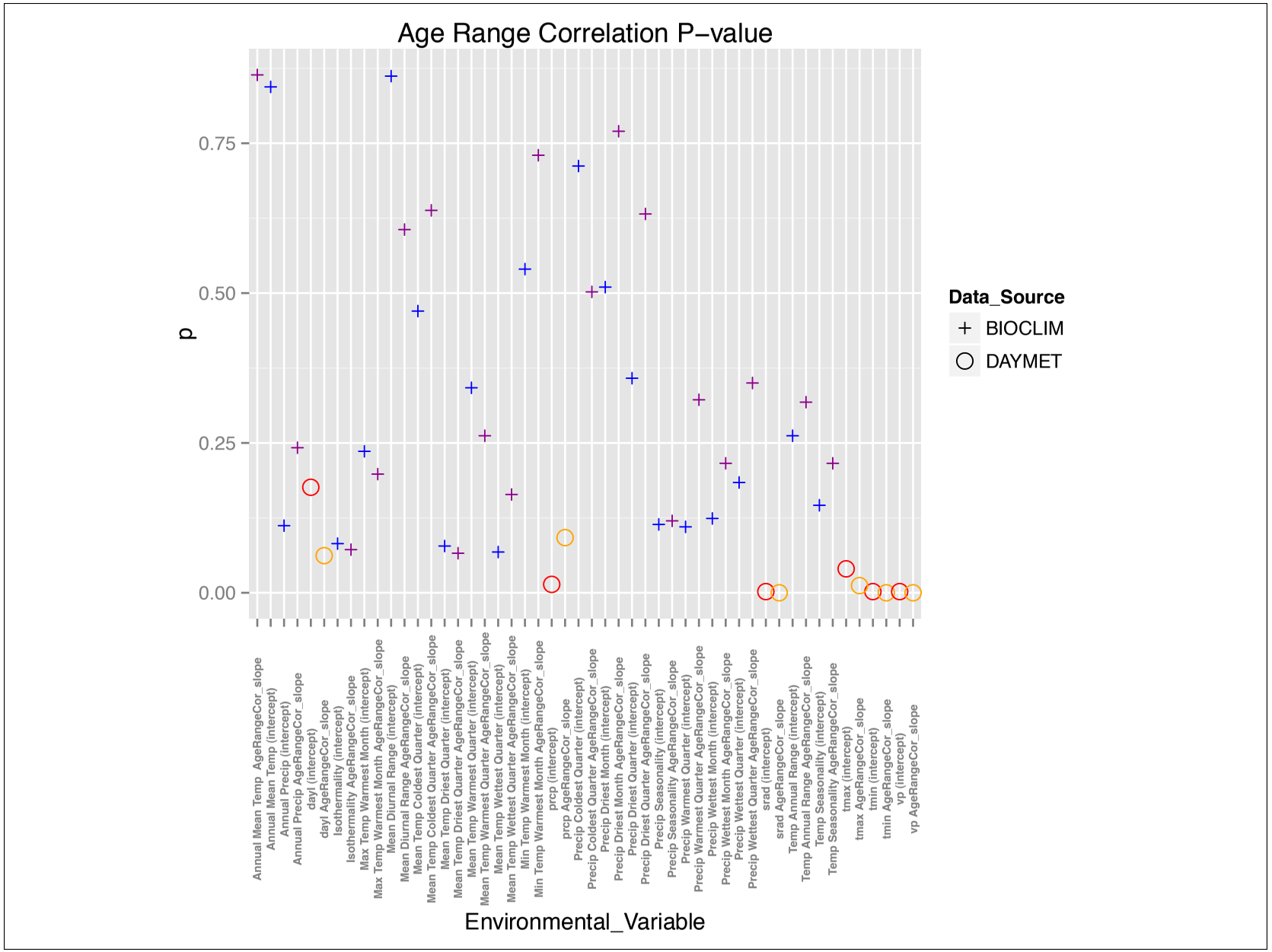
Age Range Correlation P−value
p
0.75
0.50
0.25
0.00
Environmental_Variable
Annual Mean Temp_AgeRangeCor_slope
Annual Mean Temp (intercept)
Annual Precip (intercept)
Annual Precip AgeRangeCor_slope
dayl (intercept)
dayl AgeRangeCor_slope
Isothermality (intercept)
Isothermality AgeRangeCor_slope
Max Temp Warmest Month (intercept)
Max Temp Warmest Month AgeRangeCor_slope
Mean Diurnal Range (intercept)
Mean Diurnal Range AgeRangeCor_slope
Mean Temp Coldest Quarter (intercept)
Mean Temp Coldest Quarter AgeRangeCor_slope
Mean Temp Driest Quarter (intercept)
Mean Temp Driest Quarter AgeRangeCor_slope
Mean Temp Warmest Quarter (intercept)
Mean Temp Warmest Quarter AgeRangeCor_slope
Mean Temp Wettest Quarter (intercept)
Mean Temp Wettest Quarter AgeRangeCor_slope
Min Temp Warmest Month (intercept)
Min Temp Warmest Month AgeRangeCor_slope
prcp (intercept)
prcp AgeRangeCor_slope
Precip Coldest Quarter (intercept)
Precip Coldest Quarter AgeRangeCor_slope
Precip Driest Month (intercept)
Precip Driest Month AgeRangeCor_slope
Precip Driest Quarter (intercept)
Precip Driest Quarter AgeRangeCor_slope
Precip Seasonality (intercept)
Precip Seasonality AgeRangeCor_slope
Precip Warmest Quarter (intercept)
Precip Warmest Quarter AgeRangeCor_slope
Precip Wettest Month (intercept)
Precip Wettest Month AgeRangeCor_slope
Precip Wettest Quarter (intercept)
Precip Wettest Quarter AgeRangeCor_slope
srad (intercept)
srad AgeRangeCor_slope
Temp Annual Range (intercept)
Temp Annual Range AgeRangeCor_slope
Temp Seasonality (intercept)
Temp Seasonality AgeRangeCor_slope
tmax (intercept)
tmax AgeRangeCor_slope
tmin (intercept)
tmin AgeRangeCor_slope
vp (intercept)
vp AgeRangeCor_slope
Data_Source
BIOCLIM
DAYMET

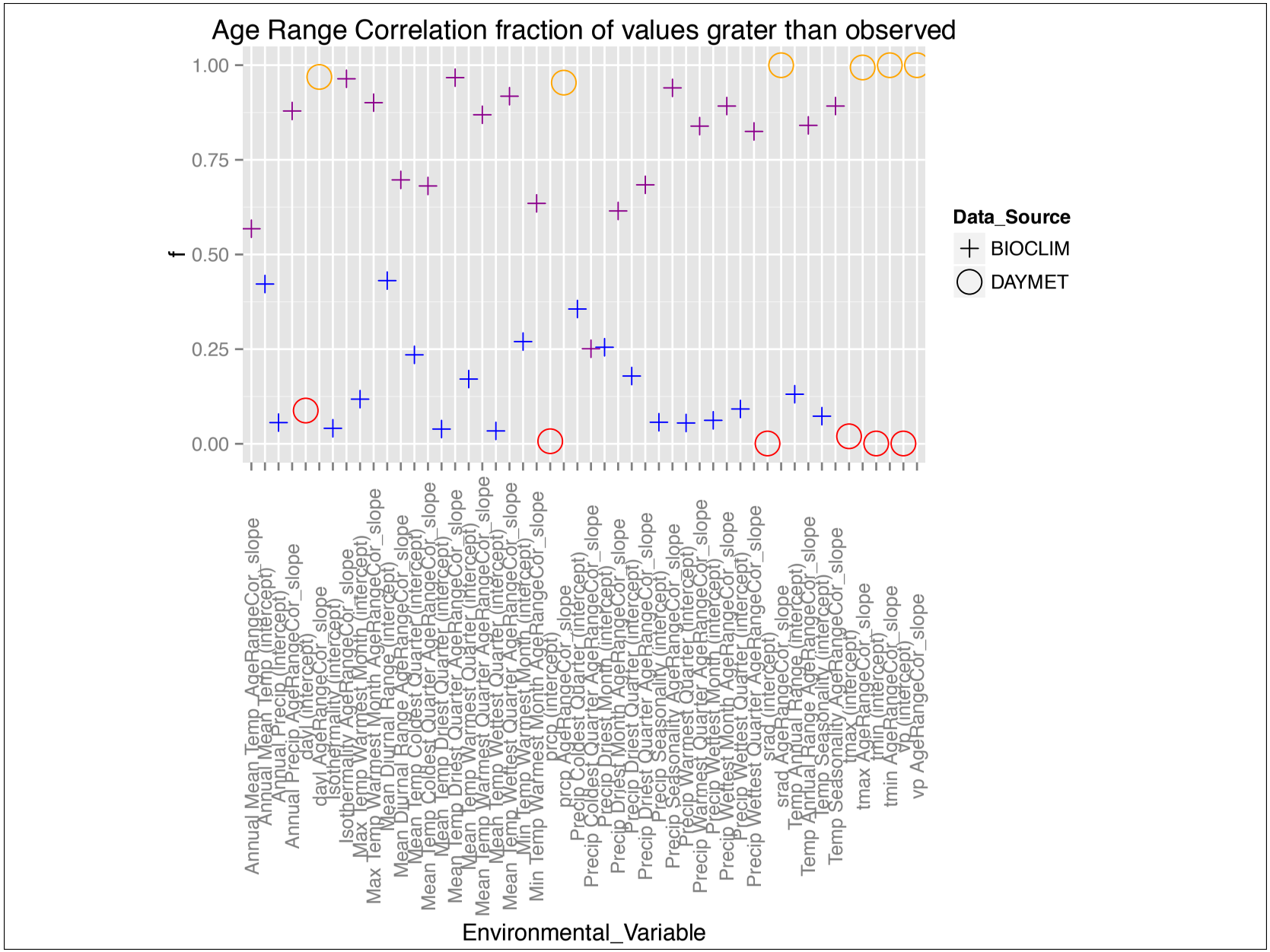
Age Range Correlation fraction of values grater than observed
f
1.00
0.75
0.50
0.25
0.00
Data_Source
BIOCLIM
DAYMET
Annual Mean Temp_AgeRangeCor_slope
Annual Mean Temp (intercept)
Annual Precip (intercept)
Annual Precip_AgeRangeCor_slope
dayl (intercept)
dayl_AgeRangeCor_slope
Isothermality (intercept)
Isothermality_AgeRangeCor_slope
Max Temp Warmest Month (intercept)
Max Temp Warmest Month_AgeRangeCor_slope
Mean Diurnal Range (intercept)
Mean Diurnal Range_AgeRangeCor_slope
Mean Temp Coldest Quarter (intercept)
Mean Temp Coldest Quarter_AgeRangeCor_slope
Mean Temp Driest Quarter (intercept)
Mean Temp Driest Quarter_AgeRangeCor_slope
Mean Temp Warmest Quarter (intercept)
Mean Temp Warmest Quarter_AgeRangeCor_slope
Mean Temp Wettest Quarter (intercept)
Mean Temp Wettest Quarter_AgeRangeCor_slope
Min Temp Warmest Month (intercept)
Min Temp Warmest Month_AgeRangeCor_slope
prcp (intercept)
prcp_AgeRangeCor_slope
Precip Coldest Quarter (intercept)
Precip Coldest Quarter_AgeRangeCor_slope
Precip Driest Month (intercept)
Precip Driest Month_AgeRangeCor_slope
Precip Driest Quarter (intercept)
Precip Driest Quarter_AgeRangeCor_slope
Precip Seasonality (intercept)
Precip Seasonality_AgeRangeCor_slope
Precip Warmest Quarter (intercept)
Precip Warmest Quarter_AgeRangeCor_slope
Precip Wettest Month (intercept)
Precip Wettest Month_AgeRangeCor_slope
Precip Wettest Quarter (intercept)
Precip Wettest Quarter_AgeRangeCor_slope
srad (intercept)
srad_AgeRangeCor_slope
Temp Annual Range (intercept)
Temp Annual Range_AgeRangeCor_slope
Temp Seasonality (intercept)
Temp Seasonality_AgeRangeCor_slope
tmax (intercept)
tmax_AgeRangeCor_slope
tmin (intercept)
tmin_AgeRangeCor_slope
vp (intercept)
vp_AgeRangeCor_slope
Environmental_Variable

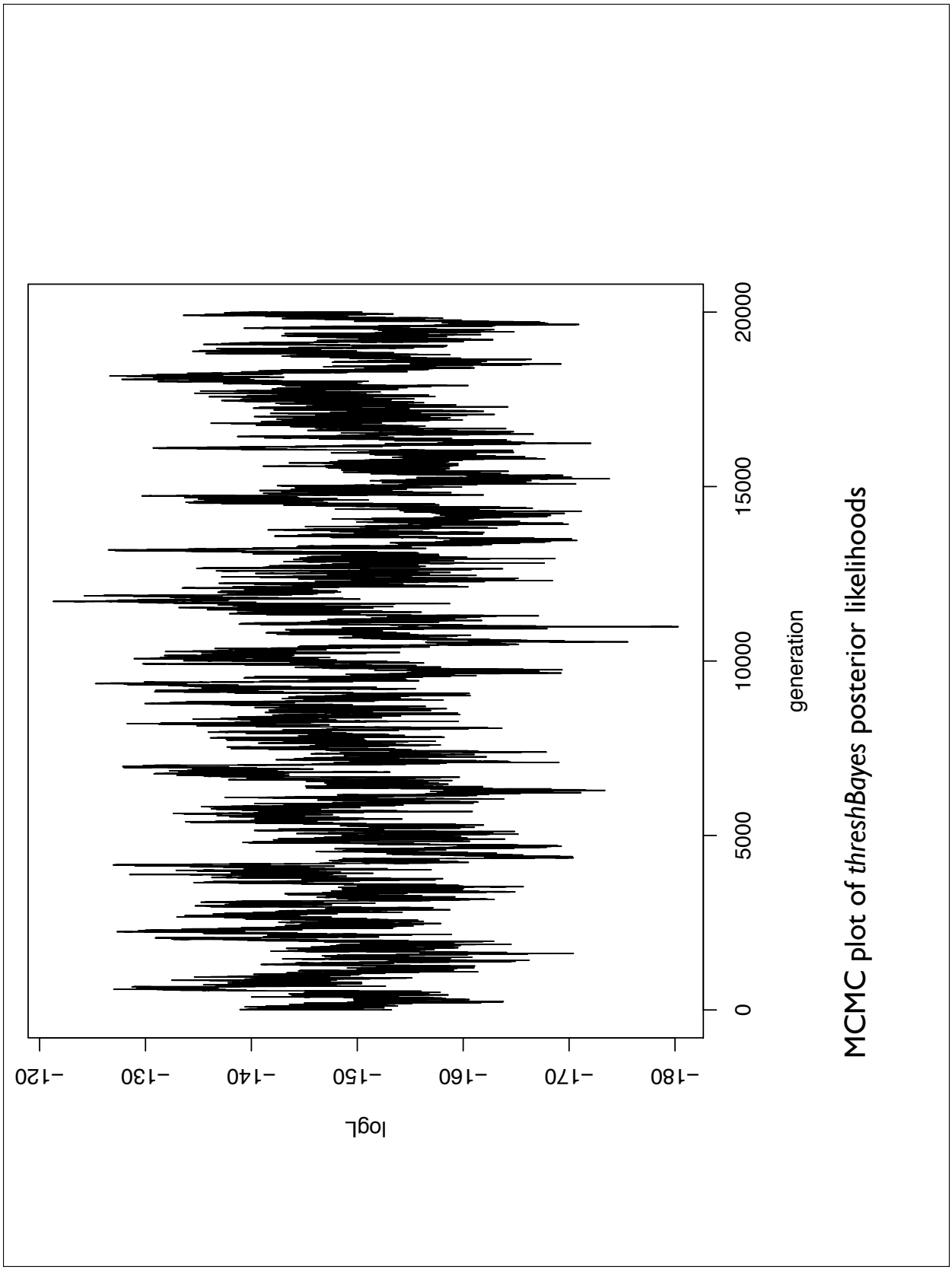
MCMC plot of *threshBayes* posterior likelihoods
logL
−120
−130
−140
−150
−160
−170
−180
0
5000
10000
15000
20000
generation

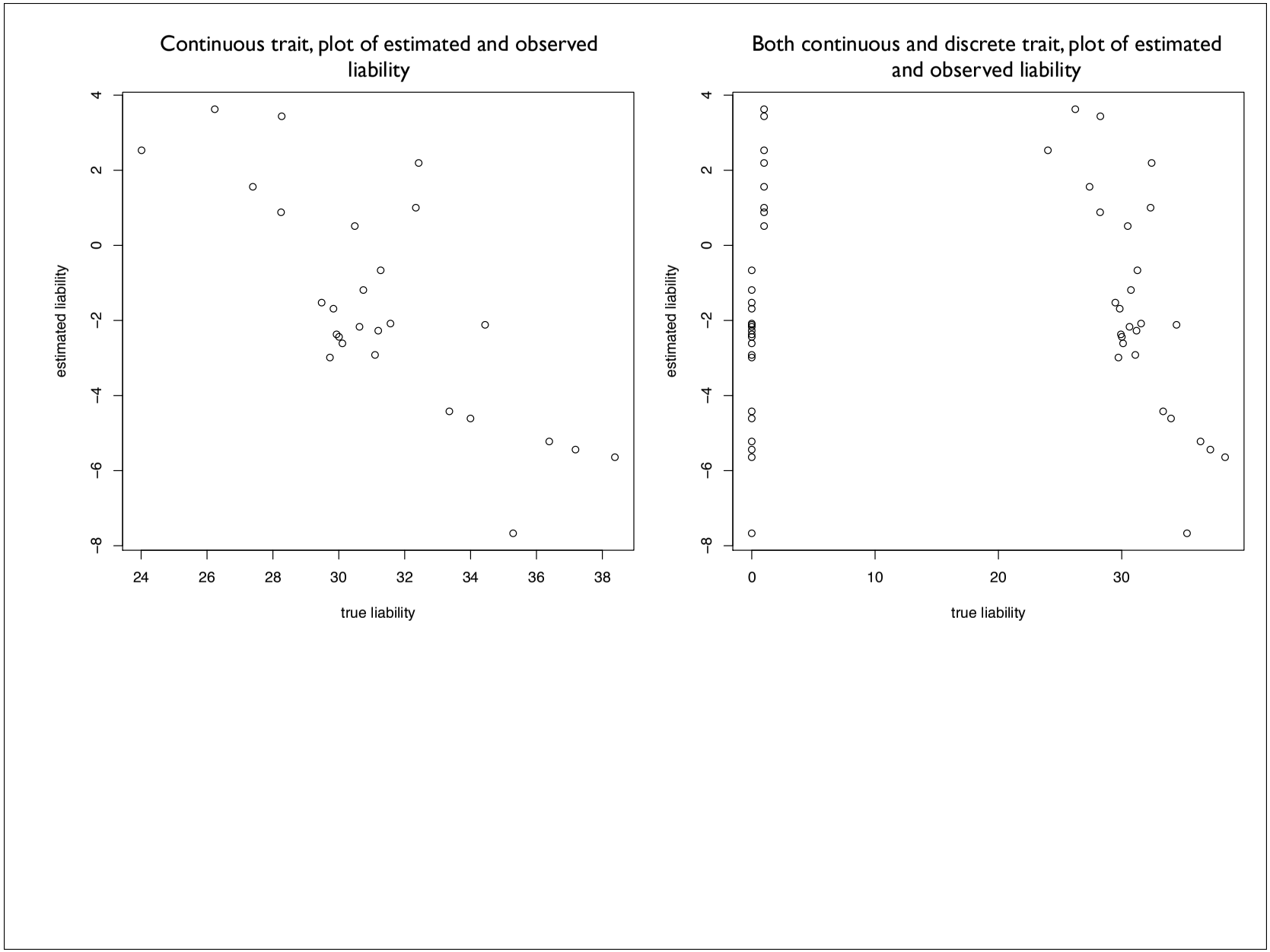
Continuous trait, plot of estimated and observed liability
estimated liability
true liability
Both continuous and discrete trait, plot of estimated and observed liability
estimated liability
true liability